

UNIVERSAL  
LIBRARY



123 432

UNIVERSAL  
LIBRARY











# TRANSACTIONS

OF THE

## AMERICAN INSTITUTE OF MINING AND METALLURGICAL ENGINEERS

(INCORPORATED)

Vol. 111

---

## INSTITUTE OF METALS DIVISION 1934

---

PAPERS AND DISCUSSIONS PRESENTED BEFORE THE DIVISION AT MEETINGS HELD  
AT DETROIT, OCTOBER, 1933 AND AT NEW YORK, FEBRUARY, 1934  
AND OCTOBER, 1934

---

NEW YORK, N. Y.  
PUBLISHED BY THE INSTITUTE  
AT THE OFFICE OF THE SECRETARY  
29 WEST 39TH STREET

## Notice

This volume is the eighth of a series constituting the official proceedings of the Institute of Metals Division of the American Institute of Mining and Metallurgical Engineers. It deals with nonferrous metals and includes papers presented at the Detroit Meeting, Oct 4-5, 1933, and the New York Meetings, Feb 19-22 and Oct 2-4, 1934.

The series is a continuation of the publications and proceedings of the Institute of Metals Division. The complete list of publications and proceedings, including the present volume, is as follows:

1908-1911 *Transactions* of the American Brass Founders' Association 1908, Vols 1 and 2; 1909, Vol 3; 1910, Vol 4; 1911, Vol 5.

1912-1916 *Transactions* of the American Institute of Metals, Vols 6-10

1917-1918 *Journal* of the American Institute of Metals, Vols 11-12

1919-1926 *TRANSACTIONS* of the American Institute of Mining and Metallurgical Engineers, Volumes 60, 64, 67, 68, 69, 70, 71 and 73.

1927-1928 *PROCEEDINGS* of the Institute of Metals Division of the American Institute of Mining and Metallurgical Engineers, two volumes, of which the latter is now designated Vol. 78 of the A I M E. *TRANSACTIONS*

1929-1934 *TRANSACTIONS* of the American Institute of Mining and Metallurgical Engineers, Volumes 83, 89, 93, 99, 104 and 111, Institute of Metals Division

COPYRIGHT, 1934, BY THE  
AMERICAN INSTITUTE OF MINING AND METALLURGICAL ENGINEERS  
(INCORPORATED)

---

PRINTED IN THE UNITED STATES OF AMERICA

THE MAPLE PRESS COMPANY, YORK, PA



## THE INSTITUTE OF METALS LECTURE

AN annual lectureship was established in 1921 by the Institute of Metals Division, which has come to be one of the important functions of the Annual Meeting of the Institute. A number of distinguished men from this country and abroad have served in this lectureship. The roll is quoted below:

- 1922 Colloid Chemistry and Metallurgy By Wilder D Bancroft
- 1923 Solid Solution By Walter Rosenham
- 1924 The Trend in the Science of Metals By Zay Jeffries
- 1925 Action of Hot Wall a Factor of Fundamental Influence on the Rapid Corrosion of Water Tubes and Related to the Segregation in Hot Metals By Carl Benedicks
- 1926 The Relation between Metallurgy and Atomic Structure By Paul D Foote
- 1927 Growth of Metallic Crystals By Cecil H Desch
- 1928 Twinning in Metals By C H Mathewson
- 1929 The Passivity of Metals, and Its Relation to Problems of Corrosion By Ulrick R Evans
- 1930 Hard Metal Carbides and Cemented Tungsten Carbide By S L Hoyt
- 1931 X-ray Determination of Alloy Equilibrium Diagrams By Arne Westgren
- 1932 The Age-hardening of Metals By Paul D Merica
- 1933 Present-day Problems in Theoretical Metallurgy By Georg Maseng
- 1934 Ferromagnetism in Metallic Crystals By L W McKechnan

## A. I. M. E. OFFICERS AND DIRECTORS

For the year ending February, 1935

President and Director, HOWARD N EAVENSON, Pittsburgh, Pa  
Past President and Director, SCOTT TURNER, Washington, D C  
Past President and Director, FREDERICK M BECKET, New York, N Y  
Vice President, Treasurer and Director, KARL EILERS, New York, N Y

### VICE PRESIDENTS AND DIRECTORS

EUGENE MCAULIFFE, Omaha, Neb	HENRY KRUMB, Salt Lake City, Utah
PAUL D MERICA, New York, N Y	EDGAR RICKARD, New York, N Y
LOUIS S CATES, New York, N Y	

### DIRECTORS

ERLE V DAVELER, New York, N Y	MILNOR ROBERTS, Seattle, Wash
HARVEY S MUDD, Los Angeles, Calif	FRANK L SIZER, San Francisco, Calif
J V W REYNDERS, New York, N Y	H A BUEHLER, Rolla, Mo
J B UMPLEBY, Norman, Okla	CHARLES B MURRAY, Cleveland, Ohio
CHARLES C WHITTIER, Chicago, Ill	BRENT N RICKARD, El Paso, Texas
ELI T CONNER, Scranton, Pa	GEORGE B WATERHOUSE, Cambridge, Mass
JOHN M LOVEJOY, New York, N Y	WILLIAM WRAITH, New York, N Y
HUGH PARK, Cobalt, Ont	

Secretary, A B PARSONS, New York, N Y

---

Assistant Secretary, EDWARD H ROBIE, New York, N Y  
Assistant to the Secretary, JOHN T BREUNICH, New York, N Y  
Assistant to the Secretary, E J KENNEDY, JR, New York, N. Y.  
Assistant Treasurer, H A. MALONEY, New York, N Y



## INSTITUTE OF METALS DIVISION

Chairman, J L CHRISTIE, Bridgeport, Conn  
 Past Chairman, T S FULLER, Schenectady, N Y  
 Vice Chairman, W M PEIRCE, Palmerton, Pa  
 Vice Chairman, W A SCHEUCH, Tottenville, N Y  
 Secretary, E M WISE  
 International Nickel Co., Bayonne, N J  
 Treasurer, W M CORSE, Washington, D C

### *Executive Committee*

H A BEDWORTH, <sup>1</sup> Waterbury, Conn	G O HIERS, <sup>4</sup> Brooklyn, N Y
D K CRAMPTON, <sup>2</sup> Marion, Conn	R H LEACH, <sup>3</sup> Bridgeport, Conn
E H DIX, JR., <sup>1</sup> New Kensington, Pa	R F MEHL, <sup>2</sup> Pittsburgh, Pa
J A GANN, <sup>3</sup> Midland, Mich	J WALTER SCOTT, <sup>1</sup> Chicago, Ill
JEROME STRAUSS, <sup>2</sup> Bridgeville, Pa	

### *Finance Committee*

	T S FULLER, <sup>3</sup> Chairman	
W. M. CORSE <sup>1</sup>	C H MATHEWSON <sup>2</sup>	SAM TOUR <sup>1</sup>
	H S RAWDON <sup>2</sup>	

### *Data Sheet Committee*

	JEROME STRAUSS, <sup>3</sup> Chairman	
R S ARCHER <sup>1</sup>	L W KEMPF <sup>2</sup>	N B PILLING <sup>1</sup>
ARTHUR PHILLIPS <sup>1</sup>		WILLIAM G SCHNEIDER <sup>1</sup>

### *Papers and Publications*

	A J PHILLIPS, <sup>1</sup> Chairman	
	R F MEHL, <sup>1</sup> Vice Chairman	
W H BASSETT, JR. <sup>2</sup>	O W ELLIS <sup>1</sup>	W H FINKELDEY <sup>1</sup>
L W KEMPF <sup>2</sup>	W M PEIRCE <sup>1</sup>	N B PILLING <sup>1</sup>
W ROMANOFF <sup>3</sup>	W A SCHEUCH <sup>2</sup>	T A WRIGHT <sup>2</sup>
	LYALL ZICKRICK <sup>3</sup>	

### *Annual Lecture Committee*

	W M CORSE, <sup>1</sup> Chairman	
E H DIX, JR. <sup>3</sup>	T. S FULLER <sup>1</sup>	PAUL D MERICA <sup>1</sup>
W. B PRICE <sup>2</sup>		SAM TOUR <sup>2</sup>

### *Membership Committee*

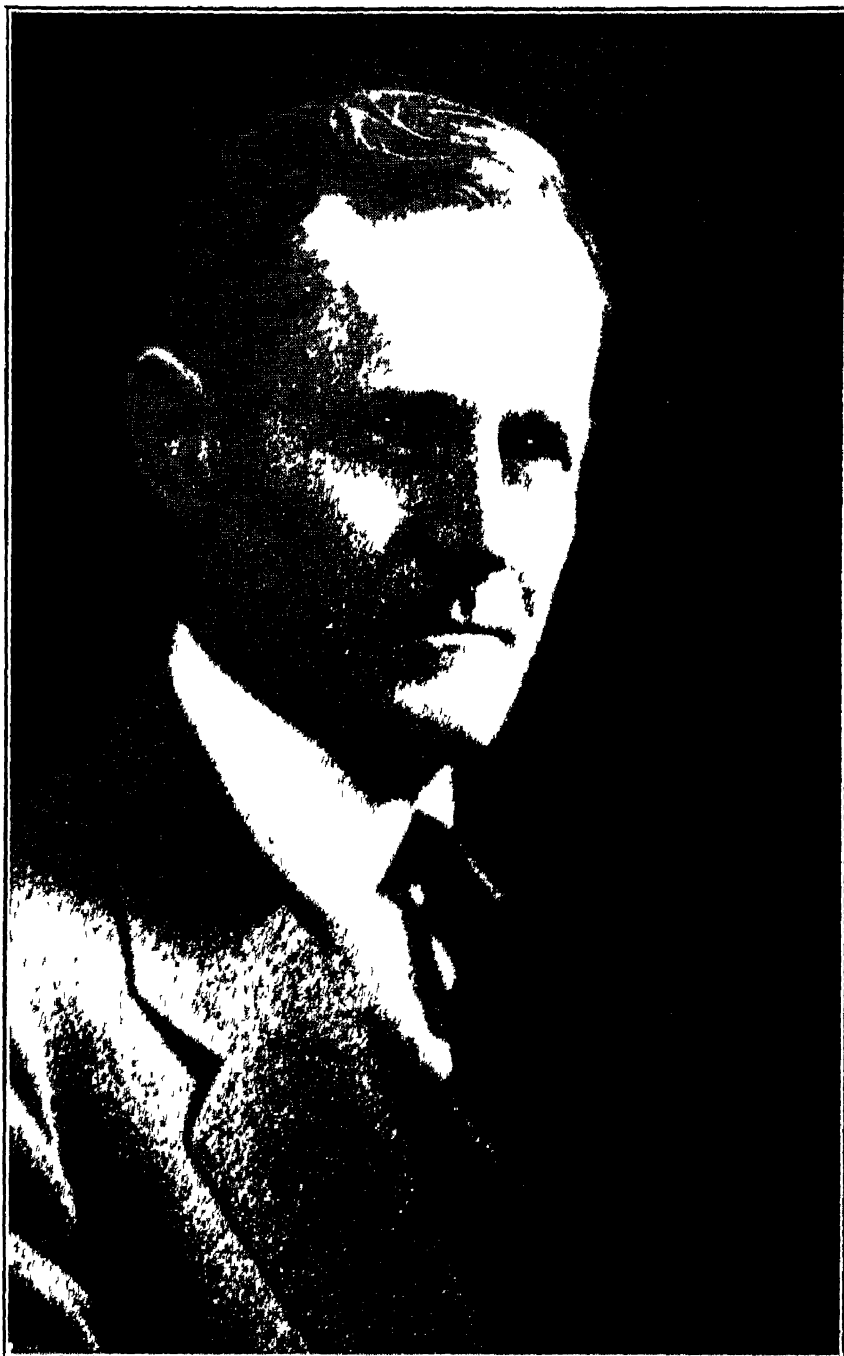
	E A ANDERSON, <sup>1</sup> Chairman	
J R FREEMAN, JR. <sup>1</sup>	J A GANN <sup>4</sup>	G. O. HIERS <sup>1</sup>
R. F. MEHL <sup>1</sup>		J. WALTER SCOTT <sup>2</sup>

### *Nominating Committee*

	SAM TOUR, Chairman	
T S FULLER	A J PHILLIPS	W. B. PRICE
	E M WISE	

<sup>1</sup> Until February, 1935    <sup>2</sup> Until February, 1936.    <sup>3</sup> Until February, 1937.





*Photograph by Bachrach*

**L. W. McKEEHAN**

*Institute of Metals Division Lecturer, 1934*

## Ferromagnetism in Metallic Crystals

By L. W. McKEEHAN,\* NEW HAVEN, CONN.

(Institute of Metals Division Lecture)

It is no longer necessary, if it ever was, for your annual lecturer to apologize for including in his remarks frequent references to the arrangement of metal atoms in crystals and for basing his arguments that metals behave as they do upon their crystal structure. Neither will any objection be raised because the large metallic crystals of which we will speak are hard to prepare and of negligible commercial interest. The particular set of physical properties we propose to discuss—ferromagnetic properties—may require more justification. Very few in this audience are primarily, or even remotely, interested in the ferromagnetic behavior of the metals they handle. By no means all of you ever deal, by choice or by necessity, with metals which display any ferromagnetism at all, and even those who study or control ferrous metallurgy must usually depend upon electrical engineers for assistance in ferromagnetic applications.

My excuse for talking about such an obvious specialty is, like all Gaul, divided into three parts. In the first place, the members of the committee who select the annual lecturer must wish the speaker to confine himself to matters he has at least thought about before he prepares his speech. In the second place, the study of ferromagnetism in crystals has, as you will soon realize, suffered in the not-too-distant past from inadequate metallurgy. Further progress probably depends upon proper use being made of the skill and knowledge of some members of the Institute of Metals Division who have not, before today, been asked to think about the problems presented here. Finally, there is at least a sporting chance that the ferromagnetic properties of a few metal crystals will give some insight into the more generally interesting properties which they share with nonferromagnetic metal crystals.

Our topic is neither ancient nor ultra modern. The Greeks did not even have a word for it, but as soon as metallographers agreed that iron at room temperature was at least predominantly crystalline, it became evident that ferromagnetism in metallic crystals had frequently been observed to exist. We will ignore this negative sort of knowledge to confine our attention to the ways in which individual crystals show ferromagnetism. We could still, if we had time, go back of the first deliberate

---

\* Director, Sloane Physics Laboratory, Yale University

† Presented at the New York Meeting, February, 1934. Thirteenth annual lecture.

tests on monocrystal specimens to comb the prior art for disclosures of peculiar magnetic behavior now traceable to then unsuspected anisotropy of crystal aggregates. Such a search, which we will not undertake, should not be necessary before about 1880, since the whole subject of ferromagnetism hardly deserved a name of its own before that date. About then Emil Warburg<sup>(1)</sup> and James Alfred Ewing<sup>(2)</sup>—the latter is still living—independently observed that sort of hysteresis which still seems inseparable from ferromagnetic behavior and which is, perhaps, the only ferromagnetic property never found in nonferromagnetics. What they discovered was that the magnetization of an iron wire at a particular intensity of the applied magnetic field depended not only upon that value of the intensity but also upon the previous succession of such values. (The technical jargon in which this discovery is reburied will be explained a little later.)

In the next 37 years the ferromagnetism of what we now call polycrystalline metal received much attention in laboratory and workshop. (It may be noticed that these words mean about the same thing.) Let us see what language, including mathematics, was in use by the time ferromagnetism in monocrystalline metal was first reported upon in 1918.

It was already clear that all magnetic phenomena could be explained—that is, rendered consistent with other phenomena supposed to be simpler—by imagining them due to the motion of electricity within what people still sometimes called “ponderable matter.” We have since given up “imponderable” matter, so can now drop “ponderable” also. In paramagnetic matter there seemed to be permanent electric currents which might be arranged in various ways by the appropriate manipulation of electric currents outside the specimen, in a near-by coil of copper wire, for example. In ferromagnetic matter traces of any previous arrangement of the permanent currents could always be detected—hence hysteresis—and if an arrangement persisted very strongly the ferromagnetic metal itself might, in the form of a so-called permanent magnet, be used to induce changes in the arrangements within other bodies.

In quantitative work there arose the usual didactic fiction, the separation of a part of the phenomenon, called a *cause*, from another part, called an *effect*. This naturally permits the formulation of laws connecting the quantity of the effect with the quantity of the cause, and this is always regarded as a triumph. The putative cause was named the magnetic field, inseparably and quantitatively connected with moving electricity. The putative effect was named the magnetization, and, as we have just said, this too is inseparably and quantitatively connected with moving electricity, being, in fact, another name for the arrangement in space of certain permanent currents in the ferromagnetic body. The horrible confusion that resulted as soon as these names took the places of

---

\* Superior figures in parentheses refer to bibliography at end of paper.

the ideas they represented, so that their real kinship was forgotten, has cursed electrical engineering and even some outlying parts of physics with interminable arguments about units, dimensions, and equations, in which proponent and opponent carefully avoided learning each other's language. Without venturing into this no-man's-land we hasten to set up some equations between quantities which everybody will measure in the same way no matter how he was brought up.

In any finite ferromagnetic body apparently at rest and in magnetic equilibrium with its surroundings, the magnetic field intensity at a point—what Van Vleck<sup>(3)</sup> calls the microscopic field intensity—depending as it must on the motion of electrons and other charged particles, no doubt varies in magnitude and direction in regions of atomic dimensions and cannot be independent of the instant in time at which its value is desired. Since the detailed study of such highly variable fields is, to say the least, beyond present experimental technique, we have to be satisfied with an average value of the field intensity taken throughout a small volume, which is still large enough to contain very many atoms. This average value—what Van Vleck calls the macroscopic field intensity—is constant in time under our proposed conditions, except for fluctuations we can safely ignore at this stage of our progress. It will, in general, be different in different parts of a ferromagnetic body. If, by very good management, it is the same in magnitude and direction everywhere in the body, we say that conditions are homogeneous.

The macroscopic magnetic field intensity we have just been defining is usually called the magnetic induction,  $B$ . Obviously it includes magnetic field intensities due not only to permanent electric currents in the volume throughout which the average extends, but also those due to remote permanent currents in the rest of the ferromagnetic body, or in adjacent bodies, or to currents artificially maintained in wires, if any such permanent or quasipermanent currents are near enough to contribute measurably to the resultant magnetic field. We now proceed to separate  $B$  into a cause and an effect, and we try to make the effect depend only upon the arrangement of permanent currents in the volume we chose in defining  $B$ . This seems a natural thing to do—though it is not—because once we have put a wholly imaginary boundary around the little volume in which  $B$  is known we insist on regarding it as a real boundary. We are willing to let any moving bit of electricity inside our boundary know directly all about the motions of its compatriots within the boundary, but we insist that it can only know about the outside universe as much as we can sum up in a magnetic field intensity which shall *cause* the little volume to be as it is. Disregarding this philosophical objection, as usual, we write, in Heaviside-Lorentz units,

$$B_{HLU} = I_{HLU} + H_{HLU} \quad [1]$$

where  $I_{HLU}$  is the intensity of magnetization (the effect!) and  $H_{HLU}$  is the

magnetic field intensity (the cause!) Notice that this is a vector equation—the three terms will usually differ in direction in the case of a crystal.

Another name for  $I_{HLO}$  is magnetic moment per unit volume, and under this title its identity in kind with a magnetic field intensity may seem at least debatable. Remember, however, that a magnetic field intensity can be computed by dividing a magnetic moment by the cube of a length and the paradox resolves itself. The likeness of magnetization and magnetic field intensity is further obscured when the same separation is made in electromagnetic units

$$\mathbf{B} = \mathbf{H} + 4\pi\mathbf{I} \quad [2]$$

We always put the cause before the effect so as to heighten the illusion. A distinctive name for  $\mathbf{I}$  is now a necessity.

In a body with a real boundary—that is, in every real body— $\mathbf{H}$  can be subdivided without much trouble into a magnetizing field intensity  $\mathbf{H}_M$  and a demagnetizing field intensity  $\mathbf{H}_D$  so that, still in vector notation,

$$\mathbf{H} = \mathbf{H}_M + \mathbf{H}_D \quad [3]$$

The magnetizing field is that part of  $\mathbf{B}$  due to permanent currents quite outside the specimen, the demagnetizing field is all the rest that has not already been segregated in the term  $4\pi\mathbf{I}$ . If this seems a very awkward definition for  $\mathbf{H}_D$ , try to find a better, which does not include one or more words we have not yet been forced to define. The essentially artificial aspect of what has just been done now appears when we discover that  $\mathbf{H}_D$  depends upon  $\mathbf{I}$ . If conditions are homogeneous  $\mathbf{H}_D$  is a linear vector function of  $\mathbf{I}$ , and there are three coordinate axes at right angles, say  $\mathbf{a}_1, \mathbf{a}_2, \mathbf{a}_3$ , with respect to which the relation between  $\mathbf{H}_D$  and  $\mathbf{I}$  takes the very simple form

$$\left. \begin{aligned} H_{D_1} &= n_1 I_1 \\ H_{D_2} &= n_2 I_2 \\ H_{D_3} &= n_3 I_3 \end{aligned} \right\} \quad [4]$$

That is, for a proper choice of axes of reference each component of  $\mathbf{H}_D$  depends only upon the corresponding component of  $\mathbf{I}$ . The coefficients  $n_1, n_2, n_3$  are the three demagnetizing factors. The choice of axes and the magnitudes of  $n_1, n_2, n_3$  depend upon the shape of the ferromagnetic body. If the demagnetizing factors are found by experiment not to be constant in a particular body, this is proof that it has not remained homogeneously magnetized.

If  $\mathbf{I}$  changes by a small amount,  $d\mathbf{I}$ , in a magnetic field of intensity  $\mathbf{H}$  the work done on the ferromagnetic material per unit volume is

$$dW = \mathbf{H} \cdot d\mathbf{I} \quad [5]$$

An equivalent equation involving only scalars is

$$dW = H_1(dI)_1 + H_2(dI)_2 + H_3(dI)_3 \quad [6]$$

It must be remembered that  $d\mathbf{I}$  is a vector the direction of which may be quite different from the direction of  $\mathbf{I}$ .

In isotropic bodies  $\mathbf{I}$  and  $\mathbf{H}$  may be parallel. They certainly would be if it were not for hysteresis, and if  $\mathbf{H}$  is varied sufficiently in magnitude while remaining parallel to itself the body will forget that  $\mathbf{H}$  ever had any other direction and  $\mathbf{I}$  will remain parallel to  $\mathbf{H}$  in spite of hysteresis. A two-dimensional drawing will then be an adequate record of simultaneous values of  $I$  and  $H$ . As  $I$  and  $H$  change, the drawing pen traces a continuous curve. In accordance with equation 6, which now has but one term on the right-hand side, the work done on the specimen, or the magnetic energy input in going from a point  $A$  on such a curve to a point  $B$  farther along on the same curve is

$$W_B - W_A = \int_A^B H dI \quad [7]$$

If we get the material into a cyclic state so that the pen continually retraces the same loop its area is the work lost per cycle, and under our fundamental assumption that all changes are quasistationary this is the hysteresis loss

$$W_h = \oint H dI \quad [8]$$

or

$$W_h = \frac{1}{4\pi} \oint H dB \quad [9]$$

in which form it is more familiar to engineers

Points inside any loop can be reached by suitable changes in  $H$  within the limits given by the tips of the loop. Sometimes a small area outside the loop is also traversable by this process <sup>(4)</sup>. The shape as well as the area of a loop depends upon the range in  $H$ , but for sufficiently great values of  $H$ , plus at one limit, minus at the other, the part of the loop near the origin is invariant with respect to the extreme values of  $H$ . The intersections of this maximal  $B$ - $H$  loop with the axes give  $B_r$ , the remanence, and  $H_c$ , the coercivity. The corresponding intersection of the maximal  $I$ - $H$  loop with the  $I$ -axis gives  $I_r$ , the remanent magnetization, but there is no accepted term or symbol for the  $H$ -intercept. Fig. 1, drawn for a magnet steel, shows the quantities just mentioned. It also shows why the magnetization  $\mathbf{I}$  was worth inventing, for it, unlike  $\mathbf{B}$  and  $\mathbf{H}$ , has a limiting or saturation value  $I_s$  beyond which it does not go. It is pleasant to think that  $I_s$  characterizes the best of all possible arrangements of the permanent electric currents in the material.

One other important line on the  $I$ - $H$  or  $B$ - $H$  plane remains to be considered. It starts at  $I = 0$ ,  $H = 0$  or at  $B = 0$ ,  $H = 0$  and is the locus traced out by the upper tip of a symmetrical hysteresis loop centered



at this origin as the range in  $H$  is slowly increased. It is called the normal magnetization curve (even when drawn on the  $B$ - $H$  plane) The ratio of ordinate to abscissa for any point on this line is the corresponding susceptibility,

$$\kappa = I/H \quad [10]$$

or permeability

$$\mu = B/H \quad [11]$$

Whether  $\kappa$  and  $\mu$  have any useful meaning for points on other  $I$ - $H$  and  $B$ - $H$  curves is rather doubtful.

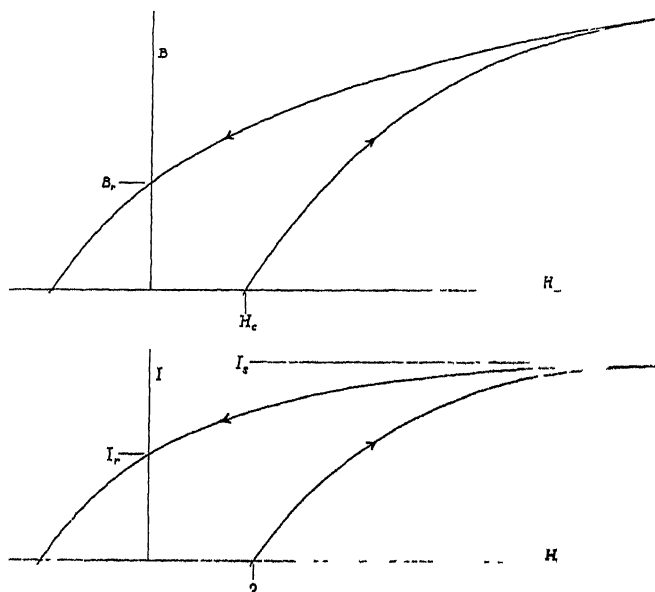


FIG 1.— $B$ - $H$  AND  $I$ - $H$  HYSTERESIS LOOPS.

In a crystal specimen the vectors  $B$ ,  $I$ ,  $H$ ,  $H_M$  and  $H_D$  generally point in five distinct directions. Even if we confine ourselves to  $B$ ,  $I$  and  $H$  it is clear that the scalars  $B_r$  or  $I_r$ ,  $H_c$ ,  $W_h$  are not adequate to a proper presentation of the data of experiment. Two-dimensional pictures can show the relations of  $I$  and  $H$ , or  $B$  and  $H$ , only in specially restricted cases. Three-dimensional diagrams or their analytical equivalents are called for. In order to save time at a later point we will explain two ways in which analytical equivalents have been devised.

If  $I$  happened to be a linear vector function of  $H$  over the whole range in  $H$  we could use the scheme already explained in getting  $H_D$  from  $I$ . There is always some range in  $H$  over which this is nearly enough true to make the analysis worth while but at least as soon as  $I/I_s$  becomes as large as  $1/3$  the increase of  $I$  with  $H$  must cease to be linear. William

Thomson, later Lord Kelvin, worked out the linear case for all crystal systems as early as 1850<sup>(6)</sup> and pointed out that his analysis would probably not apply to soft iron.

Thomson's first approximation is not too bad in hexagonal crystals but in cubic crystals it misses all the interesting facts. In any crystal whatever we can always find three rectangular axes along which  $\mathbf{I}$  is parallel to  $\mathbf{H}$ . The coefficients replacing  $n_1, n_2, n_3$  in equation 4 become the so-called principal susceptibilities  $\kappa_1, \kappa_2, \kappa_3$  according to the scheme

$$\left. \begin{aligned} I_1 &= \kappa_1 H_1 \\ I_2 &= \kappa_2 H_2 \\ I_3 &= \kappa_3 H_3 \end{aligned} \right\} \quad [12]$$

In the triclinic system  $\kappa_1, \kappa_2, \kappa_3$  are independent and the principal axes cannot be fixed from a knowledge of the crystallographic axes. In the monoclinic system one principal axis is parallel to the single symmetry axis, or perpendicular to the single symmetry plane, the azimuths of the other two principal axes have to be found by experiment. In the orthorhombic system the principal axes coincide with the crystallographic axes. In the tetragonal and hexagonal systems one principal axis is parallel to the single fourfold or sixfold axis (the latter may be a threefold axis in some classes) the other two principal axes have the same  $\kappa$  and can be taken in any azimuth. It results that the magnetic symmetry is that of a spheroid rather than that appropriate to the crystal system. In the cubic system the principal axes may be turned into any orientation with respect to the cubic axes, all three have the same  $\kappa$  and the magnetic symmetry is that of a sphere so that the crystal behaves isotropically, and  $\mathbf{I}$  remains parallel to  $\mathbf{H}$ .

It will be noticed that the linear vector function insures that  $\mathbf{I}$  is a known radius vector of a known ellipsoid when  $\mathbf{H}$  is a known radius vector of a known sphere. The ellipsoid may degenerate into a spheroid or sphere.

Real cubic symmetry in the dependence of  $\mathbf{I}$  upon  $\mathbf{H}$  requires a non-linear vector function, and the simplest improvement only goes far enough to make the  $\mathbf{I}$ -surface corresponding to a fixed value of  $\mathbf{H}$  of the fourth degree instead of the second. Symmetry requires that the equation of such a surface take the form

$$k_4(I_1^4 + I_2^4 + I_3^4) + k_{22}(I_2^2 I_3^2 + I_3^2 I_1^2 + I_1^2 I_2^2) + k_2(I_1^2 + I_2^2 + I_3^2) + k_0 = 0 \quad [13]$$

and either  $k_4$  or  $k_{22}$ , but not both, can be made equal to zero without loss of generality. Experiments might then be summarized by showing how  $k_0, k_2$ , and  $k_{22}$ , for example, vary with the magnitude of  $\mathbf{H}$ . Nobody has yet done this.

Another and less ambitious program is to measure one scalar quantity, say the magnetic energy density, for different directions of  $\mathbf{I}$  for the same magnitude of  $\mathbf{I}$  in each case. Equation 13 still holds with  $k_0$  as the scalar

in question, but since  $I_1^2 + I_2^2 + I_3^2 = I^2$  is now a constant,  $k_2$  can be dropped and we can find out whether a single value for  $k_{22}$  will satisfy all the measured values of  $k_0$ . If so, the second approximation is good enough. If not, a fourth degree solution cannot be made to fit the measurements.

One other artifice has been tried <sup>(6)</sup>. Let us suppose that  $\mathbf{I}$  is always parallel not to the actual  $\mathbf{H}$  but to a fictitious magnetic field intensity, say  $\mathbf{H} + \mathbf{M}$  where  $\mathbf{M}$  may be called a crystalline field but is certainly not a measurable magnetic field at all. We then try to express  $\mathbf{M}$  as a vector function of  $\mathbf{I}$  (a linear vector function is inadequate). If any form of function with a single arbitrary parameter fits many data we can compare materials or individual crystals in terms of this parameter.

The study of ferromagnetism in crystals needs a special technique because in the more usual sort of measurements care is taken to use specimens that make impossible any great divergence between  $\mathbf{H}$  and  $\mathbf{I}$ . Here we wish any tendency toward such divergence to have the freest possible play. The methods which Pierre Weiss developed in dealing with the nonmetallic crystals of magnetite<sup>(7)</sup> and pyrrhotite<sup>(8)</sup> have been used with minor changes by most of the investigators we have to quote on metallic crystals. Weiss himself seems never to have reported any measurements in our more restricted field of interest, but one of his pupils<sup>(9)</sup> says that some small iron crystals had been examined by his methods at Zurich some time prior to 1909 and that the tentative opinion then held there was that iron and magnetite behaved alike.

## IRON

The first classic<sup>(10)</sup> in our literature is like most classics, more frequently mentioned than read. It is by Karl Beck, a student of Weiss at Zurich, and is astonishingly complete in every respect. Many ideas which have recently been advertised as new will be found in its 70 pages. The accident of publication in a Swiss journal containing no other papers on physics and at a time (April, 1918) when most of the world was otherwise occupied, explains why it has been studied less than it deserves. It deals with iron crystals.

Two of Beck's seven crystals came from an old grate bar; the other five, including all those on which much work was done, were prepared by de Freudenreich<sup>(11)</sup> by igniting with thermit in a crucible buried in sand to insure very slow cooling. The largest crystals found on breaking up the mass were about 2 cm. on an edge and contained nearly 2 per cent of the usual impurities—here predominantly silicon<sup>(12)</sup>—not very uniformly distributed. Cleavage faces of form  $\{100\}$  guided the sawing of slabs 0.1 to 0.2 cm. thick parallel to three important planes:  $\{100\}$ ,  $\{110\}$ ,  $\{111\}$ . These were filed carefully to thicknesses ranging from 0.02 to 0.03 cm. At this stage buttons were cut out, mounted on brass

rods, and turned down to diameters ranging from 0.66 to 0.92 cm. Finally the disks were rubbed down on fine sandpaper until their thicknesses fell between 0.0060 and 0.0110 cm. Eight disks were used in the magnetic experiments.

These little iron wafers must have been pretty severely cold-worked throughout their volume, even if the original slabs had been strain-free. We may be certain, however, that the cleaved crystals were already very imperfect. Beck traced Neumann bands over the corner between two perpendicular cleavage faces to prove that they lay approximately in  $\{211\}$  positions and remarks that the angles between the traces of various sets of Neumann bands on a single cleavage face varied from point to point by as much as several degrees of arc. He concluded that either before or during the formation of these markings the crystals must have been rather badly overstrained.

Even if the disks had been perfectly cut from perfectly crystallized iron they could not have been homogeneously magnetized, for this is possible only in the case of an ellipsoid for  $I$  intermediate between 0 and  $I_s$ . For an ellipsoid the demagnetizing factors are known and for a spheroid they take relatively simple forms<sup>(13)</sup>. If  $c$  is always the rotation axis, so that  $a$  and  $b$  are equal, the prolate spheroid has  $a < c$ , and an eccentricity  $e = \sqrt{1 - a^2/c^2}$ ; the oblate spheroid has  $a > c$  and  $e = \sqrt{1 - c^2/a^2}$ . For the former the demagnetizing factors are

$$\left. \begin{aligned} n_1 = n_2 &= -2\pi \left( \frac{1}{e^2} - \frac{1 - e^2}{2e^3} \log \frac{1 + e}{1 - e} \right) \\ n_3 &= -4\pi \left( \frac{1}{e^2} - 1 \right) \left( \frac{1}{2e} \log \frac{1 + e}{1 - e} - 1 \right) \end{aligned} \right\} \quad [14]$$

or, if  $a \ll c$

$$\left. \begin{aligned} n_1 = n_2 &= -2\pi \\ n_3 &= -4\pi \frac{a^2}{c^2} \left( \log \frac{2c}{a} - 1 \right) \end{aligned} \right\} \quad [15]$$

For the oblate spheroid

$$\left. \begin{aligned} n_1 = n_2 &= -2\pi \left( \frac{\sqrt{1 - e^2}}{e^3} \sin^{-1} e - \frac{1 - e^2}{e^2} \right) \\ n_3 &= -4\pi \left( \frac{1}{e^2} - \frac{\sqrt{1 - e^2}}{e^3} \sin^{-1} e \right) \end{aligned} \right\} \quad [16]$$

or, if  $a \gg c$

$$\left. \begin{aligned} n_1 = n_2 &= -\pi^2 c/a \\ n_3 &= -4\pi \end{aligned} \right\} \quad [17]$$

We will suppose as Beck did that the values of  $n_1, n_2, n_3$  for the largest oblate spheroids inscribable in his disk specimens are sufficiently close to

the real demagnetizing factors, here not constant throughout the volume. Equations 17 apply but even after writing down for one of his best disks ( $V_2: a = b = 0.345 \text{ cm}, c = 0.0045 \text{ cm}$ )  $n_1 = n_2 = -0.129, n_3 = -12.6$ , it may not be obvious that  $\mathbf{I}$  can rotate freely in the plane of the disk although any rotation away from this plane is greatly hampered. If the metal is isotropic, with  $\kappa = 30$  or more,  $\mathbf{H}_M$  can swing  $30^\circ$  out of the plane of the disk before  $\mathbf{I}$  swings out by as much as  $30'$ . The choice of such flat specimens therefore makes it unnecessary to measure more than two components of  $\mathbf{I}$  if reasonable care is taken to keep  $\mathbf{H}_M$  in the right plane.

Even with such a flattened form the value of  $H_1$  is very much less than that of  $H_{M1}$ . In the case just cited,  $H_1 = H_{M1}/(1 - n_1\kappa)$  gives  $H_1 = 0.205H_{M1}$  for  $\kappa = 30$ . If it were not for the high value of the demagnetizing factor for a sphere ( $n_1 = n_2 = n_3 = -4\pi/3$ ) the sphere would serve much better than the disk or flat spheroid, because in a sphere any divergence between  $\mathbf{I}$  and  $\mathbf{H}$  must depend wholly upon the material, in a spheroid or equivalent disk it may depend in part upon the shape, and the exact location of  $\mathbf{H}$  itself is not easy.

Beck's choice of diametral planes of forms  $\{100\}$ ,  $\{110\}$  and  $\{111\}$  is the best possible. Each has a symmetry axis for the axis of figure and the first two also lie parallel to symmetry planes. Under these conditions the axes for the vector function relating  $\mathbf{I}$  and  $\mathbf{H}$  may be taken so as to coincide with the axes for the linear vector function relating  $\mathbf{H}_D$  and  $\mathbf{I}$ . The plane of form  $\{111\}$  is not a symmetry plane, so results for this third type of specimen are not so easy to interpret.

As we have already suggested, Beck kept  $\mathbf{H}_M$  in the plane of the disk and measured two rectangular components of  $\mathbf{I}$ , also in the plane of the disk. Let us call these  $I_P$  (parallel to  $\mathbf{H}_M$ ) and  $I_N$  (perpendicular to  $\mathbf{H}_M$ ). If we need later to refer to the suppressed third component of  $\mathbf{I}$ , perpendicular to  $\mathbf{H}_M$  and to the plane of the disk, we can call it  $I_Q$ . Beck measured  $I_P$  for various directions of  $\mathbf{H}_M$  by suddenly withdrawing the properly orientated disk from a search coil in the air-gap of the electromagnet used to produce various constant values of  $\mathbf{H}_M$ . In order to reduce the effect of hysteresis  $\mathbf{H}_M$  was reversed several times before the disk was withdrawn. He measured  $I_N$  by a torsion balance and after a different succession of  $\mathbf{H}_M$  values, so that the correction of  $I_N$  for hysteresis is not so satisfactory.

In getting  $I_N$  the torsion axis was vertical, normal to the disk at its center, and coincident with an axis about which the electromagnet producing  $\mathbf{H}_M$  could be rotated into any azimuth,  $\theta$ . When the magnet is so rotated the torque on the specimen arises from two causes, hysteresis, which makes  $\mathbf{I}$  lag behind the momentary direction of  $\mathbf{H}$  in the disk, and the crystal anisotropy which, by itself, would put  $\mathbf{I}$  ahead of  $\mathbf{H}$  as often as behind it. The torque per unit volume is

$$\mathbf{T} = \mathbf{I} \times \mathbf{H}_M \quad [18]$$

or, in scalar form

$$T = I_N H_M \quad [19]$$

Since this is proportional to the twist of the suspension wire—measured by telescope and scale—the two directions of rotation give, for a fixed  $H_M$ , two  $T$ - $\theta$  curves. The mean value of  $T$  is as free from hysteresis

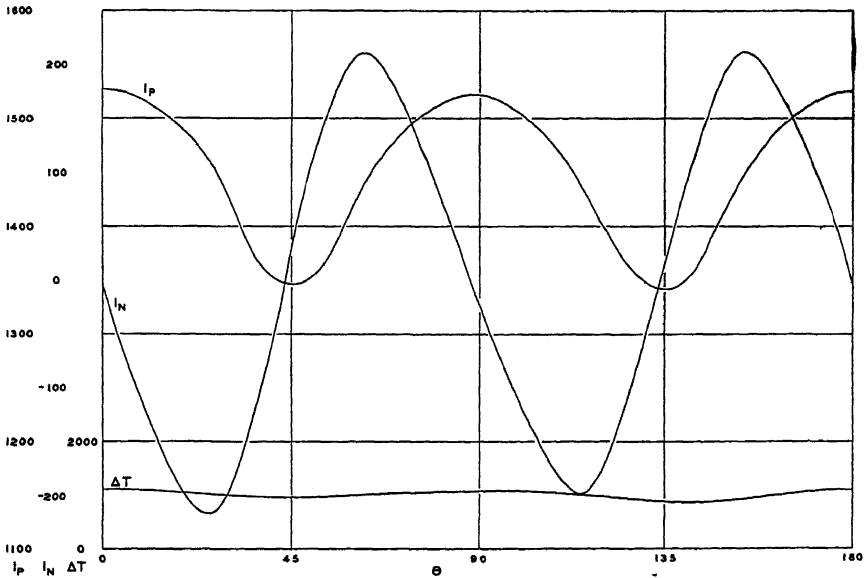


FIG 2— $I_P$ - $\theta$ ,  $I_N$ - $\theta$ ,  $\Delta T$ - $\theta$  FOR  $H_M = 392$  IN BECK'S IRON DISK {100}  
(No  $V_2$   $2a = 2b = 0.690$  cm,  $2c = 0.0090$  cm,  $n_1 = n_2 = -0.129$ ,  $n_3 = -12.6$ )  
Directions in the plane of the disk.  $\langle 100 \rangle$  at  $\theta = 0^\circ, 90^\circ$ ,  $\langle 110 \rangle$  at  $\theta = 45^\circ, 135^\circ$

effects as any we can get from such data. The area between the two  $T$ - $\theta$  curves is twice the hysteresis loss per turn.

Beck avoided the chief difficulty of the torsion balance by using so stiff a suspension that the angle of twist was generally small in comparison with  $\theta$ . This also prevented the instability in azimuth that has bothered some later users of this method of measurement.

We have selected from Beck's original paper a few curves showing  $I_P$ - $\theta$ ,  $I_N$ - $\theta$ , and  $\Delta T$ - $\theta$  ( $\Delta T$  is the separation of the two  $T$ - $\theta$  curves at a given value of  $\theta$ ) all for the same value of  $H_M$  and for the disks which he judged to be the best of each type. The basis for judgment was the symmetry of the curves, and examination of Figs. 2, 3 and 4 shows that the expected symmetry of the cubic crystal is well exhibited in each case. In redrawing Beck's curves the sign of  $I_N$  has been changed so that the convention here used makes  $I_N$  positive if  $I$  is ahead of  $H_M$ ; i. e., if the azimuth  $\phi$  of  $I$  is greater than the azimuth  $\theta$  of  $H_M$ .

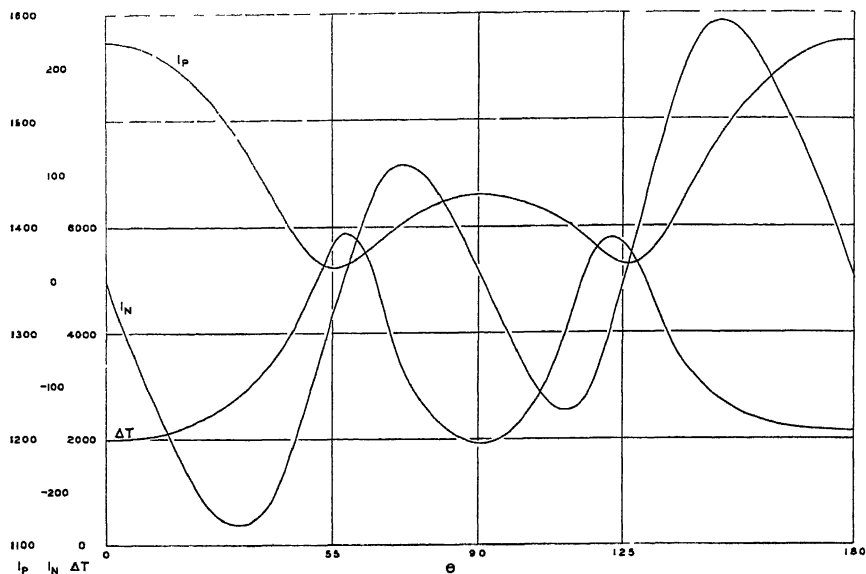


FIG 3— $I_P$ - $\theta$ ,  $I_N$ - $\theta$ ,  $\Delta T$ - $\theta$  FOR  $H_M = 392$  IN BECK'S IRON DISK {110}

(No VII,  $2a = 2b = 0.920$  cm,  $2c = 0.0085$  cm,  $n_1 = n_2 = -0.091$  [0.083 given],  $n_3 = -12.6$ ) Directions in the plane of the disk:  $\langle 100 \rangle$  at  $\theta = 0^\circ$ ,  $\langle 110 \rangle$  at  $\theta = 90^\circ$ ,  $\langle 111 \rangle$  at  $\theta = 55^\circ, 125^\circ$ .

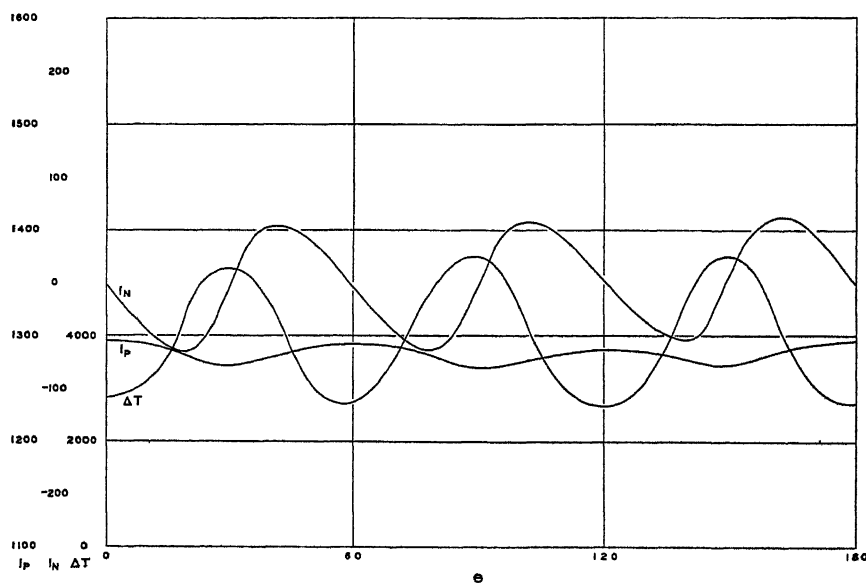


FIG 4— $I_P$ - $\theta$ ,  $I_N$ - $\theta$ ,  $\Delta T$ - $\theta$  FOR  $H_M = 392$  IN BECK'S IRON DISK {111}.

(No. VIII,  $2a = 2b = 0.764$  cm,  $2c = 0.0110$  cm,  $n_1 = n_2 = -0.142$ ,  $n_3 = -12.6$ ) Directions in the plane of the disk;  $\langle 110 \rangle$  at  $\theta = 0^\circ, 60^\circ, 120^\circ$ ,  $\langle 211 \rangle$  at  $\theta = 30^\circ, 90^\circ, 150^\circ$ .

The simplest statement that can be made about Beck's results is that magnetization is easiest along the fourfold axes  $\langle 100 \rangle$ , hardest along the threefold axes  $\langle 111 \rangle$ , and intermediate in difficulty along the twofold axes  $\langle 110 \rangle$ . This is more apparent in Fig 5, the  $I$ - $H$  curves in which are careful copies of Beck's originals. We have already seen that the area included between an  $I$ - $H$  curve and the  $I$  axis up to any specified value of  $I$  is the magnetic energy input per unit volume. Part of this is stored and part is dissipated in hysteresis. If we go to a very high value of  $I$  the dissipated part is proportionately less and we may, with Beck,

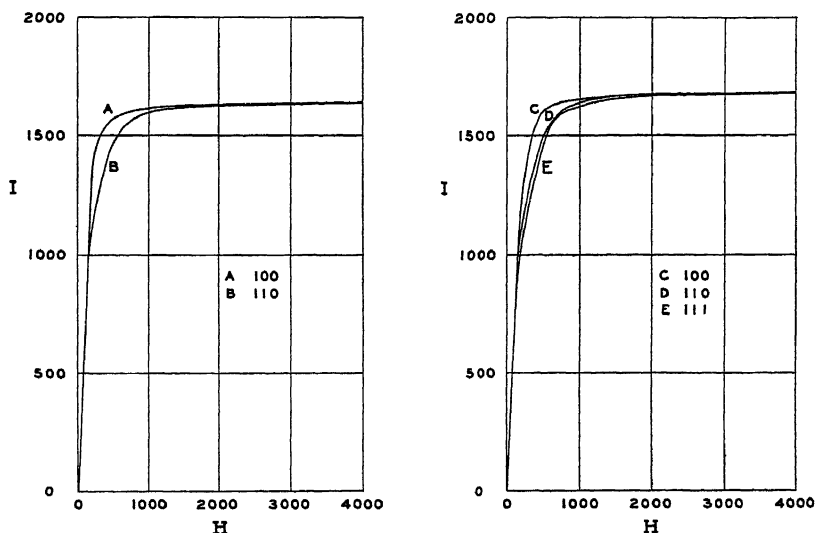


FIG 5— $I$ - $H$  ALONG AXES OF SYMMETRY IN BECK'S IRON DISKS {100}  
(No V<sub>2</sub>) A, B and {110} (No VII<sub>1</sub>) C, D, E  
Along  $\langle 100 \rangle$ , A, C, along  $\langle 110 \rangle$ , B, D, along  $\langle 111 \rangle$ , E.

neglect it in comparing different directions. The error thus committed is greater the more hysteresis losses depend upon direction. If we make  $I_s$  the upper limit of  $I$  in such an analysis we will attach to  $W = \int_0^{I_s} H dI$  a subscript denoting the common direction of  $I$  and  $H$  during the magnetizing process. From the curves of Fig 5 we can then get, for example,  $W_{110} - W_{100}$  in each of the two disks,  $W_{111} - W_{100}$  in the {110} disk only. Going back to Figs. 2 and 3 we can, as Beck proved, get other values for these energy density differences by supposing that we go from one state to the other not by way of  $H_M = 0, I = 0$  but by holding  $H_M$  constant and letting  $\theta$  change. The energy density difference is then the area under the appropriate  $T$ - $\theta$  curve, or with the proper multiplier, the area under an  $I_N$ - $\theta$  curve.



## BECK'S FINDINGS

Energy Density Difference (Erg Cm <sup>-2</sup> )	Beck's	
	{100} Disk V <sub>2</sub>	{110} Disk VII <sub>2</sub>
$W_{110} - W_{100}$	1 048 (10) <sup>5</sup>	0 786 (10) <sup>5</sup>
$W_{111} - W_{100}$		1 179 (10) <sup>5</sup>

There is one important qualitative conclusion to be drawn from the directional properties in the {111} plane. The I surface corresponding to a fixed value of  $H$  cannot be of the fourth degree but must be of some higher degree, or transcendental. Beck pointed out this fact very clearly but was inclined to think that the sixfold symmetry actually observed in the {111} disk was due to imperfections—possibly the Neumann bands—symmetrically located with respect to the crystal axes. The really excellent symmetry shown in our Fig. 4 would, on this view, be an unhappy accident.

In reviewing the rest of the experimental material we will deviate from historical order whenever this helps in grouping the results. We will, according to this plan, first mention other work on disks or oblate spheroids cut from iron crystals.

C. W. Heaps<sup>(14)</sup> measured the magnetostriction in two disks of monocrystalline 3.5 per cent silicon steel prepared by the strain-anneal method of Edwards and Pfeil<sup>(15)</sup> at the Research Laboratories of the General Electric Co. The disks were 1.48 and 1.70 cm. in diameter and 0.07 cm. thick, so they were much larger than Beck's specimens. Unfortunately the positions of the crystal axes were unknown, so that only qualitative conclusions are justified. When polycrystalline iron is magnetized the relative change of length in the direction of  $\mathbf{H}_M$ , say  $(\Delta L/L)_P$ , is at first positive, passes through a maximum value of only a few parts per million, drops to negative values and is still negative at the highest attainable  $H_M$ . The monocrystal disks were strongly anisotropic and in certain directions  $(\Delta L/L)_P$  reached a positive value as high as 30 parts per million. In other directions only negative values were observed. The effect of small inclinations of  $\mathbf{H}_M$  to the plane of the disk were surprisingly large.

W. L. Webster<sup>(6)</sup> examined the magnetization of two {100} disks cut from crystals grown by Miss Elam, who furnished the accompanying analyses. Before the magnetic testing, however, disk B was "heated in hydrogen," how long or at what temperature not being stated, and the author claims that this treatment probably removed all of the carbon and some of the sulfur. If so, the treatment must have been drastic indeed. The high phosphorus content of disk A should be especially noted.

## ANALYSES BY C F ELAM

	Disk A	Disk B
Carbon	0 048	0 105 — 0 130 (?)
Silicon	0 013	0 021 — 0 023
Sulfur	0 017	0 045 — 0 028 (?)
Manganese	0 024	0 380 — 0 440
Phosphorus	0 220	0 019 — 0 020

Webster measured  $I_P$  and  $I_N$  for various  $H_M$  at various  $\theta$ . Unlike Beck he used a torsion method for  $I_P$ , first used by Weiss<sup>(8)</sup>. The disk is hung with its plane vertical in a horizontal  $H_M$ . If  $H_M$  is in the plane of the disk, as it strictly ought to be, there is no torque on the suspension

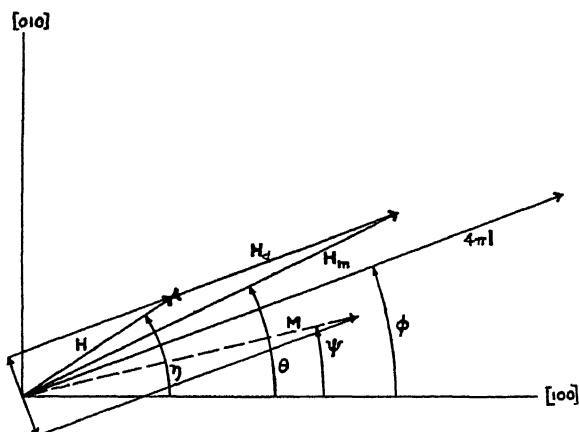


FIG 6 —WEBSTER'S CRYSTALLINE FIELD  $M$  IN  $\{100\}$  PLANE

If  $H_M$  makes a small angle, say  $5^\circ$ , with the plane of the disk, the balancing torque is

$$T_1 = I_P H_M \sin 5^\circ - I_Q H_M \cos 5^\circ \quad [20]$$

As long as  $I_Q$ , normal to the plane of the disk, is negligible in comparison with  $I_P \tan 5^\circ$ , the twist in the suspension fiber necessary to hold the disk at the fixed angle,  $5^\circ$ , increases with  $I_P$ . Finally, however, even the high demagnetizing factor  $n_3$  is incompetent to keep  $I$  practically in the plane of the disk,  $I_Q$  becomes important and the twist in the fiber must be reduced again. Webster used a graphic method, which is not entirely free from errors,<sup>(16)</sup> in getting  $I_P$ - $H$  curves from  $T_1$ - $H_M$  curves. The correction for  $H_D$  is relatively large in Webster's disks because  $n_1 = n_2 = -0.771$  for disk A,  $-0.734$  for disk B.

The results were qualitatively like Beck's. Webster had not heard of the earlier work at the time he presented his paper before the Royal Society and had seen only an abstract of it<sup>(17)</sup> prior to publication. He

invented a crystalline field  $\mathbf{M}$  to explain the divergence of  $\mathbf{I}$  from  $\mathbf{H}$ . Fig 6 illustrates the relations between  $\mathbf{H}$ ,  $\mathbf{I}$  and  $\mathbf{M}$ , which are rather complicated, even in a  $\{100\}$  plane. The direction of  $\mathbf{M}$  depends only upon the direction of  $\mathbf{I}$ . If the azimuth angles of  $\mathbf{H}_M$ ,  $\mathbf{I}$  and  $\mathbf{M}$  are  $\theta$ ,  $\phi$  and  $\psi$  measured from the nearest  $\langle 100 \rangle$  direction in the plane of the disk Webster put

$$\tan \psi = \tan^4 \phi \quad [21]$$

The magnitude of  $\mathbf{M}$  has now to be adjusted so that

$$M \sin (\phi - \psi) = H_M \sin (\theta - \phi) \quad [22]$$

The appearance of  $H_M$  and its azimuth  $\theta$ , rather than  $H$  and its so far undesignated azimuth, say  $\eta$ , needs explaining. We see that the components of  $\mathbf{H}_M$  and  $\mathbf{H}$  perpendicular to  $\mathbf{I}$  are, in fact, equal, because  $\mathbf{H}_D$  is antiparallel to  $\mathbf{I}$ . Equation 21 is equivalent to the more symmetrical equations

$$\left. \begin{aligned} M \cos \psi_1 &= M_H \cos^4 \phi_1 \\ M \cos \psi_2 &= M_H \cos^4 \phi_2 \\ M \cos \psi_3 &= M_H \cos^4 \phi_3 \end{aligned} \right\} \quad [23]$$

where  $M_H$  is a constant factor, which may be called the crystalline field intensity coefficient, and  $\phi_1, \phi_2, \phi_3, \psi_1, \psi_2, \psi_3$ , are the position angles of  $\mathbf{I}$  and  $\mathbf{M}$  with respect to the crystal axes. In the case here treated  $\psi_3 = \phi_3 = \pi/2$ . From equations 23 we see that  $M$  has its maximum  $M_H$  along  $\langle 100 \rangle$ , its minimum  $M_H\sqrt{3}/9$  along  $\langle 111 \rangle$  and a saddle-point  $M_H\sqrt{2}/4$  along  $\langle 110 \rangle$ .

As we have tried to indicate by the subscript,  $M_H$  is still a function of  $H$ . Webster found  $M_H$  (he called it  $M$ ) for a series of  $H_M$  and observed that it approached a limiting value which we will call  $M_s$ . From the form of the equations it is clear that  $M_s$  is the highest possible value of the crystalline field intensity. Webster's results showed that for disk A,  $M_s = 470$  and for disk B,  $M_s = 620$ .

It seems much more natural to make the magnitude of any crystalline field depend upon the magnitude of  $\mathbf{I}$  rather than upon the magnitude of  $\mathbf{H}$ . We suggest that this may be done by substituting for equations 22 and 23

$$K \sin (\phi - \psi) = I \sin (\theta - \phi) \quad [24]$$

$$\left. \begin{aligned} K \cos \psi_1 &= K_I \cos^4 \phi_1 \\ K \cos \psi_2 &= K_I \cos^4 \phi_2 \\ K \cos \psi_3 &= K_I \cos^4 \phi_3 \end{aligned} \right\} \quad [25]$$

This does not disturb the symmetry at all and it allows us to estimate energy density differences in terms of  $K_s$  and vice versa. The angular variation of  $K$  is such that a  $\{111\}$  disk should show variations of the sort actually observed by Beck at high  $H_M$ . The crystalline field is superior

in this respect to a fourth degree I-surface, which does not lead to such variations

Along  $\langle 100 \rangle$  the magnetic energy input per unit volume for saturation may now be written

$$W_{100} = W_0 - \frac{1}{2}K_s I_s \quad [26]$$

where  $W_0$  includes terms not depending upon the direction of I.

$$\text{Similarly} \quad W_{110} = W_0 - \frac{\sqrt{2}}{8}K_s I_s \quad [27]$$

$$W_{111} = W_0 - \frac{\sqrt{3}}{18}K_s I_s \quad [28]$$

$$\text{so} \quad W_{110} - W_{100} = \frac{4 - \sqrt{2}}{8}K_s I_s \quad [29]$$

$$\text{and} \quad W_{111} - W_{100} = \frac{9 - \sqrt{3}}{18}K_s I_s \quad [30]$$

If we put  $I_s = 1620$  (this low value is that reported by Webster) we thus obtain

Energy Density in Erg Cm <sup>-3</sup>	Webster's	
	Iron A	Iron B
$K_s I_s$	2 585 (10) <sup>5</sup>	3 410 · (10) <sup>5</sup>
$W_{110} - W_{100}$	0 836 (10) <sup>5</sup>	1 102 (10) <sup>5</sup>
$W_{111} - W_{100}$	1 044 · (10) <sup>5</sup>	1 377 · (10) <sup>5</sup>

These energy density differences are in good agreement with Beck's data if we consider the approximations involved in both experiments. We can, of course, reverse this process to find values of  $K_s$  to agree with observed energy density differences in any cubic crystal

It will be interesting to this audience to hear that the most extensive studies on ferromagnetism in metallic crystals have been carried on in a metallurgical laboratory. Kotaro Honda and his colleagues at the Research Institute for Iron, Steel and Other Metals at the Tohoku Imperial University, Sendai, Japan, have published a notable series of papers, among which one of those on iron<sup>(18)</sup> was first in point of time.

The iron crystals were grown by the strain-anneal method. The raw material, a Swedish mild steel, contained the following weight per cent of the usual impurities: C, 0.10; Si, trace; Mn, 0.40, S, 0.021; P, 0.021. Forged plates 26 by 7 by 0.6 cm. were heated four days in moist hydrogen (presumably at 950° C.) to remove carbon. After suitable stretching, to slightly less than 3 per cent permanent elongation, another three or four days at about 880° C, a little below the  $\alpha$ - $\gamma$  point, gave crystals of

large size in most cases. By careful sawing and filing three oblate spheroids with diametral planes of forms  $\{100\}$ ,  $\{110\}$  and  $\{111\}$ , respectively, were obtained. Their dimensions and least demagnetizing factors ( $n_1 = n_2$ ) were as shown in the accompanying table.

DIMENSIONS AND LEAST DEMAGNETIZING FACTORS OF OBLATE SPHEROIDS

Diametral Plane	Dimensions, Cm		$n_1 = n_2$	
	$2a$	$2c$	Computed	Observed
$\{100\}$	2 302	0 043	-0 184	-0 190
$\{110\}$	2 019	0 044	-0 218	-0 252
$\{111\}$	1 807	0 061	-0 332	-0 321

The observed demagnetizing factors were so chosen that the resultant  $I$ - $H$  curves for principal directions in each disk agreed with each other (and with  $I$ - $H$  in a prismatic monocrystal, to be mentioned later) up to about  $I = 1000$ , below which point the anisotropy is very slight.

In getting  $I_P$  and  $I_N$  only ballistic methods were used, the component measured depending upon the azimuth of a two-part search coil with respect to  $\mathbf{H}_M$ . For nonsymmetrical directions of  $\mathbf{H}_M$  the whole value of  $I_P$  was not measured but only the change in  $I_P$  when the disk was suddenly turned so that  $\mathbf{H}_M$  and the search-coil axis fell along a near-by symmetry axis. Similarly,  $I_N$  was measured for the same change in  $\theta$  with the search-coil axis normal to  $\mathbf{H}_M$ . It is clear that the hysteresis thus introduced is somewhat different from any we have yet considered. That the difference is not serious is seen from the good qualitative agreement of  $I_P$ - $\theta$  and  $I_N$ - $\theta$  curves for fixed  $H_M$  with the corresponding curves published by Beck.

The qualitative agreement is very close indeed, but there are some quantitative differences. In Beck's  $\{110\}$  disk the solitary twofold axis had minimum  $I_P$  for  $I_P < 786$  ( $I_P/\rho = 100$ ); it had a secondary maximum  $I_P$  for  $786 < I_P < 1572$  because minima now occurred near the two threefold axes. Just below magnetic saturation all three sorts of symmetry axis had higher  $I_P$  than intermediate directions, though the intervening minima were very shallow. In Honda's  $\{110\}$  spheroid the initial minimum  $I_P$  along the twofold axis is barely perceptible, the maximum does not show up until  $I_P = 1650$  and for slightly higher  $I_P$  there is a shallow minimum in this direction.

In Beck's  $\{111\}$  disk the twofold axes have maximum  $I_P$  for  $I_P < 1400$ , as in Fig. 4. For higher  $I_P$ , and particularly at  $I_P = 1500$ , these axes have minimum  $I_P$ . In Honda's  $\{111\}$  spheroid at  $I_P = 1500$  the transitional character is apparent and the deepest minima occur surprisingly near magnetic saturation.

Honda and Kaya<sup>(18)</sup> give  $I$ - $H$  curves for symmetry axes in each of the three disks, which show, more clearly than Beck's curves, the striking differences that here obtain.

Magnetostriction was measured by Honda and Mashiyma<sup>(18)</sup> both along  $H_M$  and at right angles thereto, this being the first measurement of transverse magnetostrain  $(\Delta L/L)_N$  (The longitudinal effect  $(\Delta L/L)_P$  had, as we shall see below, already been measured in rods )

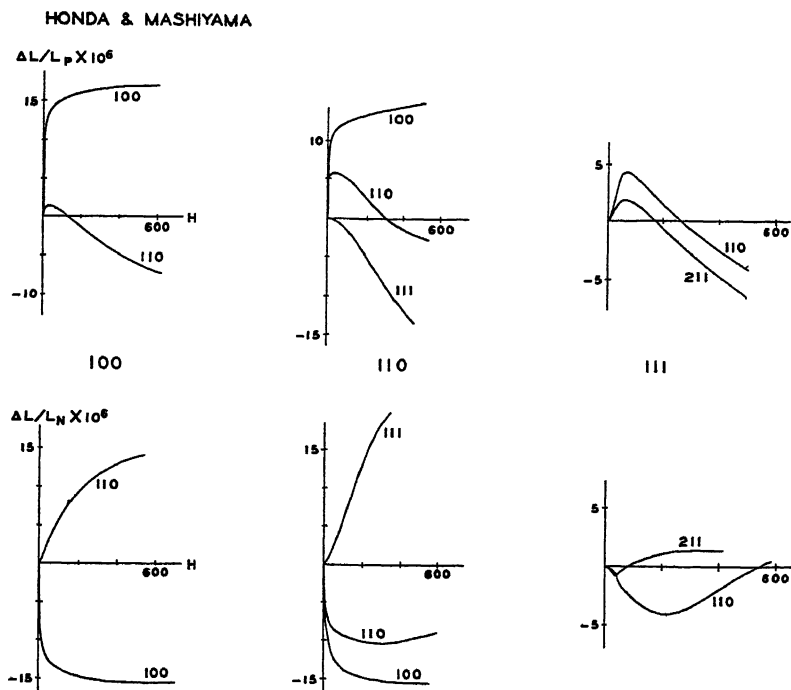


FIG 7—MAGNETOSTRAINS IN HONDA AND MASHIYAMA'S IRON SPHEROIDS

Fig. 7 presents some typical results. The curves seem to have been plotted against  $H$  rather than  $H_M$ , but, if so, use must have been made of the  $I$ - $H$  curves of Honda and Kaya. Whether this is justified in view of the more rigid clamping in the magnetostriction measurements is at least debatable. Curves showing  $(\Delta L/L)_P$  and  $(\Delta L/L)_N$  in terms of  $I$  rather than  $H$  would probably be somewhat easier to interpret.

The changes in  $I$ - $H$  curves for the three sorts of symmetry axis in the  $\{110\}$  spheroid were followed by Honda, Masumoto and Kaya<sup>(19)</sup> at temperatures ranging from  $5^\circ$  to  $770^\circ$  C. The figures are so carefully drawn that energy density differences derived from them should be especially reliable.

This concludes the list of disks and oblate spheroids of monocrystalline iron. Work on elongated specimens, prismatic or cylindrical rods, is

intrinsically easier because, except for enormous  $H_M$ ,  $I$  is constrained by  $H_D$  to be nearly parallel to the long dimension of the piece. Its measurement is accordingly easier. The trouble is that comparison of different directions for  $I$  in the crystal now requires comparison of data taken on different specimens and all the difficulties of making two pieces of metal nearly alike have to be overcome.

The first results on strips of monocrystalline iron were reported by W. E. Ruder.<sup>(20)</sup> His specimens, of silicon steel containing from 2.75 to 3.45 per cent Si, were 0.064 cm. thick, 1.27 cm. wide and 25.4 cm. long, and were annealed at 1000° C in vacuum before magnetic testing. The values of  $H$  and  $B$ , both along the length of the piece, were measured in a Burrows permeameter. This instrument is designed to keep  $H_D$  zero, so that  $H = H_M$ . About one hundred strips were tested and the positions of the crystal axes were fixed optically by observing the reflections from deeply etched surfaces. These reflections take place, in iron, at  $\{100\}$  planes. The  $B$ - $H$  curves turned away from the  $B$ -axis at  $B$  values depending upon the orientation of the crystal axes in the strip. Ruder selected  $B$  for  $H = 10$  as the index for classifying his specimens. This varied from 16,000 for  $\langle 100 \rangle$  to about 11,000 for  $\langle 111 \rangle$  with a good deal of scattering due to individual peculiarities of specimens. The low value of  $H$  at which  $B$ - $H$  curves were cut off ( $H = 190$ ) makes it difficult to estimate energy density differences, but a lower limit may be set for  $W_{111} - W_{100}$  at  $0.86 (10)^5$  erg cm.<sup>-3</sup> Part of our uncertainty results from the fact that the lowest  $B$ - $H$  curve actually reproduced does not correspond exactly to  $\langle 111 \rangle$ .

Webster<sup>(21)</sup> also measured the magnetization of some nearly rectangular rods of monocrystalline iron intended primarily for magnetostriction experiments. Their characteristics are shown herewith.

CHARACTERISTICS OF RODS OF MONOCRYSTALLINE IRON

Designation	A	B	C
Axis	$\langle 100 \rangle$	$\langle 110 \rangle$	$\langle 111 \rangle$
Length (cm.)	1.63	1.29	1.50
Mass (gm.)	0.0920	0.0602	0.1023
Mean cross-section (cm. <sup>2</sup> )	0.00725	0.00585	0.00865
$n_s$	-0.155	-0.195	-0.205
$n_s$ (recomputed)	-0.110	-0.135	-0.146

In getting the demagnetizing factor here important ( $n_s$ ) the rods—actually of nearly square but nonuniform cross-sections—were regarded as prolate spheroids of the same length and of the mid-sectional area given in the table. Using equation 14 we obtain smaller values than those given by Webster. The new values agree better with the  $I$ - $H_M$  curves he gave.

The  $I$ - $H$  curves show the now familiar succession:  $\langle 100 \rangle$ ,  $\langle 110 \rangle$ ,  $\langle 111 \rangle$ , the first giving the highest  $I$  at each  $H$ , and permit a rough calculation of energy density differences, rough because saturation was not nearly enough attained along  $\langle 110 \rangle$  and  $\langle 111 \rangle$ .

The magnetostrains  $(\Delta L/L)_P$ , here reported for the first time, were strikingly different for the three rods. Webster was also able to observe the converse effect, the effect of compression on  $I$ - $H$  curves. Since the production of homogeneous strains is much harder than the production of homogeneous  $H$ , and cannot be managed at all in the ideal spheroids we will content ourselves with saying that Webster's results are qualitatively in agreement; e.g., compression raises  $I$  if  $(\Delta L/L)_P$  is negative

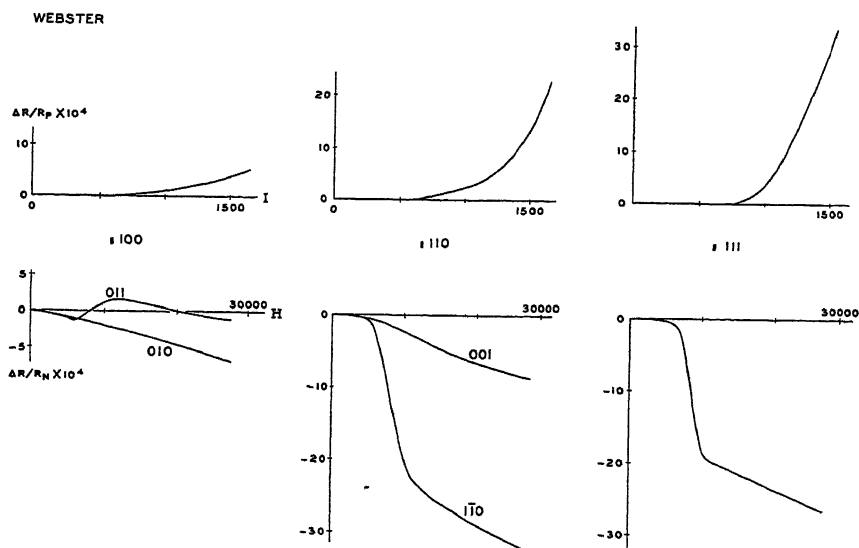


FIG 8—MAGNETORESISTANCES IN WEBSTER'S IRON RODS

Still later these three rods and some others of the same sort were used by Webster<sup>(22)</sup> in another experiment impracticable with spheroids. This was the measurement of magnetoresistance. The current vector  $i$  must, of course, be along the axis of the rod, so that again there is a longitudinal effect  $(\Delta R/R)_P$  when  $H$  and  $I$  are also in this direction, and transverse effects  $(\Delta R/R)_N$  when  $I$  is made perpendicular to the rod axis by very high transverse  $H_M$ . The longitudinal effect is the simpler. Fig 8 shows that the effect is least along the axis of easiest magnetization, greatest along the axis of most difficult magnetization, and is always positive. Any relation between magnetoresistance and magnetostrain is very obscure. The transverse effect is best considered as due to the superposition of two effects of different character. The first is a decrease of  $R$ , which is roughly proportional to  $H_M$ , the factor of proportionality



depending somewhat upon the direction of  $\mathbf{H}_V$  in the transverse plane, and which has no obvious dependence upon either the direction or magnitude of  $\mathbf{I}$ . At least for high  $H_M$  this magnetoresistance can therefore be written

$$(\Delta R/R)_{NH} = k_{NH}H \quad [31]$$

We put  $H$  rather than  $H_M$  in equation 31 because at sufficiently high  $H_M$  there is no great difference and because  $H$  is the magnetic field intensity in the region where the current flows. The values of  $k_{NH}$ , while small, are larger than is usual in nonferromagnetics. The rest of  $(\Delta R/R)_N$  seems to depend upon the direction of  $\mathbf{I}$ . We may designate it as

$$(\Delta R/R)_{NI} = (\Delta R/R)_N - (\Delta R/R)_{NH} \quad [32]$$

The direction of  $\mathbf{I}$  is not accurately known except at the limiting value of  $H_M = 27,500$  where it must be nearly parallel to  $\mathbf{H}_M$ . The data show that for most pairs of mutually perpendicular directions of  $\mathbf{i}$  and  $\mathbf{H}_M$  a rather sudden drop in  $R$  occurs between  $H_M = 5000$  and  $H_M = 10,000$ . The demagnetizing field must be of the order of magnitude of  $-2\pi I_P$  where  $I_P$  is, as usual, the component of  $\mathbf{I}$  parallel to  $\mathbf{H}_M$ . A simple calculation shows that  $I_P$  will then range from 800 to 1600 as  $H_M$  increases from 5000 to 10,000. Any large changes in  $(\Delta R/R)_F$  which occur in this range of  $I$  will therefore be associated with large changes in  $(\Delta R/R)_{NI}$  which occur between  $H_M = 5000$  and  $H_M = 10,000$ .

The relative magnitudes of these two magnetoresistances, as taken from Webster's curves, may be derived from the accompanying table. It

FOR DERIVATION OF RELATIVE MAGNITUDES

Directions of		$k_{NH}$ (10) <sup>3</sup>	$(\Delta R/R)_{NI}$ (10) <sup>4</sup>
$\mathbf{i}$	$\mathbf{H}_M$		
[100]	[010]	-3	0
	[011]	-2	+ 5
[110]	[001]	-3	0
	[110]	-5	-22
	[111]	-3	- 6
[111]	any	-4	-20

is seen at once that directions of form  $\langle 100 \rangle$  are peculiar in having no abrupt changes in resistance

Walther Gerlach<sup>(23)</sup> used the rod form in all his experiments on iron crystals. The raw material, wire 3 to 5 mm. in diameter, was prepared by Heraeus from electrolytic iron. Information regarding the analysis or details of preparation is not given. In the measurements first reported the single-crystal portions had a maximum length, in 4-mm. wire, of

12 cm., and several specimens more than 5 cm. long were available. Emphasis was first placed on the narrowness of the hysteresis loops as compared with the loop for the untreated wire, and upon the extremely low remanence  $I_r$ . Conclusions as to  $I_r$  are, to be sure, extremely difficult when the hysteresis loop is narrow, for a small underestimation of  $n_3$  reduces the apparent remanence nearly to zero. As far as low hysteresis goes Cioffi<sup>(24)</sup> has shown that this can be obtained in polycrystalline iron.

The most talked about feature of Gerlach's results is the appearance on his  $I$ - $H$  curves of abrupt changes in slope, characteristically different in wires with their lengths lying in different crystallographic directions.

Most of Gerlach's crystals had  $\langle 110 \rangle$  near the wire axis, a few had  $\langle 100 \rangle$ . No wire with  $\langle 111 \rangle$  along the axis was obtained. This preference has been observed by all experimenters who use the strain-anneal method for producing monocrystals in iron.

Arguments about corners on the  $I$ - $H$  curve center on the accuracy with which  $H_D$  can be estimated. Gerlach used a method devised by Dussler<sup>(25)</sup> which measured  $H$  close to the equator of the crystal with a belt of small search coils 1.8 cm. long and 0.118 cm. in diameter in his first tests. Dussler used still smaller coils in later experiments in an effort to get good data for short monocrystals in long wires. Under these conditions  $H_D$  changes rather rapidly in the neighborhood of the knee of the  $I$ - $H$  curve, and  $n_3$  is far from being a constant. The nature of the changes depends upon whether  $I$  is higher or lower in the crystal under test than in its immediate neighbors. Foster<sup>(26)</sup> found smooth  $I$ - $H$  curves using a double search coil<sup>(27)</sup> for  $H$ , and, with Bozorth,<sup>(28)</sup> has suggested that Gerlach's corners are due to residual errors in  $H_D$ . It must be admitted, however, that Foster's double search coil was longer and his wires smaller than the coils and wires used by Dussler, so that part of the smoothness may be an effect of averaging over a greater range in  $H_D$ , which is not the same at all points in the length of a cylindrical specimen.

In Dussler's final paper the changes in  $I$ - $H$  curves with change in temperature is followed from 20° to 850° C. The value of  $I$  at which the curves break away from the  $I$  axis is lower at higher temperature, and approximate saturation is attained at lower  $H$ , neither of which findings is unexpected. Corners persist but the straight-line portions between them become shorter.

We must not confuse Gerlach's corners, occurring at low values of  $H$  and at values of  $I$  just above that at which the curve separates from the  $I$  axis with the flattening off at  $I_r$  which permits us to get finite energy density differences. None of Gerlach's specimens is carried to complete saturation and we cannot get any useful estimate of energy density differences from his data.

Honda and Kaya<sup>(18)</sup> also studied a long monocrystalline rod (6.81 by 0.24 by 0.181 cm.), but its length was not along any symmetry axis. Its

inclination to the nearest  $\langle 100 \rangle$  direction was  $21^\circ-10'$ , to the nearest  $\langle 110 \rangle$  direction,  $28^\circ-40'$ , to the nearest  $\langle 111 \rangle$  direction,  $35^\circ-05'$ . Its  $I$ - $H$  curve is like those obtained by the same authors in a  $\langle 110 \rangle$  direction in an ellipsoid, except that the slope from  $I = 1100$  to  $I = 1700$  is more nearly uniform. Honda, Masumoto and Kaya<sup>(19)</sup> also used this specimen in their work at low and high temperatures

Honda and Mashiyama<sup>(18)</sup> studied magnetostriction in five rods about  $4.0$  by  $0.2$  by  $0.2$  cm as well as in spheroids. None of them had its length exactly along a symmetry axis and all that needs to be said about them is that they agree qualitatively with more manageable shapes

Long strip crystals were prepared by the strain-anneal method in Oberhoffer's laboratory at Aachen, and were studied first by Wolman,<sup>(29)</sup> later by Gries and Esser<sup>(30)</sup>. The magnetic measurements included what amounts to a direct compensation of  $H_d$  so that, as in Gerlach's work,  $I$ - $H$  curves may be plotted directly from the data. The low magnetic fields were handled more expertly, and the existence of hysteresis was proved in every case. Wolman showed that too large or too sudden changes in  $H$  may cause the loop apparently to collapse, and this may account for Gerlach's report of zero hysteresis. Oddly enough, Wolman, who had no crystal with its length parallel to a symmetry axis, got only smooth  $I$ - $H$  curves. Gries and Esser, who had crystals in the  $\langle 110 \rangle$  position and one nearly in the  $\langle 100 \rangle$  position, found corners. Here again saturation was not nearly enough attained to make energy density calculations interesting. A point of some importance in Wolman's report is his statement that the slightest bending resulted in a corner on an otherwise smooth hysteresis loop.

The reality of corners on  $I$ - $H$  curves in iron crystals was earnestly supported by G. J. Sizoo<sup>(31)</sup> at the Phillips Lamp Works, Eindhoven. His iron, also from Heraeus, was remelted in vacuum, and the rise of the temperature coefficient of resistance from  $5.80 \cdot 10^{-3}$  to  $6.25 \cdot 10^{-3}$  per degree Centigrade was taken as proof that some purification was thus effected. The strain-anneal process, applied to wire 1 mm. in diameter, sometimes yielded single crystals 10 to 15 cm. long. Especial care was taken to prevent mechanical deformation before or during magnetic testing by a magnetometric method. The cylindrical crystals were tapered by etching so as to approach somewhat the ideal spheroidal shape. The usual difficulty in regard to irrational indices of the wire axis was again encountered. The closest approaches to symmetrical positions for which magnetic data are reported were:  $14^\circ$  from  $\langle 100 \rangle$  for No. 18 and  $3^\circ$  from  $\langle 110 \rangle$  for No. 14. The values of  $H_c$  were small but never zero, ranging from 0.28 to 0.46 when recorded.

As to corners, Sizoo seems to over-prove his point. On a single graph of the relation between  $I$  and  $H$  which almost anyone would be satisfied to represent by a smooth curve, he finds five corners below  $I = 1100$

(at  $I = 750, 854, 921, 968$ , and  $1045$ ), and supports their validity by tables showing that straight lines between them fit the data with astonishing precision—astonishing, that is, to anyone who has tried to use a magnetometer. By somewhat rough extrapolation from  $I = 1650$  to  $I = 1725$  we can get from the two crystals mentioned above (Nos 18 and 14), a value for  $W_{110} - W_{100} = 1.04 (10)^5 \text{ erg cm}^{-3}$ .

Since leaving Honda's laboratory Kaya<sup>(32)</sup> has continued work on iron crystals in rod form, longer and better annealed (5 hr at  $800^\circ \text{C}$  in hydrogen) than before. He tries particularly to get good values for  $I_r$  and uses an ingenious scheme, recording not the intersection of the loop with  $H = 0$  but the height of the nearly horizontal upper branch of the loop just before the sudden drop in  $I$  occurs. He finds that for a dozen different crystals

$$I_r = I_s / (\cos \phi_1 + \cos \phi_2 + \cos \phi_3) \quad [33]$$

to a sufficient degree of precision. This equation permits  $I_r$  to range between  $I_s$  and  $0.577 I_s$  as the axis ranges between  $\langle 100 \rangle$  and  $\langle 111 \rangle$ . Kaya also finds a great many corners, but now, perhaps because his range in  $H$  is greater, these are all above  $I = 1100$ . As an example we quote for crystal No. 18:

Corners at		Corners at	
$H$	$I$	$H$	$I$
68 0	1226	430 0	1643
172 0	1413	574 0	1710 = $I_s$
277 0	1525		

The reality of so many abrupt changes in slope may well be doubted. A lower limit for  $W_{110} - W_{100}$  can be set at  $1.23 (10)^5 \text{ erg cm}^{-3}$  by planimetry on Kaya's curves.

The toroidal form of test specimen is excellent when the ferromagnetic material is isotropic, but is quite unsuited to studies of crystalline anisotropy. Nevertheless ring specimens were chosen by A. G. Hill<sup>(33)</sup> in an attempt to decide for or against Gerlach corners on  $I$ - $H$  curves. His idea, of course, was that  $H_D$  is everywhere zero in a uniformly magnetized toroid. In the debatable region a toroid cut from a single crystal cannot be uniformly magnetized, so Hill's idea was not a very happy one. The large crystals came from Vicker's Manchester works, but no analysis seems to have been available. From the statement that they were "composed of parallel groups of octahedral form," from their large size and from the nature of the supplier's business we are inclined to believe that they were found in the top of a large ingot. As cut (in a lathe?) the axis of each ring was of form  $\langle 100 \rangle$  and the dimensions of the two rings were:

Outside Diameter, Cm	Inside Diameter, Cm	Height, Cm
1 242	1 072	1 525
1 015	0 905	1 436

We have changed the radial thicknesses as given, "0 85 and 0 55 cm," to 0 85 and 0.55 mm so as to leave a hole in each. Hysteresis was not measurable in the smaller ring until the maximum value of  $H_M$  in a cycle became greater than 2. Up to this limit  $\mu = 37$  ( $\kappa = 2 87$ ) so that the iron was impure or strain-hardened or both. (The value of  $\mu_0$  in pure annealed iron crystals is of the order of 300 or higher.) Though no complete hysteresis loop is drawn it seems likely that such loops must have been constricted near the origin. The larger specimen seems to have been more nearly homogeneous, since no hysteresisless range in  $H_M$  was observed in it. The initial permeability at room temperature was 40, that at liquid-air temperatures was only 25. This difference is so great that it strongly suggests the supposed iron to have been, in fact, a nickel steel. The impossibility of getting consistent results above 162° C. confirms this suspicion.

Since Hill could not get  $I$  above 110 in these hard magnetic materials, he did not even approach the range in  $I$  where crystal anisotropy has been observed by others, and it is not surprising that he detected no difference in  $I$  in the parts of his search coil. This is the less astonishing when we note that there were four search coils symmetrically placed on the circumference, so that even if crystal anisotropy occurred each search coil would measure the same value of  $I$ . The only interest of this experiment to us lies in the fact that what seemed at least to be a single crystal of iron was magnetically hard and demonstrably inhomogeneous. Perhaps many of the specimens examined by others suffer from the same defects in lesser degree.

Table 1 contains the energy density differences derived from the experiments on iron crystals. The most striking thing about it is the general agreement of the entries in spite of the probably wide variation in the irons examined. Another thing to notice is that the energy densities involved here are very much greater than the hysteresis loss per unit volume per cycle in annealed iron, so that even considerable errors in fixing the position of the  $I$ - $H$  curve within the hysteresis loop have but little effect upon the directional differences here considered.

### NICKEL

The review of work on nickel crystals will be arranged in the order chosen for work on iron, first mentioning results obtained with disks or oblate spheroids, then results with rods or prolate spheroids. The extent of the literature to be covered is very much less than for iron.

TABLE 1.—*Energy Density Differences in Iron*

Observers	Specimens	$W_{110} - W_{100}$	$W_{111} - W_{100}$
		Erg cm <sup>-3</sup> (10) <sup>5</sup>	
Beck	Disk V <sub>2</sub> {100}	1 048	
Beck	Disk VII <sub>1</sub> {110}	0 786	1 179
Webster	Disk A {100}	0 836	1 044
Webster	Disk B {100}	1 102	1 377
Honda-Kaya	Spheroid {100}	1 18	
Honda-Kaya	Spheroid {110}	1 20	1 45
Honda-Masumoto-Kaya	{110} at 5° C	1 14	1 47
Ruder	Strips 3 25 S <sub>1</sub>		>0 86
Webster	Rods <100>, <110>, <111>	0 77	1 37
Sizoo	Wires No 18 and No 14	1 04	
Kaya	Rods No 18 and No 10		>1 23

W Sucksmith, H. H Potter and L. Broadway<sup>(34)</sup> melted Mond nickel shot, said to be 99.6 per cent pure, in a long cylindrical alundum crucible and crystallized the metal slowly. They cut disks of the dimensions shown in the accompanying table, trying to prevent deformation in the cutting process. Following Beck's practice, they measured  $I_P$  by ballistic galvanometer,  $I_N$  by torsion balance and corrected for rotational hysteresis

DIMENSIONS OF DISKS

Plane of Disk	Dimensions, Cm		$\eta_1 = \eta_2$
	2a	2c	
{100}	0 393	0 041	-0 908
{110}	0 388	0 041	-0 918
{111}	Dimensions not given—Six were tested		

The direction of easiest magnetization is <111> and that of hardest magnetization is <100>, exactly opposite to the order of difficulty in iron. In the {100} disk the variation in  $I_P$  is not very pronounced and the maximum value of  $I_N$  is about 20. In the {110} disk variations in both components of  $I$  are greater. In the {111} disks the expected sixfold symmetry could not be proved to exist, the values of  $I_P$  and  $I_N$  varied irregularly with  $\theta$ . Fig. 9 shows characteristic  $I_P$ - $\theta$  and  $I_N$ - $\theta$  curves of large amplitude. In comparing them with curves for iron, it should be remembered that  $I_S$  for nickel is only  $\frac{3}{4}$  of  $I_S$  for iron ( $\frac{3}{4} = 0.273$ ).

The energy density differences calculated from the published  $I$ - $H$  curves are of the opposite sign to those given in Table 1 for iron and are

about one-tenth as great. The crystalline field  $\mathbf{K}$  if defined exactly as in iron, is everywhere negative and has its maximum negative values along  $\langle 100 \rangle$ .

Kaya and Masiyama<sup>(35)</sup> obtained oblate spheroids of nickel from single crystals 7 cm. long and 2.3 cm. in diameter made by slowly lowering the melt, in vacuum, out of a vertical carbon tube electric furnace. The

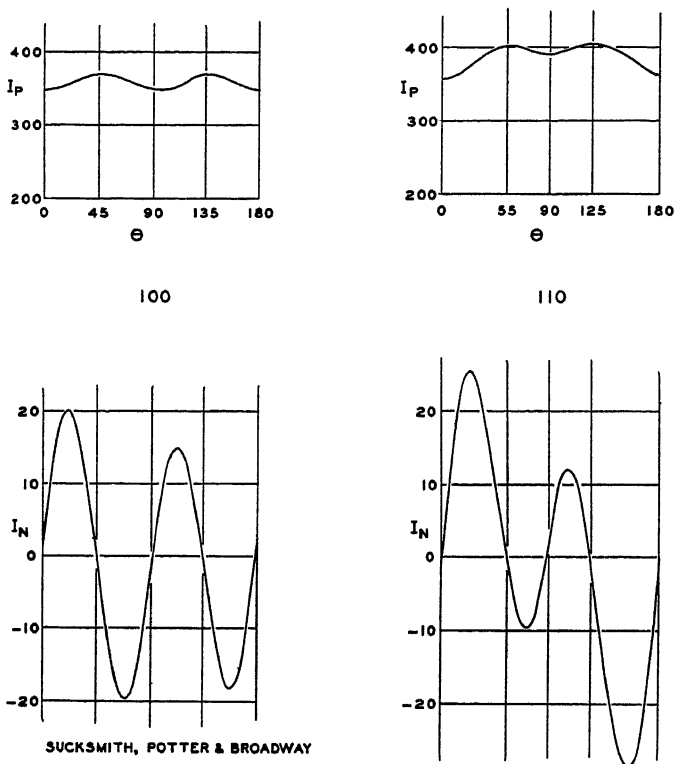


FIG. 9— $I_P$ - $\theta$ ,  $I_N$ - $\theta$ , FOR CONSTANT  $H_M$  IN SUCKSMITH, POTTER AND BROADWAY'S NICKEL DISKS {100} AND {110}.

In {100},  $H = 214$  at  $\theta = 45^\circ$  for  $I_P$ ,  $H = 246$  at  $\theta = 45^\circ$  for  $I_N$ , directions in the plane of the disk.  $\langle 100 \rangle$  at  $\theta = 0^\circ, 90^\circ$ ,  $\langle 110 \rangle$  at  $\theta = 45^\circ, 135^\circ$ . In {110},  $H = 250$  at  $\theta = 55^\circ$  for  $I_P$ ,  $H = 434$  at  $\theta = 55^\circ$  for  $I_N$ , directions in the plane of the disk;  $\langle 100 \rangle$  at  $\theta = 0^\circ$ ;  $\langle 110 \rangle$  at  $\theta = 90^\circ$ ,  $\langle 111 \rangle$  at  $\theta = 55^\circ, 125^\circ$ .

best results were obtained at a lowering rate of 10 cm. an hour. The raw material was electrolytic nickel containing the following impurities in weight per cent: Fe, 0.097; Co, 0.027; Si, 0.05; Mn, trace; S, 0.014; P, 0.0023. The spheroids were cut and filed "so as to avoid the least distortion of the crystal." Their dimensions and principal demagnetizing coefficients are shown herewith. Ballistic methods were used for  $I_P$  and  $I_N$ .

DIMENSIONS AND PRINCIPAL DEMAGNETIZING COEFFICIENTS OF NICKEL OBLATE SPHEROIDS

Equatorial Plane	Dimensions, Cm		$n_1 = n_2$
	$2a$	$2c$	
{100}	1 906	0 0634	-0 320
{110}	1 326	0 0502	-0 368
{111}	2 036	0 1063	-0 482

In spite of the care taken to prevent distortion, the susceptibility was so much less than that for well annealed polycrystalline nickel of the same purity that after a complete series of magnetic measurements the spheroids were given a one-hour anneal in hydrogen at 650° C. This

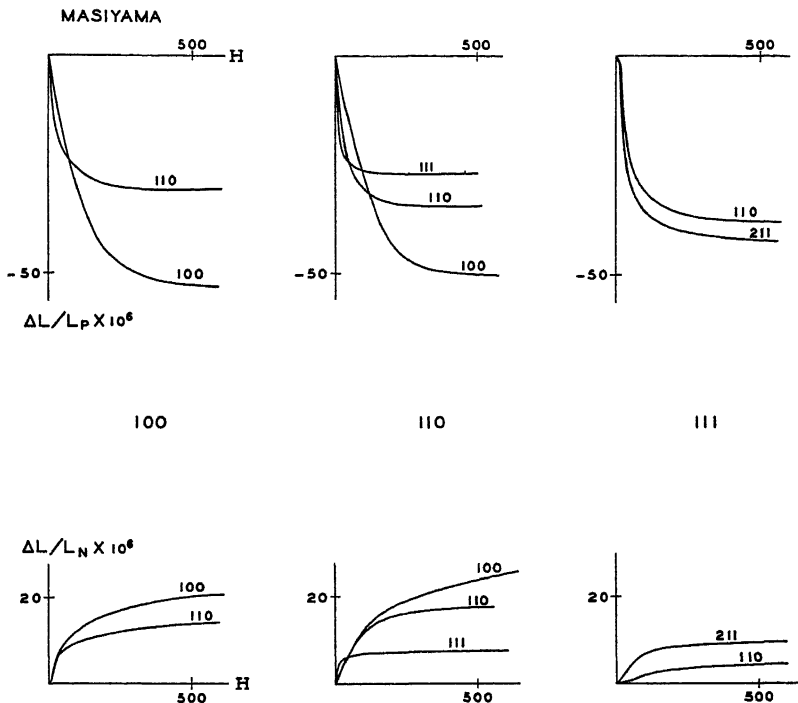


FIG 10 —MAGNETOSTRAINS IN MASIYAMA'S NICKEL SPHEROIDS

made magnetization easier in all directions and gives us our first chance to compare energy density differences in a single specimen before and after annealing. Unfortunately the first measurements are not reported for the plane of greatest interest, {110}, which contains all three types of symmetry axis. Where comparison is possible the difference due to annealing is not very great.



The results agree qualitatively with those obtained by Sucksmith, Potter and Broadway<sup>(34)</sup>, but are more self-consistent. In the {111} plane, especially, the sixfold symmetry was now clearly apparent, though the amplitudes of  $I_P$  and  $I_N$  are extremely small. Along the twofold axes in this plane, of form  $\langle 110 \rangle$ ,  $I_P$  is minimum up to about  $I_P = 350$ , then maximum up to about  $I_P = 460$ , and minimum for still higher  $I_P$  up to apparent saturation at  $I_s = 503$  for  $20^\circ \text{C}$ .

Masiyama's magnetostriction curves for the same spheroids are simpler than corresponding curves for iron.  $(\Delta L/L)_P$  is always negative,  $(\Delta L/L)_N$  always positive. There are, to be sure, considerable differences in magnitude for different crystallographic directions. Fig 10 shows that the strains attain nearly to saturation values within the range of experiment.

Kaya<sup>(35)</sup> also measured magnetoresistance in rods of the same nickel and of the dimensions given herewith. The magnetization was not

DIMENSIONS OF NICKEL RODS

Axis	Dimensions, Cm		
	Length	Breadth	Thickness
$\langle 100 \rangle$	2 6	0 125	0 125
$\langle 110 \rangle$	2 2	0 155	0 130
$\langle 111 \rangle$	1 3	0 113	0 090

measured, even for longitudinal  $H_M$ , so we cannot plot  $\Delta R/R$  as a function of  $I$ . We can tabulate the greatest observed changes for various directions of  $i$  and  $H_M$ . Average values are taken where several equivalent directions for  $H_M$  were tried. The linear variation of  $(\Delta R/R)_N$  with  $H$  at

GREATEST OBSERVED CHANGES FOR DIRECTIONS OF  $i$  AND  $H_M$ 

Directions of		$(\Delta R/R)_P$ (10) <sup>4</sup>	$(\Delta R/R)_N$ (10) <sup>4</sup>
	$H_M$		
[100]	[100]	+197	+ 58 -134
	[010]		
	[011]		
[110]	[110]	+233	+ 82 - 51 5 -100
	[001]		
	[1 $\bar{1}$ 0]		
	[1 $\bar{1}$ 1]		
[111]	[111]	+242	- 80
	[10 $\bar{1}$ ]		

high values of  $H$ , so conspicuous in Webster's work on iron, seems, at first sight, to be absent. The changes in  $R$  are relatively so much greater in nickel, however, that a  $k_{NH}$  of the order of  $3 \cdot 10^{-8}$  might easily be overlooked.

Sizoo<sup>(38)</sup> also studied nickel crystals in rod form but prepared his rods in a different way, sucking them up into a fused silica tube from a melt about  $50^\circ \text{C}$  above the melting point. We may assume that the impurities did not exceed 0.4 per cent, as this is the upper limit given in a paper<sup>(37)</sup> describing the application of the same method in preparing a series of iron-nickel alloys. The nickel crystals thus obtained, about 1 mm in diameter and up to 20 cm long, were magnetically hard. They were therefore annealed in vacuum for 24 hr or more at  $900^\circ \text{C}$ , after it had been discovered that 12 hr at  $900^\circ \text{C}$  was insufficient but that after 28 hr. at  $900^\circ \text{C}$ . a further 24 hr at  $1100^\circ \text{C}$  produced negligible changes in susceptibility.

As in Wolman's work on iron, the hysteresis loops were not markedly different in width from each other or from loops for polycrystalline nickel. The range in  $H_c$  was from 1.88 to 3.20 in different specimens. Sizoo again devotes much attention to looking for corners on  $I$ - $H$  curves, and finds them in suspicious abundance. No crystal with an axis very near to  $\langle 111 \rangle$  is reported upon, so we can set only a negative limit for  $W_{111} - W_{100}$  by considering Sizoo's crystal No. 1, which had its axis parallel to  $\langle 100 \rangle$ . This is the last value in Table 2. We can again conclude that the few available experiments are consistent.

TABLE 2 — *Energy Density Differences in Nickel*

Observers	Specimens	$W_{110} - W_{100}$	$W_{111} - W_{100}$
		Erg $\text{Cm}^{-3} (10)^4$	
Sucksmith-Potter-Broadway	Disk {100}	-1.29	
Sucksmith-Potter-Broadway	Disk {110}	-1.27	-1.70
Kaya	Spheroid {100}	-1.25	
Kaya	Same, unannealed	-1.20	
Kaya	Spheroid {110}	-1.28	-1.67
Sizoo	Rod No 1		> -2.8

### CUBIC ALLOYS

Work on the ferromagnetism of alloy monocrystals has only started. H. H. Potter's paper<sup>(38)</sup> on a Heusler alloy was the first to appear in this department of our subject. The proposed composition of his alloy corresponded to the formula  $\text{AlMnCu}_2$ , which gives the maximum value for  $I_s$ , but there was in fact a small excess of copper. The largest crystals he got by slow freezing in vacuum had a volume of about  $0.15 \text{ cm}^3$ . The

structure was cubic with  $a_0 = 5.9 \cdot 10^{-8}$  cm and with 16 atoms per unit cube. Their locations are either

$$\left. \begin{array}{ccccccc} \text{Cu} & 0 & 0 & 0 & 0 & \frac{1}{2} & \frac{1}{2} & \frac{1}{2} & 0 & \frac{1}{2} & \frac{1}{2} & \frac{1}{2} & 0 & 0 \\ & 0 & 0 & \frac{1}{2} & 0 & \frac{1}{2} & 0 & \frac{1}{2} & 0 & 0 & \frac{1}{2} & \frac{1}{2} & \frac{1}{2} & \frac{1}{2} \\ \text{Al} & \frac{1}{4} & \frac{1}{4} & \frac{1}{4} & \frac{1}{4} & \frac{3}{4} & \frac{3}{4} & \frac{3}{4} & \frac{1}{4} & \frac{1}{4} & \frac{3}{4} & \frac{3}{4} & \frac{1}{4} & \frac{1}{4} \\ \text{Mn} & \frac{1}{4} & \frac{1}{4} & \frac{3}{4} & \frac{1}{4} & \frac{3}{4} & \frac{1}{4} & \frac{3}{4} & \frac{1}{4} & \frac{1}{4} & \frac{3}{4} & \frac{3}{4} & \frac{1}{4} & \frac{1}{4} \end{array} \right\} \quad [34]$$

or

$$\left. \begin{array}{ccccccc} \text{Cu} & 0 & 0 & 0 & 0 & \frac{1}{2} & \frac{1}{2} & \frac{1}{2} & 0 & \frac{1}{2} & \frac{1}{2} & \frac{1}{2} & 0 & 0 \\ & 0 & 0 & \frac{1}{2} & 0 & \frac{1}{2} & 0 & \frac{1}{2} & 0 & 0 & \frac{1}{2} & \frac{1}{2} & \frac{1}{2} & \frac{1}{2} \\ \text{Al} & \frac{1}{4} & \frac{1}{4} & \frac{3}{4} & \frac{1}{4} & \frac{3}{4} & \frac{1}{4} & \frac{3}{4} & \frac{1}{4} & \frac{1}{4} & \frac{3}{4} & \frac{3}{4} & \frac{1}{4} & \frac{1}{4} \\ \text{Mn} & \frac{1}{4} & \frac{1}{4} & \frac{1}{4} & \frac{1}{4} & \frac{3}{4} & \frac{3}{4} & \frac{3}{4} & \frac{1}{4} & \frac{1}{4} & \frac{3}{4} & \frac{3}{4} & \frac{1}{4} & \frac{1}{4} \end{array} \right\} \quad [35]$$

of which the first seems more probable.

Magnetic tests were made entirely by torsion balance methods, since the specimens were too small for accurate measurements by ballistic methods. The three disks were the smallest ever used in such experiments. Only enough magnetic data were reported to show that the

DIMENSIONS OF ALLOY DISKS

Plane of Disk	Dimensions, Cm		$n_1 = n_2$
	$2a$	$2c$	
{100}	0.280	0.028	-0.99
{110}	0.278	0.025	-0.89
{111}	0.350	0.038	-1.07

axes of hard and easy magnetization are the same as in nickel. By measuring the area under an  $I_N$ - $\theta$  curve for high  $H_M$  we conclude that  $W_{110} - W_{100} = -2.24 \cdot 10^5$  erg cm $^{-3}$ .

Lichtenberger<sup>(39)</sup> more recently has examined a series of iron-nickel alloys of face-centered cubic structure. He used a very slender crucible, of pythagoras, or fused silica, packed with a proper mixture of 0.5-mm electrolytic iron and nickel wires. This was first raised and then lowered slowly through the hot zone of a vacuum furnace. The crucible was about 30 cm long and only from 2 to 4 mm in inside diameter. It is rather surprising to be told that alloys containing more than 60 per cent nickel undercooled and gave only polycrystal castings unless the crucible support was kept in vibration by an attached buzzer. One fears also that the metal was contaminated by the refractory, or otherwise, because too high a furnace temperature or too long a time at an otherwise suitable temperature resulted in small and pitted crystals. Surface tension was troublesome in the smaller diameters, for if the melt separated into drops they rarely coalesced again before freezing. The author states that the crystals contained less than 0.75 per cent Mn, 0.04 Si, 0.01 C, and thinks

that the total impurities may have been as low as 0.01 per cent. This may be doubted. The iron and nickel varied as much as 3 per cent from the intended composition. Cobalt was present in small amounts, if any ("less than traces"!)

Many specimens were prepared and tested, about 40 in all. Besides cylinders up to 16 cm. long in the 4-mm. diameter there were some small rings cut out of solid or cored cylinders of larger diameter. There was a decided preference for a  $\langle 100 \rangle$  direction along the crucible axis, especially in the lower range of nickel content. The whole range in nickel was from 30 to 100 per cent.

Both  $I$ - $H$  and  $(\Delta L/L)_P$ - $H$  were measured, usually in separate experiments. The very high values of  $\kappa$  which occur in the permalloy range, here included, made the measurement of  $H$  very difficult. What was done, therefore, was to use such a value of  $n_3$  in each case that the sides of the  $I$ - $H$  loop were parallel to the  $I$ -axis near the origin. Some unexplained variations in  $I_s$  may have been due to porosity or contamination. Values of  $H_c$  ranged from 0.03 to 0.7 with a mean of 0.25, there being no conspicuous correlation with ease or difficulty of magnetization as judged from the upper part of the  $I$ - $H$  curves.

Lichtenberger makes use of Akulov's so-called orientation factor

$$f = \cos^2 \phi_2 \cos^2 \phi_3 + \cos^2 \phi_3 \cos^2 \phi_1 + \cos^2 \phi_1 \cos^2 \phi_2 \quad [36]$$

Our equation 13 may, if  $I$  is constant, be written

$$W_f = W_0 + fW_{22} \quad [37]$$

where  $W_f$  is the stored energy density, and  $W_0$ ,  $W_{22}$  are constants. For  $\langle 100 \rangle$ ,  $f = 0$ ; for  $\langle 111 \rangle$ ,  $f = 1/3$ , and these are the outside limits for  $f$ . One of the tabulated differences in Tables 1 and 2 is therefore seen to be

$$W_{111} - W_{100} = 1/3 W_{22} \quad [38]$$

From Table 2 we can conclude for nickel  $W_{22} = -5 (10)^4 \text{ erg.cm.}^{-3}$ . Lichtenberger's crystal No. 81a, for which  $f = 0.050$ , and which contained 85.5 per cent Ni, has  $W_f < 1.24 (10)^4$  so that  $W_{22}$  must be algebraically greater than  $\frac{-1.24 (10)^4}{0.333 - 0.050} = -4.4 (10)^4$ . At about 60 per cent Ni,  $W_{22}$  passes through zero, for  $W_f$  is independent of  $f$ , and below this nickel content  $W_{22}$  is positive. Thus at 53.5 per cent Ni in crystal No. 61a, for which  $f = 0.000$ , we estimate  $W_f < 1.2 (10)^3$ . In this range we find no data for high  $f$  values by which we can estimate an upper limit for  $W_{22}$ .

Values of  $(\Delta L/L)_P$  are reported more fully, and clearly depend upon  $f$  at any one composition. An equation of the form

$$(\Delta L/L)_P = \Delta_0 + f\Delta_{22} \quad [39]$$

fits the observed values (at saturation) rather well. We tabulate  $\Delta_0$  and  $\Delta_{22}$  from Lichtenberger's figure. The change of sign in  $\Delta_{22}$  at about 60 per cent Ni is associated with the change in sign of  $W_{22}$  at the same composition. The change in sign of  $\Delta_{22}$  at 85 per cent Ni is not, as we

TABULATION OF  $\Delta_0$  AND  $\Delta_{22}$  FROM LICHTENBERGER'S FIGURES

Per Cent Ni	(10) <sup>6</sup> $\Delta_0$	(10) <sup>6</sup> $\Delta_{22}$	Per Cent Ni	(10) <sup>6</sup> $\Delta_0$	(10) <sup>6</sup> $\Delta_{22}$
100	-45	+63	63	+21	-21
91	-17	+28.5	59	+18	+12
85.5	-5	0	53	+13	+33
82	+10	-34.5	44	-5	+97.5
80	+11	-33	38	-7	+99
71	+18	-31.5	33	-2.5	+61.5

have seen, associated with any important change in  $W_{22}$  but rather with the zero value of  $\Delta_0$  in this region. The relations are apparently too complicated for a two-constant formula to follow in detail.

J. W. Shih, one of our students at the Sloane Laboratory, is studying crystals of the iron-cobalt alloys of the body-centered cubic structure. He has measured magnetization in oblate spheroids with diametral planes {100} and {110} cut from a crystal of 30 per cent Fe, 70 per cent Co. The easy direction for magnetization is no longer  $\langle 100 \rangle$  as in iron but is  $\langle 111 \rangle$  as in nickel. The shift is perhaps similar to that already found in iron-nickel alloys by Lichtenberger, but it would be premature to guess on this point. New methods for cutting a small spheroid very accurately and for measuring  $I_p$  in such a specimen have been devised recently in our laboratory and we hope to apply them to fill in some of the gaps apparent after this rather tedious survey of the experimental evidence.

### HEXAGONAL COBALT

Before considering experiments on hexagonal cobalt, we write down an equation for the hexagonal system which takes the place of equation 13 for the cubic system. For a linear vector function of  $I$  we must have

$$k_{12}(I_1^2 + I_2^2) + k_3 I_3^2 + k_0 = 0 \quad [40]$$

The hexagonal symmetry has been concealed by this approximation. To exhibit it we may write a fourth-degree equation

$$k_{124}(I_1^4 + I_2^4) + k_{34}I_3^4 + k_{1222}I_1^2I_2^2 + k_{322}(I_1^2 + I_2^2)I_3^2 + k_{122}(I_1^2 + I_2^2) + k_{32}I_3^2 + k_1 = 0 \quad [41]$$

in which the coefficients are not all independent. (In both of these expressions  $I_1$  and  $I_2$  are components at right angles to each other in the (001) plane, and not components along proper hexagonal axes.) We

will remark at once that equation 41 is not convenient. A transcendental surface of more manageable form and of the necessary symmetry is to be preferred.

All the work on cobalt so far reported is from Honda's laboratory. Kaya<sup>(40)</sup> studied magnetization at room temperature, Honda and Masumoto<sup>(41)</sup> continued this work at higher temperatures, Nishiyama<sup>(42)</sup> studied magnetostriction. The allotropic transformation occurs at so

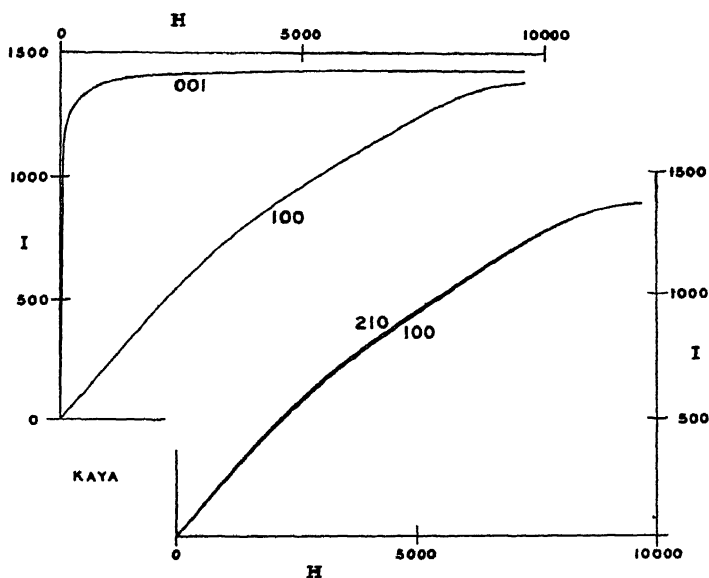


FIG 11 —  $I$ - $H$  ALONG AXES OF SYMMETRY IN KAYA'S COBALT SPHEROIDS (100) AND (001)

low a temperature (Masumoto<sup>(43)</sup> reports 470° C.) that it is very surprising to find that slow cooling of large cubic cobalt crystals formed from a slowly cooled melt gave large crystals of the low-temperature hexagonal structure. Kaya reports the following impurities in weight per cent: Fe, 0.116; Ni, trace; Mn, 0.048; Si, 0.012; C, 0.01; S, 0.010; P, 0.0124. One disk was cut in the plane (100) and one in the plane (001), not here equivalent since the sixfold axis (third index) is unique. The characteristics of the disks were.

#### COBALT DISKS

Plane of Disk	Dimensions, Cm.		$\eta_1 = \eta_2$
	$2a$	$2c$	
(100)	0.4530	0.0283	-0.706
(001)	0.4340	0.0276	-0.718

Ballistic methods were used in finding  $I_P$  and  $I_N$ .

Anisotropy is evident in the lowest magnetic fields, the hexagonal axis being the only easy direction for magnetization. This axis may be designated as direction [001] or as the normal to plane (001) but the same simple relation between line indices and plane indices holds for no other axis. Kaya's notation, which is irregular, is not followed in this review. Here [100] is the direction between closest atoms in the basal plane and [210] is perpendicular thereto in the same plane.

Fig. 11 shows  $I$ - $H$  curves for axes of symmetry. The slight but definite difference between the two sorts of twofold axis in the (001) disk is particularly interesting, since this rules out a linear vector function for the relation between  $I$  and  $H$ . We will confine our attention to energy density differences, collected in Table 3. Any detailed analysis is made more difficult by the fact that even a small deviation of  $H_M$  from the (001) plane causes  $I$  to swing through a large angle, the preference for [001] overcoming the high demagnetizing factor  $n_3$ .

Nishiyama's measurements of  $(\Delta L/L)_P$  and  $(\Delta L/L)_N$  were especially difficult because of the small diameters of the disks and the fact that very

RÉSUMÉ FOR  $H_M = 7320$ 

Direction of $H_M$	$(\Delta L/L)_P$ (10) <sup>6</sup>	$(\Delta L/L)_N$ (10) <sup>6</sup>
In (001) plane		
[100] (mean of 3)	-12 2	-35 9
[210] (mean of 3).	-14 3	-38 2
In (100) plane		
[001]	- 2 5	- 7 2
22 5° from [001] (mean of 2)	-25 7	+21 4
45° from [001] (mean of 2)	-42 7	+50 0
67 5° from [001] (mean of 2)	-31 5	+73 5
[100]	-17 7	+51 5

high  $H_M$  was necessary to approach saturation in other directions than [001]. The results are complicated and the accompanying résumé for  $H_M = 7320$  must suffice. The principal peculiarity is that the greatest strains occur for directions of  $H_M$  that do not coincide with any

CHARACTERISTICS OF PRISMATIC RODS

Direction of Prism Axis	Dimensions, Cm			$n_1$	$n^*$
	Length	Breadth	Thickness		
[001]	1 453	0 1491	0 1488	-0 293	-0 318
[100]	1 153	0 1187	0 0632	-0 207	-0 197
[210]	1 493	0 1133	0 0732	-0 157	-0 151

axis of symmetry. Besides these spheroids Nishiyama also tested some prismatic rods which had the characteristics shown herewith. Of the two values for the demagnetizing factor along the prism axis  $n_3$  is that given by Nishiyama,  $n_3^*$  is a value for a prolate spheroid inscribed in a circular cylinder of the same length and midsectional area as the prism. The longitudinal effects in these rods were as shown, again for  $H_M = 7320$  in each case. These agree well enough with the results for spheroids.

## LONGITUDINAL EFFECTS IN PRISMATIC RODS

Direction of Prism Axis	$(\Delta L/L)_P$ (10) <sup>s</sup>
[001]	- 3 5
[100]	-25 6
[210]	-27 7

Honda and Masumoto's work at higher temperatures was done on the rods last mentioned, to judge by the dimensions they report, and the  $I$ - $H$  curves are plotted on a large scale so that energy density differences can be computed with confidence. They are included in Table 3. The interesting point is the shift of the easy direction of magnetization from the hexagonal axis to any direction in the basal plane at about 270° C. Since the value of  $I_s$  dropped only from 1438 to 1366 in the range from -190° C. to +390° C., we see that this change has nothing to do with the Curie point of hexagonal cobalt, which must lie at a very high temperature.

TABLE 3.—*Energy Density Differences in Cobalt*

Observers	Specimens	$W_{100} - W_{001}$	$W_{100} - W_{210}$
		Erg Cm <sup>-3</sup> (10) <sup>s</sup>	
Kaya	Disk (100)	51 9	1 09
	Disk (001)		
Honda-Masumoto	Rods [001], [100], [210] at		
	-190° C	88 1 <sup>a</sup>	-6 3 <sup>a</sup>
	+ 12°	59 8 <sup>a</sup>	-3 1 <sup>a</sup>
	50°	45 6	-5 0
	100°	31 2	-3 2
	150°	19 2	-3 2
	200°	9 8	-2 2
	230°	4 4	-2 4
	260°	0 3	-1 3
	300°	- 4 7	0 0
	350°	-13 2	0 2
	390°	-22 0	-0 5

<sup>a</sup> These values are less accurate than the others because the areas to be measured had to be obtained by extrapolation to  $I_s$  beyond the experimental limit in  $H$ .



## THEORIES

We now have to consider how this complexity of experimental findings has been simplified by theories of one kind or another. Theories, of course, may be more or less ambitious in what they attempt to do. The simplest sort merely offers a mathematical framework in which a few numerical magnitudes replace the presentation of the data by two-dimensional or three-dimensional diagrams. We have already made some use of this first simplification in computing differences in magnetic energy density required for complete magnetization in various crystallographic directions, and have mentioned, in connection with Lichtenberger's experiments on nickel-iron crystals, Akulov's anisotropy factor  $f$ , which is intended to give a mathematical summary of the effects of the direction of magnetization upon any scalar property we please. This viewpoint has been developed by Akulov in a series of papers of which the last <sup>(44)</sup> appeared in 1930. As we have seen, this form already existed in Beck's 1918 paper, and even as early as that was shown to be inadequate to cover the variations in planes perpendicular to a threefold axis. In other words, a fourth-degree surface is too simple to provide better than a second approximation, and we seem to need further refinement in our theory. Webster's crystalline field<sup>(6)</sup> is a theoretical device of the same sort—a mere mathematical artifice—but goes a little farther in providing the necessary symmetry. (It gives an eighth-degree characteristic surface.) It has not yet been tested against a sufficient body of data to prove its general usefulness.

A second category of theories assumes from experiment the fact that certain directions in each crystal are directions of easy magnetization and attempts to explain the details of magnetization by showing how shift from one easy direction to another and deflection from any easy direction toward the direction of  $\mathbf{H}$  take place under certain added assumptions. The most important in this group is the explanation offered by Akulov<sup>(45)</sup> and by Heisenberg<sup>(46)</sup> for the magnetostriction and magnetization curves in iron. They suppose that the direction of  $I_s$  in each of the small regions which act as magnetic units—in each domain—lies along one of the six easy directions for magnetization, of form  $\langle 100 \rangle$ . In the apparently unmagnetized crystal these six directions are equally represented so that the resultant  $\mathbf{I}$  is zero. The equilibrium is disturbed by the presence of  $\mathbf{H}$  and the first thing that happens is the reversal of  $I_s$  in all those domains in which this is favored by the direction of  $\mathbf{H}$ . Such reversal is not supposed to alter the dimensions of a domain, that is, there is no magnetostrain during this stage, and the changes occur for low values of  $H$ . The corresponding rapid rise in  $I$  stops as soon as all domains have a component of  $I_s$  in the direction of  $\mathbf{H}$ . This occurs at  $I = 0.577 I_s$  for  $\langle 111 \rangle$ , at  $I = 0.707 I_s$  for

$\langle 110 \rangle$ , and at  $I = I_s$  for  $\langle 100 \rangle$ . Further increase of  $I$ , possible except for  $\langle 100 \rangle$ , requires large energy supply because in this stage it is necessary to turn  $I_s$  in each domain into an "unnatural" direction. Changes of direction through  $90^\circ$  rather than  $180^\circ$  also occur and the experimental evidence is in favor of the view that such changes are intermediate in difficulty between reversals and deviations from an easy direction.

R. M. Bozorth<sup>(47)</sup> has been able to extend this theory to cover the relations between  $I_P$  and  $I_N$  in a disk specimen. In order to get a mathematical hold upon the problem he supposes that the probability of a change from one easy direction to another depends only upon the potential energy difference for the two directions of  $I_s$  in the presence of  $H$ . The theory explains sudden changes—Barkhausen jumps—in  $I_N$  as well as in  $I_P$  and experiment<sup>(48)</sup> shows that these are abundant in polycrystalline material at about the right value of  $I$ , and that the ratio of transverse to longitudinal effects is reasonable. A search for further evidence on this point is under way in our laboratory. R. F. Clash is using a cathode ray oscillograph to reintegrate in two dimensions the rectangular components of elementary vector increments in the magnetization of a disk specimen.

C. J. Gorter<sup>(49)</sup> has recently shown that Kaya's measurements on  $I_r$  in iron agree very well with Heisenberg's hypothesis. The only care we must take is to be sure in the case of a rod that  $I_r$  remains parallel to the rod axis, and this requires that particular relation between  $I_{r1}$ ,  $I_{r2}$  and  $I_{r3}$  which leads to equation 33

Francis Bitter<sup>(50)</sup> has gone a step farther by combining in one representation the effects of crystal structure and elastic strain. He considers a fourth-degree energy surface for constant  $I$  with cubic symmetry, of the sort first discussed by Karl Beck, modified by the deformation in the way that R. Becker<sup>(51)</sup> has shown to be appropriate in the isotropic case. It was already known that an elastic strain could create so strong a preference for a given direction of magnetization that we could picture the metal as composed wholly of domains saturated one way or the other along this one direction. Bitter has given quantitative significance to this picture and suggested the mode of transition from crystal control to strain control. His theory is able to predict the effect of homogeneous strain in many cases where it has not yet been looked for and thus is subject to experimental verification or disproof.

The very interesting discovery, by Bitter,<sup>(52)</sup> that the magnetic inhomogeneity of a single crystal can be made evident by precipitating a magnetic powder upon it, has aroused much interest.<sup>(53)</sup> It is too soon to decide what influence this type of analysis will have upon the topic we are discussing. We must also leave out of account a number of

incidental experiments on ferromagnetic monocrystals that must, of course, be considered in any full discussion of the subject

When we turn to theories regarding the physical nature of the crystalline field, or whatever we choose to call the circumstances which fix the easy directions of magnetization in a given crystal, we are unable to find anything presently useful. The first proposal was that the superior stability was conditioned by the existence at each elementary magnet of a particular magnetic field intensity due to all the rest. As long as it seemed even remotely possible that magnetic fields of the right order of magnitude and the right directional properties could be explained by suitable arrangement of suitable magnetic particles—these two “suitables” weed out most of the *a priori* possibilities—this would do as a working hypothesis. We have shown, however, by rather extensive calculations<sup>(54)</sup> that none of the schemes yet proposed lead to anything of the right sort. It is not too much to say that the magnetic stability pictured in various ways by Ewing, Honda and Okubo, Mahajan, Akulov, Becker and others, does not exist in that range of  $I$  values where crystalline anisotropy is most obvious.

It will not do, either, as some have proposed, to regard crystalline anisotropy in magnetic behavior as due to crystalline defects. Without entering too deeply into a highly controversial subject, we may be given leave to doubt whether crystal imperfections can be so beautifully symmetrical as some of the effects we have just passed in review, or so similar in crystals of one element having such widely different magnetic susceptibilities and hysteresis losses. The case for residual elastic strains is no better, and for the same reason. Processes which are known to leave cold-working strains merely superpose an effect of their own upon something which appears to be inherently symmetrical.

The way of escape is open but few will have the necessary skill and strength to follow it far enough. Since Heisenberg<sup>(55)</sup> showed that the pseudomagnetic molecular field, invented by Weiss to explain ferromagnetism itself—local saturation  $I_s$  when  $H$  is zero—is probably electrostatic in origin, it has seemed likely that the molecular field should be at least slightly anisotropic. Since its magnitude at room temperature in iron is of the order of  $(10)^7$  it seems not unreasonable to find in it a directional variation of the order of  $(10)^3$ , which is all we need. We may venture to amplify this notion a little. Electrostatic forces effect magnetic control in a rather indirect way. When the magnetic elements—permanent electric currents—are identified with spinning electrons it becomes at least possible to admit that the electron pattern in a domain should be different when the magnetic axes are parallel, all in one direction, and when they are not. This is exactly what the modern theory of atomic and metallic structure demands. A metal with disposable spinning electrons in its atoms is ferromagnetic if the electrostatic poten-

tial energy turns out to be least when most of the spins are parallel. Furthermore, the electron pattern, in three dimensions, is different when the spins are parallel from what it is when they are directed at random. The only addition we need to make to this is to say that the electron pattern—which, please remember, includes the electrons that maintain the crystal structure—is dependent upon the direction of parallel spins with respect to the crystal axes. That some of the electrostatic forces vary with this direction is already clear from the presence of magnetostriction. That some of the electrons choose different paths is clear from the presence of magnetoresistance.

This suggestion, of course, is only a foundation for a proper theory. It will take good work by good men, some of whom have yet to hear of the problem, before the theory will be at all adequate. When it is, a lot of metallurgical problems will also be solved, because their solution must lie exactly in this same region, the electron patterns in and between the atoms of a metal or alloy.

## BIBLIOGRAPHY

- <sup>1</sup> E. Warburg *Ann d Physik* (1881) [3] **13**, 141–164
- <sup>2</sup> J A Ewing: *Proc Roy Soc* (1882) **34**, 39–45, *Phil Trans Roy Soc.* (1885) **176**, 523–640
- <sup>3</sup> J H Van Vleck *The Theory of Electric and Magnetic Susceptibilities*, 2 Oxford, 1932 Clarendon Press
- <sup>4</sup> T Spooner *Amer Physics Teacher* (1933) **1**, 121
- <sup>5</sup> W Thomson *Phil Mag* (1851) [4] **1**, 177–186
- <sup>6</sup> W L Webster *Proc Roy Soc* (1925) [A] **107**, 496–509
- <sup>7</sup> P Weiss *Éclairage électrique* (1896) **7**, 487–508 **8**, 56–68, 105–110; *Jnl. de phys.* (1896) [3] **5**, 435–453
- <sup>8</sup> P Weiss *Jnl de phys* (1904) [4] **3**, 194–202; (1905) [4] **4**, 469–508, 829–846; *Arch. des sci* (1905) [4] **19**, 537–558, **20**, 213–230
- <sup>9</sup> V Quittner *Ann. d Physik* (1909) [4] **30**, 289–325
- <sup>10</sup> K Beck *Vierteljahrsschrift der naturforschenden Gesellschaft in Zurich* (1918) **63**, 116–186
- <sup>11</sup> J de Freudenreich *Arch des Sci* (1914) [4] **38**, 36–45
- <sup>12</sup> C, 0 06, Si, 1 62, Mn, 0 16, P, 0 050, S, 0 040, Al—
- <sup>13</sup> J Clerk Maxwell: *A Treatise on Electricity and Magnetism*, Ed. 3, 2, 66–72, articles 437–438 Oxford, 1892 Clarendon Press
- <sup>14</sup> C W Heaps *Phys Rev* (1923) [2] **22**, 436–501
- <sup>15</sup> C A. Edwards and L B Pfeil *Jnl Iron and Steel Inst* (1924) **109**, 129–147, disc, 148–158.
- <sup>16</sup> W Sucksmith, H H Potter, L Broadway *Proc. Roy Soc.* (1928) [A] **117**, 471–485.
- <sup>17</sup> J Kunz *Nat Res Council Bull* (1922) [3] **3**, 165–213
- <sup>18</sup> K. Honda, S Kaya and Y Masuyama *Nature* (1926) **117**, 753–754, K Honda and S Kaya *Sci Rept Tohoku Imp Univ* (1926) [1] **15**, 721–753  
K Honda and Y Mashiyama. *Sci Rept Tohoku Imp Univ* (1926) [1] **15**, 755–776.
- <sup>19</sup> K. Honda, H Masumoto and S Kaya *Sci Rept. Tohoku Imp. Univ* (1928) [1] **17**, 111–130
- <sup>20</sup> W E Ruder. *Trans Amer Soc Steel Treating* (1925) **8**, 23–29
- <sup>21</sup> W L. Webster *Proc. Roy Soc.* (1925) [A] **109**, 570–584

- <sup>22</sup> W L Webster *Nature* (1926) **117**, 859, *Proc. Roy Soc* (1926) [A] **113**, 196-207, (1927) [A] **114**, 611-619
- <sup>23</sup> W Gerlach. *Phys Ztsch* (1925) **26**, 914-915, *Ztsch f Physik* (1926) **38**, 828-840, **39**, 327-331.  
E. Dussler, W Gerlach *Ztsch f Physik* (1927) **44**, 279-285  
E Dussler *Ztsch f Physik* (1928) **50**, 195-214
- <sup>24</sup> P P Cioffi *Phys Rev* (1932) [2] **39**, 363-367.
- <sup>25</sup> E Dussler. *Ztsch f Physik* (1927) **44**, 286-291, *Ann d Physik* (1928) [4] **86**, 66-94
- <sup>26</sup> D D Foster *Phys. Rev.* (1929) [2] **33**, 1071.
- <sup>27</sup> D. D Foster *Phil Mag* (1929) [7] **8**, 304-313.
- <sup>28</sup> D D Foster and R. M. Bozorth. *Nature* (1930) **125**, 525
- <sup>29</sup> W Wolman: *Archiv. f Elektrotech* (1928) **19**, 385-404
- <sup>30</sup> H Gries and H Esser. *Archiv f Elektrotech* (1929) **22**, 145-152.
- <sup>31</sup> G. J Sizoo. *Ztsch f Physik* (1929) **56**, 649-670, **58**, 718; *Physica* (1930) **10**, 1-18
- <sup>32</sup> S Kaya. *Ztsch. f Physik* (1933) **84**, 705-716.
- <sup>33</sup> A G Hill *Phil Mag* (1932) [7] **14**, 599-604
- <sup>34</sup> W Sucksmith and H H Potter: *Nature* (1926) **118**, 730-731; also reference of note 16
- <sup>35</sup> S Kaya and Y Masiyama. *Nature* (1927) **120**, 951-952.  
S Kaya. *Sci. Rept Tohoku Imp Univ.* (1928) [1] **17**, 639-664, 1027-1037  
Y Masiyama. *Sci Rept Tohoku Imp Univ* (1928) [1] **17**, 945-961
- <sup>36</sup> G. J Sizoo: *Ztsch f Physik* (1929) **57**, 106-114; *Physica* (1930) **10**, 1-18
- <sup>37</sup> G. J Sizoo and C Zwikker *Ztsch f Metallkunde* (1929) **21**, 125-126
- <sup>38</sup> H H Potter *Proc Phys Soc* (1929) **41**, 135-142
- <sup>39</sup> F Lichtenberger. *Ann. d. Physik* (1932) [5] **15**, 45-71.
- <sup>40</sup> S Kaya. *Sci Rept Tohoku Imp Univ.* (1928) [1] **17**, 1157-1177
- <sup>41</sup> K Honda and H Masumoto: *Sci Rept Tohoku Imp Univ* (1931) [1] **20**, 323-341
- <sup>42</sup> Z Nishiyama. *Sci. Rept Tohoku Imp Univ* (1929) [1] **18**, 341-357
- <sup>43</sup> H Masumoto: *Sci Rept Tohoku Imp Univ.* (1926) [1] **15**, 449-477
- <sup>44</sup> N. S Akulov. *Ztsch f Physik* (1930) **59**, 254-264; cf F. Bitter. *Phys Rev.* (1932) [2] **39**, 371-375.
- <sup>45</sup> N. S Akulov: *Ztsch f Physik* (1931) **67**, 794-807, **69**, 78-99
- <sup>46</sup> W Heisenberg. *Ztsch. f. Physik* (1931) **69**, 287-297
- <sup>47</sup> R. M Bozorth *Phys Rev* (1932) [2] **39**, 353-356, disc 375-376, **42**, 882-892
- <sup>48</sup> R M Bozorth and J. F Dillinger *Phys Rev* (1931) [2] **38**, 192-193; (1932) [2] **41**, 345-355
- <sup>49</sup> C. J Gorter *Nature* (1933) **132**, 517-518
- <sup>50</sup> F. Bitter. *Phys Rev.* (1933) [2] **43**, 655-660
- <sup>51</sup> R. Becker: *Ztsch f Physik* (1930) **62**, 253-269
- <sup>52</sup> F. Bitter: *Phys Rev* (1931) [2] **38**, 1903-1905
- <sup>53</sup> L. v Hámos and P. A. Thiessen: *Ztsch. f Physik* (1931) **71**, 442-444, (1932) **75**, 562  
W Gerlach. *Ztsch f. Physik* (1932) **74**, 128-129.  
N [S.] Akulov and M Degtiar. *Ann d. Physik* (1932) [5] **15**, 750-756.  
R Becker and H F. W. Freundlich: *Ztsch f Physik* (1933) **80**, 292-298  
K. J Sixtus: *Phys Rev.* (1933) [2] **44**, 46-51.
- <sup>54</sup> L W. McKeehan *Phys Rev* (1933) [2] **43**, 913-923, 924-930, 1022-1024, 1025-1029; **44**, 38-42, 582-584.
- <sup>55</sup> W. Heisenberg. *Ztsch. f. Physik* (1928) **49**, 619-636.

# Comparative Studies on Creep of Metals Using a Modified Rohn Test

By C R AUSTIN\* AND J R GIER,† EAST PITTSBURGH, PA

(New York Meeting, February, 1934)

IN a recent paper<sup>1</sup> the authors presented information on a refinement of the Rohn type of creep test with data on pure iron that exemplified the behavior of the apparatus. The present paper extends that work to nickel and cobalt and to the examination of the comparative high-temperature properties of two widely used commercial alloys. Careful attention has been given to the effect of plastic deformation in decreasing creep rate, using the elementary metals iron, nickel and cobalt for purposes of analysis.

In any endeavor to develop new materials for high-temperature service one soon encounters a real problem as to the sort of test to be employed in evaluating the commercial possibilities of the alloys. At one time it was considered satisfactory to determine the tensile strengths at elevated temperatures and to use these values as a criterion for the commercial application of the alloys. More recently the proportional limit has been used as a means of classification. Data obtained from a form of bend test have also shown promise as providing a "merit index" of high-temperature serviceability.<sup>2</sup>

Koerber and Pomp<sup>3</sup> state that since the influence of testing time is small, the high-temperature yield point of steel furnishes sufficiently reliable and concordant values up to about 350° C. (and a maximum of 450° C. for alloy steels) to serve as a suitable basis for comparison evaluations of materials and for judging permissible stresses. Koerber and Pomp consider, however, that above these temperatures creep limit must be substituted for the high-temperature yield point as the all-important characteristic of the material. Whatever may be their definition of

---

Manuscript received at the office of the Institute Nov 22, 1933.

\* Section Engineer, Alloys and Process Section, Research Laboratories, Westinghouse Elec & Mfg Co.

† Associated with Research Laboratories, Westinghouse Elec. & Mfg Co.

<sup>1</sup> C. R. Austin and J. R. Gier. Studies on a Modification of the Rohn Test for Investigating Creep of Metals. *Proc Amer Soc Test Mat* (1933) pt 2, 293.

<sup>2</sup> C. R. Austin and G. P. Halliwell: Some Developments in High-temperature Alloys in Nickel-cobalt-iron System. *Trans A I M E.* (1932) 99, 78

<sup>3</sup> F. Koerber and A. Pomp. High-temperature Yield Point and Creep Limit of Steel. *Stahl und Eisen* (1932) 52, 553-559.

"creep limit," there will be few engineers who will dispute the necessity for recognizing flow characteristics when evaluating metals intended for high-temperature mechanical duty.

With the exception of the type of test suggested by Rohn, and another suggested by Barr and Bardgett, all methods of creep testing are concerned with the direct measurement of strain and the deduction therefrom of the rates of creep. The Rohn test<sup>4</sup> is concerned with the measurement of temperature and depends on the following simple principle.

It is considered that if there is a suitable linking between the deformation by stretching under constant load and the temperature of the specimen, and if the test is conducted for an indefinite period, a limiting condition is approached where the temperature of the test rod has been progressively reduced to a point at which it is capable of sustaining the load without accepting further measurable deformation.

It was from a consideration of this work that the present authors concluded that the Rohn test might provide a more satisfactory means of alloy evaluation at elevated temperatures than any test hitherto suggested. Furthermore, it appeared to provide a rapid means of evaluating resistance to deformation of metals over a range of temperatures.

#### MATERIALS USED IN THE INVESTIGATION

The data were obtained on tests on iron, nickel and cobalt, on an 18 per cent chromium, 8 per cent nickel alloy and on a chrome-silicon alloy. The 18-8 alloy contained less than 0.07 per cent carbon and the nominal composition of the chrome-silicon ferrous alloy was as follows: carbon, 0.45 per cent; manganese, 0.4; phosphorus and sulfur, 0.02; silicon, 3.25; chromium, 8.5. The iron, nickel and cobalt had the compositions given in Table 1.

The silver specimens were prepared from "fine" silver. It will be noted that of the three transition elements the iron alone was of a high degree of purity. This element, together with silver and nickel, is free from allotropic change within the temperature range of the present tests. Cobalt is regarded as having a close-packed hexagonal lattice at ordinary temperatures. Between 400° and 500° C. a transformation results in the formation of a gamma cobalt with a face-centered cubic lattice.

The samples were prepared by swaging in the form of  $\frac{3}{16}$ -in. rod of uniform section and were thoroughly annealed before the test. The variations along the diameter of any test bar were less than 0.001 in. No

---

<sup>4</sup> W. Rohn, Festschrift zum 70 Geburtstag von Dr. Phil. Dr. Ing. E. L. Wilhelm Hereaus in Hanau, reviewed in the *Metallurgist* (supplement to *The Engineer*) (Feb. 28, 1930) 22.

difficulties were experienced in fabrication except in the case of cobalt. The rate of work-hardening of this element appears to be so great that it was found extremely difficult to cold-swage the metal. Frequent annealings were required and trouble was experienced in keeping the

TABLE 1.—*Chemical Composition of Iron, Nickel and Cobalt Tested*

Element	Composition, Per Cent		
	Iron	Nickel	Cobalt
Iron	99.967	0.23	0.11
Nickel		98.78	0.16
Cobalt		0.42	99.32
Copper	Tr	0.30	0.04
Carbon	0.001	0.13	0.16
Phosphorus	0.002	0.026	0.024
Sulfur	0.008	0.005	
Silicon	0.004	0.09	0.07
Manganese	0.002		0.08
Aluminum		0.010	0.010
Oxygen	0.016		

metal free from surface defects. However, satisfactory rods were finally secured.

#### FACTORS INFLUENCING TEST DATA

Factors influencing the test data, such as coefficient of expansion and changes in elastic modulus of the test rod, and temperature gradients in the test furnaces, have been fully discussed in the authors' paper cited, but it is necessary to present here information as to how the creep data are calculated and to indicate the significance of unit temperature changes in terms of creep.

In the Appendix it is demonstrated that creep may be assumed to take place over a 25-in. length of specimen while 35 in. represents the length affected by expansion and modulus changes. A new method of actually measuring changes of length due to temperature dilatation in the test furnace is also described at the end of this paper.

Assume the rate of fall in temperature during test to be  $1^{\circ}\text{C. per } 10\text{ hr.}$ , or  $0.1^{\circ}\text{C. per hour.}$  With a temperature coefficient of  $15 \times 10^{-6}\text{ in. per in.}$ , the contraction due to  $0.1^{\circ}\text{C.} = 15 \times 10^{-7}\text{ in. per in.}$  Total contraction taking place in 35 in. of the test rod is thus  $0.000054\text{ in. per hour.}$

Since the actual length of the rod remains constant, this thermal contraction is a measure of the extension by creep occurring over the



effective "gage length," assumed to be 25 in. Thus, the creep rate approximates  $2 \times 10^{-6}$  in. per in. per hour. The percentage creep per 1000 hr. would be 0.2 per cent for  $0.1^\circ \text{C. per hr.}$  fall in temperature in this case.

The above analysis with the data included in the appendix should serve to demonstrate the role of the factors discussed in the study of creep by this temperature-time method, and it should serve, further, to indicate approximately the significance in conventional creep units of the slope of the temperature-time curves as they approach an asymptotic position relative to the time axis.

### RESULTS OF TESTS ON PURE METALS

In each experiment the annealed metal was loaded at room temperature, and the temperature was raised in steps until, with the control

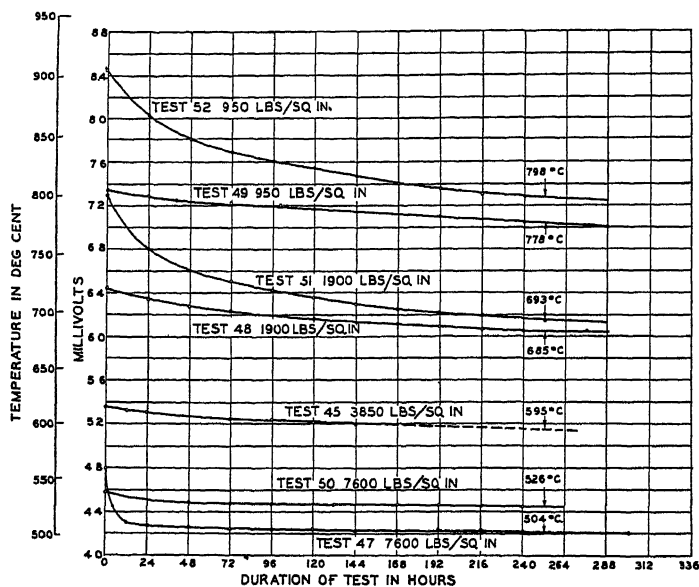


FIG. 1.—CREEP TESTS ON PURE NICKEL

mechanism working, it was clear that the test bar was exhibiting definite creep under the initially applied load. A temperature record was then taken every 2 hr. during the entire course of the test.

In Fig. 1 are presented the data obtained for nickel using four different loads. In Fig. 2, similar data are given for cobalt. Annealing of the metal followed by loading at room temperature was the procedure in all tests. For purposes of comparison a group of curves for iron, nickel, cobalt and silver, illustrating the time-temperature relationships under

different loads, have been assembled in Fig 3. It is considered that this figure illustrates the utility of the test in differentiating between metals or alloys with respect to their high-temperature strength. Drawing a comparison between iron and silver, we note that silver, with a load of 2000 lb per sq. in., and iron, with 7500 lb. per sq. in., tend to approach a limiting temperature which we have assumed to be near  $275^{\circ}\text{C}$ . The superior strength of iron is evident. In order to reduce what may be termed the load-carrying capacity of iron, within the limits of this particular experiment, to 2000 lb per sq. in. we must raise the temperature to between  $450^{\circ}$  and  $500^{\circ}\text{C}$ . Nickel has a similar load-carrying capacity at about  $675^{\circ}\text{C}$ .

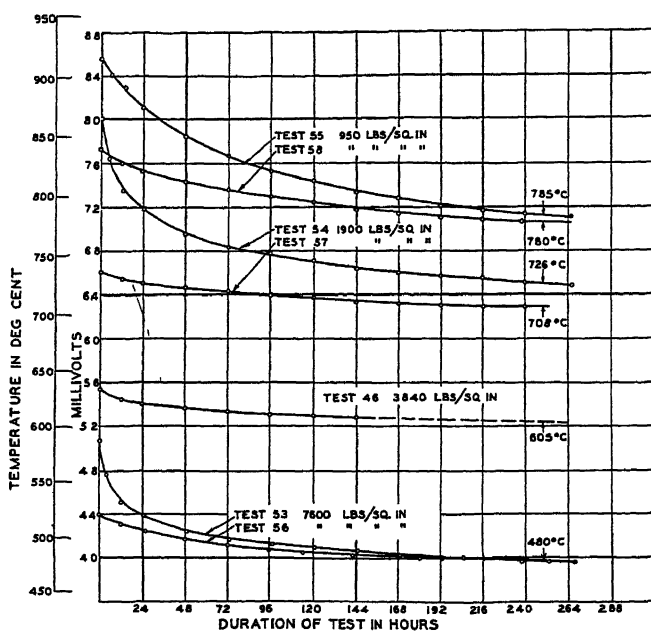


FIG 2—CREEP TESTS ON COBALT.

An interesting comparison is also found in the two curves for the iron and nickel specimens, which practically coincide. These demonstrate that at about  $680^{\circ}\text{C}$ . our nickel specimen carried a load of 1900 lb. per sq. in. compared to only 385 lb. per sq. in. for the iron. All are familiar with the fact that nickel is "stronger" than iron, which is in turn "stronger" than silver, but the data provided give us a measure (at least within the limits of experimentation) of the superiority in terms of load carrying capacity for any given temperature, or in terms of temperature to which the metal may be raised and beyond which it fails to provide the given load-carrying capacity.

These features of the test have been emphasized in order to illustrate how the test may be used to compare creep characteristics of the alloys within a comparatively short period of time

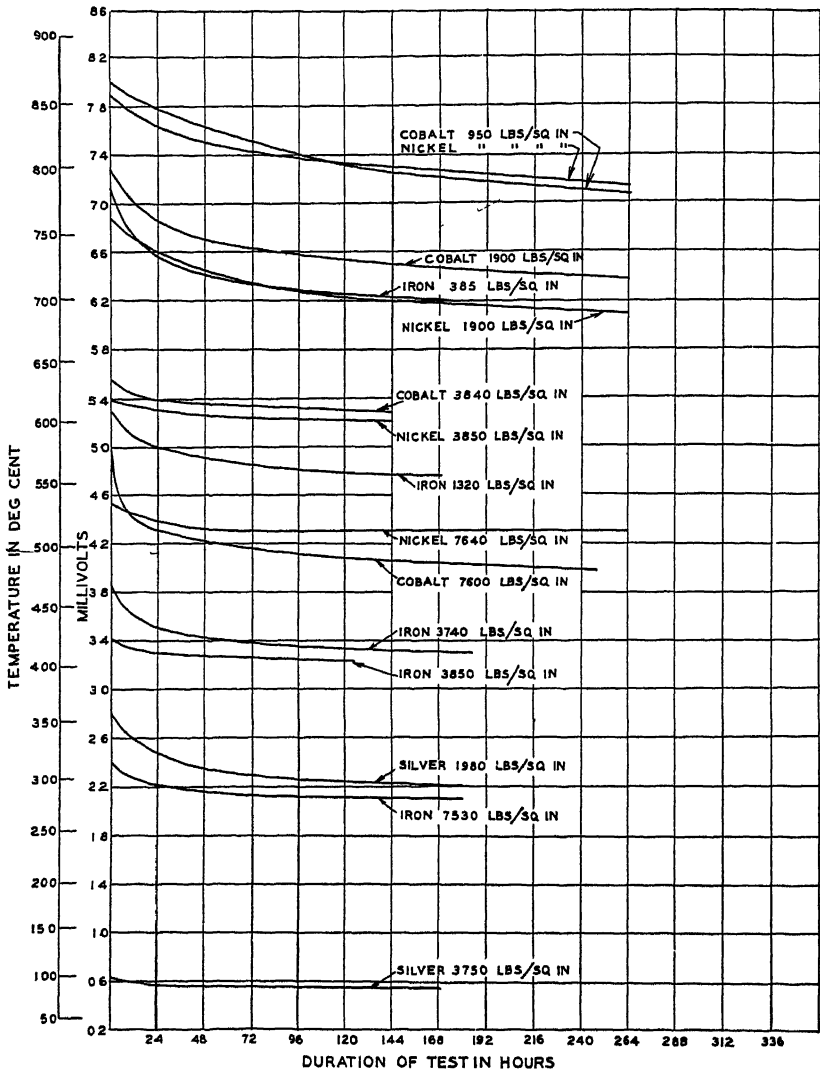


FIG 3—CREEP TESTS ON PURE METALS

### EFFECTS OF TEST PROCEDURE ON TEST RESULTS

Investigators appear to have given little attention to the effects of method of loading on the test results. Recently, in an instructive paper by White and Clarke,<sup>5</sup> attention is drawn to the marked difference in

<sup>5</sup> A E White and C L Clarke Creep Characteristics of Metals at Elevated Temperatures *Trans Amer Soc Steel Treat* (Jan 1933).

value of the stress required to produce a given rate of creep, dependent on the method of loading

In the type of test discussed in the present paper the method of loading is found to be of considerable importance in the lower temperature ranges. In the higher ranges we begin to approximate to the same end point, independent of the method of approach. In the preceding tests the specimens were loaded at room temperature and the temperature was raised in the manner described. The question as to whether a change in procedure produces any material change in results is answered by

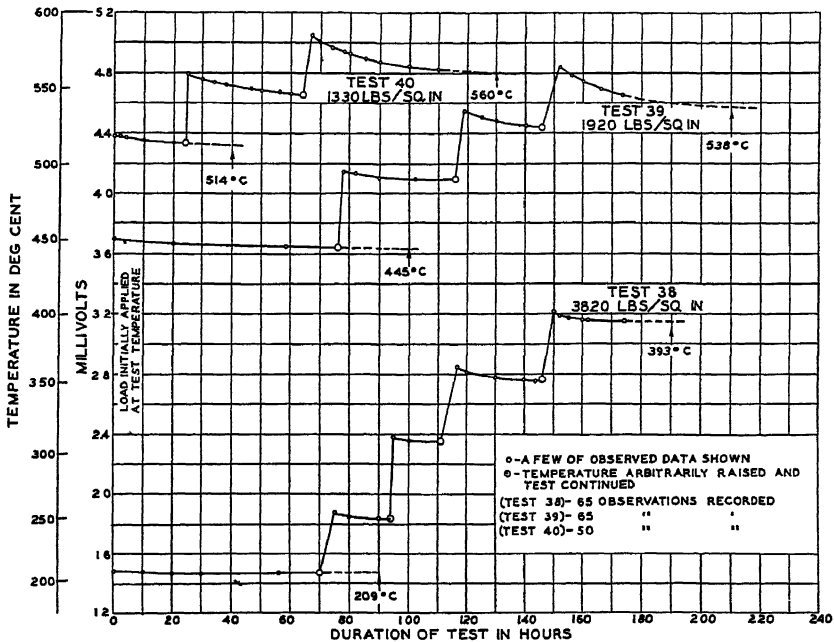


FIG 4—CREEP TESTS ON PURE IRON

reference to Fig 4, where the load was applied after reaching the minimum or first test temperature. Three test loads are considered, 3820, 1920 and 1330 lb per sq. in., all using pure iron as the test sample and hence carrying the temperature of experimentation over a fairly wide range.

The sample was heated to some predetermined temperature and loaded, and time-temperature records were taken from which to draw a segment of the "creep curve." The temperature was then arbitrarily raised some  $50^{\circ}\text{C}$ . with the load still on, and a creep curve again established. This was repeated four times for the high load.

Consider curve 38 (Fig. 4). Definite signs of creep were found between  $210^{\circ}$  and  $215^{\circ}\text{C}$  and the temperature fell  $1^{\circ}\text{C}$ . between the tenth and the thirtieth hour. The characteristic time-temperature curve is readily evident at successively increasing temperatures, and at the stage

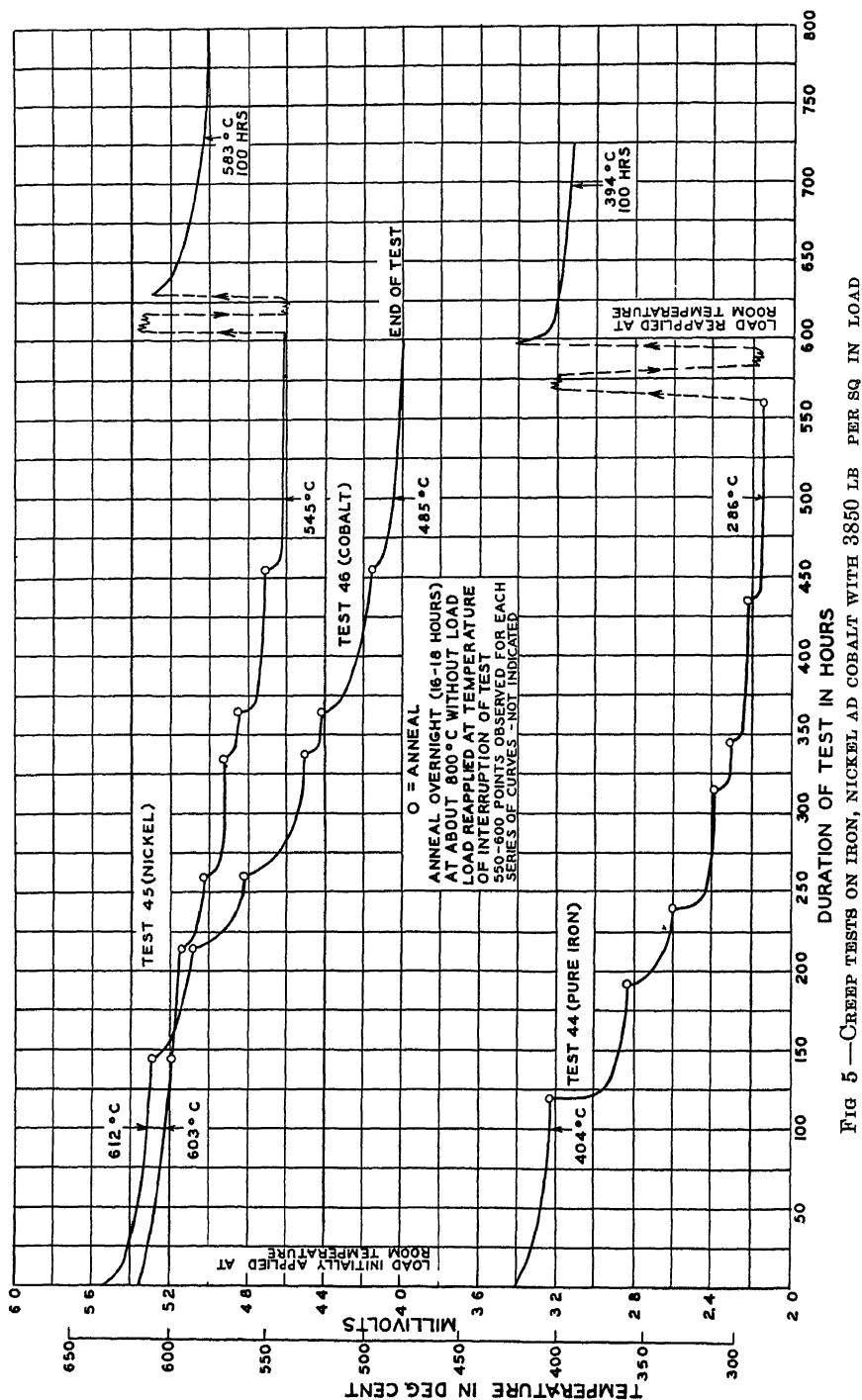


FIG 5—CREEP TESTS ON IRON, NICKEL AND COBALT WITH 3850 LB PER SQ IN LOAD

finally used a definite but small rate of creep is still found at about  $395^{\circ}\text{C}$ . Thus the time-temperature curve of pure iron for 3820 lb. per sq. in. load has been raised from  $210^{\circ}$  to  $395^{\circ}\text{C}$ , assuming equal rates of temperature change. In test 39, the similar limiting part of the creep curve has been raised from  $450^{\circ}$  to  $540^{\circ}\text{C}$  and in test 40, with only 1330 lb. per sq. in., from  $515^{\circ}$  to  $560^{\circ}\text{C}$ . The temperature differences give the values  $185^{\circ}$ ,  $95^{\circ}$  and  $45^{\circ}\text{C}$ ., respectively. Thus as the temperature increases this effect of the method of loading on the temperature to which the curves tend to become asymptotic becomes much less profound.

This interesting and important effect of creep strain is again revealed by a study of the data presented in Fig. 5. It is well known that strain induced in a metal tends to increase the resistance to creep of that metal. The profound effect of this creep strain on the creep resistance of the metal, however, is not so generally taken into account. Iron, nickel and cobalt were selected for the test under a load of 3850 lb per sq. inch.

The test rods were loaded at room temperature and raised to a temperature where creep was readily perceptible, in the manner just described. Consider test 44 on pure iron. The first part of the test shows a curve presumably asymptotic to a temperature coordinate between  $390^{\circ}$  and  $400^{\circ}\text{C}$ . After 122 hr. the load was removed, the temperature raised to  $800^{\circ}\text{C}$  and the test bar thus annealed overnight. The temperature was then restored to that existing at the time when the interruption occurred, the load reapplied, and the test continued. As soon as the rate of creep had again reached a low value, the test bar was again given the annealing treatment with the load reapplied at the second temperature of interruption. This was repeated until seven sections of the curve had been obtained.

Fig. 5 demonstrates that the temperature at which the curve was beginning to approximate a horizontal position has been dropped from  $400^{\circ}$  to  $285^{\circ}\text{C}$ . At this point the test bar was thoroughly annealed, cooled to room temperature and loaded and tested in the manner initially used. This final member of the curve gives a fair approximation to the initial member.

In test 46, with cobalt, the fall in temperature was from about  $610^{\circ}$  to  $480^{\circ}\text{C}$ . In nickel (test 45) the temperature fall was not so marked ( $600^{\circ}$  to  $545^{\circ}\text{C}$ .) and the final member of the curve suggested that the nickel was somewhat "weaker" at the end of the test than at the beginning.

#### DISCUSSION OF DATA ON PURE METALS

From the temperature-time data presented in Fig. 3 on iron, nickel, cobalt and silver, it appears that we have a useful means of comparing

the high-temperature strength of metals. All the data were obtained by similar experimental procedure and are therefore comparable.

It is considered that the important section of these creep curves, for purposes of comparison, is that where the curve begins to approximate to a position parallel to the abscissa (time). The importance of the time required to approach this condition is readily observed to be a factor dependent on temperature. Thus, the relationships established at the higher temperatures exhibit a pronounced slope (or relatively high rate of creep) even after 200 to 300 hr., while the low-temperature tests "flatten out" much more quickly. However, if the expansivity-temperature characteristics of the metals under test are approximately known and not subject to anomaly in a given temperature range under consideration, the slope of the curve provides a possible means for evaluating the rate of creep at this temperature.

Furthermore, in comparing a family of alloys or metals of similar characteristic properties, the coefficient of expansion is usually very similar, although this should be checked experimentally. The change in elastic modulus will probably follow a general similarity in the various alloys, but since the temperature ranges under consideration are usually small (a few degrees) the effect due to modulus change is practically negligible in most cases.

Under conditions of approximate similarity of temperature coefficient and modulus, the slopes of the time-temperature curves present a first approximation of relative rates of creep of the members of a group of metals, and these serve as a means of comparison, which is useful in exploratory work.

Another method that may be employed as a simple means of classification is to consider the system as one that approaches a definite limiting condition. This, of course, presupposes that rate of change of temperature of the test specimen, and therefore its creep rate, approaches zero and that a limiting temperature has been obtained below which the test sample cannot fall.

Whichever method is used, the metal is stated as being capable of holding a definite load within a limited temperature range. In Fig 6 data have been plotted derived from the temperature-time curves for iron, nickel and cobalt. These curves serve to provide a first approximation of the relationship between temperature and load-carrying capacity for the three metals. It will be recognized that the exact temperature location of these curves depends on the duration-of-test value at which the data were collected. However, the minor differences obtained on considering nickel and cobalt after 250 hr. instead of 150 hr. duration of test are readily evident from a study of this figure. Furthermore, while these metals have comparable resistance to creep at elevated temperatures, it is clear that the effect of temperature on creep resistance is

not identical. Comparable creep resistance in iron is found some 200° C below the temperature for nickel and cobalt at a given stress. It may be observed that as the temperature is increased the difference in strength decreases. This is to be anticipated, since the load-carrying capacity of all metals approximates to zero as the melting point is approached.

It seems of interest to analyze the slope of the time-temperature curves of iron, nickel and cobalt for various loads after some given period

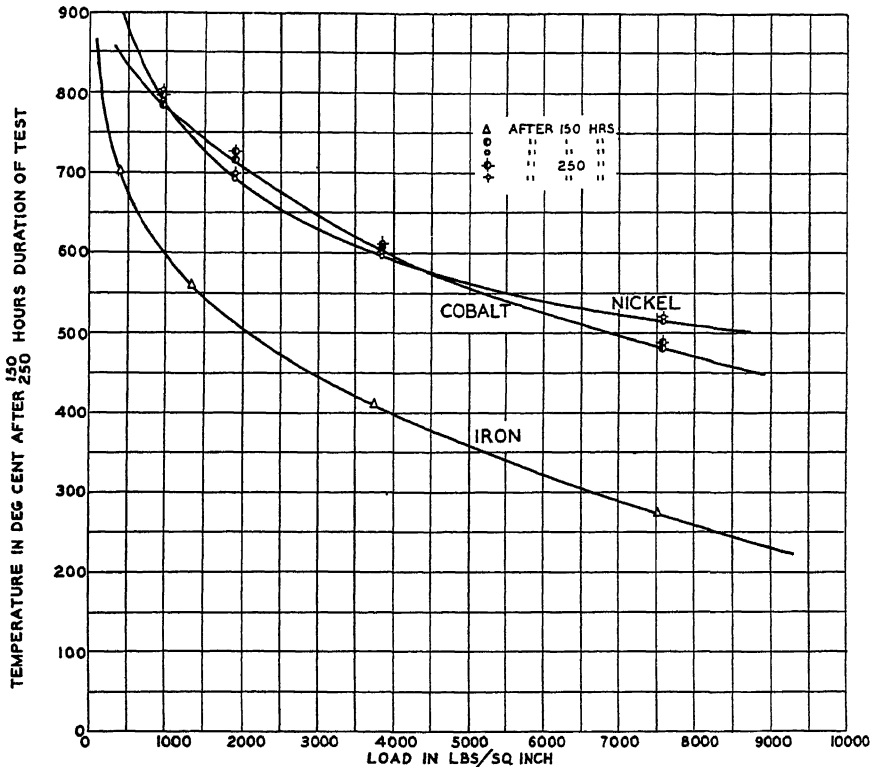


FIG 6—STRESS-TEMPERATURE RELATIONSHIP OF IRON AFTER 150 HR AND OF NICKEL AND COBALT AFTER 150 AND 250 HR. DURATION OF TEST

of test and to approximate these values in terms of creep. This has been done for each metal for each of four loads at a point on the time-temperature curve 144 hr. after start of test. A mean value of  $15.5 \times 10^{-6}$  was taken for the coefficient of expansion for iron and nickel between 300° to 700° C. and 500° to 800° C., respectively, and  $14.5 \times 10^{-6}$  for cobalt between 500° and 800° C. Instead of tabulating the data, a diagrammatic illustration is presented in Fig. 7.

If the exact relationship between stress, strain, and creep rates were known it would be possible to draw a graph showing the relationship between creep rate and temperature for constant stress. The data,



however, clearly indicate that such a relationship would show that the rate of creep increases much faster than the increase of temperature of test. This accords with general observations on effect of temperature on creep rate.

Finally, some consideration should be given to certain features of this method of testing metals at elevated temperatures brought out by a

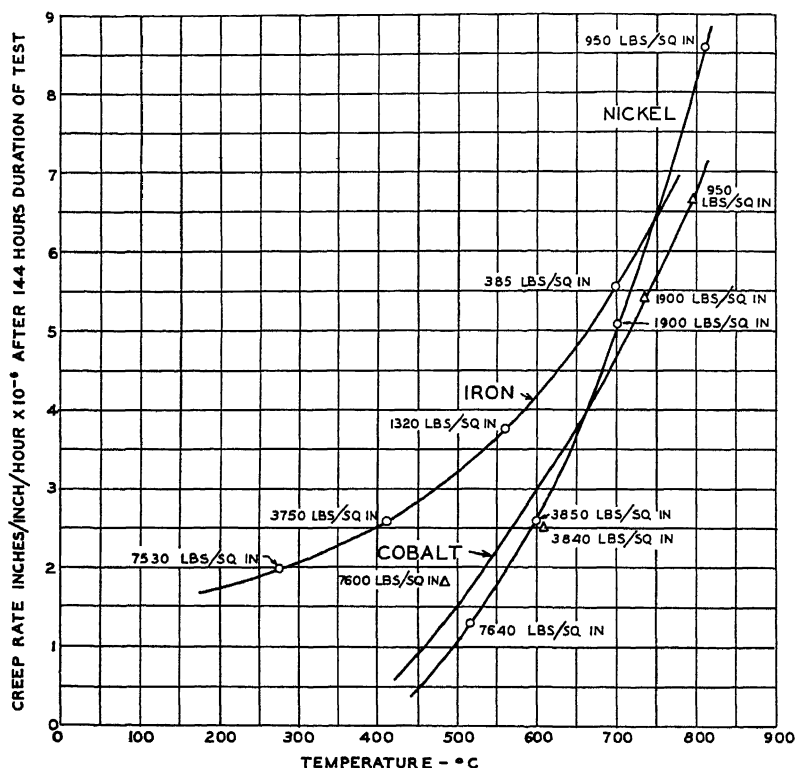


FIG 7 —RELATION BETWEEN TEMPERATURE, LOAD AND RATE OF CREEP AFTER 144 HR DURATION OF TEST FOR IRON, NICKEL AND COBALT.

study of Figs. 4 and 5. Much of the difficulty in coordinating test data on creep of metals is due to the fact that the material is constantly changing during the course of the test. In the examples already considered in the present paper, major structural changes are eliminated and we have to consider chiefly strain-hardening effects, which, naturally, are greater at temperatures below the recrystallization range.

Thus consider test 44, Fig. 5. The load was applied at room temperature after full anneal, and the six successive members of the curve obtained in the manner already described. It is important to note that the initial rate of creep in the last section of the curve at  $295^{\circ}\text{C}$ . was greater than that obtained in the first section at  $425^{\circ}\text{C}$ . This rapid

initial rate was reduced to a very small value, approximately  $0.04^{\circ}\text{C. per hour}$  ( $0.85 \times 10^{-6}$  in. per in. per hr.) in less than 10 hr. duration of test by an amount of strain-hardening corresponding to an  $8^{\circ}\text{C.}$  fall in temperature, or less than 0.0002 in. per in. elongation.

In test 38 (Fig. 4) the last branch of the curve suggests a limiting flow temperature of about  $390^{\circ}\text{C.}$  as compared with the initial one of  $205^{\circ}\text{C.}$  The rise in flow resistance for this metal is due to strain-hardening imposed on the metal during the 180 hr. duration of test.

An attempt was made to evaluate the amount of strain-hardening that raises the temperature of the load-carrying capacity of 3800 lb. per sq. in. for iron from  $210^{\circ}$  to  $390^{\circ}\text{C.}$  The records show that the total temperature fall in the five stages of the curve during creep approximates  $25^{\circ}\text{C.}$  We do not have any means of recording the elongation during the period of arbitrary rise in temperature (see Fig. 4). However, the total creep measured during the actual five stages of test gives us an elongation of only 0.000525 in. per inch.

With the load applied at room temperature and the temperature slowly raised to  $400^{\circ}\text{C.}$ , a result not very unlike that obtained in the last branch of the curve for test 38 would have been recorded. This suggestion is confirmed by the results given on tests 26, 27 and 28 in the authors' previous paper.<sup>6</sup> This point should be emphasized when one reverts to a consideration of the data presented in Fig. 3.

The analysis given here of tests 38 and 44 suggests that almost any result can be obtained, depending on the method of testing adopted. To a certain extent this is true in soft, annealed metals and it should be evident that in order to get strictly comparable temperature-time curves a given mode of test must be adopted throughout. The most logical method appeared to be that chosen for the data in Fig. 3 where the metal is loaded cold, and hence accepts all the strain-hardening that can occur during the period of increase of temperature prior to start of test.

At more elevated temperatures where approximation of the recrystallization range is begun, the magnitude of the effects of the methods of loading diminish (Fig. 4).

#### CREEP DATA ON COMMERCIAL ALLOYS

Since the previous thermal history of an alloy may be an important factor in determining the magnitude of its resistance to deformation, it was decided to conduct all creep tests on alloys in the following manner. The specimen was heated to  $950^{\circ}\text{C.}$  maintained for 1 hr., cooled in the furnace to  $800^{\circ}\text{C.}$ , loaded to the predetermined stress, and temperature readings taken every 2 hr. during the course of the test. A hydrogen atmosphere was maintained throughout.

---

<sup>6</sup> Reference of footnote 1, Fig. 9

The temperature-time curves for three different loads on 18-8 alloy and the chrome-silicon ferrous alloy are presented in Fig 8 The two-hourly recorded data on all tests are omitted for the sake of clearness

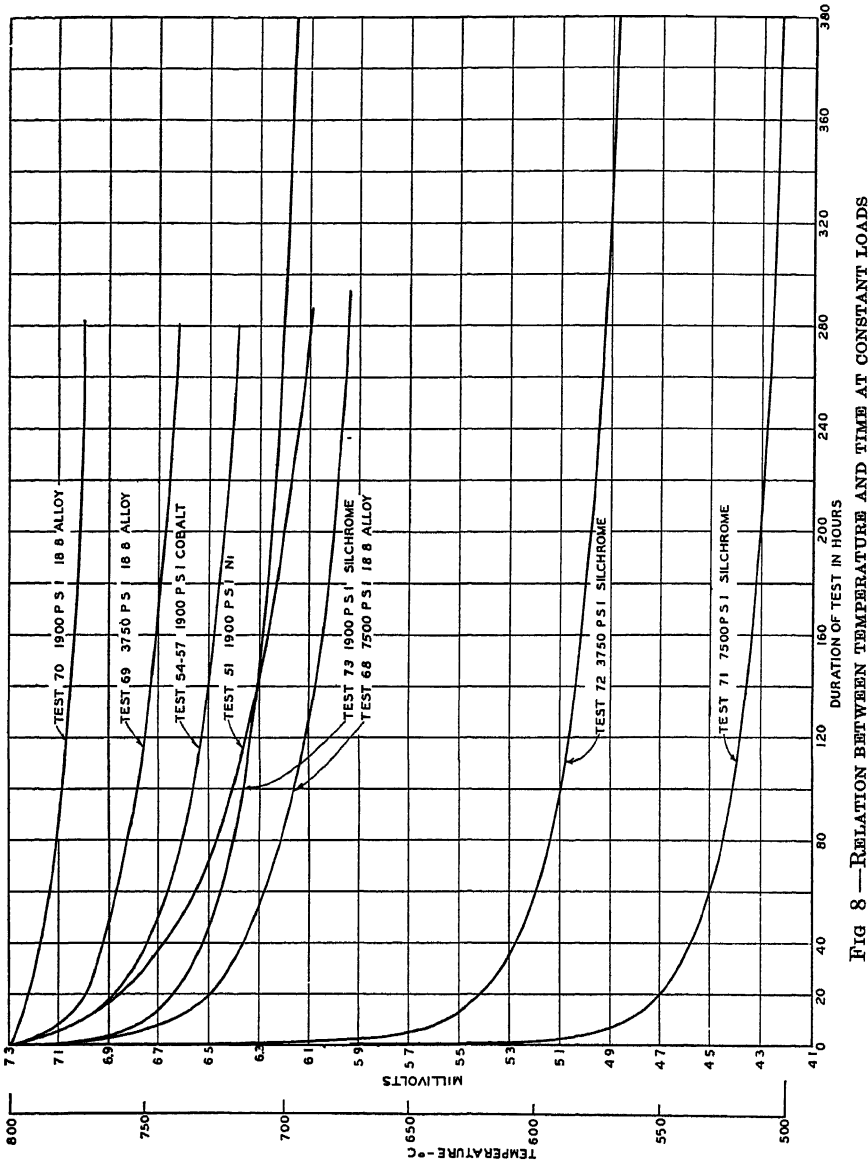


Fig 8 —RELATION BETWEEN TEMPERATURE AND TIME AT CONSTANT LOADS

Comparable tests on nickel and on cobalt (taken from Figs. 1 and 2) are also included in the diagram. The elementary metals were loaded at room temperature but since the tests considered were conducted from

800° C, it may be assumed that this second method of loading would give data comparable to that recorded for the other materials.

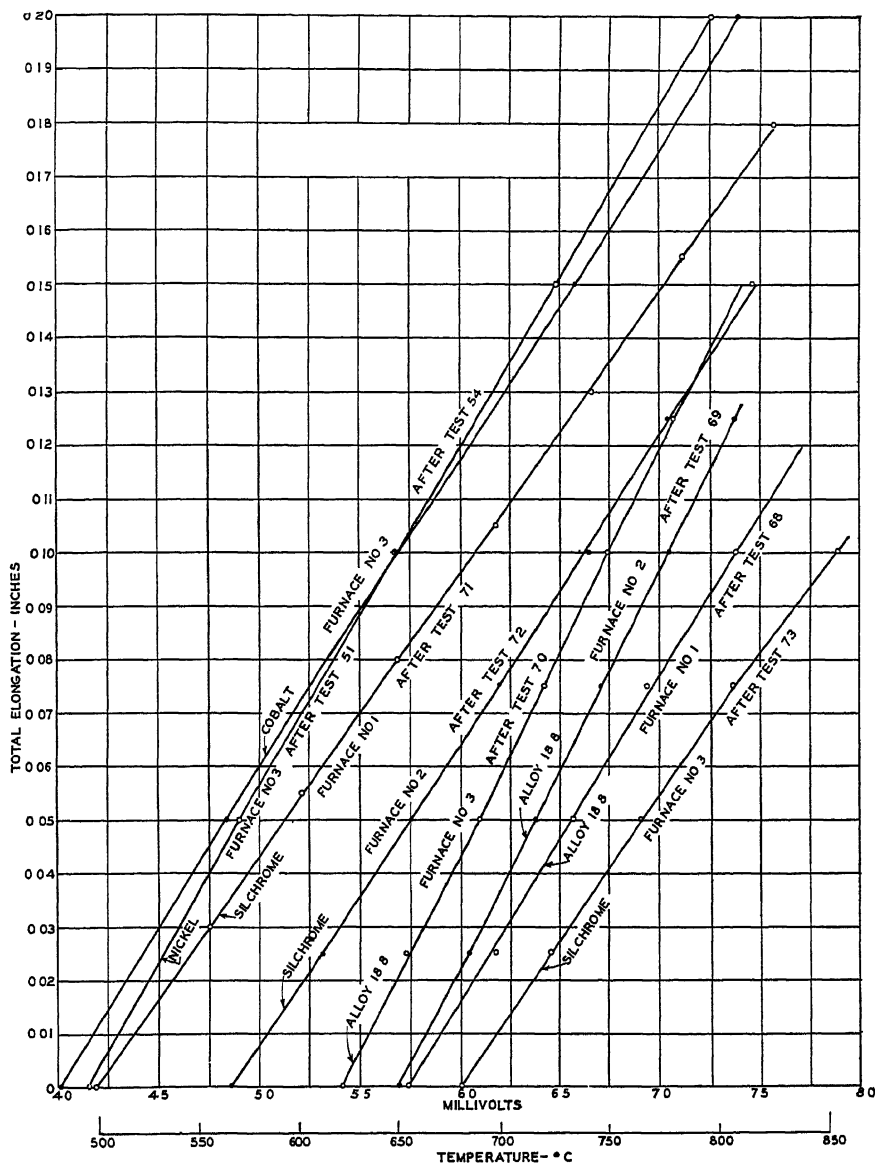


FIG 9—DILATION-TEMPERATURE RELATIONSHIPS OBTAINED IMMEDIATELY AFTER REMOVAL OF LOAD

A profound difference in creep resistance can be noticed between the 18-8 alloy and the chrome-silicon alloy. However, since these alloys are constitutionally quite different, it may be objected that these curves are not creep-time curves.

Means were devised (discussed in the Appendix) whereby the dilation-temperature relationships could be observed directly on a specimen in the furnace as set up for the time-temperature test. These experimentally determined relationships obtained immediately after removal of the load from the test indicated on the several curves are shown in Fig. 9. All tests were commenced at 800° C. (73 mv) and the decrease in length of any test bar, in the particular furnace used for the test, due to any given fall in temperature, can be read directly from the chart.

Thus, we obtain derived data for an elongation (creep) time chart by the following means. Consider test 68, which falls 1 mv (100° C.) in 55 hr. (Fig. 8). This fall in temperature corresponds to 0.062 in. (Fig. 9). In the test the actual length of the test bar remains constant, so that the change of temperature is, by way of the corresponding dilatation, a measure of creep.

The derived data for each of the eight tests have been plotted in Fig. 10, which shows flow-time curves. Each curve represents the change in amount of extension with time under constant load, but gradually decreasing temperature. The relatively low resistance to deformation of silchrome as compared to the stainless steel is as evident in these extension-time curves as it was in the temperature-time curves.

It is true, however, that although we present a series of flow-time relationships for constant stress, we are changing the temperature during the course of this test. In order to introduce this variable in the graphic data, it is only necessary to express deformation in terms of rate of extension and plot against temperature. Thus, the tangent to the total extension-time curves in Fig. 10 gives a measure of flow rate at any period in the test, which in turn establishes the temperature (Fig. 8).

The plotted data are presented in Fig. 11, where the ordinate expresses creep as a rate in inches per inch per hour, or as a percentage per 1000 hr. Temperature of test forms the abscissa.

Since it has been demonstrated that minute amounts of initial deformation have the most profound effect on rates of creep, brief reference must be made to the factor, so far as it affects the interpretation of the data in Fig. 11.

In pure iron it was shown (page 64) that strain-hardening of about 0.0002 in. per in. at 300° C. reduced the rate of change of creep to such an amount as to correspond with the end of the first stage of creep<sup>7</sup> in the conventional creep test. Furthermore, it is evident that comparisons of creep rates of metals must be made during the second stage of creep, but the magnitude of deformation per unit length prior to this is a factor of first importance when one attempts to design structures.

---

<sup>7</sup> A. E. White and C. L. Clark. Creep Characteristics of Metals at Elevated Temperatures. *Trans. Amer. Soc. Steel Treat.* (1932) 5.

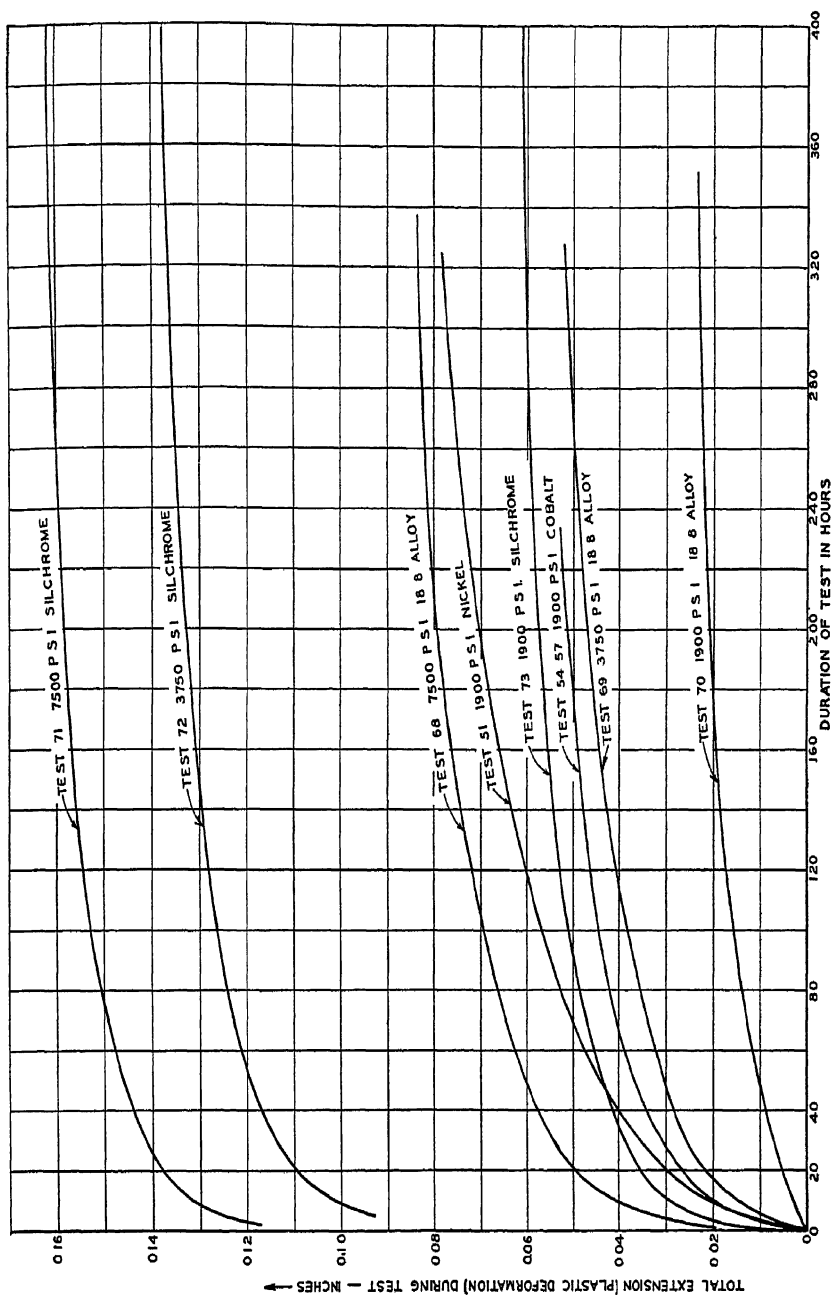


Fig 10 — Relation between extension and time at constant loads with failing temperature, derived from temperature-time curves (Fig 8) using dilatation-temperature relationships (Fig 9)

Thus, in Fig 11 it is considered that a satisfactory tentative rating of the metals shown is given when we consider the horizontal  $2 \times 10^{-6}$  in per in. per hr creep rate To each curve at this given creep rate has been appended the total deformation in inches per inch up to this stage

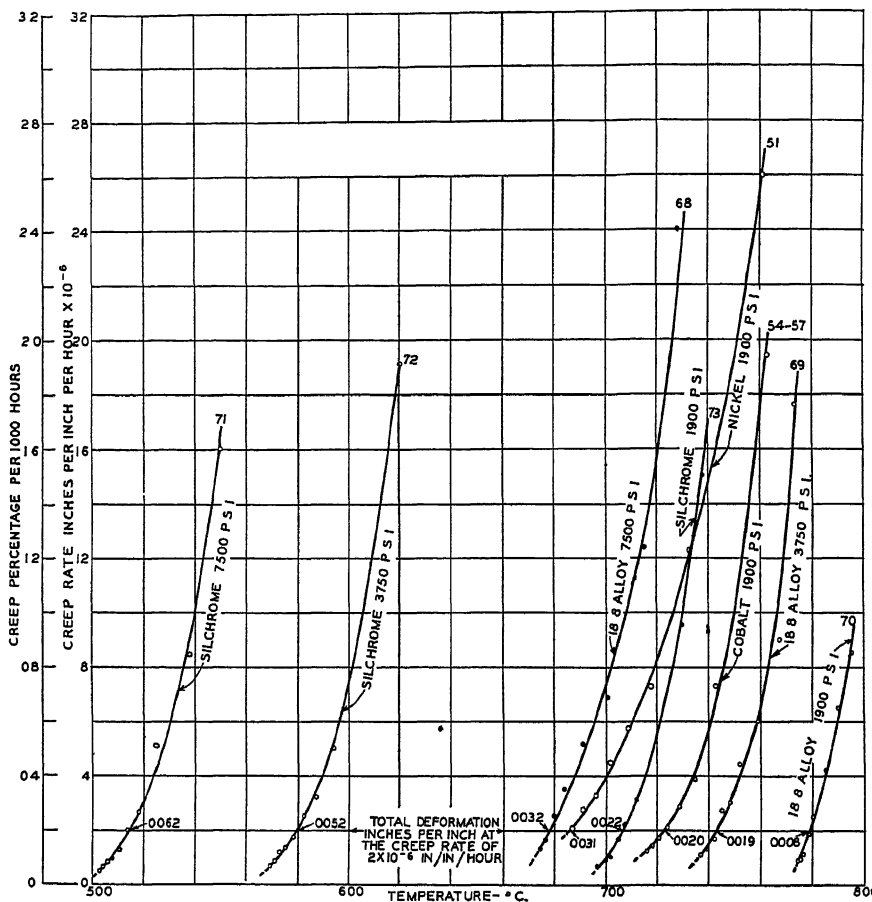


FIG 11 —RELATION BETWEEN CREEP RATE AND TEMPERATURE FOR CONSTANT LOADS  
CREEP RATES WERE DERIVED FROM CURVES OF FIG 10

of the test From the data cited and from an examination of data from conventional creep tests,<sup>8</sup> we believe that at this arbitrary rate of creep we have reached, by virtue of the initial deformations, a location comparable to the second stage of creep found in constant-temperature creep testing.

Thus, for instance from our creep-temperature curves, we see that under a load of 7500 lb per sq. in. comparable rates of creep are obtained

<sup>8</sup> P. G. McVetty: Working Stresses for High Temperature Service Amer. Soc. Mech. Engrs (1933)

for the silicon-chrome alloy and for the 18-8 alloy at 515° and 675° C. respectively

It should be emphasized that in analyzing the two alloys, no matter what portion of the creep rate-temperature curve is taken, the evaluations of the relative merits of the alloys as regards their high-temperature strength are essentially alike. Further, it may be anticipated that the characteristics of pure metals will differ from those of alloys, and this is readily evident in the curves.

In order to obtain a picture that will give a true criterion as a means of evaluation of high-temperature alloys we must observe.

1. The temperature at which the creep rate approximates to some constant value (say  $2 \times 10^{-6}$  in per in per hr) after the test specimen has accepted an initial plastic deformation safely above that likely to be observed in the first stage of creep. (Probably of the order of 0.001 in. per in. in the range of test considered.)

2. The slope or general trend of the creep rate-temperature curve below this arbitrary constant value of creep rate

In this discussion it must be remembered that we have compared the high-temperature properties of two commercial alloys within a limited temperature, in one specific state of heat treatment, with respect to their resistance to plastic deformation alone. If the temperature range were altered considerably the alloys might change the order of their rating. If resistance to various corroding media were considered, the problem would become much more complex.

### GENERAL CONCLUSIONS

1. Data have been presented on elementary metals and commercial alloys to illustrate how the temperature-time curves, obtained by means of a modified form of the Rohn test and resulting from plastic deformation, serve as a ready means of making comparisons of the creep characteristics of metals at elevated temperatures

2. A convenient means of classification has been discussed whereby an approximate relationship is expressed between load-carrying capacity and temperature for any given metal. A series of curves for iron, nickel and cobalt illustrate this method of sorting metals

3. The relationship between rate of creep and temperature with the four loads studied for iron, nickel and cobalt indicates that the rate of creep increases much faster than temperature. This accords with general observations on effect of temperature on creep rate.

4. The effects of minute amounts of plastic deformation on resistance to further creep have been studied. The importance of these effects on the modus operandi of test have been discussed, and it has been shown that they tend to assume minor importance in the higher temperature ranges.



5. In order to express the deformation-time data on the commercial alloys in terms readily understood by those associated with results obtained by the conventional constant-temperature method, the data have been expressed in a series of curves illustrating the relationship between creep rate and temperature of test for constant load. Variation in load is represented in the different curves. In discussing the evaluation of the high-temperature strengths of the alloys, the importance of initial amount of deformation on creep rate has been realized and taken into account.

6. The information and analysis of data presented in the paper appear to substantiate the contention that this modified Rohn method of testing provides a valuable means of studying the high-temperature properties of materials.

## APPENDIX

### 1. *Relative Length Effects of Furnaces on Test Rod Subject to Creep and to Dilatation and Modulus Changes*

In deducing the approximate creep rate for metals from temperature-time data in the paper it was stated that creep was effective over about 25 in. length of test while a mean value of 35 in. was subject to dilatation and modulus changes.

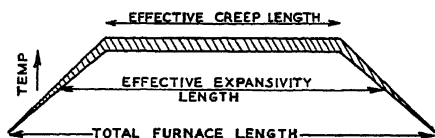


FIG 12 —GENERAL RELATION BETWEEN EFFECTIVE CREEP AND EXPANSIVITY LENGTHS

Assume temperature distribution as shown in Fig. 12. The effective expansivity gage length is 35 in. This gives a 1.4 ratio

for effective expansivity length to creep gage length. A careful study of the temperature gradient charts (previously published) will show that this ratio actually ranges from 1.41 for furnace 1 to 1.36 for furnace 3. A mean value of 1.4 is taken as representing all cases.

### 2. *Measurement of Dilatation Changes in the Test Rods*

The derivation of creep rates, from time-temperature curves, depends on the use of dilatation constants. It has been shown previously that the effect of change in elastic modulus, due to limited changes of temperature during test, is so low a percentage of that due to dilatation that for metals in the common range of temperature coefficients of expansion it can be neglected for the purpose of the present paper.

If the derived creep rates are to be reliable the basic dilatation data must be accurate.

In order to eliminate uncertainties as to the effective expansivity length, it was decided to devise means whereby the absolute total changes in the length of the test rod, between the top support and the control

mechanism below the furnace, could be measured directly. For this purpose, the screw contact attached to the lower end of the test bar, which permitted make or effected break of the heating circuit as the test rod expanded or contracted, was replaced by a micrometer contact.

Total dilatation data were obtained in the following manner. The contact was set to control the temperature below the minimum temperature of test for the given test bar in the given test furnace. When the temperature was steady the contact was raised say 0.010 in. and this permitted the temperature to rise to the constant value for that setting. Consecutive settings in this manner provided a relationship between length changes in test rod and temperature changes in the furnace.

In order to eliminate creep during this test the specimen was not loaded. To test the accuracy of the data the micrometer contact was finally screwed down an amount equal to the sum total of the increments used in the reverse operation.

Theoretically this resulted in the furnace falling to and being controlled at the starting temperature. Experimentally some hysteresis was noted, but it was only of the order of 2 or 3 per cent.

## DISCUSSION

*(L. S. Reid presiding)*

W. M. PEIRCE,\* Palmerton, Pa.—Metallurgists dealing with zinc are much interested in the subject of creep, because at much lower temperatures than those discussed in this paper creep is encountered. If we approach the study from a slightly different angle and make our tests by applying a definite load at a carefully maintained constant temperature, we find that the rate of elongation changes rapidly for a considerable period of time and then becomes constant. If we then plot these constant rates of elongation determined for a series of loads at this one constant temperature, we obtain a secondary curve from which, if it is carried out far enough, we can estimate the maximum load that the metal under test will sustain indefinitely without creep. In some cases at least that must be the ultimate aim of creep testing.

The point I wish to bring out in connection with this paper is that for zinc the time required to establish this constant rate of elongation for a fixed load and a fixed temperature is much greater than the periods of loading reported in this paper by Austin and Gier.

Have individual tests, not shown in the illustrations, been carried out for much longer periods than those described, to establish definitely the constant temperature? That is, have those tests been carried out to establish that the test period is long enough?

There is one other point, also. For zinc we have a somewhat more complicated situation with respect to the effect of deformation on the structure than is the case in a metal of the cubic system, because in zinc deformation is more likely to develop a preferred orientation in the structure. That preferred orientation, we know, can have quite a definite effect on the resistance to creep on a given axis of a test specimen. I wonder whether the authors of this paper have encountered any similar effect in the cubic metals.

---

\* Chief, Metal Research Division, New Jersey Zinc Co.

C R AUSTIN (written discussion) —There is always a certain amount of deformation necessary before much resistance to creep is developed, but the amount is dependent on the metal tested. This is well brought out in comparison between pure iron and one of the commercial alloys discussed in the paper. It is suggested that in using this temperature-decrement method we can reduce in point of time what has been called the first stage of creep. This stage is apparently necessarily long in the conventional type of creep testing, and is merely a question of the time taken while the metal is accepting deformation up to the point where is reached the constant creep rate condition indicated in the second stage.

So long as the temperature changes are not great, it is possible satisfactorily to induce this first stage of creep to occur rapidly and hence permit reaching the second stage at a much greater rate.

As regards the maximum length of time used in conducting the tests, it is true that most of the tests have been carried for periods of 200 to 250 hr where they were used more particularly for the purpose of sorting alloys, and finding out alloys that were considered worthy of further consideration by use of the conventional creep test. However, we have run a few tests up to a total period of 600 hr and found that the curves flatten out progressively. We have not arrived at the stage where a truly horizontal position obtains. As the test continues a progressively slower rate of creep is noted and the curve tends to assume a horizontal position. In the type of test under consideration it is, of course, theoretically impossible to obtain a "constant rate of creep" on account of the falling temperature.

Mr Peirce also makes reference to preferred orientation. This is certainly a matter of importance but it seems that the amount of deformation accepted by metals put into service or examined for true creep by any experimental method is so small that we do not nearly reach deformation magnitudes that can be correlated with preferred orientation. If the metal has been subject to fabrication methods that produce preferred orientation prior to test, there is little doubt that it will have a definite effect on the resistance to creep no matter what the crystallographic system to which the metal or alloy belongs, although we do not have data to substantiate this contention.

## Intermetallic Solid Solutions

By ERIC R. JETTE,\* NEW YORK, N. Y.

(New York Meeting, October, 1934)

IN thermodynamic studies of gas mixtures and liquid solutions, the respective problems have been greatly simplified by the use of two general limiting laws, Dalton's law of partial pressures and Raoult's law. It is generally recognized that these two laws have a common physical and chemical basis which may be stated as follows: The law may be expected to be strictly valid only for systems in which the different molecular species are so nearly the same in their physical and chemical properties that a molecule is unable to recognize whether its neighbor is one of its own kind or not. Positive and negative deviations from both laws are frequently encountered. The occurrence of negative deviations in both gases and liquids is ascribed to attractive forces which, in the more extreme cases, may be so large in magnitude and so highly specific in character as to lead to the formation of definite chemical compounds. Positive deviations in gases develop only at higher pressures where the intermolecular distances are so decreased that factors such as molecular size and shape, which ultimately become concerned with the repulsive forces, come into play.

In liquid mixtures, positive deviations are generally considered as due to differences in the symmetrical (nonpolar) fields of force which surround the various molecular species and which are supposed to give rise to a tendency for each species to associate with its own kind and thus to "squeeze out" the other variety. Fundamentally this also involves the existence of repulsive forces between unlike molecules. If the fields of force are unsymmetrical (polar) a tendency towards compound formation results. Stated in more exact terms, strict adherence to the law means that the "activity" (or any adequate measure of this quantity) of a component in a mixture is a linear function of the molecular (or atomic) fraction of that component between the mol fraction limits 0 and 1. A positive deviation means that the activity is greater than corresponds to the law; a negative deviation that the activity is less. The deviations from Raoult's law have been fully discussed by many writers<sup>1</sup>

---

Manuscript received at the office of the Institute May 7, 1934.

\* Associate Professor of Metallurgy, School of Mines, Columbia University

<sup>1</sup> J. Hildebrand, Solubility, New York, 1924; Chem. Cat. Co.

A. Eucken, E. R. Jette and V. K. LaMer, Fundamentals of Physical Chemistry, New York, 1925; McGraw-Hill Book Co.

on solubility so that further consideration of this point will be unnecessary.

Raoult's law is sufficiently general in nature for us to expect that it will hold for solid as well as liquid solutions. Likewise, we may expect that both types of deviation will be found in the solid solutions. Unfortunately, however, direct test of this law requires experimental determination of the thermodynamic activity or some direct measure of this quantity. This type of measurement is extremely difficult to perform on solid solutions and particularly the solid solutions encountered in intermetallic systems. The most promising method seems to be the measurement of the electromotive force of cells in which one electrode is an alloy and the other one of the two pure components. These measurements must be carried out at temperatures high enough so that diffusional processes operate at rates great enough to maintain the alloy electrode surface in equilibrium with the interior of the electrode. Successful applications of this method have recently been made by Olander<sup>2</sup> and by Wachter.<sup>3</sup> Some of the latter's results will be discussed later.

The experimental difficulties involved in the application of thermodynamic methods has led the writer to consider the results of another field of investigation—X-ray crystal structure analysis—in the effort to obtain evidence as to the type of deviation from Raoult's law shown by solid solutions. For solid solutions, Vegard<sup>4</sup> has proposed an "additivity law" which states that for two elements possessing the same crystal structure and forming a complete series of solid solutions, the lattice constants of the alloys are a linear function of the atomic composition. It follows as a corollary that when this law holds the average atomic radius in the solid solution must also be a linear function of the atomic composition; therefore, when the crystal structure and the atomic radii of the two elements are known the lattice constants of the binary alloys can be calculated simply from the chemical analysis.

The lattice constants may, of course, readily be converted to lattice volumes. Since the number of atoms in the unit lattice is known from the structure and the average weights of these atoms can be found from the composition, the density or specific volumes of the alloys may be obtained. We could, therefore, base the discussion on either of these quantities if we wished and thus obtain a direct comparison with the more extensive work on liquid solutions. However, it seems preferable to use the directly measured lattice constant or the geometrically related quantity, one-half the distance of closest approach of atoms. For the

---

<sup>2</sup> A. Olander: *Jnl. Amer. Chem. Soc.* (1931) **53**, 3577, *ibid* (1932) **54**, 3819; *Ztsch. phys. Chem.* (1933) **163A**, 107

<sup>3</sup> A. Wachter: *Jnl. Amer. Chem. Soc.* (1932) **54**, 4609

<sup>4</sup> L. Vegard: *Ztsch. physik* (1921) **5**, 17.

sake of brevity the latter will be called the effective atomic radius. Either of these quantities leads in a somewhat more direct fashion to the interpretations that follow. In view of the relation between lattice constants and densities, the range of material used for this investigation could have been extended somewhat by consulting the ordinary density data on intermetallic alloys. This was not done for two reasons: (1) The density obtained from accurate lattice constant measurements is generally conceded to approach more closely to the "true density" than densities from other methods; (2) the care with which alloys must be prepared for X-ray investigation lends confidence to the results obtained.

The additivity law is expressed by the equation:

$$a = a_A F_A + a_B F_B \quad [1]$$

where  $a_A$  and  $a_B$  are the lattice constants of elements  $A$  and  $B$  and  $F$  denotes atomic fractions. For a face-centered cube it is also possible to write:

$$a = \frac{4}{\sqrt{2}}(r_A F_A + r_B F_B) \quad [2]$$

where  $r$  is the atomic radius, there are corresponding relations for other structures. If, however, the elements  $A$  and  $B$  have different structures, it is permissible only in certain special cases to use the values of the radii calculated from the lattice constants in pure metals. The new factor that enters here is the influence of the coordination number on the effective radius of an element. This will be discussed in detail later in this article.

It seems obvious that the physical and chemical requirements that must be satisfied if the additivity law is to be fulfilled are identical with those of Raoult's law. This statement contains the major premise for what follows. If there is any tendency towards compound formation, the observed lattice constants will be less than those calculated from the additivity law. Thus negative deviations from the additivity law correspond directly to the negative deviations from Raoult's law. Positive deviations from the additivity law refer back to the more fundamental concept of repulsive forces existing between unlike atoms rather than its corollary the association of like atoms. This arises from the physical structure of the substitutional type of solid solution, the only type to be considered in this article.

Experimental proof of deviations from the additivity law demands a high order of accuracy in the determination of the lattice constants. This is particularly true in the case of positive deviations, which are small in nearly all cases. Experimental results of the requisite accuracy have fortunately been made available in researches from a number of laboratories during the last few years. With very few exceptions work prior to 1930 could not be used in this connection.

Westgren and Almin<sup>5</sup> have discussed the application of the additivity law to several intermetallic systems where compound formation occurs. It was shown that the volume per atom for intermetallic compounds was less than that calculated from the volume per atom of the pure constituents. The curves presented by these authors also give ample proof that when terminal solid solutions occur in systems with intermediate compounds, the volume per atom in the solid solutions is less than would be calculated from the additivity law. The same will be true for the lattice constant. The effect of compound formation in causing negative deviations from the additivity law may be considered as thoroughly established.

In connection with these negative deviations the question inevitably arises as to whether the "solute" is a compound or is atomically dispersed in the same way as ideal solutions. This question cannot be answered without first having an adequate conception of what characterizes a "compound" in solution, and, in particular, an intermetallic "compound" in solid solution. It does not seem possible to attain such a conception at the present. For terminal solid solutions it is not difficult to imagine "compounds" of a loose indefinite sort similar to the ion aggregates in aqueous solutions of electrolytes or "solvated" ions and molecules. Again in the terminal solid solutions it is easy to conceive of a sort of "coordinative compound" in which, however, the "coordination number" is not a characteristic property of the solute atom but is determined solely by the type of lattice in which the solute atom finds itself; i.e., 12 if in a face-centered cube, 4 if in a diamond structure, etc. But it is somewhat difficult to understand how or why there should be a sufficiently specific relation between a solute atom in, for example, a face-centered cubic lattice and one of its 12 neighbors to lead to postulating the compound  $AB$ , or for two of its neighbors to correspond to  $A_2B$ , etc. The idea of a solution of one intermetallic compound in another, such as  $AB$  in  $A_2B_3$  or  $A_2B_3$  in  $A_3B_4$ , seems even less satisfactory. These considerations apply to the substitutional type of solid solution and probably to the subtraction type.<sup>6</sup> For the interstitial type the idea of compounds in solid solution may be of greater applicability but a discussion of this point is beyond the scope of the present paper. Finally, there is no experimental evidence of a structural nature, which has come to the writer's attention, to support the idea of molecules existing as solutes in solid solutions of the substitutional types.<sup>7</sup>

---

<sup>5</sup> A. Westgren and A. Almin *Ztsch. phys. Chem.* (1929) **5B**, 14.

<sup>6</sup> G. Hagg. *Nature* (1933) **131**, 167; E. R. Jette and F. Foote *Jnl. Chem. Phys.* (1933) **1**, 29.

<sup>7</sup> The work of R. T. Phelps and W. P. Davey [*Trans. A.I.M.E.* (1932) **99**, 234] on the Ag-Al alloys, which was interpreted to mean that the compound  $Ag_2Al$  dissolved in silver, has been disproved by C. H. Barrett [*Metals & Alloys* (1933) **4**, 63].

# SYSTEMS IN WHICH BOTH ELEMENTS HAVE THE SAME STRUCTURE AND COMPOUNDS DO NOT OCCUR

In the special cases to be considered under this heading, the coordination factor is not involved. In several cases, however, superstructures are found in alloys annealed and quenched from sufficiently low temperatures. The influence of this phenomenon will be discussed in another section.

There are several examples of negative deviations from the additivity law in systems forming complete series of solid solutions. Wachter<sup>8</sup> has already called attention to the similarity in the behavior of the thermodynamic activity of silver or gold in the binary alloys of these two elements and the lattice constants of these alloys as a function of the atomic composition.<sup>9</sup> A direct comparison is given by Fig. 1. Wachter considers that his measurements are compatible with the existence of an "ordered" arrangement of the gold and silver atoms at 50 atomic percent. X-ray evidence of a superstructure in these alloys has not yet been reported. Other binary systems with complete series of solid solutions which likewise show negative deviations from the additivity law are Ag-Pt,<sup>10</sup> Ag-Pd,<sup>11</sup> and Cu-Ni.<sup>12</sup>

Several systems that obey the additivity law over the entire range of compositions are Au-Pt,<sup>13</sup> Au-Pd,<sup>14</sup> Mo-W,<sup>15</sup> Pt-Ir,<sup>16</sup> Pt-Rh,<sup>16</sup> Pb-βTi<sup>17</sup> and Sb-Bi.<sup>18</sup> For the last example the available experimental material is not of as great accuracy as for the others. The experimental difficulties are much greater since Sb and Bi are rhombohedral and the results on the Bi end of the series are none too satisfactory.

N. Ageew and D. Shoyket [Inst. of Metals, Adv. copy No. 636 (1933)] and by unpublished results obtained in the present writer's laboratory. The negative results of G. Wassermann [*Ztsch. Metallkunde* (1930) **22**, 158] in trying to prove the existence of the compound  $MgZn_2$  dissolved as molecules in aluminum may also be mentioned.

<sup>8</sup> Reference of footnote 3.

<sup>9</sup> G. Sachs and J. Weerts. *Ztsch. Physik* (1930) **60**, 481.

<sup>10</sup> C. H. Johansson and J. O. Linde. *Ann. Physik* (1930) **6**, 458.

<sup>11</sup> F. Kruger and G. Gehn. *Ann. Physik* (1933) **16**, 190, also W. Stenzel and J. Weerts. Siebert *Festschr.* (1931) 288 quoted by J. Weerts. *Ztsch. Metallkunde* (1932) **24**, 138.

<sup>12</sup> W. G. Burgers and J. C. M. Basart. *Ztsch. Krist.* (1930) **75**, 155.

<sup>13</sup> C. H. Johansson and J. O. Linde. *Ann. Physik* (1930) **5**, 762, also Stenzel and Weerts. reference of footnote 11.

<sup>14</sup> W. Stenzel and J. Weerts. reference of footnote 11.

<sup>15</sup> E. Van Arkel. *Ztsch. Krist.* (1928) **67**, 235.

<sup>16</sup> J. Weerts and F. Beck. Quoted by J. Weerts, *Ztsch. Metallkunde* (1932) **24**,

138.

<sup>17</sup> E. McMillan and L. Pauling. *Jnl. Amer. Chem. Soc.* (1927) **46**, 666.

<sup>18</sup> E. G. Bowen and W. M. Jones. *Phil. Mag.* (1930) **13**, 1029.

W. F. Ehret and M. B. Abramson. *Jnl. Amer. Chem. Soc.* (1934) **56**, 385.



Positive deviations are to be found in the systems Cu-Au,<sup>19</sup> and Cu-Pd,<sup>20</sup> in the Ag-Cu<sup>21</sup> system at both ends (broken series) and at the Fe end of the Fe-Cr<sup>22</sup> system.

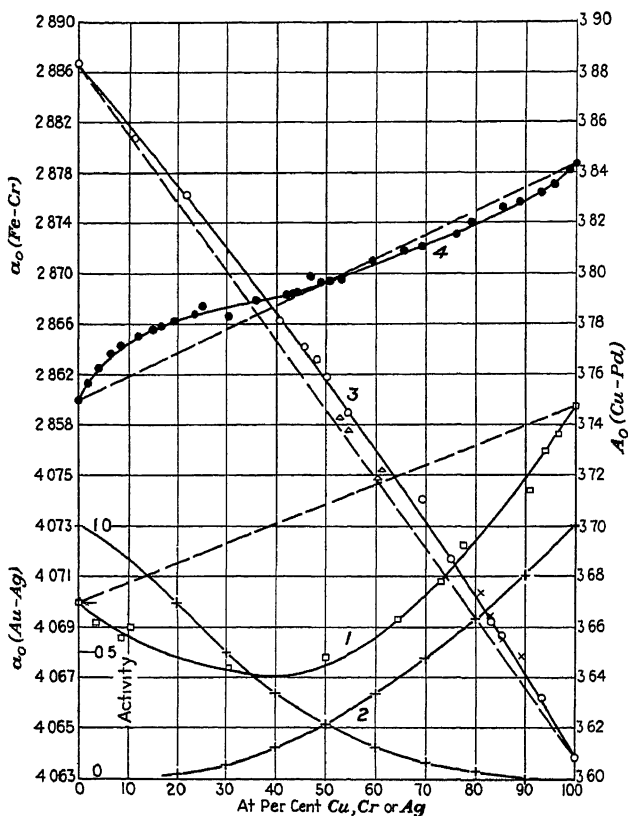


FIG. 1 — COMPARISON OF NEGATIVE DEVIATIONS FROM ADDITIVITY LAW

1.  $\square$  Au-Ag lattice constants (Sachs and Weerts)
2.  $+$  Activity curves for Au-Ag solid solutions at 200° (Wachter)
3.  $\circ$  Lattice constants of Cu-Pd solid solutions (Linde).
- $\triangle$  Lattice constants in body-centered cubic superstructure multiplied by  $\sqrt[3]{2}$ .
- $\times$  Lattice constants in face-centered cubic superstructures.
4.  $\bullet$  Lattice constants in Fe-Cr solid solutions.

The writer has not as yet been able to discern any physical quantity associated with the elements involved in these alloy systems that makes it

<sup>19</sup> E. Van Arkel and J C M Basart: *Ztsch Krist* (1928) **68**, 475.

<sup>20</sup> J. O Linde. *Ann Physik* (1932) **15**, 249 The earlier and less accurate results by S Holgersson and E Sedstrom [*Ann. Physik* (1923) **75**, 143] did not show this positive deviation

<sup>21</sup> N. Ageew, M Hansen and G. Sachs: *Ztsch Physik* (1930) **66**, 350, H. S. Megaw: *Phil Mag* (1932) **14**, 130.

<sup>22</sup> G. D. Preston: *Phil. Mag* (1932) **13**, 319.

possible to predict whether the deviations from the additivity law will be positive, negative or zero

### THE COORDINATION FACTOR

As already mentioned, besides the chemical differences between the atomic species, which lead towards compound formation, and physical differences, such as atomic size and shape, there is a third important factor peculiar to solid solutions; namely, difference in coordination number. This last factor has been discussed by Goldschmidt, Perlitz, Neuberger and others, and a review of this literature, much of which is difficult of access, has been given by Neuberger<sup>23</sup>. The factor is involved in the following way. An atom of a metal that crystallizes as a body-centered cube (W,  $\alpha$ Fe, etc.) is surrounded by eight equidistant atoms. The remaining atoms are at appreciably greater distances. In an element crystallizing as a face-centered cube each atom has 12 equidistant neighbors. In the diamond structure each atom has four equidistant neighbors, etc. The coordination numbers of the atoms in these three cases are respectively 8, 12 and 4. There is now available abundant evidence demonstrating the correctness of Goldschmidt's rule that the greater the coordination number the greater the effective radius of the atom or ion. In dealing with solid elements the atomic diameter is taken simply as the distance of closest approach. In binary or higher order compounds it will be evident that a certain amount of ambiguity will be involved in this method of obtaining atomic or ionic radii, as the case may be. However, based upon investigations on the optical properties of certain ionic crystals by Wasastjerna, a wide compilation and systematization of crystal-structure data by Goldschmidt and his co-workers, and certain theoretical investigations by Pauling<sup>24</sup>, there is now available a considerable body of data as to ionic sizes and interionic distances. The tables of ionic sizes have at least a fairly high order of consistency. For intermetallic compounds this is much less true. For either ionic or intermetallic compounds, however, these data<sup>25</sup> are of sufficient accuracy to permit some of the possible crystal structures of compounds to be eliminated with a high degree of assurance.

The determination of the change in atomic or ionic radius, particularly the former, offers a number of difficulties. Since ionic sizes are not involved in the systems dealt with in this paper the following discussion will be limited to atomic sizes in intermetallic systems.

---

<sup>23</sup> M. C. Neuberger: Ahrens Sammlung chem u chem tech. Vortrage Neue Folge 17 (1932-33)

<sup>24</sup> See Neuberger: Reference of footnote 23

<sup>25</sup> M. L. Huggins [*Chem. Rev* (1932) 10, 427] gives a summary.

Perltz<sup>26</sup> has summarized the results for intermetallic systems in which there are changes in structure from hexagonal close-packed to face-centered cube and of face-centered cube to body-centered cube. Perltz used mainly lattice constants for allotropic forms of an element, and for alloys the lattice constants for two different structures representing two phases in equilibrium. In this way it was found that in the change from close-packed hexagonal to face-centered cube, in both of which the coordination number is 12, the average change in interatomic distance for a

TABLE 1.—Calculations of Percentage Change in Radius

Structural Change		Change in Coordination No	R = $\frac{\text{radius in higher coordination}}{\text{radius in lower coordination}}$		
			Theoretical	Observed from Allotropic Change <sup>a</sup>	Mean <sup>b</sup>
Hex c p → f c cube	$\frac{c}{a} = 1.633$	12 → 12	1.000	1.0032 Co, 1.000 Ce, 1.0058 Ti, 0.9948 Ni	1.00
B c cube → hex c p		8 → 12	1.0287	1.088(?) Cr, 1.015 Zr	1.03(G)
B c cube → f c cube		8 → 12	1.0287	1.0162 Fe	1.025(P)
B c tetrag → f c cube	$\frac{c}{a} = 0.516$	6 → 12	1.099		1.04(G)
Simple cube → f c cube		6 → 12	1.123		
Diamond → f c cube		4 → 12	1.296		1.14(G)
Diamond → b c cube		4 → 8	1.260		
Diamond → b c tetrag.	$\frac{c}{a} = 0.516$	4 → 6	1.180		1.07(G)
Diamond → b c tetrag	$\frac{c}{a} = 0.537$	4 → 6	1.163	1.077 Sn	
Graphite → diamond	$\frac{c}{a} = 2.76$	3 → 4	1.263	1.083 C	

<sup>a</sup> Using radii calculated by M. C. Neuberger *Zisch Krist* (1933) **86**, 395

<sup>b</sup> (G) V. M. Goldschmidt *Zisch phys Chem* (1928) **133**, 397, recalculated to present basis

(P) H. Perltz *Acta et Comm Univ Tartuensis (Dorpatensis)* (1931) A, [4] 22

number of cases was practically zero. For the change from face-centered to body-centered cubic where the respective coordination numbers are 12 and 8, the interatomic distance decreased on the average 2.25 per cent. Goldschmidt made similar calculations for these and other changes prior to Perltz. The deviations from the average values were considerable and this fact has some significance. The forces operating between unlike atoms are not the same in solid solutions as in intermetallic compounds, nor when the same elements are in different compounds, even when the two compounds are phases in equilibrium with each other. The changes in radii with coordination number calculated in this way are not independent of chemical factors.

Another method of approach depends upon the assumption that when an atom normally possessing a certain coordination number enters into a

<sup>26</sup> H. Perltz. *Acta et Comm Univ Tartuensis (Dorpatensis)* (1931) A, [4] 22.

compound or a solid solution where its coordination number is different, the change in its effective radius is such that the volume per atom remains constant. On this basis it is possible to calculate by purely geometrical methods what the percentage change in the radius will be. Such a calculation has been made by Westgren and Almin<sup>27</sup> for the transformation from face-centered to body-centered cubic. Table 1 gives the results of a number of such calculations in terms of the ratio of the radius in the higher coordination to that in the lower. Included in this table are results observed for allotropic changes, and the mean values obtained by Goldschmidt (G) and by Perlitz (P) using data on solid solutions and intermetallic compounds. Consideration of the wide differences between observed and calculated ratios, of the large deviations in the quantitative values from the averages even in the simplest types of structure change<sup>28</sup> and of the fact that this assumption implies that there is no change of volume in an allotropic transformation, leads to the conclusion that the assumption of constant volume per atom in coordination changes is of distinctly limited usefulness in intermetallic systems.

#### SYSTEMS IN WHICH THE ELEMENTS CRYSTALLIZE IN DIFFERENT STRUCTURES BUT NO COMPOUNDS ARE FORMED

Very few systems that fall into this classification have been studied with sufficient accuracy to permit conclusions to be drawn. Fig. 2 shows the observed and calculated lattice constants for the gold-rich phase of the Au-Fe alloys<sup>29</sup>. It is quite clear that there is a definite positive deviation even when the radius of the iron atom is corrected for the change in coordination of 8 to 12 by means of the theoretical factor of Table 1. The nickel-rich solid solutions of the Ni-Cr system<sup>30</sup> also show a positive deviation from the curve when the radius is similarly corrected for coordination change which is definitely beyond the experimental error, although not necessarily beyond the range of uncertainty in the correction factor. At the chromium end of the same system, the curve corresponds to the ideal within experimental error when the nickel radius is decreased to correspond to a coordination number of 8. The atomic radii of these two elements are almost identical; that is,  $r_{\text{Ni}} = 1.2425$ ,  $r_{\text{Cr}} = 1.2465$ . The observed changes in the lattice constants in these solid solutions is almost entirely due to the influence of the coordination factor.

---

<sup>27</sup> Reference of footnote 5

<sup>28</sup> See Perlitz: Reference of footnote 26

<sup>29</sup> E. R. Jette, W. L. Bruner and F. Foote: Page 354, this volume

<sup>30</sup> E. R. Jette, V. H. Nordstrom, B. Queneau and F. Foote. Page 361, this volume

The Cu-Mn<sup>31</sup> alloys show an enormous positive deviation, which is all the more surprising because there is comparatively little difference between the face-centered cubic lattice of copper and the face-centered tetragonal lattice of  $\gamma$ Mn. In the latter structure the distance of closest

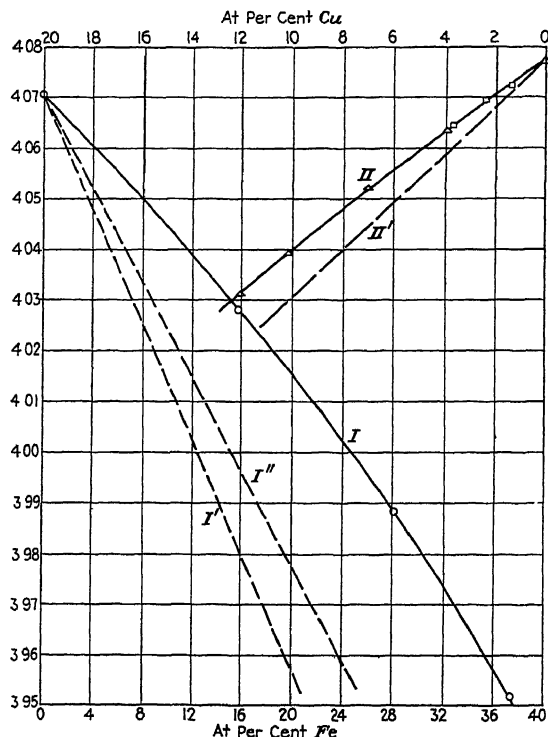


FIG. 2 — LATTICE CONSTANTS FOR GOLD-RICH PHASE OF AU-Fe ALLOYS.

Curve I. Lattice constant for solid solutions of iron in gold  
 Curve I'. Ideal curve uncorrected  
 Curve I''. Ideal curve corrected  
 Curve II. Lattice constants for solid solutions of copper in silver.  
 Curve II'. Ideal curve  
 $\Delta$  Ageew and Sachs     $\square$  Megaw.     $\circ$  Jette, Bruner and Foote

approach is given by  $d' = \frac{1}{2}\sqrt{a^2 + c^2}$  but there is a slightly longer distance between the atoms on the base of the prism, which is  $d = \frac{a}{2}$ . If the

Mn atom is ellipsoidal, the half lengths of its minor and major axes would be respectively 1.291 and 1.304 Å; the radius of the copper atom is not far different,  $r_{Cu} = 1.275$ . The average radius at the point of maximum deviation is over 1.32 Å. There is considerable justification for assuming that the coordination number in  $\gamma$ Mn is 12, although strictly speaking

<sup>31</sup> E Persson: *Ztsch phys. Chem* (1930) 9B, 25.

it should be 8. In view of the fact that the addition of copper to  $\gamma$ Mn increases the axial ratio until it approaches unity and, therefore, approaches the face-centered cubic structure, corrections for change in coordination were not made in computing the average radius.

Finally, there is the case of aluminum dissolved in magnesium.<sup>32</sup> The coordination number in both cases is 12, although magnesium has a hexagonal structure very nearly close packed and aluminum is face-centered cubic. Again comparison is facilitated by using atomic radii. The observed value for the average radius in an alloy containing 10 atomic per cent aluminum is  $1.5782\text{\AA}$  while the value calculated assuming the additivity rule is  $1.5781\text{\AA}$ . This is therefore in agreement with the additivity rule and also with the assumption of a constant volume per atom.

The writer has not found any system falling in the present classification in which negative deviation from the additivity rule occurs.

In the Fe-Si system, however, where several stable compounds are known,<sup>33</sup> the iron-rich solid solutions show an unusual behavior with respect to the variation of lattice constant with atomic composition.<sup>34</sup> The plot of these quantities shows two linear sections, which may intersect at a point at 9 atomic per cent Si or may be connected by a short curved section; the accuracy available in such measurements does not yet permit a decision to be made between these possibilities. The radius of the silicon atom in the pure element, the diamond structure, is  $1.172\text{\AA}$ . When this is corrected for the change in coordination number involved when silicon is dissolved in body-centered cubic alpha iron, we get  $1.478\text{\AA}$ . Over the first section of the plot the silicon atom appears to have a radius of  $1.211\text{\AA}$  if its radius alone is affected (see later) while for the second section it is  $1.148\text{\AA}$ . In other words, over the first 9 atomic per cent silicon the radius of this atom is greater than in pure silicon but not as great as the change in coordination number would predict. This would seem to be due to the tendency to compound formation in spite of the uncertainty of the coordination correction. Beyond 9 atomic per cent, the effect of chemical compound formation is dominant. The sudden change of direction at 9 atomic per cent is as yet not clearly understood.

#### INFLUENCE OF SUPERSTRUCTURE FORMATION ON EFFECTIVE ATOMIC RADII

Among the binary systems discussed above, superstructures are found in the Cu-Au and Cu-Pd alloys and probably in Ag-Pt alloys.

<sup>32</sup> E. Schmid and H. Seliger: *Metallwirtschaft* (1932) **11**, 409

<sup>33</sup> G. Phragmén. *Jnl. Iron and Steel Inst.* (1927) **116**, 397

<sup>34</sup> E. R. Jette and E. S. Greiner. *Trans. A.I.M.E.* (1933) **105**, 259

This last system is somewhat complex. Superstructures are found in a number of systems where definite compounds are formed; e g, the iron-rich solid solutions of the Fe-Si system.

In all cases the existence of superstructures is demonstrated by the presence of extra lines in the X-ray diffraction patterns. Frequently the superstructure is in the same crystallographic classification as the ordinary solid solution phase from which it was formed. In these cases the orderly arrangement of the atoms gives extra diffraction lines only when the scattering powers of the two atomic species are rather widely different, that is, their atomic numbers must differ by at least 10 or 15. It is therefore difficult to understand why superstructures are not observed in such systems as Sb-Bi, Au-Pd, Mo-W, Ag-Au and the gold-rich Au-Fe alloys. Phragmén<sup>35</sup> has searched unsuccessfully for such structures in the Ag-Au system as well as for the composition corresponding to  $\text{CuAu}_3$ . In one system there is a definite change of symmetry; at 50 atomic per cent in the Au-Cu alloys the superstructure is tetragonal while the statistically distributed solid solution is cubic. Dehlinger and Graf<sup>36</sup> have also found that the axial ratio of the tetragonal structure at the composition AuCu increases gradually as the annealing temperature is increased within certain limits.

The formation of the superstructure from the statistical distribution is accompanied by slight but definite contractions in the case of  $\text{AuCu}_3$ , AuCu,<sup>37</sup> and CuPd but no appreciable contraction in the case of  $\text{Cu}_3\text{Pd}$ .<sup>38</sup>

The meager store of information available on solid solutions with superstructures does not permit any certain generalizations to be made at present. As mentioned above, superstructures have not been found in a number of cases where they might reasonably have been expected, that is, in alloy systems with wide solid solution ranges and with component elements of widely different atomic numbers. The failure of the X-ray technique to reveal the presence of superstructures in these cases may, of course, be caused by using too short annealing times during the preparation of the alloys and thus failing to reach the required statistical equilibrium. If, however, we neglect this latter, somewhat too great, possibility, a consideration of the various cases where superstructures do and do not occur makes it seem reasonable to suppose that the existence of a superstructure indicates a tendency towards compound formation whether or not the lattice constant decreases during its formation from the statistical solid solution. The fact that the superstructure  $\text{Cu}_3\text{Pd}$  still shows a positive deviation from the additivity law does not eliminate

<sup>35</sup> G. Phragmén. *Teknisk Tidskr* (1926) 56, 81; *Fysisk Tidskr.* (1926) 24, 40

<sup>36</sup> U. Dehlinger and L. Graf: *Ztsch Physik* (1930) 64, 359.

<sup>37</sup> G. Sachs and J. Weerts: *Ztsch Physik* (1931) 67, 507, G. D. Preston *Jnl Inst Metals* (1932) 46, 477

<sup>38</sup> J. O. Linde. Reference of footnote 20

the possibility of finding indications of compound formation by exact thermodynamic methods. An electronic rearrangement which involves a free energy change without affecting the *average* atomic radius is possible, although this is probably an exceptional case.

Concerning the thermodynamic methods, it should be noted that at the end of his article on the Au-Ag solid solutions, Wachter<sup>39</sup> gives the following carefully stated conclusion: "The thermodynamic properties of these solid solutions are considered compatible with the existence of a regular arrangement of gold atoms in the silver crystal lattice." The effects of compound formation, regular atomic arrangement or merely an attractive force between the atoms upon thermodynamic properties differs only in degree and not in kind. Wachter's results, therefore, may indicate nothing more than the last of these possibilities. It seems to the present writer that the formation of a superstructure demands something of a more specific nature than a simple attractive force between the atoms. The X-ray evidence available at present certainly indicates that statistical distribution alone is not sufficient to account for the facts. The cases where superstructures are not found are frequently more difficult to understand than those where such structures do occur. It will be evident that the subject of superstructures is not well understood and that more experimental results from precise crystal structure and thermodynamic investigations will be needed for progress to be made.

#### MUTUAL EFFECT OF ATOMIC INTERACTIONS UPON ATOMIC RADII

Throughout the discussion we have considered the positive and negative deviations from the additivity law as tracing back ultimately to influences upon the effective radii of the atoms concerned. For the effect of change of coordination number, it was found that the entire change could, in several cases, be assigned to the radius of one of the atomic species. In most cases, however, we have simply referred to average atomic radii, these being larger or smaller than the ideal value for different pairs of atoms. Two questions arise in this connection: (1) Does the presence of a solute atom cause an immediate deviation from the ideal average radius or does the lattice constant curve approach the ideal limit asymptotically? (2) Can the deviation from the ideal average radius be assigned largely or entirely to change in the radius of the solute atom?

The experimental results so far quoted all indicate that the deviation from the ideal curve is immediate. Only one investigation (on the solution of silver in copper<sup>40</sup>) has come to the writer's attention which was

---

<sup>39</sup> Reference of footnote 3.

<sup>40</sup> H. S. Megaw. Reference of footnote 21.



sufficiently accurate and complete to indicate an asymptotic approach to the ideal curve. Miss Megaw indicates that the additivity law may be a limiting law for low concentrations, although she considers that this point is not definitely established by her results. Verification of this interpretation by experiments on other systems is necessary, of course.

Concerning the second question the answer is in the negative. At first sight it might seem reasonable, especially in systems that consist of two terminal solid solutions with an intermediate two-phase area, to consider that the solute atom alone is affected. An excellent example that this cannot be true is given by the Fe-Cr system. Both elements and the entire range of solid solutions crystallize with the body-centered cubic structure. The radii of pure iron and chromium in this structure are respectively 1.238 and 1.242 Å. At the iron end there is a pronounced positive deviation and at the chromium end a negative deviation. This means that if the Cr atom alone were affected at the iron end it would need a radius of about 1.263 Å. in order to account for the slope. The radius of the iron atom at the chromium end of the system would need to be 1.227 Å. The slope of the lattice constant curve depends upon the difference between the two atomic radii and, since this difference, 1.263 to 1.227, is greater than that for the pure elements, it is impossible to account for the observed curve between the two ends. (See Fig 1.) Had the situation been reversed—positive deviations on the chromium side and negative on the iron—it would have seemed logical to suppose that the entire curve were composed of three sections, in one of which somewhat expanded iron atoms dissolved in chromium, in the second somewhat contracted chromium atoms dissolved in iron, and the third (middle) section due to iron and chromium atoms with radii corresponding to the two terminal slopes. Since this was not the case, the only permissible conclusion is that both atomic species affect each other and from the measurements of the lattice constants merely the mean radii can be calculated.

In a theoretical treatment of cohesion in metallic crystals, Slater<sup>41</sup> introduces two kinds of forces;  $J$  forces, which are essentially Coulomb attraction forces due to interpenetration of electron shells of neighboring atoms, and  $K$  forces, which correspond to homopolar valence forces of the type involved in nonmetallic substances. In a discussion of this paper Bernal<sup>42</sup> notes the great differences in the abilities of the various metals to form solid solutions. Transition elements frequently form solid solutions of considerable extent, but the elements of the  $B$  subgroups in the periodic system and the alkali metals form solid solutions only to a limited extent. This he ascribes to the relative importance of

---

<sup>41</sup> J. C. Slater. *Phys. Rev.* (1930) **35**, 509

<sup>42</sup> J. D. Bernal. *Metallwirtschaft* (1930) **9**, 983

the  $J$  and  $K$  forces When the  $J$  forces dominate, as in the transition elements, there is no difference between solvent and solute atoms except as to size, while if the  $K$  forces dominate, solutions can be formed only when the two metals have the same outer electron configuration; e.g., Sb and Bi.

These two types of forces should also affect the form of the curve of lattice constant versus atomic composition, and it is evident that the negative deviations from the additivity rule involve primarily the  $K$  forces between unlike atoms while positive deviations refer back to the Coulombian  $J$  forces arising from the interpenetration of electron shells of unlike atoms In the case of positive deviations, this would mean that the interpenetration had not proceeded as far as would be required for the additivity law to hold, and the question arises as to what cause could be assigned to such behavior. The information available for the discussion of this point is meager. It may, however, be mentioned that in the seven systems in which positive deviations have been observed (Au-Fe, Cu-Mn, Cu-Au, Ni-Cr, Ag-Cu, Fe-Cr, Cu-Pd), after correction for the coordination factor where necessary, all the elements are members of the  $B$  subgroups or are transition elements. What seems of greater importance to the writer, however, is that at least one of the two elements involved in each system is able to exist in different valence states and that in each case the higher positive valence state involves the removal of an electron from the level below the normal valence electron level. This suggests that when an atom of potentially variable valence is in the presence of certain other atomic species, one or more of its electrons in the lower level is raised to the valence electron level, thereby decreasing the interpenetrability of the electron shells and increasing the effective atomic radius of this element In some systems, such as Ag-Cu and perhaps Ni-Cr, only one of the atomic species would be affected in this way In other systems both species may change With but few exceptions, however, variability of primary valence is a common characteristic of transition elements and members of the  $B$  subgroups, and yet in four of the systems that show ideal behavior with respect to the additivity rule, namely, Au-Pt, Au-Pd, Pt-Ir and Pb-βTl, all the elements belong in these classifications. There is no clear-cut explanation for such behavior but it must be recalled that only in exceptional cases does only one type of force exist in an interatomic or intermolecular relationship. In most cases it is probably quite safe to assume that neither negative nor positive deviations from an ideal behavior develop to the fullest extent, which would be possible if only one type of influence existed. While in the case of the Sb-Bi and Mo-W systems the ideal behavior may reasonably be ascribed to the close similarity in structures of the outer electron shells, for the four other cases just mentioned there may be nothing more than a close balance between the forces

causing the two types of deviation. In conclusion, regarding the positive deviations, it may be remarked that the factor of internal pressure difference that Mortimer<sup>43</sup> has used so successfully in explaining positive deviations in liquid solutions is of little assistance in the solid solutions thus far considered. While there are as yet insufficient data available for accurately calculating the internal pressures of solid metals, the approximate measure of this quantity, that is, the ratio of the coefficients of thermal expansion (volume) and compressibility,<sup>44</sup> leads to no useful correlation with the observed deviations. The fact that in the Fe-Cr system there are positive deviations on the Fe side and negative deviation at the Cr end is a fair indication of the complexity of the problem of solid solubility in intermetallic systems.

### SUMMARY

It is assumed that the chemical and physical requirements that must be fulfilled by solvent and solute atoms or molecules to enable solutions to obey Raoult's law are identical with those required for the additivity law of Vegard to hold for solid solutions.

A study of the results of a number of accurate determinations of lattice constants in intermetallic systems where extensive ranges of solid solution occur shows that while a number of intermetallic systems obey the additivity law, positive and negative deviations are of frequent occurrence and considerable in magnitude.

The effects of change of coordination number and superstructure formation on lattice constants are considered, and a brief discussion is given on the mutual effect of unlike atoms in the solid state upon the effective atomic radius.

### DISCUSSION

(*G. E. Doan presiding*)

R. F. MEHL,\* Pittsburgh, Pa. (written discussion).—It may seem to the casual observer that papers on the thermodynamics of alloy systems are harmless enough by way of pastime but that they are of little importance practically. However, it must be remembered that one of the greatest advances in metallurgy was made by Osmond in applying the thermodynamics developed by Roozeboom to the important systems iron-carbon and iron-nickel, resulting in the familiar constitutional diagrams we now have, upon which all of our heat treatment and indeed much of our working of alloys is based.

The study of the behavior of metals and alloys from general chemical and physical points of view, with a view to obtaining generalizations, may be regarded as the most

---

<sup>43</sup> F. S. Mortimer: *Jnl Amer Chem Soc* (1923) **45**, 633

<sup>44</sup> J. Hildebrand: Reference of footnote 1, 181.

\* Director and Professor of Metallurgy, Metals Research Laboratory, Carnegie Institute of Technology.

important single activity of the research metallurgist. We have had two examples of this sort of work this afternoon, this paper by Dr Jette and the one by Dr Fink and Mr Freche (p 304, this volume). Broad generalizations and classifications are more useful and important than any number of isolated and separate facts. Needless to say, Dr. Jette's paper leads to all this philosophizing. There is hardly a scientific field where generalizations are more difficult to formulate than that of alloy systems. Some years ago I listed all the various properties of metals that might be factors in determining the extent of solid solubility, in order to obtain a few general rules. An early attempt had been made by Rosenham but little has come of it. Despite the greater amount of data at my disposal, my effort was entirely unsuccessful. Subsequently I found that a number of people, including our chairman, Professor Doan, had made similar unsuccessful attempts. Evidently the problem is complex, but such work as this and previous work by Bernal and Hume-Rothery will in time, despite the difficulties, lead to important results.

I am inclined to believe that the behavior of metal systems with respect to the rule of mixtures can best be studied by plotting not  $a_0$ , the side of the unit cell, but the cube of this  $a_0^3$ , against atomic per cent, as I pointed out some years ago.<sup>45</sup>

Generally speaking, the cube of  $a_0$  rather than  $a_0$  itself would appear to be the proper quantity to reason about, for after all metals and alloys do exist in three dimensions. The difference in these two methods may be easily shown. If  $a_0$  for metal A is 4, and that for metal B is 2, the rule of mixtures would demand a value of 3 for a 50 atomic per cent alloy. If these same values are taken, but the cubes plotted, the value plotted for A would be 64, that for B would be 8, and that for the 50 atomic per cent alloy would be 36. The cube of the value 3, obtained above, however is 27. Thus an alloy that obeys the rule of mixtures when  $a_0$  is plotted will give a negative deviation (too low a value) when  $a_0^3$  is plotted. The example chosen is extreme but demonstrates the point. Such a method is consistent with the conventional plotting of constitutional diagrams, which calls for plotting atomic volume against atomic percentage. In my opinion Vegard's law should be expressed in this form. The difference is not appreciable except when the  $a_0$  values are quite different for the two component metals, as they are in the Cu-Au system.

The Cu-Au system is of considerable interest in this connection. The  $a_0$  values (and the  $a_0^3$  values) show a positive deviation from the rule of mixtures values, that is, they are greater than the rule of mixtures values. This would indicate the absence of any tendency to form compounds, yet the compounds  $\text{Cu}_3\text{Au}$  and  $\text{CuAu}$  are formed at low temperatures. We would expect from this that the system would show negative deviations in activity despite the positive deviations from Vegard's law and thus system might well be an exception from any simple correlation between deviations from Vegard's law and in activities. It would be very desirable to have activities measured in this system. An attempt is now being made at the Carnegie Institute of Technology to do this. The choice of a suitable fused salt electrolyte is not very easy, but appears possible.

The prediction that the Ag-Au system should form superstructures is apparently denied by experiment. It must always be remembered, however, that though our experimental researches are performed over a range of temperatures, only very rarely do we work at pressures greater than atmospheric. Several years ago I prepared a series of Ag-Au alloys for Professor Bridgman, at Harvard, for a study of the compressibility of a simple solid solution series. This system had not been included in my own earlier work on the compressibility of alloys. Professor Bridgman's measurements on these Ag-Au alloys showed that at high pressures the apparently simple

<sup>45</sup> R. F. Mehl and B. J. Maur. Chemical Affinity in Metallic Alloys, Especially Solid Solutions. A Study of Compressibility. *Jnl. Amer. Chem. Soc.* (1928) **50**, 55-73.

solid solution shows discontinuous volume curves, which might very well have been caused by compound or superstructure formation <sup>46</sup> Compared to the internal pressures that exist in this system (which we know approximately) the pressures used for measuring compressibility are not great, and we might think of the system as being on the verge of compound formation at atmospheric pressure Other alloy systems which are suspected of superstructure formation might well be studied in this way

I believe that internal pressures are of somewhat greater use than Dr Jette infers I performed some calculations on internal pressures some years ago which might be of interest in this connection <sup>47</sup> The value of the work depends on the validity of the internal pressure conception and the method of calculating internal pressure as proposed by the late Prof T W Richards This method is somewhat different from that of Mortimer and Hildebrand, and the exact justification of any of these methods physically may not be very strong, yet Professor Richards was able to correlate many important properties of metals in this way Using his method I calculated the differences between the internal pressures and the rule of mixtures values The systems Au-Pd, Cu-Ni, Cu-Au, Ag-Pd, Cu-Pd and Ag-Au were studied All of them showed an increase in internal pressure over the rule of mixture values, with the Ag-Au system showing the smallest increase Evidently all these systems show an increase in the cohesive forces, provided, of course, that the method of calculation is a justifiable one

A consideration of the forces between atoms has importance beyond purely thermodynamic considerations, particularly in connection with mechanical properties Ultimately this should be the chief usefulness in such work The process of deformation in iron may illustrate this point Iron at high temperatures deforms chiefly by slip As the temperature is lowered, slip becomes more difficult and twinning becomes the easier process Finally, at very low temperatures cleavage becomes the easiest process The rapid decrease in impact value in the neighborhood of zero degrees Centigrade is a reflection of this condition As pure iron is alloyed with chromium, the temperature of rapid fall-off in impact value increases, finally crossing room temperature at about 18 per cent chromium Evidently chromium so affects the interatomic forces that the shearing forces for slip and twinning become greater than that for cleavage

E. R. JETTE (written discussion) —The interesting and pertinent points developed by Dr Mehl in his discussion will be taken up in a somewhat different order from that in which he gave them

The possible effect of high pressures on transformations in the Au-Ag system is well taken We need to be reminded that we generally work only with the constant pressure section at one atmosphere in the more complete three-dimensional diagram temperature-composition-pressure

Dr Mehl has used the internal-pressure concept in a somewhat different manner from the author He has applied the law of mixtures to the internal pressures of a series of alloys and compared the calculated with experimental results, he was thereby enabled to draw certain conclusions regarding the cohesive forces in these alloys The author's use of internal pressures was a much more limited one. It was restricted to the use of the difference in the internal pressures of the pure metals to predict

<sup>46</sup> P W Bridgman: Compressibilities and Pressure Coefficients of Resistance of Elements, Compounds, and Alloys, Many of Them Anomalous. *Proc. Amer. Acad. Arts and Sci.* (1933) **68**, 25-93

<sup>47</sup> R. F. Mehl: Internal Pressures in Metallic Solid Solutions *Jnl. Amer. Chem. Soc.* (1928) **50**, 73-81

Interatomic Forces in Metals and Alloys *Trans. A.I.M.E.* (1928) **78**, Inst. Metals Div., 405

whether deviations from Vegard's rule should occur. It was in this sense that internal-pressure data gave little assistance. The author regrets having missed Dr Mehl's excellent papers on compressibility and internal pressure, they were read some years ago but were forgotten at the time of writing the present article.

The point that requires most discussion relates to the method of stating Vegard's rule, i.e., whether it should be in terms of the lattice constant  $a_0$  or this quantity cubed. As Dr Mehl points out, the effect of using the latter is to reduce the magnitude of the positive deviations, make the "ideal" systems show slightly negative deviations and increase the magnitude of the negative deviations. The present status of the theory of solutions in general and of solid solutions in particular permits a difference of opinion on this point.

In this connection, it should be emphasized that although Raoult's law leads to an entirely reasonable physical and mechanistic conception of the structure of a solution, its quantitative basis is found in thermodynamic studies of vapor pressure, electromotive force and other quantities that can be converted into "free energies." The other quantities such as densities, internal pressure and the like, which are sometimes used to indicate whether a solution obeys the law rather than to measure the extent of the deviation, have been introduced largely on the basis of analogy and can be used quantitatively only by means of rather rough empirical relations, if at all. Among these other quantities, which are not directly related to the free energies, are the two quantities the author has used in the paper, namely, the lattice constant and the geometrically related quantity one-half the distance of closest approach of the atoms which is conventionally called the "average atomic radius" in solid solutions. While the author has used the lattice constant much more than the radius throughout the paper, this was done mainly to avoid the recalculation of the experimental results, for the author's conclusions either quantity is suitable. However, in thinking about the phenomena discussed in the paper, the author used almost entirely the variation of the average atomic radius with composition because it seems to him that this quantity should be the most direct indication of the existence of those chemical and physical forces that will cause deviations from Raoult's law. Perhaps this point was not sufficiently emphasized in the paper.

There is much to be done on the experimental side before the questions raised by the article and Dr Mehl's discussion can be answered. The results of the experimental work on the Cu-Au system mentioned by Dr Mehl will be awaited with great interest, particularly in view of the possibility that this system (also Cu-Pd) is apt to prove difficult to classify on any basis we now know.

to a value of  $4.0285\text{\AA}$ . at the solubility limit of 5.6 per cent copper The data under A in Table 1 indicate that the parameter values of the 5 per

TABLE 1.—*Lattice Parameter Values of Copper-aluminum Alloys Prepared in Several Forms*

All specimens quenched in cold water from solution treatment at  $550^{\circ}\text{C}$ .

Specimen Form	Average Diameter, In	Method of Preparation	Composition, Per Cent	$a_0$ Value, $\text{\AA}$
			Copper	
A. Powder	0 0025	Filings from forged rod	5 03 <sup>a</sup>	4 0307
Powder	0 0035	Filings from forged rod	5 06	4 0306
Powder	0 005	Filings from forged rod	5 01	4 0305
Powder	0 007	Filings from forged rod	5 04	4 0306
Powder	0 015	Filings from forged rod	5 08	4 0308
Powder	0 033	Filings from forged rod	5 12	4 0304
Wire	0 040	Drawn from forged rod	5 07	4 0301
Wire.	0 070	Drawn from forged rod	5 04	4 0306 <sup>a</sup>
Wire	0 125	Drawn from forged rod	5 04	4 0305
Rod	} 0 25	Forged and machined	5 03	4 0324
Rod		Cast in hot graphite mold	5 09	4 0326
Rod		Forged and machined	(5 0)	4 0348 <sup>a</sup>
Rod		Chill cast, cold copper mold	5 02	4 0345 <sup>a</sup>
Rod		Cast in hot graphite mold	5 24	4 0341 <sup>a</sup>
Rod		Cast in hot graphite mold	4 80	4 0338 <sup>a</sup>
B. Wire	0 05	Drawn from forged rod	(2 40)	4 0355
Wire	0 07	Drawn from forged rod	(2 40)	4 0359
Wire	0 25	Drawn from forged rod	(2 40)	4 0374
Rod	0 50	Forged and machined	(2 40)	4 0378
C. Wire	} 0 07	Drawn from forged rod	(5 46)	4 0293 <sup>a</sup>
Wire		Cast in hot graphite mold	(5 46)	4 0294
Rod	0 25	Cast in hot graphite mold	(5 46)	4 0314
Rod	} 0 50	Cast in hot graphite mold	(5 46)	4 0337
Rod		Forged and machined	(5 46)	4 0342 <sup>a</sup>
D. Wire	0 07	Cast in hot graphite mold	(15 0)	4 0289
Rod	0 50	Cast in hot graphite mold	(15 0)	4 0333
			Aluminum	
E. Wire	0 07	Drawn from forged rod	99 95	4 0410 <sup>a</sup>
Rod	0 50	Forged and machined	99 95	4 0413 <sup>a</sup>

<sup>a</sup> Average of eight determinations

<sup>b</sup> Analyses, with exception of those in parentheses, made on part of sample exposed in X-ray determinations

cent copper alloy in the form of quenched powders and wires up to 0.125 in are constant and increase from this measurement to a maximum with

the  $\frac{1}{2}$ -in specimens. The dimension factor seems to be more important than the method of specimen preparation. After repeated treatments at  $550^{\circ}\text{C}$  the quenched specimens gave substantially the same parameter differences. The usual macroscopic etches also failed to alter these results.

The most obvious cause for the large values, perhaps, would be variations in the copper content, particularly in view of the segregation tendencies exhibited by these alloys. Careful sampling and chemical analysis of the several specimens disclosed maximum variations of 0.25 per cent copper. These differences may account to some extent for the parameter differences within any dimensional group but cannot explain the major variations. Moreover, a wrought 2.4 per cent and a cast 15.0 per cent copper alloy in the form of 0.07-in wires and  $\frac{1}{2}$ -in. rods resulted in similar  $a_0$  differences (Table 1, B and D).

A consideration of the mechanics of X-ray reflection from surfaces of different curvature indicates that the point of actual reflection from specimens of small diameter would be farther from the film than it would be for a larger specimen. This error would lead to an apparent larger parameter for the small specimens rather than to a smaller parameter as actually observed. Also, the  $a_0$  values for pure aluminum (99.95 per cent Al) in the form of 0.07-in wire and  $\frac{1}{2}$ -in rods were only 0.0003 Å. apart, a difference which, however, was consistently obtained (Table 1, E).

It seemed possible that the quench was too slow in the larger specimens; i. e., some precipitation had taken place in the quenching bath. However, the reflection lines were sharp as compared to those for alloys in which precipitation was known to have started. Alloys more drastically quenched in  $\text{CaCl}_2$ -water mixtures at  $-20^{\circ}\text{C}$ . again gave similar parameter values. Furthermore, a  $\frac{1}{2}$ -in rod at  $550^{\circ}\text{C}$ . when placed in a salt bath at  $300^{\circ}\text{C}$ . for 2 min. and then quenched in cold water gave the same  $a_0$  value. As is generally believed, precipitation in these alloys is suppressed effectively by a cold water quench.

P. Wiest,<sup>7</sup> after an investigation of gold-silver alloys, concluded that in cold-worked and annealed metal there is a critical reduction beyond which the lattice parameter is sharply changed. To test the validity of this conclusion, 5.4 per cent and 15.0 per cent copper alloys were cast in the two dimensions, 0.07-in. and  $\frac{1}{2}$ -in. rods. After quenching in cold water from the  $550^{\circ}\text{C}$  solution treatment, these specimens showed parameter differences similar to those previously noted (Table 1, C, D). These results indicate that the amount of cold working seems to be of little importance.

As previously noted, the method of specimen preparation does not seem to be a significant factor. Furthermore, the differences noted

<sup>7</sup> P. Wiest *Ztsch f Physik* (1933) 81, 121.



with specimen dimension are not related to surface-energy considerations, since from 0.125-in wire to powder passing through a 200-mesh screen the parameter values remain constant and are in accord with the data of previous studies. Finally, the variations observed from 0.125 to  $\frac{1}{2}$ -in. specimens seem comparable over a wide range of copper concentrations and may persist to some very slight degree in the 99.95 per cent aluminum.

### PRECIPITATION REACTIONS

The first precipitation studies were made by placing the specimens, quenched from 550° C., in a Hevi-Duty furnace at 300° C for successive time intervals, interrupting the treatment for parameter measurements by quenching. The reaction curves so obtained are shown in Fig. 1 (Data, Table 2). The considerably greater time required for the reaction to start in the larger specimens was a result of the longer time required for them to attain the furnace temperature. For this reason, all subsequent reaction studies were made by placing the quenched specimens individually in a salt bath, of very large volume as compared to the specimen. However, it should be noted in Fig. 1 that the  $\frac{1}{2}$ -in. rods reached a maximum lattice-parameter value some 0.0018 to 0.0020 Å. above the value for pure aluminum and that, although the  $a_0$  value dropped somewhat with time, at the end of 250 hr. it had not attained

TABLE 2.—*Reaction Rate of Different 5.0 Per Cent Copper-aluminum Specimens Heat-treated in Air at 300° C. and Quenched in Cold Water*  
Indicated by  $a_0$  Values in Ångstrom Units

Heat Treatment		0.007-in Powder	0.07-in Wire	0.50-in Forged Rod	0.50-in Chill-cast Rod	0.50-in Slow-cast Rod	1.50-in Slow-cast Rod
Time	Temperature, Deg. C						
6 weeks.	550	4.0306	4.0306	4.0348	4.0345	4.0341	4.0338
15 min	300	4.0398	4.0389	4.0335	4.0333	4.0346	4.0340
$\frac{1}{2}$ hr	300	4.0402	4.0401	4.0337	4.0338	4.0347	4.0340
1 hr	300	4.0405	4.0405	4.0349	4.0365	4.0418	4.0353
2 hr	300	4.0405	4.0408	4.0422	4.0418	4.0419	4.0422
4 hr	300	4.0405	4.0406	4.0428	4.0427	4.0426	4.0422
8 hr	300	4.0404	4.0405	4.0430	4.0430	4.0428	4.0428
30 hr	300	4.0404	4.0406	4.0428	4.0427	4.0425	4.0417
100 hr	300	4.0404	4.0400	4.0420	4.0420	4.0418	4.0417
250 hr.	300	4.0404	4.0405	4.0419	4.0420	4.0418	4.0416

the end point obtained on the small wires and powder, which exhibited a more normal reaction behavior.

The same specimens, after quenching from a re-solution treatment at 550° C. and heating at 400° C. in a salt bath, gave the  $a_0$  values shown

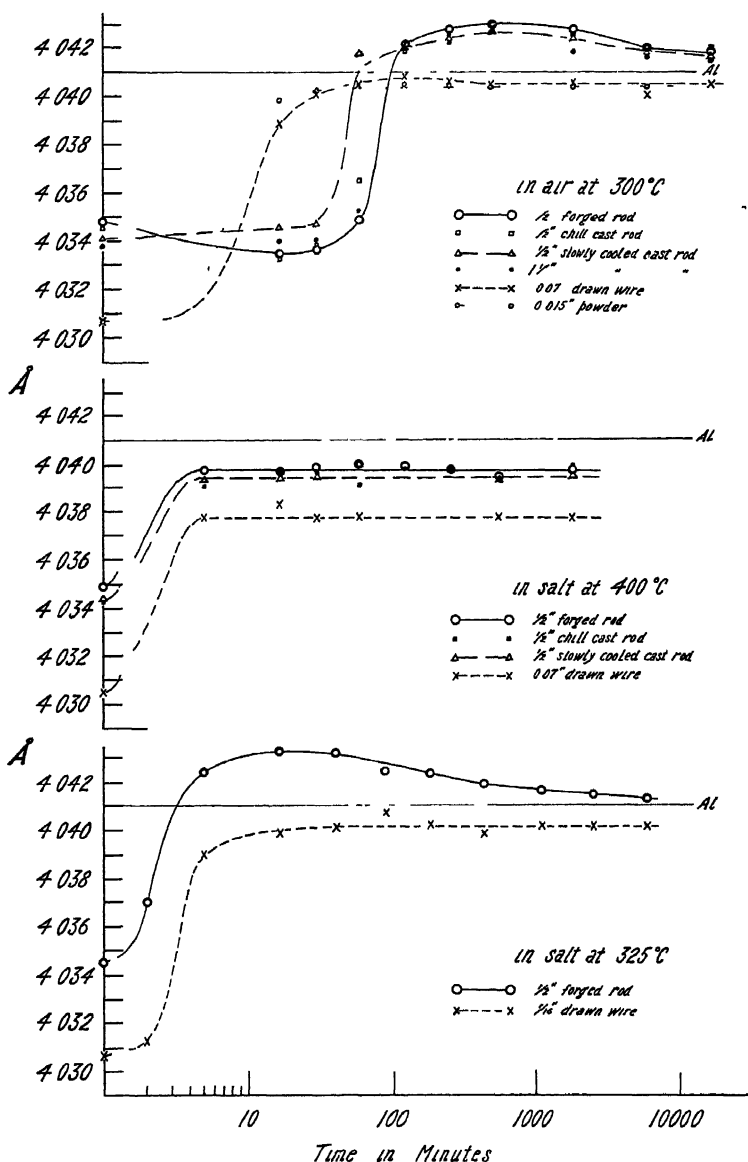


FIG. 1.—REACTION RATE OF INDICATED 5 PER CENT CU SPECIMENS.

in Fig. 1 (Data, Table 3) No maxima were observed for this temperature. The reaction seemed to be practically complete at the end of

TABLE 3.—*Reaction Rate of Different 5.0 Per Cent Copper-aluminum Specimens Heat-treated in Salt Bath at 400° C and Quenched in Cold Water*Indicated by  $a_0$  Values in Ångstrom Units

Heat Treatment		0 07-in Wire	0 50-in Forged Rod	0 50-in Chill-cast Rod	0 50-in Slow-cast Rod
Time	Temperature, Deg C				
50 hr	550	4 0305	4 0349	4 0342	4 0343
5 min	400	4 0377	4 0397	4 0390	4 0394
15 min	400	4 0383	4 0396	4 0397	4 0394
30 min	400	4 0377	4 0398	4 0396	4 0395
1 hr	400	4 0377	4 0400	4 0390	4 0400
2 hr	400		4 0399	4 0398	
4 hr	400		4 0398	4 0398	
9 hr	400	4 0378	4 0394	4 0393	4 0393
30 hr	400	4 0377	4 0397	4 0399	4 0395

5 min and the differences found in parameter values exhibited no tendency to converge but remained in the same order but of lesser magnitude, as after the solution quench

After appropriate re-solution treatments at 550° C the specimens were quenched in cold water and the precipitation reaction at 325° and 275° C was studied (Figs 1 and 2; data, Tables 4 and 5). At these

TABLE 4.—*Reaction Rate of Different 5.0 Per Cent Copper-aluminum Specimens Heat-treated in Salt Bath at 325° C and Quenched in Cold Water*Indicated by  $a_0$  Values in Ångstrom Units

Heat Treatment		0 07-in Wire	0 50-in Forged Rod
Time	Temperature, Deg C		
50 hr	550	4 0307	4 0346
2 min	325	4 0312	4 0370
5 min	325	4 0390	4 0424
15 min	325	4 0398	4 0433
40 min	325	4 0401	4 0432
1½ hr	325	4 0408	4 0425
3 hr	325	4 0402	4 0424
7 hr	325	4 0398	4 0419
19 hr	325	4 0402	4 0417
40 hr	325	4 0402	4 0416
100 hr	325	4 0402	4 0413

TABLE 5—*Reaction Rate of Specimens Heat-treated in Salt Bath at 275° C and Quenched in Cold Water*Indicated by  $a_0$  Values in Ångstrom Units

Heat Treatment		Pure Aluminum		2 4 Per Cent Cu Alloy		5 0 Per Cent Cu Alloy		Hardness <sup>a</sup>
Time	Temperature, Deg C	0 07-in Wire	0 50-in Forged Bar	0 07-in Wire	0 50-in Forged Bar	0 07-in Wire	0 50-in Forged Bar	
20 hr	550	4 0410	4 0413	4 0359	4 0378	4 0307	4 0348	{ 48 hr r t }
2 min	275					4 0306	4 0350	69 0
5 min	275			4 0362	4 0377	4 0306	4 0351	74 1
15 min	275	4 0409	4 0413	4 0366	4 0386	4 0310	4 0416	82 9
40 min	275			4 0362	4 0403	4 0394	4 0426	81 0
1½ hr	275	4 0410	4 0413	4 0379	4 0424	4 0416	4 0429	76 0
3 hr	275			4 0397	4 0427	4 0413	4 0429	73 3
7 hr	275	4 0410	4 0413	4 0401	4 0430	4 0413	4 0429	70 1
17 hr	275					4 0415	4 0424	68 7
40 hr	275			4 0404	4 0429			
100 hr	275	4 0411	4 0414	4 0406	4 0429	4 0409	4 0429	62 6

<sup>a</sup> Rockwell F scale, using  $\frac{1}{16}$ -in ball and 60-kg load

temperatures maxima similar to those shown at 300° C. were found for the  $\frac{1}{2}$ -in specimens. The parameter value decreased from this maximum with longer annealing times at 325° C. but no similar tendency

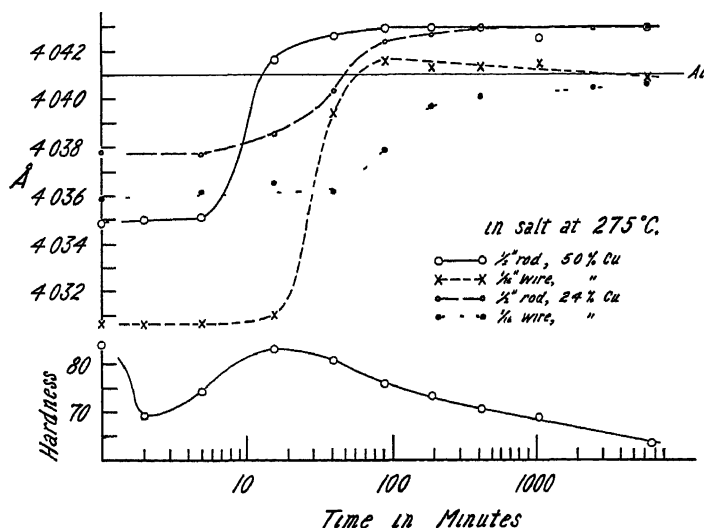


FIG 2.—REACTION RATE OF 2 4 PER CENT AND 5 PER CENT CU SPECIMENS.

was found at 275° C. up to 250 hr. In the 2 4 per cent copper alloys, quenched from a solution treatment and annealed at 275° C., the reaction took place at a considerably slower rate than in the more unstable alloys of high copper content (Fig. 2) This expected result confirms

the findings of Stenzel and Weerts<sup>8</sup> The  $\frac{1}{2}$ -in specimen reached the same maximum as that observed in the alloys of higher copper content. It should be noted that although the  $\frac{1}{2}$ -in. rods undoubtedly come up to temperature more slowly than the small wires, they always begin to precipitate somewhat earlier. To obtain additional confirmation of the anomalous effects thus far observed, the 15 per cent copper alloy, after quenching from 550° C., was given the normal precipitation treatments

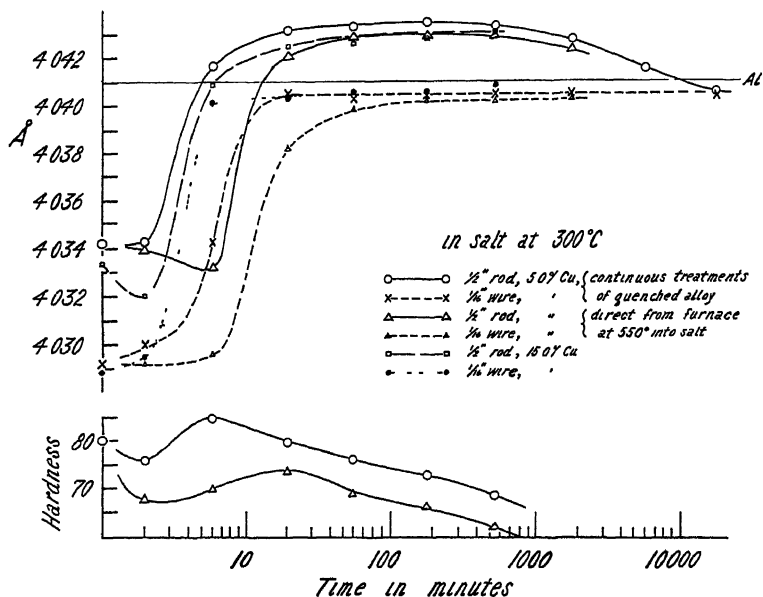


FIG 3—REACTION RATES OF SPECIMENS HEAT-TREATED IN SALT BATH AND QUENCHED IN COLD WATER

at 300° C. The same differences between large and small specimens with respect to the maximum above pure aluminum and the comparative initial reaction times were again found (Fig 3; data, Table 6).

At this point, it may be said that the general results of Stenzel and Weerts have been corroborated but the abnormally large lattice parameter was found to be markedly increased in our large specimens. It seemed desirable to extend the studies of the precipitation reaction at one temperature, 300° C. Lattice measurements of the 5.4 per cent alloy were made with the following modifications of procedure: (1) after quenching from 550° C., reheat for additive times as previously; (2) after quenching from 550° C., reheat for continuous times; (3) remove the specimens from the furnace at 550° C and rapidly transfer directly into the salt bath at 300° C.

The results of these tests are given in Fig 3 (Data, Table 6). The reaction curves for modifications 1 and 2 coincided and agreed well with

<sup>8</sup> Reference of footnote 1

the previous data, indicating that the observed maxima and earlier precipitation as found in the larger specimens are not related to a cumulative effect of reheating numerous times to the reaction temperature. For modification 3, the direct transfer from 550° to 300° C did not greatly alter the reaction curve, although two important differences should be noted; namely, the initial "incubation" drop in parameter of the 1/2-in. specimen and the later start of the reaction as compared to the quenched and reheated rods.

TABLE 6.—*Reaction Rate of Specimens Heat-treated in Salt Bath at 300° C. and Quenched in Cold Water*  
Indicated by  $a_0$  Values in Ångstrom Units

Time at 300° C	Cast 15.0 Per Cent Cu Alloy		5.4 Per Cent Cu, 1/2-in Rod Cumulative Treatments		5.4 Per Cent Cu, Continuous Treatments		5.4 Per Cent Cu, Direct from 550° C into Salt Bath at 300° C		
	0.07-in Wire	0.50-in Rod	Å	Hardness <sup>a</sup>	0.07-in Wire	0.50-in Rod	0.07-in Wire	0.50-in Rod	Hardness <sup>a</sup>
(550°)	4 0289	4 0333	4 0343	{ 48 hr r t } 80 0	4 0292	4 0342			
2 min	4 0295	4 0320	4 0343	75 9	4 0300	4 0342	4 0293	4 0340	67 3
6 min	4 0402	4 0409	4 0416	84 2	4 0343	4 0415	4 0296	4 0332	69 7
20 min	4 0403	4 0424	4 0431	79 4	4 0405	4 0421	4 0382	4 0420	73 0
1 hr	4 0406	4 0424	4 0432	76 1	4 0403	4 0432	4 0398	4 0429	68 2
3 hr	4 0406	4 0427	4 0434	72 7	4 0404	4 0428	4 0403	4 0429	66 3
9 hr	4 0409	4 0432	4 0432	67 9	4 0404	4 0432	4 0401	4 0429	62 0
30 hr			4 0427		4 0404	4 0426	4 0402	4 0424	48 3
100 hr			4 0414						
300 hr			4 0405	Qu water 100° C					

<sup>a</sup> Rockwell F scale, using 1/16-in. ball and 60-kg load.

The results thus far obtained may be summarized as demonstrating that: (1) at all temperatures employed, the 0.07-in wire specimens reacted in the more normal manner, although at 275° C even these specimens reached a maximum above pure aluminum; (2) in the 1/2-in rods, the reaction starts sooner than with the small wires and reaches a maximum at about 0.0020 Å above the parameter value for pure aluminum for all compositions studied (2.4, 5.0, 5.4, and 15 per cent copper) and for the temperatures 275°, 300°, and 325° C; and (3) the  $a_0$  value tends to decrease from the maximum point and approaches the equilibrium value at 325° and 300° C. but not at 400° and 275° C within the longest time employed.

The anomalous behavior of the larger specimens may be considered from the following viewpoints:

1. Impurities of the type causing an expansion of the aluminum lattice would function in the small wires and powders as well as in the 1/2-in. rods.

2. Errors in X-ray technique seem incapable of explaining discrepancies of the magnitude observed. The greatly blurred lines characteristic of specimens in the course of precipitation occur only on films taken along the nearly vertical part of the reaction curve. At points along the maxima, the reflection lines are fairly sharp, and in general comparable to those of the quenched solid solution alloys.

3. Structural changes in the solid solution matrix must be considered, such as the oft-alleged allotropy of aluminum.<sup>9</sup> The pure aluminum was carried through the 275° C. treatment and the same variation of 0.0003 Å between the large and small specimens was again consistently

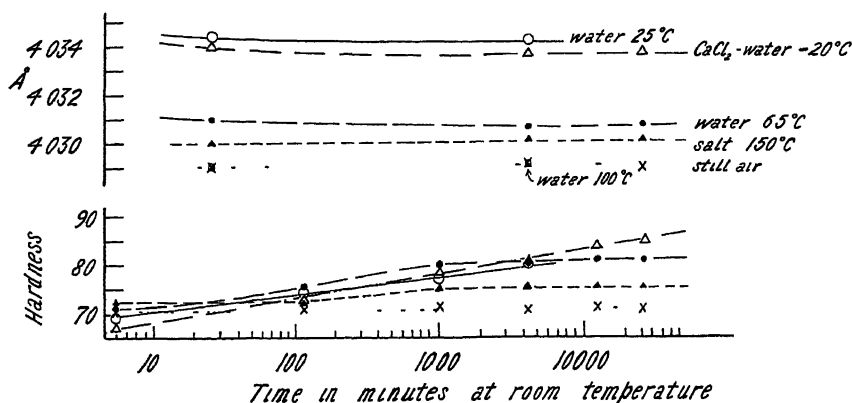


FIG 4—COURSE OF ROOM-TEMPERATURE AGING OF 54 PER CENT CU SPECIMENS QUENCHED FROM 550° C IN INDICATED MEDIA

noted, but no further changes appeared (data, Table 5). Also, there may be a change to a tetragonal lattice at this maximum  $a_0$  value, similar to the intermediate form of tetragonal martensite found in iron-carbon alloys. On a film representing a lattice constant above that of pure aluminum, parameter values calculated from different reflecting planes fell on a straight line, indicating that the lattice is still cubic. Weerts<sup>10</sup> has reported the existence of a new transitional form of  $\text{CuAl}_2$  which may appear in the temperature ranges used here. This suggested explanation also fails to explain why the  $\frac{1}{2}$ -in. rods react differently from the small wires.

It seemed probable that the anomalies appearing in the course of precipitation are related to, and perhaps originated in, the 550° C solution treatment and the subsequent quench. To further disprove the possibility of precipitation in the quenching bath, a  $\frac{1}{2}$ -in., 5.4 per cent copper specimen was quenched from 550° C. in the ordinary manner and the lattice parameter again found to be high, as previously mentioned (4.0342 Å). After drilling to form a hollow cylinder of 0.05-in. wall

<sup>9</sup> A. Schulze: *Metallwirtschaft* (1933) **12**, 667.

<sup>10</sup> Reference of footnote 3

thickness, the  $a_0$  value of the as-machined cylinder was  $4.0299\text{\AA}$ , closely approaching the 0.07-in. wire value of  $4.0292\text{\AA}$ . A subsequent treatment at  $550^\circ\text{C}$ . followed by the usual cold water quench resulted in a parameter value of  $4.0316\text{\AA}$ . These changes could not be associated with precipitation in the quenching bath but rather indicated a probable strain effect, originating with quenching, and operating to change the lattice constant in an unknown manner.

To check this hypothesis, several  $\frac{1}{2}$ -in., 54 per cent copper specimens were quenched from the  $550^\circ\text{C}$ . solution treatment in various media at temperatures of from  $-20^\circ$  to  $150^\circ\text{C}$ . The results (Fig. 4; data, Table 7), show that the large specimens cooled in still air or in boiling

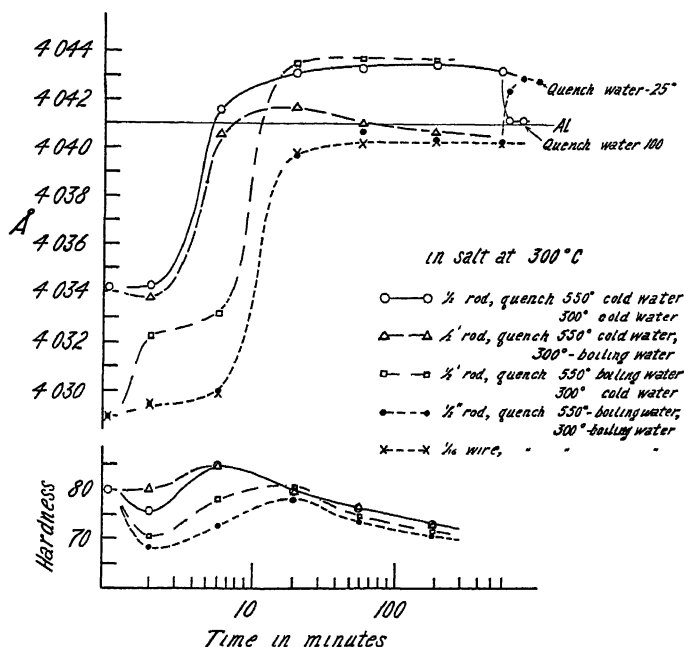


FIG. 5—REACTION RATE OF 54 PER CENT CU SPECIMENS UNDER INDICATED CONDITIONS

water had lattice parameters identical with those of the 0.07-in. wires, both dropping to a value  $0.0002\text{\AA}$ . below the previous 0.07-in. wire value. Furthermore, the X-ray photograms of these specimens had reflection lines somewhat sharper than those of more drastically quenched alloys. The data clearly indicate that strain originating in the quenching bath was responsible for the previously observed large  $a_0$  values. When these alloys were heat-treated at  $300^\circ\text{C}$ ., again quenching in boiling water from each treatment, the reaction-rate curves for the  $\frac{1}{2}$ -in. rods and the small wire specimens were identical, as shown in Fig. 5 (Data, Table 8). This curve closely corresponds to that previously found for



TABLE 7—*Course of Aging at Room Temperature Shown by Lattice Parameter and Hardness Values of  $\frac{1}{2}$ -in., 54 Per Cent Copper-aluminum Specimens Quenched from Solution Treatment at 550° C in Indicated Media*

Time at Room Temperature	CaCl <sub>2</sub> -H <sub>2</sub> O	Water			Salt	Still Air
	-20° C	25° C	65° C	100° C	150° C	25° C
Hardness 5 min	67 4	68 8	71 5	68 5	72 7	70 9
a <sub>0</sub> value 1 hr	4 0340	4 0344	4 0310	4 0290	4 0300	4 0291
Hardness 2 hr	73 6	74 3	75 2	71.0	72 4	71 9
Hardness 18 hr	78 6	76 5	80 0	74 5	75 5	71 6
Hardness 3 days	80 3	80 6	81 0	78 0	75 5	70 6
a <sub>0</sub> value 3 days	4 0336	4 0342	4 0306	4 0291	4 0300	4 0292
Hardness 9 days	84 1		81 6	78 9	75.1	71 1
a <sub>0</sub> value 9 days	4 0337		4 0307		4 0300	4 0289
Hardness 20 days	84 3		79 5		74 9	72 5
a <sub>0</sub> value 20 days	4 0336		4 0306		4 0300	4 0290
Hardness 30 days	85 3		80 9		76 6	71 3

TABLE 8.—*Effects of Various Combinations of Cold and Hot Quenches (Water at 20° and 100° C.) on Reaction Rate of  $\frac{1}{2}$ -in., 54 Per Cent Copper-aluminum Specimens in Salt at 300° C.*

Indicated by a<sub>0</sub> Values in Ångstrom Units and by Hardness Values

Time	Quenched from 550° C in Cold Water				Quenched from 550° C in Boiling Water				
	Quenched at 300° C, Cold Water		Quenched at 300° C, Boiling Water		Quenched at 300° C, Cold Water		Quenched at 300° C, Boiling Water		
	Å	Hardness	Å	Hardness	Å	Hardness	0.07-in Wire	$\frac{1}{2}$ -in Rod	Hardness
(550° C)	4 0342	80 0 (3 day, r t)	4 0342	80 4 (3 day, r t)	4 0290	78 0 (3 day, r t)	4 0290	4 0290	78 6 (3 day, r t)
2 min	4 0343	75 9	4 0338	80 2	4 0323	71 6	4 0295	4 0295	68 6
6 min	4 0416	84 2	4 0406	84 4	4 0332	77 3	4 0299	4 0300	72 6
20 min	4 0431	79 4	4 0417	79 4	4 0434	80 1	4 0398	4 0396	77 0
1 hr	4 0432	76 1	4 0411	77 4	4 0437	74 5	4 0402	4 0407	73 2
3 hr	4 0434	72 7	4 0408	73 6	4 0436	71 4	4 0403	4 0404	70 6
9 hr	4 0432	67 9					4 0402	4 0403	62 3
	1	Reheated { 2 min 1 hr } 300° C Quenched boiling water						1	Reheated { 20 min. 1 hr 3 hr. } 300° C. Quenched cold water
	4 0411							4 0424	
	4 0411							4 0430 4 0427	

the small wires, exhibits no maximum, and has approximately the shape of the theoretical curve for a reaction of the first order.

The effect of quenching strain on parameter values seems to account for. (1) the differences noted in specimens quenched from 550° C.; (2) the initial "incubation" drop occasionally noticed at the start of the precipitation treatments; (3) the differences maintained at 400° C., which is a temperature high enough to cause new strains upon each quench therefrom; and finally (4), the gradual decrease in parameters at 325° and 300° C., temperatures that appear to be high enough to eliminate ultimately the strain that originated in the quench from 550° C. and yet low enough so that additional strain on quenching from the low temperatures can gradually be at least partly relieved. Since strain is generally acknowledged to be a factor in accelerating reactions, the quenching strain seems to be a logical explanation of the earlier occurrence of the reaction consistently observed in the  $\frac{1}{2}$ -in. rods. In the course of the work it was also found that the  $a_0$  value of the  $\frac{1}{2}$ -in. specimens quenched from the heat treatments on different days were apt to vary occasionally by an amount greater than the experimental measurement error. It seems probable that these variations were real and probably were due to changes in temperature of the tap water used for quenching.

A  $\frac{1}{2}$ -in. specimen, quenched from 550° C. in cold water, was carried through the 300° C. treatments and quenched from these in boiling water, and, conversely, a similar specimen quenched from 550° C. in boiling water was treated at 300° C. and quenched in cold water. The resulting reaction curves, shown in Fig. 5 (Data, Table 8), indicate that strain originating in the quench from the solution treatment at 550° C. is an important factor determining the start of the reaction curve but that its subsequent course is determined by the quenching method from 300° C. This was further demonstrated by taking a  $\frac{1}{2}$ -in. rod at the maximum  $a_0$  point above pure aluminum and quenching in boiling water after an additional heat treatment of 2 min. at 300° C. The parameter decreased to a value approaching the true one. Again, when a  $\frac{1}{2}$ -in. specimen at a comparable point along the true or equilibrium reaction curve was reheated for additional times at 300° C. and quenched in cold water, the  $a_0$  value increased to nearly the usual maximum point above pure aluminum. These effects are also shown in Fig. 5. Finally, when the two sizes of pure aluminum were air-cooled from a high temperature, the  $a_0$  values became identical (4.0410Å). A consideration of all the data seems to indicate that in addition to the temperature of the quenching bath, two related factors function in connection with the strain effect; namely, the temperature from which the specimen is quenched and, to a smaller degree, the amount of copper in solution at this temperature.

Here it seems pertinent to refer again to the work of von Goler and Sachs and of Stenzel and Weerts,<sup>11</sup> who found parameter values above pure aluminum for aluminum-copper alloys in the course of precipitation treatments. It seems probable that the quenching strain was responsible for the results in both studies, particularly in those of the latter workers, who used specimens 5 mm in diameter. Stenzel and Weerts were inclined to believe that the strain incidental to the lattice and volume changes accompanying the precipitation of  $\text{CuAl}_2$  was responsible for their maximum values. However, strain produced by precipitation cannot be a significant factor, since in our experiment just mentioned (Fig. 5), a specimen after having completed the precipitation reaction at 300° C. attaining an equilibrium  $\alpha_0$  value, upon reheating at 300° C and quenching in cold water again showed a parameter larger than that of aluminum. With regard to the second form of  $\text{CuAl}_2$  reported by Weerts, we have no evidence, since  $\text{CuAl}_2$  lines did not appear until annealing times of over a week were employed, by which time the effect of quenching strain in causing maximum  $\alpha_0$  values had disappeared.

X-ray technique in its present state of development has proved inadequate in completely defining and evaluating the different types of lattice "distortion" or strain present in metallic materials, so that nothing has been attempted in this direction other than qualitative visual comparisons of line broadening. However, it seemed of interest to inquire into the penetration depth represented by our back-reflection photograms. The polished surface of a 5.4 per cent copper alloy, quenched from the solid solution treatment, was covered with single sheets of aluminum foil of various thicknesses, held tightly and smoothly against the alloy surface by a very thin film of vaseline. The composite specimens were X-rayed under closely controlled and identical conditions of tube current, applied voltage, exposure and development times. Reflection lines from the aluminum foil naturally increased in intensity as the foil thickness increased while the alloy lines correspondingly decreased in intensity, finally disappearing with a foil thickness of 0.004 in. Hence it appears certain that the observed effects of strain on lattice constants may apply strictly only to that lattice extending from the surface to a depth of 0.004 in. It is impossible to say with any certainty what parameter values hold in the interior of the specimen, since by any method of removing the surface layers the strain relationships existing in the interior are altered.

#### RELATED HARDNESS CONSIDERATIONS

The  $\frac{1}{2}$ -in. specimens used for lattice measurements in the preceding work were also adapted for Rockwell hardness measurements. The differences in the time required for precipitation to start in large and

---

<sup>11</sup> References of footnotes 1 and 2

small specimens as a function of previous quenching strains clearly indicate that hardness measurements, to be of significance when correlated with parameter measurements, should be made on the same specimens. Results so obtained in the course of this work seem to be worthy of mention.

Rods quenched from the solution treatment at 550° C in media at temperatures of from -20° to 150° C were allowed to age at room temperature. The lattice parameter values found, together with the accompanying hardness changes, are given in Fig. 4 (Data, Table 7). It appears that the rate and magnitude of the age-hardening process is greatly influenced by the previous quenching speed. Although perhaps it is impossible to cool a supersaturated solid solution to room temperature rapidly enough to suppress the breakdown of the metastable phase without introducing strain, the  $\frac{1}{2}$ -in rod cooled in still air seems to approach this ideal most closely. No precipitation occurred during the cooling process, as shown by the parameter value and, up to the end of 30 days, practically no hardening was observed. In the same period, marked increases in hardness were found in the other specimens, reaching a maximum in the rod cooled in a  $\text{CaCl}_2$ -water mixture at -20° C. The corresponding parameter values shown in Fig. 4 range from no change in the air-cooled rod to a small decrease in the more severely quenched specimens. The decrease does not seem, at first thought, to be connected with a precipitation process that normally would involve an increase in the  $a_0$  value. Nor can it be due to a re-solution of compound precipitated in some way by quenching stresses, since this would involve an increase in the metastability or free energy of the lattice and probably a softening effect. It seems likely that the age-hardening at room temperatures is related in an unknown manner to a partial relief of the original quenching strain. Although the parameter of the quenched specimen has decreased slightly, it is still considerably above that of the nonaging, air-cooled specimen, and it seems possible that the relief of strain has been accompanied by an actual precipitation. With one exception, the lower the lattice parameter value of the quenched alloy, the less the magnitude of room-temperature hardening. Although our data suggest the possibility of an actual precipitation, the evidence is admittedly too meager definitely to establish this point. Also, it must be remembered that these observations strictly apply only to the depth of penetration of X-rays contributing to our photograms, 0.004 in., and the depth of penetration of the Rockwell hardness penetrator (with a  $\frac{1}{16}$ -in ball, 60-kg. load). There is reason to believe that they may hold, qualitatively, throughout the cross-section; e. g., drilling out the center of the rod causes the outer layers to revert to nearly the equilibrium  $a_0$  value. The suggestion may be advanced that no room-temperature aging will occur in the high-purity aluminum-copper alloys without the presence of quenching strains and

that when these are present the age-hardening may or may not be accompanied by an actual precipitation of  $\text{CuAl}_2$

It is of interest here to consider the age-hardening of zinc-aluminum alloys. Fraenkel<sup>12</sup> reported that it was necessary to quench these alloys from temperatures considerably above the solid solubility limit in order to develop room-temperature aging at all, although the quench from just above the line should preserve the solid solution intact. P. D. Merica,<sup>13</sup> in commenting upon these results, presumed that . . . "the higher quenching temperature serves better to suppress the transformation during the first quenching treatment and consequently permits better the later development of the aging process." In view of our results, the data of Fraenkel may be reinterpreted from the viewpoint that the higher quenching temperature results in a greater strain effect and hence facilitates the subsequent aging process. A similar effect is well known in the iron-carbon alloys, which may retain considerably more austenite after a relatively slow oil quench than after more drastic quenches in water or iced brine.

Proceeding to the hardening found at 275° and 300° C., as shown in Figs. 2, 3 and 5, it will be noted that in all cases the maximum hardness value was obtained when the precipitation reaction, as indicated by parameter changes, was practically complete. This was true whether the rods were quenched in cold water when the reaction together with the hardness maximum occurred early, or whether the rods were quenched more slowly in boiling water when the precipitation together with the hardness maximum came correspondingly later, and, incidentally, with less magnitude. It seems to be generally assumed that in these alloys, even at elevated temperatures, the hardness maximum is usually obtained before any appreciable precipitation occurs. The foregoing work shows how such a result may easily be obtained if small wires are used for the parameter measurements and large specimens for the hardness tests.

In Figs. 2, 3 and 5, the "incubation" drop in hardness found by Fraenkel was again observed. However, when the air-cooled specimen that had shown no aging at room temperatures was heated at 300° C., no incubation drop was noted. This result is consistent with the rather generally accepted theory of "knot" formation (which possibly may be an actual precipitate) at room temperatures and the explanation for the "incubation" drop in hardness in the early stages at elevated temperatures; namely, the re-solution or breakdown of the "knots."

### SUMMARY

1. Aluminum-copper alloys of high purity, quenched from a full solution treatment, may have an abnormally large lattice parameter. It

<sup>12</sup> W. Fraenkel. *Ztsch. f. Metallkunde* (1930) **22**, 84

<sup>13</sup> P. D. Merica: *Trans. A I M E* (1932) **99**, 13.

has been found that this increase in lattice dimension is a result of strain induced by the stresses originating in the quenching operation. In general, our tests indicate that the parameter value is larger with increasing (a) rapidity of cooling, (b) specimen diameter, up to  $\frac{1}{2}$  in., and (c) copper concentration of the solid solution.

2. Alloys containing 5.4 per cent copper in solution and quenched most drastically, in addition to showing the most abnormally high  $a_0$  values, had the maximum age-hardening capacity at room temperatures. During the aging period, there seems to be a very slight initial decrease in parameter towards the equilibrium value, as has been found in duralumin. However, it becomes constant at a value sufficiently high to attribute the hardening process to a possible, but unproved, partial precipitation. Since stress caused the original large  $a_0$  value, it is logical to assume that the initial decrease in parameter is due to a lattice adjustment coincident with the gradual relief of stress. It is also conceivable that the opposing stress or lattice change normally associated with the separation of the segregate during aging cancels the effect of the initial tendency, hence preventing any further parameter change.

3. Similar specimens cooled slowly enough to reduce quenching strains greatly and yet sufficiently rapid to preserve the metastable solid solution exhibit no tendency to age-harden within a period (30 days) that permits almost maximum hardening in the rapidly quenched rods. Although this slow cooling treatment may merely delay the hardening reaction to a period of months or years, rather than days, the results at present suggest that strain may be an essential condition for room-temperature aging in these alloys.

4. The greater the degree of strain resulting from the solution treatment and quench, and from the degree of supersaturation, the sooner precipitation takes place at elevated temperatures (275° to 325° C.)

5. By a rapid quench from the precipitation treatment temperatures, the parameter value of the matrix solution is found to be considerably higher than that of pure aluminum. By air-cooling or quenching in boiling water from these temperatures, a normal reaction curve is obtained, indicating the probable equilibrium condition. Further reheating at the precipitation temperature followed by a drastic quench again results in the abnormally large value. Thus it appears that this condition cannot be attributed to strain induced by the precipitation of  $\text{CuAl}_2$ .

6. Irrespective of the strain condition, the maximum hardness values as determined on the X-ray specimens during reaction studies at 275° and 300° C. were attained after precipitation was practically complete.

7. Our results seem to indicate, for the aluminum-rich copper alloys at least, that quenching-strain effects, particularly in association with specimen dimensions, are far more effective in influencing param-

ter determinations than the method of specimen preparation and other factors considered

8 Since the magnitude of quenching strains is greatly influenced by specimen dimensions, all hardness measurements and other physical tests, to be of significance in relation to parameter values, should be made on the actual X-ray specimens.

## DISCUSSION

(Robert H Aborn presiding)

C S BARRETT,\* Pittsburgh, Pa (written discussion) —The many careful experiments reported in this paper prove conclusively that internal stresses are present in the authors' quenched rods, and that such stresses affect the reaction curves as determined by X-rays. It is worth while, I believe, to calculate the magnitude of the stresses in the outer fibers of these specimens. It will take but a few moments to indicate how such calculations may be made from the X-ray data given in the paper.

Quenching stresses in the outer fibers of a solid cylinder are approximately equal in the longitudinal and tangential directions, while they are always zero in the direction of the normal to the surface. If these stresses are thought of as acting on a spherical element of volume in the unstressed metal, the sphere will be deformed into an ellipsoid. By applying the theory of elasticity to this "deformation ellipsoid" it can be shown that under the conditions just mentioned, if the material is isotropic (and aluminum alloys are, approximately), the strain at an angle  $\phi$  from the normal to the surface is

$$\epsilon_{\phi} = \frac{\sigma}{E} \{ \sin^2 \phi - \nu(1 + \cos^2 \phi) \} \quad [1]$$

where  $\sigma$  is the longitudinal (or tangential) stress,  $E$  is Young's modulus, and  $\nu$  is Poisson's ratio. The strain in certain directions can be obtained from X-ray measurements of  $a_0$ , if a beam of X-rays is directed normal to the surface and is diffracted at an angle of  $\theta$  degrees, the strain at an angle of  $\phi = \frac{180 - 2\theta}{2}$  will be

$$\epsilon_{\phi} = \frac{a_0' - a_0}{a_0} \quad [2]$$

where  $a_0$  is the lattice constant of the unstressed metal and  $a_0'$  is that of the stressed metal, as calculated from the diffraction ring at  $\theta$  degrees. It happens that the data recorded in this paper were obtained by plotting  $a_0$  against  $(90 - \theta) \cot \theta$  and extrapolating to  $\theta = 90^\circ$ . This extrapolation, when applied to the particular diffraction lines used in this paper, results in a value of the lattice constant within 2 per cent of the value that would be found by diffraction at the angle  $\theta = 90$ . Therefore it is permissible to let  $\theta = 90$  in equation 1 (i.e.,  $\phi = 0$ ), and combining equations 1 and 2 the longitudinal or tangential stress is given by

$$\sigma = -\frac{a_0' - a_0}{a_0} \frac{E}{2\nu} \quad [3]$$

Substituting the proper constants for these alloys ( $E = 10,000,000$ ,  $\nu = 0.36$ ,  $a_0 = 4.029$ ), this reduces to

$$\sigma = -3,450,000(a_0' - a_0) \text{ lb per sq in} \quad [4]$$

providing  $a_0'$  and  $a_0$  are given in Ångströms. When  $\sigma$  is negative the stress is com-

---

\* Metals Research Laboratory, Carnegie Institute of Technology.

pressive This formula may be applied only to the data on specimens that have the same composition and are free from precipitation

We will now apply formula 4 to some of the experiments cited in the paper where quenching stresses have been set up without the occurrence of precipitation In Table 1, a 5.02 per cent Cu rod  $\frac{1}{2}$  in in diameter that was quenched from 550° into cold water gave an  $a_0$  0.0039 Å larger than the value for a small wire of 5.04 per cent Cu, which had been similarly treated If the 0.07-in wire contained no quenching stresses, as is very likely, this indicates that the rod had compressive longitudinal and tangential stresses of about 13,000 lb per sq in in the surface fibers The 5.46 per cent specimens listed in Table 1 show  $a_0' - a_0 = 0.0049$ , from which it follows that compressive stresses in the surface amounted to 17,000 lb per sq in The data in Table 1 indicate lower stresses for the 2.4 per cent specimens; namely, 5000 to 6000 for the  $\frac{1}{4}$ -in rod and 6000 to 7000 for the  $\frac{1}{2}$ -in rod The 15 per cent alloy of Table 1 had a stress of 15,000 lb per sq in Pure aluminum, according to the data of Table 1, was only slightly stressed by the quenching operation, the  $\frac{1}{2}$ -in rod having 1000 lb per sq in On page 104, a 5.4 per cent rod quenched from 550° in cold water gave a lattice constant 0.0043 Å larger than the same rod after drilling to a wall thickness of 0.05 in The drilling therefore released a stress of 15,000 lb per sq in in the outer layers From the data in Table 7, we can determine the effect of the quenching medium on the intensity of the surface stresses in  $\frac{1}{2}$ -in rods of 5.4 per cent alloy, as follows.

Quenching medium	Brine at -20° C	25° water	65° water	100° water	150° salt	Still air
Stress, lb per sq in compression	17,000	18,000	6,000	0	3,000	0

Summarizing, the stresses appear to increase with increasing diameter of the specimen, with increasing rate of quench, and with increasing copper content up to about 5.4 per cent Cu, after which it remains about constant In every case the surface is in compression, as would be expected from plastic deformation originating in the temperature gradients caused by the quench The authors have proved that no precipitation occurred on the surface and the fact that the surface is in compression also indicates that there is no appreciable precipitation within the specimen, for internal precipitation would tend to throw the surface into tension For if there were internal precipitation the solid solution would become lower in copper content in the interior than at the surface, and this in turn would bring about an increase in specific volume of the interior and throw the surface into tension The formation of  $\text{CuAl}_2$  particles might add to the effect, also

These conclusions confirm those of Kempf, Hopkins and Ivanso (p 158, this volume) On quite similar aluminum alloys they found outer fiber stress increasing in intensity with increasing specimen diameter, for example, an alloy of 10 per cent Cu and 1.2 per cent Fe quenched in ice water from 482° C had longitudinal compressive stress of 10,000 in a 1.45-in rod, and a stress of 20,000 in a 1.85-in rod They also found that quenching stresses increased with the rate of cooling; quenching in boiling water produced no stresses greater than 5000 lb per sq in And, finally, they found lower stresses in aluminum than in aluminum alloys

L. W. KEMPF,\* Cleveland, Ohio (written discussion)—The authors have satisfactorily explained the various effects, but for the sake of additional emphasis it might be worth while to consider the shape of these parameter curves from a slightly different viewpoint Apparently many factors affect the shape of these curves, among the

\* Aluminum Company of America



most important of which we may consider the variation in the lattice constant arising from (1) the solution or precipitation of copper, (2) the strains induced by quenching from the solution heat-treating temperature, (3) the strains induced by quenching from the reheating temperature, and (4) the variation in the rate of the relief of internal stress at the various reheating temperatures

The curve in Fig 5 for the  $\frac{1}{2}$ -in rod and  $\frac{1}{16}$ -in wire quenched from 550° C into boiling water, reheated to 300° C and quenched in boiling water, may be taken as illustrating the normal course of the changes in lattice parameter due only to solution and reprecipitation of copper at 550° and 300° C, respectively. The variations in lattice parameter induced by the strains arising from quenching from the solution heat-treating temperature are illustrated by the difference in the as-quenched parameter values of the wire and  $\frac{1}{2}$ -in rod quenched in cold water from the solution heat-treating temperature. This effect is also illustrated by the curve in Fig 5 for the  $\frac{1}{2}$ -in rod quenched from 550° C in cold water, reheated at 300° C and quenched in boiling water. The effect of drastic quenching from the reheating temperature is illustrated by the curve in Fig 5 of the  $\frac{1}{2}$ -in rod quenched from 550° C in boiling water, reheated to 300° C and quenched in cold water. The effect of the rate of stress relief is illustrated by the curves of Fig 2 for the temperature 275° C as compared with the 325° C and 400° C curves of Fig 1. At 400° C the rate of stress relief is very rapid and the differences in lattice parameter of the reheated specimens must be due only to the difference in internal strain induced by quenching the various sized specimens from the reheating temperature into cold water. At 275° C the rate of stress relief is relatively slow and the shape of the curves is considerably affected by the internal strain induced by quenching from the solution heat-treating temperature of 550° C. The relatively low rate of stress relief at temperatures in the neighborhood of 300° C may permit an accumulation of stress by repeated quenching, which the rapid rate of relief at temperatures in the neighborhood of 400° C prevents.

It is interesting to note from the curves of Fig 2 that quenching in cold water from 550° C induces appreciable internal stress even in the  $\frac{1}{16}$ -in wire. These stresses are relieved at 275° C as indicated by the gradual decrease of the parameter to a value somewhat less than that for pure aluminum. At 300° C also the rate of relief of internal stress is slow enough so that a slight amount of the stress induced in the  $\frac{1}{16}$ -in wire by quenching from the high-temperature solution treatment is preserved after considerable reheating. Apparently quenching the wire from 300° C does not result in the development of stresses of any great magnitude. At least the stresses in the wire are nowhere near as great as those developed in the  $\frac{1}{2}$ -in rod quenched from the same temperatures. At 325° C the rate of relief of stress induced by the high-temperature quench is rapid enough so that none of this effect is noticed in the curve for the wire. It is also suspected that the large parameter obtained with the  $\frac{1}{2}$ -in. rod at 325° C is principally the result of the quenching from this temperature rather than from the solution temperature.

The authors say that "the effect of quenching strain on parameter values seems to account for . . . the gradual decrease in parameters at 325° C and 300° C, temperatures that appear to be high enough to eliminate ultimately the strain that originated in the quench from 550° C and yet low enough so that additional strain on quenching from the low temperatures can gradually be at least partly relieved." It is rather difficult to understand how the strain induced by quenching from the reheating temperature can be gradually relieved inasmuch as it is established anew immediately prior to each parameter determination. Fig 5, from the data on the  $\frac{1}{2}$ -in rod quenched from 550° C. in cold water, reheated to 300° C and quenched in boiling water, shows that the strain induced by the high-temperature quench is practically eliminated in a relatively short time, whereas the strain induced by quenching in cold water from reheating temperature, as illustrated by the data on the  $\frac{1}{2}$ -in rod quenched

from 550° C in boiling water, reheated to 300° C and quenched in cold water, persists over a long period of time. The authors have demonstrated by drilling out the center of their  $\frac{1}{2}$ -in cylinders that the strain induced by quenching is thus practically eliminated. This, together with the authors' statement that the diffraction lines were generally quite sharp, indicates that the type of strain is substantially homogeneous or macroscopic. Some studies in these laboratories have indicated that this type of internal stress induced by high-temperature quenching in cold water is relieved at 300° C at a rate quite comparable with that indicated in the authors' data (Fig 5) for  $\frac{1}{2}$ -in rod quenched from 550° C in cold water, reheated at 300° C and quenched in boiling water. As indicated elsewhere (p 158, this volume), quenching large sections in boiling water results in relatively little internal stress.

The coincidence of the continuous and cumulative reheating curves of Fig 3 and Table 6 also indicates the strain induced by quenching from the reheating temperature to be a much more important factor affecting the shape of the parameter curve than the strain induced by the quench from the solution treatment. The reason for the gradual reduction in lattice parameter on continued reheating followed by quenching in cold water awaits additional data. It may be suggested that the effect may have its origin in a change in conditions, such, for example, as a gradual increase in thick-

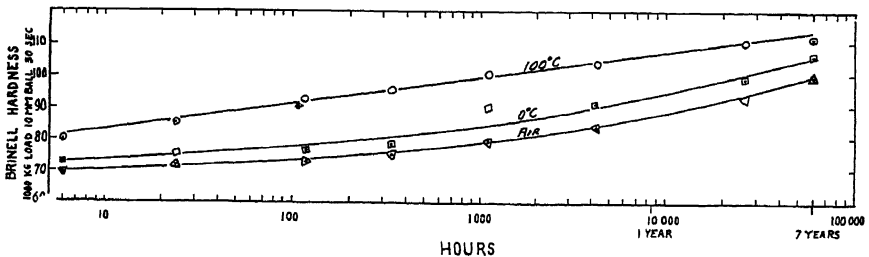


Fig 6 —AGING OF A 5.63 PER CENT COPPER ALLOY AT ROOM TEMPERATURE FOLLOWING QUENCHING AS INDICATED FROM 64 HOURS AT 545° C

ness of oxide film, which would make for lower stresses on quenching from the reheating temperature. Also, as suggested in the foregoing, there may be a gradual accumulation of stress in early shorter stages of reheating, which is eliminated in the longer periods of heating. Under these conditions the parameter should decrease to and become constant at some value above the equilibrium value, showing the effect of a single quench from the reheating temperature.

It is interesting to refer to an observed experimental result (p 163, this volume), which could not be explained at the time. We repeatedly noted an expansion of pure aluminum cylinders quenched in cold water from about 520° C. This expansion may have been due to the effect of the internal stress induced by the quenching. The expansion in pure aluminum cylinders amounted to about 0.05 per cent, which is of the same order of magnitude as the parameter differences noted by the authors. It was entirely absent on cylinders of pure aluminum quenched in boiling water.

It is to be hoped that the authors will extend their investigations to reheating temperatures more nearly comparable with those utilized for the precipitation-hardening of commercial alloys; that is to say, in the neighborhood of 150° to 200° C. The reactions within this range of temperature appear to be somewhat different, although perhaps only in degree, from those that take place at the considerably higher temperatures used in this investigation. The authors' suggestion that, in this type of alloy quenched in such a manner as to be entirely stress-free, hardening might not take place at room temperature, is worth some consideration.

The diagram of Fig 6 shows the aging of a high-purity (0.03 per cent iron, 0.03 per cent silicon) 5.6 per cent copper alloy at room temperature following quenching from an extended solution treatment at 545° C. As indicated on the curves, the alloy was quenched in water at 0° C, in water at 100° C, and cooled in a gentle breeze from an electric fan. The material was prepared by forging a chill-cast  $3\frac{1}{2}$ -in square ingot to about  $\frac{3}{4}$  in square. Aging continued over this entire period of time regardless of the manner of quenching and at approximately equivalent rates, although the hardness attained is appreciably different for the different manners of quenching. The detailed shape of the curves is probably not significant inasmuch as no attempt was made to keep the specimens at constant temperature, and it is to be expected that the aging rate varied considerably with the season of the year.

Figs 7 and 8 illustrate the progress of aging at 150° C and 170° C of the same alloy quenched in the same three manners. At these elevated temperatures the effect of

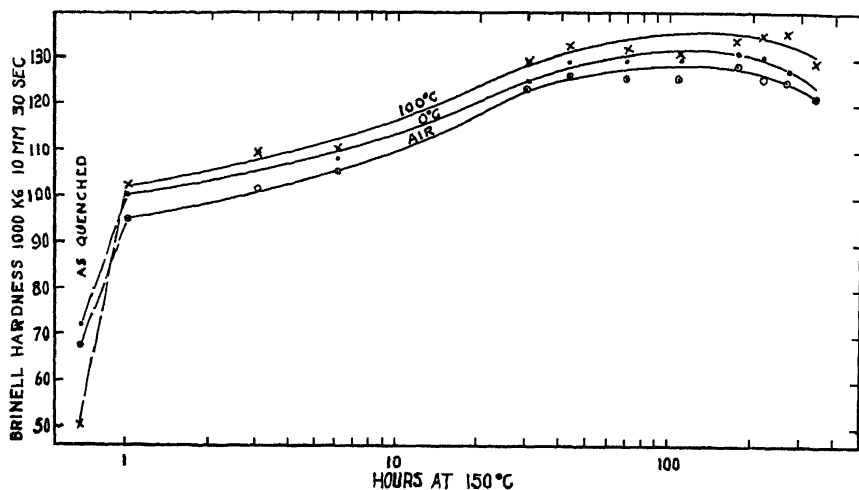


FIG 7—AGING OF A 5.63 PER CENT COPPER ALLOY QUENCHED AS INDICATED FROM 64 HOURS AT 545° C

quenching rate on aging is in general the same as at room temperature. The specimens quenched in boiling water reach and maintain the highest hardness while the material quenched in water at 0° C and cooled in air yield curves showing lower hardnesses but approximately paralleling the curve for the material quenched in boiling water. Here again the detailed shape of the curves is probably not significant, since undoubtedly they were affected by factors such as interruptions and holdings for various periods at room temperature, which we have since learned somewhat affect the course of aging at the elevated temperature.

With regard to the effect of rate of quench on the incubation period, the alloys aged for 7 years at room temperature were reheated to 170° C and the hardness determined after various periods of time. The hardness values are given in Table 9, and indicate that the rate of quenching has but little effect on the incubation period, as evidenced by the marked softening of all materials in the early stages of the reheating at 170° C. The incubation period as evidenced by softening on reheating is very fugitive at the higher temperatures, which probably accounts for the failure of the authors to note it in some of their experiments.

A. PHILLIPS and R. M. BRICK (written discussion)—Dr Barrett's calculations of the stresses in our quenched specimens are a welcome addition to our paper. We are

naturally pleased that determinations, based on our parameter measurements, show stresses of the order of magnitude found by direct measurements on similarly quenched alloys. Dr. Barrett's qualification regarding his equation 4—namely, that “this

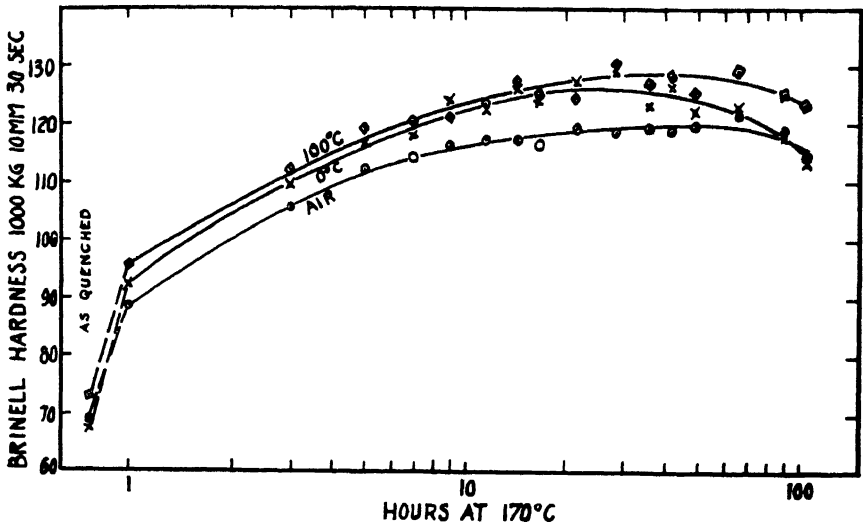


FIG 8 —AGING OF A 5.63 PER CENT COPPER ALLOY AT 170° C. QUENCHED AS INDICATED FROM 64 HOURS AT 545° C.

TABLE 9 —*Brinell Hardness of 5.63 Per Cent Copper, 0.03 Per Cent Iron, 0.03 Per Cent Silicon Alloy, Quenched as Indicated from 64 Hours at 545° C. and Aged 7 Years, 1 Month, 8 Days at Room Temperature; Reheated at 170° C (1000 Kg, 10 Mm, 30 Sec)*

Minutes at 170° C	Quenched in Water at 0° C	Quenched in Water at 100° C	Cooled in Breeze of Electric Fan
Approx 7 years at room temperature	107.7	112.8	100.6
15	91.8	90.4	85.0
30	97.4	95.1	89.9
45	100.9	98.5	94.2
60	103.6	101.5	97.9
90	106.1	102.4	99.4
120	107.0	105.0	100.0
150	107.4	105.0	100.0
180	109.8	105.7	101.8
240	110.9	109.5	104.0

formula may be applied only to data on specimens that have the same composition and that are free from precipitation”—may be somewhat misleading. This formula for obtaining the quenching stress is probably valid with composition change or in a specimen containing precipitated compound if the proper adjustment for the  $a_0$  value

is made. As a matter of fact, Dr Barrett used the formula for our 2 40, 5 04, 5 46 and 15 0 per cent copper quenched alloys and also for pure aluminum.

Mr Kempf's critical analysis of our data has been of great value in supplementing and clarifying some of the conclusions expressed in the paper. His earlier studies (p 158, this volume) in determining quenching stresses by mechanical means have proved to be of particular interest to us and we regret the omission of proper reference to this work.

In discussing the parameter curves for the heat treatments at 300° and 325° C, Mr Kempf suggests that the large parameter values for the 1/2-in specimens are due mainly to stress conditions of a cumulative nature originating in the quench from the reheating temperature, modified somewhat by stress relief at that temperature. Although we admit that such an accumulation of stress does occur, we believe it is relatively small in comparison with the relief of the stresses originating in the quench from the solution treatment. In Fig 1, a comparison of the "normal" reaction curve, as shown by the 1/16-in wire, and that for the 1/2-in rod shows the following parameter differences after the 325° C treatment

TIME AT 325° C	TIME SINCE PREVIOUS QUENCH	PARAMETER DIFFERENCE, Å
2 min		0 0058
5 min	3 min	0 0034
100 hr	60 hr	0 0009

The last value (0 0009 Å) may be considered to be the parameter increase attributable to a single quench from 325° C. The maximum difference found earlier in the heat treatment for equivalent periods is several times this value. Furthermore, in Fig 3 the coincidence of curves obtained by continuous and cumulative treatments at 300° C strengthens our belief that strain from the solution treatment quench is the important factor influencing the course of the parameter curves.

In this connection, a study of the data of Fig 5 reveals a condition not previously mentioned, namely, that when two 1/2-in rods are quenched from 550° C in boiling water (hence, substantially free from strain) and subsequently quenched from 300° C, cumulative treatments, one in cold and the other in boiling water, a nearly constant difference in parameter is obtained, as shown below.

TIMES AT 300° C	PARAMETER DIFFERENCE	TIMES AT 300° C	PARAMETER DIFFERENCE
0	0 0000	20 min	0 0038
2 min	0 0028	1 hr	0 0030
6 min	0 0032	3 hr	0 0032

It is obvious that the maximum influence of additive stresses produced by quenching from 300° C after the 20-min treatment (involving three quenches) is relatively slight.

Mr Kempf's data on the effect of quenching stresses on the room-temperature aging characteristics of these alloys are of interest, particularly since they include observations extending over a long period of time. We are not sure, however, that Mr Kempf's results disprove our suggestion that quenching stresses are an important factor in accelerating and, perhaps, actually causing, age-hardening. It is entirely possible that the circulation of air from an electric fan may result in un-uniform cooling, thereby producing cooling stresses of some magnitude. The size and shape of the specimens, not given by Mr Kempf, may also be significant in this connection.

# An X-ray Study of Orientation Changes in Cold-rolled Single Crystals of Alpha Brass\*

BY CARL H. SAMANS,† BETHLEHEM, PA

(New York Meeting, October, 1934)

THE attention of physicists and metallurgists has been directed toward the study and explanation of the deformation textures in metals for the past 15 years. In 1920 N. Uspenski and S. Konobejewski<sup>1</sup> were first able to show that the symmetrical X-ray diffraction effects that had been previously reported by E. Hupka<sup>2</sup> and others in metal foils were caused by a directed arrangement of the crystallites. Since then, the systematic study of textures resulting from the application of the pure forces of tension or compression to polycrystalline materials has been supplemented by many investigations on deformed single crystals, which have greatly added to our knowledge of deformation. However, despite the valuable information secured from these comparative studies only four investigations upon cold-rolled single crystals of any of the face-centered cubic metals have been reported in the literature. This lack of quantitative data is especially unfortunate because of the much greater practical significance of rolling textures and their effects in both cold-rolled and annealed materials. This investigation was undertaken for the purpose of specifying the deformation of rolled single crystals in the hope that such information might later facilitate the explanation of polycrystalline textures.

Of the four studies that have been made upon cold-rolled single crystals, only two are of any quantitative value. S. Tanaka,<sup>3</sup> working

---

\* A part of a dissertation presented by the author to the Faculty of the Graduate School of Yale University in partial fulfillment of the requirements for the Degree of Doctor of Philosophy. Manuscript received at the office of the Institute Sept 12, 1934

† Instructor, Department of Metallurgical Engineering, Lehigh University; formerly Junior Metallurgist, Chase Brass & Copper Co., Waterbury, Conn.

<sup>1</sup> N. Uspenski and S. Konobejewski: Lecture before Russian Physical Lebedev Society, April 30, 1920. *Jnl Russian Phys.-Chem Soc* (1922) 50 (Phys.), 173-184; *Ztsch Physik* (1923) 16, 215-217

<sup>2</sup> E. Hupka: Ueber den Durchgang von Roentgenstrahlen durch Metalle *Physikal Ztsch* (1913) 14, 623

<sup>3</sup> S. Tanaka: The Effect of Rolling on Single Crystals of Aluminum. *Mem Coll Sci., Kyoto Imp Univ.* (1927) 10A, 303.

with single crystals of aluminum prepared by the strain-annealing method, found that rolling caused the crystals to break up into microcrystals which, after heavy reductions, tended to arrange themselves according to three principal types of orientation structures. In the first of these the rolling direction corresponded to a  $[110]$  direction and the  $(001)$  planes were nearly parallel to the rolling surface. The maximum deviation from this orientation was about  $26^\circ$ , produced by a rotation of the crystals about the rolling direction. In the second,  $[112]$  directions were approximately parallel to the rolling direction while  $(110)$  planes were nearly in the rolling plane, the maximum deviation in this case being about  $28^\circ$ . The third type reported had a  $[111]$  direction parallel to the rolling direction and  $(110)$  planes nearly in the rolling plane. His results also indicated still a fourth arrangement in which a  $[111]$  direction was parallel to the rolling direction and  $(112)$  planes were nearly in the rolling plane, but proof of this was not definite.

While these results are valuable, Tanaka was able to offer no specific information concerning the manner of deformation except that, for the orientations studied, no simple relationship between the existing orientation of the crystal, the direction of rolling, and the final state of the fibrous structure could be found. However, the fact that his crystals tended to fragment even after reductions of the order of 6 per cent suggests that the strain-annealing method might not be suitable for preparing crystals to be deformed by such complex forces.

T. Sakao,<sup>4</sup> believing that Tanaka's studies had been made upon material too severely worked, sought to add to it by investigating the orientation changes in seven different single-crystal plates of aluminum after lighter reductions, using the Laue method to study the scattering of the microcrystals. His results indicated that these crystals rotated, to some extent, around an axis parallel to the surface of the specimen and perpendicular to the rolling direction, regardless of the orientation of the crystallographic axes. The maximum angle of rotation was found to increase proportionally with the reduction in thickness of the plate by rolling.

F. Wever,<sup>5</sup> and W. G. Burgers<sup>6</sup> also made X-ray studies of rolled single crystals of aluminum but their results were only used to show, qualitatively, the changes in the normal Laue pattern that are produced by cold rolling.

<sup>4</sup> T. Sakao: On the Destruction of the Single Crystal of Aluminum by the Process of Rolling. *Mem. Coll. Sci., Kyoto Imp. Univ.* (1928) 11A, 279.

<sup>5</sup> F. Wever: Ueber die Walzstruktur kubisch kristallisierender Metalle. *Mitt. a. d. K. W. Inst. f. Eisenforschung zu Dusseldorf* (1924) 5, 69, *Ztsch. Physik* (1924) 28, 69.

<sup>6</sup> W. G. Burgers: Ueber den Zusammenhang zwischen Deformations- und Bear-

## PREPARATION OF SINGLE-CRYSTAL SPECIMENS

Single crystals of 70 30 brass, made by a modification of P W Bridgman's<sup>7</sup> method of slow cooling from the melt that was developed by H. L. Burghoff,<sup>8</sup> were chosen for the experimental study. In accordance with Burghoff's findings, these were given a high-temperature homogenizing anneal to remove coring, and then five specimens, approximately 1 in long,  $\frac{1}{2}$  in wide, and  $\frac{1}{8}$  in thick, were cut out at random for the rolling experiments. The loci of their orientations are shown in stereographic projection in Fig. 1. One-quarter of each specimen was left in the undeformed condition while each of the other three-quarters was given the reductions listed in Table 1, using a set of hand rolls  $2\frac{3}{4}$  in in diameter. By giving all the reductions to the same specimen, and by being sure that the same rolling surface was uppermost for each reduction, it was felt that the greatest possible

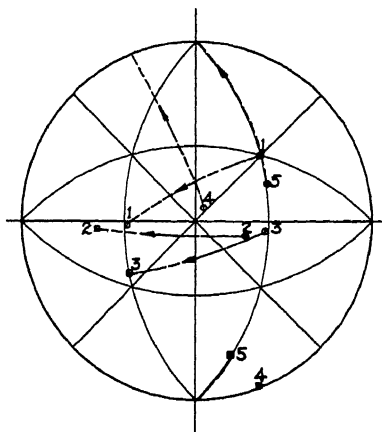


FIG 1—STEREOGRAPHIC PROJECTION SHOWING ORIENTATIONS OF FIVE SPECIMENS BEFORE COLD ROLLING

Poles of the rolling plane are represented by  $\circ$ , those of planes normal to rolling direction ( $90^\circ$  removed) by  $\square$

TABLE 1—Reductions Given to the Five Rolled Specimens

Specimen No	Original Thickness, In	Thickness after Rolling, In			Corresponding Percentage Reductions in Thickness		
		1	2	3	1	2	3
1	0 118	0 109	0 097	0 085	7 6	17 8	28 0
2	0 133	0 120	0 107	0 093	10 0	20 0	30 0
3	0 105	0 093	0 078	0 073	7 6	25 8	30 5
4	0 072	0 065	0 058	0 051	10 0	19 5	29 0
5	0 052	0 047	0 042	0 036	10 0	20 0	31 0

source of error was eliminated without impairing the value of the results in any way.

beitungs-Rekristallisationstextur bei Aluminium *Metallwirtschaft* (1932) 11, 251-255, 265-267

<sup>7</sup> P. W. Bridgman. Certain Physical Properties of Single Crystals of Tungsten, Antimony, Bismuth, Tellurium, Cadmium, Zinc, and Tin. *Proc Amer Acad Arts and Sci* (1925) 60 (6), 305

<sup>8</sup> H. L. Burghoff: The Preparation and Certain Properties of Single Crystals of Alpha Brass. M S Report, Yale University, 1930



Each of the specimens was given a deep etch in nitric acid to remove the flowed layer on the surface, and then examined using the Davey<sup>9</sup> method of X-ray analysis to determine the orientations of the individual sections, and thus follow the steps of the lattice rotation with increasing reductions. This X-ray technique is useless for higher degrees of deformation, though the orientations developed after greater reductions could, undoubtedly, be studied by simple pole-figure methods.

#### METHODS USED TO DETERMINE ACTIVE SLIP SYSTEM

If deformation by rolling be considered as a "plane parallelepipedal compression" as proposed by F. Wever and W. E. Schmid<sup>10</sup> two methods can be used to indicate the active slip plane: (1) the use of the maximum shear stress law, the validity of which has been proved for so many kinds of deformation that its application here seems quite permissible; and (2) the study of the lattice rotations.

In order to employ the first of these methods some expression for the shear stress must be secured. Other investigators, notably E. Schmid,<sup>11</sup> have used, for pure tension or compression, the expression

$$s/F = \cos \chi \cos \lambda$$

in which  $s/F$  is the ratio of the effective shear stress  $s$  to the applied force  $F$  and  $\chi$  and  $\lambda$  are the angles between the line of action of the applied force and the poles of the slip plane and the plane normal to the slip direction,<sup>12</sup> respectively, the first cosine function correcting for the effective area of the slip plane and the second for the inclination of the slip direction to the applied force. In order to apply this to plane parallelepipedal compression a further restriction must be added to that of the maximum shear stress law because of the unidirectional flow requirements. On this basis, then, the active slip system will be the one that is most highly stressed according to the above expression and that, at the same time, will produce the maximum lengthening of the specimen. The

<sup>9</sup> T. A. Wilson, *A Study of Crystal Structure and its Applications*, pt. XII. *Gen. Elec. Rev.* (1928) **31**, 612.

<sup>10</sup> F. Wever and W. E. Schmid, *Beiträge zur Kenntnis der Textur kaltverformter Metalle*. *Mitt. a. d. K. W. Inst. f. Eisenforschung zu Düsseldorf* (1929) **11**, 109; *Ztsch. Metallkunde* (1930) **22**, 133.

<sup>11</sup> W. Boas and E. Schmid, *Zur Deutung der Deformationstexturen von Metallen*. *Ztsch. f. tech. Physik* (1931) **12**, 71.

P. Rosbaud and E. Schmid, *Ueber Verfestigung von Einkristallen durch Legierung und Kaltreckung*. *Ztsch. Physik* (1925) **32**, 197.

<sup>12</sup> This expression differs from that of Schmid in the definition of the angle  $\chi$ . The angle given, complementary to his  $\chi$ , is more convenient when working with stereographic projections.

latter statement requires that the angle between the active slip direction and the plane through the normal and rolling directions be smaller for the active system than for any of the other most highly stressed systems.

In order to make use of the second method for determining the active slip plane, that of lattice rotation, it is necessary to compare the orientations of at least two successive reductions. G I Taylor,<sup>13</sup> in his noteworthy studies on the deformation of aluminum crystals by pure compression, found that the rotation of the crystallographic axes was such that the pole of the active slip plane tended to rotate along a great circle toward the pole of the plane of compression, in this case the rolling plane. It would seem logical, therefore, to expect a similar rotation to result from plane parallelepipedal compression, thus giving an indication of the active system.

An agreement between these two methods should, then, fix the active slip plane with reasonable certainty.

#### ORIENTATION CHANGES IN ROLLED CRYSTALS

For simplicity the orientations of the four quarters of each crystal have been plotted together in one composite stereographic projection, only the cube, octahedral, and dodecahedral poles being shown. In this representation the rolling plane is always considered as the plane of the projection, and the axes are arbitrarily chosen as parallel and perpendicular to the rolling direction. On this basis, the individual poles in each of the four projections of one specimen must be mutually derivable by a stereographic rotation. To conform to this restriction, in some instances, the individual projections had to be rotated a few degrees about an axis normal to the rolling plane. The required rotation was never more than about five degrees and was probably attributable to some irregularity in the rolling technique or to an error introduced by the unavoidable curling of some of the sections during rolling.

##### *Specimen 1*

In the undeformed section of this specimen an octahedral, (111), plane was nearly in the rolling plane, and a dodecahedral,  $[\bar{1}01]$ , direction was only a few degrees removed from the rolling direction. The lattice rotation with increasing reduction can best be seen from the projection of Fig. 2, the rotation of the pole (111) being shown to a larger scale in the lower left corner. From the locations of these poles shear stresses were computed, according to the equation given above, assuming a force of

---

<sup>13</sup> G I. Taylor. Distortion of Crystals of Aluminum under Compression, II.—Distortion by Double Slipping and Changes in Orientation of Crystal Axes during Compression. *Proc. Roy. Soc.* (1927) **116A**, 16



On further rotation of a similar kind, then, the stress on this system would be expected to continue to increase, eventually surpassing that on the initial system.

For some undetermined orientation, then, there will be a transfer of the slip to the system  $(111)/[10\bar{1}]$ , causing the lattice to rotate in the opposite direction about the same axis; i e., so that the pole  $(111)$  moves along a great circle toward the pole of the rolling plane

In the orientation of the section reduced 17.8 per cent this "counter-rotation" has taken place to such an extent that the first system has again become most highly stressed. After, perhaps, some further rotation the slip would be expected to be retransferred to the initial system, the rotation proceeding as in the first stage. This manner of deformation will explain satisfactorily the orientation found after 28 per cent reduction. At this stage the system  $(111)/[10\bar{1}]$  is definitely subjected to the highest stress, and it would be expected that, on further reduction, the deformation would continue to be a repetition of that previously described.

If, then, a specimen of this initial orientation continues to deform in a simple manner, the entire deformation can be explained by competitive (alternate) slip on the two systems  $(11\bar{1})/[011]$  and  $(111)/[10\bar{1}]$ . On this basis it would seem that either of two textures might be found after heavy reductions, depending upon which of these systems had been last active: (1) the  $(110)$  plane in the rolling plane and the  $[\bar{1}12]$  direction in the rolling direction, if the predominant system was  $(11\bar{1})/[011]$ ; or (2) the  $(111)$  plane in the rolling plane and the  $[\bar{1}01]$  direction in the rolling direction, if the predominant system was  $(111)/[10\bar{1}]$ . Inasmuch as in the first of these the impressed shear stresses are much higher than in the second, the  $(110) - [\bar{1}12]$  texture might be expected to be more probable.

The major steps of this deformation were confirmed by a study of three other specimens not reported here. One of these, even when rolled as much as 75 per cent, still seemed to conform to this manner of deformation, although proof of this was not entirely definite because of the limitations of the X-ray technique when used for these reductions.

### *Specimen 2*

This specimen was one of several used to study the deformation of orientations whose rolling plane is near a dodecahedral plane, when rolled in a dodecahedral direction. In this case the rolling plane made angles of  $15^\circ$ ,  $30^\circ$ , and  $33^\circ$  with  $(011)$ ,  $(111)$ , and  $(001)$ , respectively, while the rolling direction was near a  $[02\bar{1}]$  direction. The lattice rotation shown in Fig. 3 was quite different from that of specimen 1.

The shear stresses acting upon the most important systems, listed in Table 3 for the entire series of reductions, facilitate the explanation of the deformation to some extent. In the undeformed section the system  $(\bar{1}11)/[101]$  is definitely subjected to the highest stress and consequently

would be expected to become active, causing, on the basis of the rotation of specimen 1, the ( $\bar{1}11$ ) pole to rotate along a great circle toward the pole of the rolling plane. However, this rotation did not occur. Instead the

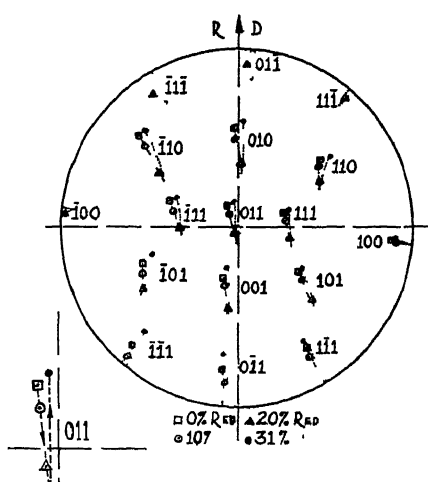


FIG. 3—COMPOSITE STEREOGRAPHIC PROJECTION SHOWING ORIENTATIONS OF FOUR SECTIONS OF SPECIMEN 2

tendency seemed to be to rotate the (011) pole toward the central position. This could result from a cooperative slip upon the two planes ( $\bar{1}11$ ) and (111), the first (and most highly stressed) system dominating the rotation while the second, by its action, tended to keep the rolling plane symmetrically located between the two.

This manner of rotation apparently has continued for a reduction of 20 per cent, at least, both slip planes being nearly parallel to the rolling direction at this point and therefore unfavorably situated for deformation. It might be expected, therefore, that the deformation

would be transferred to one or both of the other slip planes. Both of these are nearly perpendicular to the rolling plane and therefore subjected to a low shear stress. However, despite this, the final 11 per cent reduction and its resulting rotation can best be explained by a

TABLE 3.—*Shear Stresses Acting on the Most Highly Stressed Slip Systems of Specimen 2*

Slip System		Shear Stresses $s/F$ after Reductions of			
Plane	Direction	0 Per Cent	10 Per Cent	20 Per Cent	31 Per Cent
$(\bar{1}11)$	[101]	0.50	0.49	0.36	0.50
	[110]	0.36	0.39	0.45	0.27
	[0 $\bar{1}1$ ]	0.16	0.10	0.09	0.23
(111)	[ $\bar{1}01$ ]	0.43	0.42	0.36	0.47
	[ $\bar{1}10$ ]	0.24	0.30	0.45	0.21
	[0 $\bar{1}1$ ]	0.19	0.12	0.09	0.25
$(1\bar{1}1)$	[011]	0.23	0.19	0.12	0.26
	[ $\bar{1}11$ ]	0.12	0.05	0.07	0.21

cooperative slip of the two systems  $(1\bar{1}1)/[011]$  and  $(\bar{1}11)/[011]$ , tending to rotate the (0 $\bar{1}1$ ) pole toward the pole of the rolling plane.

It is difficult to predict, in view of the light reductions studied, just what textures might result from more heavily rolled specimens. If, as

seems logical, the deformation continues to take place by successive slip in the manner described above, it would be expected that they would be modifications of the ideal position: a dodecahedral plane in the rolling plane and a dodecahedral direction in the rolling direction. However, it might also be possible to secure textures derived from the position of a cube plane in the rolling plane and a cube direction in the rolling direction, provided the slip planes ( $\bar{1}\bar{1}1$ ) and ( $1\bar{1}1$ ) remained active long enough.

The transfer of the deformation to slip systems subjected to a very low shear stress was confirmed by rolling another specimen in which a dodecahedral plane was nearly in the rolling plane and a dodecahedral direction in the rolling direction. In this case slip began immediately on the perpendicular slip planes. This, strictly, is not a violation of the maximum shear-stress law, inasmuch as the most highly stressed systems (according to the compressive force alone) are unfavorably situated for producing both a reduction in thickness and a lengthening as required by the flow requirements of rolling.

### *Specimen 3*

The rolling plane of this specimen, inclined at  $5^\circ$  to the (011) plane, is near that of specimen 2, but in this case the rolling direction is only  $8^\circ$  from a  $[\bar{1}\bar{1}\bar{1}]$  direction instead of being near a  $[02\bar{1}]$  direction. This change in the rolling direction should limit the possible slip systems to  $(\bar{1}\bar{1}1)/[101]$  and  $(111)/[\bar{1}10]$ . The shear stresses acting on these two systems throughout the deformation have been listed in Table 4, with the stresses acting on

TABLE 4 — *Shear Stresses Acting on the Most Highly Stressed Slip Systems of Specimen 3*

Slip System		Shear Stresses $s/F$ after Reductions of			
Plane	Direction	0 Per Cent	7.6 Per Cent	25.8 Per Cent	30.5 Per Cent
$(\bar{1}\bar{1}1)$	$[101]$	0.47	0.40	0.42	0.51
$(111)$	$[\bar{1}10]$	0.36	0.41	0.38	0.19
$(1\bar{1}1)$	$[011]$			0.07	0.33

the system  $(1\bar{1}1)/[011]$ . According to these, the most highly stressed system would be expected to become active; i.e.  $(\bar{1}\bar{1}1)/[101]$ , causing the  $(\bar{1}\bar{1}1)$  pole to rotate toward the pole of the rolling plane.

However, instead of rotating in this simple manner, the deformation seemed to resemble that of the previous specimen. During the first stage of the deformation (up to an undetermined reduction between 7.6 and 25.8 per cent) the slip planes  $(\bar{1}\bar{1}1)$  and  $(111)$  cooperated, this action apparently continuing until the dominant plane  $(\bar{1}\bar{1}1)$  became practically parallel to the rolling direction. Then, as before, the deformation seemed to be transferred to the system  $(1\bar{1}1)/[011]$  despite the low

shear stress to which it was subjected. This system then remained active during the latter stages, thereby tending to rotate the (111) pole into the center of the projection in the manner described under specimen 1. This change in orientation with increasing reduction is indicated by the dotted lines in Fig. 4.

No definite texture can be specified from the data at hand. However, the orientation at which the slip is transferred from the initial to the secondary systems is probably near the ideal position, a (112) plane in the

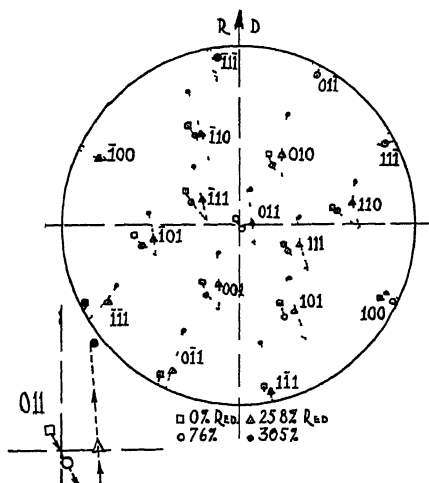


FIG 4.

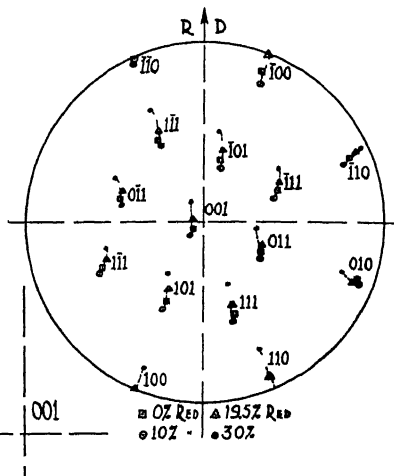


FIG 5.

FIG. 4.—COMPOSITE STEREOGRAPHIC PROJECTION SHOWING ORIENTATIONS OF FOUR SECTIONS OF SPECIMEN 3

FIG 5.—COMPOSITE STEREOGRAPHIC PROJECTION SHOWING ORIENTATIONS OF FOUR SECTIONS OF SPECIMEN 4

rolling plane and an octahedral direction in the rolling direction, so a texture of this nature might conceivably be found after heavy reductions

*Specimen 4*

Four systems are favorably located for deformation in this specimen for which a cube (001) plane is  $9^\circ$  from the rolling plane and a direction midway between  $[\bar{1}\bar{1}0]$  and  $[\bar{1}00]$  is the rolling direction. The shear stresses on these systems, listed in Table 5, would indicate that the system (111)/ $[\bar{1}01]$ , as the most highly stressed and most favorably located system, would be active during the entire reduction; i.e., up to 29 per cent. If this were so the (111) pole should tend to rotate toward the pole of the rolling plane.

However, from the projection of Fig. 5 it can be seen that the observed rotation does not entirely correspond to this although it is quite similar. During the first 10 per cent reduction, probably due to some irregularity in the rolling, either one or both of the systems  $(\bar{1}\bar{1}1)/[101]$  and  $(\bar{1}\bar{1}1)/[011]$

have been active. Because of insufficient data no further description of this stage of the deformation can be given. The reductions between 10 and 29 per cent seem to have taken place by slip on the system  $(111)/[\bar{1}01]$  as indicated by the shear stresses. However, the observed rotation could be about an axis in the rolling plane normal to the rolling direction (the transverse direction) equally as well as of the "compressive" type

TABLE 5.—*Shear Stresses Acting on the Most Highly Stressed Slip Systems of Specimen 4*

Slip System		Shear Stresses $s/F$ after Reductions of			
Plane	Direction	0 Per Cent	10 Per Cent	19.5 Per Cent	29 Per Cent
$(\bar{1}\bar{1}1)$	$[101]$	0.35	0.35	0.37	0.37
$(\bar{1}11)$	$[101]$	0.42	0.43	0.45	0.47
$(111)$	$[\bar{1}01]$	0.44	0.42	0.44	0.44
$(1\bar{1}1)$	$[\bar{1}01]$	0.33	0.33	0.37	0.31

previously discussed. The difference between these two axes is of the order of  $15^\circ$ , but whether the variation is caused by an error of measurement, by some action of the system  $(1\bar{1}1)/[\bar{1}01]$ , or by a different type of rotation cannot be entirely fixed. The insufficient data also make it difficult to specify any equilibrium texture for this initial orientation, although it would seem that a cube  $(001)$  plane would be near the rolling plane.

### *Specimen 5*

The rotation of this specimen was quite clear cut and simple to explain. In the undeformed section the rolling plane was almost on the great circle between  $(110)$  and  $(111)$ , inclined at  $15^\circ$  to the latter plane, while the

TABLE 6.—*Shear Stresses Acting on the Most Highly Stressed Slip Systems of Specimen 5*

Slip System		Shear Stresses $s/F$ after Reductions of			
Plane	Direction	0 Per Cent	10 Per Cent	20 Per Cent	31 Per Cent
$(11\bar{1})$	$[101]$	0.41	0.42	0.45	0.35
$(1\bar{1}\bar{1})$	$[011]$	0.41	0.44	0.43	0.38
$(111)$	$[10\bar{1}]$	0.23	0.27	0.35	0.44
$(11\bar{1})$	$[01\bar{1}]$	0.23	0.29	0.31	0.45

rolling direction was almost parallel to it. For this orientation, as shown by the shear stresses listed in Table 6, the systems  $(11\bar{1})/[101]$  and  $(1\bar{1}\bar{1})/[011]$  are subjected to the highest shear stress for all the orientations except the one after a 31 per cent reduction. The lattice rotation shown



in Fig 6 agrees with this, the rotation in every case being around an axis perpendicular to the great circle between  $(11\bar{1})$  and the center of the projection, i e, very nearly a transverse axis

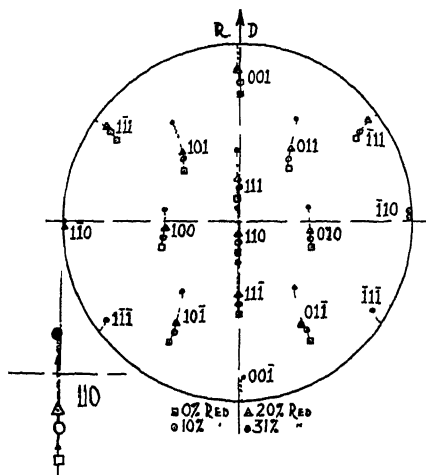


FIG 6—COMPOSITE STEREOGRAPHIC PROJECTION SHOWING ORIENTATIONS OF FOUR SECTIONS OF SPECIMEN 5

of the ideal position: a dodecahedral plane in the rolling plane and a cube direction in the rolling direction

## Summary

The lattice rotations found in rolled single crystals of five different initial orientations have been successfully explained on the basis of a "plane parallelepipedal compression" representation of the forces of rolling. In practically every case the active slip plane could be determined from both the maximum-shear-stress law and the manner of rotation which seemed to be quite similar to that reported by G. I. Taylor<sup>15</sup> for pure compression.

## THEORETICAL CONSIDERATION OF POSSIBLE TEXTURES

The number of textures possible in cold-rolled single crystals is naturally dependent upon the number of slip systems that can function. This, in turn, is definitely limited by the maximum-shear-stress law. For pure tension or compression the problem is quite simple, and the excellent work of G. I. Taylor and C. F. Elam<sup>18</sup> has shown clearly for the face-centered cubic metals that only one system can be active for orientation in a given base triangle (stereographic). For convenience their

<sup>15</sup> Reference of footnote 13

<sup>16</sup> G I Taylor and C F Elam The Distortion of an Aluminium Crystal during a Tensile Test Bakerian Lecture, *Proc Roy Soc* (1923) **102A**, 643

work is summarized in Fig 7 using the nomenclature of W Boas and E Schmid,<sup>17</sup> which will be followed hereafter

When the deforming force is made more complex, as in rolling, the problem becomes considerably more involved as, for any specific rolling plane, a change in the direction of rolling will usually require a change in the active slip system because of the criteria previously discussed. However, a consideration of the favorably located systems for any rolling direction in each of several widely different rolling planes definitely

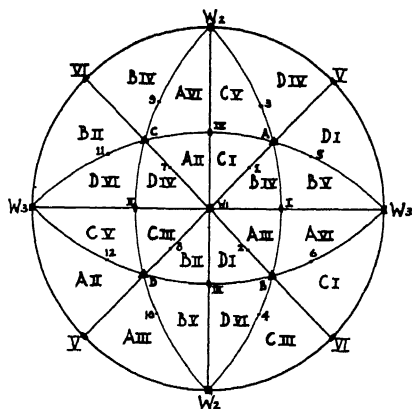


FIG 7

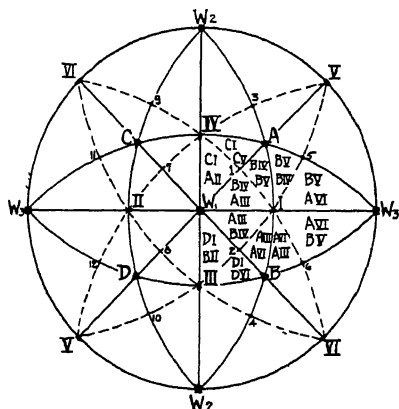


FIG 8

FIG 7 —DESIGNATION OF ACTIVE SLIP SYSTEM FOR DEFORMATION BY PURE TENSION OR COMPRESSION (*G I Taylor and C F Elam, ref 16*).

FIG 8 —DESIGNATION OF ACTIVE SLIP SYSTEM FOR DEFORMATION BY ROLLING

limited the possible active systems to one of three. This work has been summarized in Fig 8, only the favorable systems in three of the triangles being indicated for simplicity. The possible textures that can be found can then be easily specified.

Considering, for example, the triangle  $W_1$ -A-I, one of the three systems BIV, AIII, or BV will be most highly stressed, depending on the choice of rolling plane and rolling direction.

If BIV is active the rolling plane will tend to rotate toward B. This will cause an increase in the shear stress on the system AVI, eventually making this system active instead of the initial one, thereby producing a counter rotation toward A. The competition of these two systems will lead to an equilibrium position characterized by a rolling plane midway between A and B (the dodecahedral plane I) and a rolling direction on the great circle VI-IV-I-VI (the trapezohedral direction 9). Then each system will be equally stressed, and slip upon one will produce a counter-slip on the other tending to restore the lattice to the equilibrium position.

<sup>17</sup> First reference of footnote 11

The selection of *BV* or *AIII* will lead to the same final position. Slip and rotation of either one will produce an increased stress on the other, eventually causing a competition between the two. This will give an end position in which the rolling plane is near the dodecahedral plane *I*, as above, and the rolling direction is on the great circle *V-I-III-V*, the trapezohedral direction 10.

For the general case, then, of any rolling plane and any rolling direction, there is only one possible end position—a  $[112]$  direction in the rolling direction and a  $(110)$  plane in the rolling plane. Some variation in this ideal position, such as is found for all textures, might be expected, of course.

In addition to the general case discussed above there are three special cases, in which two systems are nearly equally stressed, which must be considered. In these the pole of the rolling plane is near the boundaries of the base triangle, and the rolling direction is nearly parallel to the great circles constituting these boundaries.

1. Rolling plane near the great circle between *A* and *I*, rolling direction parallel to it.

The systems *BIV* and *BV* will be subjected to the highest stresses. Action of these will cause a rotation of the rolling plane toward *B*, at the same time increasing the stress on *AIII* and *AVI*. The eventual competition between these two sets will lead to the texture—a dodecahedral,  $(110)$ , plane in the rolling plane, and a cube,  $[001]$ , direction in the rolling direction. Specimen 5 falls within the limits of this special case.

2. Rolling plane near the great circle between *W1* and *A*, rolling direction parallel to it.

Between 1 and *A*, the systems *BV* and *CV* will be most highly stressed, slip on them causing a rotation of the rolling plane toward *W1*. Between 1 and *W1*, the systems *AII* and *AIII* will be most highly stressed, slip on them causing a rotation toward *A*, i.e. toward 1. Because of this opposition the final position will be, clearly, a trapezohedral,  $(112)$ , plane in the rolling plane (plane 1) and an octahedral,  $[111]$ , direction in the rolling direction.

3. Rolling plane near the great circle between *W1* and *I*, rolling direction parallel to it.

This set of orientations, of which specimen 2 is an example, had to be investigated by actual experiment, not fully reported here, because of the peculiar nature of the deformation. For rolling planes near *I*, as mentioned previously, there is no system favorably located for deformation. The slip planes *A* and *B* are nearly parallel to the rolling direction and thus are unable to produce by rotation both a decrease in thickness and an increase in length, while the planes *C* and *D* are nearly perpendicular to the rolling plane and thus subjected to a low stress. In spite of this, the systems *CI* and *DI* were found to become active, causing the rolling

plane to rotate toward  $W1$ , thereby building up an increasing tendency to slip on the systems  $AII$  and  $BII$ . For rolling planes near  $W1$  the systems  $AII$  and  $BII$  are most highly stressed, causing by their action a rotation of the rolling plane toward  $I$ .

Specimens falling in this group can, therefore, give either of two textures, depending upon the degree of rolling and the original rolling plane: (1) a cube,  $(001)$ , plane near the rolling plane and a cube,  $[010]$  direction in the rolling direction; or (2) a dodecahedral,  $(011)$ , plane in the rolling plane and a dodecahedral,  $[0\bar{1}1]$ , direction in the rolling direction.

These five textures do not agree in every respect with those reported by Tanaka.<sup>18</sup> However, the discrepancies are easily explainable when it is remembered that his observations were, apparently, made upon only a few specimens that had been given one heavy reduction.

Under these conditions it can be seen that Tanaka's  $(110)$ - $[111]$  could be explained as a variation of the  $(110)$ - $[112]$  texture, the angle between  $[111]$  and  $[112]$  being only  $19^{\circ}30'$ . Likewise, a position near the  $(100)$ - $[110]$  texture could be attained by a specimen such as described above under case 1, in which the systems  $BV$  and  $CV$  had predominated; i.e., the rolling plane had been carried beyond 1 toward  $W1$ .

### CONCLUSIONS

By rolling alpha brass single crystals of any possible orientation, one of three slip systems will be active, depending on the choice of rolling plane and direction. The lattice rotations resulting from this deformation will lead to a variation of one of the following ideal positions

Texture	Rolling Plane	Rolling Direction
1	$(110)$	$[112]$
2	$(110)$	$[001]$
3	$(110)$	$[0\bar{1}1]$
4	$(001)$	$[010]$
5	$(112)$	$[111]$

### ACKNOWLEDGMENTS

The investigations outlined in this paper were carried out at the Hammond Laboratory, Yale University, under the direction of Prof C H Mathewson, to whom the author is greatly indebted. Sincere thanks are also due to Dr D K Crampton, Director of Research of the Chase Brass & Copper Co, Waterbury, Conn, for his interest and encouragement, and to Mr A J Smith, of the Hammond Laboratory, for his assistance in the X-ray analysis.

<sup>18</sup> Reference of footnote 3

## DISCUSSION

*(John T. Norton presiding)*

W P DAVEY,\* State College, Pa (written discussion) —It is only by working out the mechanics of various orientation changes that we can hope to have a rational picture of the rolling process. Orientation work on single crystals will eventually explain what happens in the mechanical working of ideal polycrystal material. We should soon be able to work backwards from the preferred orientation of rolled polycrystal metal to a picture of the nature of the metal itself. Every paper of the type of Dr Samans' puts us just that much closer to the goal.

M GENSAMER,† Pittsburgh, Pa (written discussion) —Because we, at the Metals Research Laboratory in Pittsburgh, have under way a program of research on the crystallographic mechanism of the deformation of iron, and because we are going to begin our researches on single crystals of iron, we are much interested in papers of this type. I have no doubt that Dr Samans' conclusions are correct, but I think it unfortunate that he did not take advantage of this opportunity to elaborate on the methods of Boas and Schmid, to which he refers, particularly since Boas and Schmid's account of their calculations and stereographic manipulations is too brief, and, because in German, not easily available. There is no doubt of the value of this paper and others like it, and I think it unfortunate that a little more space could not be given to a clearer description of the methods by which the author arrived at his conclusions.

C H SAMANS (written discussion) —I endeavored to write as clearly as possible, but, owing to the limited space available, this effort was apparently not entirely successful. Unfortunately, it is inherent in crystallographic studies of this nature that the methods of explanation shall become quite complex. It is really essential that the reader spend considerable time in making himself thoroughly familiar with the methods and with the subject matter before a good understanding can be secured.

Dr Gensamer suggests that the methods of Boas and Schmid should have been elaborated upon. This was not considered wise because of the fact that Boas and Schmid's paper dealing with polycrystalline textures differed from this single-crystal study in many respects; namely, in the manner of lattice rotation and in the number of slip systems involved. The coincidence that the two methods lead to similar end positions because of other effects should not mislead one in considering the manner of deformation.

Since this paper was intended to be only a contribution to the study of single crystals, it was not considered entirely suitable to go into a discussion of the explanations of polycrystalline deformation at this time. It seemed to the author that this would rather tend to becloud the issue and that polycrystalline and commercial textures could be better discussed in a separate paper.

---

\* Professor of Physical Chemistry, Pennsylvania State College

† Metals Research Laboratory, Carnegie Institute of Technology

# Influence of a Grain Boundary on the Deformation of a Single Crystal of Zinc

BY RICHARD F. MILLER,\* NEW HAVEN, CONN

(New York Meeting, October, 1934)

The investigations of large-grained specimens carried out by Polanyi and Schmid,<sup>1</sup> Sykes,<sup>2</sup> Goucher,<sup>3</sup> Yamaguchi,<sup>4</sup> Gough, Cox, and Sopwith,<sup>5</sup> Carpenter and Elam,<sup>6</sup> Aston,<sup>7</sup> and others have shown qualitatively that grain boundaries restrain the deformation of adjacent crystals

But whether or not the influence of the grain boundary is confined to the glide planes intersected by the boundary has not been demonstrated in any of these investigations, nor has there been carried out any quantitative analysis of the influence of a boundary on the deformation of a crystal. Indeed, the specimens employed in the previous work contained so many complicating factors that it would have been difficult to observe any variation of the extent of the influence of the grain boundaries in relation to their size. The specimens were small, the grain boundaries irregular and at no particular angle to the specimen axis or the

---

Manuscript received at the office of the Institute August 17, 1934. The paper is an abstract of a thesis submitted in partial fulfillment of the requirement for the degree of Doctor of Science from the Massachusetts Institute of Technology, June, 1934.

\* Research Assistant in Metallurgy, Yale University

<sup>1</sup> M. Polanyi and E. Schmid. *Über die Struktur bearbeiteter Metalle*. *Ztsch f tech Phys* (1924) **5**, 580.

<sup>2</sup> W. P. Sykes. *Effect of Temperature, Deformation, Grain Size and Rate of Loading on Mechanical Properties of Metals*. *Trans AIME* (1920) **64**, 780.

<sup>3</sup> F. S. Goucher. *On the Strength of Tungsten Single Crystals and its Variation with Temperature*. *Phil Mag* (1924) **48**, 229.

Studies on the Deformation of Tungsten Single Crystals under Tensile Stress. *Ibid.*, 800.

<sup>4</sup> K. Yamaguchi. *Effect of Grain Boundary upon the Hardness of Aluminum*. *Sci Papers, Inst Phys Chem Res (Tokyo)* (1927) **6**, 271.

<sup>5</sup> Gough, Cox, and Sopwith. *A Study of the Influence of the Intercrystalline Boundary on Fatigue Characteristics*. *Jnl Inst of Metals* (1933) **53**, clvii-clxxxviii.

<sup>6</sup> H. C. H. Carpenter and C. F. Elam. *Crystal Growth and Recrystallization in Metals*. *Jnl Inst of Metals* (1920) **24**, 83.

*Production of Single Crystals of Aluminum and Their Tensile Properties*. *Proc Roy Soc* (1921) **100-A**, 329.

<sup>7</sup> R. L. Aston. *Tensile Deformation of Large Aluminum Crystals at Crystal Boundaries*. *Proc Camb Phil Soc* (1927) **23**, 549.

crystallographic axes, the deformation caused to occur was often of a complex nature, and the presence of impurities and cold working further obscured the true effect of the grain boundary

In regard to these previous investigations, Gough<sup>8</sup> stated

There exists certain indirect evidence that the increased resistance to shear afforded in the neighborhood of an inter-crystalline boundary is due to slip interference or inhibition, it should be possible to devise a critical test to examine this idea in relation to varying grain size

In the present investigation, such a critical test was made possible by eliminating the complicating factors prevalent in earlier work. A grain boundary of definite size and in a definite position was caused to encounter a simple type of glide in a single crystal of zinc, whereupon the characteristic features of the encounter became apparent

### PRODUCTION OF SPECIMENS

Zinc was selected as the most suitable metal on which to examine the behavior of a grain boundary because it has only one plane (0001) of preferred glide, as shown by Mark, Polanyi, and Schmid,<sup>9</sup> and it is obtainable in a pure state. Also, it possesses a low recrystallization temperature (below room temperature), and is particularly ductile and free, between 100° and 200° C, from irregular effects of cold working, at which temperatures large single crystals can be elongated to uniform bands with small loads

The single crystals were produced from Horsehead zinc (99.99 per cent pure) by a modification of the Bridgman<sup>10</sup> method of gradual solidification from the melt. The specimens were grown cylindrical in form and large enough (10 in long and  $\frac{1}{2}$ -in dia) to allow the glide process to be directly observed by noting the changes in the position of the traces of the glide layers

A bi-crystal, with its grain boundary transverse to the axis of the specimen, could not be produced by the Bridgman method, because the hexagonal structure of the zinc tended to make an oblique boundary between the two single crystals

<sup>8</sup> H. J. Gough. Crystalline Structure in Relation to Failure of Metals. (Edgar Marburg Lecture, 1933) *Proc Amer Soc Test Mat* (1933) **33**, pt II

<sup>9</sup> Mark, Polanyi, and Schmid. Vorgänge bei der Dehnung von Zinkkristallen *Ztsch f Phys* (1922-1923) **12-13**, 58

<sup>10</sup> P. W. Bridgman. Certain Physical Properties of Single Crystals of Tungsten, Antimony, Bismuth, Tellurium, Cadmium, Zinc, and Tin. *Proc Amer Acad Arts and Sci.* (1925) **60**, 305.

In order to obtain a single crystal terminated at one end by a transverse grain boundary, the specimens were removed from the furnace

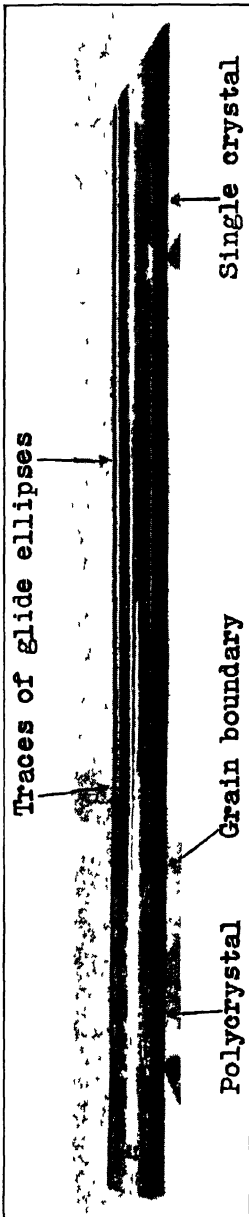


FIG 1—SPECIMEN READY FOR ELONGATION. The traces of the glide layers, developed by cooling strains, are indicated by arrows. The right end of the single crystal was cleaved along a basal plane after chilling in liquid air. The specimen was etched with sodium sulfate and chromic acid.

when five-sixths of their length had been changed into a single crystal, and while the remaining one-sixth was still molten. Since the freezing zone in the furnace was uniform and at right angles to the direction of lowering, the specimens consisted, when cool, of about 6 in. of cylindrical single crystal terminated at one end by a transverse grain boundary adjoining polycrystalline metal. For the purposes of this investigation, such a specimen is an effective substitute for a bi-crystal, since if the latter could be produced and subjected to elongation, the crystal with the more ductile orientation would undergo deformation while the other crystal, having a stronger orientation, would maintain its shape undeformed, as does the polycrystalline part of the specimens employed.

After cooling, the specimens were etched with a solution of chromic acid and sodium sulfate. The tapered ends of the single crystals were chilled in liquid air, and cleaved with a needle parallel to the basal plane. A specimen, ready for elongation, is shown in Fig 1.

#### DEFORMATION OF SPECIMENS

The specimens, held in suitable clamps, were elongated by means of a dead load



FIG 2—PARTIALLY ELONGATED SINGLE CRYSTAL CLEAVED PARALLEL TO BASAL PLANES AFTER CHILLING IN LIQUID AIR. NATURAL SIZE.

applied at a uniformly slow rate with an apparatus somewhat similar to that employed by Mark, Polanyi, and Schmid<sup>11</sup>. The elonga-

<sup>11</sup> Reference of footnote 9



tion was carried out at 180° C because it was found that specimens tested at room temperature suffered from irregular cold-working effects and broke before uniform elongation could be produced. During the elongation, the polycrystalline section of the specimens did not deform measurably. The single-crystal section elongated to a uniform band by the simple flexural gliding process described by Mark, Polanyi, and Schmid, who showed that the ratio of the sines of the initial and final angles ( $\alpha$

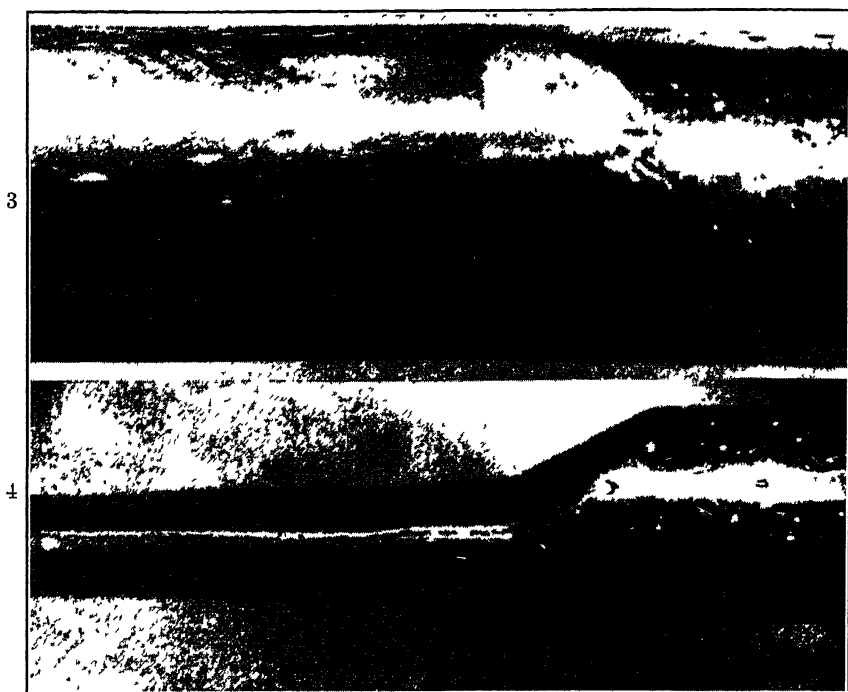


FIG 3—PLAN VIEW OF TRANSITION ZONE, SPECIMEN No 224  $\times 43$   
 FIG 4—SIDE VIEW OF TRANSITION ZONE, SPECIMEN No 224  $\times 35$

and  $\alpha'$  respectively) of the basal planes relative to the specimen axis is directly proportional to the elongation ( $e = l'/l = \sin \alpha / \sin \alpha'$ )

Only specimens in which a glide direction coincided with the direction of action of the shearing component of the applied force were chosen for examination, since it is only in such specimens that the basal glide planes remain in the same crystallographic zone from the beginning to the end of the elongation.

Polanyi and Schmid<sup>12</sup> showed that every basal plane is not equally susceptible to the gliding process, but that several thousand atom layers act together as unit blocks in gliding over other unit blocks or "glide layers."

<sup>12</sup> Reference of footnote 1



adjoining part of the uniform band  $JMKL$  to the left. It was observed that the grain boundary prevented any deformation of the crystal in the region  $FPT$ . From simple geometrical relationships, a formula was derived for distance  $PQ$  in terms of the original diameter  $d$  of the single crystal, the original angle  $\alpha$  of the basal planes relative to the axis of the specimen, and the final angle  $\alpha'$  of the basal planes relative to the axis of the band

$$d = \frac{PQ}{\tan \frac{\alpha + \alpha'}{2}} + \frac{PQ}{\tan (90 - \alpha)} \quad [1]$$

The distance  $PQ$ , calculated with the aid of this formula, is 0.139 in., and the distance  $PQ$  measured on the photograph (Fig. 4) is 0.14 in. The calculated and the measured distances  $PQ$  thus agree closely.

Angle  $HTF$  varies with the original position of the basal plane relative to the specimen axis and with the amount of elongation. Its magnitude was calculated with the aid of the following formula, derived from Fig. 5

$$\text{angle } HTF = \frac{\alpha + \alpha'}{2} = \frac{56.5^\circ + 17^\circ}{2} = 36.7^\circ \quad [2]$$

Angle  $HTF$ , measured with a protractor on the photograph or the tracing, amounts to  $37^\circ$ .

The grain boundary does not hold motionless the entire extent of the glide layers it intersects; the ends of the intersected glide layers (region  $TOMP$ ) have been bent through the same angle  $(\alpha - \alpha')$  as have the glide layers that are not intersected by the grain boundary. In order to have passed through this flexure, these glide layers have slipped over one another, the traces of the motion of the glide layers are visible on the specimen from  $T$  to  $M$ . However, examination of the specimen and the tracing seems to show that the amount of glide that has taken place on the ends of these intersected glide layers is less than the normal amount that has taken place in the uniform band.

The band does not assume a uniform cross-section until point  $M$  is passed, going from right to left in Fig. 5. Point  $M$  is the end of the first glide layer not directly intersected by the grain boundary. It is thus evident that the influence of the grain boundary is confined to the glide planes that it directly intersects.

No formula for distance  $MS$  could be obtained from Fig. 5, but a formula for the equivalent distance  $JS$  was quite readily obtained from Fig. 6, which is drawn to show the hypothetical production of a band by translational instead of flexural gliding, using the same values for  $d$ ,  $d'$ ,  $\alpha$ , and  $\alpha'$  as were observed on the actual specimen 224. In Fig. 6, the band assumes a uniform cross-section to the left of line  $JM$ . The maximum extent of the effect of the grain boundary in restraining the

deformation of the single crystal could thus be said to be the distance  $JS$ , which was discovered to be identical with the length  $MS$  of Fig 5, both in length and position. At first glance, the agreement seemed to be a remarkable coincidence, but examination of four different specimens in the same manner proved the genuineness of the agreement. Thus,

$$JS = MS = d \cos \alpha' \frac{\cos(\alpha - \alpha')}{\sin \alpha} \quad [3]$$

Applying formula 3 to specimen 224, the extent of the influence of the grain boundary was calculated to be 0.355 in. Distance  $MS$ , measured by the photograph (Fig. 4) of the specimen, was 0.35 in. The legitimacy of applying a formula derived from considerations of translational

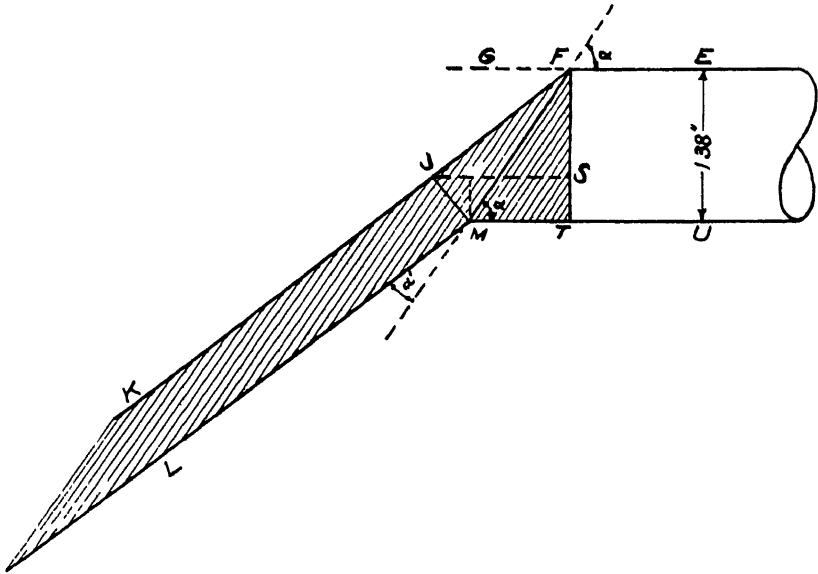


FIG 6 —SCHEMATIC DIAGRAM SHOWING PRODUCTION OF BAND BY TRANSLATION GLIDING, SPECIMEN 224

gliding to actual conditions of flexural gliding is established by the fact that the values for the distances  $PQ$  and  $MS$ , measured directly on the photographs of four specimens, were found to agree within 0.02 in. with the calculated values. This agreement is as close as could be expected, considering that  $PQ$  and  $MS$  could not be measured closer than 0.01 or 0.02 in. on the photographs. Tabulation of observations is given in Table 1.

### SUMMARY

The influence of the grain boundary is confined to glide planes that it directly intersects, and is composed of two distinct parts.

1 The glide layers in the region *FPT* (Fig 5) are held motionless, and the maximum extent of this influence is the distance *PQ* (formula 1)

2 In the region *PTM*, the glide layers have not been prevented from passing through a flexure and sliding over one another a small amount, but they have been restrained from sliding over one another the normal amount required to form a uniform band The maximum extent of the influence of the grain boundary is *MS* (formula 3) The extent of the influence of the boundary is thus seen to vary in a regular way with the size of the grain boundary *d*, the amount of the deformation ( $\alpha'$ ), and the original orientation (ductility) of the single crystal ( $\alpha$ )

TABLE 1 — *Observations on Deformation of Single Crystal of Zinc*

	Specimen 213	Specimen 224	Specimen 235	Specimen 245
<i>d</i> , in	0 405	0 399	0 332	0 322
Final load, lb	84 5	26 0	22 0	50 6
$\alpha$ , deg	56 0	56 5	44 4	42 0
$\alpha'$ , deg	12	17	15	13
Elongation observed per cent	280	180	166	200
Elongation calculated, per cent	284	186	170	197
<i>PQ</i> observed, in	0 11	0 14	0 13	0 12
<i>PQ</i> calculated, in	0 137	0 139	0 12	0 114
<i>MS</i> observed, in	0 31	0 35	0 48	0 39
<i>MS</i> calculated, in	0 345	0 355	0 400	0 410
Angle <i>HTF</i> observed, deg	33	37	30	30
Angle <i>HTF</i> calculated, deg	34 2	36 7	29 7	27 5

The position of line *HT*, itself a grain boundary, also may be predicted (formula 2)

## DISCUSSION OF RESULTS

If the single crystal is homogeneous, the glide layers intersected by the grain boundary would be intrinsically the same as the glide layers elsewhere in the crystal, and the resistance to shear would be the same throughout the lattice The reason that the glide layers in region *FPT* (Fig 5) remained motionless during the elongation may have been

because the grain boundary altered the stress distribution in the single crystal, and the shearing stress never reached the minimum critical value in this region. Thus it may appear that the function of a grain boundary is not to increase the resistance to shear of the adjacent crystal, but to decrease the shearing stress acting upon it.

In Fig 5, it is seen that glide is prevented in region *FPT* only so long as the grain boundary (the material on the other side of the boundary) maintains its shape undeformed. If a true bi-crystal were being tested, region *FPT* would maintain its shape only until deformation began to take place in the adjacent crystal.

Speculating as to the mechanics of deformation of a polycrystal, it seems probable that the crystallites of more ductile orientation could not deform (since all their glide planes are intersected by some boundary) until the load increased to such an extent that deformation was produced in the strongest crystals. Jeffries' "slip interference" theory might thus be extended in its application to polycrystals.

#### ACKNOWLEDGMENT

The investigation discussed in this paper was carried out at the Massachusetts Institute of Technology, under the direction of Dr Robert S. Williams, to whom the author is indebted for his continued interest and inspiration.

#### DISCUSSION

(*John T. Norton presiding*)

C. H. MATHEWSON,<sup>1</sup> New Haven, Conn.—This is a very interesting demonstration of the action of slip in a single crystal of zinc. I think the author is to be congratulated on his skill in preparing these large crystals and stretching them, and on the success with which he has been able to analyze the changes in the crystal.

One might say that Galileo invented a telescope so that he could study the solar system, but Dr. Miller brought his solar system down to the laboratory bench and made it perform under close observation. What I am trying to indicate is that the earlier work by Mark, Polanyi and Schmid was done with small single crystals in wire form, and while it gave us, undoubtedly, very important and accurate information concerning the slip phenomena in single crystals and was a classical contribution, yet there is a good deal of benefit, it seems to me, to be secured by magnifying the phenomena, as has been done here.

The thing that interests me most of all is the observation so clearly made here that these slip planes in contact with the polycrystalline area shown in Fig 5 are restrained, viz., actually prevented from slipping throughout part of their length, but they do slip in the region of their lower extremities. In other words, we can anchor a group of slip planes, yet they may slip and change the shape of the crystal. Of course, this is a characteristic of the flexural gliding illustrated here. It is the same thing as holding a pack of cards firmly at one end and then bending the pack at the other end, so that the individual cards in this region must slide on one another.

---

\* Professor of Metallurgy, Yale University

The fundamental geometrical requirement that seems to be satisfied in Fig 5 is that the triangle  $PNT$  have the same area as the triangle  $MPT$ . In other words, the lower portions of the restrained glide layers move around corners located on the line  $HT$  and assume the position of equal area,  $MPT$ , which apparently is called for by the distribution of forces in pulling the crystal.

One hopes, in reading papers of this sort devoted to the mechanism of crystal plasticity, to find something quantitatively describing the size of the slip lamellae. That is about the most interesting thing left with very little of a definite explanation in sight. Apparently, nothing of this sort can be obtained from the present experiments, and we do not know, indeed, whether the slipping is confined to blocks of certain width or whether every plane slips on the adjacent plane. One thing indicating that the latter situation may possibly be realized is that apparently there is no twinning at all of the lamellae as they are bent around the corner, so to speak. This seems very suggestive to me because I have done considerable work with zinc in the past and one very definite observation is that sections of zinc crystals isolated by cleavage along basal planes very promptly twin when bent even slightly in the fingers. The twinning planes lie in the neighborhood of  $45^\circ$  to the basal surfaces, and they function on the least provocation. It may be that in the flexural gliding observed here every plane does glide and that during this process of gliding and flexing the twinning phenomenon cannot manifest itself. In other words, blocks of unaltered crystal substance may be necessary to permit twinning.

Quantitatively, in the literature of crystal mechanics about all that we can find about the block-slipping process is the determination of specific shear, or the ratio of the amount of shear to the distance between blocks. Of course, a given ratio can correspond to a very long slip on wide blocks, a very short slip on narrow blocks, or almost no slip at all where every plane functions.

Again, I wish to congratulate the author on placing before us this large-scale experimental material which, undoubtedly, will be of considerable value in the study of this general subject of crystal mechanics.

R. F. MEHL,\* Pittsburgh, Pa. (written discussion) —I should like to add my compliments concerning the beauty of these experiments. Much of the work in this field has been done on very fine, almost threadlike samples, precise measurements on such crystals are very difficult and the work often lacks precision for this reason. Well formed large crystals, such as Dr. Miller has used, are much preferable.

It seems to me that the most desirable sort of information now to be obtained from the study of the mechanical properties of single crystals is that relating to the critical stresses for the initiation of the processes of slip, twinning and cleavage. Some data are available on the critical shearing stresses for slip, but the data clearly show that the values obtained are greatly dependent upon the speed of loading. In fact, an inspection of the stress-elongation curves from which points of critical shearing stress for slip have been read show that this quantity is not well defined. Some of these curves actually show initially a negative elongation in loading, so that the stress-elongation curve intersects the ordinate axis twice before taking a normal course, evidently because of nonaxiality of loading. Furthermore, the curves are irregular, and picking a true yield point is a very uncertain operation. I do not believe that a true yield point has as yet been truly demonstrated. The proper way to attack the problem would be to perform static loading or creep tests. A true yield point would be shown by a low stress level below which no yielding took place. Such an experi-

---

\* Director, Metals Research Laboratory and Professor of Metallurgy, Carnegie Institute of Technology

ment on well formed large crystals with close attention to auality of loading would furnish valuable information

So far as I know, there have been no measurements attempted for critical shearing stress for twinning. A study of critical shear for slip, for twinning, and for cleavage, over a wide range of temperature, performed as suggested, would furnish really valuable information. Furthermore, the effect of increasing degrees of cold work should be studied. It is by no means certain that cold work affects all these properties to equal or proportionate degrees.

C. H. MATHEWSON—In connection with Dr. Mehl's remarks, I think I have recently seen a paper by Dehlinger in which it was shown that crystals grown directly from the melt had quite a different threshold stress from those grown by the strain-anneal method.

L. W. MCKEEHAN,\* New Haven, Conn.—The paper contains about 400 lines, and I have an objection to only one of them, so do not regard the objection as representing a generally unfavorable reaction.

The author says that no formula for the distance  $MS$  could be obtained in Fig. 5. The mathematics are accused of incompetency, but all the meat was not put into the mathematical sausage machine. I suggest that a piece of information that has not been made use of, as far as I can see in the formula, is that the axis of the deformed band on the left seems to coincide in each case with the axis of the undeformed polycrystal on the right. If that condition is introduced, it will provide the missing parameter, or the missing fixation for the point  $M$ .

J. T. NORTON,† Cambridge, Mass.—I have been privileged to watch the development of these experiments and watch the doubts grow into more or less certainties. I am sure the author is to be congratulated in giving us such a simple mechanical picture of what goes on when a crystal is deformed. The usual method in the past, when we did not understand the deformation, was to lay the discrepancy to the grain boundaries. We will not be able to do that any longer because we have such a simple conception of process as a result of this investigation.

R. F. MILLER (written discussion)—As Dr. Mehl has pointed out, the isolation of mechanical phenomena on these large single crystals seems to offer a field for research of considerable promise. A definite yield point was noted in the single crystals employed, and it is hoped that a detailed examination of similar specimens will disclose the threshold values for shear and twinning.

The author is indebted to Dr. McKeehan for his suggestion. Further study of the region of restrained glide will no doubt yield interesting results.

---

\* Director, Sloane Physics Laboratory, Yale University

† Associate Professor of Physics and Metals, Massachusetts Institute of Technology



# Crystal Orientations Developed by Progressive Cold Rolling of an Alloyed Zinc

By M L FULLER\* AND GERALD EDMUNDS,† PALMERTON, PA

(New York Meeting, February, 1934)

THE fundamental mechanism of the deformation of zinc has been thoroughly described by several prominent investigators, particularly Mark, Polanyi, and Schmid,<sup>1</sup> Mathewson and Phillips,<sup>2</sup> and Schmid and Wassermann.<sup>3</sup> The deformation of zinc occurs primarily through slip along basal planes  $\{00\ 1\}$ , and secondarily through twinning on pyramidal planes of the form  $\{10\ 2\}$ . In addition to these basic studies on single crystals, there have been a number of determinations<sup>4,5</sup> of preferred orientations developed in rolled, polycrystalline zinc. In no case, to our knowledge, has there been described the development of oriented structures in zinc as a result of a systematic series of rolling treatments. The work included in the present paper shows the changes in orientation produced in a zinc alloy by successively increasing degrees of cold-rolling reduction. This alloy has the same crystal form, hexagonal close-packed, as zinc, but its susceptibility to hardening for a given degree of working is much greater because of its higher recrystallization temperature.

## EXPERIMENTAL PROCEDURE

### *Composition of the Alloy and Rolling Treatment*

The alloy used in this investigation consisted of zinc of 99.9 per cent purity to which 1 per cent of copper and 0.01 per cent of magnesium had been added.

---

Manuscript received at the office of the Institute Dec 1, 1933

\* Investigator, X-Ray Laboratory, Research Division, The New Jersey Zinc Co

† Investigator, Rolling Mill Section, Research Division, The New Jersey Zinc Co

<sup>1</sup> H. Mark, M. Polanyi and E. Schmid *Ztsch f. Phys.* (1922) **12**, 58

<sup>2</sup> C. H. Mathewson and A. J. Phillips *Proc. Inst. Met. Div., A. I. M. E.* (1927), 143

<sup>3</sup> E. Schmid and G. Wassermann *Ztsch f. Phys.* (1928) **48**, 370

<sup>4</sup> E. Schmid and G. Wassermann *Metallwirtschaft* (1930) **9**, 698

<sup>5</sup> E. Schmid and G. Wassermann *Ztsch f. Metallkunde* (1931) **23**, 87

V. Caglioti and G. Sachs: *Metallwirtschaft* (1932) **11**, 1.

M. A. Valouch *Metallwirtschaft* (1932) **11**, 165.

H. Mark: *Ztsch f. Krist.* (1925) **61**, 75.

T. A. Wilson and S. L. Hoyt *Trans. A. I. M. E.* (1928) **78**, Inst. Met. Div., 241.

Cast bars were rough rolled by the usual hot rolling practice, annealed, cold-rolled with a total reduction of 50 per cent, reannealed and finish-rolled, cold, with total reductions of 30, 50 and 80 per cent to a final thickness for each coil of 0.040 in. Throughout the cold rolling the coils were allowed to cool between successive passes. Additional metal of the same gage was prepared in the annealed condition from the coils given the 50 per cent final cold-rolling reduction. In this paper the several varieties of metal are referred to as "annealed," or 30, 50 or 80 per cent samples, corresponding to the amount of final cold rolling.

### *Determination of Orientations*

The first investigators of the oriented crystal structures in worked metals sought to establish single orientations to which all crystals approximated. It was found that in most cases no such simple structure existed. Owing to the complexity of the orientation systems, a method of representing them graphically became necessary for their proper description and study. The most effective and generally used graphic method has been the pole figure (Flächenpolfigur) method of F. Wever.<sup>6</sup> In this method a stereographic projection of the poles of an individual form of lattice planes is made for all the orientations shown by X-ray diffraction analysis to be present. The regions including the projected points constitute the pole figure.

Throughout this paper the basal plane {00 1} is the only one for which pole figures are given. One more figure, preferably that of a prismatic plane, is required for a complete definition of structure. It is fortunate that only the orientation of the basal plane is of major importance, since the X-ray evidence for types of preferred orientation of such planes as would add to the description of the structures given is indefinite and in some cases nonexistent.

The technique of preparing the rolled strips for X-ray examination, the experimental details of the X-ray method, and the plotting of the pole figures have been described by the authors in another paper.<sup>7</sup>

### *Correlation of Orientation Structures with Deformational Characteristics of Monocrystalline Zinc*

The development of oriented crystal structures in the rolling of polycrystalline metal depends upon the fundamental mechanism of deformation of the individual crystals, the mechanical effects of the crystals upon one another, the applied stresses, the internal distribution

---

<sup>6</sup> F. Wever. *Ztsch. f. Phys.* (1924) **28**, 69.

F. Wever: *Trans. A. I. M. E.* (1931) **93**, Inst. Met. Div., 51.

<sup>7</sup> G. Edmunds and M. L. Fuller: *Trans. A. I. M. E.* (1932) **99**, 75.

of stresses, and the nature of the external deformation of the metal. Because of these and other factors which influence the development of this anisotropic structure, it may seem futile to attempt to explain the mechanism of its formation during rolling. It will be shown in this discussion, however, that the general structures found can be rationalized in terms of the known mechanism of the plastic deformation of single crystals and the external deformation of the metal.

The deformation of single crystals of zinc by basal slip takes place by gliding of blocks of the crystal, parallel to the basal plane, in a direction of closest atomic packing of the lattice, i. e., in a direction normal to a plane of the form  $\{110\}$ . The gliding movement is simultaneously accompanied by a rotation of the slipping lamellae about an axis in the basal plane perpendicular to the direction of slip. This reorientation in rolling must be such that the change in shape of the deforming crystal conforms with the external change of form<sup>8</sup> of the strip. Hence the tendency of this slip rotation process will be to reorient the crystals toward that position in which the basal plane is parallel to the rolling plane and the direction of closest atomic packing is parallel to the rolling direction. The ultimate position that the crystals would assume as a result of the slip-rotation process was not reached in the experiments reported here, since the crystals were reoriented by twinning before reaching it.

Twinning in zinc takes place as a result of a shearing stress along planes of the form  $\{102\}$  whereby an atomic rearrangement takes place forming a crystal bearing a definite orientation with respect to the parent crystal. In the alloyed zinc used in the present study the angle between the principal or trigonal axes of the two crystals is  $93^{\circ} 26'$  and the twins have a  $\{102\}$  plane in common. All or parts of a crystal may reorient by twinning. The maximum possible extension of a crystal by twinning is, according to calculation, approximately 7 per cent. Further extension may take place, however, by basal slip in the twinned crystal if it is suitably oriented.

The orientation structures produced in the rolled metal will be the result of the deformation processes of slip-rotation and twinning as produced by the stresses of rolling and as limited by the change in external shape undergone by the strip.

## CHANGES IN ORIENTATION STRUCTURE PRODUCED BY COLD ROLLING

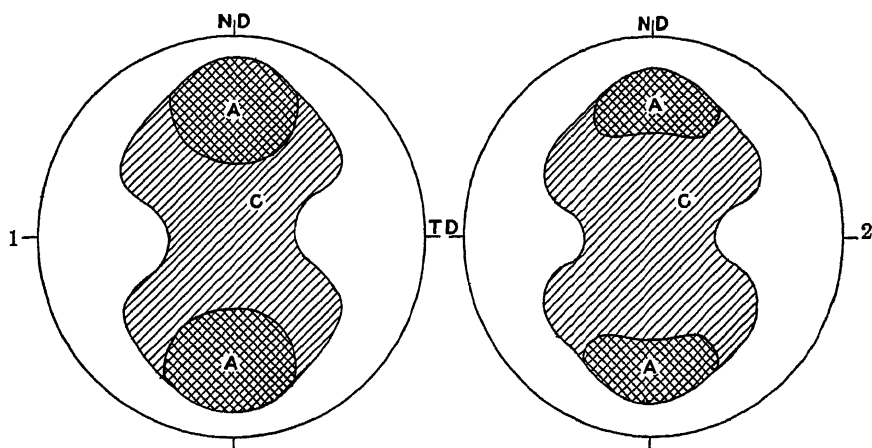
### *Experimental Results*

Basal-plane pole figures depicting the orientation structures in the cold-rolled alloyed zinc are shown in Figs 1 to 8. These figures are

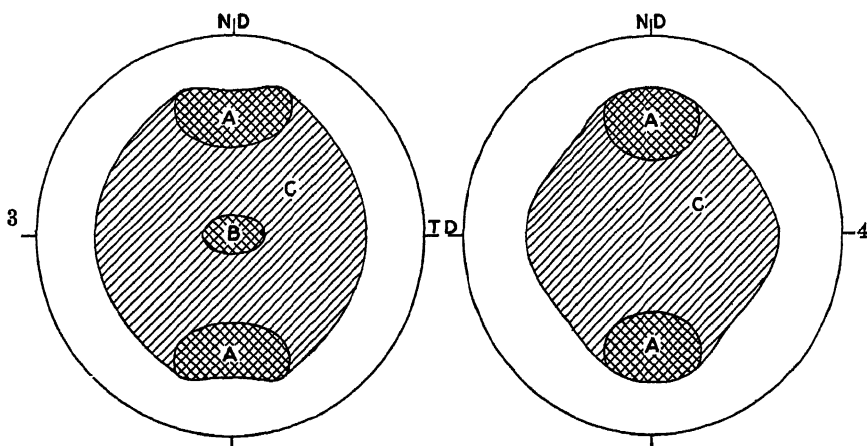
---

<sup>8</sup> The change of form in rolling consists of a lengthening in the direction of rolling with a corresponding decrease in thickness of the material. Width changes are small enough to be ignored in the present considerations.

representative of the metal intermediate between the surface and the center of the strip. The intermediate section was chosen because it is probably more representative of the deformation throughout the entire strip than sections at or near the surface or center. Pole figures of two coils from each rolling treatment are given to indicate the degree of reproducibility experienced.



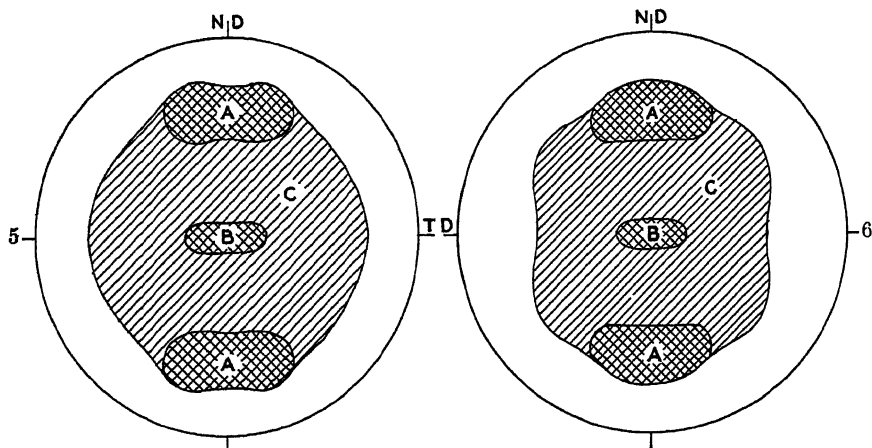
FIGS. 1 AND 2—BASAL PLANE POLE FIGURES OF STRUCTURE IN ANNEALED STRIP



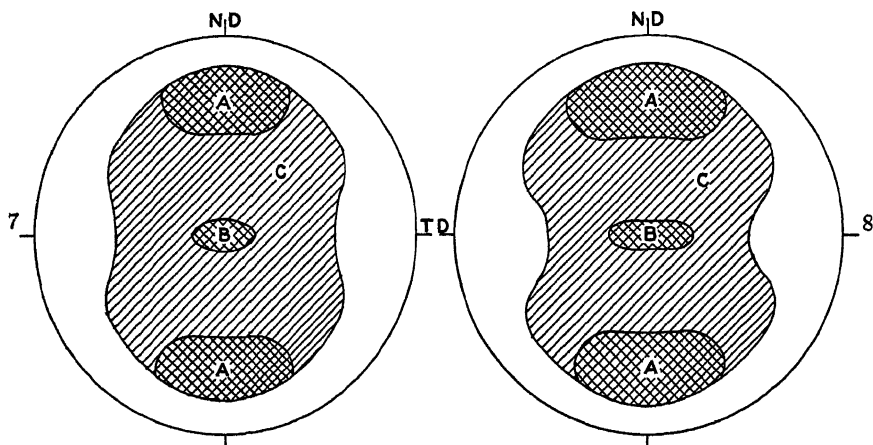
FIGS. 3 AND 4—BASAL PLANE POLE FIGURES OF STRUCTURE AFTER 30 PER CENT REDUCTION.

The plane of projection of the pole figures is the plane including the direction normal to the surface of the strip ( $N.D.$ ) and the across rolling or transverse direction ( $T.D.$ ). The transverse direction lies parallel to the surface of the strip and perpendicular to the rolling direction. The shaded areas include all the orientations present, the cross-hatched areas having the greater density of crystal population than those cross-lined.

Three orientation types were developed in these specimens, designated *A*, *B* and *C*. No attempt is made to indicate on the figures the variation among the several rolled strips in relative densities of crystal population in areas *A*, *B* and *C*. As the amount of rolling increases, the number of crystals in the areas of high concentration, *A* and *B*, increases at the expense of *C*. Thus the ratio of the density of *A* to that of *C* in the 30 per



FIGS. 5 AND 6—BASAL PLANE POLE FIGURES OF STRUCTURE AFTER 50 PER CENT REDUCTION



FIGS. 7 AND 8—BASAL PLANE POLE FIGURES OF STRUCTURE AFTER 80 PER CENT REDUCTION

cent strip is greater than in the recrystallization orientation of the annealed strip that served as the starting material for the cold-rolling experiments. The region *B* is not present in the annealed strip and is only weakly developed in the 30 per cent strip. Indeed, region *B* is not always produced by this reduction, as shown by its presence in one and not in the other of the 30 per cent samples. However, in the 50 and 80 per

cent strips, the region *B* is densely populated as well as region *A*, with correspondingly lesser density in region *C*

### *Discussion of Structure Changes*

As the metal is deformed, the slip-rotation process causes the crystals to reorient toward the position in which the basal planes are parallel to the rolling plane. (This position on the pole figures is at the extremes of the vertical diameter.) However, as the crystals approach this orientation, the stresses of rolling are evidently such as to produce a reorientation by twinning, since the ultimate position by slip is not reached. The

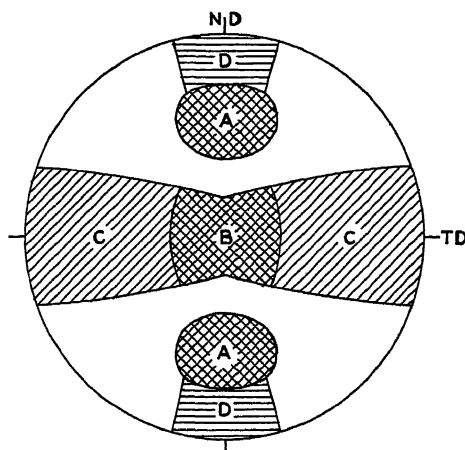


FIG 9—BASAL PLANE POLE FIGURE INDICATING SOME TWINNING REORIENTATIONS POSSIBLE DURING ROLLING

region of orientations at *A* is developed by crystals that have deformed by slip-rotation. Crystals that reach or pass beyond the outermost limits of region *A* form twins.

The general nature of the twinning reorientations is represented in an arbitrary manner in Fig. 9. The regions *A* are those found experimentally into which the crystals move by slip-rotation. The regions *D* are those into which crystals tend to move by slip-rotation but from which they are removed by twinning. The crystallographically possible orientations derived by twinning from *D* are the regions *B* and *C*. Of the six possible twin orientations into which any crystal in *D* may reorient to *B* and *C*, one is most likely to occur. This twinning position is in the area *B*, because of the requirement that the reorientation conform to the external change in dimensions of the strip.<sup>9</sup> The position in this area for a given

<sup>9</sup> Schmid and Wassermann (reference of footnote 4) have shown in a stereographic projection the nature of the changes in length, whether shortening or lengthening, which would occur by twinning during the rolling process.

basal-plane orientation in  $D$  will depend upon the position of the (close-packed) lattice line common to the crystal and its twin.

Crystals that reach area  $B$  of Fig 9 may reorient by slip-rotation if the stresses are sufficient. Crystals in orientations at or very near the center of the pole figure are not in a favorable position for deformation by either mechanism, as is demonstrated by the fact that with the progress of rolling a small area at the center of the pole figure becomes more and more densely populated. In position  $B$  the basal plane is perpendicular to the rolling direction. From such a position, twinning could not take place, since the strip would then increase in thickness or width whereas actually it is forced to decrease in thickness during rolling. Crystals in this area, therefore, tend to remain fixed in orientation.

The literature on the rolling structure of zinc has not reported the existence of the orientation type  $B$ . This probably is due to the fact that these other studies have dealt with unalloyed zinc. The lesser tendency for recrystallization to take place during rolling in the alloyed zinc of the present study accounts in part for the development of this special orientation structure. Another factor that would affect the rolling structure is that the stress required to produce slip relative to that required to produce twinning may be different between alloyed and unalloyed zinc. No data are available on this.

The less densely populated region  $C$ , which exists in all of the specimens included in this paper, consists of crystals which in general are suitably oriented for further deformation. This region is being continually replenished by twinning. The large number of possible twinning positions, and subsequent slip-rotation from these positions, causes area  $C$  to be large compared to the more highly preferred areas  $A$  and  $B$ .

No crystals are in positions near the primitive circles of the pole figures. While these positions must have been present in the cast structures, crystals so oriented are readily removed by twinning and presumably were so removed by the stages of rolling prior to those included in these experiments. Crystals are not oriented into these positions during rolling by either slip or twinning.

The differences in the shapes of the various regions for the several strips may be due to any of several factors. For example, the processes of slip and twinning may be altered by variations in degree of strain-hardening, by the action of neighboring grains upon one another, or by differences in grain size.

### SUMMARY

The crystal orientations developed by the progressive cold rolling of a zinc alloy have been investigated. Cold rolling yields three types of preferred orientation, one of which has not previously been reported in the literature. These structures have been rationalized with the funda-

mental mechanisms of the deformation of zinc crystals and the changes of form undergone by the metal during rolling

### ACKNOWLEDGMENT

The writers wish to express appreciation for assistance given by other members of the Research Division, The New Jersey Zinc Co., during the course of the investigation and in the preparation of the manuscript.

### DISCUSSION

(*Wheeler P. Davey presiding*)

C S BARRETT,\* Pittsburgh, Pa (written discussion)—Unalloyed zinc has a rolling structure in the surface layers different from that in the interior, and characterized by uniform distribution of orientations about the normal to the sheet surface<sup>10</sup> Have the authors made any observations on this point with their alloy?

It should be pointed out that pole figures in this paper indicate that the alloyed zinc recrystallizes with a preferred orientation (Figs 1 and 2 are of the orientation after annealing); furthermore, that this orientation is almost identical with the orientation produced by rolling. The similarity of all pole figures in the paper implies this, although a definite proof would require a pole figure not given in the paper; namely, one determined for the sheet as rolled and before annealing. This would hardly have been expected from Mathewson and Phillips' observations<sup>11</sup> on zinc which had been annealed following a hot rolling and which showed an approximately random orientation of grains. Perhaps zinc is another of those metals, like silver, of which the recrystallization structure depends upon the temperature of recrystallization. The authors have not given in the paper the annealing temperature used.

It would be of interest to see a calculation of the anisotropy of the tensile strength, elastic modulus, electrical resistance, etc., for this alloy, the calculation to be based on the author's pole figures together with the measured physical properties of single crystals. One wonders if the difference between the pole figures in this paper and the earlier ones for unalloyed zinc would make a significant difference in the anisotropy of the physical properties. Probably more quantitative data on the density of crystal population in the different pole-figure areas would be necessary for such a study, for the calculations of anisotropy that have been made from qualitative pole figures<sup>12</sup> are not highly accurate; greater accuracy can be expected only when the distribution within the areas on the pole figure is determined. Complete pole figure data would include not only the outlines of areas but contours of density within the areas.

The authors suggest that the addition of alloying elements to zinc changes the relation between the stress to initiate slip and the stress to produce twinning. There is a large and almost unexplored field for research in the relation between the stress condition that produces twinning and the condition that produces slip. Probably the temperature of deformation and the speed of deformation are closely related to this question for most metals (definitely so in iron); also, the presence of alloying

---

\* Metals Research Laboratory, Carnegie Institute of Technology.

<sup>10</sup> Schmid and Wassermann. Reference of footnote 5.

<sup>11</sup> C. H. Mathewson and A. J. Phillips. Reference of footnote 2.

<sup>12</sup> For example, by Schmid and Wassermann for zinc (reference of footnote 5) and by J. Weerts for rolled and re-crystallized copper [*Ztsch f Metallkunde* (1933) 25, 101].



elements in solid solution or as particles precipitated from solid solution or otherwise distributed, still further to be considered is the factor of strain-hardening—perhaps not only the increase with deformation of the stress necessary to produce slip but also of the stress necessary to produce twinning. While experiments in this field to be successful would have to be planned with some care, I believe there is hope for establishing curves showing the relation of several of these factors. If and when such data become available, they will be immediately useful in the interpretation of deformation structures. The authors have shown this in the present paper; the differences between the pole figures for their alloy and the usual ones for zinc can be ascribed to the effect of the alloying elements upon recrystallization and upon the stresses required for twinning and for slip.

M L FULLER—In reply to Dr Barrett, the surface orientation reported in the literature by Schmid and Wassermann, and also by ourselves in a previous paper, was not found in this investigation. We have examined a number of samples rolled similarly to this and in no case did we find such a condition. The metal strip was examined at the surface, midway between the surface and center, and at the center of the specimen. The particular cold-rolling treatment used was such that there was not much difference in orientation structure throughout the thickness of the strip.

The annealing treatment given was well above the recrystallization temperature, the annealing temperature being  $325^{\circ}\text{C}$  and the recrystallization temperature about  $200^{\circ}\text{C}$ .

Dr Barrett has pointed out something we failed to mention; namely, that there really is a recrystallization structure indicated in the first sample. Figs 1 to 8 show this. Prior to the annealing given in the case of Figs 1 and 2, the material had received a 50 per cent cold-rolling reduction. In other words, the samples corresponding to Figs 1 and 2 were derived by an annealing of the samples of Figs 5 and 6. Figs 1 and 2 represent the recrystallization structure, the concentration of crystals at the central area *B* having disappeared and the area *A* having grown at the expense of area *B* during the recrystallization.

We have not attempted the calculation of physical properties of the strip due to the anisotropy in crystal orientation, such a calculation would be very interesting. We have planned to investigate the ratio between the stress required to produce slip and that required to produce twinning, but have not yet found the time. It certainly would be of great value to us to know that ratio.

We have observed, in studying pole figures of this type, that the position of the areas *A* will vary, depending upon the rolling treatment. This variation may be due in part to a change in the relative stress required to produce slip and twinning. The more nearly the basal planes of the crystals are allowed to become parallel to the surface of the strip, the greater must be the force required to produce twinning relative to that required to produce slip.

R W DRIER,\* Houghton, Mich.—The author mentioned that the results of progressive working, that is, percentage of oriented material in fiber structures, is not spoken of frequently in literature. Professor Thomassen and Mr. Pearl, at the University of Michigan, did some work several years ago on depth of working in brasses, which were machined with tools of varying degrees of dullness. This undoubtedly could be classed as progressive working.

W A. Wood has correlated, in the *Philosophical Magazine*, the degree of orientation in cold-drawn copper wires with various amounts of reduction. He mentioned the percentage of the diameter that was core, varying from 50 per cent for a 40 per cent reduction to 40 per cent for a reduction of about 90 per cent.

---

\* Michigan College of Mining and Technology.

Schmid and Wassermann, also Glocker, mention varying amounts of worked structure with progressive deformation. This was shown also in some work done at the Michigan College of Mining and Technology in correlating the conductivity and cell orientation in cold-drawn copper.

Did you find any variation in the amount of preferred orientation from surface to surface?

M. L. FULLER—We appreciate these additional references to the literature. We are familiar with those, and in the paper it was stated that we were referring only to the literature on zinc, where there had been a number of determinations on single samples of material, but no systematic investigation of a progressive series of rolling treatments. With respect to the difference from surface to surface, I take that to mean difference at various points in the same sheet. Is that what you mean by that question?

R. W. DRIER—Does the intensity of the orientation, or the type of preferred orientation, vary as you examine the sheet from one rolled surface to the other?

M. L. FULLER—I think I answered that previously when I said that we had examined similarly rolled material at both the surface and underneath the surface and found very little difference. However, a difference is readily developed by other rolling treatments, as we reported in an earlier paper before the Institute.

C. H. SAMANS, Waterbury, Conn. (written discussion)—Data of this nature dealing with commercial reductions are of great value to the practical metallurgist who is endeavoring to explain other phenomena on the basis of textures.

There is one point in the discussion of the structure changes that should be brought up more for the purpose of clarification than criticism. In the explanation of area *B*, the statement is made that "crystals in this area tend to remain fixed in orientation." It seems scarcely possible that, in an aggregate subjected to the forces of cold rolling, any crystal of a hexagonal metal could remain fixed in orientation. Despite the fact that orientations in area *B* are poorly situated for deformation by slip, because of the low shear stress acting on them, it seems only logical to say that they must deform by this process, since twinning, the only other known method, is excluded because of thickness changes. Because there is only one slip plane in this system the metal obviously cannot deform without rotation. Therefore the crystals must rotate, thereby proceeding to positions more favorable for slip, and so on. If crystals are removed from the area *B* by slip and rotation and the area, despite this, becomes more intense with heavier reduction, it would seem that it must be replenished by the twinning of orientations in another intense area. To supply these twins we have only area *A*, and primary twinning from points in area *A* cannot account for area *B*, because of the angular relationships between the basal planes in the twinned and untwinned crystals, i.e.,  $93^{\circ} 26'$ .

However, there is an alternate solution of this problem. Fig 10a is a stereographic projection of a hexagonal crystal, with its basal pole at the center and a slip direction vertical, showing the original basal plane and the positions of the basal planes for all possible twins of the first two generations. In Fig 10b this projection has been rotated until the basal plane of the original crystal falls into area *A* of the author's Fig 8. Fig 10c is a reproduction of Fig 8 and in Fig 10d, Figs. 10b and c have been superimposed without the crosshatching. Considering Fig 10d, then, it will be seen that if a basal plane in area *A* is twinned there are six possible orientations of its primary twins. Positions 1, 2, 4 and 5 are favorably located for deformation by slip and account nicely for area *C*. Twins in positions 3 or 6 are very unfavorably situated for deformation, their basal plane being nearly parallel to the rolling direc-

tion and within  $30^\circ$  of the perpendicular to the rolling plane. Since they cannot deform by slip it seems logical that they would immediately be re-twinned into positions in area *C* or area *B*. This process of secondary twinning would cause a decrease in thickness and a corresponding increase in width, which is not at all impossible. The practically immediate formation of the secondary twins accounts for the fact that these primary orientations are not found by the X-ray. On this basis, then, all of the orientations are explained.

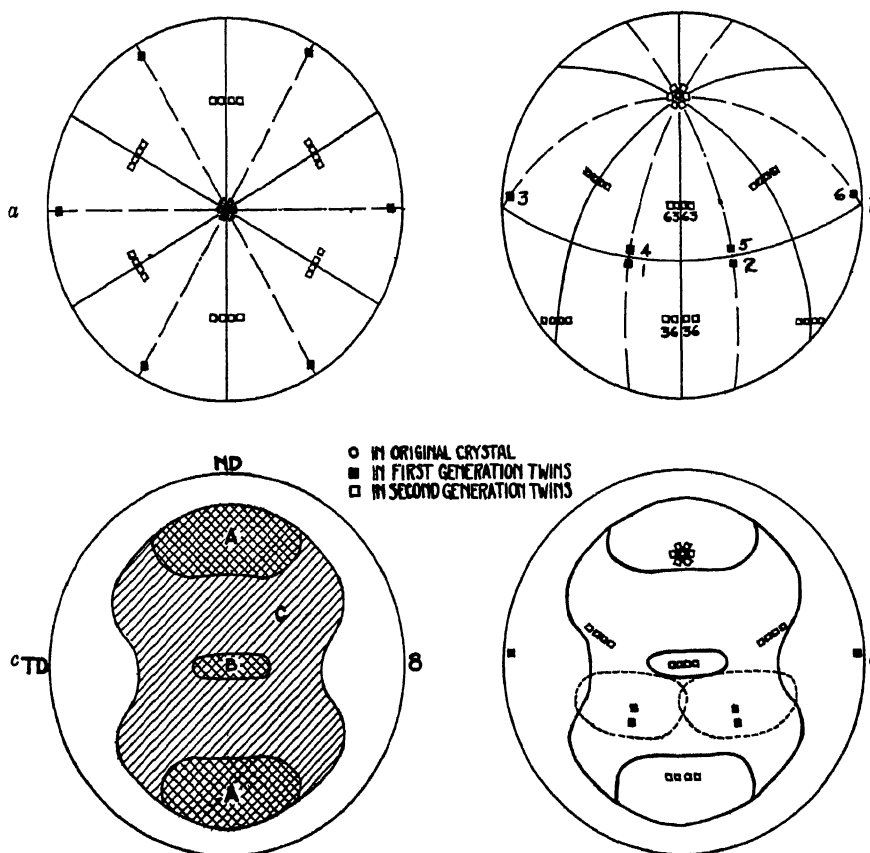


FIG. 10.—SYMBOLS FOR POLES OF BASAL PLANES

M. L. FULLER AND G. EDMUNDS (written discussion).—Mr. Samans has presented a carefully developed stereographic analysis of possible twinning reorientations which are capable of placing crystals in the area *B* of the pole figures. The authors agree with Mr. Samans' statement that the crystals in area *B* will not remain absolutely fixed in orientation. The point, which we believe was clearly stated on page 152, is that the unfavorable nature of the orientations in area *B* for either slip or twinning reduces the probability of reorientation for these crystals. In effect, the gross deformation of the metal is mostly carried on by crystals outside of area *B*.

With respect to the mechanism by which crystals are oriented to position *B*, which Mr. Samans proposes, the authors differ on two points and therefore believe

that the mechanism suggested in the paper by means of Fig 9 is the more valid solution. In the first place, the orientation of the original crystal which Mr Samans has indicated in Figs 10c and d is probably not an orientation from which twinning is likely to occur. Referring to Fig 9 and the explanation thereof in the text of the paper, it is evident that a crystal in the orientation which Mr Samans has selected as the original crystal of Figs 10c and 10d is not likely to deform by twinning. Such a crystal will probably deform by slip rotation, eventually reaching the outermost limits of region A and passing into region D (see Fig 9). Crystals in region D reorient by twinning. Of the various possible twinning positions, those most likely to occur are included in the area B, since only such twinning reorientations are compatible with the external change in form of the metal. (See footnote 8.) The second point in Mr Samans' hypothesis with which the writers disagree is in connection with the first generation twins in positions 3 and 6. The first generation twins, 1, 2, 4 and 5, are much more likely to form than 3 and 6, for the reason that twinning to the former positions produces a thinning and lengthening of the rolled strip whereas twinning to the latter positions produces a widening of the strip which is not consistent with the general deformation taking place in rolling. It does not seem likely that crystals would have reoriented by twinning to positions 3 and 6 when positions 1, 2, 4 and 5 are so much more consistent with the external deformation taking place.

## Internal Stresses in Quenched Aluminum and Some Aluminum Alloys\*

By L W KEMPF,† H. L. HOPKINS† AND E V IVANSO,‡ CLEVELAND, OHIO

(New York Meeting, February, 1934)

A BALANCED system of internal stress is set up in any metallic structure by plastic deformation below the annealing temperature. The internal stress induced by cold rolling or other fabricating processes is generally recognized and its magnitude is known to be, within certain limits, a function of the degree of cold deformation. The plastic deformation that may accompany rapid cooling from elevated temperatures may not materially change the form of the product. The internal stresses so induced are not, therefore, so evident and nonrecognition of their presence has at times led to engineering failures.

The heat treatment of aluminum alloys is a relatively new art and little information is available regarding the magnitude of stresses induced during the commercial heat treatment of aluminum alloy products. As the industrial use of aluminum increases, it is inevitable that products of increasingly large volume will be required. It has become necessary in the present commercial utilization of aluminum to heat-treat castings and forgings weighing hundreds of pounds. One of the factors governing the magnitude of internal stresses arising from rapid cooling from elevated temperatures is that of the size of the structure being treated. Some of the other factors are cooling rate, elastic properties of the alloy, thermal expansivity, thermal conductivity, and the presence or absence of phase changes. Practically all aluminum alloys have a high coefficient of thermal expansion and some are capable of developing relatively high elastic limits. On the other hand, all commercial aluminum alloys have relatively high thermal conductivities, no invariant phase changes, and the quenching temperatures are comparatively low. In the absence of invariant phase changes involving change in the type of crystallographic lattice, the fundamental basis for the development of internal stress

---

Manuscript received at the office of the Institute Nov. 29, 1933

\* Part of this work was carried out by E. V. Ivanso in the laboratories of, and submitted to, Case School of Applied Science as a thesis in partial fulfillment of the requirements for the degree of Master of Science in Metallurgical Engineering.

† Aluminum Research Laboratories, Aluminum Company of America.

‡ Formerly Assistant Instructor, Department of Mathematics, Case School of Applied Science.

during rapid cooling from an elevated temperature is the time rate of heat transfer from the interior to the exterior of the section. With this consideration in mind it is easy to estimate qualitatively the manner in which a variation in any one of the factors listed above will affect the development of internal stress. Thus, for example, it is to be expected that the high thermal conductivity of aluminum alloys should make for low internal stress. An understanding of the process of the development of internal stress during cooling places a tool in the hands of the heat-treater which may change what is sometimes considered an unmitigated evil into an asset. Thus Greene<sup>1</sup> has shown that the internal stresses in quenched heading and drawing dies can be so directed as to strengthen the die in service. Welty<sup>2</sup> has directed to useful purposes the internal stresses developed in quenching hollow cylinders of aluminum alloy. These considerations prompted an attempt to determine in a more quantitative manner the effect of heat-treating variables on the magnitude of the internal stresses induced during heat treatment.

Considerable attention has been devoted to the distribution and magnitude of the internal stresses in heat-treated steel products. The magnitude of stresses in quenched steel has been examined by Hoyt,<sup>3</sup> Scott<sup>4</sup> and Heyn.<sup>5</sup> A more complete analysis of the distribution of such stresses has been made by Sachs<sup>6</sup> and Greene.<sup>7</sup> Grogan and Clayton<sup>8</sup> have studied the internal stresses in quenched aluminum alloys and their relation to stability of heat treatment. This report contains the results of an investigation of the magnitude of internal stress induced in aluminum alloys by quenching from elevated temperatures. The effect of various heat-treating factors was examined. Some results are also included regarding the removal of stress by annealing.

## EXPERIMENTAL PROCEDURE

### *Longitudinal Stresses*

A common method of determination of internal stresses depends upon mechanically removing parts of the body, which disturbs the stress

<sup>1</sup> O. V. Greene: Estimation of Internal Stress in Quenched Hollow Cylinders of Carbon Tool Steel. *Trans. Amer. Soc. Steel Treat.* (1930).

<sup>2</sup> G. D. Welty: U. S. Patents 1638898 and 1688300.

<sup>3</sup> S. L. Hoyt: Stresses in Quenched and Tempered Steel. *Trans. Amer. Soc. Steel Treat.* (1927) 11, 509.

<sup>4</sup> H. Scott: Origin of Quenching Cracks. U. S. Bur. Stds. *Sci. Paper* 513

<sup>5</sup> E. Heyn: Physical Metallography. Trans. by M. A. Grossman. New York, 1925. John Wiley & Sons.

<sup>6</sup> G. Sachs: Der Nachweis innerer Spannungen in Stangen und Rohren. *Ztsch. f. Metallkunde* (1927) 352.

<sup>7</sup> Reference of footnote 1.

<sup>8</sup> Grogan and Clayton: Dimensional Stability of Heat Treated Aluminum Alloys. *Jnl. Inst. Metals* (1931) 45, 157.

equilibrium and results in deformation of the remaining metal. Measurement of the deformation permits the estimation of the internal stresses in the portion removed

In a right cylindrical rod, the measurement of internal stresses induced by quenching from elevated temperatures is made possible by the fact that the stresses are generally symmetrical about the longitudinal axis. For solid pieces such as bars, rods, etc., a method for determining internal stresses developed by Howard<sup>9</sup> and Heyn<sup>10</sup> consists in machining off concentric layers of metal and measuring the resulting linear contraction or expansion. Given the length changes, the actual internal stress in each layer can be computed by means of the formula:

$$S_n = \frac{E}{L^1} \times \frac{d_n^2(L_n - L_0) - d_{n-1}^2(L_{n-1} - L_0)}{d_{n-1}^2 - d_n^2}$$

$S_n$  = stress in  $n$ th layer, lb. per sq. in

$E$  = modulus of elasticity, 10,000,000 lb per sq in.

$L^1$  = length turned down.

$d_n$  = diameter of turned down part after  $n$ th cut.

$d_{n-1}$  = diameter of turned down part after  $(n - 1)$ th cut

$L_0$  = initial length of bar.

$L_n$  = length of bar after  $n$ th cut.

$L_{n-1}$  = length of bar after  $(n - 1)$ th cut

This is a modification of Heyn's formula by Merica and Woodward.<sup>11</sup> Reference should be made to the original papers for the development of this formula. It will be sufficient to state that it is based on the equilibrium between the tensile and compressive forces in a given piece and is derived from the definition of Young's modulus:

$$E = \frac{L_0 \times S}{L - L_0}$$

where  $E$  = modulus of elasticity,

$S$  = average stress, lb. per sq. in.,

$L_0$  = original length of specimen,

$L - L_0$  = change in length of specimen.

Specimens were cast as ingots about 8 cm. square by 30 cm. long, in chill molds. Nominal compositions of the aluminum and aluminum

<sup>9</sup> J E Howard Tests on Harveyized Bars. Tests of Metallurgy, Watertown Arsenal, 285, 1893

<sup>10</sup> E Heyn Internal Stresses in Cold Wrought Metals, and Some Troubles Caused Thereby. *Jnl. Inst. Metals* (1914) 12, 3-37.

<sup>11</sup> P. D Merica and R. W Woodward: Failure of Brasses U. S. Bur. Stds. *Tech. Paper* 82 (1917).

alloys are listed in Table 1. The resulting bars were then machined to the desired size, the ends being faced parallel and perpendicular to the longitudinal axis of the bar. The bars ranged from about 26 to 29 cm. in length, and from about 5 to 7 cm. in diameter.

TABLE 1—*Nominal Composition of Alloys*

Alloy No	Composition, Per Cent					
	Copper	Iron	Silicon	Magnesium	Nickel	Aluminum Minimum
Pure Al						99 97
122	10 0	1 2		0 2		87 00
195	4 0	0 70	0 70			93 00
142	4 0			1 5	2 0	90 00
355	0 75	0 25	5 00	0 5		92 00
25S	4 5	0 75	0 8			92 00
51S	0 20	0 60	1 0	0 6		96 50

To remove any casting and machining stresses, the specimens were annealed at 650° F. (343° C) and furnace-cooled. Subsequent determinations showed the bars to be practically free from internal stress after this treatment. Fig. 3 shows the distribution of stresses in a pure aluminum rod after the annealing treatment.

Length measurements were made with a 100-cm end-comparator of Swiss make, using a standardized Invar meter bar for reference. The graduation is such that readings can be made directly to 0 0001 cm. and even 0 00001 cm. may be readily estimated. It was determined experimentally that readings could be duplicated to well within  $\pm 0.0001$ . Although the measurements were recorded to the fifth decimal place, the last figure has but little significance.

Measurements were made at four spots about midway between the periphery and the center of the cross-section of the specimen. The positions of these four spots were indicated by scratches and all subsequent measurements were made at these positions. Three readings were made at each spot, disturbing the settings of the cross-hairs in the measuring microscope between consecutive readings. The average of these three readings was taken as the length of the specimen between the specific pair of spots. This procedure was repeated at the other three positions. As a check, the entire procedure was repeated a second time. Thus the length of the piece was taken as the average of 24 readings.

It was noted in the above procedure that the second set of readings usually indicated a slightly larger specimen than the first. This was attributed to the increase in temperature of the specimen during manipulation. A mercury-in-glass thermometer in constant contact with the



specimen indicated the average increase in temperature to be about  $0.5^{\circ}\text{C}$ . The maximum increase noted was  $1.0^{\circ}\text{C}$ . The average of the specimen temperature at the beginning and end of the determination was taken as the temperature of measurement. This method of determining the

TABLE 2.—*Heat Treatments*

Alloy	Specimen No	Treatment
Pure Al	A-2	As prepared
Pure Al	A-4	Quenched in oil from $900^{\circ}\text{F}$ . ( $482^{\circ}\text{C}$ )
Pure Al	A-5	Quenched in boiling water from $900^{\circ}\text{F}$ ( $482^{\circ}\text{C}$ )
Pure Al	A-7	Quenched in ice water from $900^{\circ}\text{F}$ ( $482^{\circ}\text{C}$ ).
122	C-2	As prepared.
122	B-4	Quenched in oil from $900^{\circ}\text{F}$ . ( $482^{\circ}\text{C}$ .)
122	B-6	Quenched in boiling water from $900^{\circ}\text{F}$ ( $482^{\circ}\text{C}$ )
122	B-8	Quenched in ice water from $900^{\circ}\text{F}$ ( $482^{\circ}\text{C}$ ).
122	C-3	Quenched in ice water from $900^{\circ}\text{F}$ ( $482^{\circ}\text{C}$ ).
122	C-5	Quenched in ice water from $950^{\circ}\text{F}$ ( $510^{\circ}\text{C}$ ).
122	C-6	Same as C-5
122	C-8	Quenched in ice water from $900^{\circ}\text{F}$ ( $482^{\circ}\text{C}$ ), annealed at $440^{\circ}\text{F}$ ( $226^{\circ}\text{C}$ )
122	C-10	Quenched in ice water from $900^{\circ}\text{F}$ ( $482^{\circ}\text{C}$ ), annealed at $500^{\circ}\text{F}$ ( $260^{\circ}\text{C}$ ).
122	C-12	Quenched in ice water from $900^{\circ}\text{F}$ ( $482^{\circ}\text{C}$ ), annealed at $608^{\circ}\text{F}$ ( $320^{\circ}\text{C}$ )
195	D-1	Quenched in ice water from $960^{\circ}\text{F}$ ( $515^{\circ}\text{C}$ ).
195	D-2	Quenched in boiling water from $960^{\circ}\text{F}$ ( $515^{\circ}\text{C}$ )
355	D-3	Quenched in ice water from $980^{\circ}\text{F}$ . ( $526^{\circ}\text{C}$ )
355	D-4	Quenched in boiling water from $980^{\circ}\text{F}$ ( $526^{\circ}\text{C}$ )
142 (Y)	Y-1	Quenched in ice water from $960^{\circ}\text{F}$ ( $515^{\circ}\text{C}$ ).
142 (Y)	Y-2	Quenched in ice water from $960^{\circ}\text{F}$ ( $515^{\circ}\text{C}$ ), annealed at $440^{\circ}\text{F}$ . ( $226^{\circ}\text{C}$ )
51S	51SC	Quenched in cold water from $1000^{\circ}\text{F}$ . ( $538^{\circ}\text{C}$ )
51S	51SH	Quenched in boiling water from $1000^{\circ}\text{C}$ ( $538^{\circ}\text{C}$ )
25S	960C	Quenched in cold water from $960^{\circ}\text{F}$ . ( $515^{\circ}\text{C}$ ).
25S	930H	Quenched in boiling water from $930^{\circ}\text{F}$ ( $498^{\circ}\text{C}$ ).

temperature of measurement is probably accurate to  $\pm 0.25^{\circ}\text{C}$ . With a unit increase in length of aluminum of about 0.000024 per degree Centigrade, this corresponds to an error of about  $\pm 200$  lb. per sq. in. with a cut of 0.3 cm from the diameter of a specimen 20 cm long. The error, of course, decreases with larger cuts. All measurements were corrected to  $24^{\circ}\text{C}$ .

To minimize the change in temperature of the specimen during measurement it was stored in the constant-temperature measuring room for 20 hr. before measurement. The temperature of the specimen, as indicated by a thermometer in contact with it, reached the temperature of the room usually within about 5 hours.

The measured cylinders were heated at 900° to 980° F (482° to 526° C) and cooled at various rates to room temperature by quenching in one of three different mediums, ice water, boiling water, or oil at room temperature. Table 2 lists the heat treatments to which the various specimens were subjected.

Length measurements were made on a group of specimens of pure aluminum and 122 alloy before and after they had been subjected to the various heat treatments Table 3 shows the length changes in the

TABLE 3—*Dimensional Changes Due to Heat Treatment*

Specimen No	Original Length, Cm	Length after Heat Treatment, Cm	Difference, Cm	Per Cent Change
A-5	28 11149	28 11095	-0 00054	-0 0019
A-7	28 15591	28 16945	+0 01354	+0 0484
B-4	28 18814	28 17628	-0 01186	-0 0424
B-6	28 19390	28 18019	-0 01371	-0 0490
B-8	28 12299	28 10063	-0 02236	-0 0860
C-3	26 40756	26 40173	-0 00583	-0 0224
C-5	26 40720	26 37981	-0 02739	-0 1052
C-6	26 40884	26 38113	-0 02771	-0 1066
C-8	26 40901	26 41024	+0 00123	+0 0047
C-10	26 40910	26 40898	-0 00012	-0 0005
C-12	26 41287	26 40904	-0 00383	-0 0147

specimens caused by the heat treatment. To determine the dimensional stability of these heat-treated aluminum alloys during aging at room temperature, length measurements were made on specimens of the alloys after various periods of aging up to about 8 days. The dimensional changes appeared to be well within the total experimental error. An example of such determinations is given in Table 4. These results are in agreement with those reported by Grogan and Clayton.

After the initial length and diameter measurements had been made, a layer of definite thickness was machined from the pieces and the measuring process repeated. Thus, concentric layers were machined from the bars and length determinations were made after every cut until the diameter of the bar became too small to allow further machining without distortion. Care was used in the machining operation to prevent any plastic deformation. To prevent deformation due to the ordinary "dog," a close-fitting lead collar was placed around one end of the

cylinders and the dog then lightly fastened over this, the friction of the collar being sufficient to hold the piece tightly

TABLE 4.—*Dimensional Changes Due to Aging 122 Alloy at 75° F. (24° C) after Quenching from 900° F. (482° C.)*

Sample B-7

Hours after Heat Treatment	Length, Cm	Difference, Cm
21	28 10365	
42	28 10346	-0 00019
71	28 10342	-0 00004
93	28 10343	+0 00001
188	28 10336	-0 00007
Total		-0 00029

The machined bars gradually assumed a dumbbell-like form as shown in Fig 1. The cuts were made over length  $L^1$ , and the length changes due to the cut were measured over length  $L_n$ . With each cut, the stress in each layer was removed with it, hence the remaining stress in the bar

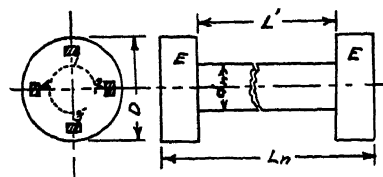


FIG 1—DIAGRAM SHOWING HOW SPECIMENS ASSUME A DUMBELL SHAPE AFTER A NUMBER OF CUTS.

Cross-hatched areas represent measuring spots

redistributed itself to attain a condition of equilibrium, and a length change of the bar resulted. The end portions,  $E$ , were not cut and did not contribute to the length change. However, the length change due to the cut  $L^1$  was transmitted through the piece and was measured over the entire length  $L$ .

By the application of Heyn's formula the stress in each machined layer was calculated. Several examples of the data and calculated stresses are given in Table 5. In the interests of space conservation the data for all the specimens are not reproduced but are available in the authors' files. To illustrate the distribution of the stresses in each piece, the average stress in each layer was plotted against one-half the cross-sectional area of the machined specimen, as shown in the diagrams in Figs. 3 to 10.

Many of the treatments were repeated in order to determine the actual experimental error in handling the material. Fig. 6 shows stresses resulting in the 122 alloy specimens

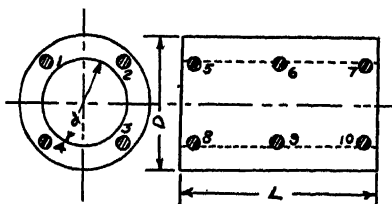


FIG 2—DIAGRAM OF CYLINDERS AFTER A NUMBER OF LAYERS HAVE BEEN REMOVED FROM CENTER

Cross-hatched circles represent measuring spots

C-5 and C-6 after they were quenched in ice water from 950° F (510° C.). Only a small variation between stresses in corresponding positions will be observed, and this is true of the other repeat specimens.

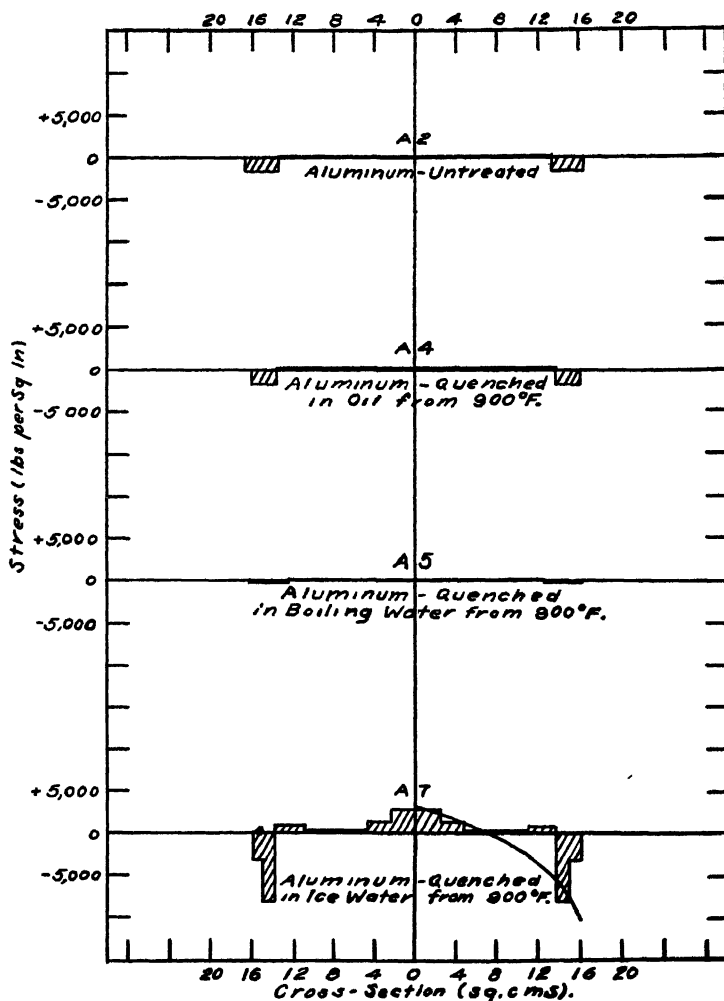


FIG 3—STRESS DIAGRAMS OF PURE ALUMINUM AFTER VARIOUS TREATMENTS.

Since the ordinates of the diagrams represent stress and the abscissas represent cross-section areas, the enclosed areas in the diagrams represent forces. Those below the zero line indicate a negative or compressive force, while those above the zero line indicate positive or tensile force. Since the internal forces in each piece are in equilibrium, the tensile force equals the compressive forces, consequently in each case the area below the zero line should equal the area above the zero line. The curved lines

are sketched in the diagrams as a guess of the probable distribution of stress, assuming that it varies smoothly from a maximum in compression at the surface through zero at about one-half the distance, on the basis

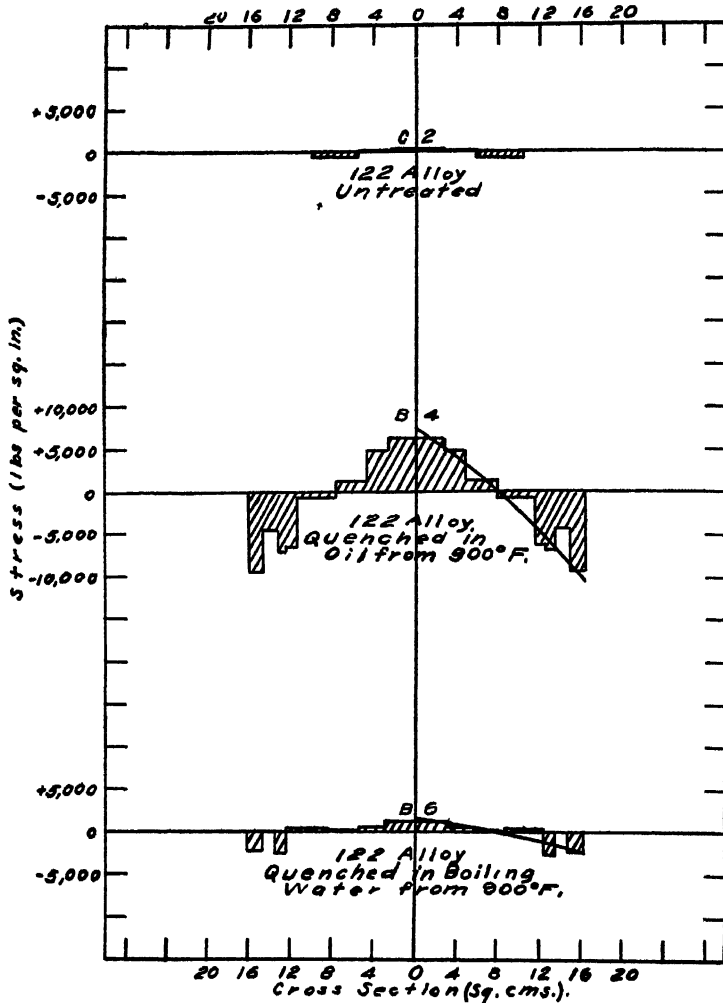


FIG. 4—STRESS DIAGRAMS OF 122 ALLOY SHOWING EFFECT OF QUENCHING IN OIL AND BOILING WATER

of cross-sectional area, between center and outside, to a maximum in tension at the center. It follows that the smaller the cuts, other experimental conditions remaining constant, the more accurately will the stress distribution be determined. Owing, however, to the limitations of the experimental methods, small cuts yield relatively great errors in stress determinations, and a depth of cut was chosen that would bring about

readily measurable changes in dimensions. Hence, the computed stresses are the average stresses in the cross-section of the individual layers

It should be noted that although the theoretical limitations of the formulas do not appear to justify measurements yielding stresses less

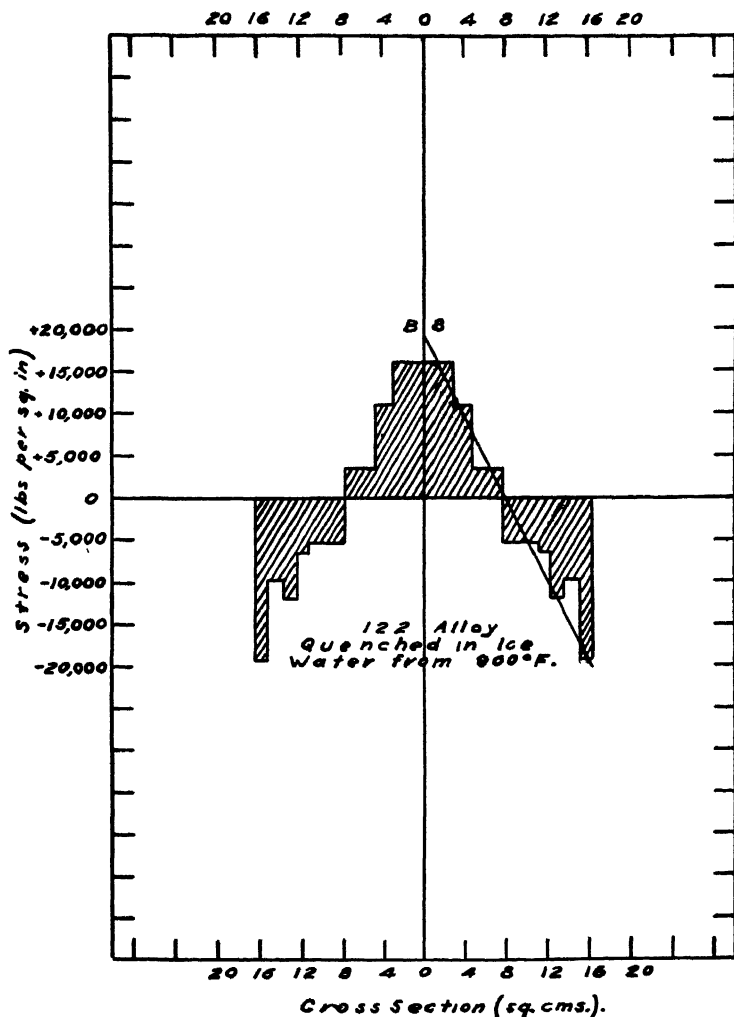


FIG. 5—STRESS DIAGRAM OF 122 ALLOY SHOWING EFFECT OF QUENCHING IN ICE WATER FROM 900° F (482° C)

than several thousands of pounds per square inch, still the consistency of these data, as well as those reported by other investigators using these methods, would seem to warrant recording the stresses to the nearest hundred pounds.

*Traaxial Stresses*

An estimation of the directional magnitude of the internal stresses was obtained utilizing the method described by Sachs.<sup>12</sup> This method consists in boring out the cores of cylinders, one axial layer at a time, so that

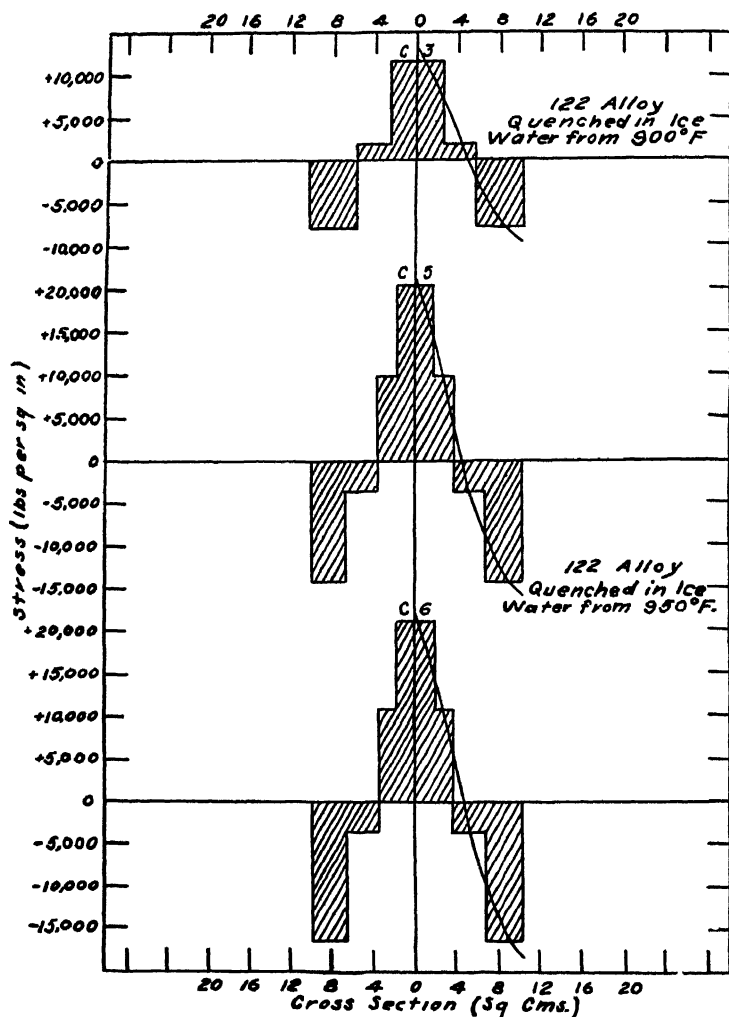


FIG 6—STRESS DIAGRAMS OF 122 ALLOY SHOWING EFFECT OF QUENCHING IN ICE WATER FROM 900 (482° C) AND 950° F. (510° C).

the longitudinal, transverse and radial stresses may be determined from the resulting variations in length and diameter. The internal stresses in each layer can be computed from the following formulas:

<sup>12</sup> Reference of footnote 6

*Longitudinal Stress:*

$$S_L = \frac{E}{1 - \gamma^2} \left[ (F_b - F) \frac{\Delta(\alpha + \gamma\beta)}{\Delta F} - (\alpha + \gamma\beta) \right]$$

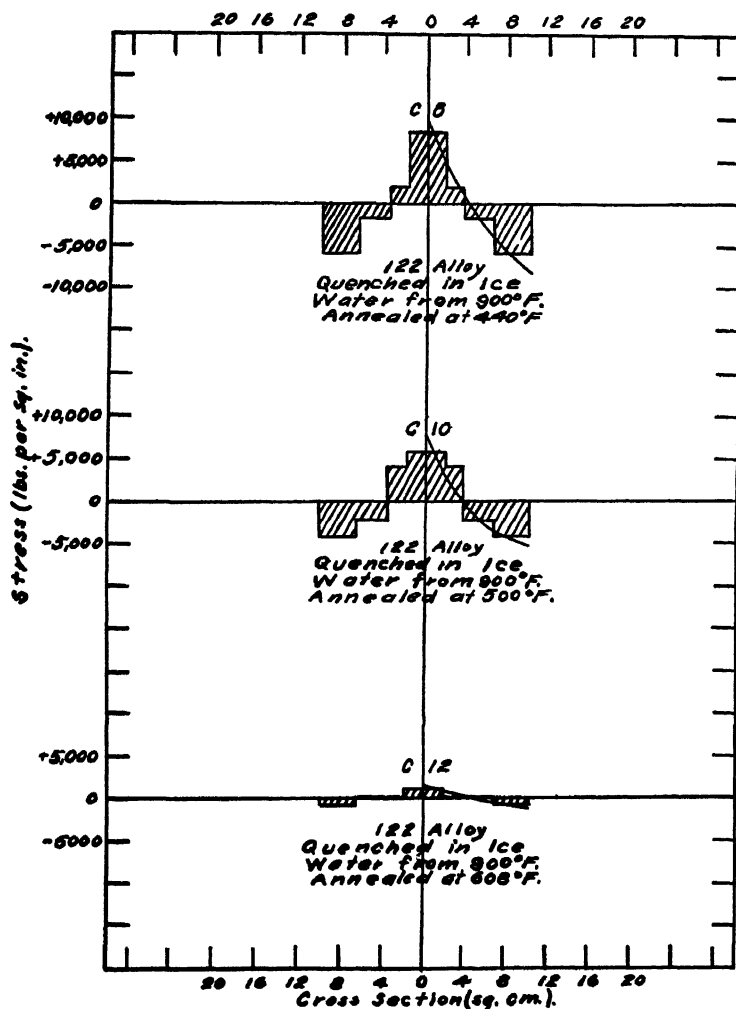


FIG. 7.—STRESS DIAGRAMS OF 122 ALLOY SPECIMENS SHOWING EFFECT OF ANNEALING ON REMOVAL OF INTERNAL STRESS.

*Tangential Stress:*

$$S_T = \frac{E}{1 - \gamma^2} \left[ (F_b - F) \frac{\Delta(\beta + \gamma\alpha)}{\Delta F} - \frac{F_b + F}{2F} (\beta + \gamma\alpha) \right]$$

*Radial Stress:*

$$S_R = \frac{E}{1 - \gamma^2} \left[ \frac{(F_b - F)}{2F} (\beta + \gamma\alpha) \right]$$



where

$\Delta$  = differential sign,

$E$  = modulus of elasticity (10,000,000 lb. per sq in.),

$\gamma$  = Poisson's ratio (0.36),

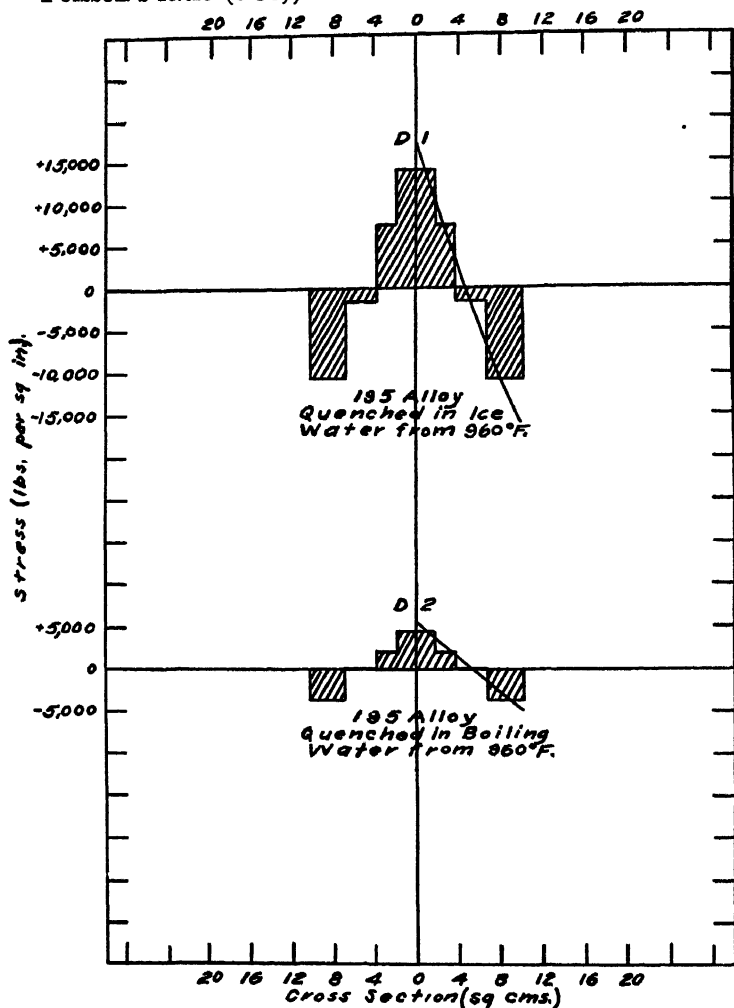


FIG. 8.—STRESS DIAGRAMS OF 195 ALLOY AFTER QUENCHING IN ICE WATER AND BOILING WATER FROM 960° F. (515° C.).

$$E^1 = \frac{E}{1 - \gamma^2} = 11,489,000,$$

$F_b$  = complete cross-section of undrilled cylinder,

$F$  = drilled-out cross-section,

$\Delta F$  = cross-section of one drilled layer,

$\alpha$  = unit length change,

$\beta$  = unit diameter change.

Solid cylinders about 7 in. long by 7 in. in diameter were carefully machined from hot-rolled 51S and 25S alloys. The compositions of the alloys are given in Table 1.

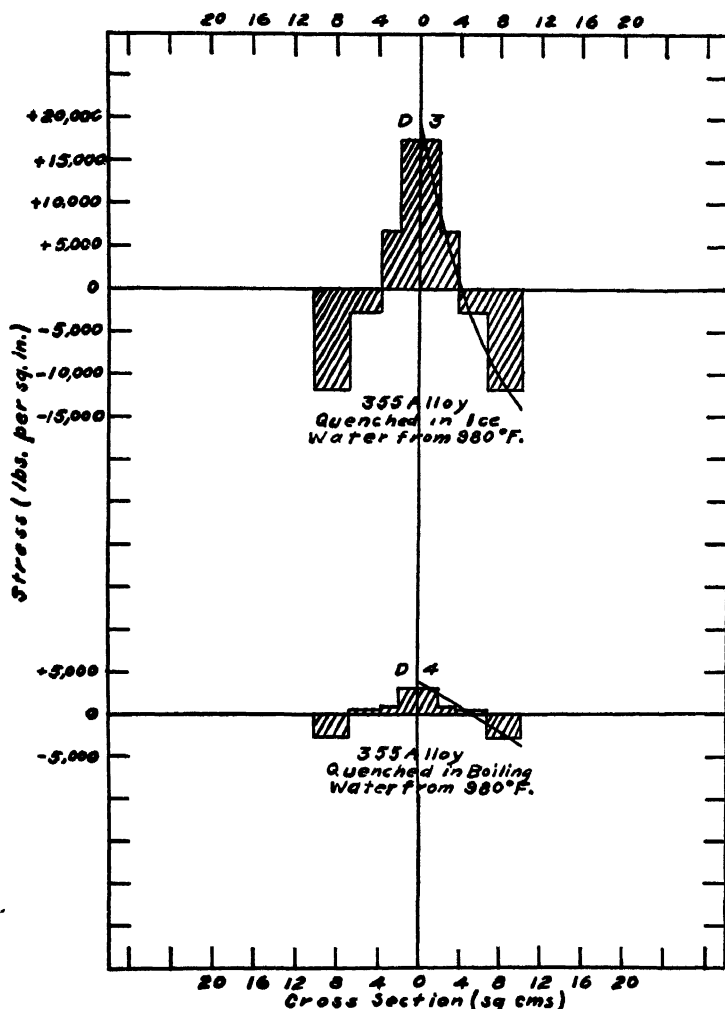


FIG. 9 —STRESS DIAGRAMS OF 355 ALLOY AFTER QUENCHING IN ICE WATER AND BOILING WATER FROM 980° F. (526° C.).

Stresses remaining from fabrication were removed by annealing the cylinders at 650° F. (343° C.). Measurements were made with a micrometer to 0.0001 in., taking necessary precautions and correcting for temperature as previously described. The locations where the measurements were taken are shown in Fig. 2. Subsequent dimensional measurements were taken on the same places. It may be somewhat confusing

that the measurements in this portion of the investigation were made in inches while those in the portion first described were in centimeters. This was unavoidable with the instruments available and it was considered that the labor involved in transposition was unwarranted in view of the

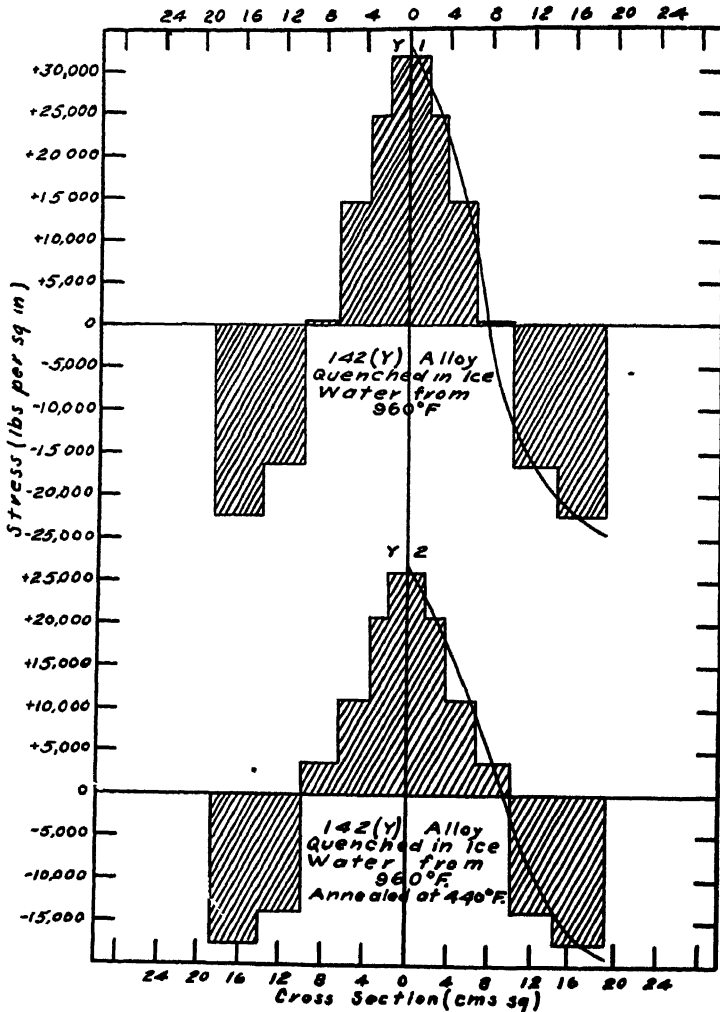


FIG 10—STRESS DIAGRAM OF 142 ALLOY SHOWING EFFECT OF QUENCHING AND ANNEALING ON INTERNAL STRESS

chances for error. Table 2 gives the quenching treatments for the various specimens.

Dimensional changes were determined after the quenching operation, and after each boring operation. The core of each cylinder was bored out so that the inside diameter was 2, 3, 4, 5 and 6 in, within 0.002 in. Care was exercised in the boring operation to prevent distortion. Examples of

TABLE 5—*Dimensional Changes and Stress in 122 Alloy Specimens*

Treatment	Number of Layers, $n$	Diameter of Bar, $n$ th Cut, $d_n$ , Cm	Length of Cut $L_1$ , Cm	Length of Bar $L_n$ , Cm	Length Change $L_n - L_0$ , Cm	Stress* $S_n$ , Lb per Sq In
C-2 As prepared	0	5 0810		26 41067		
	1	3 8085	20 91	26 40973	-0 00094	- 600
	2	2 5401	20 98	26 40960	-0 00107	+ 400
	Core					+ 600
B-6 Quenched in boiling water from 900° F (482° C)	0	6 4339		28 18000		
	1	6 1486	20 49	28 17959	-0 00042	- 2,300
	2	5 8946	20 61	28 17954	-0 00046	0
	3	5 6387	20 61	28 17904	-0 00096	- 2,600
	4	4 6830	20 67	28 17905	-0 00095	+ 500
	5	3 7248	20 67	28 17831	-0 00169	- 200
	6	2 7736	20 67	28 17759	-0 00241	+ 400
	Core					+ 1,300
B-8 Quenched in ice water from 900° F. (482° C)	0	6 4384		28 10056		
	1	6 1537	20 41	28 09710	-0 00346	-19,400
	2	5 9241	20 41	28 09538	-0 00518	- 9,800
	3	5 6366	20 71	28 09244	-0 00812	-11,900
	4	5 3813	20 71	28 09042	-0 01014	- 6,600
	5	4 4296	20 71	28 08074	-0 01982	- 5,300
	6	3 4722	20 71	28 07308	-0 02748	+ 3,600
	7	2 7754	20 74	28 06961	-0 03095	+11,100
	Core					+16,100
C-8 Quenched in ice water from 900° F (482° C), annealed at 440° F (226° C)	0	5 0858		26 41024		
	1	4 1328	21 30	26 40443	-0 00581	- 5,700
	2	3 1790	21 37	26 39818	-0 01206	- 1,600
	3	2 2235	21 37	26 39333	-0 01691	+ 3,700
	Core					+ 8,500

\* Positive sign indicates tension; negative, compression.

TABLE 6.—*Dimensional Changes in Cylinder No. 960*  
25S Quenched in Cold Water from 960° F (515° C)

Inside Diameter of Cylinder* In	Length, In	Length Change, In	Diameter, In	Diameter Change In
0	6.9019		7 1587	
2	6 9024	+0 0005	7 1597	+0 0010
3	6 9030	+0 0006	7 1606	+0 0009
4	6 9038	+0 0008	7 1617	+0 0011
5	6 9046	+0 0008	7 1630	+0 0013
6	6 9060	+0 0014	7 1660	+0 0030

\* Inside diameter was machined to  $\pm 0.002$  in

the dimensional changes and the calculated stresses after boring operations may be obtained from Table 6. The magnitude of the stresses in each layer was plotted against the bored-out cross-sectional area, and it

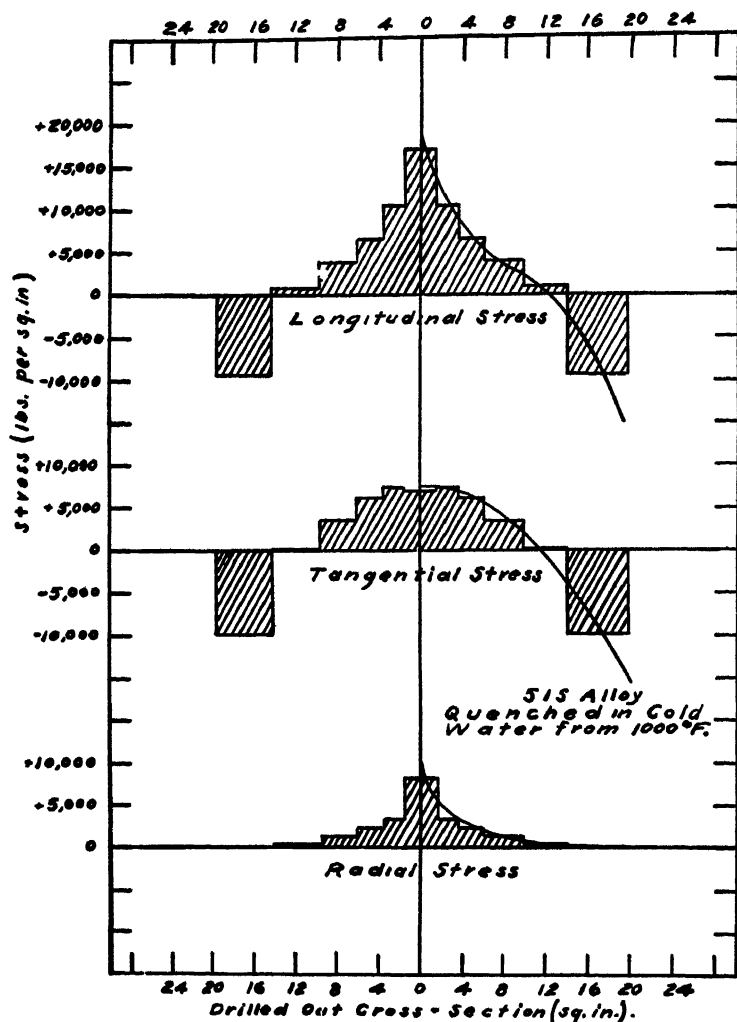


FIG. 11—STRESS DIAGRAMS OF 51S ALLOY AFTER QUENCHING IN COLD WATER FROM 1000° F (538° C)

will be observed from Figs. 11 to 14 that the type of stress diagram is similar to those obtained from the specimens measured longitudinally only.

#### DISCUSSION OF RESULTS

The data indicate that aluminum and aluminum alloy products rapidly cooled from elevated temperatures may contain internal stresses of considerable magnitude. It should be emphasized that the conditions

producing high stresses were, by intention, extremes. The average section of heat-treated castings and forgings is considerably thinner than those used in this investigation. Commercial products are never

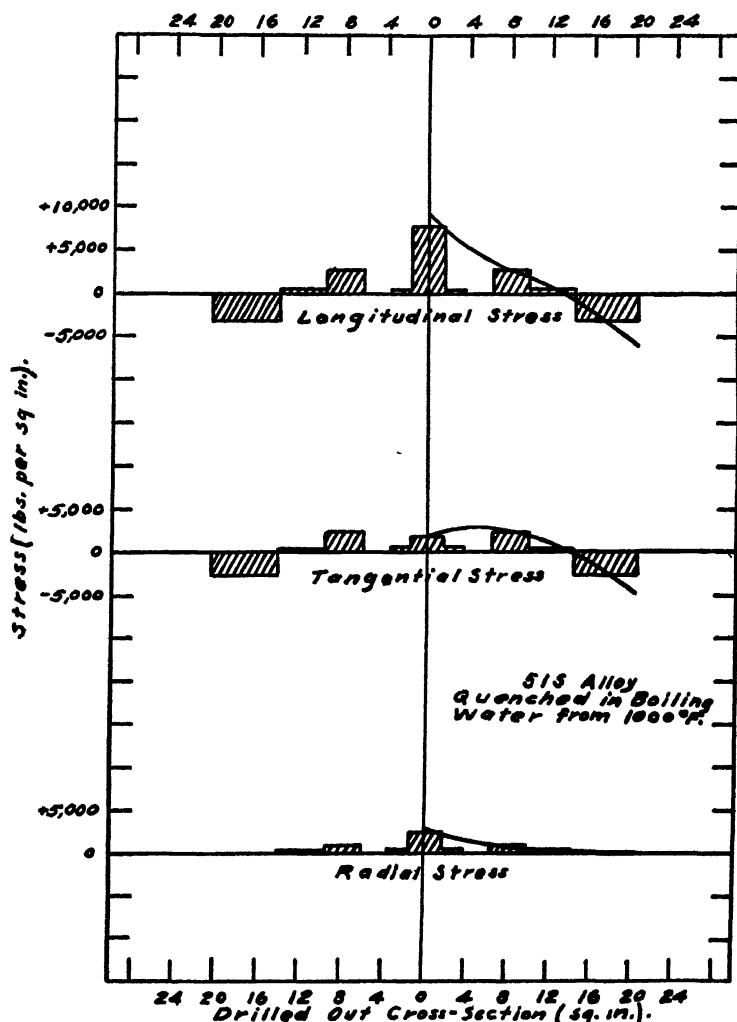


FIG 12—STRESS DIAGRAMS OF 51S ALLOY AFTER QUENCHING IN BOILING WATER FROM 1000° F (538° C)

quenched from a temperature as high as 1000° F. into water at 32° F. This selection of extreme conditions is justified by the limited accuracy of the method. One of the conclusions to be drawn from the results obtained by the use of unusual conditions is that in the heat treatment of aluminum alloys an intimate knowledge of the process and the exercise of reasonable care are necessary for attaining optimum properties.

In the specimens examined during this investigation, the maximum stresses occurred at the surface and at the center of the specimen, the stresses at the surface being compressive and at the center tensile in

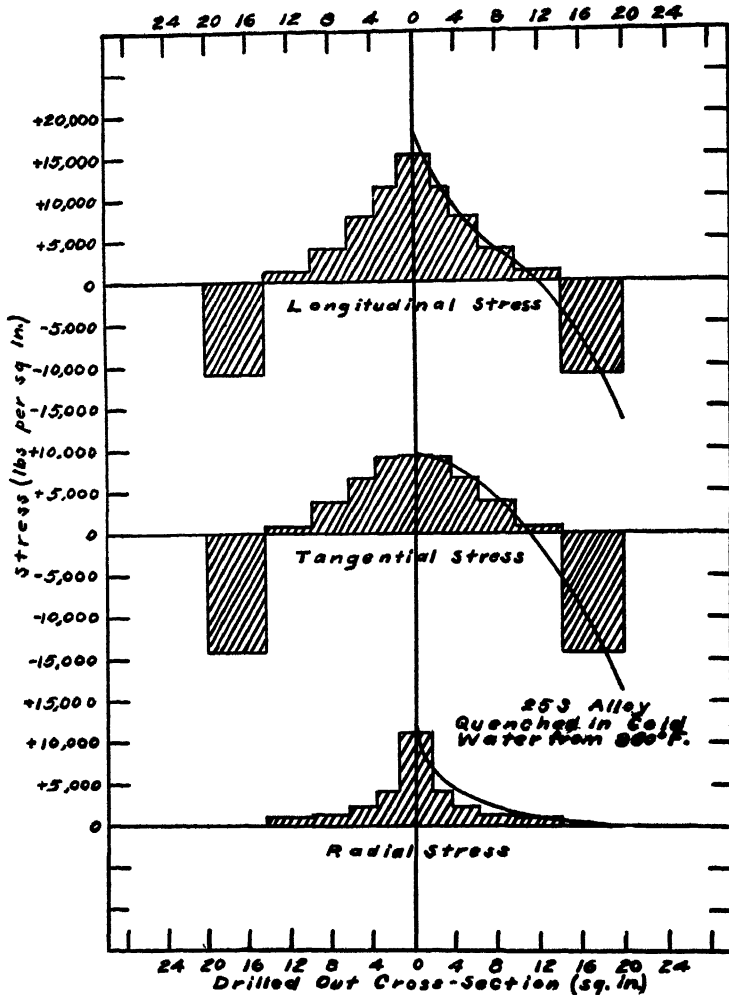


FIG 13—STRESS DIAGRAMS OF 25S ALLOY AFTER QUENCHING IN COLD WATER FROM 960° F. (515° C)

nature. The points of zero stress generally occur about halfway between the center and circumference on the basis of cross-sectional area. Linearly these points are about 0.3 the distance from circumference to center of the cylinders. In right cylinders of approximately equal diameter and length, the stresses longitudinal to the axis of the cylinder usually achieve the highest unit magnitude. The tangential stresses are about equal to

the radial stresses at the center of any given specimen and both the latter are of a lower intensity than the longitudinal stress

The normal dimensional changes to be expected on rapidly cooling a slender cylinder from an elevated temperature are a decrease in length and

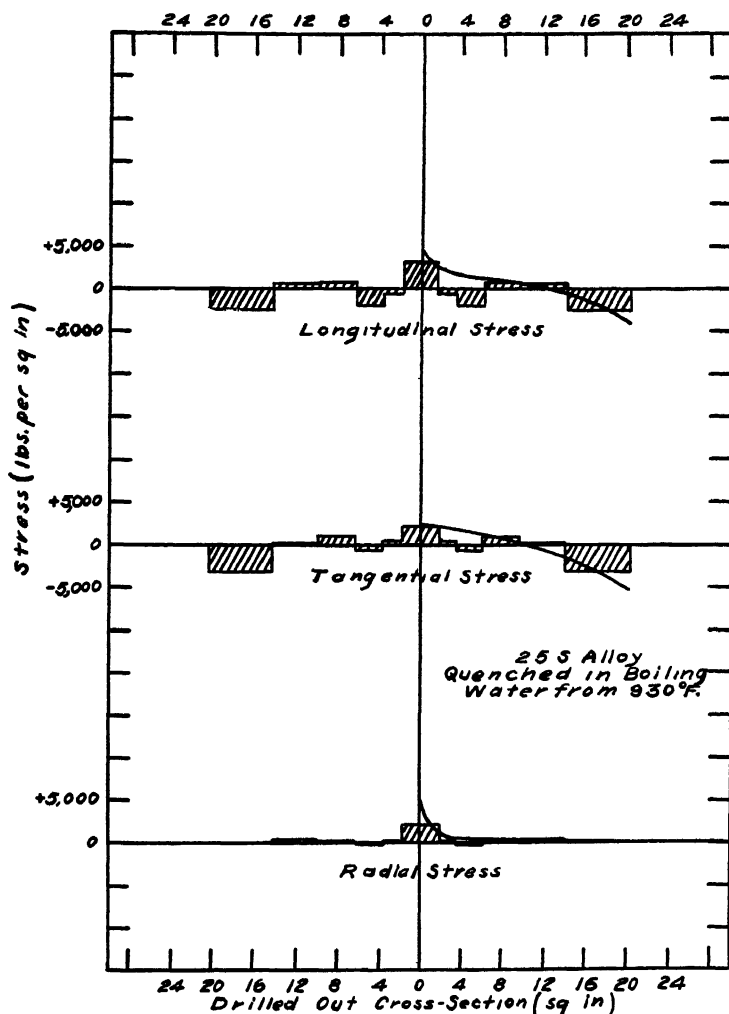


FIG 14 —STRESS DIAGRAMS OF 25S ALLOY AFTER QUENCHING IN BOILING WATER FROM 930° F. (498° C)

increase in diameter This general tendency was noted in all the quenched specimens with the exception of the pure aluminum cylinders quenched in ice water. These specimens all exhibited an increase in length. The changes in diameter were within the error of measurement This unexpected observation was repeatedly checked. No explanation is offered here for its occurrence.



The intensity of internal stress varies with the rate of cooling. The three different rates of cooling used in this investigation were brought about by quenching in water at 32° F (0° C), oil at about 77° F (25° C), and water at 212° F (100° C). The rate of cooling brought about by these quenching mediums decreases in the order named. Under any specific set of conditions the stresses induced by quenching in ice water are greater than the stresses induced by quenching in oil, which in turn are greater than the stresses induced by quenching in boiling water. With the fastest rate of cooling, quenching in water at 32° F (0° C), from extreme temperatures, the internal stresses approach in value the yield stresses of the various alloys. With a more usual rate of cooling, quenching in water at 212° F (100° C), the maximum stresses are of the same order of magnitude as the experimental errors. These effects are illustrated in the curves for specimens A-4, A-5 and A-7 (Fig 3) and B-4, B-6 and C-3 (Figs 4 and 6).

The rate of cooling will increase with increase in quenching temperature and it is therefore to be expected that the internal stresses will be a function of the quenching temperature. For an illustration of this effect, the curves for C-5 and C-6, Fig 6, may be compared with the curves for specimen C-3. These specimens were all of about the same size and all quenched in ice water. The increase in internal stress with an increase of 50° F. in quenching temperature is very marked.

The effect of size of specimen on the magnitude of the internal stresses may be estimated by comparing the curve for B-8 with that for C-3. It will be noticed that the larger specimen develops the highest internal stresses.

The elastic properties of the alloy are probably most important in determining the magnitude of the internal stresses. The stresses induced in a pure aluminum specimen are decidedly lower than those induced in any alloy under similar conditions.

The data on the series of specimens annealed at increasing temperatures following quenching in ice water from 900° F (482° C) indicate that with this time at temperature (20 hr) relief of the internal stress is more complete the higher the temperature. A limited investigation in these laboratories of the time effect in the reduction of internal stresses by annealing indicates that with a specific stress the rate of relief is a semilogarithmic function of the temperature. Also, at a specific temperature the rate of stress relief is a function of the magnitude of the stress as well as of the time. At temperatures below about 440° F (226° C.), hundreds of hours are necessary to bring about a 50 per cent reduction in the stress, while at 575° F (302° C) a few minutes will practically eliminate all internal stress. It is obvious under these circumstances that annealing treatments cannot be employed to reduce internal stresses in aluminum alloys induced by heat treatment without

simultaneously eliminating the beneficial effects of the heat treatment on mechanical properties

From a practical standpoint it is probably most important to note that under certain conditions of heat treatment structures of these dimensions may be produced with little or no internal stress. It is recognized, of course, that commercial products are usually composed of sections of widely varying thickness and of considerable complication, and it is to be expected that the internal stresses induced by heat treatment will vary with the degree of complication of the structure. The conditions, however, for minimum internal stresses are indicated and the application of such conditions in the heat treatment of commercial products should result in a minimum of internal stress. In the commercial heat treatment of aluminum alloy castings and forgings it is the general

TABLE 7—*Computed Stresses in Cylinder No. 960<sup>a</sup>*  
25S Quenched in Cold Water from 960° F (515° C)

Inside Diameter or Cylinder, In	Stress, Lb Per Sq In		
	Longitudinal	Tangential	Radial
2	15,100	9,400	11,200
3	11,400	9,200	4,200
4	7,800	6,700	2,300
5	4,000	3,800	1,400
6	1,400	900	1,200

<sup>a</sup> All values to be taken as positive indicating tension, unless designated negative indicating compression

practice to quench in hot water. Also, when heat treatments are carried out at temperatures appreciably higher than necessary for complete solution of the constituents concerned, it is customary to cool the product in the furnace to about the equilibrium temperature before quenching. These are the conditions for minimum internal stress; consequently but little trouble has been encountered from this factor in the application of these products.

### SUMMARY

1. The conditions utilized commercially in the heat treatment of aluminum alloy castings and forgings are such as to produce in simple shapes stresses of the same order of magnitude as the errors of the methods used in this investigation.

2. Under extreme conditions, involving the quenching in ice water of heavy sections from temperatures considerably above those used in ordinary practice, stresses of the same order of magnitude as the yield strength of the alloy may be induced in the heat-treated product.

3 The magnitude of stresses induced by heat treatment are influenced by the mechanical and physical properties of the alloy, the rate of cooling, and the volume and geometry of the specimen

4 Stresses in simple shapes are compressive in the surface and tensile at the center of the specimen

5 In cylindrical specimens the longitudinal stresses are of a higher order of magnitude than the tangential and radial stresses which are about equal at the center of the specimen

6 To bring about in relatively short periods of time a substantial reduction in internal stress, reheating to temperatures in excess of about 500° F (260° C) is necessary.

## DISCUSSION

(*L. S. Reed presiding*)

C. S. BARRETT,\* Pittsburgh, Pa (written discussion) —I believe there has been no paper published in this country on the measurement of internal stresses that equals this one in excellence of technique. Prior to 1927 only inferior methods were available, such as the method of Heyn mentioned in this paper. Since that date the accurate method of Sachs has been available but has remained practically unused in this country, chiefly because it is so time-consuming and costly.

No one will deny that much useful information can be obtained from methods of internal stress analysis that yield only approximate data. Most of the facts now known about internal stress have been learned by the exact methods of analysis developed by Heyn, Hatfield and Thirkell, Anderson and Fahlman, Merica and Woodward, Fox, Crampton, Templin, Mather and others. But the assumptions underlying these methods are frequently invalid, and it is not surprising that there has been much controversy over the validity and interpretation of the results obtained by their use. Buchholtz and his associates at the Forschungsinstitut der Vereinigte Stahlwerke have recently made a number of comparative tests of the best known methods and have demonstrated the superiority of the Sachs method, they are using it throughout their extensive series of researches now being published in the German metallurgical journals. There is only one other method that compares favorably with it, that is the one proposed in 1932 by Dawidenkow, which appears to hold considerable promise for tubular specimens, but which has seen little use thus far.

---

\* Metals Research Laboratory, Carnegie Institute of Technology

# Structure and Origin of the Copper-cuprous Oxide Eutectic

By L. W. EASTWOOD,<sup>4</sup> Houghton Mich

(Detroit Meeting, October, 1933.)

THE structure of eutectics has been studied by a number of investigators, and the complexity of the structural relationship of the components has been agreed upon, especially that of the "eutectic colony," type III of Portevin's<sup>1</sup> classification. This paper does not attempt to alter the present classifications of eutectics, rather, it discusses the relationship between the macrostructure and the microstructure of the copper-cuprous oxide eutectic, and describes in detail the mechanism of the formation and the structure of the eutectic. Further, throughout the entire discussion it attempts to point out certain misconceptions in regard to the interpretation of the observed structure of the copper-cuprous oxide eutectic, one of the so-called "eutectic colony" types, and to correlate as much as possible the work done by the writer with that done by other investigators.

Of the three types of eutectics listed by Portevin,<sup>2</sup> the eutectic colony type has presented the greatest difficulty in interpretation. Although the copper-cuprous oxide eutectic is typical of the eutectic colony type in appearance, it may not be truly representative because the copper forms about 96 per cent of the eutectic and the cuprous oxide about 4 per cent. The interpretation of the origin and structure of the "eutectic colony" given here is strictly limited, therefore, to the copper-cuprous oxide eutectic.

## MACROSTRUCTURE

Fig 1 shows the macrostructure of the eutectic at 3 diameters, the melt having been chill-cast into an iron mold, the resulting specimen sawed into two parts and the section polished and etched with the usual mixture of hydrogen peroxide and ammonium hydroxide. This specimen contains 0.48 per cent oxygen and is only slightly hypereutectic. If such a melt is allowed to cool slowly, large macrograins will form without the columnar structure of Fig 1 and the well-known phenomenon of liquation will occur, forming copper oxide dendrites at the top and copper

---

Manuscript received at the office of the Institute Sept 5, 1933

\* Instructor in Physical Metallurgy, Michigan College of Mining and Technology

<sup>1</sup> A. M. Portevin, *The Structure of Eutectics*, *Jnl Inst of Metals* (1923) 29, 239. Abst., *Engineering* (1923) 115.

<sup>2</sup> Reference to footnote 1

dendrites and eutectic at the bottom. Referring again to Fig. 1, it is evident that the eutectic forms large columnar macrograins much as a pure metal does. That the copper in these macrograins has the same orientation throughout and therefore composes individual crystals is proved by the following:

1 The macrograins etch similarly throughout their individual areas, adjoining macrograins etching differently in accordance with their difference in orientation, analogous to pure metals



FIG. 1—MACROSTRUCTURE OF COPPER-CUPROUS OXIDE EUTECTIC  $\times 3$

2 Deep etching shows etching pits of similar orientation throughout each individual macrograin, but of different orientation in adjoining macrograins

3 A polished surface slowly deformed produces slip bands, these bands being continuous and straight across a macrograin but changing direction at the macrograin boundary

#### MICROSTRUCTURE

Portevin<sup>1</sup> describes the copper-cuprous oxide eutectic as follows:

Viewed under magnification insufficient to resolve clearly the eutectic particles, a network approximating to polyhedra is revealed by polished and etched sections, this structure being the arrangement of "complex grains" analogous to the crystal grains of a metal. Viewed under high magnification, these grains themselves are seen to consist of a radiating or more strictly, diverging cluster of closely spaced threadlike particles of the eutectic.

Close examination of the copper-cuprous oxide eutectic in reference to its macrostructure reveals that the "complex grains" described by

<sup>1</sup> Reference of footnote 1

Portevin are not analogous to the crystal grains of a metal, but are the intersections of the polished surface with the branches of the eutectic dendrite, or macrograin. The numerous polyhedra within the eutectic grain are called "complex grains" by Portevin and "eutectic colonies" by others, however, because there has been some confusion in the use of both of these terms, the polyhedra will be designated as "intersections" in this paper. This term has the desirable feature of describing the origin and nature of the network observed in the eutectic grain. It is the eutectic grain, or macrograin, that forms in a manner analogous to that in which the crystal grain of a pure metal forms.

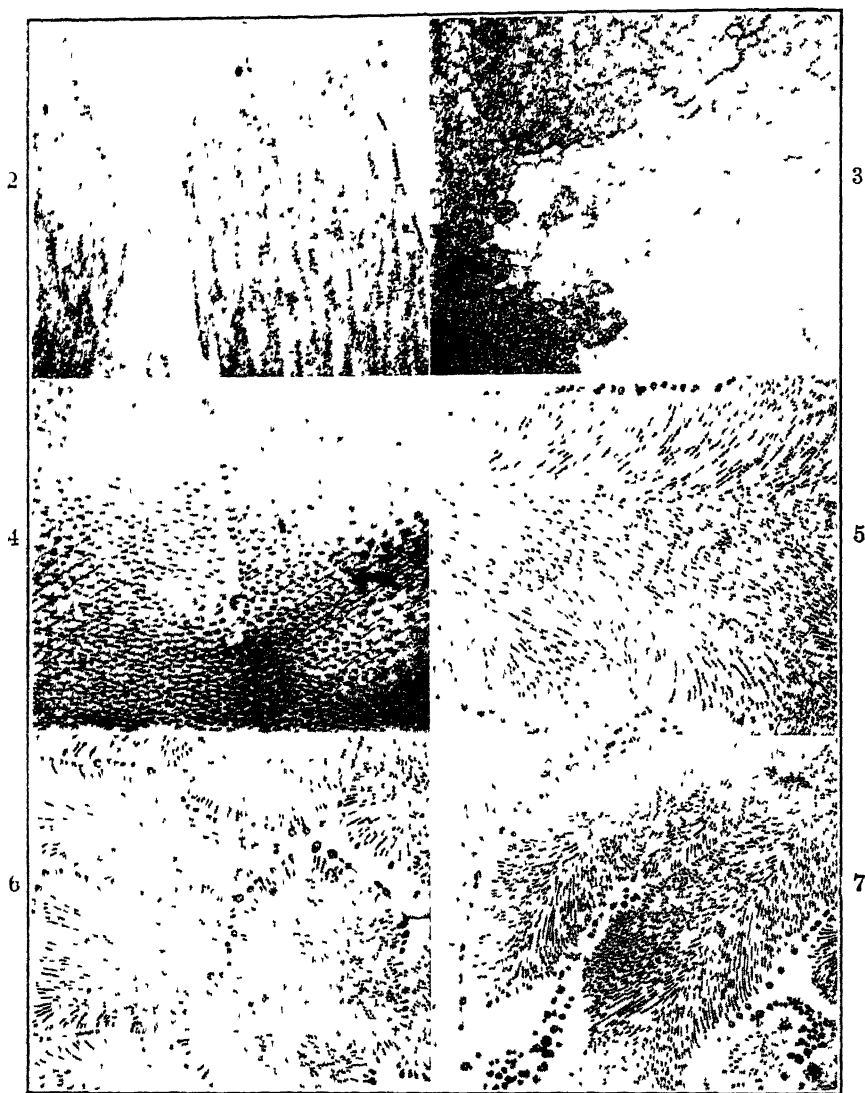
Fig 2, a nearly longitudinal section of parts of four eutectic grains of the specimen of Fig 1, shows the longitudinal and therefore elongated intersections within the eutectic grains. The light eutectic grain near the center best illustrates the longitudinal section of the main axes which grew into the melt at right angles to the mold wall. Fig 3, a cross-section of the eutectic grains, shows the numerous small equiaxed intersections within a few eutectic grains. The polished section of this specimen was made on a plane parallel to the mold wall. When viewed at high magnification, within the intersections are observed the diverging clusters of the cuprous oxide particles of the eutectic. The intersections are easily explained by the fact that the eutectic develops by the growth of a main axis which branches off to form secondary and tertiary axes, just as does the growing dendrite of a pure metal or solid solution. If the structure is columnar, produced by chill casting, the axes having a crystallographic direction of growth conducive to the greatest speed of crystallization shoot into the melt with one or more main axes parallel to the direction of crystal growth at right angles to the mold wall. The cross-section of these axes produces the equiaxed intersections of Fig 3, and a longitudinal section produces the elongated ones of Fig 2.

A grain of pure copper forms in a manner similar to the forming of the eutectic grain with its numerous branches, yet the exterior boundary of these branches—the last portions of the grain to form—cannot be observed in the pure metal because of the similar orientation and composition of the grain. If a very small amount of impurity, such as bismuth, is added, the exterior of the branches of the dendrite is clearly delineated by the particles of the impurity. However, in the case of the eutectic these boundaries between adjacent branches of the eutectic dendrite are clearly marked by the following:

- 1 The coarsening of the portion of the eutectic last to solidify. This phenomenon, pointed out by Brady,<sup>4</sup> is explained by Portevin as the result of the decreased rate of solidification of the last portions to solidify, the decreased rate being due to heat of solidification liberated

---

<sup>4</sup> F L Brady. The Structure of Eutectics. *Jnl Inst of Metals* (1922) **28**, 369. Abst., *Engineering* (1922) **114**.



FIGS 2-7

FIG 2—NEARLY LONGITUDINAL SECTION OF PARTS OF FOUR EUTECTIC GRAINS OF SPECIMEN SHOWN IN FIG 1  $\times 75$

FIG 3—CROSS-SECTION OF EUTECTIC GRAINS  $\times 75$

FIG 4—SLIP BANDS PASSING CONTINUOUSLY ACROSS BOUNDARY AND THROUGH ADJACENT SECTIONS  $\times 400$

FIG 5—CUPROUS OXIDE IN LONGITUDINAL SECTION OF EUTECTIC DENDRITE BRANCH  $\times 300$

FIG 6—RODS IN LONGITUDINAL SECTION, SHOWING RADIAL STRUCTURE NEAR PERIPHERY OF INTERSECTION  $\times 200$

FIG 7—SECTION ALONG A-B OF FIG 8A  $\times 200$

Original magnifications given, photomicrographs reduced 25 per cent.

by the portions first to solidify. The writer believes that this coarsening of the exterior may also be due in part to the greater space near the periphery as compared with the interior of the branch of the dendrite in which the copper oxide rods diverge.

2 The difference in orientation of the cuprous oxide rods in adjacent branches of the eutectic dendrite, as explained below.

3 The numerous and comparatively large spheroids of cuprous oxide in the copper shell that forms the boundary between adjacent branches of the eutectic dendrite.

These three causes of the demarcation of the adjacent branches of the eutectic dendrite are clearly shown in Figs 5, 6 and 7. In Fig 4 slip bands passing continuously across the boundary and through two adjacent intersections without interruption or change in direction show the copper in these to be of the same crystallographic orientation and hence part of the same grain.

The boundary between adjacent eutectic grains is similar to that between adjacent intersections in the same grain, except that the former is divided by a dark sharp line when the surface is etched deeply while no such line can be developed for the latter, since there is no grain boundary. The dark fine line in Figs 6 and 7 is the boundary between adjacent eutectic grains, only parts of two of the latter being visible in these photographs. A comparison can be readily made between this boundary and the one separating adjacent intersections in the same eutectic grain.

#### MORPHOLOGICAL RELATIONSHIP OF CUPROUS OXIDE AND COPPER IN EUTECTIC

When viewed at a magnification sufficient to resolve the individual constituents of the eutectic, the diverging clusters of cuprous oxide within the intersections are observed. Close examination of the columnar grains and of grains on polished sections at right angles has determined the form and position of the cuprous oxide in reference to the direction of growth of the copper dendrite. The copper is the directing constituent of the eutectic, and when a columnar grain is being formed axes of growth of the copper portion of the eutectic dendrite shoot into the melt at right angles to the mold wall. These axes fill out and form branches, which grow until they encounter adjacent branches of the same dendrite or of other dendrites. During the growth of the copper dendrite portion of the eutectic, the oxide that is being precipitated simultaneously assumes a fairly definite orientation. The oxide is present as either spheroids or rods, the former being favored by a more rapid rate of solidification than the latter. Hence, the first portion of the oxide to form—that portion nearest the central part of the branch of the copper dendrite—is likely to be spheroidal when chill-cast, while the



oxide formed in the periphery of the branch will tend to form rods, which grow out at an angle of about  $45^\circ$  to the direction of axial growth. These rods grow out from the exterior of the growing branch of the copper dendrite, and when the last portion at the exterior solidifies they "turn back," or become fluted, and approach an angle of nearly  $90^\circ$  to the direction of axial growth. A schematic representation of the appearance of the cuprous oxide in a longitudinal section of a eutectic dendrite branch is sketched in Fig 8a and a photograph of such a section is shown in Fig 5. Fig 8 represents only one axis of the eutectic dendrite with the full line representing a boundary between adjacent eutectic dendrites. The rest of the boundary marks adjacent intersections within the same grain and the arrow indicates the direction of axial growth. If a cross-section of such a branch is made, the ends of the rods will be observed except near the outer edge, where the rods curve back to nearly  $90^\circ$  to the direction of growth. Here the rods will be seen in longitudinal

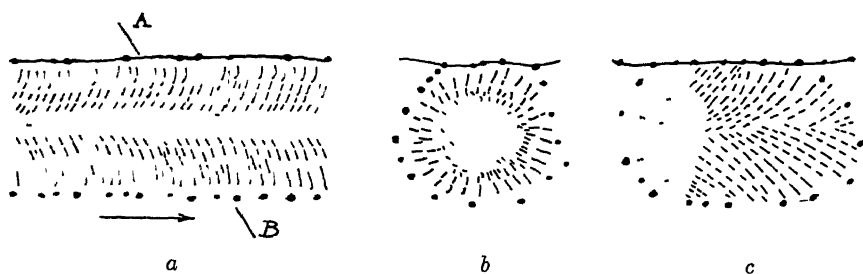


FIG 8—SCHEMATIC REPRESENTATION OF APPEARANCE OF CUPROUS OXIDE

section and will give rise to a radial structure near the periphery of the intersection. A schematic sketch of such a section is illustrated by Fig 8b and a photograph in Fig 6. If a branch is cut at any other angle, various "fan" shapes will be observed, depending upon the angle at which the section intersects the direction of axial growth. Fig 8c represents a section along A-B of Fig 8a, Fig 7 is a photograph of such a section.

If the specimen has been produced by slow cooling without chilling, the cuprous oxide rods will be pronounced and numerous branches of the dendrite will form. A random section through such a dendrite produces a great many different angles of intersection with the direction of axial growth and develops numerous "fan" and "radial" structures of the so-called "eutectic colony."

The form and structure of the eutectic crystals are usually independent of the existence of primary crystals of either copper or cuprous oxide except when the melt is cooled in a manner that permits surfusion. The copper surfsuses more than the oxide, and when rapid solidification occurs in a melt of hypereutectic, eutectic, or slightly hypoeutectic

composition it forms halos of copper about the cuprous oxide dendrites. Rapid cooling not only causes surfusion but also produces smaller eutectic grains, which are of a finer structure within themselves, the cuprous oxide appearing as very small rounded particles that can be resolved only with difficulty. Occasionally very fine cuprous oxide rods can be observed near the periphery of the intersection even after solidification at an extremely rapid rate.

The eutectic grains reveal alternate dark and light areas, giving rise to a mottled or wavy appearance when viewed at low magnification, especially by oblique illumination such as that used in Fig. 1. The mottled appearance is due to the distribution of the cuprous oxide particles, these being concentrated in thick clusters of spheroids corresponding to the darker portions of the eutectic grain. The lighter regions coincide with the portions of the dendrite containing less oxide. The darker regions, which contain the thick clusters of oxide spheroids, are especially pronounced where the main axis sends off a secondary axis. The secondary axes occur periodically along the main axes and give rise to the alternate light and dark areas that cause the wavy appearance. Because of the nature of its origin, this structural feature is most characteristic of a polished and etched longitudinal section of the columnar grains of a chill casting.

Hargreaves<sup>5</sup> investigated the lead-tin eutectic and decided from his observations before and after deformation of the eutectic by hammering that the component of the eutectic present in the greater amount forms grains similar to those of a pure metal. He called these grains "crystal grains," but designated the other component of the eutectic by the morphological term "eutectic colony." He concluded that the "crystal grain" may embrace: (1) part of one, (2) one, or (3) more than one "eutectic colony." According to his terminology, the copper forms the "crystal grain" and the cuprous oxide forms the "eutectic colony." Further, according to his classification the copper-cuprous oxide eutectic belongs to either the second or the third class, belonging to the former, however, only when it has solidified with extreme rapidity as is the case when the melt is poured into an ice-brine mixture.

The view taken in this paper differs considerably in some respects from that taken by P. Siebe<sup>6</sup> who also observed the radial structure of chill-cast copper of eutectic composition, but who apparently confused the radial macrograins with the intersections. He explained the coarsening at the boundaries of the intersections by assuming them to have

---

<sup>5</sup> F. Hargreaves, Notes on the Crystallization of the Lead-Tin Eutectic, *Jnl Inst of Metals* (1927) 37, 106.

<sup>6</sup> P. Siebe, Einige metallographische Beobachtungen an Kupferoxydul im Kupfer, *Ztsch. f. anorg. Chem.* (1926) 154.

grown by the formation of foam cells of pure copper, the eutectic solidifying within from the exterior to the interior

The writer has made an attempt to correlate the macrostructure with the microstructure, his opinion being that this is necessary to a complete understanding of eutectic structures. It is to be regretted that this phase of investigation has not been given more attention in the published work on this subject. Just how applicable the interpretation given here is to the other eutectics of Portevin's type III must remain undecided until further work is completed.

## DISCUSSION

*(Cyril Stanley Smith presiding)*

L. L. WYMAN,\* Schenectady, N. Y.—I believe that Mr. Eastwood said that on the surface of the sample the small-grain structure was probably due to the low rate of cooling. I am a little inclined to disagree with him there. I think the size of grains in the melt that is cooling down is primarily a function of the conditions present that either foster or do not foster the formation of nuclei, which in itself causes the formation of a grain. I rather seriously doubt that the condition of the slow rate of cooling might give rise to that small grain structure in this particular kind of material. I think we are dealing rather with particular conditions that foster grain growth or the initiation of grain growth by the formation of nuclei.

R. F. MEHL,† Pittsburgh, Pa. (written discussion)—Although perhaps not directly related to Mr. Eastwood's paper, I should like to point out that one factor may be operative in determining the structure of eutectics, which has not been considered by those interested in the subject. It seems possible, at least in some eutectic structures, that a unique relationship in orientation may exist between the lattices of the components in the eutectic and that this relationship may well determine, at least partly, the growth form of the eutectic structure. There is at present no evidence for the existence of such a relationship, but there are many suggestions from other types of phenomena that such a relationship may obtain. Thus we have reason to believe that gases adsorbed on the surface of metal catalysts form a lattice layer congruent with the lattice of the metal catalyst, we know that the molecules of insoluble organic acids, spread into a film on water, take preferred orientations, with the (COOH) groups pointed into the water, we have data showing that one crystal growing on top of another (the so-called overgrowths), like sodium nitrate on calcite, assumes an orientation determined by the crystallographic relationships obtaining between the two lattices, and we have ample evidence that such crystallographic relationships exist between the initial and final phases in a solid-solid transition or precipitation. Although we have no direct evidence for such relationships in eutectics, I have observed in many eutectics that the predominant component within a single eutectic grain or island frequently is continuous, without grain boundary, and that the external form of the eutectic structure within this grain or island shows some regularity. The problem is interesting and not difficult in methods of attack.

It is time that the older theories of the formation of eutectics be revised. It seems quite certain that eutectics—and eutectoids—do not form by alternate deposition of the two components by reason of reciprocating supersaturation. Observations

---

\* Research Laboratory, General Electric Co.

† Director, Metals Research Laboratory, Carnegie Institute of Technology

on lamellar eutectics show that the lamellar structure often, if not always, grows in the direction of the lamellae, as if both components were depositing simultaneously. Recent studies on eutectoids by our chairman, Dr. Smith and by E. C. Bair show that the lamellar eutectoid structures produced upon the decomposition of the beta phase in the copper-zinc system, and in the steels of eutectoid composition, definitely grow in directions that lie in the plane of the lamellae and not perpendicular to this plane.

The possibility of orientation relationships in eutectoids is simpler to conceive than in eutectics, we have recently shown that ferrite in pearlite takes its orientation from the original austenite, and presumably there is a relationship in orientation between the ferrite and cementite. Such an inheritance in orientation in eutectics is impossible, since the mother phase is a liquid, and we must look to overgrowths for a more completely analogous case.

A. J. PHILLIPS,\* Maurer, N. J.—If I understood the author correctly, the formation of the woody structure of Fig. 1 is dependent upon the arrangement of a second phase in the copper; that is, the cuprous oxide eutectic. However, I have seen the same structure in many samples of copper that were so free from cuprous oxide or any other phase that a microscopic examination at 75 diam. revealed crystals of copper only. It would therefore seem that there must be some more fundamental explanation of this typical woody structure than that advanced by the author.

C. S. SMITH,† Waterbury, Conn.—I too have seen the "woody structure" in extremely pure cast copper. I had assumed that it was due to some sort of periodic change in orientation, possibly caused by shrinkage strains, and was not necessarily due to oxide eutectic colonies.

L. W. EASTWOOD—Since my statement relative to the size of the eutectic grains at the top of the eutectic ingot was inadequate, I am pleased that Mr. Wyman has called it to my attention. The rapid cooling at the mold walls would produce supercooling and the formation of nuclei as Mr. Wyman suggests. The rapid growth of the crystals to large size is due to the rapid transfer of heat to the mold wall parallel to the growth of the crystals. The absence of such conditions at the top would necessitate smaller crystals there.

I want to thank Dr. Mehl for his remarks relative to the crystal orientation relationships of the two phases in a binary eutectic, particularly since the subject has interested me and only lack of time has, up to now, prevented investigation. I quite agree with Dr. Mehl in his remarks relative to the simultaneous precipitation of the two constituents, as will be evident from the statement near the bottom of page 185.

In regard to the "woody" structure observed by Dr. Phillips in low-oxygen copper, I doubt whether this phenomenon can have any connection with that observed in the eutectic as illustrated in Fig. 1. Close examination shows that the darker portions of the eutectic contain smaller and more numerous  $\text{Cu}_2\text{O}$  particles—a condition that depends upon their position in the eutectic dendrite, as explained in the paper.

A. M. PORTEVIN,‡ Paris, France (written discussion)—The thorough and conscientious study which Dr. Eastwood has made of the eutectic of copper oxide and copper is a very useful contribution to the knowledge of eutectic structures in general.

As a matter of fact, there exists some confusion due to the various expressions employed in describing the structure of eutectics of type 3 of our classification—the

\* Superintendent, Central Research Laboratory, American Smelting & Refining Co.

† In charge, Copper Alloys Research Laboratories, American Brass Co.

‡ Professor, Ecole de Soudure Autogene

§ Translated from the French

type of the eutectic designated as "madrepore" or as the "eutectic colony." According to authors the designations "eutectic colony," "complex grains," "eutectic grains," and "macrograins" are also used, but are applied with various meanings. The intention to apply these in a precise and practical sense would be to adopt the following designations:

1 *Grains of Solidification*—Under "grains of solidification," "macrograins" or "complex grains," we intend individual crystals, or crystalline units, formed by solidification—those which appear micrographically with the same essential characteristics as the grains forming the structure, or macro-structure, by the solidification of cast metals. Each individual is characterized by the crystalline unit of orientation of the principal constituent or director of the eutectic—that which one may identify by the uniformity of the crystalline characteristics, i.e., uniformity of the direction of the slip planes, the shape of etching pits, characteristics that change decidedly when one considers a neighboring grain. These grains are separated by boundaries forming a network of fine, definite lines.

2 *Eutectic Colonies*—This term applies to all the groupings of two constituents of the eutectic in groups more or less divergent or radiating toward the periphery (following the orientation of the micrographic section of which Dr. Eastwood and we ourselves have shown schematic representations. See particularly Fig. 8 of Dr. Eastwood's monograph as well as Fig. 10 of our monograph). Usually the two components of the eutectic are more developed at the periphery of the eutectic colonies, in such a manner that the contours of these colonies form a cellular network of which the meshes are distinguished by difference of direction and by the enlargement and the spacing of the terminating elements or peripheries of the two constituents. This demarcation between adjacent colonies is neither so definite nor so distinct as that of the macrograins of solidification.

These eutectic colonies might equally well be termed "cells," for reasons that will be given later. Their grouping forms that which we have termed the "madrepore" structure because of the similarity in its appearance to the madrepores, especially those of fossil coral formations.

There are, however, two structural entities in the solid eutectic: (1) The crystals determined by the difference of the crystalline orientation of the main constituent are separated by a network of very fine lines, (2) that which is determined structurally by the distribution of the second constituent and whose elements, colonies or eutectic cells, form a second, cellular network.

These two structures are superposed, the crystalline grains admitting of several colonies, a single colony or a fraction of a eutectic colony.

If the first structure is of crystalline origin and entirely analogous to the macrograins of solidification of metals, especially those which form the directing or preponderant part of the eutectic  $\text{Cu-Cu}_2\text{O}$ , it seems that the distribution of the second constituent in these grains cannot be completely assimilated by the one that resulted in a dendritic crystallization of the principal constituent—like that of the metals or solid solution. As a matter of fact, the dendritic directions in a grain are rectilinear and their relative orientation follows the laws of crystallographic orientation and in general is conducted according to the quaternary axes of the cube (axis of the octahedron) in the cubic system. This is hardly in agreement with the inward curve of the filaments and grains or the alignments formed by the particles of the second constituent, or with the radial distribution which it assumes in the group—this being a distribution very different from that of the particles that result from dendritic segregation.

<sup>7</sup> Reference of footnote 1

Here, however, one should have the intervention of a second phenomenon, and this second structure, peculiar to the eutectic colonies, leads to a consideration of the cellular vortex as set forth in the work of Benard, Dazere and Lord Rayleigh. This should include as well the thermal convections in heating and cooling liquids.

"A cellular structure" forms within the liquid,<sup>8</sup> in each cell the trajectories of the flow are closed curves disposed radially around the axial line which expand toward the periphery or "partition" of the cells. (Regions where there are no currents.) The currents in the liquid modify the concentration and consequently the diffusion in the liquids. This occurs in such a way that they direct the distribution of eutectic particles according to their trajectories at the moment of the formation of the eutectic particles in the liquid, and as a result they tend to increase the radial distribution and the peripheral accumulation.

The filiform (threadlike) particles of the eutectic become fine and delicate as the rapidity of crystallization  $V_c$  increases, for the latter depends upon the diffusion in the liquid. At the edges of the cells there is a decrease of  $V_c$ , at the same time as an increase of temperature.

In support of this hypothesis we hasten to point out the surprising analogy between Fig. 2 in Dr. Eastwood's monograph and a photograph of lead obtained by Cartaud and published by Osmond.<sup>9</sup> The effect of the picric acid in solution in acetone was to disclose a microscopic cellular network with thickening of the lines into knots, as well as another network with far larger meshes formed by the fine lines of the boundaries of the primary crystals.

The first network is entirely similar to that formed by the contour of the eutectic colonies and the second by the boundaries of the macrograms of solidification.

In the last work published before his death, Cartaud<sup>10</sup> writes concerning this figure: "cells and crystals show a distinct relation between them, the regions of similar crystalline orientation have this type of mesh which is cellular in form, and also the specific arrangements which show a crystal to be like an aggregate of similar cells similarly disposed—the latter, however, at close inspection, is only apparent. The crystalline boundaries pass freely through the cells and do not follow at all the wavy line which marks the edge of the regions of the same cellular mesh."

The chemical etching and the lines of slip determined by the mechanical deformations allow the identification of the second network with the intercrystalline network of the actual structure and show nothing in the wavy lines except evidence of a previous structural condition. The crystalline boundaries have followed the edges of the cellular regions of similar mesh. This is the reason they cut the primary, marginal cells. Therefore, according to Cartaud, when the lead came into contact with a cold surface there was a relation between the "embryonic structure" and the actual, crystalline, "adult structure."

If certain of these conclusions of Cartaud are questionable, it is nevertheless true that the role of the vortex in the liquid is undeniably in the formation of certain

<sup>8</sup> These cellular vortices represent the most stable of three systems of vortices according to the viscosity and thermal conductivity of a liquid of thermal gradations. With Benard, one distinguishes: (1) the system of vortices in bands (strip vortices), a permanent system that is stable when the flow of heat is very small, (2) the system of cellular vortices—a stable system that comes nearest to geometric perfection for the average flow of heat and average viscosity, (3) the system of chain-like vortices—the most unstable of all. This develops when the viscosity is very low and the flow of heat very great.

<sup>9</sup> Les Recherches de G. Cartaud sur le Passage de l'État Liquide à l'État Solide. *Rev. de Met.* (1907) 4, 827, Fig. 31.

<sup>10</sup> *Comptes rend.* (1904) 140, 428.

crystallites Cartaud decided that there is decided relation between the cells and crystals although the crystalline boundaries freely traverse the cells

At least, one may say that the formation of cells, vortices, and crystals is dependent upon mutual physical conditions, i.e., exterior chilling, thickness, thermal conductivity, viscosity and agitation in liquid. It is not surprising that there is a connection between the two phenomena and that an "accommodation" takes place between the process of amorphous formations and crystalline formations (between the cellular network of liquid whirling and the cellular network of solidification)

This interrelation is probably much closer in the case of the solidification of eutectics, because the low speed of crystallization is weaker since it is under the influence of diffusion, which is under the action of the liquid currents, which persist, attenuated and deformed, in the liquid that surrounds them

The filiform constituents tend to follow the direction of the radiating threads which spread toward the periphery, that is to say, toward the "partitions" where the motion of the liquid is stopped

The similarity is remarkable between the figures shown by Benard and the pictures of the sections normal to the direction of elongation of the cells, on the other hand, one may not push the comparison too far, because Benard's experiments were performed upon liquid layers and he was much more concerned about the solidification of a liquid mass than about the study of eutectics

In this notation upon the evolution of the structure of metals Cartaud<sup>11</sup> cites the eutectic of copper oxide and copper as an exact example in support of the identification of the cells of the metals with the cell—vortices of Benard. In support of this, he mentions a photomicrograph of the work of Heyn which appeared in 1900.<sup>12</sup> He declares that the grains (lamellae) are well arranged, like the threads of Benard's vortices seen in cross-section and materialized by the two phases of the alloy

However, it is not only because of an analogy of structure that we have given the name "madrepore" to the type of structure to which the eutectic of copper oxide and copper belongs—we have been struck by the similarity of structure of numerous eutectics with these calcareous forms in which the numerous canalicules containing the living material may well represent the constituent enveloped by the eutectic, especially since they expand on parallel lines, diverge and swell to their extremities in the lime skeleton that represents the enveloping constituent of the eutectic. Another category of these madrepores, the "meandrines," on the contrary, have a skeleton of lime formed of wavy layers, or partitions, which contain living matter in bands. This whole arrangement recalls to a striking degree the eutectics of copper phosphide and copper. In accord with the statement of Renny Perrier, Benard emphasizes that in these walls or partitions, or places of no flow, the vortices of the third type reproduce exactly the complicated forms of the walls of the meandrines, the identity adhering rigorously to the minutest detail

We wish to congratulate Dr. Eastwood upon his work and to thank him for this opportunity to develop our ideas upon the origin of the structure of eutectics of the third type, the madrepore type, or the eutectic colony, which allows the theory of the superposition of two successive physical phenomena—cellular whirling of convection and crystallization, which nevertheless are interrelated, from the results of which a certain adaptation of two structures is established

L. W. EASTWOOD—The author appreciates the interest on the part of M. Portevin and his presentation of his views on the cellular growth of metals, a theory maintained by many continental European metallurgists since the work of Benard and Cartaud more than 30 years ago

<sup>11</sup> Reference of footnote 10

<sup>12</sup> Reference of footnote 9, 826

The explanation of the so-called "cells," which are observed on some metals cast in very thin sheets, does not necessitate an explanation different from that which accounts for ordinary crystal growth, i.e., growth by the formation of axes. The evidence of crystal growth by the formation of axes is abundant, as is shown principally by the very common observation of dendrites (1) on the surface of cast pure metals, (2) in polished and etched heterogeneous as-cast solid solutions, and (3) as primary crystals in a eutectic matrix. By this clearly established mechanism of crystal growth, the occurrence of the cells in cast thin sheets is readily explained without having to introduce any conjectural theory involving crystal growth by cell formation.

The cells observed upon the surface of some fusible metals, particularly lead, when cast into very thin sheets are formed by the contraction of the remaining liquid after the axes are formed. The formation of dendritic axes and their appearance in relief on the surface of cast metals is a common occurrence. When the metal is cast into thin sheets many crystals begin to form, each with many branching axes which form first as the skeleton of the crystal. The contraction during solidification leaves these first-formed axes in relief on the surface, each axis in relief forming a "cell," the exterior of which is lower than the interior, as would be expected. Careful examination shows the periphery of the cell to be lower than the rest, and for this reason alone it is possible to observe the cells. This is confirmed by the statement of Osmond<sup>13</sup> that polishing and etching removes the cells, which can then no longer be observed. The exterior of the axial framework marks the boundary of the crystal, the exterior of the marginal cells being coincident with the crystal boundary. Very frequently, however, the grain boundary of lead is found to cut through the cells rather than around them. This is readily accounted for because the grain boundary shifts, the original irregular grain boundary, which passes around the cells, is unstable, as a result of (1) the cooling strains set up by the severe method of casting and (2) the greater surface area, and hence greater surface energy, of the irregular grains. As a result of this instability, combined with the fact that lead recrystallizes at about room temperature, new grains are formed, the straight or curved boundaries of which may approximate the old ones, as illustrated by Fig. 32 in the paper by Osmond. In some cases entirely new boundaries are formed. The new grains are bounded by plain or curved surfaces typical of recrystallized metals rather than by the usual wavy ones of unrecrystallized cast lead. The new grain boundaries quickly form in the cast sheet before they reach room temperature after casting. The instability of the grain boundaries of lead is further attested by the statement of Osmond that frequently the grain boundaries occur in duplicate or triplicate. This phenomenon, also observed by the author, is due to the fact that sometimes the traces of the grain boundary are left in their former positions. This phenomenon has been observed frequently, particularly by Carpenter and Elam.<sup>14</sup>

Further evidence of the mode of "cell" formation described above follows:

- 1 If a thin strip of lead cast on glass is examined, "cells" are observed on the surface exposed to the air. On the side next to the glass one can frequently see small dendritic axes in relief. It is evident, then, that these grains at least are formed by the development of an axial framework. It is not logical that other adjacent crystals cooled under similar circumstances should form by so revolutionary a process as that postulated by the theory of cell growth.

- 2 Frequently the "cells" observed on the surface of lead cast in thin sheets are not circular in cross-section but greatly elongated. In fact they may extend entirely

---

<sup>13</sup> Reference of footnote 9, 819.

<sup>14</sup> Carpenter and Elam, *Crystal Growth and Recrystallization in Metals*, *Jnl Inst of Metals* (1920-22) **24**, 83-131.



across the surface of the grain. Obviously these are longitudinal sections of axes of columnar crystals whose growth has been preponderantly in one direction and without much branching. These are entirely analogous to the longitudinal intersections of Figs. 2, 5 and 8a. When the cells appear nearly spherical in cross-section they are produced by the observation of cross-sectional or nearly cross-sectional axial intersections. Such sections are entirely analogous to Figs. 3, 4, 6, 7, 8b and 8c. As would be expected, by this mechanism of crystal formation all the cells in a given original grain are of similar shape, although as explained above, the new grain boundary in lead does not always follow this division.

3. When the slope of the glass plate is decreased and a slightly thicker lead sheet is cast, both "cells" and the usual form of dendritic axes remain in relief in close juxtaposition. Both the dendritic crystals and the cells solidified under similar conditions, and therefore it is illogical to suppose the cells to be formed by the mechanism of cell growth. Their only difference is orientation and the relation of the surface to the position of primary axes.

Since the vortices of convection of Benard are said to account for the cellular growth, and since the evidence against cellular growth is considerable, it follows that any attempt to explain the shape and position of the cuprous oxide rods in the eutectic by the shape and position of the vortices in the cells must also be subject to the objections discussed above. Furthermore, it is difficult to imagine the fanciful condition of convection currents whereby all the numerous orientations of the cuprous oxide rods within one small crystal could have been influenced by similarly oriented convection currents, the orientation of the latter apparently being in entire disregard to the direction of gravity.

The mere fact that the cuprous oxide rods are curved does not preclude the possibility that they were formed by "rectilinear" process, i.e., by the development of an axial framework. The internal arrangement of the atoms is entirely rectilinear, though the exterior form may be distorted or bent. Thus Fig. 1 shows macrograins bent upwards, a peculiarity of growth caused by the shape of the isothermal surfaces in the cooling liquid.

The author has endeavored to explain the mechanism of growth of the crystals without attempting to explain the cause of this mechanism or the reason for the shape and position of the cuprous oxide particles in the eutectics. The latter is difficult to determine and it is hoped others may join M. Portevin in presenting their views.

F. HARGREAVES,\* Southampton, England (written discussion).—The author is to be congratulated on having given the first clear account of the crystallization of a eutectic. He has described the mechanism of formation of "chill" crystals. To render this complete the orientation of the oxide forming the "intersections" together with the crystallographic relation between the individual intersections require to be described. Such a task will be very difficult.

In the case of the cadmium-zinc eutectic, it is possible to show at will the orientation of either constituent. The fundamental factor in such cases as this is the relation between the electrochemical potentials of the two constituents in the etching agent applied.

Mr. Eastwood's paper deals with chill crystals in which, of course, the direction of growth is known, but it is very probable that more complex relations exist in the case of non-chill crystals. In pure metals the latter grow from independent nuclei and spread in all directions, i.e., they grow from a center. When, however, it is sought to apply similar ideas of growth to non-chill crystals of the eutectic of, say, lead-tin or cadmium-tin the continuity of the eutectic pattern through several orienta-

\* Chemist, Southern Railway

tions of one of the constituents presents a problem that appears insoluble on the assumption that the usual mechanism of crystal growth is in operation

It is rather surprising that Mr Eastwood finds the eutectic crystals usually independent of the primary crystals of either constituent. I would have expected in this case that the eutectic crystals would be on the same lattice as any primary copper crystals that happened to be present. A similar thing happens in the case of the lead-tin eutectic when tin is present as primary crystals but not when lead is the primary constituent.<sup>15</sup>

L W EASTWOOD (written discussion) —The problem encountered when attempting to determine the mechanism of growth of non-chill copper-cuprous oxide eutectic crystals is somewhat more complex, as Mr Hargreaves observes, than when studying columnar, or chill, crystals. The branches of the non-chill eutectic crystals grow in all directions from a starting nucleus, a given axis of the copper portion of the eutectic dendrite grows in a definite direction, and the relationship noted in the paper between this direction and the position and shape of the cuprous oxide rods is valid for the growth of non-chill crystals also. The principle difference is in the number of axes. A chill crystal has primary axes extending at right angles to the chilling surface without much branching. On the other hand, a non-chill crystal exhibits a great deal of branching. Hence a polished section through such a crystal shows a greater variety of "intersections", this gives the impression of greater complexity though the mechanism of growth in so far as the relationship of the constituents is concerned is similar to that of chill crystals, the only difference being that the non-chill eutectic is coarser.

---

<sup>15</sup> Hargreaves and Hills. Work Softening and a Theory of Intercrystalline Cohesion. *Jnl Inst of Metals* (1929), **41**, 257.

## Influence of Silver on the Softening of Cold-worked Copper

BY H C KENNY,\* HUBBELL, MICH, AND G L CRAIG,† COLUMBUS, OHIO

(New York Meeting, February, 1934)

THE annealing or softening temperature of cold-worked copper is appreciably increased by almost unbelievably small amounts of silver. As indicated by some data in this paper, the softening temperature of high-conductivity, tough-pitch copper may be increased from 200° to 350° C by the addition of only 15 oz per ton (0.052 per cent) of that element. Because it has this higher annealing temperature as compared with the silver-free metal, silver-bearing copper finds considerable use in industry. For example, when hard-rolled copper is used in operations that involve soldering or tinning, silver-bearing copper insures against loss of strength, whereas silver-free copper becomes "dead soft."

Yet—though several investigators, beginning with Caesar and Gerner<sup>1</sup> in 1916, have shown that small amounts of silver do definitely raise the softening temperature of copper—data are lacking on the problem: What is the specific influence of different amounts of silver on this temperature? It was to help in filling this gap in the knowledge of what might be termed "alloy coppers" that the data given herein were obtained.

The softening of cold-worked copper depends, of course, on a number of factors, of which the composition of the material is only one. Other highly important factors are the degree to which the material is cold-worked and the time it is held at the annealing temperature. The method of cold working and the grain size of the metal produced are also significant. All these variables were taken into account in the investigation reported here, and the influence of silver on the electrical conductivity and on the working was also considered.

The coppers used in the softening tests were Lake coppers melted and cast by the Calumet and Hecla Consolidated Copper Co. The wires were fabricated by the Roebling Wire Co. and the sheets were rolled at the Battelle Memorial Institute. Partial analyses of some of the coppers are listed in Table 1, with their electrical conductivities.

---

Manuscript received at the office of the Institute Nov. 22, 1933

\* Calumet and Hecla Consolidated Copper Co.

† Battelle Memorial Institute

<sup>1</sup> G. V. Caesar and G. C. Gerner, "The Annealing Properties of Copper at Temperatures Below 500° C, with Particular Reference to the Effect of Oxygen and of Silver," *Trans. Amer. Inst. Metals* (1916) **10**, 208-248.

## SOFTENING DURING SHORT-TIME ANNEALS

Annealing or softening temperatures of copper sheet cold-rolled 2, 4 and 6 B & S gage numbers (20, 37 and 50 per cent reduction in thickness)

TABLE 1—*Analysis and Electrical Conductivity of Typical Samples of Lake Copper*

Sample No	Silver		Oxygen, Per Cent	Electrical Conductivity, Per Cent of International Standard
	Oz per Ton	Per Cent		
1	0 36	0 001	0 053	101 0
2	6 8	0 023	0 059	100 8
3	10 5	0 035	0 068	100 5
4	15 3	0 052	0 060	100 6
5	20 2	0 069	0 048	100 7
6	25 5	0 086	0 048	100 6
7	30 0	0 103	0 067	100 2
8	35 6	0 122	0 068	100 1
9	38 6	0 132	0 056	100 1

are shown in Fig 1 These temperatures apply to an annealing period of  $\frac{1}{2}$  hr Softening was measured by means of Rockwell hardness tests. The softening temperature was taken as that at which the hardness-

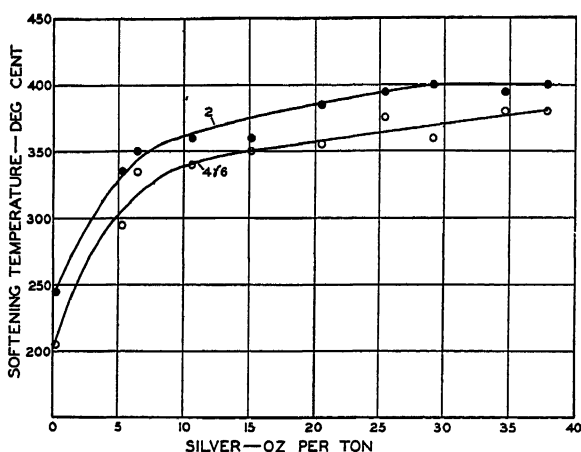


FIG 1—INFLUENCE OF SILVER ON SOFTENING TEMPERATURE OF COPPER SHEET ROLLED 2, 4 AND 6 B & S NUMBERS HARD  
Numbers on curves refer to reduction in gage

temperature curve became practically parallel to the hardness axis The hardness dropped suddenly when what is termed the "softening temperature" was reached.

As the curves indicate, there is no detectable difference in the softening temperature of the material rolled 4 numbers hard and that rolled 6 numbers hard, but the softening temperature of the material rolled 2 numbers hard is 30° C higher than that of the more severely cold-worked materials. For a heating time of  $\frac{1}{2}$  hr the addition of 10 oz per ton

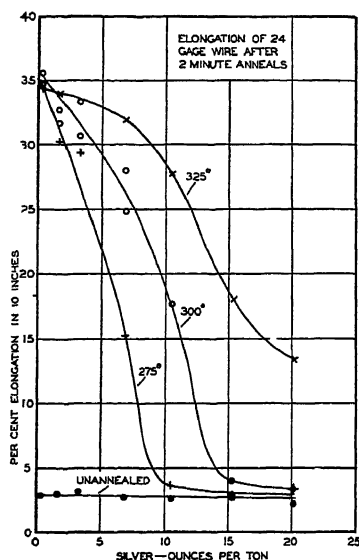


FIG 2

FIG 2 —ELONGATION OF 24-GAGE (0.020-IN) WIRE AFTER 2-MIN ANNEALS AT SEVERAL TEMPERATURES

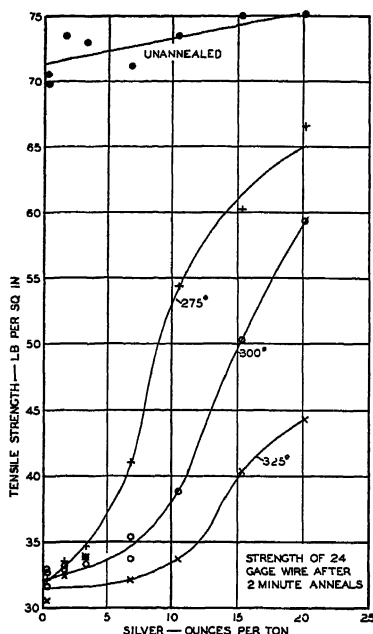


FIG 3

FIG 3 —TENSILE STRENGTH OF 24-GAGE (0.020-IN) WIRE AFTER 2-MIN ANNEALS AT SEVERAL TEMPERATURES

(0.034 per cent) of silver increases the softening temperature by approximately 130° C. A further increase in silver content increases the softening temperature but slightly.

The tensile properties of silver-bearing copper wires annealed for 2-min. periods in a salt bath are shown in Figs 2 and 3. The wires were 0.020 in. in diameter (24 B & S gage) and had been drawn without annealing from hot-rolled rods  $\frac{5}{16}$  in in diameter. Even at a temperature of 325° C the severely cold-worked wires containing over 15 oz per ton (0.052 per cent) silver were not completely softened by the 2-min. anneal.

#### SOFTENING DURING TINNING

Tensile specimens  $\frac{1}{2}$  in wide with a gage length of 2 in were cut from 0.020-in (24 B & S gage) sheet that had been cold-rolled 2, 4 and 6

B & S gage numbers hard. The tensile properties of these specimens are shown in the third and fourth columns of Table 2. Tensile specimens from each sheet were inserted in a jig and immersed for 10 sec in a 60-40 lead-tin bath maintained at 360° C. The tensile properties of the tinned samples are shown in the last two columns of Table 2, and the percentage loss in strength due to tinning (actually due to heating in the lead-tin bath) is shown in Fig 4. For sheets rolled 2 or 4 numbers hard, 10 oz per ton (0.034 per cent) of silver effectively prevented softening, but for sheet rolled 6 numbers hard 15 oz. per ton (0.052 per cent) of silver was required

#### SLOW SOFTENING AT LOW TEMPERATURES

According to data secured by Zeerleder and Bourgeois,<sup>2</sup> cold-drawn, silver-free copper gradually loses its strength when held for a long time at a temperature as low as 80° C., and when it is used as overhead transmission lines the heating resulting from the current will soften the wire. Those authors found that a sample of cold-drawn wire was completely softened when kept at 80° C. for 41 days.

For the present investigation, in order to determine the influence of silver on the rate of softening of copper at comparatively low temperatures during long periods of time, a special tube furnace was constructed in which the temperature was controlled by a bimetal thermostat. The wires used in the tests were cold drawn without annealing from  $\frac{5}{16}$ -in hot-rolled rod to 16 B & S gage (0.050 in) and were comparable to those tested by Zeerleder and Bourgeois. Samples were kept at 150° C. for as long as one year and at 200° C for 150 days. At intervals five wires of each composition were removed, and their strengths determined.

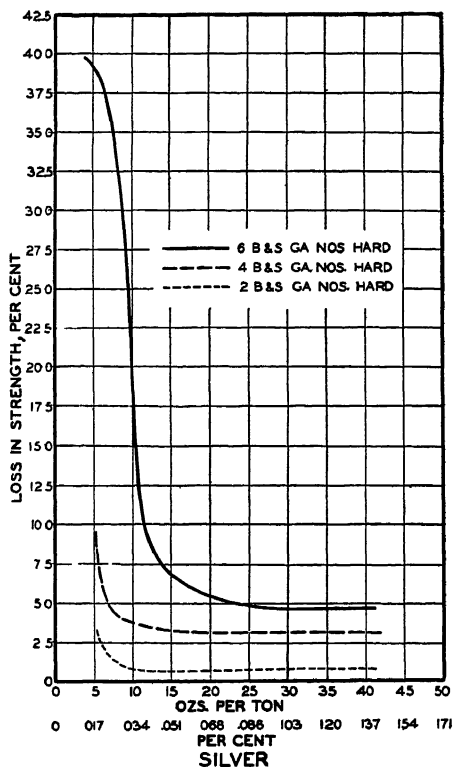


FIG 4—INFLUENCE OF SILVER ON LOSS IN STRENGTH RESULTING FROM TINNING

<sup>2</sup> A v Zeerleder and P Bourgeois Effect of Temperatures Attained in Overhead Electric Transmission Cables *Jnl Inst Metals* (1929) **62**, 321-329

The results of the tests at 150° C for periods up to 200 days are shown in Fig 5 Strengths for longer times are not shown, because no real drop in strength occurred between 200 and 365 days The wire contain-

TABLE 2.—*Effect of Silver on Loss in Strength of Copper Due to Tinning*

Silver		Before Tinning		After Tinning	
Oz per Ton	Per Cent	Tensile Strength, Lb per Sq In	Elongation in 2 In, Per Cent	Tensile Strength, Lb per Sq In	Elongation in 2 In, Per Cent
2 B & S Gage Numbers Hard (20.6 per cent reduction)					
5.3	0.018	40,900	13.9	39,700	14.0
6.5	0.022	39,300	13.5	38,800	15.8
10.7	0.037	38,900	16.4	39,000	16.5
15.1	0.052	40,100	16.9	40,000	16.6
20.5	0.070	40,300	15.3	39,800	13.8
25.4	0.087	40,800	12.5	40,200	14.5
29.15	0.100	39,800	16.0	40,000	13.5
34.7	0.119	40,400	14.6	40,600	14.4
37.8	0.130	40,900	12.3	41,000	14.8
4 B & S Gage Numbers Hard (37.1 per cent reduction)					
5.3	0.018	49,200	2.5	44,600	7.0
6.5	0.022	48,400	2.2	46,100	5.4
10.7	0.037	49,400	2.75	47,700	3.8
15.1	0.052	49,600	2.9	48,100	4.5
20.5	0.070	50,700	2.75	48,700	4.3
25.4	0.087	50,500	2.75	49,200	3.3
29.15	0.100	50,800	2.5	49,400	3.3
34.7	0.119	51,100	2.4	49,200	4.4
37.8	0.130	51,300	2.6	49,000	3.4
6 B & S Gage Numbers Hard (50.0 per cent reduction)					
5.3	0.018	55,000	1.6	34,200	38.4
6.5	0.022	54,600	1.3	34,200	36.5
10.7	0.037	54,600	1.6	45,700	7.6
15.1	0.052	54,500	1.6	51,200	3.2
20.5	0.070	55,500	1.6	52,600	3.0
25.4	0.087	55,500	1.6	52,700	2.3
29.15	0.100	55,500	1.6	53,000	2.1
34.7	0.119	56,000	1.6	53,300	2.4
37.8	0.130	56,000	1.6	53,700	2.3

ing only 0.36 oz per ton (0.001 per cent) of silver was completely softened in a few days at 150° C. and that containing 6.8 oz. per ton (0.023 per

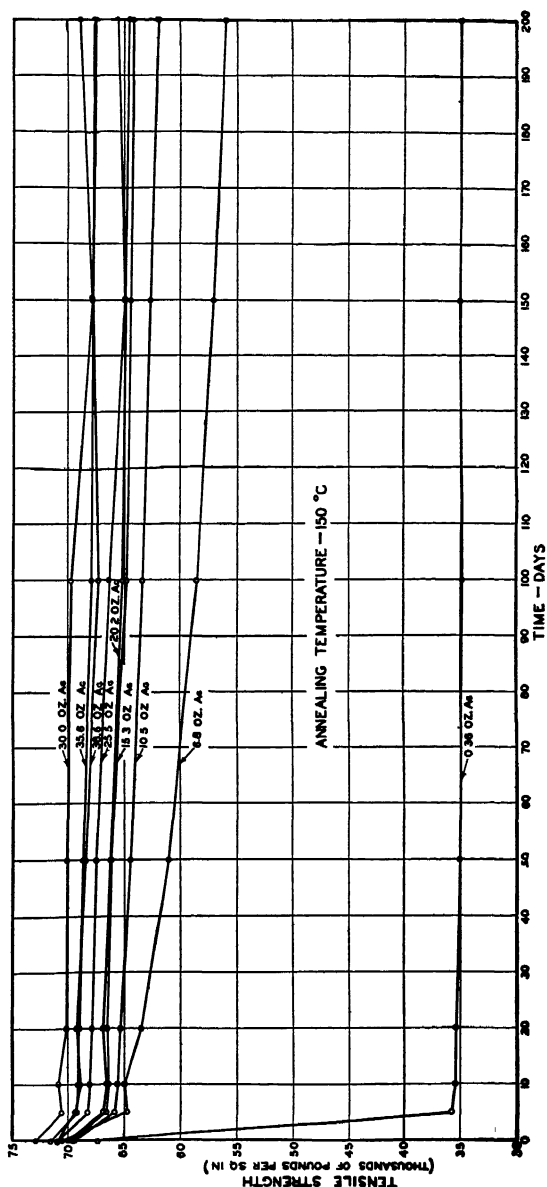


FIG 5.—TENSILE STRENGTH OF 16-GAUGE (0.050-IN.) WIRE AFTER HEATING FOR LONG PERIODS AT 150° C. Numbers on curves may be converted to percentage by multiplying by 0.00343

cent) was appreciably softened toward the end of the test. Wires containing more silver, on the other hand, were but slightly affected, and a year at 150° C gave no indication that they would ever become “dead



soft" at this temperature. Extrapolation, however, is unwarranted, and all that can be said is that the strength curves for wires containing over 10 oz per ton (0.034 per cent) of silver were *apparently* horizontal between 150 and 365 days.

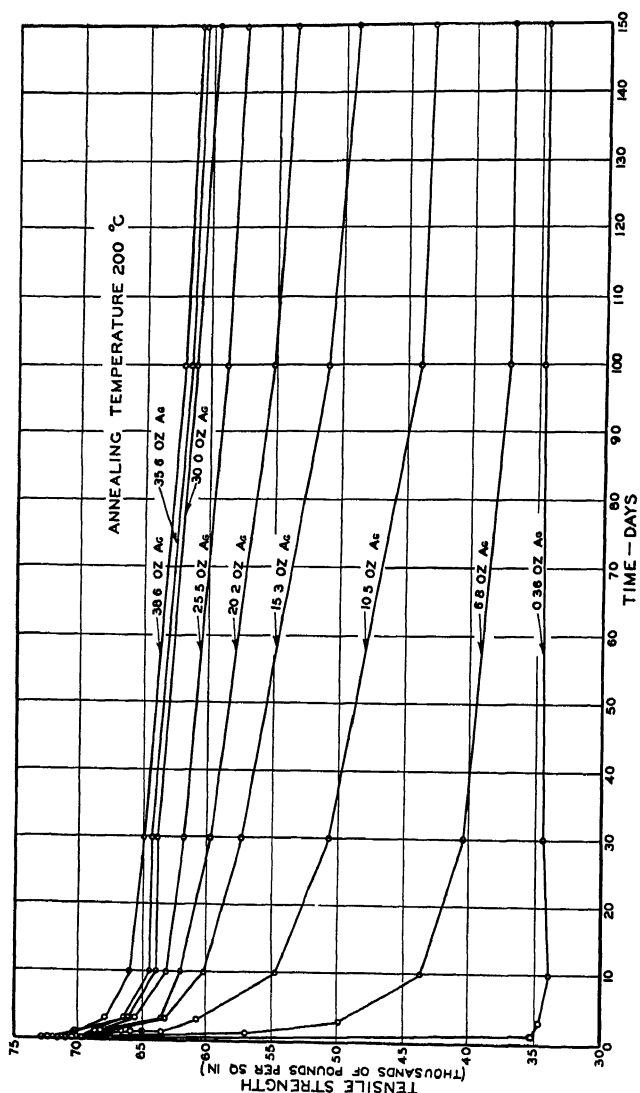


FIG 6.—TENSILE STRENGTH OF 16-GAGE (0.050-IN) WIRE AFTER HEATING FOR LONG PERIODS AT 200° C  
Numbers on curves may be converted to percentage by multiplying by 0.00343

As shown in Fig. 6, all wires were softened when held at 200° C for 200 days, and none of the strength curves appeared to become horizontal. There was, however, a marked diminution in the rate of softening as the silver content increased.

## MECHANICAL AND ELECTRICAL PROPERTIES

The data in Table 2, third and fourth columns, indicate that as much as 38 oz per ton (0.13 per cent) of silver has but little effect on the tensile properties

The electrical conductivity, as appears from Table 1, is not appreciably lowered by increasing amounts of silver. The thermal conductivity, which bears a constant relation to the electrical, is likewise but slightly affected. The increase in annealing temperature being secured with the least sacrifice in conductivity, silver-bearing copper has proved a most appropriate metal in radiator construction and other similar uses

## SUMMARY

A small fraction of one per cent of silver in high-conductivity tough-pitch copper increases the softening temperature of the cold-worked material. The silver is effective in raising the softening temperature both for very short anneals and for heating times of months. The softening temperature increases rapidly until the silver content reaches 10 oz per ton (0.034 per cent), and then slowly with further increase in silver content. Cold-worked copper containing almost no silver is completely softened on heating for a few days at 150° C., while copper of the same hardness containing over 10 oz per ton (0.034 per cent) of silver is not greatly softened when maintained at this temperature for a year. As much as 40 oz per ton (0.14 per cent) of silver has no adverse effect on the mechanical properties, nor does it lower the electrical conductivity appreciably.

## DISCUSSION

*(Carleton S. Harloff presiding)*

R. A. WILKINS,\* Rome, N. Y.—It would seem that the article under consideration would have presented data of more quantitative finality had the specimens been prepared by the addition of silver to carefully refined electrolytic copper in which the oxygen content had been reduced to a minimum consistent with freedom from residual deoxidant. It is recognized that certain impurities, such as arsenic, antimony, etc., might have a bearing on the properties being studied. It would not appear justifiable to assume the absence of all such impurities in Lake Copper and the data presented do not indicate that their absence was determined.

J. L. CHRISTIE,† Bridgeport, Conn.—It seems to me that this particular paper is representative of a type that is very valuable for the Institute to present. As Mr. Gregg said in presenting the paper for the authors, most of us who are interested have known for a long time that silver raises the annealing point of copper, and here we have for our files a large amount of quantitative information on the subject. It seems to me that the authors were very wise in selecting for their tests sheet metal

---

\* Director of Research and Development, Revere Copper and Brass Inc.

† Metallurgist, Bridgeport Brass Co.

rolled two, four and six numbers hard and wires drawn considerably harder than that, in other words, forms of copper and conditions of copper in which we are all interested practically

J L GREGG, \* Columbus, Ohio —We are investigating something more than Mr Wilkins thinks should be studied We worked on prime Lake coppers, and the purity, I believe, should be guaranteed by the conductivity reported in Table 1

---

\* Battelle Memorial Institute

## Copper Embrittlement, III

By L. L. WYMAN,\* SCHENECTADY, N. Y.

(Detroit Meeting, October, 1933)

PREVIOUS studies<sup>1</sup> by the writer dealing with the embrittlement of copper have been concerned with the behavior of various pure and deoxidized coppers when exposed to an oxidation-reduction cycle, and the consequent evaluation of these materials on the basis of their resistance to this action. No attention was devoted to the variations in penetration of embrittlement with time, when these copper materials are exposed to a strong reducing gas, such as hydrogen, nor to the variations in oxygen penetration, with time and temperature, into the "pure" coppers.

The cause of the embrittlement is the reduction of the oxygen in the copper by the hot reducing gas, so that a consideration of time, temperature, the occurrence of hydrogen and oxygen must be given. For the purpose of differentiating some of the involved factors, the present work may be divided into two separate series of experiments. The first of these deals with the oxidation of purified coppers under various conditions and then the subjection of these to a standard hydrogen treatment. The second series concerns the reduction, under different conditions, of tough-pitch coppers of several oxygen contents.

The resulting data will give the rates of oxidation, and of reduction, for the materials involved. The first series of experiments will reveal how rapidly copper may become oxidized, while the second series will indicate how rapidly embrittlement will penetrate into an oxygen-containing copper when it is exposed to hydrogen at different temperatures.

### MATERIALS

For the purpose of determining these variables, three types of material were selected, to cover the extremes in the ranges of materials commercially obtainable.

The first class of materials is represented by an oxygen-free copper, as well as the high-purity vacuum-melted copper<sup>2</sup> used in previous work. These materials were selected to determine the variation of oxidation with time and temperature, by oxidizing these coppers under various combinations of these factors, and noting the effect as indicated by a

---

Manuscript received at the office of the Institute July 5, 1933

\* Research Metallurgist, General Electric Co

<sup>1</sup> L. L. Wyman: Copper Embrittlement. A. I. M. E. Preprint (1931)

<sup>2</sup> L. L. Wyman: Copper Embrittlement, II. Trans. A. I. M. E. (1933) 104, 141.

standard hydrogen treatment to cause embrittlement. To determine the resistance to oxidation with time, the same double-deoxidized copper previously studied<sup>3</sup> was selected (containing 0.026 per cent residual silicon).

The studies on the reduction, the second series of experiments, were made on three samples of tough-pitch copper, containing respectively 0.026, 0.042, and 0.060 per cent oxygen, which were subjected to various reduction treatments to ascertain the variation of penetration of embrittlement with time and temperature.

All of the coppers were in the same condition, having been cold-rolled from a 0.5-in. ingot section to a 0.125-in. sheet. The hydrogen used was "line" hydrogen, produced by electrolysis, and carrying as impurity some 1 per cent moisture and under 0.2 per cent oxygen. The gas flow was approximately 1025 liters per hour.

### OXIDATION-REDUCTION TESTS

#### *Methods*

The pure coppers and the deoxidized coppers were heated for varying periods of time from 5 to 240 min. at temperatures from 200° to 900° C, in an electric muffle furnace, the door of which was permitted to be slightly open to insure ample air supply. After having been air-cooled, the samples were heated in a 3-in. hydrogen tube furnace at 800° C for 15 min., and then quenched.

Owing to the various air treatments, the pure and deoxidized coppers have oxygen penetrated into them to different depths, dependent upon the treatments. Consequently, the standard hydrogen treatment to which these samples were subjected will cause an embrittlement, or open grain structure, in the copper to that depth of penetration reached by the oxygen during the series of air treatments.

Long experience with these oxidation-reduction tests has shown that neither an increase in time of exposure to the hydrogen at a given temperature, nor an increase in the temperature of the hydrogen treatment will cause a material difference in the depth of embrittlement in these "pure" coppers that have been given a definite oxidation. In addition, standard samples that have been run repeatedly to determine any variation fail to deviate more than 0.001 inch.

Thus it seems conclusive that the reduction of the oxygen that the copper has taken up is complete.

These penetration data, then, will show the variation of oxygen penetration with time and temperature, as indicated by the action of hydrogen on this oxygen to produce the apparent embrittlement.

The damage that can be done to the oxidized or oxygen-bearing coppers by such a reducing treatment is extreme, and will, therefore,

---

<sup>3</sup> Reference of footnote 2

amply cover any commercial brazing, soldering, sealing, or bright-annealing operation.

For the different heat treatments, all samples to be treated at a given temperature were put into the furnace together, and the individual samples removed at the definite time intervals

The determinations of the penetration of the embrittlement were made microscopically, at 500 diameters magnification, by observing the depth below the exposed surfaces at which open grain structure was in evidence. On properly prepared samples this limit is readily observed, as may be seen in Figs. 1 and 2

### Results

For ease of interpretation, the results of these experiments have been represented graphically. The ordinates are the two variables of time and penetration, each curve depicting the variation at the indicated temperature. Although the rate of penetration curves that may be derived from these same data are of great value, the actual penetrations have the more practical value and therefore are presented. Figs. 4 to 6 inclusive show the variations of depth of oxygen penetration with time and tem-

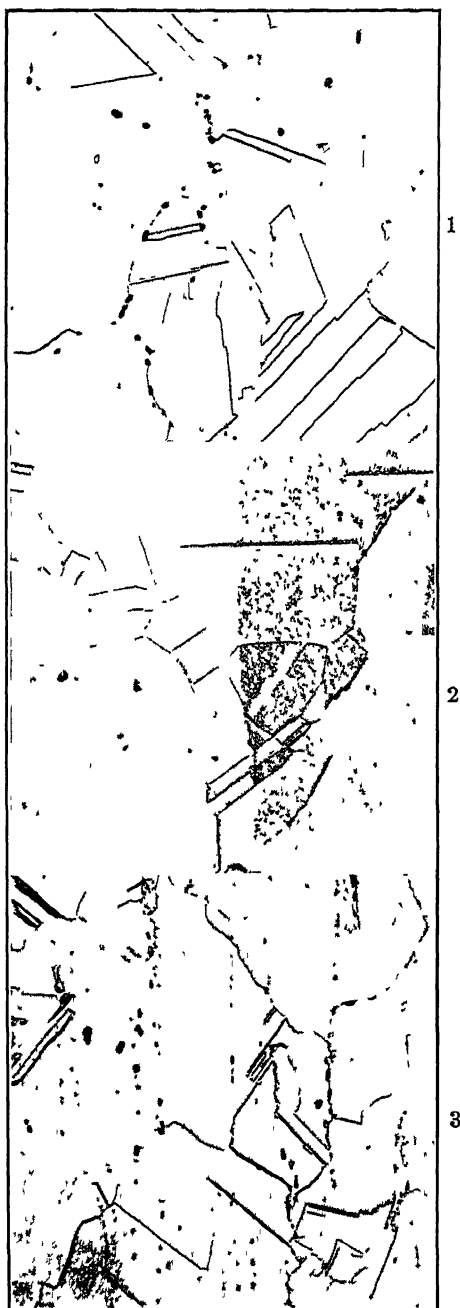


FIG. 1—OXYGEN-FREE COPPER  
60 MIN AT 700° C IN AIR PLUS 15 MIN  
AT 800° C IN HYDROGEN

FIG. 2—DOUBLE-DEOXIDIZED COPPER  
60 MIN AT 900° C IN AIR PLUS  
15 MIN AT 800° C IN HYDROGEN

FIG. 3—COMMERCIAL COPPER,  
0.042 PER CENT OXYGEN 50 MIN AT  
700° C IN HYDROGEN

All sulfuric dichromate etch Original magnification 500, reduced 50 per cent

perature, as judged by the depth of open grain structure, caused by the hydrogen treatment

Figs. 4 and 5 show the embrittlement of the vacuum-fused copper and the oxygen-free copper, respectively. These two materials are nearly duplicates in their reaction to the heat treatments. The differences occur in that the oxygen-free copper is somewhat embrittled at 500° C after one hour, while the vacuum copper is unscathed by this treatment

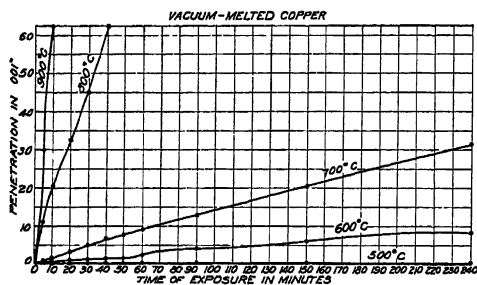


FIG 4.

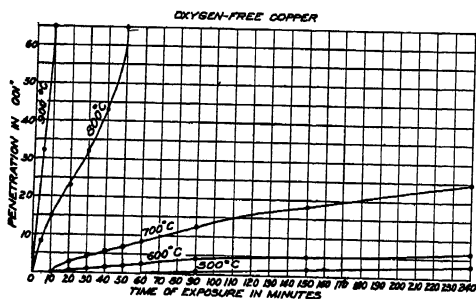


FIG 5

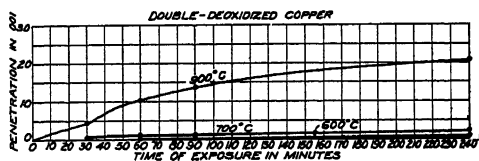


FIG 6.

Figs. 4-6—PENETRATION OF EMBRITTLEMENT DUE TO HYDROGEN AT 800° C FOR 15 MIN., AFTER OXIDIZING IN AIR AT TIMES AND TEMPERATURES INDICATED

At temperatures of 600°, 700°, and 800° C, the vacuum copper has slightly deeper penetration. At 900° C. the curves are nearly identical. It will be noted that the oxygen-free copper showed initial embrittlement occurring at periods of over one hour at 500° C. Although the vacuum copper gave no reaction at 500° C, both of these coppers give similar results throughout the 600° C. treatments.

Fig. 6 shows the results obtained on the double-deoxidized copper, and the curves are entirely different from the previous instances. In

this case there is no indication of any action at 500° C, and at 600° C the maximum penetration is only 0.0005 in. The results at 700° and 900° C are correspondingly low, and the 900° C curve for the deoxidized copper approximates the 700° C curves for the pure coppers

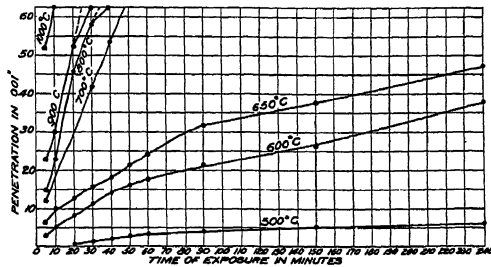


FIG 7

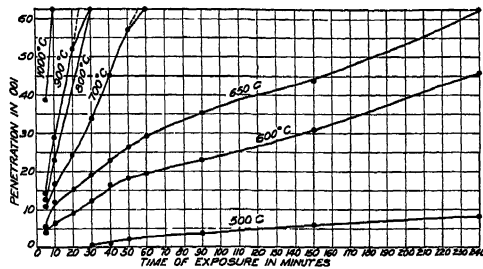


FIG 8.

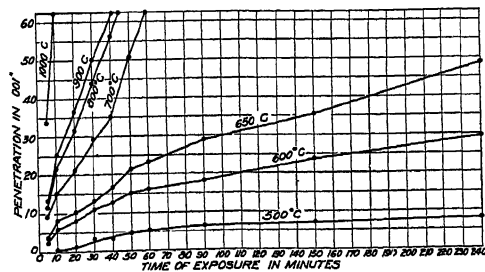


FIG 9

FIGS 7-9 — PENETRATION OF EMBRITTLEMENT IN COMMERCIAL COPPER DUE TO HYDROGEN TREATMENTS AT TIMES AND TEMPERATURES INDICATED

Fig 7, 0.026 per cent oxygen; Fig 8, 0.042 per cent oxygen; Fig 9, 0.060 per cent oxygen

## REDUCTION TESTS

### Methods

As previously mentioned, this series of tests was carried out on a set of three tough-pitch coppers of different oxygen contents, in order to determine the variations of embrittlement with time and temperature.



These oxygen-bearing samples were heated in hydrogen for varying periods of time from 5 to 240 min., at temperatures from 200° to 1000° C. and then quenched. These treatments will cause a reduction of the  $\text{Cu}_2\text{O}$  in the copper, leaving voids and open grain structure.

The procedure in this series of tests paralleled those used in the preceding tests in that all samples to be treated at a given temperature were treated simultaneously. The determination of the embrittlement penetration, also made microscopically at 500 diameters magnification, had as its criterion the nearest approach to the surface at which  $\text{Cu}_2\text{O}$  was observed, as shown in Fig. 3.

In dealing with these commercial coppers, the oxygen is already present as  $\text{Cu}_2\text{O}$  and the position within the sample at which  $\text{Cu}_2\text{O}$  as such is first observed indicates the depth of penetration of the hydrogen under the conditions of testing. It is, of course, important that the first appearance of  $\text{Cu}_2\text{O}$ , as such, be taken as the criterion, as that is the indication at least of incomplete reduction.

### Results

The curves that show the penetrations observed in this second series of experiments have the same coordinates previously used, but in this case the results show the penetrations as a function of the depth of reduction accomplished by the hydrogen at the various test conditions, as judged by the presence of  $\text{Cu}_2\text{O}$  as such. The curves for these oxygen-bearing coppers are shown in Figs. 7, 8 and 9, representing, respectively, the coppers containing 0.026, 0.042, and 0.060 per cent oxygen. These results are all close to each other and leave very little to choose between them.

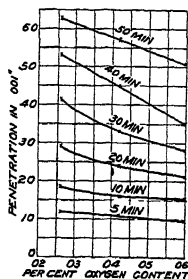


FIG. 10—PENETRATION OF EMBRITTLEMENT IN COMMERCIAL COPPERS, DUE TO HYDROGEN TREATMENTS AT 700° C FOR PERIODS INDICATED, SHOWING EFFECT OF OXYGEN CONTENT ON DEPTH OF EMBRITTLEMENT

With these materials, it can be seen that there is an appreciable penetration at 500° C., in contrast to the previous results, and that the penetrations at temperatures below 900° C. are considerably greater than noted with the first sets of materials. Above this temperature the reverse seems to be true.

The significance of the slight differences in these curves is shown in Fig. 10, which shows the replotted data contained in the other curves, and which will be discussed later.

### INTERPRETATION

The penetration curves, as a whole, show several points of practical value. In the first place, it is patent that the double-deoxidized copper is far superior to any of the other materials at any of the temperatures

used. This is direct confirmation of previous work.<sup>4</sup> This outstanding characteristic has proved to be of immense practical value in operations wherein copper, of necessity, must be subjected to high temperatures in oxidizing and reducing atmospheres

The next point of interest lies in the fact that the pure coppers have considerably higher resistance to embrittlement, in their oxidized condition, than do the commercial coppers, at temperatures below 800° C. At 800° C. and above, the embrittlement is so rapid that small choice remains between any of these five lots of material

Another noteworthy feature concerns itself with the rate of embrittlement. In the pure coppers, there is a decided increase in the rate of embrittlement from 700° to 800° C. On the other hand, there is also a "break" in rate in the commercial coppers, to a greatly increased rate, but it occurs between 650° and 700° C. To state this in more practical terms, operations that might safely be carried on at 700° C. with the pure coppers might well ruin a similar piece made from tough-pitch copper, particularly where either the utmost strength per section is demanded or where thin stock or wire is involved

As stated previously, this series of tests included treatments as low as 200° C. in order to ascertain definitely whether or not copper could be damaged at these temperatures. This is answered definitely by the fact that even after exposure for a period of 4 hr. at 400° C. none of these materials gave indication of embrittlement.

In order to corroborate these results, several of the samples treated at lower temperatures were bend-tested and fractured, with no observable indications of embrittlement. Additional bend tests were made on samples in order to check the microscopically observed embrittlement. This was accomplished by making a sharp bend in the test sample, which would cause a cracking open of the embrittled shell. The results in every instance corroborated the observed penetration of embrittlement.

Another observation of some import lies in the nature of the embrittlement, or the structure of the damaged material. It was noted that at temperatures below the 700° C. treatments in hydrogen, the damaged structure consisted of "porous" grain boundaries due to the reduction of  $\text{Cu}_2\text{O}$  with insufficient resultant pressure to blow open the entire boundary. At temperatures of 800° C. and above, the damaged structure is literally blown open, the grains being actually separated in many cases.

A review of the previous work on this subject brings forth the studies of Bassett and Bradley,<sup>5</sup> dealing with the action of an illuminating gas on copper containing about 0.015 and 0.075 per cent oxygen, and the work

---

<sup>4</sup> Reference of footnote 2

<sup>5</sup> W. H. Bassett and J. C. Bradley. Action of Reducing Gases on Heated Copper. *Trans. A. I. M. E.* (1926) **73**, 755

of Pilling<sup>6</sup> on copper containing some 0.05 per cent oxygen when exposed to hydrogen, as well as the studies of Smith and Hayward,<sup>7</sup> using hydrogen

The curves drawn from the data of Bassett and Bradley show a fair agreement of their 0.015 per cent oxygen copper with the curves of the 0.026 per cent used in these experiments. The penetrations found by Bassett and Bradley in the approximate 0.075 per cent oxygen copper are slightly lower than those observed herein with 0.06 per cent oxygen-bearing material.

When Pilling's results<sup>8</sup> on the rates of diffusion of gases through copper are considered, it may be well to interpret the penetrations obtained in terms of hydrogen alone. Inasmuch as the illuminating gas used by Bassett and Bradley contained 38 per cent hydrogen, the most rapidly diffusing gas present, it is small wonder that the results should be in agreement. Nevertheless, it is of considerable value to know that throughout the range of temperatures involved there seems to be no great difference in the reaction of oxygen-bearing coppers to hydrogen and illuminating gas, so far as the resultant embrittlement is concerned.

Comparing the results of the present work to those obtained by Pilling, it is found that there is close agreement of results at temperatures of 700° C. and above. The results obtained by Pilling at 650° and 500° C. are definitely higher than those obtained in the present experiments. It must be considered, however, that Pilling's results cover but short periods of time.

The work of Smith and Hayward provides no direct comparison other than that furnished by their 0.10 per cent oxygen in the forged condition. The results are in agreement *below* 700° C., but at and above this temperature the present experiments indicate a decided increase in penetration, or rate of penetration, which is not evident in the curves by Smith and Hayward.

The data obtained from the tough-pitch coppers show the effect of the oxygen content on the depth of deoxidation. These results are plotted in Fig. 10, for values at 700° C.

### CONCLUSIONS

The results obtained from this series of experiments have shown definitely that:

1. Neither pure copper when oxidized, or deoxidized, nor tough-pitch copper up to 0.06 per cent oxygen is embrittled by hydrogen at temperatures of 400° C. or below at four hours

---

<sup>6</sup> N. B. Pilling. The Action of Reducing Gases on Hot Solid Copper. *Jnl. Franklin Inst.* (1918) **186**, 373.

<sup>7</sup> C. S. Smith and C. R. Hayward: The Action of Hydrogen on Hot Solid Copper. *Jnl. Inst. Metals* (1926) **36**, 211.

<sup>8</sup> Reference of footnote 6.

2. (a) The rate of oxygen penetration into "pure" copper decreases markedly below 800° C

(b) The rate of hydrogen penetration into oxygen-bearing copper decreases markedly below 700° C

Consequently, up to about 800° C, the coppers containing no oxygen are superior to tough-pitch coppers for resistance to the embrittling action of oxidation-reduction cycles

3 The embrittlement due to pure hydrogen is of the same order of magnitude as that caused by illuminating gas (Bassett and Bradley).

4. The rate of embrittlement or deoxidation due to hydrogen decreases with the depth of penetration.

5 The elimination of oxygen by purifying processes or by means of deoxidation of the copper is advantageous in resistance to the embrittling action of reducing gases

#### ACKNOWLEDGMENT

The writer wishes to express his appreciation of the valuable services rendered by Mrs C. B Brodie and Mr M D Collins in the processing of these experiments

#### DISCUSSION

*(Cyril Stanley Smith presiding)*

S ROLLE,\* New York, N Y (written discussion)—We wish to congratulate Mr Wyman on the thoroughness of his investigation and his persistent pursuit of the effect of oxidizing and reducing treatments on copper as evidenced by this, the third, paper in a series on this subject His work has been of great value to us and undoubtedly to users of these high-grade coppers

We have assumed that the oxygen-free copper tested by Mr Wyman was OFHC, produced by the United States Metals Refining Co If this is so, we are in a position to confirm in general the results with respect to oxygen-free copper reported in the present paper Our metallurgical department has been concerned for some time with an investigation of oxide penetration into OFHC copper under various conditions at different temperatures The specimens used have been sections of  $\frac{5}{8}$ -in dia rod hot-rolled and cold-drawn in a commercial mill Unfortunately, the work has not progressed sufficiently to present any quantitative data at this time, but, as said before, the trend of our results appears to check his

In our opinion Mr Wyman's work has amply demonstrated that copper containing some residual deoxidant more satisfactorily resists oxide penetration than "pure" coppers which are also free from oxygen but contain no residual deoxidant In this connection there are one or two questions we would like to ask Mr Wyman to comment upon

We wonder whether the specimens of oxygen-free copper and vacuum-melted copper, as well as the oxygen-bearing coppers, revealed as clearly defined a line indicating the extent of the zone of hydrogen embrittlement as is exhibited in the photomicrograph of double-deoxidized copper reproduced in Fig 2 Further, was

---

\* Mining and Metallurgical Engineer, Oxygen-Free Copper Department, United States Metals Refining Co

the "band" effect found in the double-deoxidized copper observed in any other specimens examined?

We were extremely interested to note Mr Wyman's observation (p 211, next to last paragraph) that at temperatures below 700° C hydrogen embrittlement took the form of minute holes in the grain boundaries instead of an extended separation of the crystals We have frequently observed this phenomenon ourselves and would be interested in any theory Mr Wyman has developed to account for this difference in the result of hydrogen treatment

It has been noted that the specimens of  $\frac{1}{8}$ -in thick copper sheet examined by Mr. Wyman were prepared by cold rolling from cast material  $\frac{1}{2}$  in thick While we in no way intend to question the validity of the results obtained, more particularly since our own work, as far as it has gone, appears on the whole to confirm Mr Wyman's results, still we are of the opinion that a similar investigation of copper samples prepared by ordinary commercial practice would be of extreme interest It seems to us by no means impossible that specimens prepared in the manner described might react to the oxidation-reduction treatments somewhat differently from copper processed in quite another manner, for example, by hot rolling from a cake of normal dimensions and finishing by cold rolling in a commercial mill

We are certain that an investigator of Mr Wyman's competence has tested a large number of samples before reporting results of his experiments However, in evaluating investigations of different kinds of copper, it is well to bear in mind that as far as we are informed no continuous processes have been developed for making copper castings other than that used to produce OFHC This implies that it is necessary to obtain representative samples from a great number of batches of material, such as vacuum-melted copper or copper treated with deoxidizers, in order to have a suitable comparison with OFHC, of which only relatively few samples are necessary on account of the uniform quality of the metal inherently resulting from a continuous operation

C S SMITH,\* Waterbury, Conn—I noticed, in one of Mr Wyman's photomicrographs, that the extreme edge of a specimen of oxygen-free copper that had been heated in an oxidizing atmosphere had a much smaller grain size than the center Is this due to a restriction of grain growth in the oxidized zone? One would expect that heating cold-worked or fine-grained pure copper under suitable conditions would cause rapid oxidation of the outer layers with restriction of further grain growth, while the metal well below the surface would remain unchanged in composition and have opportunity for normal grain growth I wonder if this is a general phenomenon, and if small superficial grains in an "oxygen-free" copper can be considered as a definite indication of oxidation

L L WYMAN (written discussion)—In reply to Mr Rolle's first question, I have never noticed any of the so-called banding in the oxygen-free and vacuum-melted copper Within the scope of the work that we have done and with the etchants used—we essentially use the dichromate and sulfuric acid solution in this type of work, and sometimes the ammonium peroxide oxygen—we have never found the so-called band effect in these essentially pure coppers They do, however, occur in some of the deoxidized coppers Fig 11 shows silicon-deoxidized copper in which this banding is very pronounced It is not the double-deoxidized copper, nevertheless it shows it very clearly

In regard to the difference in the nature of this blowing up in the boundaries, I believe that when just these little pot-holes are found, as compared to the whole grain boundaries being blown up, the difference is due to two factors, individually

---

\* In charge, Copper Alloys Research Laboratories, American Brass Co

or collectively In the first place, the amount of the cuprous oxide at that particular place to be reduced is a vital factor, for whatever amount is there at that particular temperature is certainly going to result in the formation of a certain amount of water vapor The more  $\text{Cu}_2\text{O}$  there is, the more water vapor will be formed Secondly, the temperature of the particular sample must be taken into consideration, because the higher the temperature the greater the volume any given amount of water vapor would occupy, the generated pressure would be higher, and capable of greater destruction. In my opinion, the difference noted above is due to the latter cause more than to anything else

Concerning the differences that might be brought out between the material that is cold-rolled from a  $\frac{1}{2}$ -in ingot section and material that had been completely

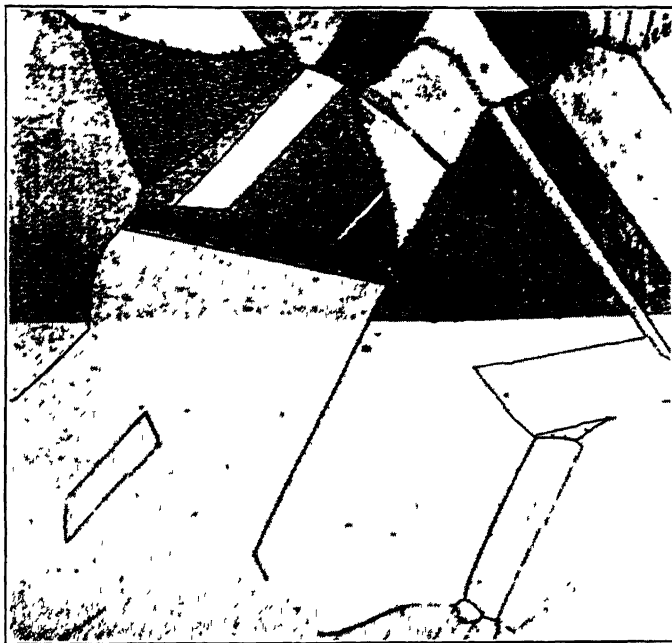


FIG 11 —SILICON-DEOXYDIZED COPPER, AIR-ANNEALED AT 900°C. FOR 15 MINUTES PLUS HYDROGEN ANNEAL AT 800°C FOR 15 MINUTES

mill-processed, in none of the samples of this material did I find any differences whatsoever

Figs 12 and 13 show two samples, received at different times, of the commercial oxygen-free copper The material that in this paper has been called "oxygen-free copper" was the OFHC copper

Perhaps Mr Rolle might have in mind the fact that if a material had been very severely overworked and possibly torn apart in cold rolling, there would be reason to suspect there might be differences in the reaction of the material, because really it is not a solid piece of copper, it is one that is very severely damaged However, none of the samples used in any of the embrittlement experiments have shown overworking

In regard to Dr Smith's statement concerning the fine-grained structure near the outside edge, I agree with him that that is a very common occurrence Under



As received      Air-annealed at 900° C 15 minutes      Annealed in an, 900° C, 15 mm + hydrogen anneal, 800° C, 15 min      COMMERCIAL STRIP      X 250

FIGS 12 AND 13—TWO SAMPLES OF OXYGEN-FREE COPPER

the conditions of this test materials such as the vacuum copper and the oxygen-free copper are prone to form extremely large grains. Nearly always the outside layers of those materials still have a fine-grained structure, when the embrittlement is partial. Total embrittlement, on the other hand, seems to cause restricted growth of even the center grains. I might say that it is characteristic of that material during such oxidation or oxidation reduction cycle to form a fine grain outside, and yet to have very large grains inside. To some extent this can also be noticed in the deoxidized material.

C S SMITH—Would you say the fine grain outside was a definite indication that the material had been oxidized? Would you regard the presence of the fine-grained rim as definite indication that the material had been oxidized?

L L WYMAN—I would seriously suspect that that had happened



# Strength and Aging Characteristics of the Nickel Bronzes

By E M WISE\* AND J T EASH†, BAYONNE, N J

(New York Meeting, February, 1934)

THE practice of adding moderate quantities of nickel to a variety of bronzes has been employed by foundrymen for many years with several objects in view. In some instances it was desired to harden the alloy, in others it was to increase the fluidity or to improve the solidity of the castings, or to refine their grain. These important matters have been considered in detail by Pilling and Kihlgren<sup>1</sup> and by numerous other workers cited by them, and with the exception of the first will not be considered in the present communication.

The possibility of reducing the cost of bronze by replacing a portion of the tin with nickel received attention some years ago by Burgess and Woodward,<sup>2</sup> and, as will be shown later, offers attractive savings in cost under present conditions.

The age-hardening characteristics of the nickel bronzes of appropriate compositions have been known for some time and were mentioned by Price, Grant and Phillips<sup>3</sup> and discussed by Wise<sup>4</sup> in connection with their paper. These matters are further considered in recent patents,<sup>5</sup> and are becoming of commercial importance in the production of high-strength castings.

The equilibrium relations existing in the high-copper region of the copper-nickel-tin system have been carefully studied by Eash and Upthegrove,<sup>6</sup> and in somewhat less detail by Veszelka.<sup>7</sup> The observa-

---

Manuscript received at the office of the Institute, Dec 1, 1933

\* Assistant Manager, Research Laboratory, The International Nickel Co

† Metallurgist, Research Laboratory, The International Nickel Co

<sup>1</sup> N B. Pilling and T E Kihlgren. Some Effects of Nickel on Bronze Foundry Mixtures. *Trans and Bull Amer Foundrymen's Assn* (1931) **39**, 93-110

Casting Properties of Nickel Bronzes. *Trans American Foundrymen's Association* (1932) **40**, 289-309

<sup>2</sup> G K Burgess and R W Woodward. A Symposium on the Conservation of Tin. *Trans A I M E* (1919) **60**, 180

<sup>3</sup> W B. Price, C G Grant and A J Phillips. Alpha Phase Boundary of the Copper-nickel-tin System. *Trans A I M E* (1928) **78**, Inst Met Div, 511-513

<sup>4</sup> E M Wise. *Trans A I M E* (1928) **78**, 514-517

<sup>5</sup> E M Wise. U S Patent 1816509 (1931) and U S Patent 1928747 (1933).

<sup>6</sup> J T Eash and C Upthegrove. The Copper Rich Alloys of the Copper-Nickel-Tin System. Submitted as a Doctor's Dissertation to the University of Michigan, April 15, 1932, also *Trans A I M E* (1933) **104**, 221-249

<sup>7</sup> J Veszelka. Investigation of Equilibrium Relationships of Further Alloyed

tions of Veszelka, however, check quite closely with those of Eash and Upthegrove. The alpha domain of the pure ternary alloys at 1436° F. (780° C.) and at 572° F. (300° C.), as determined by the former workers, is shown in Fig. 1. This change in the alpha domain with the temperature is responsible for the remarkable age-hardening properties exhibited by these alloys.

#### SCOPE OF PRESENT DISCUSSION

1. The alloys considered range from 0 to 12.5 per cent tin and from 0 to 15 per cent nickel, together with numerous alloys containing both tin and nickel.

2. The methods employed for the production of the test castings are briefly outlined while the tensile properties obtained are given in detail. It is shown that the presence of nickel leads to improved properties and decreased alloy cost. The properties of alloys of constant cost (that of the 88-10-2 alloy) are considered, and it is found that the maximum properties in sand castings are obtained with 5 per cent tin and 8 per cent nickel.

3. The aging characteristics of the sand-cast nickel bronzes are studied in detail and data are presented regarding the physical properties of the annealed and aged sand-cast alloys many of which develop tensile strengths in excess of 90,000 lb per sq in., coupled with an elongation of 15 per cent. The relation between the tensile strength, proportional limit and the elongation of the 7.5 per cent nickel 8 per cent tin alloy after various aging treatments is presented.

4. The effects of various additions to the 7.5 per cent nickel 8 per cent tin alloy are considered in reference to their influence upon the strength and aging characteristics.

5. The fatigue strength of the sand-cast heat-treated 7.5 per cent nickel 8 per cent tin alloy was found to be about 18,000 lb per sq in. at 16,000,000 cycles.

6. The practical considerations dictating the use of the nickel bronzes are briefly considered.

7. The production and aging characteristics of the wrought nickel bronzes are described and the remarkable tensile properties exhibited by these relatively inexpensive alloys; namely, tensile strengths of the order of 135,000 lb. per sq. in. for annealed and aged alloys and 170,000 lb per sq. in. for the hard-rolled and aged alloys, are indicated. The relation between the tensile strength, proportional limit and elongation of the wrought 7.5 per cent nickel 8 per cent tin alloy resulting from various aging treatments is shown.

## ALLOYS STUDIED

The nickel and tin contents of the alloys studied are set forth in Fig 1 The present discussion will be devoted to alloys containing up

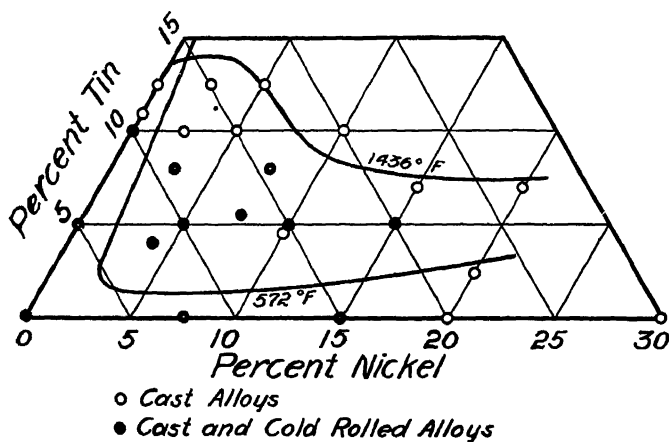


FIG 1—COMPOSITIONS OF ALLOYS STUDIED HEREIN AND ALPHA-PHASE BOUNDARY AT 1436° F AND 572° F AS DETERMINED BY EASH AND UPTEGROVE

to 15 per cent of nickel The interesting properties of the alloys of higher nickel content may be considered later.

The charges were made up from copper, nickel, and tin of high commercial purity, 2.4 per cent zinc and 0.30 to 0.35 per cent manganese were added normally Analyses indicated that substantially complete recoveries of nickel and tin were effected and that approximately 2 per cent of zinc and 0.25 per cent manganese were retained Barium was employed as a deoxidizer, sometimes in conjunction with other elements It was found that where 0.1 per cent barium was added to foundry melts, from 0.003 per cent to 0.005 per cent was recovered, and where 0.1 per cent was added to Ajax melts 0.013 per cent was recovered, and where 0.05 per cent was added 0.008 per cent was recovered

## PRODUCTION AND TENSILE PROPERTIES OF SAND CASTINGS

In view of the fact that a major portion of the bronze used is employed in the form of sand castings, our principal attention was devoted to the study of such castings It was desired to determine the properties of well-fed castings and to produce as many bars per pound of metal as was feasible. A pattern was developed which meets these requirements The standard casting employed is shown in Fig. 2 This weighed

22 lb and produced four tensile bars having minimum diameters of 0.7 in., which were machined to the standard 0.505 by 2-in. gage length specimens.

Most of the melts considered here were made in a 40-lb Ajax high-frequency furnace. Crucible melts (of 180 lb each) of some of the alloys were made in an oil-fired pit furnace, and these indicated as good or better properties than those of the Ajax melts.

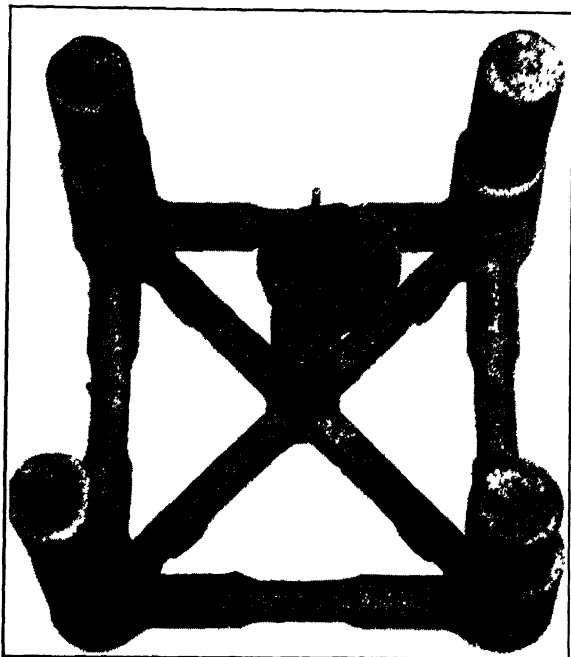


FIG 2 —TENSILE BAR CASTING

A detailed study was made of the 7.5 per cent nickel 8 per cent tin alloy to determine the best method of processing the melt, the proper deoxidizer, and the optimum pouring temperature, to avoid the presence of the intercrystalline shrinkage cavities and discolored grain fractures which are apt to be present in sand-cast bronze. It may be noted that the presence of a small amount of intercrystalline shrinkage sharply reduces the ductility of the hard alloys while it exercises much less influence upon the strength and hardness. These studies, which will be reported later, indicated that in the case of this alloy the best pouring temperature was 390° F. over the liquidus and that it was desirable to oxidize the molten cupronickel prior to adding the more reactive elements and to make a final addition of 0.05 to 0.1 per cent barium. The melt was held about seven minutes after the deoxidation and was then poured into green sand molds and into  $\frac{3}{4}$  by 2 by 9 in. cast-iron ingot molds for

strip rolling The presence of a charcoal cover was found to be highly detrimental to this alloy. Certain modifications in melting procedure were made in the alloys as the composition was changed, but a pouring temperature approximately 390° F over the liquidus was maintained in all cases These details are indicated in the appendix The procedures employed are undoubtedly susceptible to further improvement, but in general the castings produced may be considered to be good and to represent the properties of sound test bars of the type indicated in Fig 2

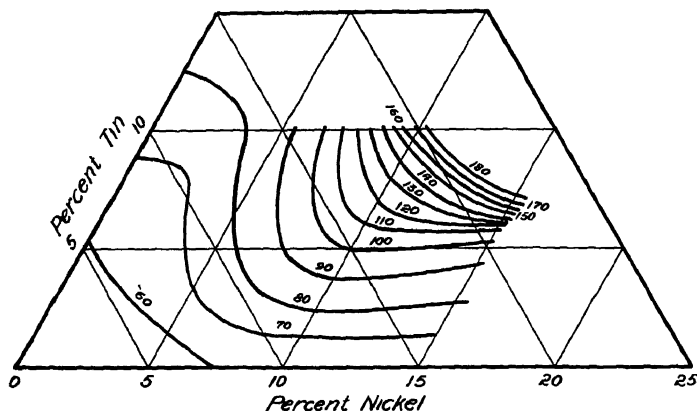


FIG 3—BRINELL HARDNESS OF SAND-CAST NICKEL-BRONZE ALLOYS

The properties of the alloys tested in the as-cast state are summarized<sup>8</sup> in Figs 3 to 6 As noted above, these castings were poured at about 390° F above the liquidus

It is apparent that the tensile strength, proportional limit and hardness increase almost directly with the nickel content over the usual range of tin content The ductility, as measured by the elongation, is, in general, increased over that of the straight bronze by the addition of nickel up to 5 to 7 per cent, and thereafter decreases at a moderate rate, depending upon the tin content It is evident that an excellent combination of properties can be secured over a wide range of compositions. For example, ultimate strengths ranging from 45,000 to 70,000 lb per sq. in, yield strengths<sup>9</sup> from 20,000 to 40,000 lb per sq

<sup>8</sup> It should be noted that the Brinell hardness values for the cast alloys are based upon the use of a 10-mm ball and a 500-kg load for all alloys possessing a hardness of 100 or below and upon the use of a 1000-kg load for the harder alloys The Brinell values for wrought alloys were derived from Rockwell readings and were found to check closely with the actual Brinell values of thick samples

<sup>9</sup> The yield strength is the stress at which the bronze exhibited a limiting permanent set of 0.2 per cent in 2 in It was determined by "The Set Method" described in A S T M Designation E8-32T *Proc Amer Soc Test Mat* (1932) **32**, 956.

in , proportional limits from 15,000 to 25,000 lb per sq in , and elongations from 10 to 45 per cent, can be attained

The most useful range of compositions for alloys to be used in the as-cast state depends upon the tin content and the ductility require-

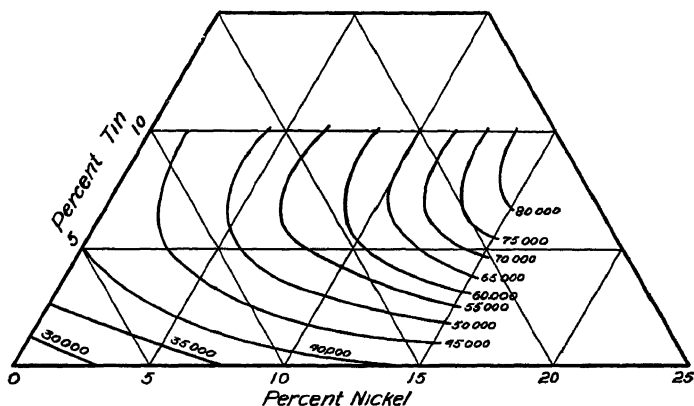


FIG. 4—ULTIMATE STRENGTHS OF SAND-CAST NICKEL-BRONZE ALLOYS

ments Thus, if an elongation greater than 10 per cent were required, the alloys containing 10 per cent of tin might contain up to about 6 per cent of nickel, while in the 5 per cent tin alloys the nickel content would extend up to 10 or 15 per cent, provided that the melting fa cili

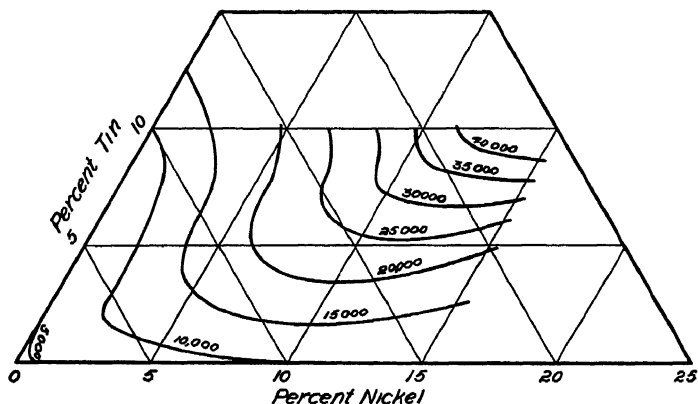


FIG 5—PROPORTIONAL LIMITS OF SAND-CAST NICKEL-BRONZE ALLOYS

ties are adequate to secure the requisite pouring temperatures for the latter alloys

#### PROPERTIES THAT CAN BE SECURED AT A CONSTANT METAL COST AND REDUCTION IN COST THAT CAN BE SECURED BY REPLACEMENT OF A PORTION OF TIN BY NICKEL

The improvement in properties that can be obtained at constant metal cost through the replacement of a portion of the tin by nickel is

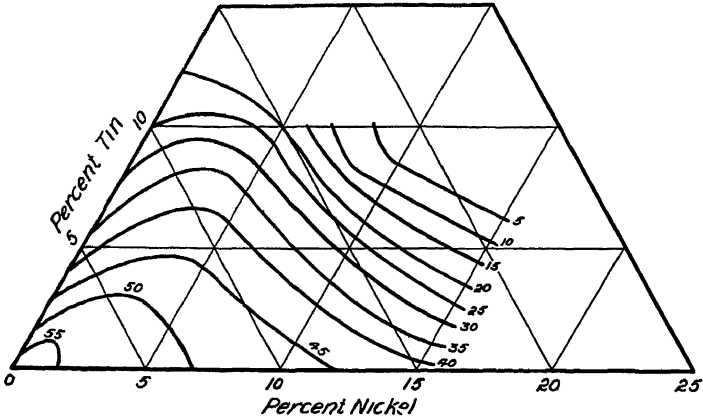


FIG 6 —PERCENTAGE ELONGATION IN 2 INCHES OF SAND-CAST NICKEL-BRONZE ALLOYS.

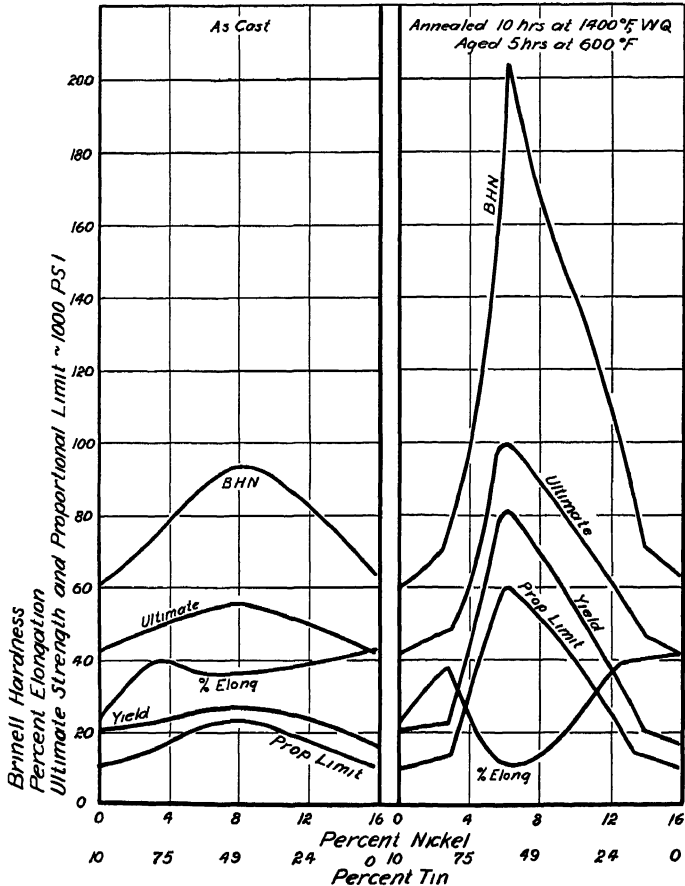


FIG 7 —TENSILE PROPERTIES OF SAND-CAST AND HEAT-TREATED NICKEL-BRONZE ALLOYS OF EQUAL COST.

made evident by Fig 7, which represents a cut across the property surfaces connecting the points 10 per cent tin, 0 per cent nickel, and 15.8 per cent nickel, 0 per cent tin, which are of equal metal cost<sup>10</sup> It is evident that the maximum properties, namely, a Brinell hardness of 93, an ultimate strength of 55,000 lb. per sq. in., a yield strength of 27,000 lb. per sq. in., a proportional limit of 22,000 lb. per sq. in., and an elongation of 35 per cent are exhibited in an alloy containing 8 per cent nickel and 5 per cent tin

From Figs 3 to 6, it is evident that if the application is such that the strength of a straight tin bronze is adequate, equal strength properties can be secured in cheaper alloys by a reduction in tin content and the introduction of a moderate amount of nickel to maintain the strength For example, properties even better than those typical of the 88-10-2 bronze, which indicated a Brinell hardness of 74, an ultimate strength of 43,000 lb. per sq. in., a yield strength of 20,000 lb. per sq. in., a proportional limit of 10,000 lb. per sq. in., and an elongation of 25 to 30 per cent, can be obtained by using a less expensive alloy containing 5 per cent tin, 5 per cent nickel and 2 per cent zinc

This alloy possesses a Brinell hardness of 75, an ultimate strength of 49,000 lb. per sq. in., a yield strength of 22,800 lb. per sq. in., a proportional limit of 13,500 lb. per sq. in., and an elongation of 44 per cent, and would cost about 6 per cent less per pound than the 88-10-2 alloy If heat treatment is employed, the properties of this 5 per cent nickel, 5 per cent tin alloy can be further increased to a Brinell hardness of 136 to 171, an ultimate strength of 74,000 to 84,000 lb. per sq. in., a yield strength of 53,000 to 66,000 lb. per sq. in., a proportional limit of 40,000 to 47,000 lb. per sq. in., and an elongation of 16 to 28 per cent.

The microstructure of the sand-cast alloys of constant cost is altered considerably as tin is replaced by nickel A small quantity of excess  $\alpha + \delta$  eutectoid is present in the 88-10-2 alloy The replacement of tin by nickel up to 3 per cent nickel causes the amount of the secondary phase to decrease while the  $\alpha + \delta$  eutectoid is replaced by a clear phase,  $\theta$  Further additions of nickel to about 7.5 per cent cause an increase in the amount of excess  $\theta$  and the occurrence of a small amount of  $\theta$  precipitated in a lamellar form similar to pearlite, which, incidentally, should be good material for a bearing metal As the nickel content is still further increased, the amount of the excess phase decreases and finally the typical cored structure of the cupronickel solid solution is obtained

The replacement of tin by nickel (along the constant cost line) causes a gradual rise in the liquidus from 1825° F (995° C.) (that of the 88-10-2 alloy) to 2130° F. (1165° C.), the liquidus of the 15.8 per cent nickel-copper alloy, containing 2 per cent of zinc.

---

<sup>10</sup> Assuming the following metal prices. copper, 9 cents per pound, nickel, 35 cents and tin, 50 cents



## AGING CHARACTERISTICS OF THE CAST NICKEL BRONZES

The increase in hardness of sand castings cut from the ends of the tensile bars, first homogenized by heating at 1400° F for 5 or 10 hr , as

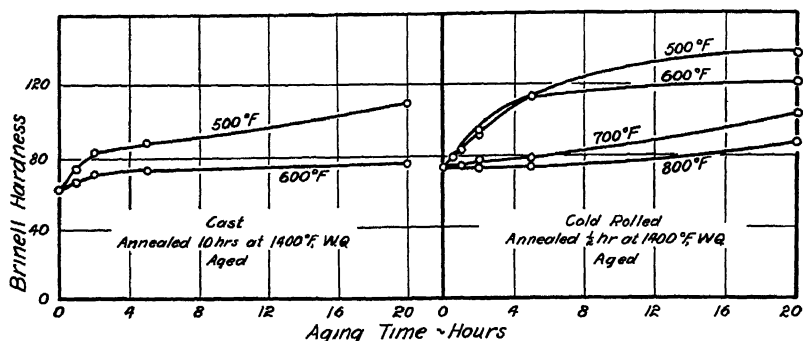


FIG. 8.—EFFECT OF AGING TIME AND TEMPERATURE ON BRINELL HARDNESS OF BRONZE CONTAINING 4 PER CENT NICKEL AND 4 PER CENT TIN

indicated, water-quenched and then aged at various temperature levels, is shown in Figs 8 to 13. Associated with these curves are data on the behavior of rolled, annealed, quenched, and aged alloys of the same compositions.

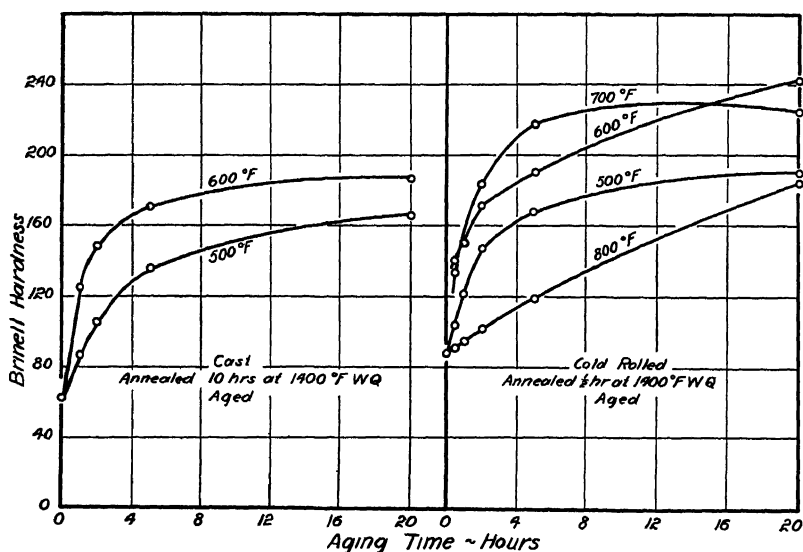


FIG. 9.—EFFECT OF AGING TIME AND TEMPERATURE ON BRINELL HARDNESS OF BRONZE CONTAINING 5 PER CENT NICKEL AND 5 PER CENT TIN

The variation in the shape of the aging curves with the composition of the alloy appears to be due largely to two factors; namely, the degree of supersaturation and the composition of the matrix.

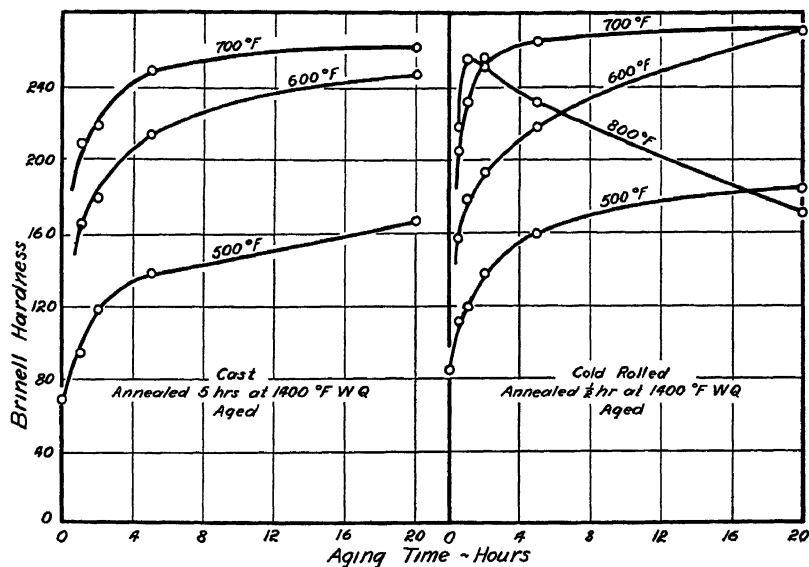


FIG 10—EFFECT OF AGING TIME AND TEMPERATURE ON BRINELL HARDNESS OF BRONZE CONTAINING 75 PER CENT NICKEL AND 5.5 PER CENT TIN.

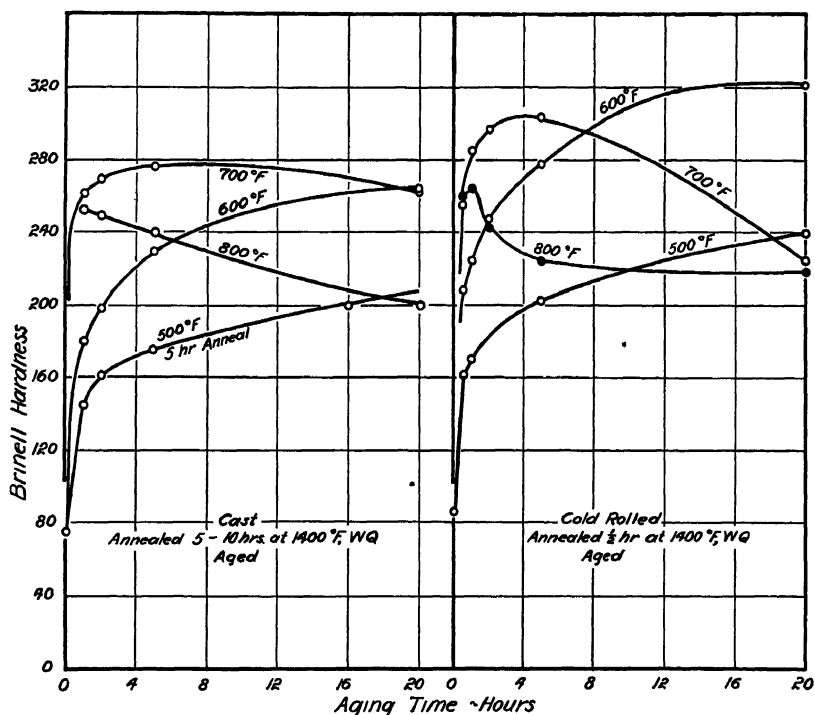


FIG 11—EFFECT OF AGING TIME AND TEMPERATURE ON BRINELL HARDNESS OF BRONZE CONTAINING 75 PER CENT NICKEL AND 8 PER CENT TIN

The alloys containing much of the precipitable phase tend to age more rapidly, while an increase in the nickel content of the matrix tends

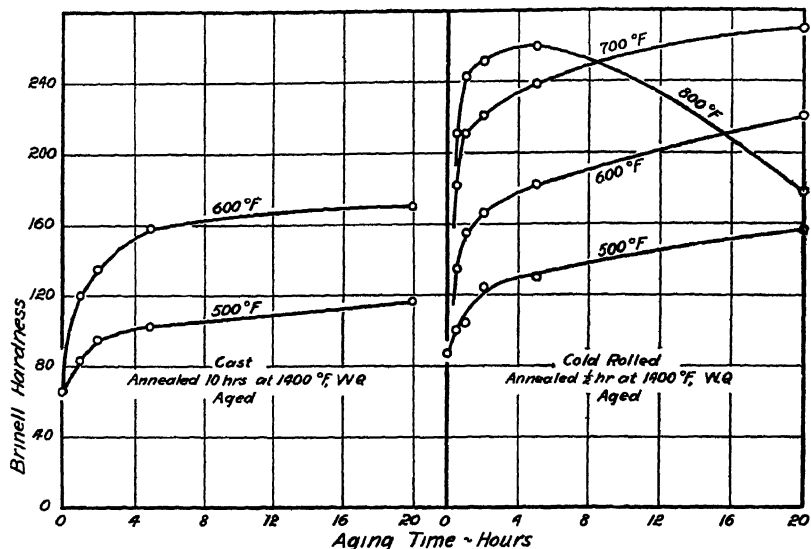


FIG. 12.—EFFECT OF AGING TIME AND TEMPERATURE ON BRINELL HARDNESS OF BRONZE CONTAINING 10 PER CENT NICKEL AND 5 PER CENT TIN.

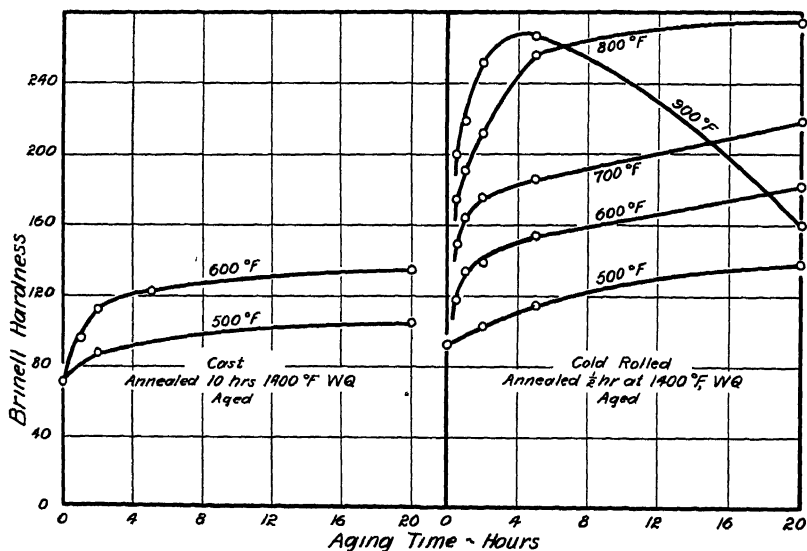


FIG. 13.—EFFECT OF AGING TIME AND TEMPERATURE ON BRINELL HARDNESS OF BRONZE CONTAINING 15 PER CENT NICKEL AND 5 PER CENT TIN

to retard the aging; or, what amounts to much the same thing, requires a higher aging temperature to secure effective hardening in a constant time interval. The alloys that are only mildly supersaturated (such

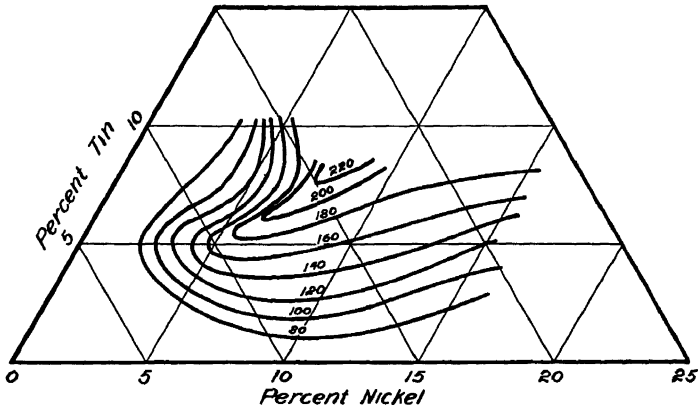


FIG 14—BRINELL HARDNESS VALUES OF CAST NICKEL-BRONZE ALLOYS ANNEALED 10 HR AT 1400° F, WATER-QUENCHED AND AGED 5 HR AT 600° F

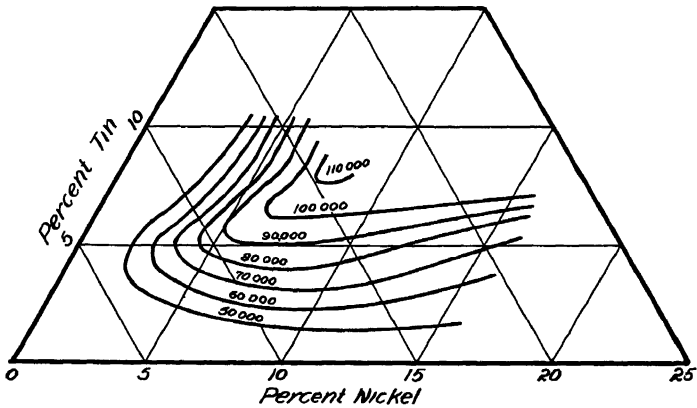


FIG 15—ULTIMATE STRENGTHS OF CAST NICKEL-BRONZE ALLOYS ANNEALED 10 HR AT 1400° F, WATER-QUENCHED AND AGED 5 HR AT 600° F

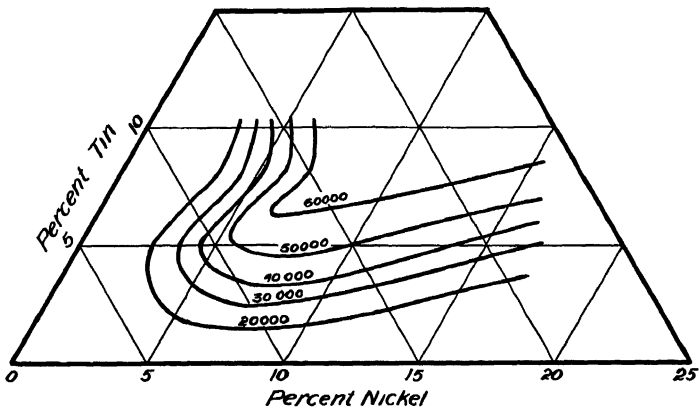


FIG 16—PROPORTIONAL LIMITS OF CAST NICKEL-BRONZE ALLOYS ANNEALED 10 HR. AT 1400° F, WATER-QUENCHED AND AGED 5 HR AT 600° F

as the 5 per cent nickel, 5 per cent tin composition) harden slowly even at the higher temperatures, whereas those containing more of the precipitable theta constituent (such as the 75 nickel, 8 per cent tin alloy) tend to overage at the higher temperatures, such as 800° F

It will likewise be noted that the cold-rolled and annealed alloys tend to age a little more vigorously than the corresponding castings. This is due probably to the slight lack of homogeneity in the castings, and perhaps to their coarser grain size as compared with the rolled and annealed material

Certain of these cast alloys are very responsive to aging. For example, the hardness of the heat-treated 75 per cent nickel, 8 per cent tin alloy can be increased from about 75 to 277 Brinell hardness, an increase of 270 per cent, by an appropriate aging treatment

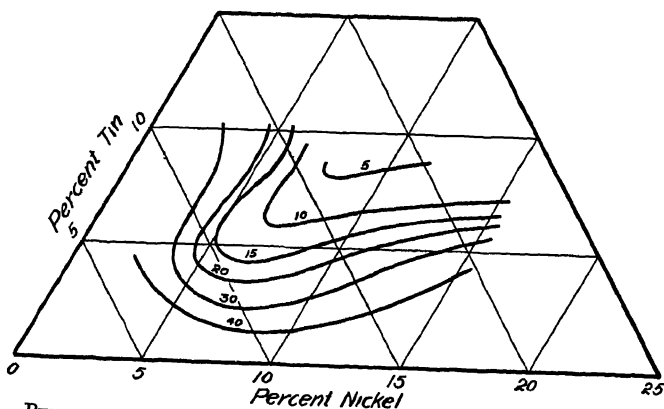


FIG 17—PERCENTAGE OF ELONGATION 2 IN INCHES OF CAST NICKEL-BRONZE ALLOYS ANNEALED 10 HR AT 1400° F, WATER-QUENCHED AND AGED 5 HR AT 600° F

A summary of the properties of the hardenable cast alloys that were homogenized at 1400° F for 10 hr, water-quenched and then aged at 600° F for 5 hr. and water-quenched, is presented in Figs 14 to 17. This aging treatment is not the optimum for all of the alloys but permits a reasonable comparison between alloys to be made. The marked increase in strength, proportional limit and hardness over the same alloys in the as-cast state is evident. The shapes of the curves in Figs. 14 to 17 suggest that the age-hardening is due to the precipitation of a phase containing equal weights of nickel and tin, which would correspond to the compound  $\text{Ni}_2\text{Sn}$ .

The properties of the aged alloys having a constant cost (that of the 10 per cent tin bronze) are shown in Fig 7. The maximum properties in the heat-treated alloys of this constant-cost series are obtained in an alloy containing equal amounts of nickel and tin; namely, 6 per cent of each. At this composition the following combination of properties is developed. a Brinell hardness of 200, an ultimate strength of 100,000 lb

per sq in, a yield strength of 82,000 lb per sq in, a proportional limit of 60,000 lb per sq in, and 10 per cent elongation. The ultimate strength and proportional limit are 130 and 500 per cent respectively above the corresponding properties of 88-10-2 bronze, which possesses the same metal cost.

In the vigorously hardenable alloys, such as the 75 per cent nickel, 8 per cent tin alloy, a considerable reduction in elongation occurs when the aging is carried to excess. However, by properly adjusting the heat

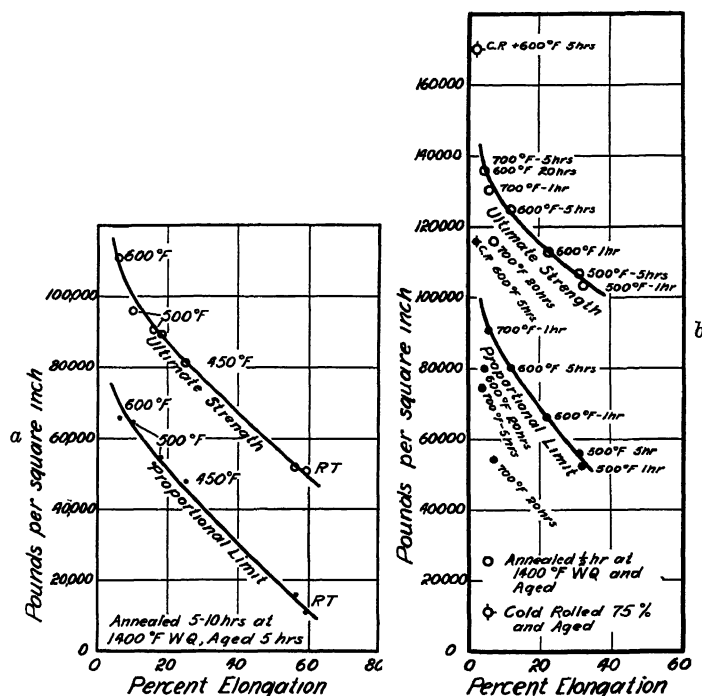


FIG 18—RELATION BETWEEN ULTIMATE STRENGTH, PROPORTIONAL LIMIT, AND PERCENTAGE ELONGATION OF ALLOY CONTAINING 75 PER CENT NICKEL AND 8 PER CENT TIN

a Heat-treated sand castings b Heat-treated wrought strip

treatment an excellent combination of properties can be secured in heat-treated castings of this alloy. This may be seen in Fig 18, which depicts the relationship between the ultimate strength, proportional limit and elongation of both the cast and wrought 75 per cent nickel, 8 per cent tin alloy after various heat treatments. It is evident that tensile strengths in excess of 90,000 lb per sq. in, coupled with proportional limits of over 50,000 lb per sq. in, and an elongation of over 15 per cent, can be secured in properly heat-treated sand castings of this alloy. For engineering purposes, plots of this type are most useful because they permit a ready evaluation of the strength properties that can be secured

with the degree of toughness that may be required to secure adequate reliability

In the studies that have been presented concerning the cast alloys, initial homogenizing treatments were employed which developed the

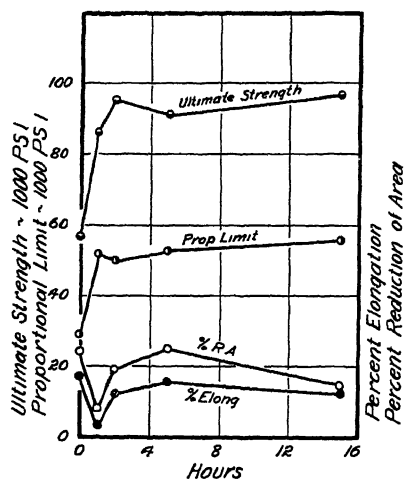


FIG 19—EFFECT OF ANNEALING TIME AT 1400° F ON TENSILE PROPERTIES OF SAND-CAST 75 PER CENT NICKEL, 8 PER CENT TIN ALLOY SUBSEQUENTLY QUENCHED AND AGED 5 HR. AT 500° F

full-strength properties attainable. However, for some purposes, particularly where bearing properties are required, it may be desirable to retain a portion, at least, of the heterogeneity of the casting, with some sacrifice in strength and hardness. This can be done by using a shorter homogenizing cycle or by lowering the homogenizing temperature or by omitting the homogenizing treatment entirely, the casting being aged as it comes from the sand. The latter procedure gives rise to only moderately good properties in sand castings, although it is more effective with chill castings, but homogenizing treatments of as short as 2 hr at 1400° F, followed by

aging, give excellent properties. These matters will be made clear by reference to Fig 19, in which the influence of the prior homogenizing treatment upon the properties of the subsequently aged 75 per cent nickel, 8 per cent tin alloy is shown.

The influence of the homogenizing treatment upon the microstructure of the sand-cast 75 per cent nickel, 8 per cent tin alloy is shown in Fig. 20. Only a small amount of the excess theta phase remained after annealing 5 hr at 1400° F. Normal aging at 500° F had no effect upon the microstructure of the homogenized alloy.

The rate of cooling from the homogenizing treatment is likewise of some importance—air cooling being feasible for small castings—but it does slightly reduce the strength and elongation finally attained upon aging. Determinations of the dimensional changes occurring during heat treatment of several tensile bars indicated that annealing the sand-cast 75 per cent nickel, 8 per cent tin alloy for 5 hr at 1400° F, followed by quenching, caused an expansion of about 0.0015 in per inch, while the subsequent aging at 500° F for 5 hr caused the homogenized alloy to shrink 0.0006 in per inch. These two effects would no doubt tend to more nearly neutralize each other with more drastic aging treatments. In products machined before aging, a small correction may be applied

to compensate for the contraction that will occur on aging. However, most castings will be machined subsequent to aging, so that it will seldom be necessary to consider the small dimensional changes noted above.

#### EFFECTS OF VARIOUS ADDITIONS ON AGING CHARACTERISTICS OF THE 7.5 PER CENT NICKEL, 8 PER CENT TIN ALLOY

Table 1 shows the effects of small additions of other metals on the physical properties of the quenched and aged 7.5 per cent nickel, 8 per cent tin alloy. These melts were processed in the manner previously described; i.e., oxidation of the cupronickel followed by the deoxidation of the entire melt with 0.1 per cent barium. Silicon or chromium additions of 0.1 to 0.15 per cent proved detrimental, while 1 per cent lead produced an exceedingly inferior casting. The low properties of the latter undoubtedly resulted from the fusion of the lead during heat treatment. Chromium and lead likewise retarded the aging rate. Two per cent iron retarded the rate of aging and lowered just slightly the properties obtained. The removal of the zinc had little effect upon the alloy, while increasing it to 10 per cent was quite harmful in the castings studied. It is possible that a modification of procedure

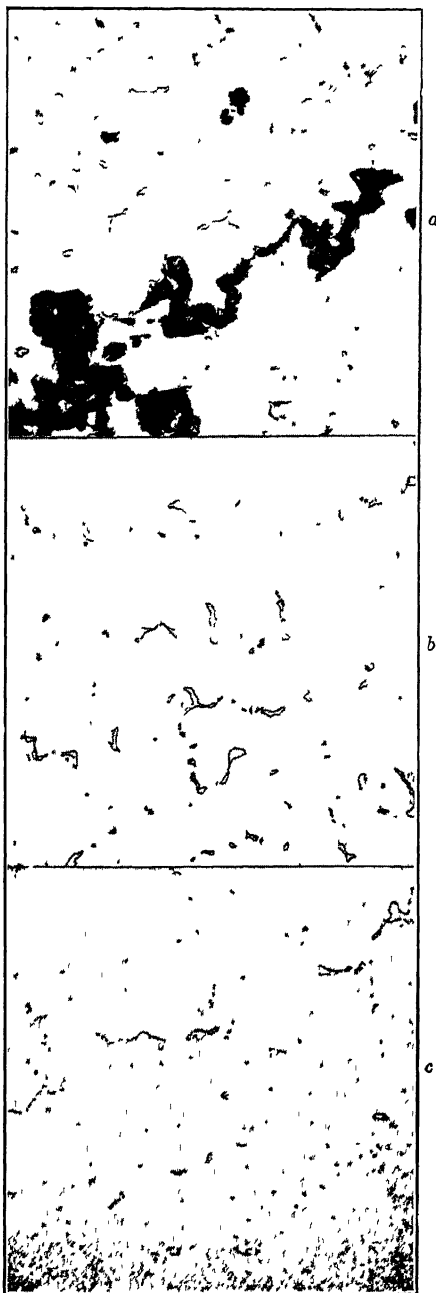


FIG. 20—MICROSTRUCTURES OF 7.5 PER CENT NICKEL, 8 PER CENT TIN SAND-CAST ALLOY ETCHED WITH ACID FERRIC CHLORIDE ( $\times 100$ ).

a. As cast

b. Annealed 1 hr at 1400° F, quenched and aged 5 hr at 500° F.

c. Annealed 5 hr at 1400° F, quenched and aged 5 hr. at 500° F.



would give rise to better properties in the high-zinc content alloys. The manganese content was found to be critical. The complete elimination of manganese resulted in castings with lower properties than normal, while increasing it above the optimum content (0.25 per cent) to 0.5 and 2 per cent, likewise resulted in inferior properties.

TABLE 1—*Effect of Slight Variations in Composition on the Aging Characteristics of the 7.5 Per Cent Ni, 8 Per Cent Sn, 2 Per Cent Zn, 0.25 Per Cent Mn Alloy\**

Composition, Per Cent, 7.5 Ni, 8 Sn +			Pour- ing Temp., Deg F	Annealing (Water Quenched)		Aging		Ultimate Strength, Lb per Sq In	Proportional Limit, Lb per Sq In	Elonga- tion, Per Cent in 2 In	Reduction of Area, Per Cent	Brinell Hard- ness
Zn	Mn	X		Deg F	Hr	Deg F	Hr					
2	0.25	0.15 Cr	2264	1400	5	500	5	75,000	50,000	2	6	160
2	0.25	2 Fe	2300	1400	5	500	5	92,000	56,000	8	17	162
0	0.25		2327	1400	5	500	5	91,500	56,500	8.5	18.5	182
10	0.25		2282	1400	5	500	10	66,700	43,500	1.5	3	169
2	0.25	0.1 Si	2300	1400	5	500	5	82,500	47,500	7.5	12.5	178
2	0.25	1 Pb	2300	1400	5	500	5	36,000	24,500	0	0.5	181
						700	3					
2	0		2300	1400	5	500	10	85,300	46,000	5.5	9.5	166
2	0.5		2300	1400	5	500	5	75,600	46,000	2.5	12.5	183
2	2		2300	1400	5	500	5	68,000	38,000	2.5	12	152
2	0.25		2300	1400	5	500	5	95,000	58,000	9	15	193

\* The melts were made in the Ajax induction furnace utilizing an unlined clay-graphite crucible. The cupronickel was oxidized with 0.05 per cent  $\text{Cu}_2\text{O}$ . The melts were deoxidized with 0.1 per cent Ba.

#### FATIGUE STRENGTH OF CAST AND AGE-HARDENED 7.5 PER CENT NICKEL 8 PER CENT TIN ALLOY

Samples for fatigue testing were produced from castings made from Ajax furnace melts utilizing the 7.5 per cent nickel 8 per cent tin alloy. The mold employed was of the type shown in Fig. 2, with the exception that the bar diameter was reduced to 0.46 in. The bars were annealed 5 hr at 1400° F, water-quenched and aged 5 hr at 500° F. One bar from each mold was machined to a tensile bar having a diameter of 0.300 in., which was the diameter of the minimum section of the standard R. R. Moore fatigue specimens used in the research. The properties of the tensile bars were slightly higher than those ordinarily obtained from the standard tensile bars made from Ajax melts.

The results of the fatigue tests are shown in Fig. 21. Tests on three bars that were unbroken after some 16,000,000 cycles indicated that the fatigue limit was at least 18,000 lb per sq in for 16,000,000 cycles. The ratio of fatigue strength to ultimate was found to be 0.20. It is believed that this ratio is susceptible to considerable increase by certain modifications of casting technique and aging treatment.

## PRACTICAL CONSIDERATIONS

From the preceding data, it is evident that the nickel bronzes possess remarkably good properties even in the as-cast state and are very responsive to heat treatment. The high proportional limit and hardness which can be so simply and inexpensively secured open up entirely new fields for nonferrous castings and offer new tools to progressive foundrymen. Furthermore, and importantly, it must be emphasized that this type of alloy derives its properties from the presence of nickel and tin

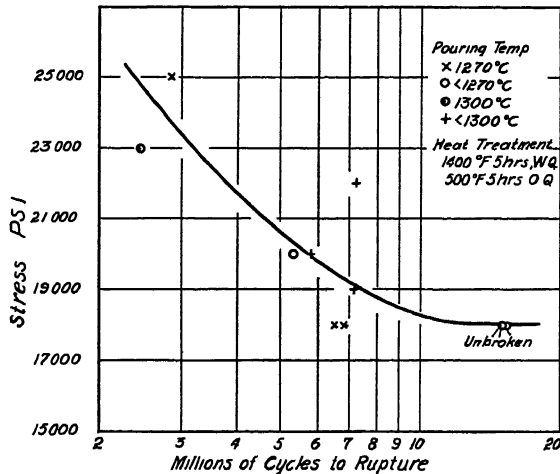


FIG 21 —FATIGUE STRENGTH OF A CAST AND AGE-HARDENED 7.5 PER CENT NICKEL, 8 PER CENT TIN ALLOY

both of which are well known to foundrymen and are generally available at moderate cost, and are recovered almost completely during melting and remelting. Both nickel and tin are compatible with practically all of the foundry bronze mixtures in current use. As a result, the admixture of nickel-bronze scrap with other bronze will do no harm, and in most cases will actually improve the properties of the mixture, which is not the case with certain other alloys that have been proposed.

## PRODUCTION OF THE WROUGHT ALLOYS

A number of the more interesting alloys were produced in the form of chill-cast ingots  $\frac{3}{4}$  by 2 by 9 in. The ingots were homogenized by a treatment at 1300° or 1400° F., depending upon the composition,<sup>11</sup> for 2 or 4 hr, followed by water-quenching, and were then cold-rolled utilizing reductions of about 50 per cent between anneals. Intermediate anneals at 1300° F for 1 hr were employed.

<sup>11</sup> With the exception of the tin-free 7.5 per cent nickel-copper alloy all the chill-cast ingots containing 5 per cent or more of nickel were initially homogenized at 1400° F for 4 hr. The others were annealed 2 hr at 1300° F.

## AGING CHARACTERISTICS OF ROLLED AND ANNEALED ALLOYS

The samples utilized for the aging series were 0.075 in thick and were annealed at 1400° F for 30 min, water-quenched and aged as indicated. The hardness-time curves for temperatures of 500° F. and upward have been presented in Figs 8 to 13 inclusive. The general effect of increasing the amount of precipitable phase can be observed by comparing Figs 8, 9 and 11, relating to the 4 per cent nickel, 4 per cent tin, 5 per cent nickel, 5 per cent tin, and 7.5 per cent nickel 8 per cent tin alloys, respectively. The maximum hardness attained increases rapidly over this composition range and reaches the very respectable value of 320 Brinell hardness for

TABLE 2—*Tensile Properties of Rolled,\* Annealed and Aged Nickel-bronze Alloys*

Composition, Per Cent		Heat Treatment				Physical Properties			
		Annealing (Quenched)		Aging (Quenched)		Derived Brinell Hardness	Ultimate Strength, Lb per Sq In	Proportional Limit, Lb per Sq In	Elongation, Per Cent in 2 In
		Deg F	Hr	Deg F	Hr				
0	0	1,400	½			38	32,800	7,300	48
0	5	1,400	½			70	44,700	13,100	64
0	8	1,400	½			78	55,000	10,200	73 5
0	10	1,400	½			84	62,000	15,200	67
3	8	1,400	½	600	5	99	64,900	33,400	71
4	4	1,400	½	600	5	113	66,000	25,600	25
5	5	1,400	½	600	5	200	100,000	30,900	23 5
7 5	0	1,400	½			61	41,000	7,700	43
7 5	5 5	1,400	½	600	5	236	109,400	62,200	29 5
7 5	5 5	1,400	½	700	1	240	112,600		19 5
7 5	5 5	1,400	½	700	5	265	124,000	91,200	8 5
7 5	5 5	1,400	½	700	20	281	126,000	72,000	4 5
7 5 <sup>b</sup>	8	1,400	½	500	1	189	103,500	52,300	32
7 5	8	1,400	½	500	5	227	107,000	56,000	31
7 5	8	1,400	½	600	1	239	113,200	66,400	22
7 5	8	1,400	½	600	5	292	125,400	79,800	11 5
7 5	8	1,400	½	600	20	314	136,400	80,000	4
7 5	8	1,400	½	700	1	297	130,700	91,000	5
7 5	8	1,400	½	700	5	301	135,700	74,500	3 5
7 5	8	1,400	½	700	20	239	116,000	53,900	6 5
7 5 <sup>b</sup>	8	1,400	½	800	5	208	106,800	36,000	8
7 5 <sup>b</sup>	8					257	128,000	65,500	2 5
7 5 <sup>b</sup>	8			600	5	392	170,000	115,900	1 5
10	5	1,400	½	600	5	197	100,000	48,200	22
15	0	1,400	½			68	45,500	8,500	41
15	5	1,400	½	600	5	162	89,400	39,000	30

\* Cold-rolled 50 per cent

<sup>b</sup> Cold-rolled 75 per cent

the 7.5 per cent nickel, 8 per cent tin alloy aged at 600° F. for 20 hr. The greater tendency for the highly supersaturated alloys such as the 7.5 per cent nickel, 8 per cent tin alloy to overage, as compared to the 4 per cent nickel, 4 per cent tin or 5 per cent nickel, 5 per cent tin alloy, has already been noted. In connection with the behavior of the latter marginal alloys, the influence of the change in solid solubility with the aging temperature should not be overlooked.

Figs. 10, 12 and 13 relate to the 7.5 per cent nickel, 5.5 per cent tin; 10 per cent nickel 5 per cent tin, and 15 per cent nickel, 5 per cent tin

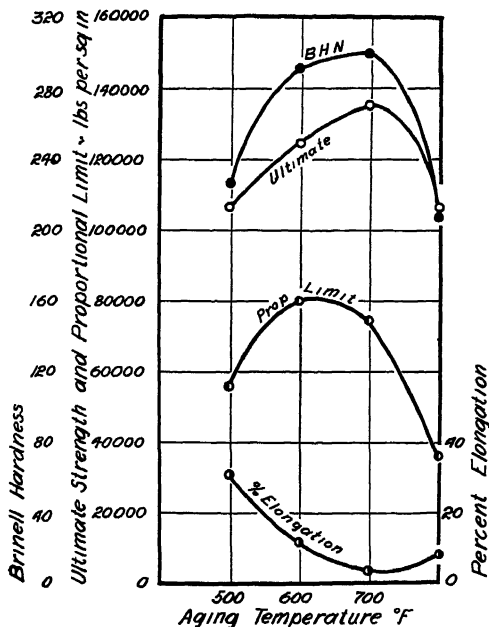


FIG. 22.—EFFECT OF AGING TEMPERATURE ON ROLLED AND ANNEALED 7.5 PER CENT NICKEL, 8 PER CENT TIN ALLOY.

alloys, respectively, which develop nearly identical maximum hardness values and possess a comparable degree of supersaturation, show that the rate of hardening and the tendency to overage decrease with the nickel content. This effect is emphasized when the nickel content exceeds 10 per cent.

#### TENSILE PROPERTIES OF ROLLED, ANNEALED AND AGED ALLOYS

The significant tensile properties of the rolled alloys after a variety of treatments are presented in Table 2. The properties of the 7.5 per cent nickel, 8 per cent tin alloy annealed  $\frac{1}{2}$  hr at 1400° F, quenched and then aged for 5 hr at various temperatures are shown in Fig. 22. A tensile strength in excess of 135,000 lb per sq in, a proportional limit of about 75,000 lb per sq in, and a Brinell hardness of about 300,

coupled with an elongation of 3.5 per cent, result from aging for 5 hr at 700° F.

### AGING PROPERTIES OF HARD-ROLLED ALLOYS

The aging characteristics of two of the very hardenable alloys—namely, the 7.5 per cent nickel, 8 per cent tin, and the 15 per cent nickel, 5 per cent tin alloys—homogenized at 1400° F, then cold-rolled with

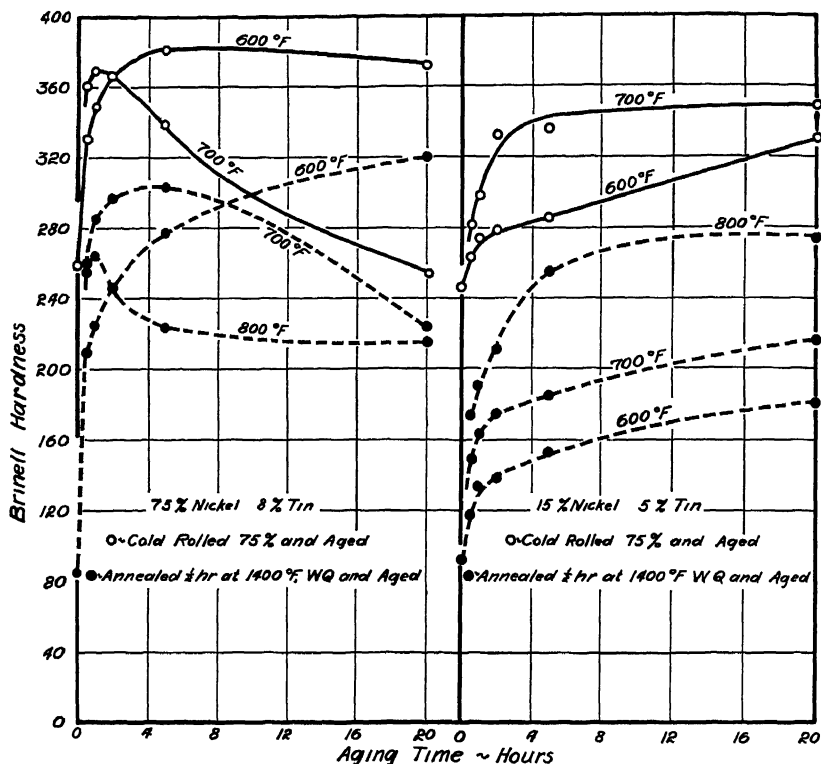


FIG. 23—COMPARISON BETWEEN AGE-HARDENING OF ANNEALED AND HARD-ROLLED (75 PER CENT REDUCTION) SAMPLES OF 7.5 PER CENT NICKEL, 8 PER CENT TIN ALLOY AND 15 PER CENT NICKEL, 5 PER CENT TIN ALLOY

75 per cent reduction, and aged after this hard rolling, are presented in Fig. 23. On the same plots are presented the corresponding data for the same alloys initially annealed at 1400° F. for 1/2 hr and then water-quenched and aged.

The cold-rolled alloys age more rapidly and the maximum Brinell hardness attained is 60 to 75 points higher than that of the initially annealed alloys. The hardness of the unaged 7.5 per cent nickel, 8 per cent tin alloy cold-rolled with 75 per cent reduction was 260 Brinell, which was raised to 382 by aging at 600° F. for 5 hr. The initial hardness

of the 15 per cent nickel, 5 per cent tin alloy was 247 Brinell, and was raised to 350 by aging at 700° F for 20 hours

The tensile strength of the 7.5 per cent nickel, 8 per cent tin alloy cold-rolled with 75 per cent reduction was 128,000 lb per sq in, and the proportional limit was 65,500 lb per sq in, coupled with 2.5 per cent elongation. After aging at 600° F for 5 hr, the tensile strength was found to be 170,000 lb per sq in, the proportional limit was 116,000 lb per sq in, the elongation was 1.5 per cent, while the Brinell hardness was 392, which was slightly higher than the similarly treated sample previously discussed.

The high elastic properties of these age-hardenable alloys, their amenability to cold working in the soft state, their ready machinability, particularly after slow cooling, and their low metal cost, suggest many applications where properties superior to the usual brasses and bronzes are required.

#### RELATION BETWEEN TENSILE STRENGTH, PROPORTIONAL LIMIT AND ELONGATION OF WROUGHT 7.5 PER CENT NICKEL, 8 PER CENT TIN ALLOY

The strength properties of the 7.5 per cent nickel, 8 per cent tin alloy, annealed at 1400° F for ½ hr, quenched and aged at temperatures ranging from 500° to 700° F for 1 to 20 hr, are shown in Fig. 18. It is evident from these curves that certain relationships exist between the elongation, ultimate strength and proportional limit, and that a high degree of toughness coupled with high elastic properties can be secured, also, that over a reasonable range at least, temperature and time appear to be nearly equivalent in their effects. It must be emphasized, however, that overaging is shown earlier in the drop in the proportional limit than in the ultimate strength and Brinell hardness, and that this drop in strength properties due to slight overaging is not associated with much increase in elongation. The shapes of these curves are similar to those of the same alloy in the cast and heat-treated form, however, the tensile strengths of the wrought material are about 25 per cent higher than those of the cast alloy when treated to produce the same elongation, while the proportional limits are 28 to 40 per cent higher. Curves of this nature are very useful in fixing the proper balance between the elastic properties and the toughness which may be required to secure adequate reliability.

#### ACKNOWLEDGMENTS

The authors desire to express their thanks to Mr. A. J. Wadhams, Manager of the Development and Research Department of The International Nickel Co., Inc., for permission to present the results of this research. The very efficient assistance of Mr. Erich Fetz in conducting much of the experimental work herein reported is acknowledged with

pleasure. They also welcome this opportunity to acknowledge the many helpful suggestions which were made by Mr. E. R. Darby, Chief Metallurgist, the Federal Mogul Corporation, Detroit, Mich., and to thank Mr. B. Clements, Chief Metallurgist, The Curtiss Wright Corporation, Paterson, N. J., for his very valuable help in carrying out certain tests.

APPENDIX.—*Tensile Properties of Cast and Heat-treated Nickel-bronze Alloys<sup>a</sup>*

Composition, Per Cent	Melting Proce- dure <sup>b</sup>		Deoxidizers, Per Cent Added	Pouring Temperature		Heat Treatment			Ultimate Strength, Lb per Sq In	Propor- tional Limit, Lb per Sq In	Yield Strength (0.2 Per Cent Permanent Set), Lb per Sq In	Elonga- tion, Per Cent in 2 In	Reduc- tion of Area, Per Cent
	Ni	Sn		Deg F	Deg C	Annealing (Water Quenched)	Aging (Quenched)	Burnell Hard- ness No					
0	0	0	0 05 P	2,296	1,258			43	25,900	4,000	9,000	57	68
0	5	5	0 05 P	2,246	1,230			59	40,000	7,000	18,000	37 5	34
0	10	10	0 025 P + 0 025 Ba	2,228	1,220			74	43,200	10,000	20,000	25	
0 <sup>c</sup>	12 5	12 5	0 025 P + 0 05 Ba	2,181	1,194			80	45,300	10,500	22,500	19	24
2 5	10	10	0 025 P + 0 075 Ba	2,296	1,258			75	46,500	10,000	22,000	27 5	21
2 5	10	10	0 025 P + 0 075 Ba	2,296	1,258	1400	600	59	43,200	12,000	21,500	33	39
3	8	8	0 025 P + 0 05 Ba	2,332	1,278			72	46,500	14,000	21,600	38	42
3	8	8	0 025 P + 0 05 Ba	2,332	1,278	1400	600	78	46,600	17,000	25,800	36	32
4	4	4	0 025 P + 0 05 Ba	2,327	1,275			69	43,800	15,000	19,000	45	47
4	4	4	0 025 P + 0 05 Ba	2,327	1,275	1400	600	110	63,500	26,000	39,000	30	40
5	5	5	0 05 P + 0 05 Ba	2,323	1,273			75	48,850	13,500	22,800	44	50
5	5	5	0 05 P + 0 05 Ba	2,323	1,273	1400	500	136	74,000	40,000	53,000	27 5	29
5	5	5	0 05 P + 0 05 Ba	2,323	1,273	1400	600	171	84,000	47,500	66,000	16	26
7 5	0	0	0 05 P + 0 05 Mg	2,403	1,317			61	35,000	10,000	16,000	37	60
7 5	5 5	5 5	0 05 P	2,347	1,286			165	56,500	24,000	29,400	36	34
7 5	5 5	5 5	0 05 P	2,347	1,286			213	103,900	50,000	64,500	22 5	34
7 5	5 5	5 5	0 05 P	2,347	1,286	1400	500	105	58,000	25,000	34,000	18	18
7 5 <sup>d</sup>	8	8	0 05 Ba	2,300	1,260	5	650	100	55,650	21,000	32,000	25	29
7 5	8	8	0 05 Ba	2,282	1,250			165	81,500	48,000	64,000	25	36
7 5	8	8	0 05 Ba	2,327	1,275	1400	5	179	89,650	55,000	76,000	18	34
7 5 <sup>d</sup>	8	8	0 1 Ba	2,327	1,275	1400	600	228	111,150	66,000		6	7
7 5	8	8	0 1 Ba	2,332	1,288	1400 <sup>e</sup>	5	500 <sup>e</sup>	86,000	48,000	63,000	11 5	19
10	4 5	4 5	0 05 P + 0 05 Ba	2,350	1,288				57,000	25,000	34,000	34	43
10	4 5	4 5	0 05 P + 0 05 Ba	2,350	1,288	1400	5	177	89,000	63,000	68,500	16	24
10	5	5	0 05 P + 0 05 Ba	2,390	1,310			101	55,700	16,500	28,500	30	29
10	5	5	0 05 P + 0 05 Ba	2,390	1,310	1400	500	102	62,200	26,500	38,000	34	35



APPENDIX.—Tensile Properties of Cast and Heat-treated Nickel-bronze Alloys.<sup>a</sup>—(Continued)

Composition, Per Cent	Melting Proce- dure <sup>b</sup>	Deoxidizers, Per Cent	Pouring Temperature		Heat Treatment			Ultimate Strength, Lb per Sq in	Propor- tional Limit, Lb. per Sq in	Yield Strength (0.2 Per Cent Permanent Set), Lb per Sq in	Elonga- tion— Per Cent in 2 in	Reduc- tion of Area, Per Cent
			Deg F	Deg C	Annealing (Water Quenched)	Aging (Quenched)	Brinell Hard- ness No					
Ni	Sn				Deg F	Hr	Deg F	Hr				
10	5	0 05 P + 0 05 Ba	2,390	1,310	1400	10	600	5	159	84,000	17 5	20 5
10	10	0 025 P + 0 075 Ba	2,327	1,275					170	64,400	0 5	2
10	10	0 025 P + 0 075 Ba	2,327	1,275	1400	10	600	5	203	82,250	1	2
15	0	0 05 P + 0 05 Mg	2,498	1,370					63	40,650	42	44
15	5	0 05 P + 0 05 Ba	2,444	1,340					91	71,750	12	14
15	5	0 05 P + 0 05 Ba	2,444	1,340	1400	10	600	5	121	70,500	39	40 5
15	7	0 05 P + 0 05 Mg	2,399	1,315					173	81,000	1 5	4
15	7	0 05 P + 0 05 Mg	2,399	1,315	1400	5	600	5	171	77,400	4	9
20	0	0 025 P + 0 05 Mg	2,486	1,352					59	42,800	44	54
20	2 5	0 025 P + 0 075 Ba	2,496	1,369					70	47,750	26	33
20	2 5	0 025 P + 0 075 Ba	2,496	1,369	1400	10	600	5	65	38,000	34	36
20	7	0 1 Ba	2,444	1,340					144	78,100	7	10
20	7	0 1 Ba	2,444	1,340	1400	10	600	5	160	85,000	21	24
20	7	0 1 Ba	2,444	1,340	1600	7	600	1	207	96,000	14	24
30	0	0 025 P + 0 05 Mg	2,547	1,397					63	45,000	42	47

<sup>a</sup> Ajax induction furnace melts unless indicated otherwise<sup>b</sup> Melting procedure A Unlined clay-graphite crucible Cupronickel not oxidizedB Unlined clay-graphite crucible Cupronickel oxidized with 0 05 per cent Cu<sub>2</sub>OC Clay-graphite crucible lined with magnesia Cupronickel oxidized with 0 05 per cent Cu<sub>2</sub>O Covered with glass slag<sup>c</sup> No zinc was added and the manganese content was reduced to 0 1 per cent<sup>d</sup> Foundry melt<sup>e</sup> Air-cooled

## DISCUSSION

(*Carleton S Harloff presiding*)

D J MACNAUGHTAN,\* London, England (written discussion) —The authors have shown in this interesting and valuable paper how to obtain outstanding improvements in the mechanical properties of nickel bronzes by the application of suitable heat treatment, whereby they become high-grade engineering materials. This is due chiefly to the fact that while securing a marked improvement in the tensile properties the authors have also obtained a great improvement in the elastic properties as shown by the high proportional limits of some of the heat-treated alloys.

As this is likely to open up new applications, it would be valuable to have data relating to electrical conductivity, resistance to corrosion and erosion, the resistance to scaling under heat, and the mechanical properties at elevated temperatures. As quenched and aged alloys are usually stable under heat up to a temperature very close to the aging temperature, it is to be expected that the alloys should maintain their mechanical properties even after considerable periods of exposure at temperatures up to 600° F. It would be useful to know whether the authors have confirmed this.

The fatigue range appears to be unduly low. As the tests were carried out on material in the "as-cast" state this is likely, as the authors suggest, to be due to defective cast structure. It would, therefore, be useful to have information concerning the fatigue properties of the wrought alloys.

In this country (Great Britain) the casting temperatures for ordinary bronzes are usually 50° to 100° C lower than those given in the paper, and as the casting temperature is usually considered to be rather critical it would be interesting to hear why the authors used such a high casting temperature.

While the paper establishes the improvements that can be obtained by adding nickel to the straight tin bronzes, the beneficial effect of small quantities of tin on cupronickel alloys is strikingly demonstrated. Thus the properties of cupronickels containing 10 to 15 per cent nickel appear to be markedly improved by additions of tin not exceeding 5 per cent.

The economic factors referred to in the paper may apply to present conditions in the United States as regards metal prices, but it remains to be seen how long these conditions will last. It certainly does not apply in many countries. Thus in Great Britain the economic advantages claimed by the authors would not be secured by replacing tin by nickel. Apart from all question of cost, however, the authors have shown that there exists a series of alloys containing appreciable amounts of both nickel and tin, which are to be distinguished very clearly from either of the binary series and in which the properties may be manipulated by heat treatment to give values greatly in excess of those obtained by the use of either metal alone. The diagrams in Figs 14 to 17 clearly show that the maximum strength is obtained when nickel and tin are present in approximately equal amounts, and the advantages obtained by this combination seem to be so great that the relative prices of nickel and tin must be considered as of minor importance. It is to be hoped that the authors' further investigations will throw some light on the nature of the constituent that makes heat treatment possible, since an exact knowledge of the nature of this phase would have both theoretical and practical interest.

R H STONE,† Swissvale, Pa (written discussion) —Referring to the following quotation "Most of the melts considered here were made in a 40-lb Ajax high-frequency furnace. Crucible melts (of 180 lb each) of some of the alloys were made

\* Director of Research, International Tin Research & Development Council

† Chemical Engineer, Vesuvius Crucible Co.

in an oil-fired pit furnace, and these indicated as good or better properties than those of the Ajax melts" Did the authors base this conclusion on experimental data or qualitative observations comparing the properties of the metal melted by the two different methods and would they care to elaborate a little on this statement?

E M WISE AND J T EASH (written discussion) —We desire to thank Mr Macnaughtan for his kind remarks and for his suggestions concerning the applications of these materials to engineering uses We have not had occasion to investigate the properties of the alloys at elevated temperature, but have noted that an alloy that had been partially aged by heating at 500° for 5 hr showed a further increase in strength and slight reduction in elongation after being reheated at 400° F for 116 hr It may be noted that rate of aging may be altered by adjusting the base composition, and that the presence of small amounts of certain addition elements markedly reduces it

The fatigue limit of the wrought alloys has not been determined but will doubtless be materially higher than for the cast material reported in the present paper The pouring temperature employed was selected after considerable investigation of the influence of this factor on the properties of test castings It does appear to be higher than is customary, but actually it proved to be the most suitable for alloys of maximum interest and for the particular test pattern employed, presumably because it resulted in a sufficient thermal gradient to secure progressive solidification and good feeding

The nature of the constituent responsible for the age-hardening, which appears to contain nearly equal quantities of tin and nickel, may be more apparent after the nickel-tin system has been re-examined

In reply to Mr Stone's question, it may be stated that the relative strength and ductility of melts made in clay graphite crucibles heated by electricity or by combustion were comparable In view of the fact that the atmosphere during melting was definitely oxidizing in both instances and the other melting conditions were not too dissimilar, this result was not unexpected

## Testing the Drawing Properties of Rolled Zinc Alloys

BY E H KELTON\* AND GERALD EDMUNDS,† PALMERTON, PA

(New York Meeting, February, 1934)

THE purposes of this paper are to describe the use of adjustable cut and draw tools as a control test of drawing properties and to point out that no other well-known test or combination of tests determines this quality in zinc and zinc alloys.

Rolled zinc has been used for making drawn articles, particularly battery cans, for many years. The development of rolling treatments satisfactory for these purposes followed the usual course of trial and error experimentation depending upon cooperation with customers to determine what type of material was suitable.

A quick test of drawing quality was highly desirable, of course. Scleroscope hardness and temper,<sup>1</sup> having no apparent relation to drawing quality, were used simply to check the duplication of rolling treatment and grade of metal. The dynamic ductility<sup>1</sup> test, on the other hand, was believed to be so like the drawing operation as to provide a reliable index and came to be taken as the criterion of good drawing properties. Faith in this test was strengthened by the fact that metal having the highest ductility was more satisfactory for operations, such as the manufacture of battery cups, that required several redraws.

No distinction was made at that time in specifying metal as to whether it was to be subjected to simple cut and draw, redrawing or forming operations. It developed, however, that in some grades of metal the highest ductility did not coincide with the most satisfactory quality when the material was used for a single draw.

When zinc-base alloys, with their wider ranges of effective rolling treatments, came into increased use, their dynamic ductility and drawing quality appeared to have no connection whatever. Furthermore, comparisons of known drawing quality with other physical properties of the metal, including tensile strength, elongation and dynamic cold bends, were fruitless in yielding any clear relationship. Almost any test value produced in one piece of metal could be duplicated by another rolling or annealing treatment with attendant different drawing characteristics.

---

Manuscript received at the office of the Institute Dec 1, 1933

\* Chief Investigator, Rolling Mill Section, Research Division, The New Jersey Zinc Co

† Investigator, Rolling Mill Section, Research Division, The New Jersey Zinc Co

<sup>1</sup> A S T M Standard Specifications for Rolled Zinc B69-29

Since it was felt that more exact information on drawing quality was essential, a double-acting commercial drawing press was secured and cut-and-draw tools made for two gages of metal. It was hoped originally that the comparative drawing characteristics of samples of metal could be measured by determining the limiting partial draw if the metal failed on a full stroke of the draw punch. In other words, the stroke of the drawing punch was progressively shortened until the metal did not fail. This method was wholly unsatisfactory.

Another set of tools having greater "take-in" was then built.<sup>2</sup> This made it possible to grade a given sample as good, fair or poor. The results obtained clearly indicated the value of this method of testing and the desirability of having available tools for any thickness of metal and any reasonable take-in. Complete sets of tools for all common thicknesses and reductions would be both expensive and unwieldy. Moreover, the time necessary to change tools would seriously interfere with the speed and efficiency of testing. Accordingly, tools were designed by which cut-and-draw cups approximately  $1\frac{1}{2}$  in. in diameter could be made with take-ins of 40,  $42\frac{1}{2}$ , 45,  $47\frac{1}{2}$  and 50 per cent merely by changing the cutting punch and die. This change with all necessary readjustments required not over 10 min. A set of 15 draw punches was made, suitable for drawing any common thickness of metal from 0.012 to 0.080 in. Interchanging punches required 20 to 30 min. The number of punches could, of course, be increased to handle metal of almost any reasonable thickness but probably would require additional draw dies having radii suitable for the extremes of thickness.

With this set of combination tools, set-up accuracy could be maintained to a remarkably high degree, since the relative positions of both the blankholder and die remained the same when the punches or cutting tools were changed. In addition to this, the adjustment nuts on the blankholder slide were graduated into thousandths of an inch in order to facilitate making uniform original set-ups and uniform changes in holding pressure.

Fig. 1 shows a section view of the so-called "combination" cut-and-draw tools. The interchangeable cutting punch and die and the drawing punch are indicated. In making these tools every known device was used to increase the drawing take-in, since a high degree of perfection is easier to duplicate than an unknown degree of imperfection. The punches were turned from 1.20 to 1.30 carbon steel to within 0.020 in. of the final diameter (approximately 1.5 in.). They were then hardened and tempered, and ground to the final diameter. In this grinding, the drawing ends were tapered 0.001 in. in the last  $1\frac{1}{4}$  in. to facilitate stripping the

---

<sup>2</sup> "Take-in" is used here as the difference between blank diameter and cup diameter divided by the blank diameter.

cup The shanks, radii, and ends of the punches were finished with the highest polish possible with crocus paper

The punch radii chosen were those that gave the best drawing results on each particular thickness of metal For metal thicknesses 0.012 to

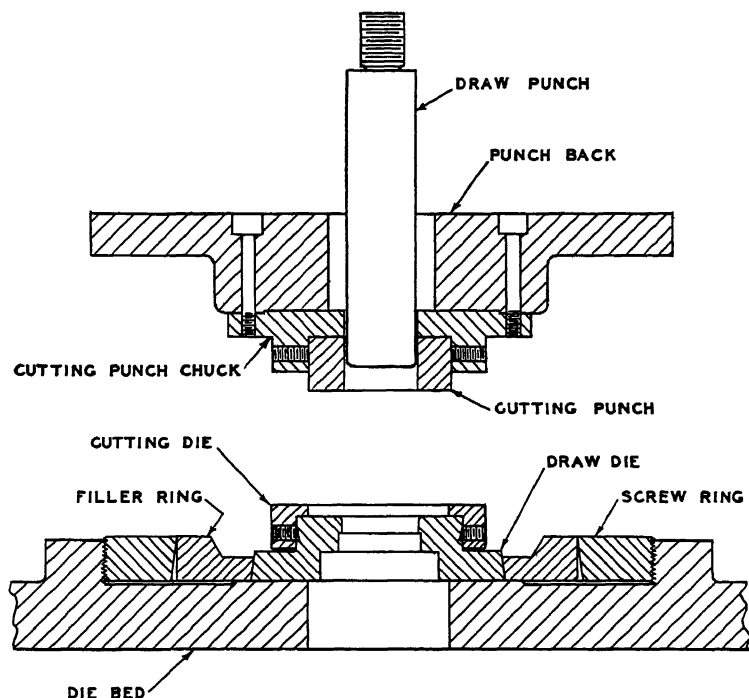


FIG 1 —COMBINATION CUT-AND-DRAW TOOLS.

0.016 in., the radius was  $\frac{3}{32}$  in ; for 0.018 to 0.022-in metal the radius was  $\frac{7}{64}$  in ; and for 0.024 to 0.040-in metal the radius was  $\frac{9}{64}$  in A  $\frac{1}{8}$ -in. punch radius was used on heavier metal up to 0.080 in but very little work was done in this range

After considerable experimentation, a standard clearance of exactly the original metal thickness between the punch and die was adopted For example, for drawing 0.020-in metal a punch diameter of 1.5205 in. and a die diameter of 1.5605 in. were used. This was found to give good results and to avoid the complications of thickening or pinching due to more or less clearance than the standard adopted.

The draw die was made of the same material as the punch and given practically the same sequence of heat-treating and finishing operations. The face of the die was ground with a slight taper, so that there was 0.001 in. more clearance between the holding punch and die at the periphery than at the aperture. This aids in preventing the formation of wrinkles and thus improves the drawn cups

A draw-die radius of  $\frac{1}{8}$  in gave the best results for metal thicknesses from 0.012 to 0.040 in. As indicated by the range of thicknesses tested on this die, there seemed to be considerable leeway in the choice of the best radius for any particular metal thickness.

Extreme care was necessary in grinding the interchangeable parts in order to secure exact fits. Preliminary tests were entirely successful in that no overlapping of cutting edges occurred.

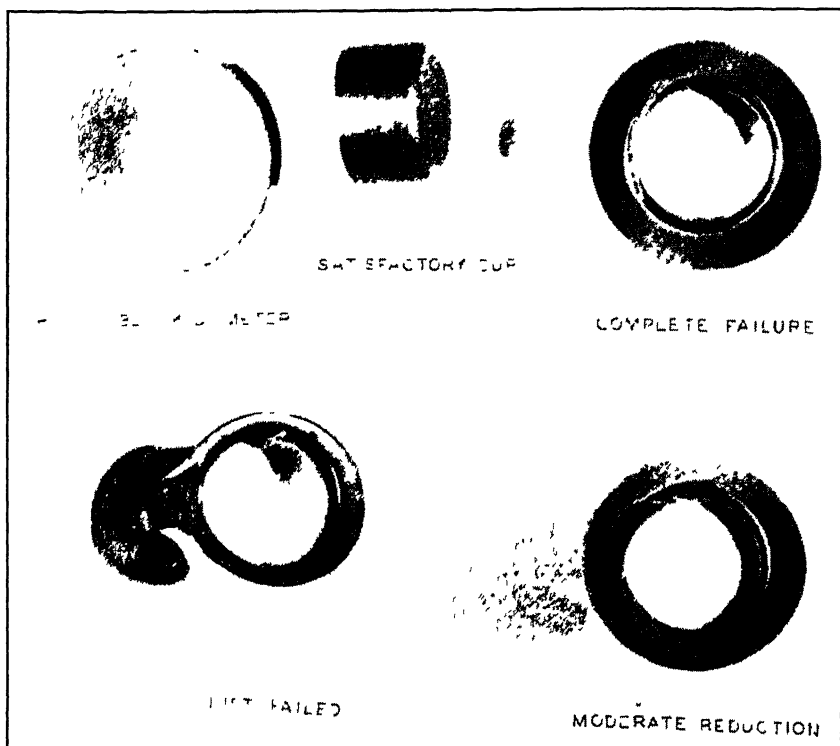


FIG 2—SATISFACTORY CUP AND VARIOUS STAGES OF FAILURE

After some experimentation with various lubricating oils and soap solutions, a standard grade of machine oil was found that gave consistent results over a wide range of surface conditions. The oil was applied to the surface of the metal and then allowed to drain off for several minutes before drawing in order to secure a thin even film of lubricant.

All drawing tests were performed at room temperature (70° F.), care being taken to allow cold or hot coils plenty of time to reach room temperature before testing.

It was found desirable to determine the maximum take-in more closely than the 2.5 per cent limits described above. This was accomplished

by testing with the next larger blank than could be drawn successfully, and noting the relative reduction in diameter before failure of the cup

Fig 2 illustrates the original blank, a satisfactory cup, a test that "just failed," one that withstood a "moderate reduction" and one that was reduced only slightly before failure. The just-failed metal was estimated to have a maximum take-in of 1 per cent less and the moderate-reduction metal was estimated to have a maximum reduction of 2 per cent less than metal that would have just withstood this operation. Thus, metal "just failing" on the 45 per cent tools was rated as 44 per cent, and a "moderate reduction" on the same tools was rated as a 43 per cent take-in.

Finally, on samples of which part of the blanks of a certain size drew successfully, while the remainder failed either completely or by "necking," the maximum probable value of the sample was estimated from Table 1 of arbitrary values, which were subtracted from the take-in of the test being made. Thus in a test of 10 blanks, of which 3 drew successfully, 4 failed completely, and 3 necked on the 47.5 per cent take-in blank, the estimated drawing quality is  $47.5 - 0.8 = 46.7$  per cent.

TABLE 1—*For Estimation of Maximum Take-in on Cut-and-draw Tests Based on Tests of 10 Blanks*

No of Cups Necked	Number of Cups Failed										
	0	1	2	3	4	5	6	7	8	9	10
0	0	-0.5	-0.6	-0.7	-0.8	-0.9	-1.0	-1.0	-1.0	-1.0	-1.0
1	-0.2	-0.5	-0.6	-0.7	-0.8	-0.9	-1.0	-1.0	-1.0	-1.0	
2	-0.3	-0.5	-0.6	-0.7	-0.8	-0.9	-1.0	-1.0	-1.0		
3	-0.4	-0.5	-0.6	-0.7	-0.8	-1.0	-1.0	-1.0			
4	-0.5	-0.6	-0.7	-0.8	-0.9	-1.0	-1.0				
5	-0.5	-0.6	-0.7	-0.8	-0.9	-1.0					
6	-0.5	-0.6	-0.7	-0.8	-0.9						
7	-0.6	-0.7	-0.8	-0.9							
8	-0.6	-0.7	-0.8								
9	-0.6	-0.7									
10	-0.6										

These methods of arbitrary rating assisted considerably in comparisons of rolling and annealing treatments.

A zinc alloy, which had been given cold-rolling reductions up to 80 per cent, was tested in both the as-rolled and annealed conditions. Fig 3 shows the comparative results when the various properties of the as-rolled metal are plotted against the percentage of cold reduction by rolling after a complete annealing. In Fig 4, the properties of the same material after a further complete annealing are plotted against the cold



reductions this metal received before the annealing. These graphs show more clearly than words can describe the lack of similarity between drawing characteristics and any other property. The ranges of the numerical values are given in Table 2. The graphs also show that the maximum drawing quality is not realized with either the softest metal or the metal having the highest dynamic ductility in this particular alloy.

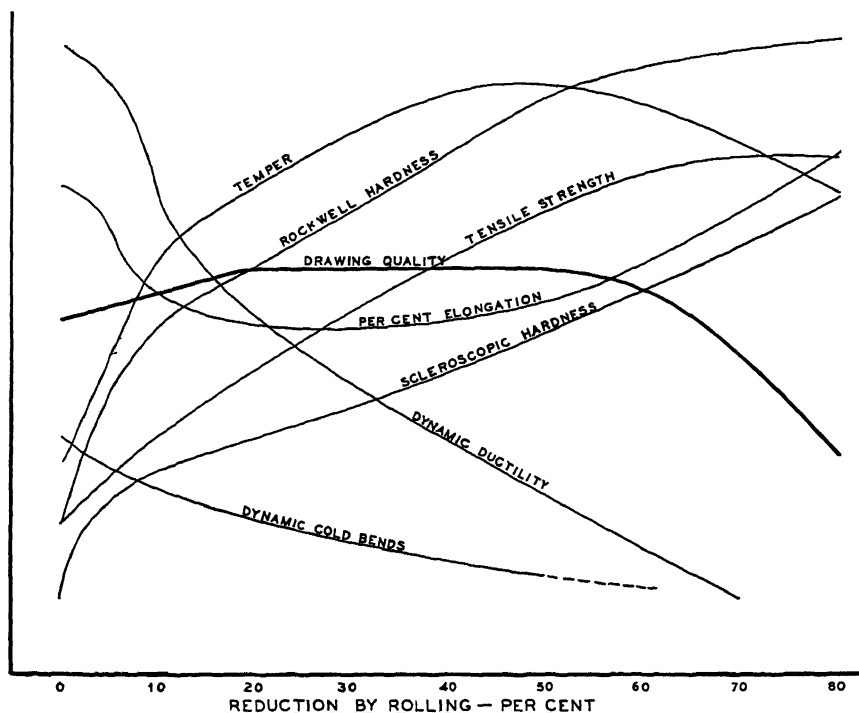


FIG 3.—RELATIVE PHYSICAL PROPERTIES OF AS-ROLLED METAL VERSUS REDUCTION BY ROLLING

High-grade zinc alloy U S P 1716599, containing 1 per cent Cu and 0.01 per cent Mg, 0.040-in. thick. Ordinate values for curves are given in Table 2.

Investigation has shown that this same situation exists in other grades of zinc and zinc alloys.

Where several redrawing operations are required it is necessary, of course, to sacrifice maximum take-in on the cut-and-draw operation in order to obtain metal sufficiently soft to stand the redrawing operations without annealing. Several sets of redrawing tools capable of taking the cups through five redrawing operations were constructed. These tools made possible a determination of the comparative redrawing characteristics of cups produced by different treatments or from different alloys. No attempt has been made (as was done with the single-draw test) to determine the limiting take-in.

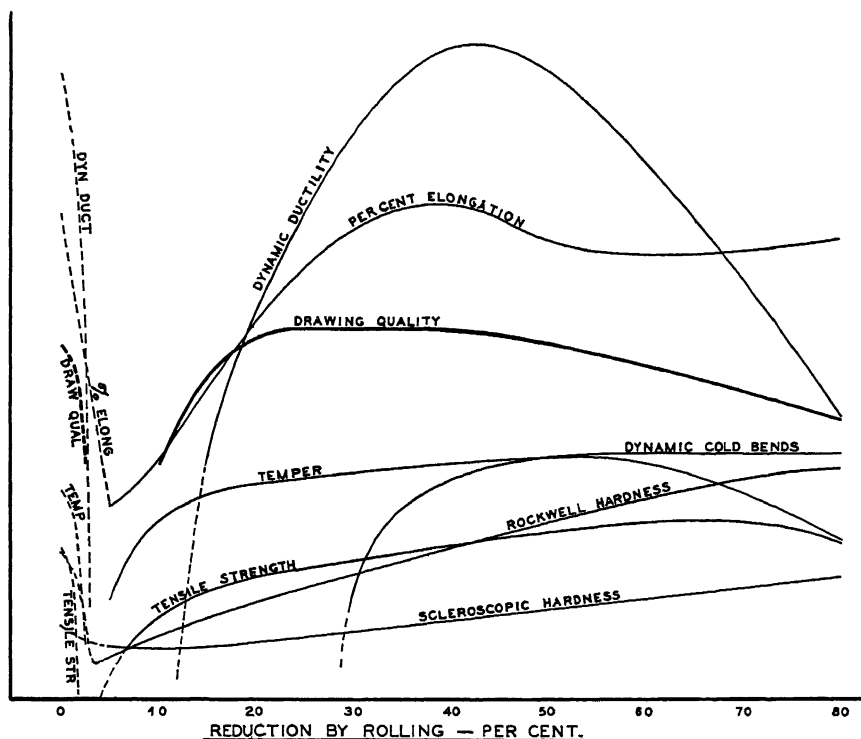


FIG 4—RELATIVE PHYSICAL PROPERTIES OF ANNEALED METAL VERSUS REDUCTION BY ROLLING

Same zinc alloy as in Fig 3 Ordinate values for curves are given in Table 2

TABLE 2—Range of Numerical Values in Graphs of Figs. 3 and 4

Property	Treatment	Range	Points per 1-in Division
Scleroscope hardness	As rolled	17-33	4
	Annealed	16-19	4
Rockwell <sup>a</sup> hardness	As rolled	72-97	5
	Annealed	66-77	5
Dynamic ductility	As rolled	327-384	10
	Annealed	322-387	10
Temper	As rolled	36 6-51 8	4
	Annealed	32-37 8	4
Dynamic cold bends	As rolled	5+-2 2	2
	Annealed	5+-2 0	2
Tensile strength	As rolled	27,000-49,500	6,000
	Annealed	21,000-34,000	6,000
Per cent elongation	As rolled	20-38	10
	Annealed	4 5-35	10
Drawing quality	As rolled	38 5-48	5
	Annealed	39 4-46 2	5

<sup>a</sup> Rockwell B scale,  $\frac{1}{16}$ -in ball, 60-kg. load.

Formed articles, in general, required soft material of the highest dynamic ductility. Forming is considered here as an operation in which the cup is not pushed through the die because of a projecting flange or collar. Many of these operations approach the dynamic ductility test in principle in that the blank is held so tightly that all shaping is done by stretching the metal

It has been our experience that the details of toolmaking differ considerably in different plants, that one diemaker will attain a desired result by one device while another will attain the same end by employing an entirely different principle. It is our belief that the details of die design are unimportant as long as duplication of results can be obtained. That duplication of results can be obtained on the tools described above has been proved to the authors' satisfaction by frequent check tests on standard coils of materials saved for this purpose. When used as a control test, duplication of results by other plants would not be essential. It is quite possible too that these particular tools would not provide satisfactory results on other metals where different clearances, punch and die radii and degrees of polish might be required.

Other investigators have developed machines for testing the drawing qualities of metals. Some of these machines yield valuable information on the stresses and pressures involved in drawing. The accurate determination of drawing quality alone, however, seems to be most economically and dependably accomplished by means of the combination tools described above.

#### ACKNOWLEDGMENTS

The authors wish to acknowledge the assistance of Mr. J. Ruzicka and Mr. N. Wolfe in this work and the very great help given by the Scovill Manufacturing Co., Waterbury, Conn., in providing tools, equipment and expert advice.

#### DISCUSSION

*(L. S. Reid presiding)*

S. TOUR,\* New York, N. Y.—Has the author attempted to calculate along the lines of Dr. Sommer's work, and to see whether or not Dr. Sommer's numerical formula applies to this zinc alloy?

G. EDMUNDS—We have not made any such calculations. You must consider, of course, in the case of zinc and its alloys, that metals are being dealt with which must be tested under conditions, particularly speed, that are comparable to the application. Dr. Sommer's work is limited to determining properties of the metal by stress-strain and alloy diagrams and predicting drawing quality on the basis of these tests, which can only be made at rather slow speeds as compared to the drawing operation. For that reason we have not even attempted to make such calculations

---

\* Vice President, Lucius Pitkin, Inc.

S TOUR—That answers it to some extent. Although Dr Sommer's work is based on actual curves, based on what he calls slow tensile tests, yet he interprets those in terms of the drawability in an eyelet machine of brass, copper, nickel, aluminum, steel, and so on. Certainly in an eyelet machine we do not have a slow drawing process. If his work can be interpreted in terms of eyelet machine work on copper and brass, why cannot it also be interpreted in the case of zinc?

G EDMUNDS—The point that I intended to bring out is that zinc is more susceptible to variations in strength and elongation and other properties with rates of working than are any of the other metals you have just mentioned, and for that reason we are so much further removed from the drawing test in the case of making tensile determinations on zinc than we would be were we working on iron or brass and such metals. I do not, of course, want to say that we do not feel there is any possibility of applying Dr Sommer's methods to zinc. We only think that it is more difficult and perhaps a little further removed from the realm of practical application in the case of this metal.

J L CHRISTIE, \* Bridgeport, Conn.—Did not the authors find that their tests were very much affected by small variations in the gage of the metal? I know we made some tests of a somewhat similar nature on brass and found that variations in gage were very important.

G EDMUNDS—We have found slight differences due to gage. In that matter, I think possibly the best thing to do is to refer you to the work of Dr Ream, in which measurements have been made of the effect of punch-die clearances. The effect is rather considerable where the clearance is small, and, of course, we are working in that range. But we find that generally the failures are caused by the first deformation rather than the final draw. For that reason, the slight changes in gage between the individual tools that we use do not have a great enough effect to affect our results seriously. The tools that we are using have punch diameters which throughout the most useful ranges vary by only 0.002 in. in clearance; that is, 0.004 in. in diameter.

---

\* Metallurgist, Bridgeport Brass Co

# Equilibrium in the Lead-zinc System with Special Reference to Liquid Solubility

BY R. K. WARING,\* E. A. ANDERSON,\* R. D. SPRINGER\* AND R. L. WILCOX,\*  
PALMERTON, PA

(New York Meeting, October, 1934)

A KNOWLEDGE of the mutual liquid solubility of zinc and lead is of importance in various phases of zinc metallurgy. The determination of this solubility has been the subject of numerous investigations, but unfortunately the results vary widely, particularly at higher temperatures, and it has been impossible to decide what data are most reliable. It was decided to investigate the matter and in view of the disagreement in the published results, it was felt necessary to take rather unusual precautions to insure the reliability of the data. For this reason determinations were made by four different methods, and the procedures of several of the previous investigators were duplicated.

The previously used methods can be divided into two classes: methods involving freezing the entire melt and taking samples of the lead-rich and zinc-rich phases in the solid state,<sup>1,2</sup> and methods in which the samples are taken while the bath is liquid and at the desired temperature.<sup>3,4</sup>

Data obtained by methods involving freezing the entire melt show much lower solubility of lead in zinc than methods in which the liquid is sampled at temperature. The latter method was used by Spring and Romanoff<sup>5</sup> and by Hass and Jellinek.<sup>6</sup> The results of these two investigations are in agreement at temperatures near the melting point but at higher temperatures Hass and Jellinek find a higher mutual solubility.

The low-temperature section of the zinc-lead equilibrium diagram is given by Peirce and Anderson.<sup>7</sup> The diagram is based on the data of Hodge and Heyer,<sup>8</sup> Arnemann,<sup>9</sup> and Peirce.<sup>10</sup>

---

Manuscript received at the office of the Institute July 17, 1934

\* Research Division, The New Jersey Zinc Co

<sup>1</sup> Wright and Thompson: *Proc. Royal Soc.* (1891) **49**, 156

<sup>2</sup> Matthiesson and Bose: *Proc. Royal Soc.* (1861) **11**, 430

<sup>3</sup> Spring and Romanoff: *Ztsch. anorg. Chem.* (1896) **13**, 29

<sup>4</sup> Hass and Jellinek: *Ztsch. anorg. allg. Chem.* (1933) **212**, 356

<sup>5</sup> Reference of footnote 3

<sup>6</sup> Reference of footnote 4

<sup>7</sup> Peirce and Anderson: *National Metals Handbook* (1933) 1428

<sup>8</sup> J. M. Hodge and R. H. Heyer: *Metals & Alloys* (1931) **2**, 29-7

<sup>9</sup> P. T. Arnemann: *Metallurgie* (1910) **7**, 201-211

<sup>10</sup> W. M. Peirce: *Trans. A. I. M. E.* (1923) **68**, 767-95.

## SUMMARY

The solubility curve was established from data obtained by four methods, all of which gave results that are in agreement to within the experimental error. The solubility was found to be higher and the temperature of complete miscibility in all proportions lower than that reported by any previous investigators.

Experiments were performed which prove conclusively that methods involving freezing the melt before sampling are unreliable owing to extremely rapid settling of lead during the cooling period.

The procedures of Hass and Jellinek and of Spring and Romanoff were duplicated and strong evidence obtained that both of these procedures provide inadequate opportunity to reach equilibrium.

The eutectic temperature was determined by thermal analysis and checks the value of Hodge and Heyer exactly. The monotectic composition and temperature were determined. The values are 417.8° C and 0.7 per cent lead as compared with 417.7° C. and 0.94 per cent lead obtained by Heycock and Neville.<sup>11</sup> The data are presented in Fig 1 and Table 1.

TABLE 1.—*Mutual Solubility of Lead and Zinc*

Temperature, Deg C	Per Cent Pb in Zn	Per Cent Zn in Pb	Temperature, Deg C	Per Cent Pb in Zn	Per Cent Zn in Pb
417.8	0.7	2.0	650	9	8
450	1.4	2.3	700	15	12
500	2.3	3	750	24	19
550	4.0	4	775	32	26
600	5.9	6	790	Complete miscibility	

## EXPERIMENTAL PROCEDURE

After considerable preliminary experimentation, the following methods of measuring solubility were used:

*Method 1*—Pure zinc (99.99+ per cent Zn) and C.P. lead (99.9+ per cent Pb) were weighed in the desired proportion to make 500 grams of metal and melted together in a closed-end silica tube  $\frac{7}{8}$  in. inside diameter by 7 in. long. The metal was covered with a molten mixture of potassium iodide and potassium chloride to retard oxidation and vaporization. The melt was brought to the desired temperature and then agitated continuously for 2 hr. by means of a silica rod with a loop on its end. The rod was moved up and down 200 times a minute by

<sup>11</sup> C. T. Heycock and F. H. Neville *Jnl. Chem. Soc.* (1892) **61**, 888-914, (1897) **71**, 383-422.

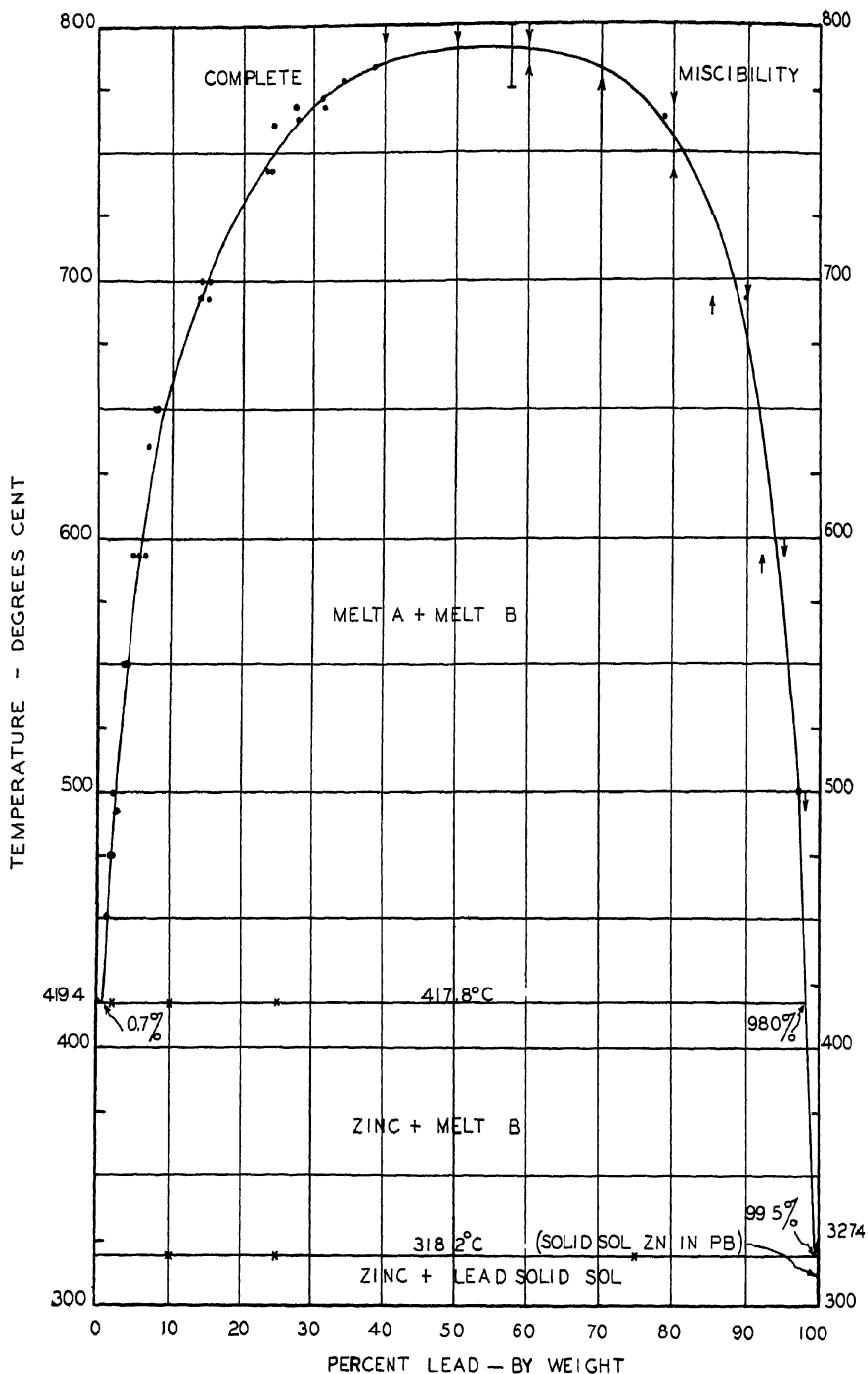


FIG 1—LEAD-ZINC EQUILIBRIUM DIAGRAM

means of a simple motor-driven mechanism. The stroke was  $2\frac{3}{4}$  in., which provided continuous and thorough agitation of the liquid. After the agitation period the melt was allowed to settle for 2 hr. before sampling. The sample was taken by dipping through the flux and just below the metal surface with a small silica ladle, which held about 6 grams of metal. The ladle was brought to the same temperature as the melt before it was allowed to touch the metal. The liquid sample was poured into water and the entire sample analyzed for lead to avoid the possibility of selecting a nonrepresentative sample.

The temperature was determined by means of a platinum thermocouple with the junction located just outside the silica tube containing the melt. Experiments showed that the temperature at this point was about  $7^{\circ}\text{C}$  higher than the temperature in the melt. This correction was applied to the data shown in Table 2.

TABLE 2.—*Data Obtained by Method 1*

Temperature Deg C	Pb		Temperature Deg C	Pb	
	Per Cent	Average Per Cent		Per Cent	Average Per Cent
493	2 0	2 0	761	24.4	24 4
593	4 8		768	27 2	
593	6 1		768	27.4	27 3
593	5.6	5 5			
			771	31.2	31 2
693	14 9				
693	13 9		778	34 1	34 1
693	13 7				
693	14 1	14 2	783	38 5	38 5
743	23 2				
743	23 7				
743	23 1	23 3			

The method of sampling was not suited to obtaining samples of the lead-rich phase. The composition of this phase was therefore determined indirectly, by varying the original proportion of lead and zinc in the melt and dipping samples from both layers. The sample dipped from the top layer was usually reliable and gave the composition of the zinc-rich phase, but the sample dipped from the bottom layer was contaminated when drawn through the top layer. When both samples contained the same proportion of lead as the original mix complete miscibility had been obtained. An arrow was then placed on the equilibrium diagram (Fig. 1), pointing down to indicate that the neces-



sary temperature for complete miscibility was below that point. If, on the other hand, the sample from the top layer contained less lead than the original mix and the sample from the bottom layer contained more lead, miscibility was not complete. In this case an arrow was placed on the diagram pointing up. The solubility curve must lie between such arrows and can be located as closely as desired by adjusting the composition of the original mixes or the temperatures. Since the chief purpose of this investigation was to determine the composition of the zinc-rich phase, the curve was fixed only approximately, as shown by the arrows in Fig 1. The composition of the lead-rich phase was, however, determined directly at 693° and at 770° C. by tapping metal from the bottom of the container. The lead contents were 89.9 and 78.8 per cent, respectively, as shown by the points on the equilibrium diagram.

In order to be sure that the 2-hr. agitation period was sufficient to reach equilibrium, the authors performed experiments in which equal parts of lead and zinc were completely dissolved at 800° C. and the bath then cooled to a lower temperature. Samples taken at the lower temperatures checked the values obtained by the usual procedure. Thus the equilibrium was approached from both sides and the same values obtained.

Another possible source of error is insufficient settling time after the agitation period. To investigate this, the time for settling was varied from 1 to 4 hr. without causing any change in the lead content of the samples. The 2-hr. period, therefore, appears to be adequate.

The chemical analyses, necessary in all four methods, were performed by the Testing Department, New Jersey Zinc Co. The accuracy was checked frequently by making up mixtures containing accurately weighed amounts of lead and zinc. In all cases the analyses proved to be correct to within a few tenths of one per cent.

*Method 2.*—The second method was similar in its essentials to the first method except that no agitation was used, so that solution was obtained by diffusion perhaps aided by some convection. It is believed, however, that convection was negligible so that the time required to reach equilibrium gives an indication of the diffusion rate.

About 6 lb. of an alloy of 60 per cent zinc and 40 per cent lead was melted in a graphite crucible. The melt was covered with a mixture of potassium chloride and potassium iodide, brought to 700° C. and held for 1 hr. A sample was then taken from the top layer with a silica ladle. The sampling procedure was the same as in method 1 except that the size of the sample was about 50 grams. This procedure was duplicated at 700° C. for a series of time up to 120 hr. The results are shown in Table 2. The average value obtained at 700° C. by method 1 is 15 per cent, thus giving an excellent check.

TABLE 3 — *Data Obtained by Method 2*

Time, Hr	Pb, Per Cent	Time, Hr	Pb, Per Cent
1	1 6	19	12 5
3	4 4	48	15 2
5½	9 4	120	14 0
6½	11 0		

*Method 3* — The third method was chosen to avoid sampling with the silica ladle as well as mechanical agitation. The apparatus comprised two Pyrex glass tubes  $\frac{7}{8}$  in. in diameter and 3 in. long. The tubes were closed at one end and connected in the middle by a Pyrex tube  $\frac{3}{8}$  in. in diameter and  $\frac{3}{4}$  in. long. The tubes joined in this manner produced a glass vessel in the form of a letter H. In melting down the charge, the required amount of lead was placed in one side of the H and the remainder of this side, as well as the other side, was filled with zinc. The zinc level was brought above the horizontal connecting tube so that it was full of zinc. The H-vessel was held at temperature in a furnace for sufficient time to reach equilibrium by diffusion. The connecting tube was then broken and the liquid metal allowed to run out until the level had reached the bottom of the connecting tube. The liquid metal remaining in the bottom portion of the H-vessel on the zinc side was poured into water and the entire sample analyzed for lead. The results obtained are given in Table 4.

TABLE 4.—*Data Obtained by Method 3*

Temperature, Deg C	Time, Hr	Pb		Temperature, Deg C	Time, Hr	Pb	
		Per Cent	Average Per Cent			Per Cent	Average Per Cent
450	500	1 3	1 2	635	335	6 6	6 6
450	500	1 0		650	72	7 7	
500	420	2 7	2 7	650	200	8 0	8.0
				650	400	8 1	
550	400	3 8					
550	450	3 5	3 7				
550	450	3 8					

In order to obtain a sample of the lead-rich phase with the H-vessel, a  $\frac{1}{8}$ -in. dia. tube was joined to the side of the main tube containing the lead about  $\frac{1}{4}$  in. from the bottom. The vessel was filled and held at temperature in the manner previously described. A sample of the lead-rich phase was secured by breaking the  $\frac{1}{8}$ -in. dia. tube while at

temperature in the furnace. The first few drops of metal that ran out were discarded, and the next 50 grams taken as a sample. Three determinations were made at 500° C. The results are given in Table 5

TABLE 5—*Solubility of Zinc in Lead by Method 3*

Time, Hr	Zinc, Per Cent	Average
195	3 0	3 0
335	2 8	
360	3 1	

*Method 4.*—The fourth method of determining solubility depended on the difference in opacity of lead and zinc to X-rays. A fused quartz cell, 25 mm square and 1 mm wide inside, was filled with a mixture of lead and zinc. The cell was heated in a specially constructed furnace and a beam of X-rays was passed through it and photographed. The difference in absorption made the two layers stand out sharply when solution was incomplete. Only one experiment was performed<sup>12</sup>. The cell contained 57.5 per cent lead, which was found to be in complete solution at 790° C. and to exhibit two layers at 780° C. The determination was made with both ascending and descending temperature, thus insuring attainment of equilibrium. The temperature measurement, in the very small furnace used, was probably not accurate to better than 10° C., so the temperature of complete miscibility, as determined by this experiment, is between 770° and 800° C. This is indicated in Fig. 1 by the vertical line at 57.5 per cent lead.

#### COMPARISON OF THE FOUR METHODS

A comparison of the results obtained by the four methods is given in Table 6, which shows that the four methods give results in excellent agreement. The largest discrepancy occurs at 650°, where method 1 gives 9.6 per cent lead in solution in zinc and method 3 gives 8.1 per cent. It is believed that this discrepancy is not significant, however, since the accuracy in this region of the curve is not better than about 2 per cent. The chief source of error is the determination of the true temperature of the melt. It is estimated that the error in this determination is about 10° C. Such an error makes little difference in the amount of dissolved lead at low temperatures but of course becomes more important as the curve approaches horizontal.

In methods 1 and 4 equilibrium was approached from both the high-lead and the high-zinc side and in methods 2 and 3 the time allowed

<sup>12</sup> This experiment was carried out with the assistance of Mr. M. L. Fuller, Investigator, Spectroscopic and X-Ray Laboratory, New Jersey Zinc Company

TABLE 6.—Average Results Obtained by Each Method

Temperature, Deg C	Method 1		Method 2	Method 3		Method 4
	Zn Layer	Pb Layer	Zn Layer	Zn Layer	Pb Layer	
500	2 2	97		2 7	97	
550	3 7	96		3 7		
600	5 9	94		5 1		
650	9 6	92		8 1		
700	15 3	88	14 6			
785						b
790	a	a				

<sup>a</sup> Complete miscibility in all proportions

<sup>b</sup> 57 per cent lead completely in solution at this temperature.

for diffusion was increased until no further change occurred. This provides conclusive evidence that equilibrium was attained

#### REPETITION OF PROCEDURES OF PREVIOUS INVESTIGATORS

The data presented in this paper indicate a substantially higher solubility of lead and zinc, at the higher temperatures, than those obtained by any previous investigators. It was thought that the data could be accepted with greater confidence if the reasons for the discrepancies were known.

Methods in which the melt is frozen before the samples are taken are obviously open to the objection that some of the lead in the top or zinc-rich layer may settle out during the freezing period. A series of experiments was performed in which mixtures of lead and zinc were sealed in silica tubes and held at temperatures from 800° to 1000° C. for various periods of time with and without agitation. At the end of the period, the tube was plunged into water to freeze the metal quickly. The metal cylinder thus formed was cut into sections and the sections analyzed for lead. Regardless of the proportion of lead used, the time, the temperature and the amount of agitation, the top section never contained more than 2 or 3 per cent lead. Lower sections contained progressively increasing quantities of lead. The chemical analyses were confirmed qualitatively by microscopic examination.

It is concluded that all methods involving freezing the bath before separating the two immiscible layers are unreliable.

The method of Spring and Romanoff involved melting the metals in a crucible, holding at temperature for 2 hr. during which time the melt was stirred with a carbon rod every  $\frac{1}{2}$  hr. for 10 min. The melt was then allowed to stand for 15 min. at temperature and sampled with a ladle. Spring and Romanoff report the temperature of complete miscibility as 945° C. At 700° C. their value for the solubility of lead in



position of thermal arrests The results are believed to be accurate to better than  $0.1^{\circ}\text{C}$ .

The eutectic temperatures, which are shown on the equilibrium diagram, Fig 1, are in excellent agreement with the value for the zinc monotectic reported by Heycock and Neville and for the lead eutectic reported by Hodge and Heyer.

Cooling curves were also run on alloys containing 0.25 and 0.5 per cent lead, giving temperatures of  $419.3^{\circ}$  and  $418.4^{\circ}\text{C}$ ., thus locating two points on the liquidus curve. The melting point of zinc,  $419.4^{\circ}\text{C}$ ., gave another point. The liquidus curve was drawn through these three points and extrapolated until it intersected the monotectic horizontal. The intersection occurred at 0.7 per cent zinc, which is the monotectic composition; that is, the composition of the zinc-rich liquid phase in equilibrium with pure solid zinc and the liquid lead-rich phase. This is shown in the enlarged section of the equilibrium diagram (Fig 2).

## DISCUSSION

(*W. L. Fink presiding*)

E E SCHUMACHER,\* New York, N Y —Is there any possibility that through the use of the very efficient stirring methods described an emulsion of lead in zinc was formed which would apparently be homogeneous and result in correspondingly high solubility values?

R K WARING —We considered the possibility of an emulsion seriously, in view of the rather violent agitation. We feel that method 2, where we had no agitation, and method 3, where we had the H-tube and the lead diffused through an arm and come down slowly to the other side, removes any possibility of an emulsion.

---

\* Bell Telephone Laboratories.

# The High-zinc Region of the Copper-zinc Phase Equilibrium Diagram

By E. A. ANDERSON,\* M. L. FULLER,\* R. L. WILCOX\* AND J. L. RODDA,\* PALMERTON, PA.

(New York Meeting, October, 1934)

THE copper-zinc phase equilibrium diagram has been the subject of many investigations. Until recently, however, the boundary of the terminal solid solution of copper in zinc (eta) has not been thoroughly investigated. This paper reports determinations of the solid solubility of copper in zinc at temperatures from 100° to 400° C, the course of the liquidus and solidus for the eta solid solution and determinations of the peritectic temperature and peritectic point for the reaction between epsilon and the melt to form eta.

The liquidus of the eta phase was determined by thermal analysis and the solidus by the microscopical examination of specimens quenched from temperatures above and below the solidus. The temperature of the peritectic horizontal was obtained by thermal analysis and the composition at the peritectic point was determined by extrapolation of the solid solubility boundary of the eta phase to the peritectic horizontal.

The solid solubility boundary of the eta solid solution was investigated very carefully. Particular care was used to achieve equilibrium in the alloys at each temperature selected. The X-ray, electrical conductivity and microscopical methods were used in determining the solid solubility limits.

The X-ray method measures the changes in the solvent lattice with increasing solute content and in this manner locates the composition of the alloy at which no further change in the solvent lattice takes place, the limit of solid solubility. The method of electrical conductivity measures the conductivity of the alloys of a graded series of compositions, whereby the solubility limit is indicated by a discontinuity in the conductivity-composition relationship. The microscopical method distinguishes, by direct inspection, between the homogeneous solid solution alloys and those having a secondary constituent in addition to the solid solution phase, and thus indicates from the examination of a series of alloys the solid solubility limit.

---

Manuscript received at the office of the Institute July 17, 1934.

\* Research Division, The New Jersey Zinc Co

The three methods are distinct in principle from one another. The X-ray method confines its examination to the solid solution phase whose limits of homogeneity are being investigated, the conductivity technique embraces the entire alloy, and the microscopical method detects directly the presence of the secondary phase.

The present paper demonstrates the effective manner in which these three methods complement one another toward the precise determination of the phase boundary and toward the indication of whether or not a true state of equilibrium exists in the alloys under examination.

### EARLIER INVESTIGATIONS

The most generally accepted determination of the solid solubility boundary of the  $\eta$  solid solution was reported from this laboratory by W. M. Peirce<sup>(1)\*</sup> in 1923. By microscopical observations, the limit at 400° C. was found to be between 1.81 and 1.95 per cent copper and at 300° C. at about 1.5 per cent copper. Conductivity determinations corresponding to an undetermined equilibrium temperature, probably lower than 300° indicated a solubility of 1.25 per cent copper.

D. Jitsuka,<sup>(2)</sup> in 1927, published the results of his work, which included microscopical studies of alloys annealed at 300° and 400° C. He concludes that the boundary is approximately vertical at 1.5 per cent copper.

Various workers<sup>(3-8)</sup> have placed the limit at or near the peritectic temperature between 2 and 3 per cent copper.

A number of papers describing X-ray studies have appeared, most of which are concerned principally with the elucidation of the structures of the alloy phases and not with quantitative determinations of phase boundaries.

Contemporaneous with the present investigation, there have appeared papers by E. A. Owen and L. Pickup<sup>(9-11)</sup> and by M. Hansen and W. Stenzel<sup>(12)</sup> in which X-ray technique has been used for the quantitative fixation of the solid solubility boundary. The work of Owen and Pickup<sup>(10)</sup> was carried out only at 380° C. at which temperature the indicated solubility is between 2.0 and 2.85 atomic per cent copper, 2.7 atomic per cent (2.63 weight per cent) being suggested by these authors as the most probable value.†

M. Hansen and W. Stenzel<sup>(12)</sup> in their paper report the results of a detailed investigation of the boundary from 150° to 400° C. They

---

\* Superior figures in parentheses refer to the bibliography at the end of the paper.

† The various values (2.0, 2.5 and 2.85) obtained by Owen and Pickup are based on atomic volumes and lattice parameters calculated from the same experimentally measured interplanar spacings. It would have been better if Owen and Pickup had estimated the solid solubility directly from the interplanar spacings, thus avoiding the errors inherent in calculation.



employed the X-ray method for the determination and checked the results by microscopical studies. This work was done upon specimens quenched from the temperature at which the solubility was sought after an annealing of the duration shown in Table 1

TABLE 1—*Solid Solubility of Copper in Zinc According to M. Hansen<sup>†</sup> and W. Stenzel*

Temperature, Deg C	Solubility Limit, Per Cent Cu		Time of Anneal, Hr
	Atomic, Per Cent	Weight, Per Cent	
150	0.52	0.51	245
200	0.79	0.77	102
250	1.15	1.12	55
300	1.56	1.53	22
350	2.00	1.95	7
400	2.42	2.41	1-3

The temperature of the peritectic horizontal and the fixed limits of concentration at this temperature have been determined by other workers as listed in Table 2

TABLE 2—*Published Data on Epsilon + Liquid  $\rightleftharpoons$  Eta Peritectic*

Peritectic Temperature, Deg C	Concentration, Per Cent Cu		Source
	Peritectic Point	Extreme Points	
419	1.8 2.5	2.0	W. C. Roberts-Austen <sup>(13)</sup> E. S. Shepherd <sup>(3)</sup>
425			V. E. Tafel <sup>(4)</sup>
425	3	13	N. Parravano <sup>(5)</sup>
426			J. L. Haughton and K. E. Bingham <sup>(6)</sup>
423		2.0 13	O. Jitsuka <sup>(2)</sup>
423	2.0	1.5 12.5	O. Bauer and M. Hansen <sup>(7)</sup>
423			R. Ruer and K. Kremers <sup>(14)</sup>
424	2.66		M. Hansen and W. Stenzel <sup>(12)</sup>

#### PREPARATION OF ALLOYS, CASTING AND ROLLING TREATMENT

Alloys of the following analyzed copper contents were prepared: 0.21, 0.42, 0.50, 0.58, 0.73, 0.79, 0.99, 1.14, 1.30, 1.55, 1.75, 2.01, 2.25, 2.60 and 2.93 weight per cent copper

The C. P. zinc used analyzed 0.0008 per cent lead, 0.003 per cent cadmium and 0.005 per cent iron, no tin being detected. The added alloying material was a copper-zinc alloy of 15.5 per cent copper content

made from electrolytic copper and C P zinc. A typical alloy prepared from these materials contained the following impurities by analysis: Fe, 0.005 per cent, Pb, 0.002 per cent; Cd, 0.0047 per cent.

From a temperature of 450° C, the alloys were cast into iron molds at 150° C. as 10 by 3 by  $\frac{5}{8}$ -in. slabs and 6 by  $\frac{7}{8}$ -in. rods.

The slabs were hot-rolled to 0.250 in., annealed one week at 350° C (after which no cored structure could be detected microscopically), hot-rolled to 0.040 in. and cold-rolled in passes of 0.003 in. to a final gage of 0.020 in.

From the cold-rolled alloys were cut specimens for X-ray measurement, microscopical examination, conductivity determinations and chemical analysis in such a manner as to provide a representative sampling of the strip. The specimens were cut from the cold-rolled strips prior to subsequent heat treatments.

## HEAT TREATMENTS

### *Preliminary Annealings*

Specimens of the rolled alloys for X-ray, conductivity and microscopical studies were given a flash annealing treatment of 2 min. in oil at 300° C. prior to the reannealing treatments. This treatment was determined by trial to produce a uniform equiaxed grain structure under which conditions the tendency to grain growth in subsequent annealings is minimized.

Some of each rolled alloy was reserved for the reannealing treatments without the previously mentioned flash annealing.

The cast rods, 6 by  $\frac{7}{8}$  in., intended for microscopical study and determination of the solidus, were annealed one week at 400° C. and quenched. This treatment was designed to produce a uniform composition throughout the casting.

### *Further Heat Treatments*

*Conductivity Specimens.*—Four strips of each alloy (35.4 in. long by  $\frac{1}{2}$  in. wide), which had been flash-annealed, were reannealed prior to conductivity measurements. The reannealing was carried out in a tube furnace of sufficient length to permit heat treatment without bending the strips and of temperature uniformity sufficient to maintain the specimens at a uniform temperature throughout. The specimens were contained in an iron pipe within the furnace tube. To this pipe the water supply could be connected, and by flushing the pipe with water at the completion of an annealing, while the pipe was still in the furnace, the alloys were rapidly and effectively quenched. An atmosphere of nitrogen

was maintained in the iron pipe during the annealing at 300° and 400° C. to prevent excessive oxidation of the alloys.

In order that the annealing time should be sufficient to produce a state of equilibrium at the annealing temperature, the specimens were annealed at each temperature until conductivity measurements of the alloys showed no change with additional annealing. This procedure for determining the necessary time of annealing was not entirely successful, as will be explained later in the paper. The failure of the three methods of examination to agree on the solid solubility limit at certain temperatures exposed the insufficiency of certain of the original anneals but the discrepancies were removed later by additional heat treatment.

The original schedule of annealings is listed in Table 3. All of the specimens were submitted successively to the several annealing treatments, starting with the 100° C annealing and following with the 150°, 200°, 300° and 400° C. annealings

TABLE 3 —*Schedule of Annealings Given the Conductivity Strips*

TEMPERATURE, DEG. C.	DURATION OF ANNEALING, DAYS
100	35
150	32
200	26
300	20
400	7

After the investigation of the solid solubility at 100° and 150° C. with conductivity, X-ray and microscopical methods, as will be described in detail later, further heat treatments at these temperatures became necessary, since the alloys were obviously supersaturated. Owing to lack of time, the 100° C. work on the conductivity strips was not carried out, and at 150° C it was decided to approach an equilibrium state by a special annealing procedure. This experiment consisted of an annealing successively of seven days at 400° C, a gradual lowering of the temperature of the annealing furnace to 100° C. over a period of 28 days, maintenance of the 100° C temperature for seven days, followed by an annealing of 27 days at 150° C and quenching. This procedure was designed to slowly relieve the condition of supersaturation produced by the annealing above the final temperature of 150° C. to the extent of an undersaturation with respect to equilibrium at 150° C, followed by final annealing at 150° C to remove this undersaturation.

*X-ray Specimens.*—The specimens for X-ray examination were taken from the same cold-rolled and flash-annealed material from which the conductivity strips were cut. They received annealings simultaneously with the conductivity strips according to the schedule of Table 3.

The X-ray examination was carried out on the alloys while they were at the temperature of test, for reasons that will be discussed later. There-

fore it was necessary that the X-ray specimens be maintained in the annealing furnace until the time of examination. Owing to the practical impossibility of subjecting a large number of alloys to X-ray diffraction photography immediately following the original annealings, the total annealing time for the X-ray specimens was considerably longer than the schedule of Table 3, and quite varied. It developed, however, that this extra annealing was advantageous, primarily because the X-ray specimens thus received adequate annealing at 150° C., the originally scheduled annealing of 32 days having proved inadequate, and secondly, the widely varied periods of annealing for a given series, without loss of consistency in the X-ray results, gave assurance that the annealings employed were sufficient. The particular annealings of the X-ray specimens were as follows:

100° C.: The original annealings for the various specimens totaled 35 to 67 days, but the equilibrium condition was not reached. Later it was found that annealings of one year's duration produced an apparent state of equilibrium in alloys well oversaturated initially, but not in alloys moderately oversaturated. This work will be discussed in detail later.

150° C.: The total annealing time at 150° C. received by the several X-ray specimens varied from 43 to 101 days. The annealing was in two stages; first, the original annealing of 32 days followed by one month at room temperature, and, second, the remainder of the annealing up to the time of the X-ray examination.

200° and 300° C.: After the original annealings of 26 days at 200° C. and 20 days at 300° C., followed by quenching, the specimens were replaced in annealing furnaces at the temperature of the former annealing and allowed to remain there until the time of X-ray examination. The total annealing time thus received varied from 33 to 159 days at 200° C. and from 101 to 180 days at 300° C. for the various specimens.

400° C.: The procedure of continuous annealing employed at 200° and 300° C. was not used at 400° C. lest the grain growth accompanying long annealing at this temperature become excessive. Accordingly, following the original annealing of seven days at 400° C., the specimens were allowed to remain at room temperature until at least a week prior to the start of the X-ray exposure. By this procedure the total annealing varied from 13 to 23 days for the several specimens.

*Microscopic Specimens.*—Three groups of specimens were prepared for microscopical examination: cast, cold-rolled and flash-annealed. The cast specimens were cut from the cast rods which had been annealed one week at 400° C. and quenched. The cold-rolled specimens were cut from the original cold-rolled strips. The cold-rolled and flash-annealed specimens were cut from the original cold-rolled strips and then flash-annealed. It is important to note that in these three groups three different conditions are represented prior to the reannealing treatments.

Successively lower equivalent temperature conditions are represented by the cast, flash-annealed, and cold-rolled specimens in the order named, because of the previous thermal histories

The cast and cold-rolled specimens were given an annealing according to the schedule in Table 4. Separate specimens were used for each annealing treatment. The flash-annealed specimens were annealed at the same time as the conductivity specimens and received the annealings listed in Table 3.

TABLE 4—*Original Annealings for Microscopic Specimens*

Temperature, Deg. C	Duration of Anneal, Days	
	Cast Specimens	Cold-rolled Specimens
100	42	42
150	39	38
200	21	21
300	14	14
400	7	7

During the course of the investigation, the possibility of specimens having altered at room temperature between the time of quenching and microscopical inspection was considered. In such cases where a considerable time had elapsed between the time of quenching and the time of examination, the specimens were replaced in the furnace at a convenient time and reannealed. In no case, on which a decision was based, did more than 36 hr. elapse between the quenching and microscopical examination.

The 300° and 400° C. reannealings of the flash-annealed specimens were not adequate to produce a state of equilibrium consistently in all of the specimens, since some of the alloys showed a heterogeneous structure, although their composition was within the range of homogeneity indicated by the other two groups of microscopic specimens and by the X-ray and conductivity results. The 300° and 400° C. specimens were therefore annealed further to remove this discrepancy, by which reannealing practical agreement was obtained.

For the above reasons, the total annealing times of the microscopic specimens were longer than those originally scheduled and listed in Tables 3 and 4. These total annealings are listed in Table 5, and on the basis of specimens thus annealed the final conclusions were drawn.

*Thermal Analysis.*—For the thermal analysis of the liquidus and the epsilon-eta peritectic horizontal, samples were cut from the original cold-rolled strips and melted down in the manner to be described later.

After the cooling-curve data on each melt were obtained the alloy was analyzed for copper. The analyzed compositions of the several

TABLE 5—*Total Annealings of Microscopic Specimens*

Temperature, Deg C	Duration of Annealing, Days		
	Cast Specimens	Cold-rolled Specimens	Flash-annealed Specimens
100	77	60	68
150	39	38	43
200	66	52	26
300	14	14	41
400	7	7	14

alloys were 0 55, 1 00, 1 30, 1 70, 2 05 and 2 90, compositions differing but little from the original analysis on the rolled alloys

*Solidus Determination.*—The determination of the solidus by the microscopical examination of quenched alloys was made on specimens cut from the cast rods after the seven days' annealing at 400° C

## METHODS OF EXAMINATION

### *X-ray Method*

The study of alloy equilibria at elevated temperatures is carried out customarily by examining the alloys after quenching from annealing at elevated temperature. Since this type of study is always open to the suspicion that the quenched specimen is not truly representative of the conditions that existed at the elevated temperature, it seemed advantageous to make the examinations by one of the three methods while the alloys were at the temperature of test. Of the several methods employed in the present investigation, the X-ray method was most conveniently adapted to examination of the alloys at temperature.

An X-ray diffraction camera, of the back reflection type, described by G Sachs and J. Weerts,<sup>(15)</sup> was used. This has proved to be an excellent experimental arrangement for the precise measurement of lattice dimensions. The manner of mounting and heating the specimen should be reported, however, for a complete description of this investigation.

The plane alloy specimen,  $\frac{3}{4}$  by  $\frac{3}{4}$  by 0 020 in., was mounted normally to the incident X-rays at a distance of about 7 5 cm. from a plane, photographic film. Maintenance of the specimen uniformly at the temperature of test was achieved by means of an electrically heated nichrome ribbon radiator mounted  $\frac{1}{8}$  in. behind the specimen. An iron-constantan thermocouple was made by attaching the two elements as  $\frac{1}{64}$ -in. wires to either side of the irradiated area, this area acting as the electrical coupling of the two elements. The electromotive force of the couple was measured periodically with a potentiometer during the course of an exposure.

At 300° and 400° C oxidation of the alloy was minimized by maintaining an atmosphere of nitrogen about the specimen during the exposure. For this purpose, the side of the specimen and heater unit toward the X-ray tube was encased in a small metal box through which nitrogen was

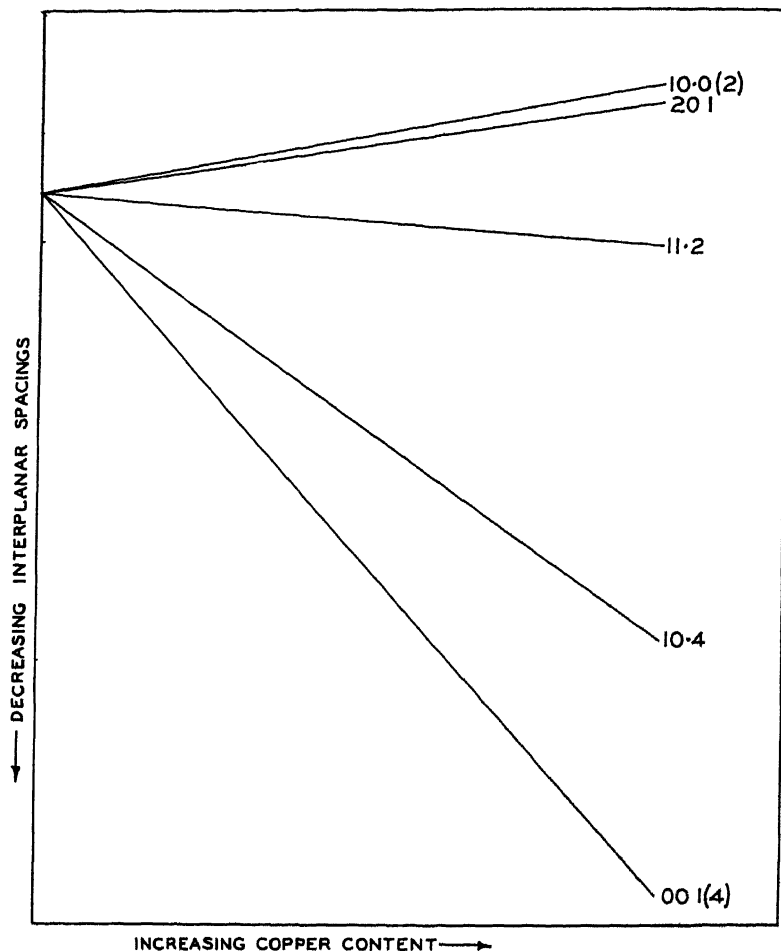


FIG. 1—RELATIVE CONCENTRATIONAL SENSITIVITY OF FIVE INTERPLANAR SPACINGS IN  $\eta$ TA COPPER-ZINC.

passed. The box was fitted with a cellophane window for the transmission of the X-rays to and from the specimen.

Because of the large crystals that result from the long annealing of zinc alloys the rotation of the Sachs-Weerts film holder was not alone sufficient to record the necessary number of reflections for a satisfactory powder pattern. To overcome this trouble, to the specimen and heater

unit was imparted a continuous reciprocating translation over a path of  $\frac{1}{4}$  in during the X-ray exposure

When copper enters into solid solution with zinc, a large contraction of the zinc lattice results in a direction normal to the basal plane and a small expansion results in directions parallel to the basal plane with corresponding intermediate contractions or expansions in intermediate directions. This effect has been noted before<sup>(16,17,12)</sup> and is probably typical of solid solutions of this type

This phenomenon imposes the experimental requirement that the X-radiation be chosen such that interplanar spacings showing large solute concentrational sensitivity be measured. To this end, the characteristic radiation from a chromium target X-ray tube was employed, the tube being fitted with a chromium-plated copper target. Under these conditions, the 00 1 (4), 11 2 and 10 0 (2) reflections from the alpha doublet and the 10 4 and 20 1 reflections from the beta wave length may be recorded from the eta solid solution. Fig 1 shows diagrammatically the relative concentrational sensitivities of the five interplanar spacings. Since the 00 1 (4) and 10 4 reflections are evidently best adapted for this work, the exposure time was regulated to record these two reflections consistently, the 20 1 and 10 0 (2) reflections of low intensity being not always recorded

#### *Electrical Conductivity Method*

The electrical conductivity measurements were made with a Kelvin double bridge. The alloy strip (35.4 by 0.5 by 0.020 in.) was maintained at a uniform temperature at or very near 20° C by means of a circulating oil bath, the temperature of which was determined to the nearest 0.01° C.

Balancing the bridge with a Leeds & Northrup type H S galvanometer, measurements were made at three different combinations of the fixed resistances, the value of the variable resistance being determined three times for each combination. Using four strips of each alloy, the average conductivity was based on 36 readings. The readings were corrected to a temperature of 20.00° C, the temperature coefficient of electrical conductivity of 0.00378 ohms per ohm per degree Centigrade being assumed for all the alloys. The maximum deviation from the mean in measuring the conductivity of any one strip was 0.05 per cent.

The results from an entire series of alloys corresponding to one equilibrium temperature were plotted against copper content, the discontinuity in the curve being taken as a measure of the solid solubility limit.

#### *Microscopical Method*

Cross-sections of the cast rods and of the rolled samples were selected for the planes of polish. All microspecimens were rough ground on a belt



sanding machine, dry polished on four grades of emery paper, then wet polished with four specially prepared graded abrasives <sup>(18)</sup>

The specimens were etched in a chromic acid-sodium sulfate etching solution of which the composition in most cases was 20 grams  $\text{CrO}_3$ , 15 grams  $\text{Na}_2\text{SO}_4$  and 100 c c water.

All the microspecimens were carefully examined at a magnification of about 1400 with a Zeiss metallographic microscope and photomicrographs were made at 1000 diameters. As previously noted, the photomicrographs were taken within 36 hr of the annealing and quenching treatment.

### *Thermal Analysis*

Cooling curves were obtained by a refined procedure for which the authors are indebted to Mr C F Homewood, of this laboratory, who developed the procedure and apparatus, and to Mr J R Bossard, who made the measurements. A separate paper describing Homewood's method will be published elsewhere, and only a brief description need be included here.

The alloys were melted in a Pyrex-lined graphite crucible in an electric furnace. The melt was heated to approximately  $525^\circ\text{C}$ , after which the thermocouples were placed in position. The temperature of the furnace was reduced gradually by means of a motor-driven rheostat at a rate of  $1.3^\circ\text{C}$  per minute. After  $495^\circ\text{C}$  had been reached, periodic temperature readings were taken from carefully calibrated iron-constantan couples with a White potentiometer.

Two temperature readings were taken, the temperature of the melt and the difference in temperature between the melt and the outer surface of the crucible. The temperatures at the thermal arrests were taken from the alloy-temperature data. The differential temperature provided a sensitive check on the position of the arrests indicated by the temperature changes of the melt. The temperatures of the halts were determined by this procedure to the nearest  $0.1^\circ\text{C}$  at the peritectic horizontal and to the nearest  $0.2^\circ\text{C}$  at the liquidus.

### *Solidus Determination*

The course of the solidus was determined by the microscopical examination of a series of alloys annealed and quenched from temperatures in the neighborhood of the solidus. The specimens were  $\frac{3}{4}$  in long and  $\frac{7}{8}$  in in diameter as cut from the cast rods, previously annealed seven days at  $400^\circ\text{C}$ . A calibrated chromel-alumel thermocouple was inserted in a hole, 0.040 in dia and  $\frac{1}{2}$  in deep, drilled in the end of each specimen. The thermocouple was calibrated before and after each annealing.

The specimens were suspended in a vertical tube furnace by means of a 0.008-in. dia nickel wire and the temperature was raised slowly over a

period of 1 hr to 419° C. The alloys were held at this temperature to within 0.3° C for ½ hr and quenched. Rapid quenching was effectively obtained by cutting the suspension wire and allowing the specimen to fall freely into ice water. The quenched specimens were examined microscopically and significant areas were photographed.

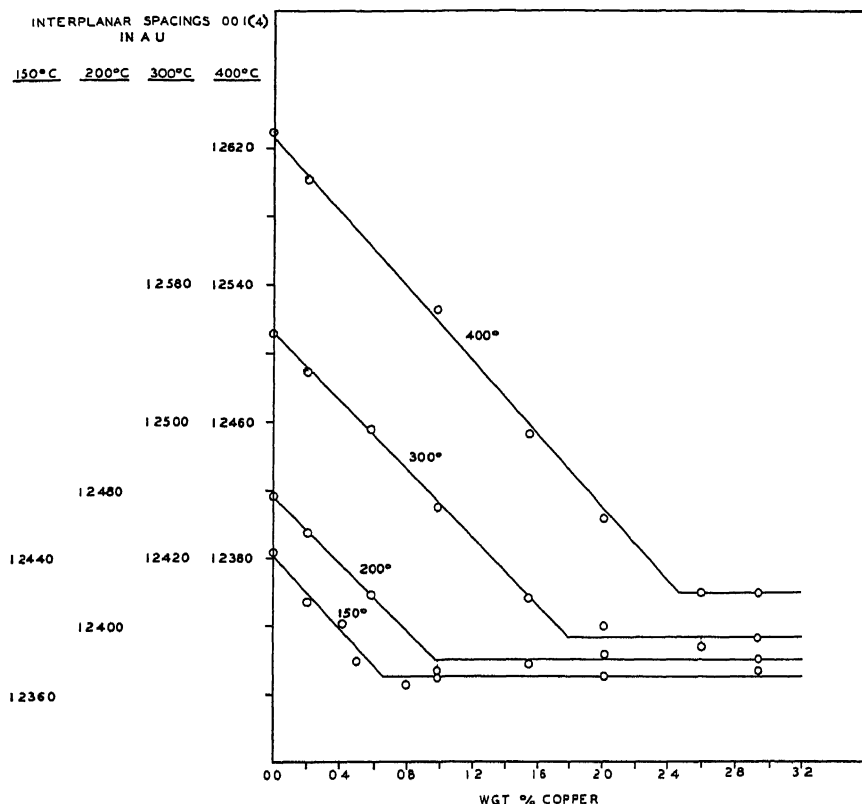


FIG. 2.—VARIATION OF 001(4) IN ETA SOLID SOLUTION OF COPPER IN ZINC, WITH COMPOSITION.

This procedure was repeated at successively higher temperatures until the microscope showed the alloys to have contained liquid prior to the quenching.

## RESULTS

Curves showing the variation of the 001 (4) and 10 4 interplanar spacings of the eta solid solution with the copper content of the alloy at 150°, 200°, 300° and 400° C. are shown in Figs 2 and 3. Each point represents the average of measurements on two X-ray diffraction patterns from separate specimens. The solubility limits indicated are listed in Table 6.

TABLE 6—*Solubility Limits of Copper in Zinc as Indicated by X-ray Method*

Temperature, Deg C	Solubility in Weight Per Cent Cu		
	00 1(4)	10 4	Average
150	0 65	0 67	0 66
200	0 97	0 97	0 97
300	1 78	1 80	1 79
400	2 46	2 60	2 53

Figs 2 and 3 and Table 6 do not contain X-ray data corresponding to equilibrium at 100° C, for the reason that the final measurements at 100° C were not made at temperature. An initial annealing of one to

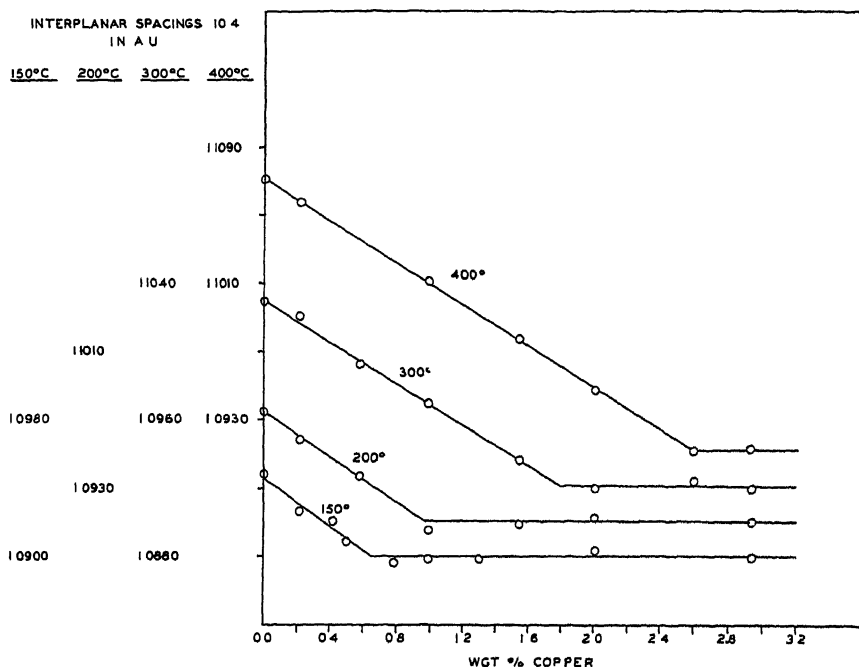


FIG 3—VARIATION OF 10 4 IN ETA SOLID SOLUTION OF COPPER IN ZINC WITH COMPOSITION

two months at 100° C. was not sufficient to produce equilibrium. According to this annealing, the indicated solubility was 1.48 per cent. Annealing for approximately one year at 100° C was sufficient to reduce the copper content of the solid solution phase from a maximum of 1.48 per cent to 0.3 per cent in alloys having a total copper content of 1.30 per cent or more. Alloys containing 0.99 and 0.58 per cent total copper were not completely relieved of their supersaturation after this extremely long

annealing It is apparent from these data that the solubility at room temperature is about 0.3 per cent Whether or not further annealing would reduce this figure is not known, but it seems unlikely Estimating the copper contents of the  $\eta$  phase on the basis of a previously determined curve showing the variation of lattice dimensions with copper content, the results of Table 7 were obtained

TABLE 7—*Annealing of Supersaturated Alloys at 100° C*

Total Copper Content of Alloy, Per Cent	Copper Content of $\eta$ Solid Solution, Per Cent	
	Annealing 1 to 2 Months	Annealing 1 Year
2.01	1.48	0.31
1.75	1.48	0.29
1.30	1.30	0.29
0.99	0.99	0.74
0.58	0.58	0.50

Curves showing the variation of electrical conductivity with copper content at 150°, 200°, 300° and 400° C are shown in Fig. 4 The discontinuities in the several curves indicate the solubility limits listed in Table 8

TABLE 8—*Solubility Limits of Copper in Zinc as Indicated by Electrical Conductivity Method*

TEMPERATURE, DEG C	SOLUBILITY IN WEIGHT, PER CENT CU
150	0.68
200	1.05
300	1.74
400	2.36

The results of the microscopical study may be reported best by the listing of Table 9, which gives for each group of alloys the compositions of the alloy of maximum copper content which was homogeneous  $\eta$  solid solution and of the alloy of minimum copper content, which was heterogeneous, showing the  $\epsilon$  phase in addition to  $\eta$ . As it was described earlier in the paper, the microscopical study was made on three groups of specimens. (1) cast alloys annealed first at 400° C and then reannealed at 100°, 150°, 200° and 300° C, (2) cold-rolled alloys annealed at 100°, 150°, 200°, 300° and 400° C, and (3) cold-rolled and flash-annealed (300° C) alloys annealed at 100°, 150°, 200°, 300° and 400° C

In Fig. 5 are reproduced typical photomicrographs of alloys on either side of the boundary. These microspecimens were taken from the group that had been cold-rolled. The first segregation takes place principally at the grain boundaries in particles whose size becomes greater with an

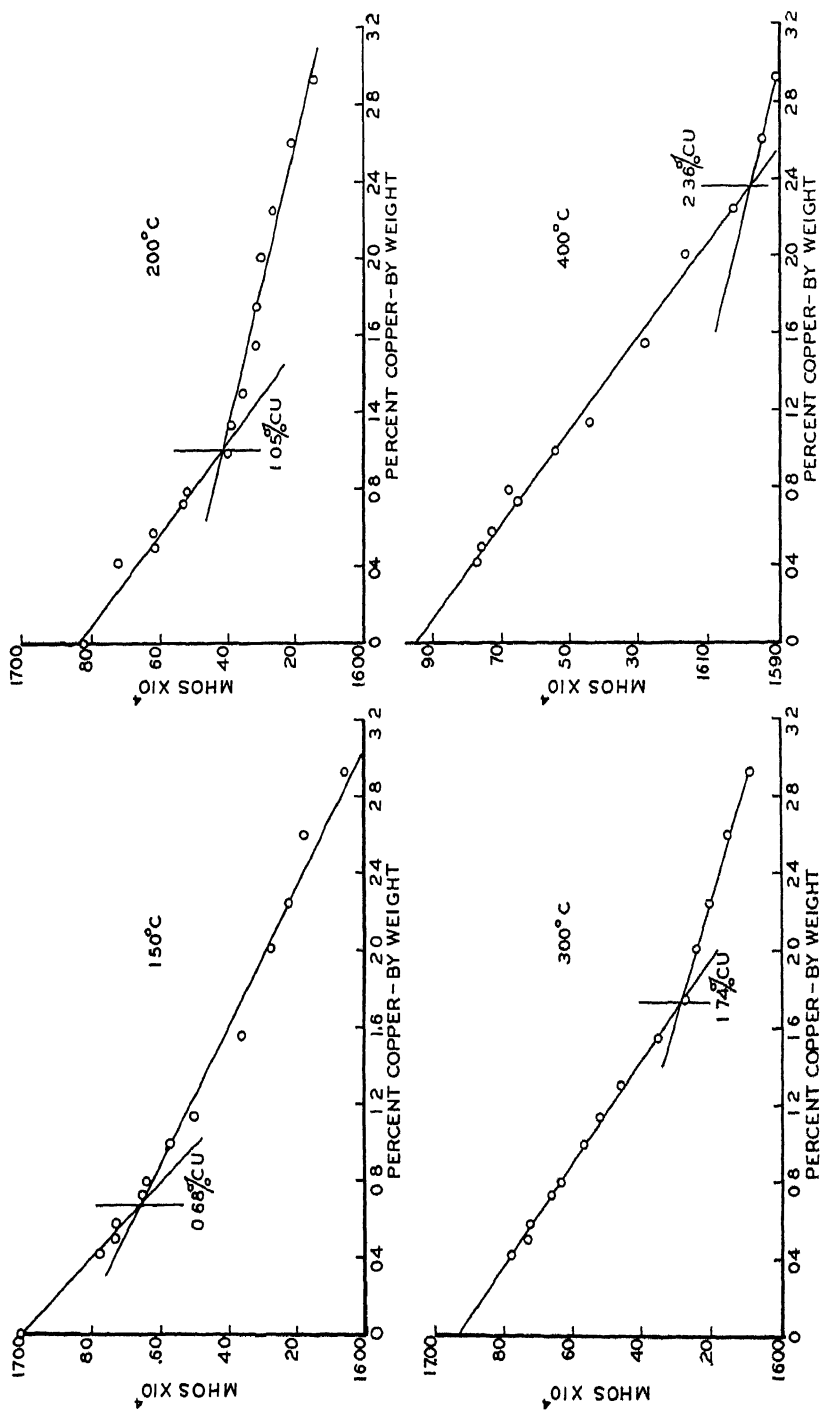


FIG. 4 — VARIATION OF ELECTRICAL CONDUCTIVITY WITH COPPER CONTENT IN QUENCHED SPECIMENS AT EQUILIBRIUM



increase in the annealing temperature. At concentrations well above the solubility limit the segregate structure is of the Widmanstätten type, a crystallographic analysis of which appeared in an earlier publication<sup>(19)</sup> from this laboratory.

TABLE 9—*Solid Solubility Limits of Copper in Zinc as Indicated by Microscopical Method*

Temperature, Deg. C	Percentage of Copper					
	Cast		Cold-rolled		Cold-rolled and Flash-annealed	
	Homogeneous	Heterogeneous	Homogeneous	Heterogeneous	Homogeneous	Heterogeneous
100	0.42	0.50	0.21	0.42	0.21	0.42
150	0.58	0.73	0.58	0.73	0.58	0.73
200	0.79	0.99	0.79	0.99	0.79	0.99
300	1.55	1.75	1.55	1.75	1.75	2.01
400	2.25	2.60	2.25	2.60	2.01	2.25

The minute markings or dots on the photomicrographs of the alloys within the range of eta homogeneity may be due in part to lead and iron, whose solubility in zinc is extremely small, and in part to an etching effect.

The results of the thermal analysis, in which cooling curves were made on a series of alloys, are listed in Table 10.

TABLE 10—*Thermal Arrests Occurring during Cooling of Copper-zinc Alloys in the Epsilon + Liquid  $\rightleftharpoons$  Eta Peritectic Region*

COMPOSITION OF ALLOY, WEIGHT PER CENT CU	THERMAL ARRESTS, DEG. C
0.55	420.2
1.00	421.9
1.30	422.8
1.70	424.3
2.05	430.0, 424.5
2.90	457.4, 424.5

Fig. 6 shows photomicrographs of alloys annealed and quenched from temperatures in the neighborhood of the eta solidus. Specimens that had partly melted prior to the quenching are easily identified from the photomicrographs.

## CONSTRUCTION OF THE PHASE EQUILIBRIUM DIAGRAM AND DISCUSSION

### *Solid Solubility Curve*

The solubility limits of copper in zinc as determined by the X-ray and electrical conductivity methods are plotted in Fig. 7, together with the

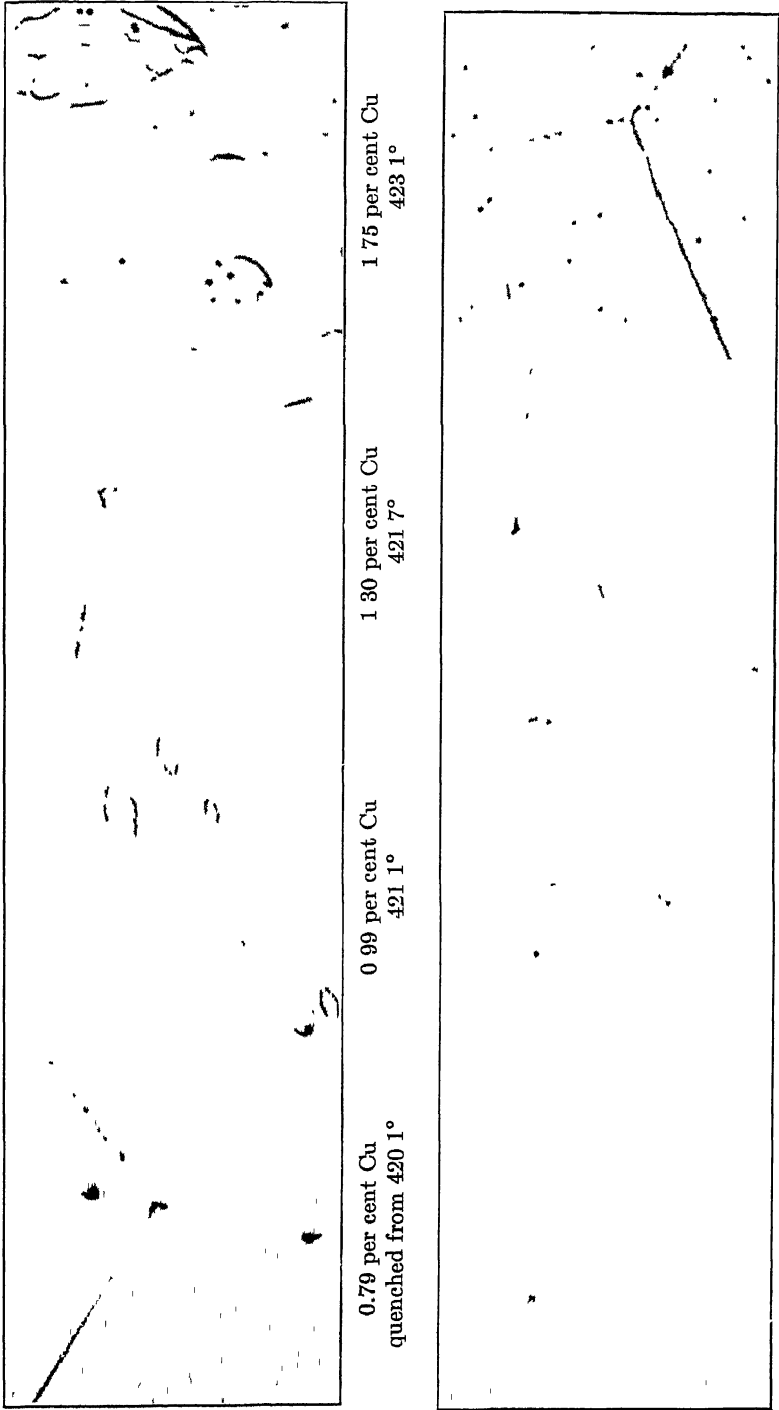


FIG 6 —ALLOYS QUENCHED FROM NEIGHBORHOOD OF ETA SOLIDUS X 500



microscopical observations. A curve has been drawn representing the most probable course of the boundary as based on the present work. The results of the X-ray and electrical conductivity methods are in excellent agreement at 150°, 200° and 300° C. The agreement at 400° C is not as good, the limit indicated by the X-ray method lies between 2.46 and 2.60 (average 2.53) and that indicated by the conductivity method is 2.36 per cent. The microscopical study found the limit to be between 2.25 and 2.60 per cent on the cast and cold-rolled specimens, and for the flash-annealed specimens the limit is apparently lower, 2.01 to 2.25 per cent. If the specimens for the microscopical study and the conductivity work were not effectively quenched from the 400° annealing, a solubility limit lower than that indicated by the X-ray method might well be expected, since the X-ray measurements were made while the alloy specimens were at 400° C. On the other hand, the experimental difficulties in getting precise X-ray measurements so close to the melting point of a metal are greater than at lower temperatures as is shown by the fact that the agreement between the 10.4 and 00.1 (4) measurements (Table 6) is not as good as that experienced at the lower temperature.

After careful consideration, the curve was drawn as in Fig. 7, which favors the X-ray value at 400° C slightly and gives equal weight to both X-ray and conductivity values at the lower temperatures. Extrapolated to the peritectic temperature, a solubility of 2.68 per cent is indicated at the peritectic point.

Regarding the microscopical findings, it is apparent from the data in Table 9 that there is not complete agreement between the three groups of specimens.

At 100° C the 0.42 per cent copper cast specimen is homogeneous  $\epsilon$ , whereas the corresponding alloy in the other two groups is heterogeneous. The cast specimen is apparently supersaturated because of an annealing inadequate for the relief of supersaturation in the coarse crystals resulting from the earlier annealing at 400° C. The lower bracket of 0.21 to 0.42 per cent copper was therefore plotted on Fig. 7.

At 150° and 200° C the microscopical results are in complete accord. For the 0.99 per cent copper alloy at 200° C, very little of the  $\epsilon$  phase was evident from a thorough study of a large area on the plane of polish. The appearance of the alloy microstructures in the range of composition near the limit at 200° C indicated on Fig. 7 suggests that the limit is closer to 0.99 per cent than 0.79 per cent, in agreement with the X-ray and conductivity results.

At 300° C. a discrepancy is apparent, since the 1.75 per cent copper alloy is heterogeneous in two cases, cast and cold-rolled groups, and homogeneous in the cold-rolled and flash-annealed group. However, since the solubility limit from the X-ray and conductivity work is approximately at this composition, it is not surprising to find that the

1.75 per cent copper alloy, heat-treated in three different manners, is not consistently homogeneous or heterogeneous. The limits indicated by the microscopical study are therefore plotted as between 1.55 and 2.01 per cent copper, on Fig 7

At 400° C, the flash-annealed specimens are at variance with the other two groups. Since it seems evident from the X-ray and conduc-

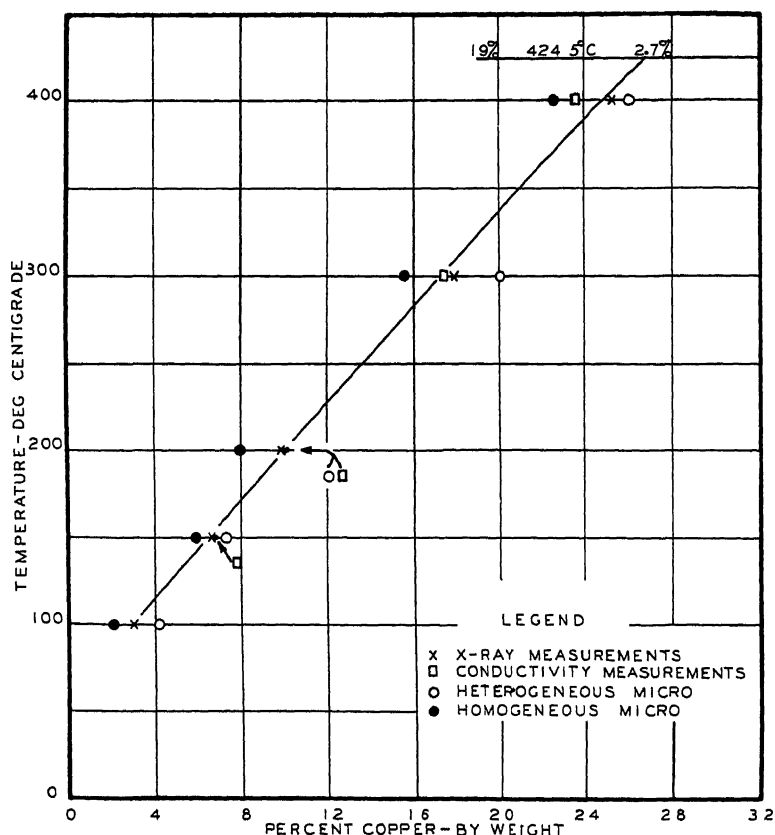


FIG 7—PHASE BOUNDARY OF ETA SOLID SOLUTION

tivity work and from the microstructure of the cast and cold-rolled specimens that the solubility limit must be over 2.25 per cent copper, the microscopical limit has been represented on Fig. 7 between 2.25 and 2.60 per cent copper

The most probable solubility limits of copper in zinc as obtained from Fig. 7 are given in Table 11

#### *Peritectic Region*

Fig 8 shows the equilibrium diagram in the region of the peritectic as plotted from the thermal analysis and microscopical study made on

TABLE 11—*Solubility Limits of Copper in Zinc*

TEMPERATURE DEG C	COPPER, WEIGHT PER CENT
100	0 30
150	0 65
200	1 00
300	1 72
400	2 48

alloys in this zone The melting point of pure zinc, 419.4° C, is taken from a precise determination previously made in this laboratory The

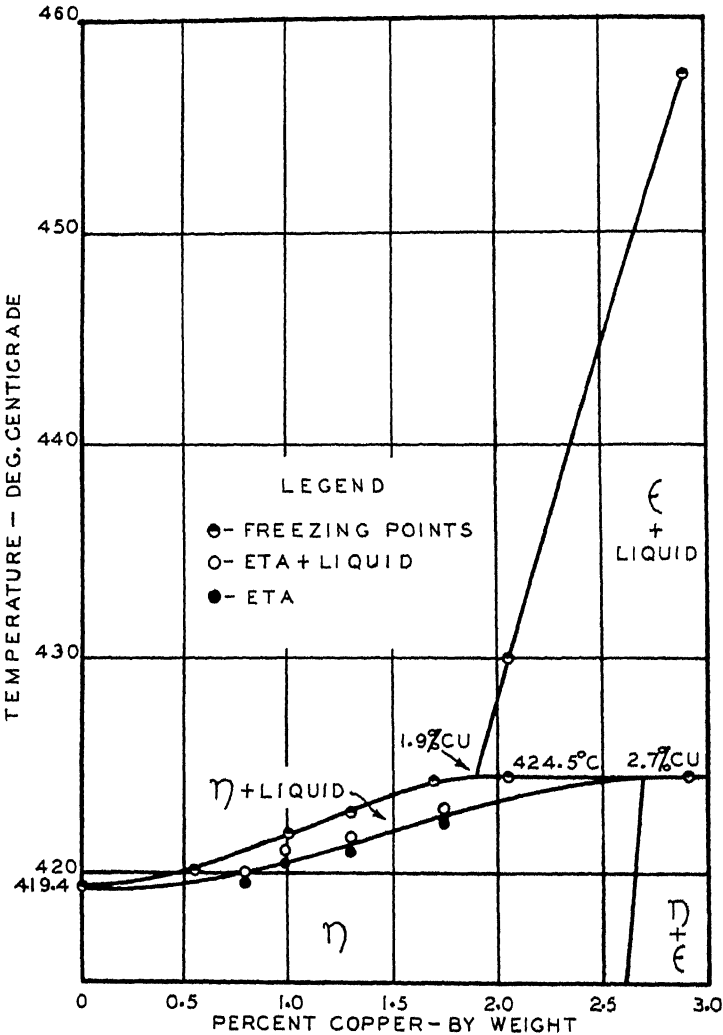


FIG 8—PERITECTIC REGION OF ETA SOLID SOLUTION.

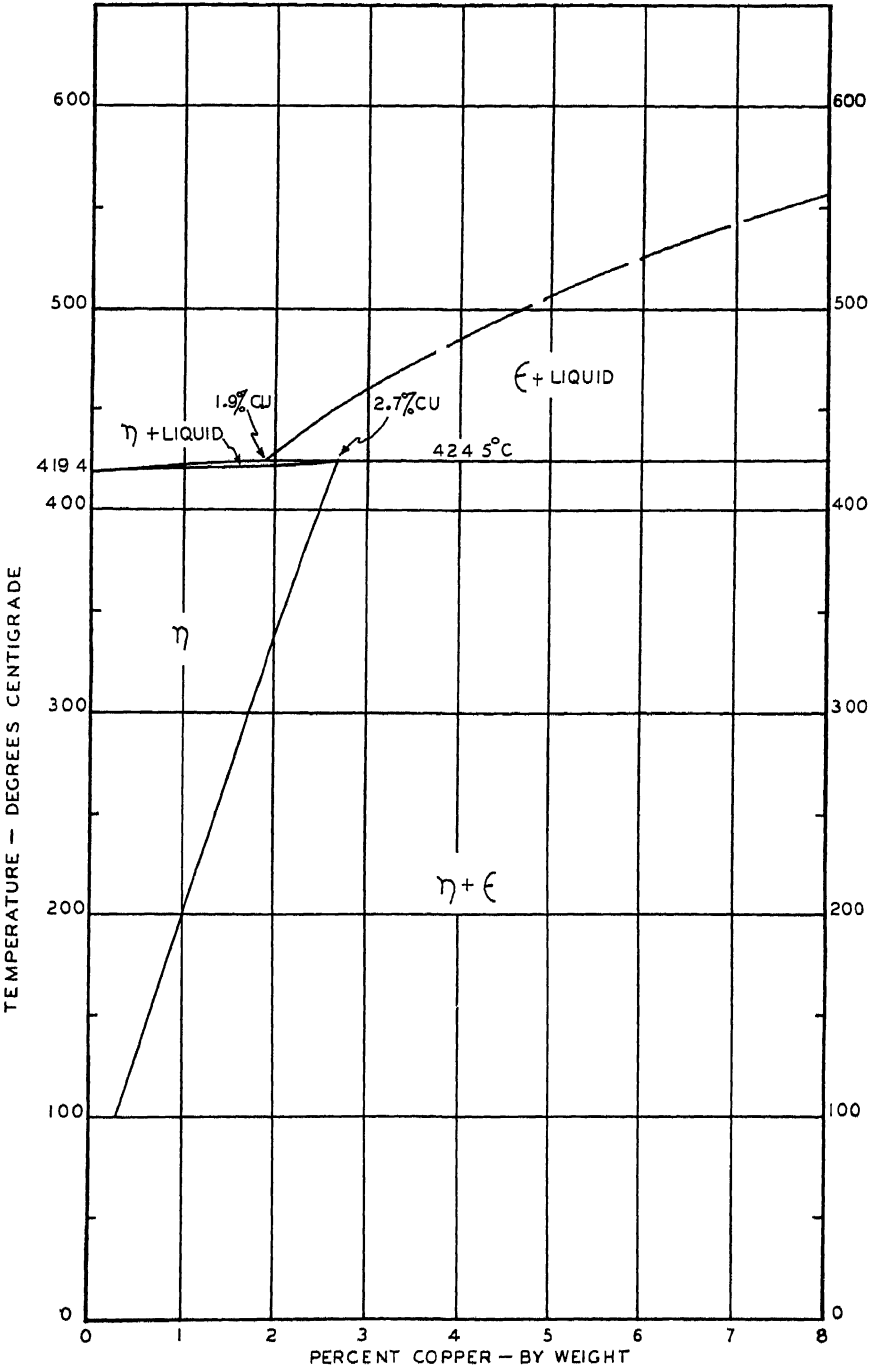


FIG 9 —PHASE EQUILIBRIUM DIAGRAM OF ZINC-RICH PORTION OF ZINC-COPPER SYSTEM

point of intersection of the eta liquidus with the peritectic horizontal at 424.5° C is at the composition 1.9 per cent copper, the peritectic point being taken from Fig. 7 as 2.68 per cent copper.

A phase equilibrium diagram based on the results of this paper is presented as Fig. 9. In constructing the liquidus above the epsilon plus liquid region, the point of 11.5 per cent copper and 594° C for the high-copper terminus of this boundary as given by O. Bauer and M. Hansen<sup>(7)</sup> was taken into consideration.

#### COMPARISON OF RESULTS OF PRESENT PAPER WITH EXISTING DATA IN THE LITERATURE

The course of the liquidus and solidus and the temperature of the peritectic horizontal are in substantial agreement with the work of O. Bauer and M. Hansen<sup>(7)</sup> and M. Hansen and W. Stenzel<sup>(12)</sup>.

The solid solubility limits are not in complete agreement with those of M. Hansen and W. Stenzel,<sup>(12)</sup> particularly at 200° and 300° C, at which temperatures they obtain much lower values. Their annealing times were much shorter (Table 1). In the event that the maximum amount of copper in solid solution was high prior to their reanneals, inadequate reannealing would tend to yield higher results than those reported by the present authors. The results of Hansen and Stenzel, however, are lower. The discrepancy may be explainable on the theory of Phillips and Brick (discussed in detail later in the paper), but no grain-size measurements of Hansen and Stenzel's alloys are available for this purpose. The peritectic point given by Hansen and Stenzel of 2.66 per cent is in good agreement with that of this paper, 2.68 per cent copper.

It is interesting to note that Hansen and Stenzel had difficulty in achieving equilibrium at 100° C. After failing to reach equilibrium after 180-hr annealing, they discontinued the attempt.

#### ON THE ATTAINMENT OF EQUILIBRIUM

This investigation has revealed how easily the experimenter in the domain of physical metallurgy may be led to erroneous conclusions because of insufficient diversity in the preparation of the alloy specimens and lack of multiplicity in methods of examination. Any one set of alloys examined by any one method would have indicated a different phase boundary for the eta solid solution than the one presented in this paper. In spite of unusually long annealing treatments given the specimens initially, a state of equilibrium was not reached in several cases to which reference has already been made. The final agreement between the three methods of examination upon specimens having undergone a diversity of heat treatments is evidence to show that the results presented

correspond to equilibrium conditions. The authors consider that their experimental observations on the methods of approach to and attainment of a state of equilibrium are a major contribution of the paper and wish therefore to discuss this point in detail.

After the original reannealing of the cold-rolled and flash-annealed alloys of 35 days at  $100^{\circ}\text{C}$ , the X-ray and conductivity methods indicated a solubility of about 1.5 per cent copper, whereas microscopical study on specimens similarly treated showed a solubility less than 0.42 per cent copper. Evidently, the bulk of the  $\eta$  phase contained a maximum of 1.5 per cent copper but some of the  $\eta$  had precipitated a portion of its excess copper as  $\epsilon$ , since the latter was evident in the microstructures of all alloys 0.42 per cent copper and higher. Annealing of an additional month produced further precipitation according to microscopical examination, and yet not sufficient of the  $\eta$  had changed to note an effect on the X-ray pattern. An annealing of one year's duration at  $100^{\circ}\text{C}$  was required to bring the X-ray observations in accord with the microscopical work. Even this treatment was insufficient to relieve completely the supersaturation of the  $\eta$  phase in alloys only slightly supersaturated (Table 7). It is interesting to note that the  $100^{\circ}\text{C}$  microscopic specimens, on which data are given in Table 9, are not at equilibrium and yet the indicated solubility limit of 0.21 to 0.42 per cent copper is in agreement with the X-ray data on alloys given the one-year annealing. It is not certain whether the longer annealing has produced equilibrium but it seems likely that in specimens 1.30 per cent copper and higher equilibrium has virtually been reached. It is not to be expected, however, that microscopic analysis will always indicate the true solubility limit in such cases of supersaturation, proof of which is given by the cast specimens, of which the 0.42 per cent copper alloy remained homogeneous.

In view of the obviously slow rate at which the copper in supersaturated  $\eta$  segregates as  $\epsilon$ , the flash-annealed specimens must have had up to 1.5 per cent copper in solid solution prior to the reannealing. After 35 days at  $100^{\circ}\text{C}$  the maximum copper content of  $\eta$  was still 1.5 per cent. The conductivity strips were annealed 32 days at  $150^{\circ}\text{C}$  following the  $100^{\circ}\text{C}$  annealing, after which conductivity measurements indicated a solubility of about one per cent copper as contrasted to a limit between 0.58 and 0.73 per cent copper indicated by the microscope for  $150^{\circ}\text{C}$ . Apparently the 32-day annealing was insufficient to produce a state of equilibrium. The agreement among the X-ray measurements on specimens annealed variously from 43 to 101 days, and the agreement with the microscopical work, is evidence that the annealing accorded the alloys was sufficient after 43 days. Later confirmation of this limit at  $150^{\circ}\text{C}$  was obtained by reannealing the conductivity strips by very slow cooling from  $400^{\circ}\text{C}$ , as described earlier in the paper. The latter result was 0.68 per cent copper.

Following the 32-day annealing at 150° C, the flash-annealed specimens were annealed at 200° C for 26 days. From the original conductivity measurements, after the 150° C treatment the copper content of the eta phase prior to the start of the 200° C annealing must have been up to a maximum of 1 per cent. Since the solubility at 200° C is approximately 1 per cent, there was little, if any, supersaturation to be relieved in this annealing.

At 300° and 400° C, the X-ray and conductivity results were in agreement with one another after the original annealings of 20 and 7 days, respectively, for the conductivity specimens, and 101 to 180 days and 13 to 23 days, respectively, for the X-ray specimens. Apparently the conductivity specimen annealings of 20 and 7 days at 300° and 400° C, respectively, were adequate. Microscopical study of flash-annealed specimens that were reannealed at 300° and 400° C for the same periods as the conductivity specimens revealed that some of the epsilon in alloys below the solubility limit had not been completely absorbed. The amount of epsilon unabsorbed must have been small, however, since further annealing which affected solution of additional epsilon did not raise the limits of homogeneity higher than the limits determined by the X-ray and conductivity measurements.

In the cold-rolled and flash-annealed specimens equilibrium was approached in the reannealing treatments at 100° and 150° C by relief of supersaturation, at 200° C the alloys were apparently only slightly supersaturated prior to the annealing, and at 300° and 400° C equilibrium was approached by the redissolution of the epsilon precipitated at the lower temperatures.

The maximum copper content of the eta phase in the cold-rolled specimens which had not been flash-annealed was not determined, so that it is not possible to state the manner of approach to equilibrium undergone by these specimens. It is interesting to note that at no temperature did the microscopical observations on the cold-rolled specimens disagree with the final results of the X-ray and conductivity methods. This suggests that equilibrium is most readily attained by the reannealing of cold-rolled material.

The segregation of epsilon from the eta solid solution results in an increase in the average atomic volume of the alloy, or in effect the alloy must expand to relieve the internal pressure resulting from the segregation. In the redissolution of epsilon in eta, the reverse takes place. It has been suggested by our colleague, G. Edmunds, that this phenomenon may influence the rate of segregation of epsilon and its redissolution. The internal pressure to be overcome when epsilon segregates from eta may greatly retard this segregation as compared to the reverse process. Experimental confirmation of the very low rate at which segregation occurs has been obtained in this investigation.

## ON DISTRIBUTION OF SEGREGATED EPSILON IN ETA MATRIX

It has been observed frequently that segregation of a secondary phase from a solid solution takes place most readily at points of strain such as at twin bands and grain boundaries. It has been noticed, in the investigation on which this paper is based, that epsilon appears at the grain boundaries and not to any considerable extent within the crystal in alloys containing only a small amount of excess copper. Where the amount of copper in excess of the solubility limit is large, the distribution of the segregate frequently provides an interesting structure.



FIG 10 —PHOTOMICROGRAPH OF 1.55 PER CENT COPPER ALLOY SHOWING DISTRIBUTION OF SEGREGATED EPSILON  $\times 500$

Heat treatment Cold-rolled and flash-annealed  
 35 days at 100° C and quenched  
 32 days at 150° C and quenched  
 37 days at 200° C. and quenched

Fig 10 is a good example of this particular structure. This specimen was one of the cold-rolled and flash-annealed series and had a total copper content of 1.55 per cent copper. The specimen had been annealed 35 days at 100° C, 32 days at 150° C and 37 days at 200° C. Prior to these annealings, the specimen had been a practically homogeneous eta solid solution. The 100° C annealing reduced the copper content of the eta phase slightly, the 150° C treatment probably reduced it to about one per cent and the 200° C annealing brought the solid solution composition definitely to 1 per cent copper.

It will be noticed on the photomicrograph that large particles of epsilon are situated at the grain boundaries, a large number of small



particles are distributed within the central area of the grain and the area of the grain adjacent to the boundary is devoid of segregate. Apparently the excess copper in the supersaturated  $\eta$  solid solution migrated rapidly to the grain boundaries where large crystals of  $\epsilon$  were developed, leaving the adjacent matrix free of its condition of supersaturation and without a segregate structure. The central area of the grain, having no preferred point of segregation, developed a uniformly distributed segregate structure probably by the simple atomic movements hypothesized for Widmanstätten structures<sup>(19)</sup>

An intermediate stage in the process of segregation may be hypothesized in which the material adjacent to the grain boundaries has reached equilibrium while the material in the central portion of the grain is still supersaturated. A natural effect of such a condition would be to lengthen the time required to reach complete equilibrium in the case of coarse-grained alloys as compared to finer grained material.

A striking example of this incomplete segregation is furnished by this investigation in the case of the work at 100° C. On the flash-annealed material, the X-ray and conductivity methods showed that after 35 days annealing at 100° C the alloys were capable of holding in solid solution nearly 1.5 per cent copper, whereas the microscopical work definitely detected precipitated  $\epsilon$  in alloys as low as 0.42 per cent copper content. If the grain size of the 100° specimens had been smaller, equilibrium might have been reached more quickly.

The fact that this case of incomplete segregation was not interpreted as equilibrium was due to the use of several methods of examination rather than one.

#### ON THE GRAIN BOUNDARY EFFECT

A. Phillips and R. M. Brick<sup>(20)</sup> have clearly stated and offered experimental evidence to support a theory of a new factor in polycrystalline alloy equilibria, namely, the influence of the relative amount of grain-boundary areas on the solubility limits in solid phases. In effect their work shows that the larger the grain size in polycrystalline metal, the greater will be the solid solubility. A similar phenomenon was observed by P. Wiest,<sup>(21)</sup> who noted that single crystals were capable of retaining larger amounts of solute than polycrystalline metal.

It has not been possible in the present investigation to study this effect. It may be possible for us to report on this question at some later time. In order, however, that the present data may prove useful in the event of such a study, all of the specimens used in the X-ray work have been subjected to a grain-size measurement, microscopically. The average grain sizes of the  $\eta$  solid solution in the X-ray specimens are listed in Table 12.

TABLE 12—*Grain Sizes of Eta Phase in X-ray Specimens<sup>a</sup>*

Temperature, Deg C	Mean Grain Size, Mm	Average Deviation from Mean, Mm
100	0 028	±0 007
150	0 034	±0 009
200	0 027	±0 016
300	0 037	±0 003
400	0 090	±0 005

<sup>a</sup> At 300° and 400° C many of the specimens below the solubility limit contained very large crystals and are not included in this table. Those alloys beyond the solubility limit, however, showed the grain sizes given in the table.

## SUMMARY

A determination of the high-zinc portion of the copper-zinc phase equilibrium diagram has been made. The peritectic zone of the eta and epsilon phases has been carefully determined. The results do not differ largely from those of previous investigations, but the refined experimental techniques used have made possible a precise location for the several boundaries, for the peritectic temperature and for the fixed points of concentration.

The solid solubility of copper in zinc has been investigated in detail using X-ray, electrical conductivity and microscopical methods of examination upon alloy specimens prepared according to several different procedures. The solid solubility boundary was then determined from 100° to 400° C, extrapolation being made to the peritectic horizontal.

The difficulty with which equilibrium conditions in solid phases are reached has been emphasized. The very effective manner in which the X-ray, electrical conductivity and microscopical methods have combined in the study of alloy phase equilibria has been demonstrated.

## ACKNOWLEDGMENT

The authors express their appreciation for assistance during the course of the investigation and in the preparation of the manuscript, which was given by other members of the Research Division, The New Jersey Zinc Company.

## BIBLIOGRAPHY

- <sup>1</sup> W M Peirce *Trans A I M E* (1923) **68**, 767-795
- <sup>2</sup> D Jitsuka *Ztsch f Metallkunde* (1927) **19**, 396-403
- <sup>3</sup> E S Shepherd *Jnl Phys Chem.* (1904) **8**, 421-434
- <sup>4</sup> V. E Tafel. *Metallurgie* (1908) **5**, 343-352, 375-383, 413-430
- <sup>5</sup> N. Parravano: *Gazz Chim Ital* (1914) 475-502
- <sup>6</sup> J L Haughton and K E Bingham *Proc Roy Soc* (1921) **99**, 47-69
- <sup>7</sup> O Bauer and M Hansen. *Ztsch f Metallkunde* (1927) **19**, 423-424
- <sup>8</sup> W. Broniewski and J Strasburger: *Rev de Mét* (1931) **28**, 19-29, 79-84
- <sup>9</sup> E A Owen and L Pickup *Proc Roy Soc* (1932) **137**, 397-417
- <sup>10</sup> E A Owen and L Pickup *Proc Roy Soc* (1933) **140**, 179-191

- <sup>11</sup> E A Owen and L Pickup *Proc Roy Soc* (1933) **140**, 191-204
- <sup>12</sup> M Hansen and W Stenzel *Metallwirtschaft* (1933) **12**, 539
- <sup>13</sup> W C Roberts-Austen *Proc Inst Mech Engrs* (1897) 31-100
- <sup>14</sup> R Ruer and K Kremers *Ztsch f anorg u allge Chem* (1930) **184**, 193-231
- <sup>15</sup> G Sachs and J Weerts *Ztsch f Physik* (1930) **60**, 481-490
- <sup>16</sup> A Westgren and G Phragmén *Phil Mag* (1925) **50**, 311
- <sup>17</sup> E A Owen and G D Preston. *Proc Phys Soc* (1923) **36**, 49
- <sup>18</sup> J L Rodda *Trans A I M E* (1932) **99**, 149-158
- <sup>19</sup> M L Fuller and J. L. Rodda *Trans A I M E.* (1933) **104**, 116-130
- <sup>20</sup> A Phillips and R M Brick *Jnl Franklin Inst* (1933) **215**, 557-577
- <sup>21</sup> P Wiest *Ztsch f Physik* (1932) **74**, 225-253

# Equilibrium Relations in Aluminum-nickel Alloys of High Purity

BY WILLIAM L. FINK\* AND L. A. WILLEY,\* NEW KENSINGTON, PA.

(New York Meeting, October, 1934)

NICKEL is used as an alloying element in several complex commercial aluminum alloys, among which are found some very interesting properties, such as relatively high strength at elevated temperatures, relatively low coefficient of expansion, the absence of permanent growth, ability to take a good polish, and a bright, pleasing as-cast surface. For that reason the aluminum-nickel system was included in the list of binary aluminum systems that are being studied as a preparation for the investigation of more complex commercial alloys.

This paper is the fifteenth of a series from the Research Laboratories of the Aluminum Company of America reporting the results of investigations of equilibrium relations in aluminum-base alloys of high purity. The aluminum-nickel equilibrium diagram from 0 to 18 per cent nickel was determined, using the purest material available.

## PREVIOUS INVESTIGATIONS

The entire aluminum-nickel system was studied thermally and microscopically by Gwyer.<sup>1</sup> At the aluminum end of the system he found the intermetallic compound  $\text{NiAl}_3$ . He found a eutectic at 6 per cent nickel with a melting point of  $630^\circ\text{C}$ . A slight thermal arrest, which he could not explain, was also noted in alloys from 2.5 per cent to 41.9 per cent nickel at  $550^\circ\text{C}$ .

Bingham and Haughton,<sup>2</sup> in a later investigation of alloys of aluminum with copper and nickel found the eutectic concentration of the binary aluminum-nickel system at about 5.3 per cent nickel. The melting point of the eutectic was about  $633^\circ\text{C}$ , or slightly higher than that found by Gwyer. Although the solid solubility of nickel in aluminum could not

---

Manuscript received at the office of the Institute June 15, 1934

\* Aluminum Research Laboratories

<sup>1</sup> A. C. G. Gwyer. Alloys of Aluminum with Copper, Iron, Nickel, Cobalt, Lead and Cadmium. *Ztsch f anorg Chem* (1907) **57**, 113-153.

<sup>2</sup> K. E. Bingham and J. L. Haughton. The Constitution of Some Alloys of Aluminum with Copper and Nickel. *Jnl Inst Metals* (1923) **29**, 71.

be determined accurately on account of the impurities in the aluminum, they found it to be less than 0.25 per cent nickel at 600° C

#### PREPARATION AND CHEMICAL ANALYSIS OF ALLOYS

Electrolytically refined aluminum<sup>3</sup> (99.985 per cent aluminum) and electrolytically refined nickel (99.938 per cent nickel) were used in the preparation of the alloys for this investigation. The analyses are given in Table 1. A nickel-rich alloy (approximately 15 per cent nickel) was the first made. Aluminum was heated to between 900° and 1000° C in a plumbago crucible and the nickel was introduced. The nickel dissolved slowly but completely in that temperature range. The alloy was thoroughly stirred and chill-cast into notch bars.

For thermal analysis, 200 grams of each alloy were prepared in a straight-walled graphite crucible 4 cm. inside diameter by 10 cm. deep. In each case the alloy was thoroughly stirred and the cooling curve immediately taken. A small Hoskins electric furnace was used. The cooling-curve ingot was remelted, stirred and a portion for chemical analysis was cast in a cold iron mold (75 by 40 by 5 mm.). The remainder of each alloy was cast in a cold graphite mold, similar to the crucible in size and shape. These ingots were used for microscopic study of the cast structures.

TABLE 1—*Analysis of Alloys*

Alloy No	Composition, Per Cent					Alloy No	Composition, Per Cent				
	Si	Fe	Cu	Ni	Other Elements		Si	Fe	Cu	Ni	Other Elements
M4619		0.13	0.02	99.38	Co, 0.26 C, 0.21	Y3218				8.09	
Y2550				1.02		Y3219				9.08	
Y2551				2.01		Y3220				10.18	
Y2552				3.07		Y3221	0.03	0.06	0.02	15.69	
Y2553				4.05		Y3628	0.005	0.007	0.003		
Y2554				5.06		Y3629	0.005	0.007	0.003	0.01	
Y2837				5.26		Y3630				0.03	
Y2838				5.46		Y3631				0.05	
Y2555				5.67		Y3632				0.07	
Y2556				6.38		Y3633				0.09	
Y3216	0.004	0.008	0.003			Y3634				0.11	
Y3217	0.01	0.03	0.01	7.09		Y3635				0.14	
						Y3636	0.006	0.010	0.003	0.19	

The alloys for the determination of the solid solubility of nickel in aluminum were prepared by melting 600 grams of each, stirring thoroughly, skimming and chill-casting into the analysis slab mentioned above and into an ingot weighing approximately 480 grams (10 by 9 by 2 cm.)

<sup>3</sup> F. C. Frary, *Electrolytic Refining of Aluminum*, *Trans. Amer. Electrochem. Soc.* (1925) 47, 275.

*Chemical Analysis*—The chemical analyses were obtained on drillings from the 5-mm chill-cast slab of each alloy used for thermal analysis or for the determination of the solid solubility. The dimethylglyoxime method was used for the determination of nickel.<sup>4</sup> The results of the analysis are given in Table 1.

### SOLIDIFICATION

*Thermal Analysis*—Cooling curves were taken according to the practice recommended by the Bureau of Standards.<sup>5</sup> Table 2 gives the temperatures of primary and eutectic arrests.

TABLE 2—*Thermal Analysis*

Alloy No	Ni, Per Cent	Primary Solidification, Deg C	Eutectic Solidification, Deg C	Alloy No	Ni, Per Cent	Primary Solidification, Deg C	Eutectic Solidification, Deg C
Y2550	1.02	656.0	639.1	Y2555	5.67		640.0
Y2551	2.01	653.2	639.9	Y2556	6.38		640.6
Y2552	3.07	648.2	639.4	Y3217	7.09	643.0	639.5
Y2553	4.05	645.4	640.0	Y3218	8.09	664.8	640.2
Y2554	5.06	641.8	639.8	Y3219	9.08	677.6	640.3
Y2837	5.26	641.0	639.8	Y3220	10.18	690.4	639.7
Y2838	5.46	640.4	639.9	Y3221	15.69	753.9	

*Eutectic Horizontal*—From the thermal analysis of 13 alloys ranging in composition from about 1 per cent to about 10 per cent nickel, it was found that the average temperature of eutectic solidification was 639.9° C. This is about 10° C higher than that found by Gwyer.<sup>6</sup> The difference was probably caused by the lower purity of Gwyer's alloys.

*Hypoeutectic Liquidus*—The hypoeutectic liquidus was also determined by thermal analysis. The results show that the liquidus is uniformly lowered with increasing quantities of nickel up to 5.6 per cent. At this point the liquidus intersects the eutectic horizontal.

*Hypereutectic Liquidus*—As in previous work on similar systems, the hypereutectic liquidus could not be determined accurately by cooling curves because of appreciable undercooling. The method actually used was that of analyzing samples taken from the melt in equilibrium with precipitated  $\text{NiAl}_3$ , a method that in earlier work gave excellent results.<sup>7,8</sup>

<sup>4</sup> Standard Methods of Analysis, Aluminum Company of America.

<sup>5</sup> U. S. Bur. Stds. *Tech. Paper* 170 (1921) 193.

<sup>6</sup> Reference of footnote 1.

<sup>7</sup> H. J. Miller, The Penetration of Brass by Tin and Solder with a Few Notes on the Copper-tin Equilibrium Diagram, *Jnl. Inst. Metals* (1927) **37**, 188.

<sup>8</sup> W. L. Fink, K. R. Van Horn and P. M. Budge, Constitution of High-purity Aluminum-titanium Alloys, *Trans. A. I. M. E.* (1931) **93**, Inst. Metals Div., 421.

Approximately 10 kg of an alloy containing 20 per cent nickel was heated to 1000° C to insure complete solution of the compound. The temperature was then lowered to 805° C and held at that temperature for approximately 2 hr (previous tests showed that this time was sufficient to insure complete precipitation and settling of the solid phase). Two samples of the saturated liquid were then obtained from the skimmed surface of the melt, after which the temperature was again lowered and the procedure repeated. The results from 805° to 646° C are given in Table 3. The extrapolation of the data to the eutectic temperature (639.9° C) indicates a eutectic composition of 5.8 per cent nickel.

TABLE 3 —*Solubility of Nickel in Liquid Aluminum*

Sample No	Temperature, Deg C			Time at Temperature		Nickel, Per Cent
	Max	Min	At Time of Sampling	11r	Min	
Y3202-1	805.0	802.2	804.8	2	19	17.88
Y3202-2	805.0	802.2	804.8	2	44	17.78
Y3203-1	736.1	729.8	736.1	1	32	11.75
Y3203-2	736.1	729.8	733.8	1	57	11.83
Y3204-1	699.8	697.3	698.3	1	49	9.20
Y3204-2	699.8	697.3	697.3	1	59	9.15
Y3205-1	654.5	652.8	654.3	1	25	6.47
Y3205-2	654.5	652.8	654.3	1	35	6.49
Y3206-1	646.8	646.1	646.8	1	45	6.25
Y3206-2	646.8	646.1	646.1	1	55	6.26

*Eutectic Concentration*—It has been shown that the hypoeutectic liquidus, as determined by cooling curves, intersects the eutectic horizontal at 5.6 per cent nickel and that the hypereutectic liquidus, as determined by the solubility method, intersects the horizontal at 5.8 per cent nickel. Considering these data the eutectic may be placed at 5.7 per cent nickel.

#### THE INTERMETALLIC COMPOUND

Crystals of the compound occurring in aluminum-rich alloys were separated from an alloy containing 15.7 per cent nickel. The alloy was first melted and slowly cooled through the solidification range to obtain large, well formed crystals. This alloy was then made the anode in a solution containing approximately 1 per cent citric acid, 0.1 per cent secondary sodium phosphate and 0.5 per cent sodium chloride. The applied potential was 4.2 to 4.7 volts. This dissolved the aluminum matrix, leaving clean, unattacked crystals of the compound. An analysis showed that these crystals contained 41.8 per cent nickel. This is in good agreement with the formula  $\text{NiAl}_3$ , which contains 42.0 per cent



FIG 1—HYPOEUTECTIC ALLOY CONTAINING 4.05 PER CENT NICKEL (Y2553-A7266D).  
 $\times 100$

Specimen from ingot cast in cold graphite mold. Shows primary aluminum solid solution dendrites in eutectic network. Etched with 0.5 per cent  $H_2F_2$ .

FIG 2—HYPEREUTECTIC ALLOY CONTAINING 8.09 PER CENT NICKEL (Y3218-A7268D).  
 $\times 100$

Specimen from ingot cast in cold graphite mold. Shows primary  $NiAl_3$  constituents in eutectic matrix. Etched with 0.5 per cent  $H_2F_2$ .

FIG 3—HYPEREUTECTIC ALLOY CONTAINING 7.09 PER CENT NICKEL (Y3217-A1563).  
 $\times 500$

Specimen from ingot cast in cold graphite mold. Shows in more detail primary  $NiAl_3$  constituents and eutectic structure. Etched with 0.5 per cent  $H_2F_2$ .

FIG 4— $NiAl_3$  CRYSTALS, 41.7 PER CENT NICKEL (Y4240-A7281).  $\times 5$

Crystals, from slowly cooled ingot containing 15.7 per cent nickel, obtained by electrolytic separation. Shows dendritic form of  $NiAl_3$  needles.



nickel by weight The formula  $\text{NiAl}_3$  is also in agreement with the findings of Gwyer

### STRUCTURE OF ALUMINUM-RICH ALUMINUM-NICKEL ALLOYS

The cast hypoeutectic alloys show primary aluminum-nickel solid solution dendrites in a eutectic network Fig 1 shows the microstructure of such an alloy (4.05 per cent nickel) cast in a cold graphite mold Fig 2 shows the primary crystals of  $\text{NiAl}_3$  in a polished section of a chill-cast 8.09 per cent nickel alloy Figs 1 and 2 show that the chill-cast eutectic is extremely fine and is not completely resolved at a magnification of 100 diameters The eutectic structure as well as a form of the primary  $\text{NiAl}_3$  constituent is shown at 500 diameters in Fig 3

The alignment of the particles of primary constituents shown in Fig 2 has been observed in other aluminum alloy systems It was believed that these particles were connected outside of the plane of polish Electrolytic separation of constituents gives a good opportunity to study these crystals in three dimensions Fig 4 shows one of the electrolytically separated crystals A polished section through such a featherlike structure would, of course, give the appearance of a group of disconnected particles

In a polished section of the aluminum-rich aluminum-nickel alloys, the  $\text{NiAl}_3$  phase appears as a light gray constituent with a slightly purple tinge in the unetched condition Several of the standard etches for aluminum alloys<sup>9</sup> give characteristic colors to the constituents In an aqueous solution of 0.5 per cent  $\text{H}_2\text{F}_2$  the constituent first turns to a light blue color and with a longer period of etching turns to brown and finally to black About the same change in color is obtained using an etching reagent of 10 per cent  $\text{NaOH}$  at  $70^\circ\text{C}$ , or one containing 0.5 per cent  $\text{H}_2\text{F}_2$ , 1.5 per cent  $\text{HCl}$  and 2.5 per cent  $\text{HNO}_3$  A 25 per cent  $\text{HNO}_3$  solution at  $70^\circ\text{C}$  does not color or attack the constituent

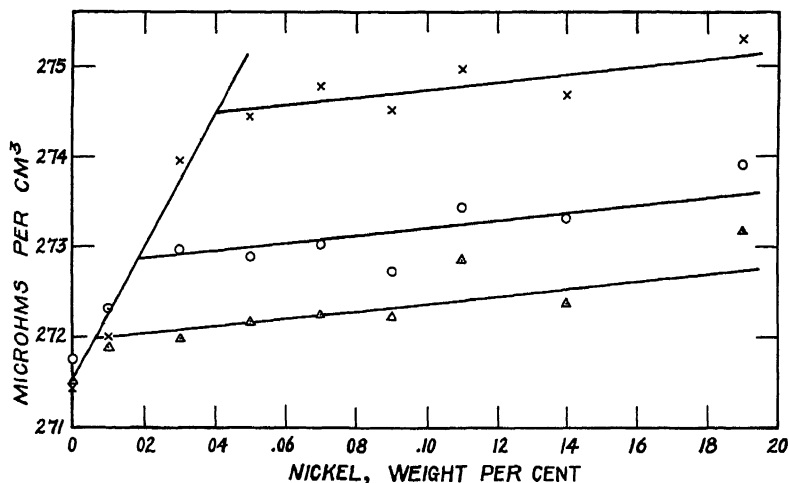
### SOLID SOLUTION

The electrical resistivity method was employed in determining the solid solubility curve for nickel in aluminum and the results were checked by microscopic examination

The ingots described earlier in the paper were hot-rolled to 6-mm slabs immediately after casting These slabs were annealed for 48 hr at  $590^\circ\text{C}$  and cold-rolled to 22-gage sheet (0.64 mm). Strip specimens 25 by 500 mm were cut from the sheet and milled to 19-mm width to be used for determining the electrical resistivity. Small samples of the sheet were also prepared for solution heat treatment and subsequent microscopic examination

<sup>9</sup> F Keller and G W Wilcox Polishing and Etching of Constituents of Aluminum Alloys *Metal Progress* (April, 1933)

The solution heat treatment of all specimens was carried out in a Leeds & Northrup Homo furnace. To reduce variation of temperature, an aluminum block (10 cm inside diameter, 20 cm outside diameter and 53 cm long) was used in the Homo furnace. While the variation in temperature outside the block was as great as  $\pm 5^{\circ}\text{C}$ , the temperature within the aluminum block varied not more than  $\pm 1^{\circ}\text{C}$  either with



- X Heat treated 67 hr at  $625^{\circ}\text{C}$ . and quenched  
 O Heat treated 67 hr at  $625^{\circ}\text{C}$ ., cooled to  $570^{\circ}\text{C}$ ., held 47 hr and quenched.  
 Δ Heat treated 67 hr at  $625^{\circ}\text{C}$ ., cooled to  $505^{\circ}\text{C}$ ., held 50 hr and quenched

FIG 5 — ELECTRICAL RESISTIVITY-CONCENTRATION CURVES

respect to time or location. The procedure followed in heat-treating the specimens was as follows.

Group 1, Y3628 to Y3636 inclusive, 67 hr at  $625^{\circ}\text{C}$  and quenched

Group 2, Y3628 to Y3636 inclusive, 67 hr at  $625^{\circ}\text{C}$ , cooled to  $570^{\circ}\text{C}$  in  $2\frac{1}{2}$  hr, held 47 hr and quenched

Group 3, Y3628 to Y3636 inclusive, 67 hr at  $625^{\circ}\text{C}$ , cooled to  $570^{\circ}\text{C}$  in  $2\frac{1}{2}$  hr, held 47 hr, cooled to  $505^{\circ}\text{C}$  in 2 hr, held 50 hr and quenched

The electrical resistivity measurements were made very soon after the specimens were quenched, to avoid any errors that might be introduced by possible precipitation in the alloys at room temperature, although subsequent measurements revealed no change upon room-temperature aging. During the resistance measurements, the specimens were immersed in a kerosene bath thermostatically controlled at  $25^{\circ}\text{C}$ . The resistance was determined by measuring the drop in potential across the specimen and a standard 0.001 ohm resistance, which were connected in series. A Leeds & Northrup type K potentiometer was employed for these measurements.

Fig 5 shows the resistivity-concentration curves for these alloys after the heat treatments at 625°, 570° and 505° C. The breaks in the curves representing the limit of solid solubility occur at 0.040, 0.018 and 0.006 per cent nickel, respectively.

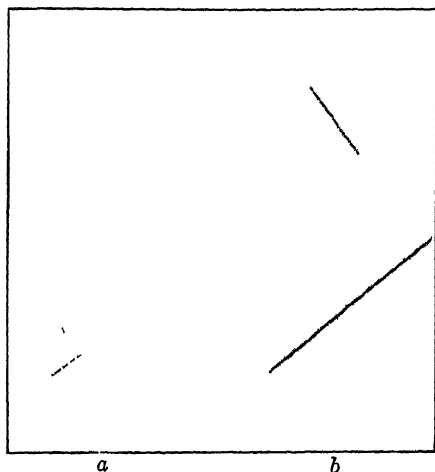


FIG 6—0.03 PER CENT NICKEL ALLOY (Y3630-A1944D-A1945D)

Specimen heat-treated 67 hr at 625° C, slowly cooled to 505° C, held 50 hr and quenched in cold water. Etched with 0.5 per cent  $H_2F_2$ .

a  $NiAl_3$  constituents precipitated from solid solution in form of fine needles or thin plates along crystallographic planes.  $\times 100$   
b Portion of same field at higher magnification.  $\times 500$

Microscopic examinations of the small specimens that were heat-treated with the resistivity specimens checked the results obtained by the electrical resistivity method. The 0.03 per cent nickel alloy showed only solid solution after the heat treatment at 625° C, whereas the 0.05 per cent nickel alloy showed small particles of  $NiAl_3$ . After heat treatment at 570° C, the 0.03 per cent nickel alloy showed particles of  $NiAl_3$ . After heat treatment at 505° C, both the 0.01 and 0.03 per cent nickel alloys showed the presence of this constituent. The  $NiAl_3$  that was precipitated from solid solution occurred as fine needles or thin plates along crystallographic planes. Fig 6 shows this structure in the 0.03 per cent nickel

alloy with the final heat treatment at 505° C.

#### AGE-HARDENING PROPERTIES OF HIGH-PURITY ALUMINUM-NICKEL ALLOYS

Although nickel is only slightly soluble in solid aluminum, the percentage variation of the solubility with temperature is large, therefore it seemed probable that these alloys would be susceptible to age-hardening. A series of alloys (0.01 to 0.19 per cent nickel) were given heat treatments suggested by the solid solubility curve. Substantial age-hardening was found. As an example, the Brinell hardness number (12.61 kg, 1.59-mm ball) of the 0.03 per cent nickel alloy was 17.7 after heating at 625° C and water quenching. After the same specimens had been artificially aged for 8 hr at 265° C the Brinell hardness number had increased to 26.0. Fig. 7 shows the hardness concentration curves for the entire series of alloys after the same thermal treatments.

Two aging temperatures were investigated, 200° and 265° C. Age-hardening takes place at 200° C, but a maximum value of hardness is not

attained even after 60 hr. at this temperature; whereas a maximum is reached in from 15 to 20 hr at 265° C Fig 8 shows the hardness of the

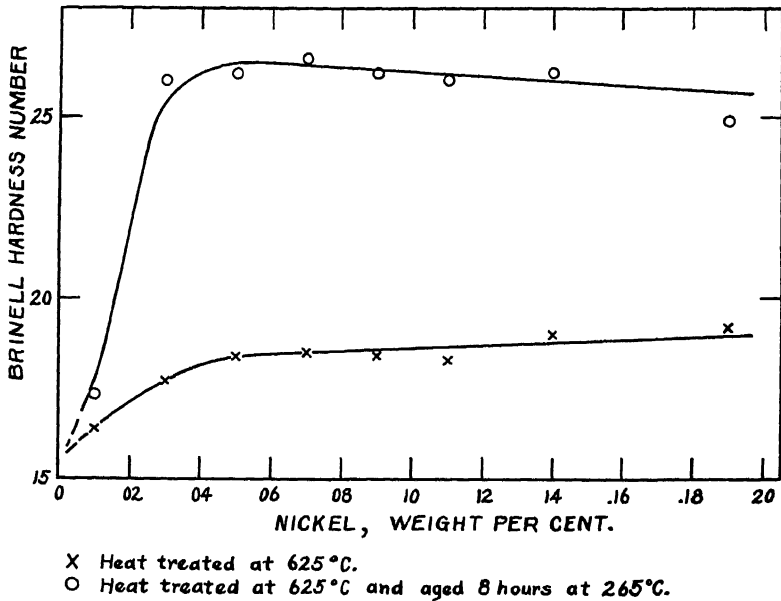


FIG 7—HARDNESS-CONCENTRATION CURVES FOR SERIES OF ALUMINUM-NICKEL ALLOYS

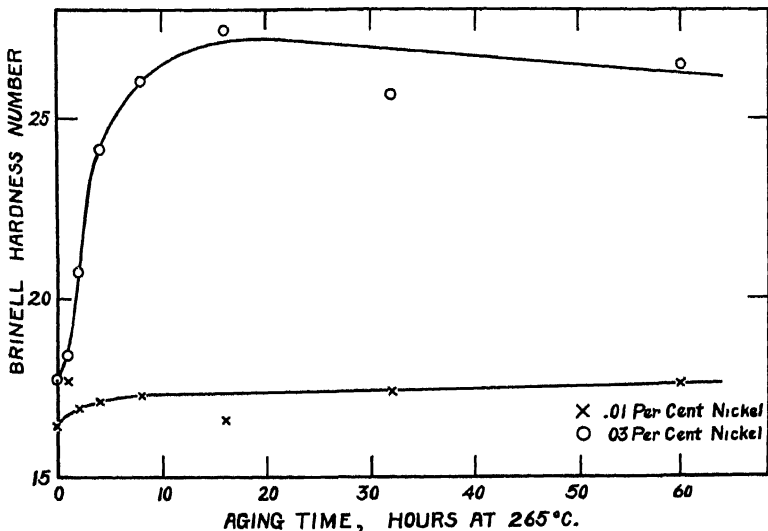


FIG 8—EFFECT OF AGING TIME AT 265° C ON HARDNESS OF HEAT-TREATED ALUMINUM-NICKEL ALLOYS.

heat-treated 0.01 per cent and the 0.03 per cent nickel alloys after aging at 265° C. for various times Only a slight increase in hardness occurs in the 0.01 per cent nickel alloy

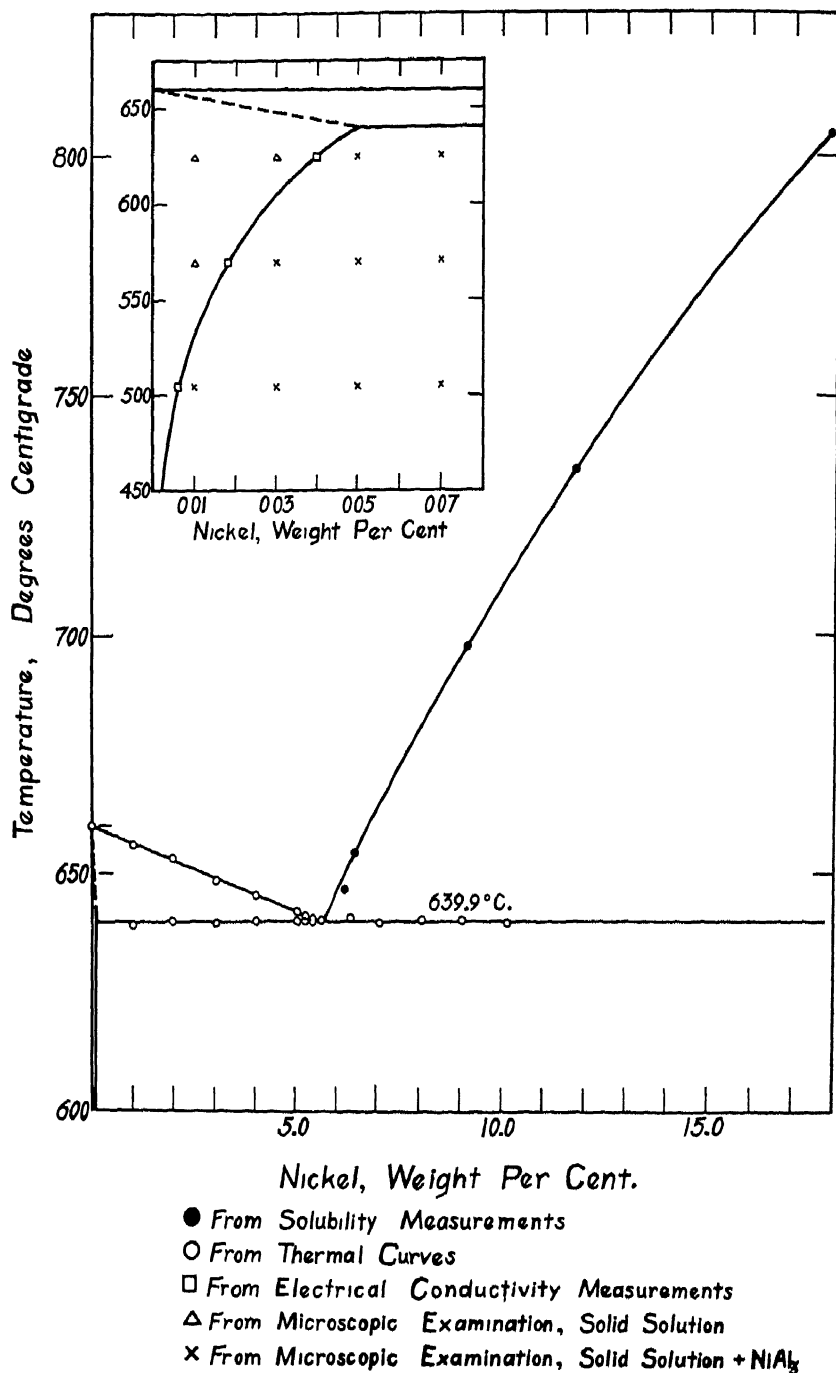


FIG 9 —ALUMINUM END OF ALUMINUM-NICKEL EQUILIBRIUM DIAGRAM.

## SUMMARY

The equilibrium relations of high-purity aluminum-rich aluminum-nickel alloys has been investigated from 0 to 18 per cent nickel as described above, and the results are summarized in the diagram of Fig 9. The eutectic between  $\text{NiAl}_3$  and the aluminum solid solution occurs at  $639.9^\circ\text{C}$  and 5.7 per cent nickel. The inset shows the solid solubility curve on a larger scale. As the curve shows, the solid solubility of nickel in aluminum decreases from 0.05 per cent at the eutectic temperature to 0.005 per cent at  $500^\circ\text{C}$ .

It was found that the aluminum-nickel alloys are subject to age-hardening, as might be expected from the shape of the solid solubility curve.

## ACKNOWLEDGMENT

The authors desire to express appreciation to Mr. H. V. Churchill and Mr. R. L. Templin, under whose direction the chemical analysis and the mechanical tests, respectively, were made. The authors are also indebted to Dr. H. R. Freche for the electrolytic separation of the aluminum-nickel constituent.

## DISCUSSION

(C. E. Swartz presiding)

H. G. CARTER,\* Watertown, Mass.—The author mentioned that he had difficulty in polishing the alloys, due, I presume, to extreme softness. He said that he finally obtained a method for getting a polish so that the particles could be clearly revealed. I wonder if he would give a little bit of that method? It would be interesting not only in this type of work but in the polishing of other soft materials in which there are small segregates.

W. L. FINK.—Unfortunately, the difference between the successful method and the unsuccessful method cannot be very readily described. It is largely a question of the small differences introduced by the man who is doing the polishing, such as the speed of the wheel, pressure on the specimen, the amount of water and abrasive used, the depth of the microtome cut, et cetera.

However, I might briefly present the method that we use. Most of the work is done on sheet material, and several different samples of sheet are clamped by means of bolts into a composite specimen. This composite specimen is machined down with a sharp microtome to obtain a nice, smooth, flat surface. Rather large cuts are first taken and then as the surface becomes flat, smaller and smaller cuts are taken so that the surface distortion is reduced as much as possible. The sample is then taken to the first polishing wheel on which are used kitten's ear broadcloth and No. 600 aluminum polishing powder. Then it is taken to the final polishing wheel on which are used duveteen and calcined magnesium oxide. It is very important to remove any particles of magnesium carbonate that may have formed in the magnesium oxide powder.

---

\* Associate Physicist, Watertown Arsenal

# Correlation of Equilibrium Relations in Binary Aluminum Alloys of High Purity

## A REVIEW OF PREVIOUSLY PUBLISHED DATA FROM THE ALUMINUM RESEARCH LABORATORIES

BY WILLIAM L FINK\* AND H R FRECHE,\* NEW KENSINGTON, PA

(New York Meeting, October, 1934)

THE investigation of aluminum alloy systems prior to 1923 was severely handicapped by the low purity of the best aluminum available. However, by that time, the electrolytic purification of aluminum had been developed by the Aluminum Company of America,<sup>(1)</sup> and in May, 1923, there was initiated, under the direction of E. H. Dix, Jr.,<sup>(2)</sup> a program for the investigation of the aluminum-alloy systems using the purest electrolytically refined aluminum. Up to the present time 15 papers<sup>(3)</sup> have been published, most of which are on the binary aluminum systems. Work is now in progress on the ternary systems, and it seems probable that most of the future work will be on ternary systems. Therefore this survey of the binary aluminum systems investigated up to the present time (the sixteenth paper of the series) concludes the first phase of this program.

Certain qualitative relations between corresponding portions of the various binary diagrams as well as between different parts of the same diagram were noted some time ago by R. S. Archer.<sup>(4)</sup> In the present paper these relations and others are considered quantitatively by the application of well-known thermodynamic equations or by newly discovered empirical relations.

No attempt will be made here to present the history of the development of the thermodynamic equations defining equilibrium or their application to metallic systems, although a list of references is given at the end of this paper for those who are interested in this phase of the subject. Two thermodynamic equations, which will be employed extensively in this paper, are:

$$\log_e x' = -\frac{L}{RT} + C \quad [1]$$

---

Manuscript received at the office of the Institute Aug. 28, 1934.

\* Aluminum Research Laboratories

† References are at the end of the paper

$$\log_e \left( \frac{x_l}{x_s} \right) = \frac{L}{R} \left( \frac{1}{T_0} - \frac{1}{T} \right) \quad [2]$$

where the letters have the following meanings:

- $x'$ , mol fraction of alloying element,
- $x_l$ , mol fraction of solvent in liquid phase,
- $x_s$ , mol fraction of solvent in solid phase,
- $L$ , molal heat of solution,
- $R$ , gas constant
- $T$ , temperature, deg. abs.,
- $T_0$ , freezing point of solvent, deg. abs.,
- $C$ , integration constant.

Equation 1, which was first developed by Le Chatelier,<sup>(5)</sup> gives the relation between the concentration of a solution and the temperature, when the

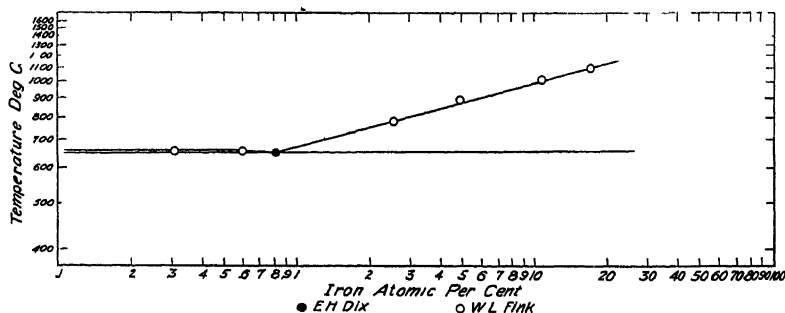


FIG 1 —ALUMINUM END OF ALUMINUM-IRON EQUILIBRIUM DIAGRAM

The diagrams are all plotted with coordinates  $1/T$  and  $\log x'$ . Diagrams plotted in usual way were omitted, to save publication costs.

precipitating phase is a pure element or compound. Equation 2, which was first developed by Van Laar,<sup>(6)</sup> gives the same relation when the precipitating phase is a solid solution. In the derivation of both these equations the assumptions are made that the solutions are perfect—that is, the activity is equal to the mol fraction—and that the heat of solution remains constant over the temperature range considered.

Considering the assumptions involved, it would not be surprising to find that the equations were of very limited application. However, the success of Andrews and Johnston,<sup>(7)</sup> Yap,<sup>(8)</sup> and Tammann and Oelsen<sup>(9)</sup> with certain applications to metal systems encouraged such an attempt in correlating the data on the binary aluminum systems.

#### SOLID SOLUBILITY AND HYPEREUTECTIC LIQUIDUS CURVES

Providing the assumptions mentioned above are substantially valid, the solid solubility and hypereutectic liquidus curves should be defined



by equation 1, since the precipitating phases are in both cases of substantially constant composition. The simplest method to check this point is to plot the equilibrium diagram using as coordinates  $1/T$  and  $\log$

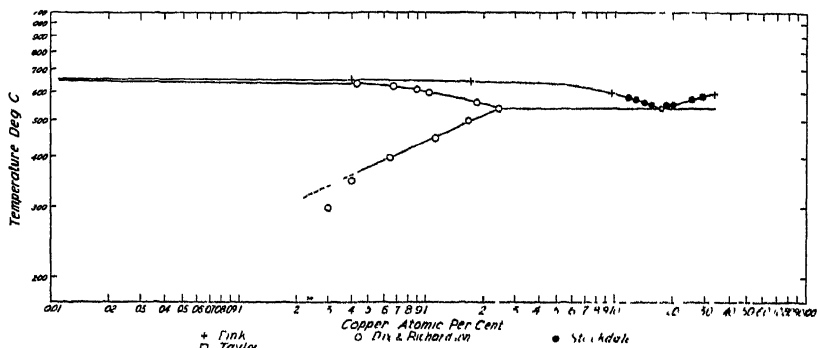


FIG 2—ALUMINUM END OF ALUMINUM-COPPER EQUILIBRIUM DIAGRAM

$x'$ . Figs 1 to 9 give the diagrams of some of the binary aluminum systems plotted in this way. Some data from outside sources have been included when the samples were made with high-purity aluminum or

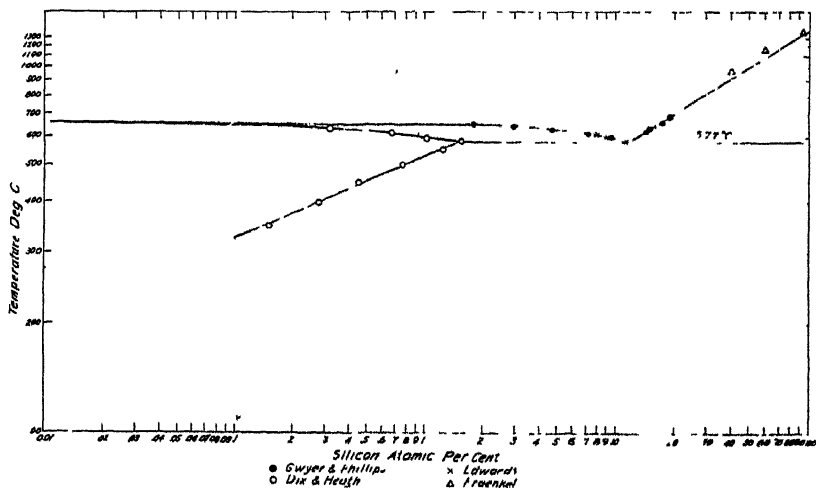


FIG 3—ALUMINUM END OF ALUMINUM-SILICON EQUILIBRIUM DIAGRAM.

when there was experimental evidence that the effect of the impurities was relatively small. It is evident from these curves that the experimental data for both the solid solubility and the hypereutectic liquidus curves closely approximate straight lines. The data from which the

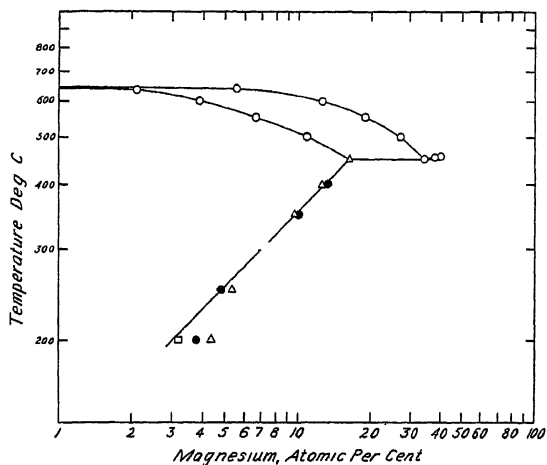


FIG 4—ALUMINUM END OF ALUMINUM-MAGNESIUM EQUILIBRIUM DIAGRAM.

△ Dix and Keller	• Schmid and Siebel
○ Hanson and Gayler	□ Willey

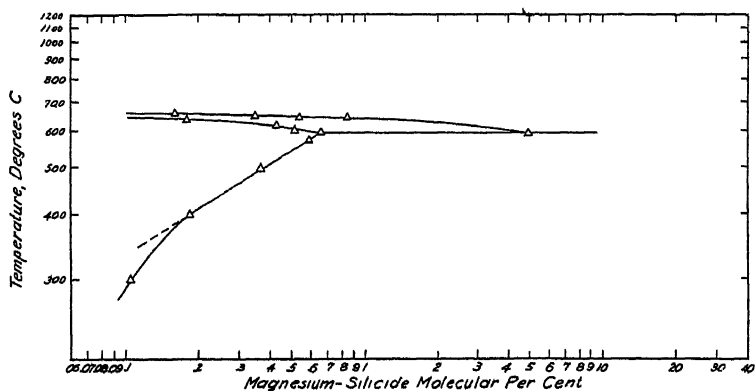


FIG. 5—ALUMINUM END OF ALUMINUM-MAGNESIUM SILICIDE EQUILIBRIUM DIAGRAM  
 $\Delta$  Dix, Keller and Graham

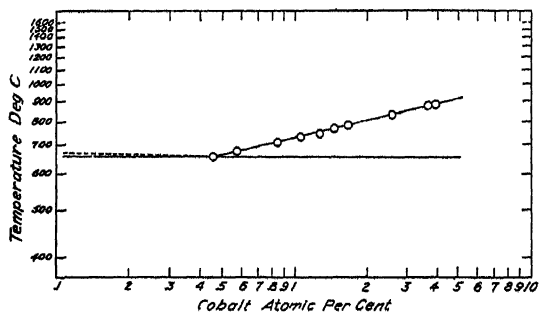


FIG. 6 — ALUMINUM END OF ALUMINUM-COBALT EQUILIBRIUM DIAGRAM.  
○ Fink and Freche

solid solubility curves and the hypereutectic liquidus curves were plotted are given in Tables 1 and 2

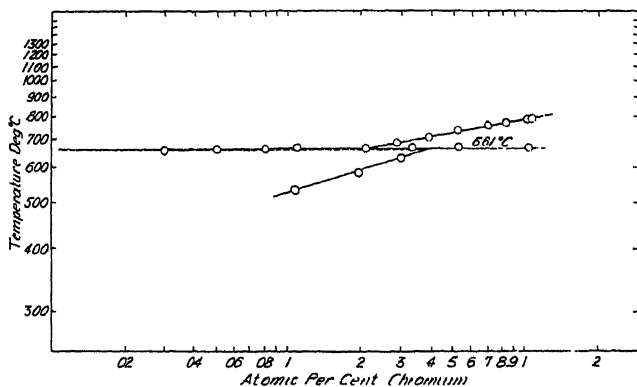


FIG. 7—ALUMINUM END OF ALUMINUM-CHROMIUM EQUILIBRIUM DIAGRAM  
O Fink and Freche

The experimentally determined solid solubility at the lower temperatures in the aluminum-copper system and the aluminum-magnesium silicide and aluminum-magnesium systems are at higher concentrations

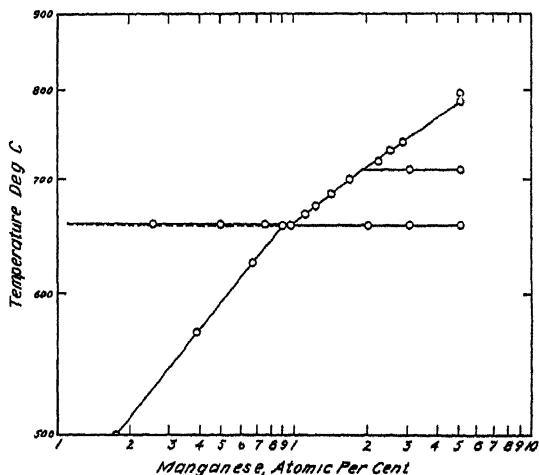


FIG. 8—ALUMINUM END OF ALUMINUM-MANGANESE EQUILIBRIUM DIAGRAM.  
O Fink and Willey

than those indicated by the straight lines. It is believed that this is due largely to a failure to obtain equilibrium at these low temperatures. For example, at the time this work was begun, the value for the solubility of magnesium in aluminum at 200° C. was high (4.0 per cent). L. A.

Wiley, of these laboratories, attempted to check this point and had difficulty in obtaining equilibrium. By repeated alternate cold rolling

TABLE 1.—*Data on Solid Solubility Curves*

System	Temperature		$\frac{1}{T}$	Weight Per Cent	Atomic Per Cent $x'$	$\log_{10} x'$	Slope of Solubility Curve $\frac{\Delta \frac{1}{T}}{\Delta \log_{10} x'}$		
	Deg C (t)	Deg K (T)					Calculated From Points	Calculated From Equation and point $x$	Estimated From Fig 13
Al-Ni	640	913	0 001095	0 050	0 0230	8 3614 $x$			
	625	898	0 001114	0 040	0 0184	8 2644°			
	570	843	0 001186	0 018	0 0083	7 9176	1 97 $\times 10^{-4}$	1 97 $\times 10^{-4}$	1 97 $\times 10^{-4}$
	500	773	0 001294	0 005	0 0023	7 3613°			
Al-Cr	661	934	0 001071	0 77	0 401	9 6029			
	630	903	0 001107	0 61	0 318	9 5017° $x$			
	580	853	0 001172	0 38	0 198	9 2962	2 98 $\times 10^{-4}$	2 79 $\times 10^{-4}$	2 82 $\times 10^{-4}$
	530	803	0 001245	0 21	0 109	9 0386°			
Al-Mn	658	931	0 001074	1 82	0 902	9 9552			
	626	899	0 001124	1 35	0 669	9 8255° $x$			
	570	843	0 001186	0 78	0 387	9 5872	2 98 $\times 10^{-4}$	3 16 $\times 10^{-4}$	3 16 $\times 10^{-4}$
	500	773	0 001294	0 36	0 177	9 2479°			
Al-Si	577	850	0 001176	1 65	1 587	0 2006			
	550	823	0 001215	1 30	1 250	0 0969° $x$			
	500	773	0 001294	0 80	0 769	9 8861	3 88 $\times 10^{-4}$	4 00 $\times 10^{-4}$	4 03 $\times 10^{-4}$
	450	723	0 001383	0 48	0 462	9 6642°			
	400	673	0 001486	0 29	0 279	9 4454			
	350	623	0 001605	0 17	0 164	9 2133			
	300	578	0 001745	0 10	0 096	8 9828			
	200	473	0 002114	0 05	0 048	8 6818			
Al-Cu	548	821	0 001218	5 65	2 478	0 3940			
	540	813	0 001230	5 30	2 320	0 3656° $x$			
	520	793	0 001261	4 70	2 049	0 3116			
	500	773	0 001294	4 10	1 781	0 2508			
	450	723	0 001386	2 60	1 120	0 0492	4 55 $\times 10^{-4}$	4 58 $\times 10^{-4}$	4 74 $\times 10^{-4}$
	400	673	0 001486	1 56	0 640	9 8074			
	385	658	0 001520	1 25	0 534	9 7277°			
	350	623	0 001605	1 00	0 427	9 6301			
	300	573	0 001745	0 70	0 298	9 4752			
Al-Mg	200	473	0 002114	0 50	0 213	9 3291			
	451	724	0 001381	14 9	16 26	1 2111			
	400	673	0 001486	11 5	12 59	1 1000°	9 94 $\times 10^{-4}$	9 17 $\times 10^{-4}$	10 05 $\times 10^{-4}$
	350	623	0 001605	8 7	9 56	0 9803° $x$			
	300	573	0 001745	6 4	7 05	0 8481			
	250	523	0 001912	4 9	5 41	0 7329			
	200	473	0 002114	4 0	4 32	0 6355			
	200	473	0 002114	2 9	3 21	0 5060			

and annealing at 200° C. equilibrium was finally approached. The solid solubility so obtained (2.9 per cent) lies much nearer the straight line as shown in the diagram of Fig. 4.

TABLE 2—Data on Hypereutectic (or Hyperperitectic) Liquidus Curves

	Temperature		$\frac{1}{T}$	Weight Per Cent	Atomic Per Cent, $x'$	$\text{Log}_{10} x'$
	Deg C ( $t$ )	Deg K ( $T$ )				
Al-Ti	948	1221	0 0008190	1 39	0 787	9 8960
	901	1174	0 0008518	1 06	0 600	9 7779
	846	1119	0 0008937	0 71	0 401	9 6030
	806	1079	0 0009268	0 51	0 288	9 4582
	742	1015	0 0009552	0 32	0 180	9 2562
	700	973	0 0010277	0 21	0 118	9 0722
	675	948	0 0010549	0 16	0 090	9 9549
Al-Cr	790	1063	0 0009407	2 07	1 084	0 0351
	785	1058	0 0009452	1 96	1 026	0 0112
	770 <sup>a</sup>	1043	0 0009588	1 595	0 833	9 9209
	753 <sup>a</sup>	1026	0 0009746	1 36	0 710	9 8511
	729 <sup>b</sup>	1002	0 0009980	0 973	0 507	9 7049
	702 <sup>a</sup>	975	0 0010256	0 75	0 392	9 5931
	694 <sup>a</sup>	967	0 0010341	0 65	0 339	9 5305
	685 <sup>a</sup>	958	0 0010438	0 565	0 294	9 4680
Al-Mn	740	1013	0 0009871	5 78	2 924	0 4660
	731	1004	0 0009960	5 26	2 654	0 4238
	720	993	0 0010070	4 62	2 323	0 3660
	699	972	0 0010288	3 44	1 719	0 2353
	686	959	0 0010428	2 90	1 445	0 1599
	675	948	0 0010549	2 51	1 248	0 0963
	668	941	0 0010627	2 26	1 123	0 0502
Al-Co	877	1150	0 0008696	8 28	3 967	0 5985
	875	1148	0 0008711	7 68	3 667	0 5643
	832	1105	0 0009050	5.53	2 609	0 4184
	780	1053	0 0009497	3 64	1 699	0.2302
	767 <sup>a</sup>	1040	0 0009615	3 185	1 483	0 1711
	748 <sup>a</sup>	1021	0 0009794	2 725	1 269	0.1035
	734 <sup>a</sup>	1007	0 0009930	2 383	1 105	0 0434
	728 <sup>a</sup>	1001	0 0009990	2 145	0 993	9 9970
	709 <sup>a</sup>	982	0 0010183	1 825	0 845	9.9288
	675 <sup>a</sup>	948	0 0010549	1 21	0 557	9 7461
Al-Fe	781	1054	0 0009488	4 87	2 413	0 3825
	891	1164	0 0008591	9 77	4 970	0 6963
	1022	1295	0 0007722	19 87	10 606	1 0292
	1105	1378	0 0007257	29 85	17.041	1 2315
Al-Ni	646 45	919 45 <sup>a</sup>	0 0010876	6 255	2 975	0 4735
	654 3	927 3 <sup>a</sup>	0 0010784	6 48	3 086	0 4894
	697 8	970 8 <sup>a</sup>	0 0010301	9 175	4 566	0 6595
	734.95	1007 95 <sup>a</sup>	0 0009921	11 79	5 787	0 7623
	804 8	1077 8 <sup>a</sup>	0 0009278	17 83	9 070	0 9576

<sup>a</sup> Average of two experimental points<sup>b</sup> Average of four experimental points<sup>c</sup> Average of three experimental points

## HYPOEUTECTIC LIQUIDUS AND SOLIDUS CURVES

Since the solid phase in equilibrium with the melt along the hypoeutectic liquidus is usually a solid solution, equation 2 should apply

provided the assumptions made in the derivation of the equations are substantially correct. The accuracy with which this equation represents the data can then be determined by plotting the liquidus of the system using as coordinates

$$\frac{1}{T} \text{ and } \log \frac{x_l}{x_s}$$

As mentioned,  $x_l$  is the mol fraction of aluminum in the liquid phase and  $x_s$  is the mol fraction of aluminum in the solid phase. Obviously those

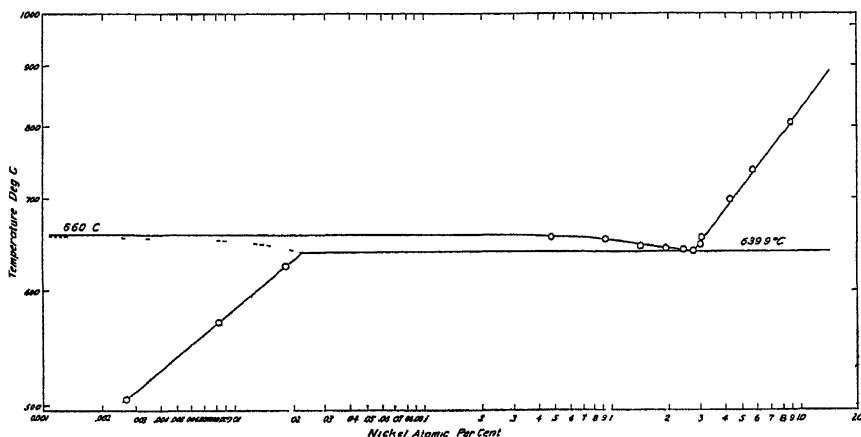


FIG. 9.—ALUMINUM END OF ALUMINUM-NICKEL EQUILIBRIUM DIAGRAM.  
○ Fink and Willey

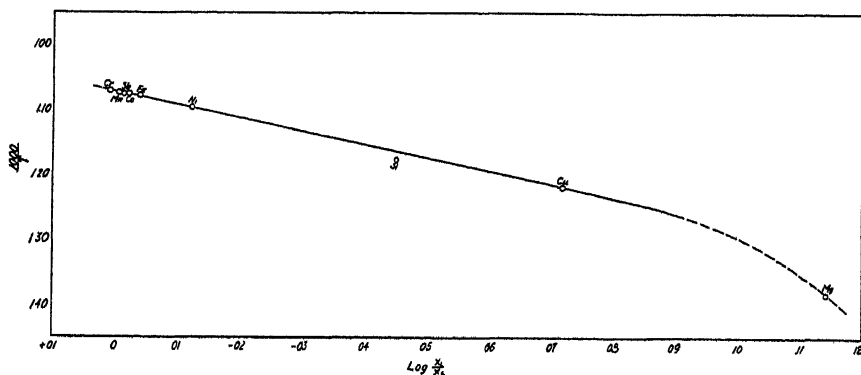


FIG. 10.—RELATION BETWEEN EUTECTIC CONCENTRATION, SOLID SOLUBILITY AT EUTECTIC TEMPERATURE, AND TEMPERATURE OF EUTECTIC

liquidi to which the equation applies will be linear when so plotted, and will all coincide. The most accurately known points (those at the eutectic temperature) are given in Table 3 and are plotted in Fig. 10. It is evident that they satisfy the equation except for the aluminum-

magnesium system and the aluminum-magnesium silicide system. The aluminum-silicon system deviated slightly. The deviation in the aluminum-magnesium system is really to be expected in view of the high concentration involved, and the large temperature range covered. It is really surprising that the aluminum-silicon and aluminum-copper systems conform as closely as they do to the straight line. The aluminum-magnesium silicide system will be considered in a later paper

TABLE 3.—Data on Eutectic Concentration and Solid Solubility at the Eutectic Temperature

System	Eutectic Temperature		$\frac{1}{T}$	Eutectic			Solid Solubility		
	Deg C (t)	Deg K (T)		Weight Per Cent	Atomic Per Cent	$x_1$	Weight Per Cent	Atomic Per Cent	$x_2$
Al-Tl	665	938	0 001066	1 5*	0 847	0 99153			
Al-Cr	661	934	0 001071	0 41*	0 213	0 99787	0 77	0 401	0 99599
Al-Mn	658 5	931 5	0 001073	1 95	0 967	0 99033	1 82	0 902	0 99098
Al-Sb	657	930	0 001075	1 1	0 246	0 99754	0 1	0 022	0 99978
Al-Co	657	930	0 001075	1 0	0 460	0 99540	0 02	0 009	0 99991
Al-Fe	655	928	0 001078	1 7	0 828	0 99172	0 02	0 009	0 99991
Al-Ni	640	913	0 001095	5 8	2 750	0 97250	0 05	0 023	0 99977
Al-Si	577	850	0 001176	11 6	11 20	0 88800	1 65	1 587	0 98413
Al-Cu	548	821	0 001218	33 0	17 28	0 82720	5 65	2 478	0 97522
Al-Mg	451	724	0 001381	33 7	36 06	0 63940	14 9	16 260	0 83740

\* Peritectic weight per cent used

Since  $x_2$  at the eutectic temperature is equal to 1 minus the solid solubility of the solute at that temperature, equation 2 is of wide application. It gives a relation between the solid solubility at the eutectic temperature, the eutectic concentration, and the eutectic temperature.

#### EMPIRICAL RELATIONS

In addition to the thermodynamic relations just mentioned, a number of empirical relations have been found. It was previously pointed out by Mr. Archer that the lower the eutectic temperature, the higher the solid solubility. It has since been found that if the logarithm of the eutectic lowering is plotted against the logarithm of the atomic per cent of solute in solution at the eutectic temperature a straight line can be drawn through most of the points (Fig. 11). The only element considered in this paper that gives a eutectic lowering for which this relation does not hold within experimental error is manganese. Of course chromium, which produces no lowering, cannot be plotted.

After the equilibrium diagrams were plotted as illustrated by Figs. 1 to 9, it was noted that the slope of the solid solubility curve seemed to vary in a rather regular manner from one system to another. On further inspection it was found that the slope of the solid solubility curve was a

function of either the eutectic lowering or the atomic per cent solute in solution at the eutectic temperature for all of the elements that fall on the straight line of Fig 11. It was thought that if the solid solubility

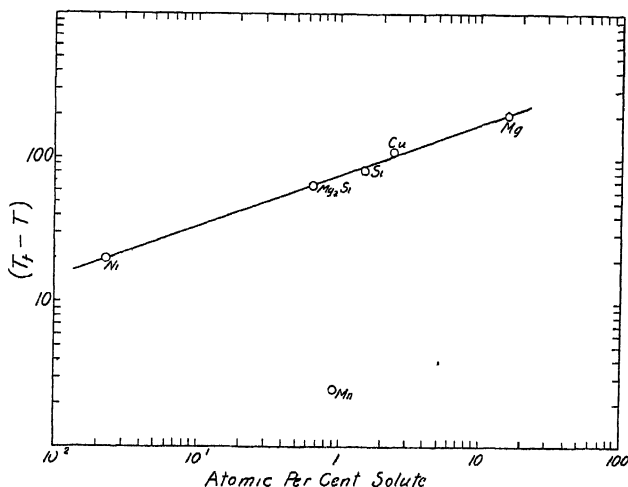


FIG 11 —RELATION OF SOLID SOLUBILITY TO EUTECTIC LOWERING.

and the temperature were considered as independent variables, it might be found that the slope of the solid solubility line for all the binary systems could be expressed in terms of these two variables. This was found to

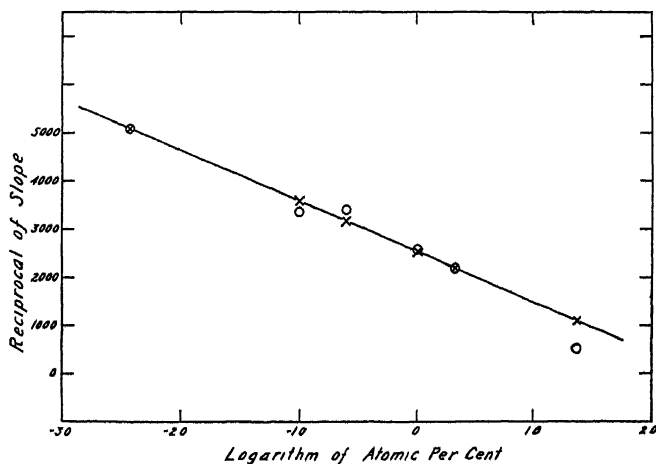


FIG. 12.—RELATION OF SLOPE OF SOLID SOLUBILITY CURVES OF DIFFERENT SYSTEMS TO ATOMIC CONCENTRATION OF SOLID SOLUTIONS ( $1/T = 0.00125$ ).

× Average estimated from curves

○ Slope calculated from two experimental points

be true, and several empirical relations and alignment charts were constructed, which gave the slope of the solid solubility line within experimental error for all of the elements, including manganese and chromium.



The most fundamental relation is probably that shown in Fig. 12, in which the reciprocal of the slope  $1/S$  is shown to be a linear function of the log of the concentration of the solute  $x'$ . By plotting different curves for a series of temperatures, the following approximate slopes

$\left(\frac{\partial \log x'}{\partial \frac{1}{S}}\right)_{\frac{1}{T}}$  are obtained.

$\frac{1}{T}$	$\left(\frac{\partial \log x'}{\partial \frac{1}{S}}\right)_{\frac{1}{T}}$
0 0011	-0 0008
0 0012	-0 0009
0 0013	-0 0010
0 0014	-0 0011
0.0015	-0 0012

by inspection:  $\left(\frac{\partial \log x'}{\partial \frac{1}{S}}\right)_{\frac{1}{T}} = 0.0003 - \frac{1}{T}$

or 
$$\frac{1}{S} = \frac{\log x'}{0.0003 - \frac{1}{T}} + K$$

If the value of  $K$  is determined for different values of  $T$  and  $\frac{1}{K}$  is plotted against  $\frac{1}{T}$ , it is found that  $\frac{1}{K}$  is a linear function of  $\frac{1}{T}$ . From the curve the value of  $\frac{1}{K}$  can readily be determined as

$$\frac{1}{K} = 0.417 \frac{1}{T} - 0.000125$$

or 
$$K = \frac{T}{0.417 - 0.000125T}$$

Therefore the slope of the solid solubility curve can be determined from any one point on the curve by substituting in the formula:

$$\frac{1}{S} = \frac{\log x'}{0.0003 - \frac{1}{T}} + \frac{T}{0.417 - 0.000125T}$$

or 
$$\frac{1}{S} = \frac{T \log x'}{0.0003T - 1} + \frac{T}{0.417 - 0.000125T}$$

It was also found that the relation of the slope of the solid solubility curve to  $\frac{1}{T}$  and  $\log x'$  could be shown very simply graphically. If all the solid solubility curves are plotted on one sheet of paper (using the coordinates previously described) the curves can all be drawn to intersect at a common point as shown in Fig 13. Knowing the point of intersection, the slope, of course, can be graphically determined from one point on the solubility curve.

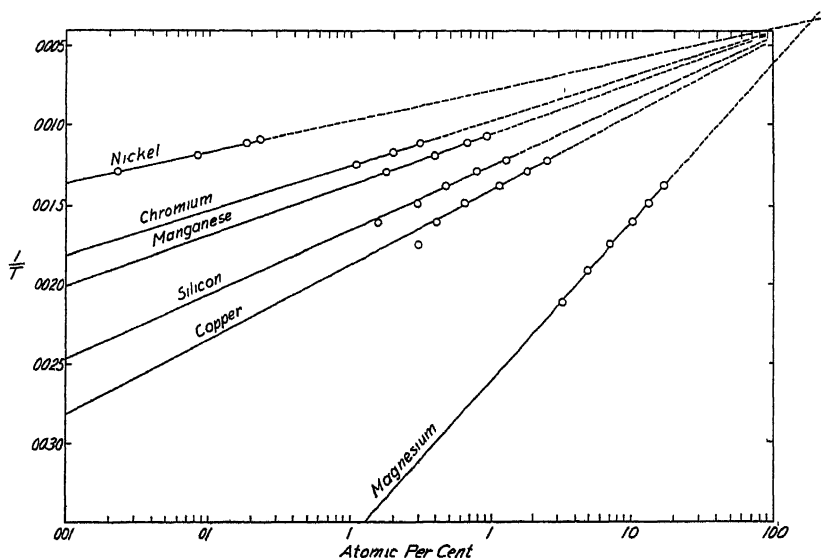


FIG 13 —SOLID SOLUBILITY CURVES OF ALL SYSTEMS, SHOWING GRAPHICALLY RELATION BETWEEN SLOPES OF DIFFERENT CURVES

In Table 1 are given the slopes determined from two experimental points, calculated by the equation from one point, and measured on the graph of Fig. 13.

#### VALUE OF ABOVE RELATIONS

The curves, tables, and equations given above furnish a very satisfactory method of summarizing the data on a series of alloy systems. Moreover, such a satisfactory agreement between the experimental data and the thermodynamic equations gives added confidence concerning the accuracy of the results.

There is also considerable theoretical significance. Although most of the solutions are so concentrated that they cannot be considered as perfect solutions, equations that were derived for perfect solutions satisfactorily generalize the data.

Not only do these relations apply to aluminum-alloy systems, but from the meager data we have they seem to apply also to other alloy

systems. Consequently they may furnish criteria to appraise data in the literature, check experimental work, and select alloy systems for careful revision.

It is also evident that equilibrium diagrams of the aluminum ends of binary aluminum systems can be drawn with a very few experimental points. Two points on the hypereutectic (or hyperperitectic) liquidus, the eutectic (or peritectic) temperature, and one point on the solid solubility curve suffice. It is believed that diagrams so constructed from a few carefully determined points, using alloys of high purity, are in general more accurate than the diagrams found in the literature summarizing work which was done with impure materials.

#### ACKNOWLEDGMENT

The authors are indebted to the many present and past members of the staff of the Aluminum Research Laboratories who have collaborated in the series of investigations that have yielded the data reviewed in this paper; to Mr. R. S. Archer and Mr. F. Keller, whose observations initiated the attempt to correlate the data, and to Mr. E. H. Dix, Jr., who has directed the work on high-purity aluminum-alloy systems since its inception.

#### REFERENCES

- 1 F. C. Frary. Electrolytic Refining of Aluminum. *Trans. Amer. Electrochem. Soc.* (1925) **47**, 275.
- 2 E. H. Dix, Jr.. Note on the Microstructure of Aluminum-Iron Alloys of High Purity. *Proc. Amer. Soc. Test Mat.* (1925) **25**, 120.
- 3 Previous publications of this series:  
 E. H. Dix, Jr. Reference 2  
 E. H. Dix, Jr. and H. H. Richardson. Equilibrium Relations in Aluminum-copper Alloys of High Purity. *Trans. A.I.M.E.* (1926) **73**, 560.  
 E. H. Dix, Jr. and W. D. Keith. Equilibrium Relations in Aluminum-manganese Alloys of High Purity. *Proc. Inst. Metals Div., A.I.M.E.* (1927) 315.  
 E. H. Dix, Jr. and A. C. Heath, Jr.. Equilibrium Relations in Aluminum-silicon and Aluminum-iron-silicon Alloys of High Purity. *Trans. A.I.M.E.* (1929) **83**, 164.  
 E. H. Dix, Jr. and F. Keller. Equilibrium Relations in Aluminum-magnesium Alloys of High Purity. *Trans. A.I.M.E.* (1929) **83**, 351.  
 E. H. Dix, Jr., F. Keller and L. A. Willey. Equilibrium Relations in Aluminum-antimony Alloys of High Purity. *Trans. A.I.M.E.* (1931) **93**, 396.  
 E. H. Dix, Jr., F. Keller and R. W. Graham. Equilibrium Relations in Aluminum-magnesium Silicide Alloys of High Purity. *Trans. A.I.M.E.* (1931) **93**, 404.  
 W. L. Fink and K. R. Van Horn. Constituents of Aluminum-iron-silicon Alloys. *Trans. A.I.M.E.* (1931) **93**, 383.  
 W. L. Fink, K. R. Van Horn and P. M. Budge. Constituents of High-purity Aluminum-titanium Alloys. *Trans. A.I.M.E.* (1931) **93**, 421.  
 W. L. Fink and K. R. Van Horn. Equilibrium Relations in Aluminum-zinc Alloys of High Purity. *Trans. A.I.M.E.* (1932) **99**, 132.

- W L Fink and H R Freche Equilibrium Relations in Aluminum-cobalt Alloys of High Purity *Trans A I M E* (1932) **99**, 141
- E H Dix, Jr, G F Sager and B P Sager Equilibrium Relations in Aluminum-copper-magnesium and Aluminum-copper-magnesium Silicide Alloys *Trans A I M E* (1932) **99**, 119
- W L Fink and H R Freche Equilibrium Relations in Aluminum-chromium Alloys of High Purity. *Trans A I M E* (1933) **104**, 325
- E H Dix, Jr, W L Fink and L A Willey Equilibrium Relations in Aluminum-manganese Alloys of High Purity, II *Trans. A I M E* (1933) **104**, 335
- W L Fink and L A Willey Equilibrium Relations in Aluminum-nickel Alloys of High Purity *A I M E Tech Pub* 569 (1934)
- 4 R S Archer Chapter III in *The Aluminum Industry* (Edwards, Frary and Jeffries) **2**, 113 New York, 1930 McGraw-Hill Book Co
- 5 Le Chatelier *Compt rend* (1894) **118**, 638, 709
- 6 Van Laar *Ztsch phys Chem* (1906) **55**, 435
- 7 Andrews and Johnston *Jnl Inst Met* (1924) **32**, 385
- 8 Yap, Chu-Phay *A I M E Tech Pubs* 381 and 397 (1931)
- 9 Tammann and Oelsen *Ztsch anorg Chem* (1930) **186**, 257

#### BIBLIOGRAPHY ON HISTORY OF APPLICATION OF THERMODYNAMIC LAWS TO ALLOY SYSTEMS

- Blagden *Phil Trans* (1788) **78**, 277
- Raoult *Compt rend* (1882) **94**, 1517; (1887) **104**, 1430, *Ann. Chim Phys* (1883) (5) **28**, 137, (1884) (6) **2**, 66, *Ztsch phys Chem* (1888) **2**, 353
- Van't Hoff *Ztsch phys Chem.* (1887) **1**, 481, (1890) **5**, 322
- Van der Waals: *Ztsch phys Chem* (1888) **2**, 463
- Tammann: *Ztsch phys Chem.* (1889) **3**, 441
- Silow *Ztsch phys Chem* (1889) **3**, 605
- Ramsay *Jnl. Chem Soc* (1889) **55**, 521.
- Meyer *Wied. Ann* (1890) **40**, 244.
- Schroeder *Ztsch. phys Chem* (1893) **11**, 449.
- Le Chatelier: *Compt rend* (1894) **118**, 638, 709
- Heycock and Neville: *Proc Roy Soc* (1896) **60**, 160, and *Jnl Chem Soc* (1890) (1897).
- Dahms: *Ann. phys. Chem* (1898) (II), **64**, 507
- Von Juptner *Stahl und Eisen* (1898) **18**, 506, 1039, and (1899) **19**, 23.
- Van Laar. *Proc K. Acad Wetensch Amsterdam* (1903) **5**, 424, and (1903) **6**, 21.
- Roozeboom Die heterogenen Gleichgewichte, pt II, 270 (1904).
- Mazzatto: *Nuovo Cim* (1907) **13**, 80; (1908) **15**, 401
- Taylor: *Jnl Amer Chem Soc* (1923) **45**, 2865
- Hildebrand, Hagness Taylor: *Jnl Amer Chem Soc* (1923) **45**, 2828.
- Andrews and Johnston: *Jnl Inst Metals* (1924) **32**, 385
- Kordes: *Ztsch anorg Chem* (1926) **154**, 93; (1927) **167**, 97; (1927) **168**, 177; (1928) **169**, 246; (1928) **173**, 1; and *Ztsch. phys Chem* (1931) **158**, 1
- Jeffery: *Trans Faraday Soc.* (1930) **26**, 86, 581-588; (1933) **29**, 550.
- Tammann and Oelsen: *Ztsch anorg Chem* (1930) **186**, 257
- Yap, Chu-Phay. *A I M E Tech Pubs* 381, 382, 397 (1931)
- Korber and Oelsen *Archiv für das Eisenhüttenwesen* (1931) **5**, 569.
- Wagner and Engelhardt *Ztsch phys Chem* (1932) **159**, 241
- Seltz. *Jnl Amer Chem Soc.* (1934) **56**, 307.

## DISCUSSION

(*Kent R. Van Horn presiding*)

R. F. MEHL,\* Pittsburgh, Pa.—I think there is no question that generalizations like this are extremely useful. I think that Dr. Fink and I agreed in discussion that it should not be implied that the solutions concerned are ideal, the method used is essentially a difference method, giving no information on the ideality of the solutions. If such generalizations as this can be made for aluminum alloys, can they also be made for alloys of other base metals?

W. L. FINK.—Nothing very extensive has been tried along that line, but at one time in connection with work we were doing on solders for aluminum, we attempted to get information on some of the equilibrium diagrams of the metal systems involved. We tried this method and as far as we could crosscheck, we seemed to get very good results. I am not prepared to say definitely that these generalizations do apply to other systems.

L. W. MCKEEHAN,† New Haven, Conn.—I think we should be very careful in dealing with empirical formulas, no matter how well they fit over a limited range, when it comes to extrapolation. In particular is that true in the case of a logarithmic formula, where the quantity of which the logarithm is taken has physical limitations, like atomic per cent. Therefore, perhaps we should not be surprised on the last diagram to see an important intersection occurring at perhaps 120 atomic per cent, which would otherwise alarm us. This is merely a plea for care in applying empirical formulas beyond the range in which their validity seems to fit.

I have no doubt as to the usefulness of these formulas, agree that they are entirely justified over the range of compositions dealt with, and over some range on each side of it, but extreme extrapolation here, as everywhere, is dangerous.

A. J. FIELD,‡ New York, N. Y.—I was interested to see in the logarithmic curves that apparently you get zero solubility at a certain temperature. In the case of silicon it appeared to me to be 300°, which is about what one would expect from electrical conductivity measurements.

Have you any correlation on the temperature at which you get zero solubility with all of these various constituents? It seems to me that the method is extremely useful in so far as simple diagrams, such as the aluminum diagrams that were shown, are concerned. But in a complicated system, such as the copper-zinc system, for instance, where there are useful alloys extending over a great part of the entire range, I would suppose that the method would not be so easy to apply.

W. L. FINK.—Since these curves are plotted on a logarithmic scale, the temperature necessary to get zero solubility depends upon the value selected to represent zero solubility. A selection of different values, such as  $\frac{1}{100}$  or  $\frac{1}{1000}$ , or  $1/10,000$  atomic per cent, makes quite a difference in the temperature.

---

\* Director, Metals Research Laboratory, and Professor of Metallurgy, Carnegie Institute of Technology.

† Director, Sloane Physics Laboratory, Yale University.

‡ The British Aluminum Company Limited

# The Lithium-magnesium Equilibrium Diagram\*

By OTTO H. HENRY AND HUGO V. CORDIANO, BROOKLYN, N. Y.

(New York Meeting, February, 1934)

THE purpose of this investigation was to determine the equilibrium diagram of the lithium-magnesium pair as a first step in studying the possible usefulness of these alloys as ultra-light structural materials.

## REVIEW OF THE LITERATURE

The behavior of lithium towards magnesium was first investigated by Masing and Tammann.<sup>(1)†</sup> In order to prevent oxidation the alloys were made in iron tubes under an atmosphere of hydrogen; temperatures were measured with a glass-protected thermocouple. These investigators found that lithium and magnesium form two series of solid solutions separated by a miscibility gap between 85 and 95 per cent magnesium; that the alloys with 81 and 95 per cent magnesium showed a homogeneous structure under microscopic examination, while the alloy with 89 per cent magnesium contained two distinguishable crystallites; that the curve indicating the beginning of crystallization rises from the melting point of lithium to that of magnesium; and that no compounds of lithium and magnesium are formed. The equilibrium diagram was not plotted because no definite data were obtained for determining the solidus and the position of the miscibility gap in the solid state. The difficulties encountered in this investigation were: (1) that it was necessary to heat them as high as the melting point of magnesium in order to obtain homogeneous melts, at such temperatures the alloys attacked the glass protecting the thermocouple; and (2) that at temperatures above 400° C. the lithium united with the hydrogen to form lithium hydride, thus contaminating the alloys. By applying the same methods as those used in the lithium-magnesium system, Masing and Tammann determined the equilibrium diagram of the

---

\* Abstract of a thesis presented by Hugo V. Cordiano in partial fulfillment of the requirements for the degree of Bachelor of Mechanical Engineering at the Polytechnic Institute of Brooklyn, and done under the direction of Otto H. Henry, Assistant Professor of Mechanical Engineering. This thesis was conducted under a scholarship grant of the New York Chapter of the American Society for Steel Treating and in 1933 was awarded the annual prize of the American Society of Mechanical Engineers for the best student paper.

Manuscript received at the office of the Institute Sept. 29, 1933

† References are to bibliography at end of paper

lithium-sodium, lithium-potassium, lithium-cadmium, and lithium-tin systems<sup>(2)</sup> of alloys

In the thermal analysis of the lithium-copper system, S. Pastorello<sup>(3)</sup> used a method similar to that used by Masing and Tammann. The lithium-copper alloys were prepared by fusion in a Ni-Cr steel crucible under an atmosphere of argon, and the cooling curves were obtained by temperature measurements with a Pt-PtRh thermocouple and a Hartman and Braun galvanometer. Several preliminary fusions were carried out until the contamination of the alloys by the Ni-Cr steel crucible was such that no appreciable error in the temperature measurements was introduced. The system was checked by an X-ray examination of the alloys. Pastorello also determined the lithium-silver diagram<sup>(4)</sup> by applying the same two methods that were used in his previous analysis of the lithium-copper system.

Another method of making lithium alloys was used by W. Fraenkel and R. Hahn in their investigation of the lithium-zinc system.<sup>(5)</sup> Zinc alloys containing up to 9 per cent lithium were melted in a porcelain crucible lined with magnesia under a protective flux of lithium chloride and lithium carbonate. The zinc was first melted; lithium was then introduced under the surface to prevent loss by oxidation. Higher lithium alloys were not made because they are brittle and tarnish rapidly.

This review of the literature on the behavior of lithium towards other metals suggests two possible methods of making lithium-magnesium alloys. The first method is to use a controlled atmosphere, the second is to use a protective flux. These methods will be considered later.

#### APPARATUS AND MATERIALS USED IN PRESENT INVESTIGATION

In the present investigation, the alloys were melted in a small low-pressure gas furnace. An electric furnace of the resistance type was used to obtain heating and cooling curves. This gave an average heating rate of about 8° C. per minute and a cooling rate of about 7° C. per minute.

For the determination of temperatures, a chromel-alumel thermocouple of 20-gage wire was employed together with a 1000-ohm internal resistance Thwing millivoltmeter. A millivoltmeter was used instead of a potentiometer because it provides continuous temperature indication and is easily manipulated. The thermocouple tip was not placed in direct contact with the alloys but was inserted in an iron tube, for reasons that will be explained later. The wires near the welded tip of the thermocouple were insulated from each other and from the iron tube by whipping them together with a figure-eight winding of asbestos cord, leaving  $\frac{1}{2}$  in. of the tip free to make contact with the walls and bottom of the iron tube. The protecting tubes were made with a diameter of 0.2 in. and a wall thickness of 0.01 in. A calibration of the thermocouple when the

tip was in direct contact with the molten metals showed a difference of about  $1^{\circ}\text{C}$  at the melting point of tin and  $2.5^{\circ}\text{C}$  at the melting point of magnesium, the direct contact giving the higher readings. However, the use of the iron tube did not introduce any error in the results of this investigation because the calibration curve was obtained for the same conditions that were used in determining the critical points of the alloys.

Magnesium was supplied by the Dow Chemical Co., Midland, Mich., and had the following composition: Mg, 99.910 per cent; Al, 0.028, Fe, 0.035; Si, 0.020, Ni, 0.003, Mn, 0.004. Lithium, supplied by the Maywood Chemical Works, Maywood, N. J., was 99.9 per cent + lithium.

### DEVELOPMENT OF METHOD OF PREPARING ALLOYS

The method of making alloys of lithium and magnesium depends wholly upon the properties of these metals. When lithium is heated in air, it burns quietly with a bright flame yielding  $\text{Li}_2\text{O}$ , and at a red heat it unites with hydrogen, forming  $\text{LiH}$ , which is quite stable. It also unites with nitrogen, forming  $\text{Li}_3\text{N}$ , and it burns when heated in chlorine, bromine, iodine, sulfur vapor or dry carbon dioxide. Lithium has an atomic weight of 6.94, a specific gravity of 0.534, a melting point of  $186^{\circ}\text{C}$  and a boiling point of  $1400^{\circ}\text{C}$ . Magnesium melts at  $651^{\circ}\text{C}$  and boils at  $1120^{\circ}\text{C}$ . The specific gravity is 1.74 and its atomic weight is 24.32.

The oxidizing tendency of lithium and of magnesium demands a method of making the alloys that will keep them from burning at elevated temperatures. Previous investigators fulfilled this requirement by using a controlled atmosphere or a protective flux. In investigations where a protective flux was used alloys higher than 12 per cent lithium were not made.

In the present investigation an attempt was made to use a flux for making lithium-magnesium alloys. In selecting such a flux it is necessary to select salts in which the metal radicals are electropositive to lithium. If this is not done, the lithium will replace the metals that are electronegative to itself in their salts; this will introduce a loss of lithium and bring about a contamination of the alloys with the displaced metals. This fact materially limits the salts that can be used as a flux.

The equilibrium diagrams of the salts of metals electropositive to lithium were reviewed and it was found that potassium and sodium chlorides form a series of solid solutions with a minimum melting point of  $661^{\circ}\text{C}$  at 50 mol per cent of sodium chloride; that lithium and sodium chlorides form a series of mixed crystals with a minimum melting point of  $552^{\circ}\text{C}$  at 50 mol per cent of sodium chloride, and that lithium and potassium chlorides form a simple eutectic system with a eutectic melting temperature of  $361^{\circ}\text{C}$  and a eutectic composition of 58 mol per cent of potassium chloride. The eutectic composition of the combina-



tion last mentioned appeared to be a good mixture for a flux from the standpoint of the low melting point and the stability of the salts at higher temperatures

Alloys of 5 and 10 per cent lithium were made by melting the metals in a nichrome crucible under a protective flux of lithium chloride and potassium chloride. The lithium was introduced under the surface of the molten magnesium in capsules made from magnesium rod. An examination of vertical sections of these alloys under the microscope showed that the 10 per cent lithium alloy was slightly segregated in spite of the stirring that it received in the molten state. The low specific gravity of lithium caused the upper part of the alloy to be higher in lithium than the lower. The flux served its purpose by completely surrounding the molten mass in spite of its slightly greater specific gravity. However, on making alloys of 15, 20 and 25 per cent lithium, segregation increased with the rise in lithium content, and the 20 and 25 per cent alloys oxidized rapidly on stirring. This experience indicated that it would be impossible to make

higher lithium alloys by this method, but it established the fact that this flux can be used for making these alloys up to about 15 per cent lithium if the proper alloying technique is employed.

The elimination of the method of using a flux suggests trial of the possibilities of using a controlled atmosphere of inert gas, or the use of a vacuum. Knowing the chemical activity of lithium with gases such as hydrogen, nitrogen and carbon dioxide, it follows that the use of argon or helium remains. The use of a vacuum was not considered

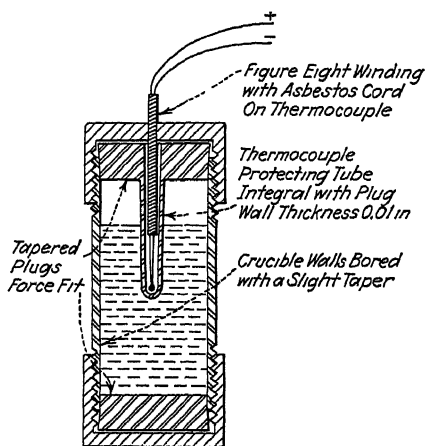


FIG 1—SKETCH OF CRUCIBLE USED IN MAKING LITHIUM-MAGNESIUM ALLOYS

since magnesium vaporizes rapidly in a vacuum at elevated temperatures

However, a satisfactory method of preparing the alloys was developed which required neither an inert gas nor a vacuum. This method consisted essentially of melting the alloys in a sealed low-carbon steel crucible in which at least 80 per cent of the air had been displaced by the component metals. A sketch of this crucible is shown in Fig 1, which also indicates the provision for measuring temperatures. The following reasons justify this method of preparing the alloys.

- 1 The calibration curves show that the measurements of temperature through an iron tube were in very close agreement with those taken with the thermocouple tip in direct contact with the molten metals. It follows,

therefore, that pressure variations within the crucible are too small to affect the temperature of the thermal arrest points

2 When the crucibles were opened the surface of the high-lithium alloys was bright, but shortly after exposure to the air they began to tarnish.

3 It was possible to heat the alloys to high temperatures and shake them well, thereby forming homogeneous melts

4 The solid alloys were homogeneous and showed no signs of being oxidized any more than would be expected from the small amount of air entrapped in the crucible. A simple calculation shows that if all the entrapped air were nitrogen and reacted only with lithium, which is the worst condition, 0.003 grams of lithium would be lost, an amount that is insignificant when compared to the weight of the alloys employed

5 Chemical analysis showed the alloys to have a composition that checked very closely with the as-weighed composition. This check showed that there were no losses of either lithium or magnesium. A test for iron showed the presence of only a trace of that metal

The progress of this work was considerably retarded, because in most cases the thermocouple protecting tubes broke when an attempt was made to get them out of the solidified alloys. The protecting tubes were made integral with the plugs so that an extra joint would be eliminated. The tube walls could have been made thicker, but this was not done because it would have obliterated the sharpness of the breaks in the heating and cooling curves

#### PREPARATION OF ALLOYS

The fact that lithium is very ductile made it possible to fill the crucible with the component metals so that most of the air was displaced. During this operation the plug with the iron tube was in place, and the second plug was forced into the other end of the crucible after it had been filled with the desired weights of the metals. The force applied to the tapered plugs caused a very tight fit. All alloys made had approximately the same volume and varied in weight from 35 grams at the magnesium end of the series to 15 grams at the lithium end. After the ends of the crucible were capped the whole unit was placed in a gas furnace and heated to about 700° C. The mixture was held at this temperature for about 15 minutes, during which time the alloy was shaken well and turned over at intervals of a few minutes. The crucible containing the molten alloy was then placed in an electric resistance furnace, which had been heated to 700° C, and allowed to cool. The thermocouple tip was inserted into the protecting tube while at 700° C. so that temperature-time readings could be obtained during the cooling

## HEATING AND COOLING-CURVE DATA

The collection of cooling-curve data consisted of recording a series of temperature time readings. Time and millivoltmeter readings were recorded at intervals of 0.2 mv (approximately  $5^{\circ}\text{C}$ ) and the curves were plotted during the cooling. When a temperature arrest point was reached, readings were taken at more frequent intervals. In most cases the cooling curves were obtained twice for the same alloy and the critical temperatures checked exactly in almost every alloy. In alloys in which the agreement was not exact the greatest difference was found to be about  $2^{\circ}\text{C}$ . Cooling curves for 38 alloys were obtained by this method.

After a few cooling curves had been collected it was found that they gave no clear indication of the solidus outside of the range from 5 to 10 per cent lithium. It was necessary, therefore, to apply some other method for determining the solidus. The quenching method was eliminated with little consideration. This method consists of heating an alloy to some elevated temperature, quenching it from that temperature in some cold medium, and examining the polished specimen under the microscope. If the structure shows no sign of being quenched from above the solidus, the alloy is reheated to a higher temperature, quenched, polished, and again examined under the microscope. This process is repeated until the polished specimen gives an indication that it was quenched from above the solidus line. The reason for not using this method in determining the solidus for lithium-magnesium alloys is that the alloys above 15 per cent lithium are difficult to polish and that they react with water.

The method of determining temperature arrest points from heating curves was next tested by running heating curves for pure zinc and pure magnesium. The heating-curve points were found to check exactly with the cooling-curve points. These results led to the adoption of this method for determining the solidus. To obtain a good heating curve it was necessary to heat the specimen uniformly and to raise the temperature at a steady rate. The electric resistance furnace used for this work fulfilled these requirements. This method of determining the solidus was found to be convenient, for on completing a cooling curve a heating curve was obtained by reheating the same alloy and recording the necessary data. A second cooling curve was then obtained by recording data during the second cooling. Heating curves for 26 alloys were obtained by this method. The heating-curve and cooling-curve data are given in Table 1.

The thermal curves for the alloys between 25 and 50 per cent lithium showed weak but definite temperature-arrest points, but this is to be expected because the solidification range in those alloys is wide. Thirteen heating and cooling curves were obtained with the aid of a Leeds & Northrup recording potentiometer in order to confirm the results obtained

by the millivoltmeter method. The temperature-arrest points obtained by this method checked closely those obtained by the other method

TABLE 1 — *Results of Thermal Analysis by Millivoltmeter*

Alloy No	Li, Per Cent by Wt	Liquidus, Deg C	Transition, Deg C	Solidus, Deg C
1	2 1	638		
2	2 6	635		617
3	3 85	622		606
4	4 0	618		
5	4 85	615		590
6	6 0	608	591	591
7	6 57	607	590	590
8	7 05	602	589	589
9	7 51	598	593	593
10	8 0		591	591
11	9 0		591	591
12	9 93		591	591
13	10 5		591	588
14	11 0		591	
15	11 5		591	581
16	12 5		593	577
17	13 1	589		
18	13 4	590		573
19	14 1	586		566
20	15 0	581		
21	16 0	578		542
22	17 8	567		514
23	20 2	555		
24	24 9	517		413
25	30 7	472		
26	33 0	453		329
27	38 0	419		295
28	39 6	407		288
29	46 0	362		262
30	55 0	306		235
31	60 0	282		227
32	64 8	262		219
33	70 5	245		210
34	75 1	234		206
35	80 0	226		204
36	85 0	218		200
37	90 0	211		194
38	94 4	201		193

Temperature measurements by the millivoltmeter method were found to be more consistent than those obtained with the recorder because in the latter method the paper might shift on the rotating drum. These data are given in Table 2.

TABLE 2—*Results of Thermal Analysis by Recording Potentiometer*

Alloy No	Li, Per Cent by Wt	Liquidus, Deg C	Transition, Deg C	Solidus, Deg C
39	3 86	620		604
40	5 6	606	588	
7	6 57	603	588	
41	8 55	596	591	
16	12 5		591	581
18	13 4	587		570
19	14 1	587		565
42	19 0	558		499
43	26 9	501		389
44	36 8	421		304
45	50 0	335		246
46	76 3	222		202

TABLE 3—*Alloys Used for Heat Treating*

ALLOY No	Li, Per Cent by Wt
47	5 05
6	6 00
48	10 00
49	10 20
50	10 40

## MICROSCOPIC EXAMINATION

The preparation of specimens for microscopic examination was carried out in three stages. first, a flat surface was obtained by filing, second, the surface was ground on Nos. 1, 0, 00 and 000 emery paper to a fair degree of smoothness, and third, the specimen was polished on a wet, rotating felt-covered disk, rouge being used as the polishing medium. The surface obtained by polishing showed very fine scratches which were easily removed by etching with a 10 per cent solution of nitric acid in alcohol. Many different etching reagents were experimented with, and a dilute ammonium chloride solution gave the best results. The etching process consisted, therefore, of removing the scratches with nitric acid followed by an ammonium chloride etch to contrast the two phases.

The alloys, which were slowly cooled to room temperature, showed under microscopic examination that lithium and magnesium form a solid solution, alpha, up to 4.9 per cent lithium, that above 4.9 per cent lithium a second phase, beta, begins to appear as a broken network around the crystals of alpha, that as the percentage of lithium increases the beta phase increases until the 10.5 per cent alloy shows very few small crystals of the alpha phase in the grain boundaries and within the beta crystals. The alloys containing from 10.9 to 15 per cent lithium showed only the beta phase. Alloys above 15 per cent lithium were not studied micro-

scopically because they tarnish in the air and react with water. A series of photomicrographs of the alloys is shown by Figs 2 to 9 inclusive.

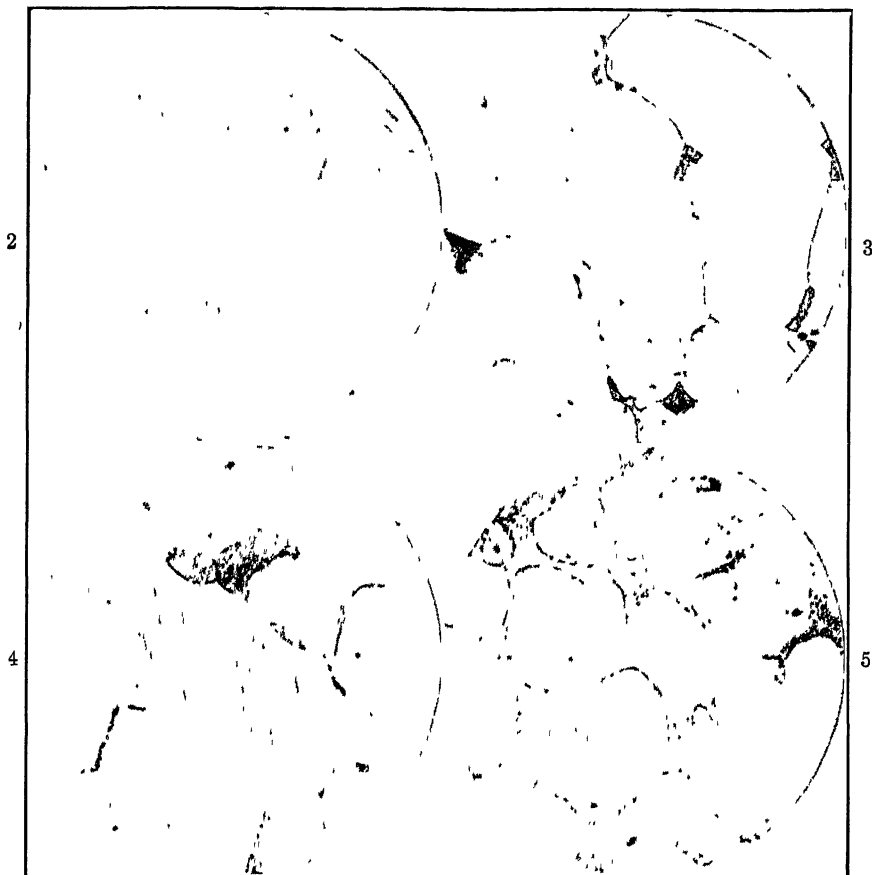


FIG 2—LITHIUM, 4 PER CENT. STRUCTURE SHOWS CRYSTALS OF ALPHA SOLID SOLUTION. NITRIC ACID ETCH.  $\times 100$

FIG. 3—LITHIUM, 5.05 PER CENT. BROKEN NETWORK OF BETA BEGINS TO SURROUND ALPHA CRYSTALS.  $\times 100$

FIG 4—LITHIUM, 6 PER CENT. LIGHT CONSTITUENT IS PRIMARY ALPHA, DARK CONSTITUENT, BETA SOLID SOLUTION.  $\times 100$

FIG 5—LITHIUM, 7 PER CENT. PRIMARY CRYSTALS OF ALPHA SURROUNDED BY A NETWORK OF BETA.

Figs 3, 4, 5 ammonium chloride on nitric acid etch

#### DETERMINATION OF SOLUBILITY LIMITS IN SOLID STATE

From the microscopic examination of adjacent alloys the percentage composition of the solid solubility limits at room temperature was determined by interpolation to be 4.9 per cent lithium for the alpha phase and 10.6 per cent lithium for the beta phase. (See Fig 9 for representative microstructure.) In order to determine these limits for higher temperatures the following quenching experiments were conducted.

Alloys containing 5.05, 6.0, 10.0, 10.2 and 10.4 per cent lithium were heated to  $400^{\circ}\text{C}$ , held at that temperature for  $2\frac{1}{2}$  hr and quenched in water. A second set of these same alloys was heated to  $550^{\circ}\text{C}$ , held at that temperature for  $1\frac{1}{2}$  hr and quenched in water. A third set of



FIG 6—LITHIUM, 8.5 PER CENT. DARK CONSTITUENT IS BETA SOLID SOLUTION, LIGHT CONSTITUENT IS ALPHA.  $\times 100$

FIG 7—LITHIUM, 9 PER CENT. DARK CONSTITUENT IS BETA SOLID SOLUTION, LIGHT CONSTITUENT IS ALPHA.  $\times 100$

FIG 8—LITHIUM, 9.9 PER CENT. ALPHA CRYSTALS IN A MATRIX OF DARK BETA SOLID SOLUTION.  $\times 100$

FIG 9—LITHIUM, 10.4 PER CENT. HELD AT  $550^{\circ}\text{C}$  FOR  $1\frac{1}{2}$  HR AND QUENCHED IN WATER.  $\times 500$

Ammonium chloride on nitric acid etch

the same alloys and one containing 5.6 per cent lithium were heated to  $580^{\circ}\text{C}$ , held at that temperature for 2 hr. and quenched in water. During each heat treatment the alloys were heated under a flux of lithium and potassium chlorides to prevent oxidation. After each quenching the alloys were polished and examined under the microscope. The 5.05,

5.6 and 6.0 per cent lithium alloys showed no change on being quenched from all temperatures up to 580° C, indicating that the solid solubility line for the alpha phase is nearly vertical.

In heat-treating the 10.0, 10.2 and 10.4 per cent lithium alloys for determining the limits of solid solubility of the beta phase, intracrystalline precipitation appeared in all the quenched specimens. This precipitation indicated that some alpha had been dissolved by the beta phase at elevated temperatures, and that the quenching was not drastic enough to prevent precipitation at ordinary temperatures. The following results led to the conclusion that the limit of solid solubility of the beta phase is virtually a straight line from 10.6 lithium at room temperature to 9.9 per cent lithium at 591° C. The alloys containing 10.0, 10.2 and 10.4 per cent lithium showed primary crystals of alpha before heat treating. On quenching from 550° C the 10.0 per cent alloy was the only one to show primary alpha crystals. No trace of alpha crystals was found in these alloys when quenched from 580° C. This structure is illustrated by Fig. 9.

#### CHEMICAL ANALYSIS

In making the alloys of lithium and magnesium, losses by oxidation and vaporization were prevented by the use of an enclosed crucible. Each of the resulting alloys, therefore, should have had a composition corresponding to the weights of the component metals used. This was proved to be true by the chemical analysis of a few alloys and therefore it was not necessary to analyze all of them. Before any analysis could be made, however, it was necessary to find a method of separating these metals quantitatively.

TABLE 4 — *Magnesium Analyses by Multiple Precipitation Method*

Mg as Weighed, Per Cent	Per Cent Mg by First Precipitation	Per Cent Mg by Second Precipitation	Per Cent Mg by Third Precipitation
94.79	96.25	94.95	94.95
94.79	96.27	94.95	94.94
89.8	90.25	89.86	89.84
89.8	90.30	89.88	89.84

The difficulty of separating lithium and magnesium is mentioned in many textbooks, together with the fact that lithium does not behave like the other alkali metals but more like magnesium. A survey of the literature showed that many attempts to analyze for lithium in the presence of magnesium were successful only for small amounts of the metal. However, Dinwiddie<sup>(6)</sup> employed a multiple precipitation method which was found to be satisfactory. Representative results obtained by this method of analysis are shown in Table 4. These results show that the



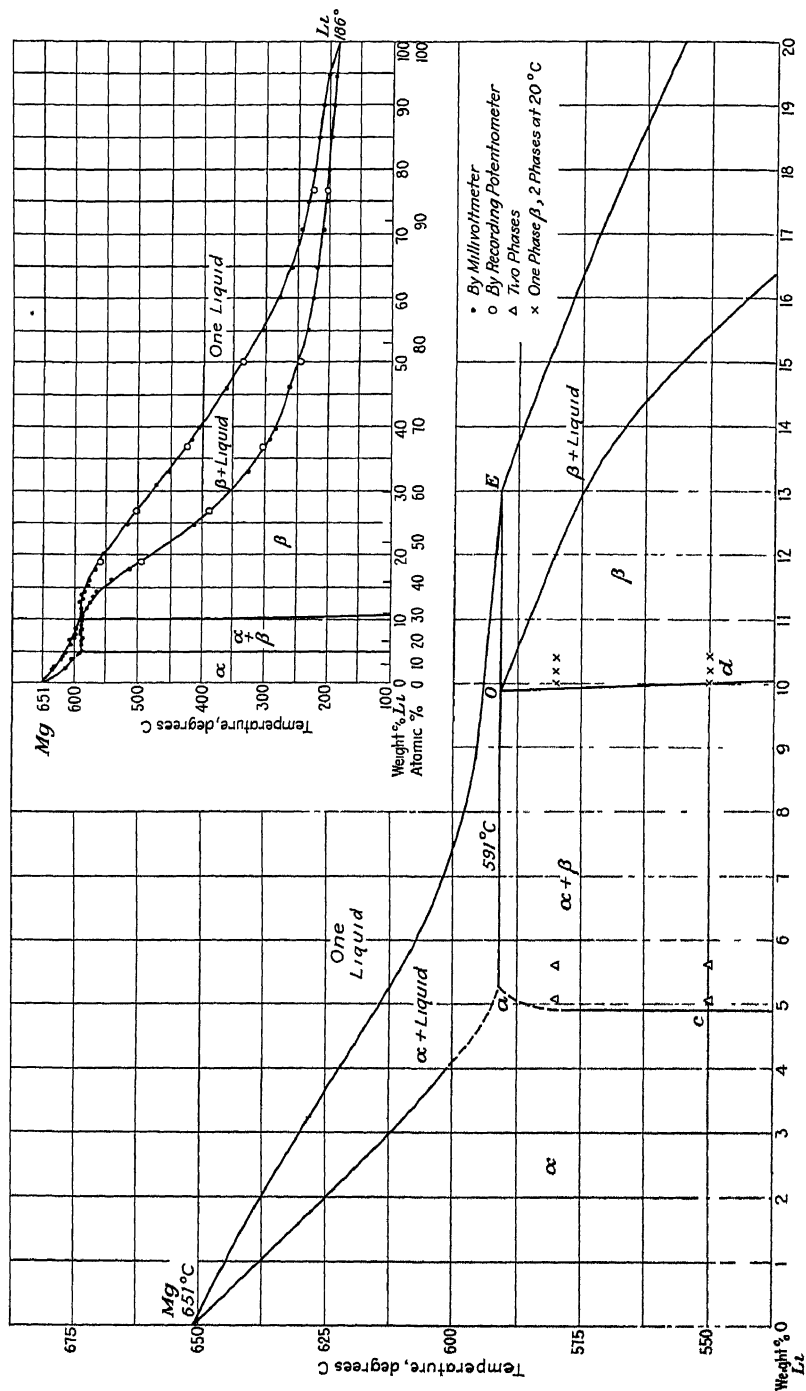


Fig 10—CONSTITUTION OF LITHIUM-MAGNESIUM ALLOYS

as-weighed composition is accurate to within the limits of experimental error

### THE EQUILIBRIUM DIAGRAM

The results of the series of experiments mentioned in the foregoing sections are plotted in Fig 10. It is to be seen that lithium and magnesium are soluble in the liquid state and partially soluble in the solid state, and that the curves of primary solidification intersect at a transition point *E*, corresponding to the "peritectic reaction"

### SUMMARY AND CONCLUSION

The equilibrium diagram for the lithium-magnesium system of alloys has been determined. The liquidus was obtained from a series of cooling curves, the solidus from a series of heating curves, and the limits of solid solubility from a series of heat-treating and quenching experiments. While it is probable that the time of annealing was not sufficiently long to obtain equilibrium, it is felt that the solid solubility limits as indicated are substantially correct. The diagram shows that lithium and magnesium are completely soluble in the liquid state, that they are partially soluble in the solid state, and that there is a transition where a peritectic reaction takes place.

Having determined the equilibrium diagram, the next step will be an investigation of the mechanical properties of these alloys and the possibility of improving them by mechanical working and heat treating. Results of such an investigation, which is now in progress, will be published later.

### BIBLIOGRAPHY

- 1 and 2 G. Masing and G. Tammann. The Behavior of Lithium Towards Sodium, Potassium, Tin, Cadmium, and Magnesium. *Ztsch f anorg Chem* (1910) **67**, 183-199.
- 3 S. Pastorello. Thermal Analysis of the System Lithium-copper. *Gazz Chim Ital* (1930) **60**, 988-992; *Chem Abs* (1931).
- Thermal Analysis of the System Lithium-silver. *Idem* (1931) **61**, 47-51; *Chem Abs* (1931).
- 4 S. Pastorello. Röntgenographic Analysis of the System Lithium-silver. *Gazz Chim Ital* (1930) **60**, 493-501; *Chem Abs* (1931).
- 5 W. Fraenkel and R. Hahn. The Constitution of Zinc-lithium Alloys. *Metallwirtschaft* (1931) **10**, 641-642; *Chem Abs* (1931).
- 6 Dunwiddie. The Separation of Lithium from Magnesium by Means of Ammonium Carbonate in Alcoholic Solution. *Amer Jnl Sci* (1915) **25**, 662.
- 7 J. Czochralski and E. Rassow. Binary Alloys of Lead and Lithium. *Ztsch f Metallkunde* (1927) **11**, 111-112; *Chem Abs* (1927).
- 8 P. Assmann. Improving Lithium-aluminum Alloys. *Ztsch f Metallkunde* (1926) **18**, 51-54; *Chem Abs* (1926).
9. J. A. Gann. Magnesium Industry's Lightest Structural Metal. *Jnl Soc Automotive Engrs.* (1931).

- 10 H P Pulsifer Magnesium—Its Etching and Structure *Trans A I M E* (1928) 78, Inst Metals Div, 461
- 11 G K Burgess On Methods of Obtaining Cooling Curves *U S Bur Stds*, 5, Reprint 99
- 12 G H Gulliver Metallic Alloys; Their Structure and Constiuction Griffin London, 1919
- 13 L Guillet and A Portevin Introduction to the Study of Metallography and Macrography Bell London, 1922

## DISCUSSION

(*Wheeler P Davey presiding*)

J A GANN,\* Midland, Mich —This piece of work covers a series of alloys regarding which we have had very little information in the past There are one or two specific questions I would like to ask, more from the practical standpoint It was pointed out in the text that alloys containing approximately 15 per cent or more lithium were fairly rapidly attacked by water during the polishing operation Have any experiments been made to determine the stability of alloys containing smaller amounts of lithium? The work indicates that probably such alloys with smaller amounts of lithium, particularly in the region of solid solution, might be used from a constructional standpoint

H V CORDIANO —The alloys seemed to be fairly stable at 5, 6, 7, up to 10 per cent lithium In some cases, when we made the alloys in a flux and some of the flux remained on the alloy, oxidation continued rapidly through the flux As we know, if any salts remain in the alloys they oxidize or corrode rapidly No tests have been made on the low-lithium alloys, but that work is now being done I cannot say anything with regard to the strength of the alloys in that range

J A GANN —Were the alloys containing 5 to 7 per cent lithium as stable as pure magnesium?

H V CORDIANO —From the work I have done, it seems that way I have had some pure magnesium in contact with the same flux after having melted it, and it corroded as much as the other alloys did

W P DAVEY,† State College, Pa —Have you any information as to the chemical nature of the alloys? Have you any evidence as to whether the lithium and the magnesium tend to react together, or do you have evidence that they remain as separate chemical entities?

O H HENRY —I have no particular evidence, but from the appearance of the microstructure, it looks as though distinct solid solutions are formed and, according to other investigators, no chemical compounds are formed Masing and Tammann and some others also considered that phase of it

At approximately 10 per cent lithium the alloy is quite stable. I have some small pieces more than two years old, which have been handled more or less continuously, and they still show some luster From that standpoint, they really look better than unalloyed magnesium

---

\* Metallurgist, Dow Chemical Co

† Professor of Physical Chemistry, Pennsylvania State College

## Notes on the Cadmium-nickel System

BY CARL E SWARTZ\* AND ALBERT J PHILLIPS,\* MAURER, N J

(Detroit Meeting, October, 1933)

IN the course of a recent investigation<sup>1</sup> to develop a more satisfactory white-metal bearing alloy, a number of alloy systems were studied. The cadmium-nickel system showed characteristics desirable in a bearing alloy, and the system was therefore studied in some detail.

### EXPERIMENTAL METHOD

Alloying cadmium with nickel offered no serious difficulty. After melting the cadmium, clean sheet nickel was added while the temperature was maintained at 500° to 600° C. A few crystals of ammonium chloride<sup>2</sup> served to clean the nickel when the latter did not "wet" readily.

In preparing the individual alloys for thermal and microscopic investigation, a "hardener" containing about 10 per cent nickel was used.

### THERMAL EXPERIMENTS AND APPARATUS

Time-temperature cooling curves were made by standard methods. Globe electrolytic cadmium was added to the hardener to make a melt of the desired composition weighing between 100 and 200 grams. This charge was placed in a Pyrex test tube, 1 by 10 in., closed with a rubber stopper carrying a thermocouple sheath and quartz stirring rod. The assembly was lowered to a depth of about 4½ in. into an electric resistance pot furnace containing a No. 0000 clay-graphite crucible (to catch the melt in case of a break in the test tube). After the tube was clamped in this position, an asbestos-magnesia mixture was loosely packed in the furnace around the tube and a "halved" cover of transite placed on top. This left at least 5 in. of the test tube protruding from the furnace.

When the alloy had melted, the thermocouple was adjusted so that the hot junction was ½ in. from the bottom of the test tube. The melt was stirred thoroughly for several minutes to insure composition homogeneity and absence of thermal gradients.

---

Manuscript received at the office of the Institute June 15, 1933

\* Central Research Laboratory, American Smelting and Refining Co.

<sup>1</sup> C. E. Swartz and A. J. Phillips. A Comparison of Certain White-metal Bearing Alloys, Particularly at Elevated Temperatures. Amer. Soc. Test. Mat. *Preprint* 30 (1933).

<sup>2</sup> Where larger quantities of alloy were desired a zinc chloride flux was used. Analyses of these lots showed a zinc content in the order of 0.01 per cent.

The thermocouple sheath and stirrer were made from quartz tubing of  $\frac{1}{16}$ -in bore, thin wall, satin surface. The thermocouple elements were 0.010-in diameter, platinum-platinum 10 per cent rhodium wire. Insulation inside the sheath was effected by thin glass tubing drawn to fit over the wire snugly. The cold junction (in a water-filled vacuum bottle) was connected through mercury contacts to potentiometer leads. The potentiometer used read directly to 0.05 millivolt.

During cooling a one-minute cycle was used. Stirring was carried out for 15 sec using a frequency of about 160 strokes per minute, and an

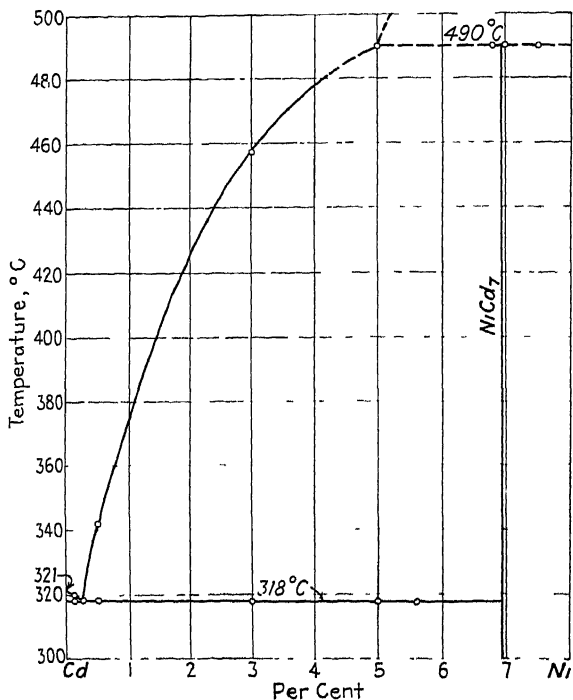


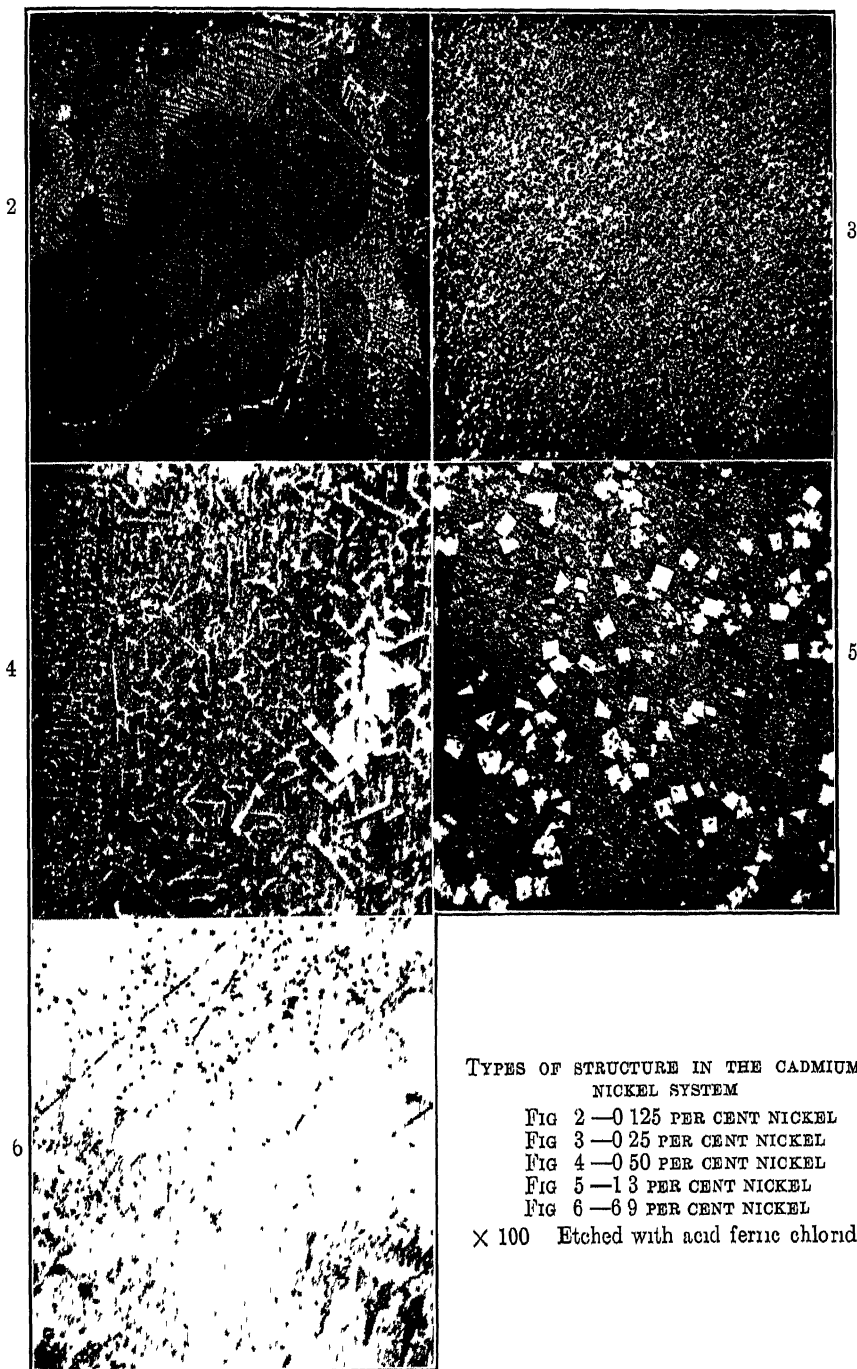
FIG 1—CONSTITUTIONAL DIAGRAM OF THE CADMIUM-RICH END OF THE SYSTEM CADMIUM-NICKEL

amplitude such that the stirrer would just reach the surface of the melt each stroke. After a 30-sec interval, the potentiometer was read. The data were plotted in the conventional time-temperature curves and liquidus critical points were detected by slight changes of slope. Microstructures consistent with the thermal data were obtained in every case.

#### DISCUSSION OF DATA

Certain differences were noted between the constitution diagram as published by Voss,<sup>3</sup> and the data obtained in the present investigation.

<sup>3</sup> Voss *Zisch. f. anorg. Chem.* (1908) **57**, 34.



TYPES OF STRUCTURE IN THE CADMIUM-  
NICKEL SYSTEM

FIG 2—0.125 PER CENT NICKEL

FIG 3—0.25 PER CENT NICKEL

FIG 4—0.50 PER CENT NICKEL

FIG 5—1.3 PER CENT NICKEL

FIG 6—6.9 PER CENT NICKEL

× 100 Etched with acid ferric chloride

1. A eutectic melting at  $318^{\circ}$  C. was found at 0.25 per cent Ni.

2. The compound is richer in cadmium than indicated by the formula  $\text{NiCd}_4$ , and if simple in composition has a formula of  $\text{NiCd}_7$ .

Fig. 1 shows the constitutional diagram and data as far as the investigation has been carried. The dotted portions are beyond the limit of usefulness of the alloy for bearings and have been less accurately located than the rest of the diagram.

Figs. 2, 3, 4, 5 and 6 show the various types of structure in the system. In Fig. 2, which shows an alloy containing 0.125 per cent Ni, the primary constituent is cadmium; the eutectic of cadmium and  $\text{NiCd}_7$  is the light-colored laminated structure. Fig. 3, representing an alloy containing 0.25 per cent Ni, shows only a uniform eutectic structure. In Fig. 4 an alloy containing 0.5 per cent Ni is shown. The excess  $\text{NiCd}_7$  has crystallized into plates and skeleton cubes in the eutectic matrix. Fig. 5 is an alloy containing 1.30 per cent Ni showing definitely shaped cubes of  $\text{NiCd}_7$ . This material was found to have excellent properties when used as a bearing alloy.<sup>4</sup> An alloy containing 6.9 per cent Ni is shown in Fig. 6. Of the two hard, brittle phases shown the lighter is probably  $\text{NiCd}_7$ , while the darker is a compound richer in nickel. Attempts to isolate the compound  $\text{NiCd}_7$  have been unsuccessful, owing partly to the slow rate of diffusion between the solid phases arising from a probable peritectic reaction.

#### SUMMARY

A eutectic melting at  $318^{\circ}$  C. has been found in the system cadmium-nickel. Its composition is 0.25 per cent Ni, 99.75 per cent Cd. Its components are cadmium, and a cadmium-nickel compound.

This compound is richer in cadmium than previously reported, and if simple in composition has a formula of  $\text{NiCd}_7$ .

---

<sup>4</sup> C. E. Swartz and A. J. Phillips Reference of footnote 1.

# Solubility of Oxygen in Solid Copper<sup>†</sup>

BY F N RHINES<sup>†</sup> AND C H MATHEWSON,<sup>‡</sup> NEW HAVEN, CONN

(New York Meeting, February, 1934)

DESPITE the large amount of study which has been devoted to the subject our present knowledge of the copper-oxygen system remains incomplete and unsatisfactory in many respects. This applies particularly to those regions in which solid metallic copper exists. The primary object of the present paper is the contribution of new information relative to the solid solubility of oxygen (or cuprous oxide) in copper at atmospheric pressure, together with certain observations in the low-pressure regions of the system. It seems appropriate also to present a brief summary of the outstanding previous work on the constitution of mixtures of copper with its lowest oxide in order to show the relation between the new facts and the system as a whole.

The earliest recorded investigations of the copper-oxygen system are those of M S Lucas<sup>(1)</sup>§ and of M Chevallot<sup>(2)</sup> in 1819 and 1820. Lucas believed that liquid copper is capable of dissolving its oxide, but neither he nor Chevallot was able to furnish convincing proof of this property. It was not until 1866 that T Graham<sup>(3)</sup> definitely established the existence of such a solubility. Nine years later W Hampe<sup>(4)</sup> measured its extent and roughly outlined the copper-rich portion of the system. The first really precise examination of the constitutional relationship between copper and cuprous oxide, however, was that of E Heyn<sup>(5)</sup> who in 1900 published a temperature-concentration diagram covering the range from 0 to 10 per cent of cuprous oxide at atmospheric pressure. Within these limits of composition cuprous oxide was found to dissolve in liquid copper, forming at 3.4 to 3.5 per cent a eutectic which melted at 1065° C. R E Slade and F D Farrow<sup>(6)</sup> extended these studies to mixtures of higher oxygen content. They discovered that between 20 and 95 per cent of cuprous oxide the metal and oxide form two liquid phases at a monotectic reaction of 1195° C. The span of the binuquidal region diminishes slightly

---

\* From a part of a dissertation presented by F N Rhines to the Faculty of the Graduate School of Yale University in partial fulfillment of the requirements for the degree of Doctor of Philosophy. Manuscript received at the office of the Institute Dec 1, 1933.

<sup>†</sup> Assistant in Metallurgy, Yale University

<sup>‡</sup> Professor of Metallurgy, Yale University

§ References are to bibliography at end of paper



at higher temperatures. More recent investigations by H. S. Roberts and F. H. Smyth<sup>(7)</sup> and by R. Vogel and W. Pocher<sup>(8)</sup> have shown that the above results are substantially correct. The last named authors place the monotectic reaction temperature at 1200° C and the concentrations of the two liquid layers at 15 and 95 per cent of cuprous oxide, respectively. The melting point of cuprous oxide is given by Roberts and Smyth as 1235° C at 0.6 mm Hg. At lower temperatures under atmospheric pressure oxygen can combine with cuprous oxide to form cupric oxide and even in an atmosphere of nitrogen, according to Vogel and Pocher, slow cooling causes the cuprous oxide associated with copper to decompose, forming the copper-rich solid solution and cupric oxide. They place the thermal boundary between the regions of stable cupric and cuprous oxides at approximately 375° C.

Although no solid solubilities in any portion of the system were observed by the early investigators, there seems to have been a general recognition among metallurgists of the capacity of solid copper to dissolve oxygen. The measurement of its extent was first attempted by D. Hanson, C. Marryat and G. W. Ford<sup>(9)</sup> who placed the limit at less than 0.009 per cent oxygen at 1000° C. Vogel and Pocher<sup>(8)</sup> presented microscopic evidence of the solid solubility and gave a saturation value of 0.08 per cent of oxygen at 950° C. Very recently N. P. Allen and A. C. Street<sup>(10)</sup> have quoted an unpublished research by T. Hewitt in which the solubility limit was fixed at 0.005 per cent of oxygen at 500° C. The values found in the present investigation are of the same order of magnitude as those of Hanson, Marryat and Ford<sup>(9)</sup> and Hewitt,<sup>(10)</sup> but differ widely from the figure given by Vogel and Pocher<sup>(8)</sup>. However, a probable cause of the disagreement with this latter figure has been indicated in the following discussion.

A graphic summary of the observations quoted above is presented in the temperature-concentration diagram of Fig. 1. E. Heyn's<sup>(4)</sup> data for the freezing points to the left of the binodal region, Slade and Farrow's<sup>(6)</sup> boundaries of this region and Vogel and Pocher's<sup>(8)</sup> monotectic reaction temperature (1200° C.) are used in this diagram. The solid solubility limit is drawn from the new data of the present paper. Similar diagrams extending to the composition of pure cupric oxide have been published by Roberts and Smyth<sup>(7)</sup>, Vogel and Pocher<sup>(8)</sup> and M. Randall, R. F. Nielsen and G. H. West.<sup>(11)</sup>

#### DETERMINATION OF SOLUBILITY LIMIT OF OXYGEN IN SOLID COPPER

In beginning the work on the measurement of the solid solubility of oxygen in copper several courses of procedure were considered. The ideal method would be the study of the equilibrium pressure at known temperatures in a system of known composition, or of the equilibrium composition of a regulus in contact with oxygen at a known pressure and temperature.

The range of pressures in which such equilibria can be attained is necessarily limited to those below the triple curve  $\text{Cu}-\text{Cu}_2\text{O}-\text{Gas}$  (curve 5, Fig. 5). At higher pressures the gas phase can no longer remain in equilibrium with the copper-solid solution and a true equilibrium can be attained only between the solid phases copper-solid solution and copper oxide. Thus the solid solubility of oxygen in copper may be considered

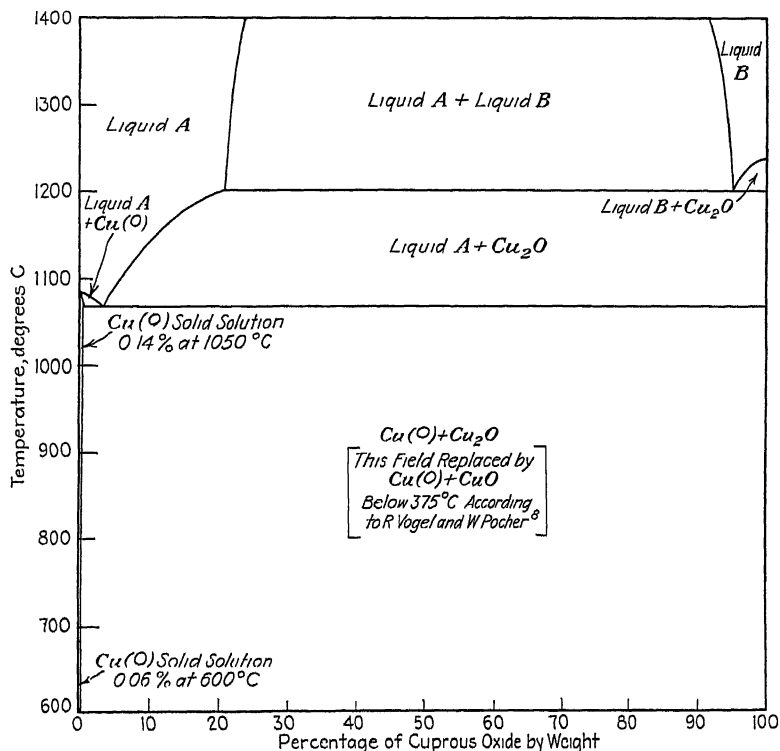


FIG. 1 —COPPER-CUPROUS OXIDE CONSTITUTIONAL DIAGRAM FROM THE BEST AVAILABLE DATA

to be constant with respect to (ordinary, nondeformational) pressures in excess of those represented on curve 5, Fig. 5. If gas is continually made available to the system at these elevated pressures, as by heating copper in air, saturation of the metal with oxygen will be accompanied by slow oxidation and scale formation, but under favorable conditions it should be possible properly to identify the saturated but unoxidized copper-oxygen solid solution.

The problem of measuring the solubility in the region in which pressure is a principal variable is one involving serious experimental difficulties, since the pressures will be of the order of  $10^{-4}$  mm. of Hg at  $1065^\circ\text{C}$  and much lower at lower temperatures. No equipment for directly obtaining

such pressures was available and such indirect expedients as the use of mixtures of an inert gas and oxygen, or the decomposition products of water vapor were thought to be undesirable, the former because of proven difficulties in the way of maintaining a sufficiently delicate control of composition, and the latter because the results might be vitiated by the presence of hydrogen in the system. It was decided, therefore, to limit the investigation to those regions in which pressure is not a factor

To this end two courses of procedure seemed to be open. The lowest temperature at which an alloy of known oxygen content was found to become homogeneous at an effectively non-oxidizing pressure above the Cu:Cu<sub>2</sub>O Gas curve could be taken as a point on the saturation curve, or oxygen-free copper could be exposed to the action of oxygen, or cuprous oxide, for an extended period at a definite temperature, the composition at saturation being determined by a final analysis

At the start of the work the first of these methods seemed to give the greatest promise of success. Assuming the determination of 0.08 per cent oxygen at 950° C. made by Vogel and Pocher<sup>(8)</sup> to be correct, the attainment of saturation should be detectable by microscopic means. The preparation and analysis of a series of alloys with compositions varying between 0 and 0.1 per cent of oxygen presented no difficulties. However, it soon became evident that the solubility was very much less than 0.08 per cent, indeed, was so small that a microscopic determination of its value was out of the question. This necessitated the abandonment of the method.

Fortunately, the circumstances which made the first approach unworkable favored the second procedure. The small amount of solubility together with the considerable speed of diffusion to be expected at elevated temperatures made it seem probable that complete saturation of a specimen of copper, of not too great thickness, could be attained in a reasonably short length of time. This proved to be the case and a series of saturation points at temperatures between 600° C. and 1050° C. have been established in this manner.

#### EXPERIMENTAL PROCEDURE

The copper used in the following experiments was secured from the Raritan Copper Works in the form of thin dense sheets of electrolytically refined metal specially selected for its purity. In order to eliminate all traces of sulfur it was redeposited in a nitrate electrolyte and was finally heated in a stream of dry hydrogen for the removal of oxygen. Melting was carried out in vacuum using chemically pure alumina crucibles furnished by the Norton Co. and capable of holding about 200 grams of copper. When liquid the metal was again subjected to the action of hydrogen and was finally degassed by heating to 1300° C. in a vacuum of the order of one micron. Solidification was allowed to take place in the

crucible under vacuum. A chemical analysis of metal so treated showed a copper content of 99.99+ per cent and a spectroscopic analysis<sup>||</sup> revealed the presence of no appreciable quantity of any impurity.

The ingots prepared in this way were rolled into sheets of thickness varying between  $\frac{1}{8}$  and  $\frac{1}{4}$  in, depending upon the severity of the expected oxidation. They were then exposed to free access of air at a definite temperature ( $\pm 10^\circ \text{C}$ ) in a Hevi Duty muffle furnace for periods varying between one day and three weeks. Because of the proven insolubility of nitrogen in copper it is not supposed that the use of an atmosphere of air instead of pure oxygen has in any way affected the results. Upon removal from the furnace the specimens were quenched in water. As much scale as possible was removed mechanically and the remainder was dissolved with nitric acid. This treatment was followed by washing successively with water, alcohol and ether before sampling for analysis. Great care was always exercised in avoiding the presence of visible surface oxide or mechanically trapped particles.

The analytical procedure followed was that described as the indirect method by W. H. Bassett and H. A. Bedworth<sup>(12)</sup>. It consists in measuring the loss of weight suffered by the sample of oxygen-bearing copper upon reduction with hydrogen at an elevated temperature. Owing to the purity of the metal used it was found unnecessary to make a determination of the sulfur content; this result, when measurable, must be subtracted from the loss of weight before calculating the oxygen content. The apparatus and technique were checked on numerous occasions by running a sample of copper which had been carefully standardized by several prominent analysts. The values reported for its oxygen content are tabulated here in order to illustrate the degree of accuracy to be expected from the method.

ANALYST	OXYGEN, PER CENT
A	0.033
B	0.036
C	0.0368
Authors	0.037

The limit of variation between analyses run by a single operator is probably not greater than  $\pm 0.001$  per cent.

In practice, between 25 and 50 grams of copper chips cut at slow speed on a shaper were used for a single sample. Ignition was carried out in a silica glass bulb heated with a gas burner and supplied with a continuous flow of pure dry hydrogen. A treatment of two hours duration was found to be ample. All analyses were run in duplicate and the results were discarded when they failed to check within  $\pm 0.001$  per cent.

---

<sup>||</sup> The authors are indebted to Dr. C. S. Smith, of the American Brass Co., for the spectrographic analyses.

In the measurement of quantities as small as those considered here numerous ordinarily insignificant sources of error become important. The ever present danger of contaminating the metal with oxygen during the preparation of the original ingot is obvious and usually easily avoided, or, if it does occur, is readily detected. The enormous effect which exceedingly small quantities of metallic impurities can have upon the solubility value was well demonstrated by an instance in which a small amount of ordinary electrolytically refined copper was accidentally introduced into a melt. The oxygen figure in this case was less than half that expected.

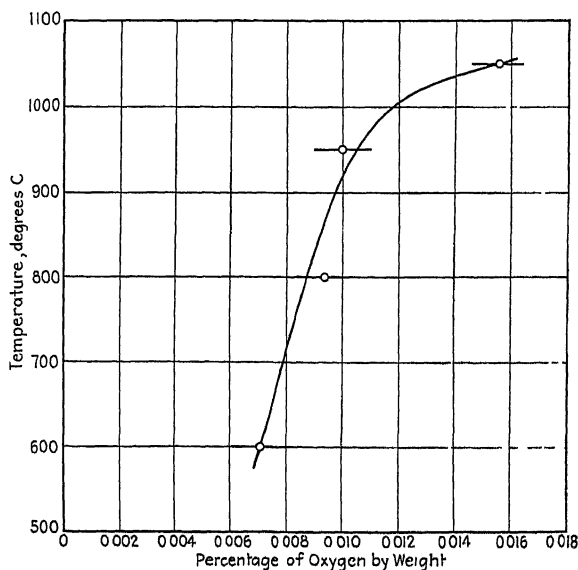


FIG. 2—SOLID SOLUBILITY OF OXYGEN IN COPPER. HORIZONTAL LINES THROUGH DATA POINTS INDICATE PROBABLE LIMITS OF ANALYTICAL ERROR.

The most troublesome sources of error, however, are those connected with the sampling and analysis. In spite of every precaution, particles of free oxide would occasionally find their way into the analytical samples and cause high results. This was particularly true of specimens of copper saturated at the higher temperatures where the surface oxidation is extremely severe and occasionally produces crevasses and deep pits in the surface of the metal. Even the matter of weighing presented unusual difficulties because of the extreme accuracy required. The large surface of the ignition bulb in which the samples were weighed made the temperature equilibrium in the balance such an important factor that it was found expedient to allow at least an hour for the system to come to equilibrium before a final weighing could be made.

The solubility limit of oxygen in copper was determined at four temperatures: 600°, 800°, 950° and 1050° C. In each case successive speci-

mens were saturated for periods of increasing duration until an end point was reached. The averages of the analyses believed to represent a state of saturation at each temperature are plotted in the diagram of Fig. 2 and a smooth curve has been drawn between them. Justification for not passing the curve exactly through the points is derived from the probable error of analysis of  $\pm 0.001$  per cent. See Table 1 for the actual values.

TABLE 1—*Data on Solubility Limit of Oxygen in Copper*

Temperature, Deg C	Saturation, Days	Oxygen, Per Cent	Average Oxygen, Per Cent
600	7	0.0071	0.0071
600	14	0.0070	
600	21	0.0071	
800	5	0.0093	0.0094
800	11	0.0096	
950	3	0.0092	0.0100
950	7	0.0107	
1050	1	0.0156	

It is evident from Table 1 that the accuracy of the determination is greater for the points at 600° and 800° C than for those at higher temperatures. Nevertheless, the point at 950° C. is believed to be correct within the limit of error specified. The value given for 1050° C represents the only one of numerous attempted determinations at that temperature in which there was no suspicion of contamination by free oxide particles. The location of that point must, therefore, be considered uncertain.

The shape of the solid solubility curve is interesting in its similarity to those found in the bimetal systems. It at once suggests the possibility of a precipitation of cuprous oxide in the solid metal when a piece of copper saturated at a high temperature is reannealed at a lower temperature. Attempts to reveal this behavior by use of the ordinary metallographic technique failed repeatedly, probably because the particles were too small. Finally a procedure was discovered which seemed to give indirect evidence of the precipitation of cuprous oxide. This consisted in etching a polished specimen alternately with 10 per cent copper ammonium chloride solution and concentrated nitric acid saturated with chromic acid. Pieces of oxide-free copper or copper saturated with oxygen and quenched from the saturation temperature were attacked quite evenly by this etch and presented a clean, unbroken surface upon microscopic examination. However, when particles of oxide were present the etch violently attacked the metal in their immediate neighborhood leaving pits considerably larger than the particles of oxide them-

selves, which, if the etch was not too prolonged, were often seen standing out in the center of the depressions. Metal that had been saturated in

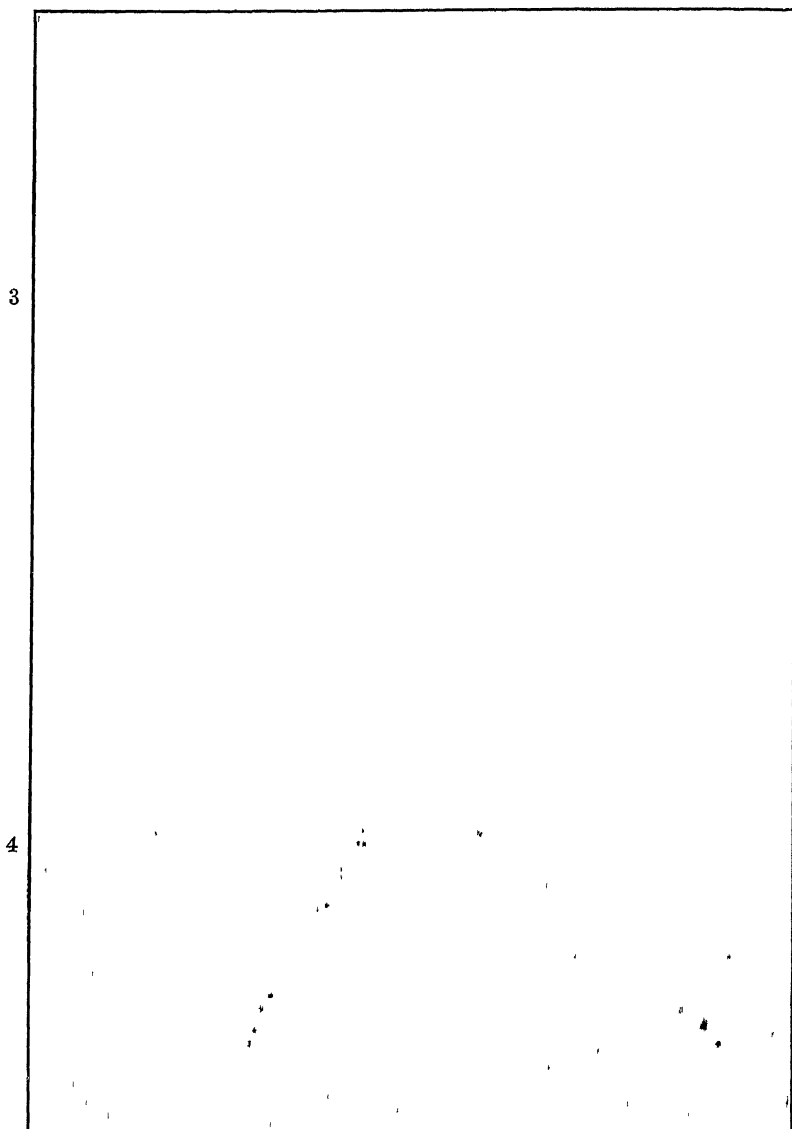


FIG. 3—OXYGEN-FREE COPPER HEATED 12 HR. IN AN OXIDIZING ATMOSPHERE AT  $1050^{\circ}\text{C}$  AND QUENCHED IN WATER  $\times 500$  SPECIAL ETCH, PAGE 343

FIG. 4—SAME SPECIMEN AS FIG. 3, GIVEN AN ADDITIONAL AGING TREATMENT OF 24 HR. AT  $400^{\circ}\text{C}$   $\times 500$  SPECIAL ETCH, PAGE 343

air at a temperature above  $1000^{\circ}\text{C}$  and subsequently annealed at  $400^{\circ}\text{C}$ . was found to show a large amount of fine surface pitting distributed in a manner typical of precipitates when etched according to the above

procedure These effects are illustrated in the micrographs of Figs. 3 and 4 Efforts to detect an age-hardening effect met with no success

#### EXPERIMENTS AT REDUCED PRESSURES

It has been mentioned previously that an attempt was made to measure the solid solubility limit of oxygen in copper by homogenizing a series of reguli of known compositions at a fixed temperature In these experiments it was desired, of course, to avoid changes in composition This, it was thought, might be accomplished by annealing in the best vacuum available, i e, 1 to 10 microns, which pressure, although well above the supposed decomposition pressure of cuprous oxide, should greatly retard the surface oxidation of the metal It was with some surprise, however, that specimens of copper annealed under these conditions at temperatures ranging from 500° to 1050° C were observed to be entirely free from surface oxide This suggested a possible loss of oxygen from the alloys and a series of simple experiments designed to explore this possibility was undertaken

A charge of one gram of chemically pure cuprous oxide contained in a cup made from our own high-purity copper foil was heated for 24 hr at 1000° C under a vacuum of 2.5 to 4 microns Upon removal from the furnace it was found that the surface layer of oxide had been reduced to copper A calculation based upon the total loss in weight and the final oxygen content indicated that 8.73 per cent of the oxide had been lost by vaporization and 23.27 per cent by decomposition As a correction for the presence of the copper foil a blank cup was employed. Evidently oxygen could be lost from cuprous oxide under the conditions existing in the furnace tube

Next it was desired to discover whether oxygen alloyed with copper could be dissipated in a similar manner Accordingly, two pieces of copper, one containing 0.2291 per cent of oxygen and the other only 0.0035 per cent, were annealed in vacuum under the same conditions as in the previous experiment At the end of the treatment the first specimen was found to have lost weight to the extent of 0.0916 gram out of a total of 52.7862 grams while the other lost only 0.0023 gram out of 44.1993 grams Analysis of these specimens showed a decrease in the oxygen content of the first to 0.1551 per cent while the change in the second specimen was less than the sensitivity of the measurement From these figures it was calculated that the oxide-rich specimen had lost 6.06 per cent of its oxygen by vaporization of cuprous oxide and 26.08 per cent as oxygen gas Compensation for the loss of weight due to the vaporization of copper itself has been made in this calculation by assuming that the total loss in weight of the low-oxygen specimen resulted from that cause. The correction thus effected, however, is small and does not influence the qualitative interpretation of the results.



Several possible explanations of the behavior of cuprous oxide demonstrated here may be suggested. First, the decomposition pressure of cuprous oxide may actually be of the order of 1 micron. This seems highly improbable because it would require an error of nearly 10,000 per cent in the thermodynamical calculations of this decomposition pressure. Second, the gage pressure may bear no relation to the partial pressure of oxygen in the system, because of stagnation of the atmosphere of the furnace chamber. Finally, there may be a reducing atmosphere present owing to the back diffusion of oil vapors from the Cenco Megavac pump used in these experiments.

Presuming the first possibility to be eliminated it remained to distinguish between the latter two. For this purpose an air leak was arranged at the end of the furnace most remote from the vacuum connection. This was adjusted to allow a positive but very small flow of air through the furnace at the same time maintaining a fairly high vacuum. Copper foil cups of cuprous oxide were again placed in the chamber and heated at a temperature of  $1000^{\circ}\text{C}$  as in the former experiment. On the first trial the leakage allowed was so small that the pressure increased to only 6 microns. Upon examination it was found that the outside of the copper foil had been oxidized, but since the opening in the top of the cup had been turned away from the direction of the oncoming flow of air the surface layer of cuprous oxide was again reduced to copper. In a second run the flow of air was increased until the vacuum fell to 40 microns. Here the copper foil was heavily oxidized and the cuprous oxide showed no sign of reduction. An analysis of the contents of the cup revealed a loss of oxygen by volatilization of oxide amounting to 9.14 per cent in 24 hr at  $1000^{\circ}\text{C}$ . Since the back diffusion of oil vapor against a flow of air sufficient to oxidize copper foil and at a temperature of  $1000^{\circ}\text{C}$ , as existed under the first set of conditions, seems very improbable, we venture to conclude that the reduction of the cuprous oxide in this instance was caused by actual decomposition in a localized zone of oxygen-impoverished atmosphere maintained by the enveloping walls of the copper cup.

Besides the observation described above, of the decomposition of solid cuprous oxide, which if correctly interpreted is of some theoretical importance, several points brought out in these experiments seem worthy of brief comment. In the first place it is interesting from a practical point of view to note that oxygen can be removed from solid copper without the use of gaseous reducing agents which leave the metal quite unsound. Numerous specimens of copper deoxidized in this way were examined microscopically and found to be free from porosity. Again it may be worthy of note that cuprous oxide was lost from the pure powdered compound and from the alloy by volatilization and decomposition in about the same ratio. Perhaps this indicates that the oxygen

is combined with copper in its migration through the copper lattice prior to vaporization at the surface

Of more immediate importance, however, is the bearing of these observations upon the solid solubility determination made by Vogel and Pocher<sup>(8)</sup> It will be recalled that the value obtained by these investigators was nearly eight times as great as the corresponding value shown on our solubility curve, Fig 2 Their method of measurement consisted in heating a specimen of copper containing about 0.1 per cent of cuprous oxide "in an air-tight sealed tube in an atmosphere of purified nitrogen at a temperature of 950° C" After annealing to equilibrium at this temperature the sample was quenched and the amount of oxide remaining out of solution was estimated microscopically, the difference between this amount and the original composition being taken as the solid solubility. It is not clearly stated that a chemical analysis was made after the heat treatment Evidently oxygen and cuprous oxide vapor were evolved from the surface of the copper and, since cuprous oxide at high temperatures reacts freely with silica, or other available refractories from which this tube may have been made, its vapor pressure was doubtless kept sufficiently low to allow a considerable loss from the copper matrix, thus vitiating the solubility figure

Although it is perhaps unwarranted to place a strict physical interpretation upon these fragmentary experiments, the primary purpose of which was to act as a guide in setting up suitable conditions for proceeding with the solubility determination of oxygen in copper, it may be of interest to examine the general arrangement of pressure-temperature curves which they seem to require A brief résumé of the related aspects of the system is given below.

#### PRESSURE-TEMPERATURE-CONCENTRATION RELATIONSHIPS OF THE SYSTEM COPPER-CUPROUS OXIDE

The simplest and most satisfactory graphic survey of the constitution of a binary system as affected by pressure and temperature is given by the pressure-temperature projection of the triple curves Although such a projection does not show the concentration values associated with the projected points and curves it is possible, owing to the systematic nature of the changes, to develop by inspection of the pressure-temperature diagram a complete series of typical pressure-concentration, or temperature-concentration diagrams (the diagrams so commonly used in metallography) on the basis of a few guiding assumptions of important concentration values. The principles and methods used in such studies have been discussed in much detail by H. W. Bakhuys Roozeboom and his collaborators in the well-known volumes entitled *Die heterogenen Gleichgewichte* Further illustration is offered by the analysis of Vogel

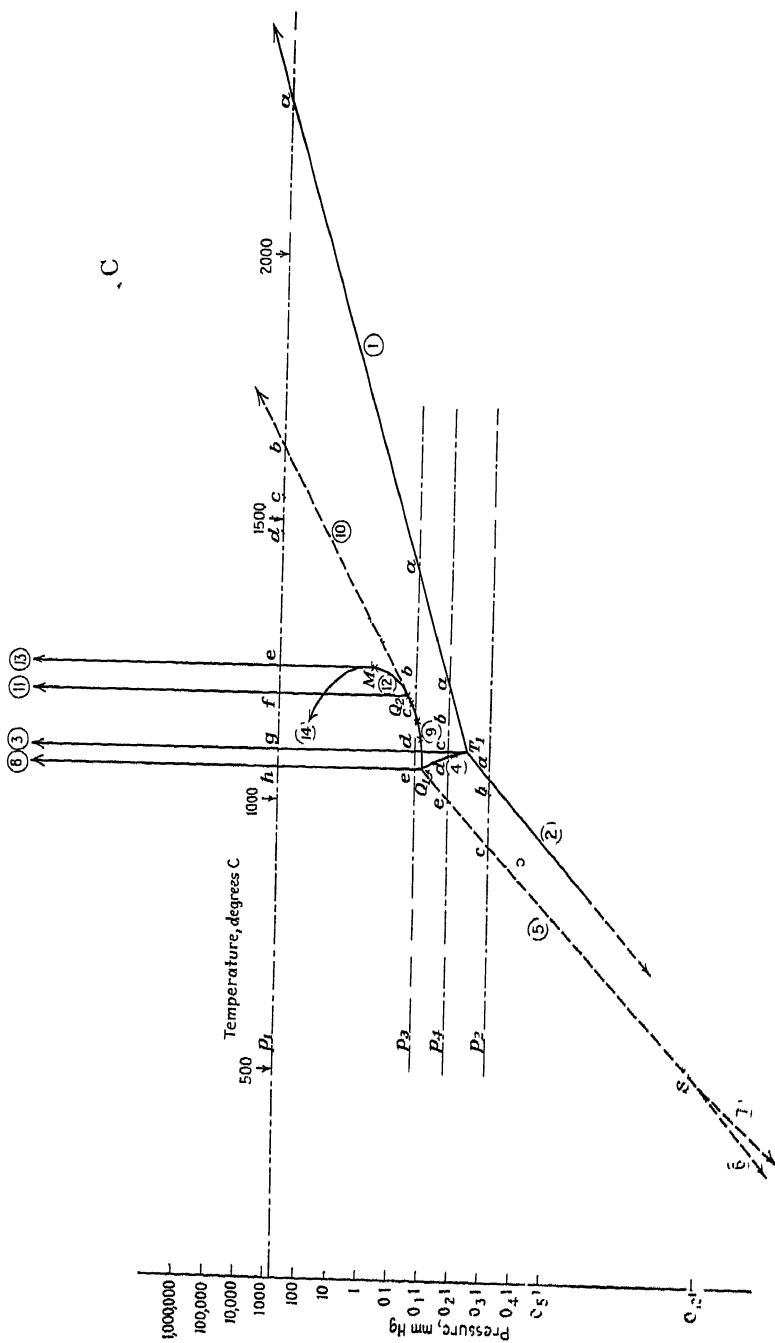


Fig 5—PROVISIONAL PRESSURE-TEMPERATURE DIAGRAM OF SYSTEM COPPER-CUPROUS OXIDE  
 Crosses represent data from Roberts, and Smyth (7). The dotted circle represents a dissociation pressure of  $\text{Cu}_2\text{O}$   
 calculated by Stockdale (13). Curves 1 and 2 are drawn from numerous data contributed by Randall, Nielsen and West (11)

and Pocher<sup>(8)</sup> of the present copper-oxygen system, but chiefly in the region  $\text{Cu}_2\text{O}-\text{CuO}$

Only fragmentary information relative to the constitution of the copper-cuprous oxide system at pressures other than atmospheric is now available and no complete diagrammatic assembly of this information is known to us. Nevertheless, a provisional diagram believed to give a good general outline of conditions in this system is shown in Fig. 5

Randall, Nielsen and West<sup>(11)</sup> have tabulated the values, obtained from the publications of numerous investigators, of the vapor pressure of solid and liquid copper at various temperatures. By extrapolation to the melting point of copper, the triple point  $T_1$  is found to lie at approximately 0.00059 mm Hg and  $1084^\circ\text{C}$ . The boiling point of copper at atmospheric pressure is given by H. C. Greenwood<sup>(13)</sup> as  $2310^\circ\text{C}$ . These data are represented graphically in curves 1, 2 and 3 of Fig. 5. By plotting pressures logarithmically the boiling and sublimation curves, 1 and 2, become ideally straight lines. For the lack of specific information defining the slope of the melting curve 3 this has been drawn vertically, which is known to be a close approximation in similar cases.

There seems to be little reason to doubt that the compound cuprous oxide can dissociate below the temperature, approximately  $1235^\circ\text{C}$ , at which it melts in the air. It, therefore, has no true triple point, but instead a minimum melting point  $M$  and a maximum sublimation point  $S$ , between which this decomposition can take place.<sup>(14)</sup> The location of the minimum melting point has been approximated by Roberts and Smyth<sup>(7)</sup> at  $1235^\circ\text{C}$  and a pressure of 0.06 mm Hg. No determination of the position of the maximum sublimation point is available. Qualitatively it may lie either in the region of the diagram in which liquid and solid cuprous oxide exist, or in that in which no liquid oxide is present. That is, it may lie either to the right or the left of the quadruple point  $Q_1$  upon one of the triple curves along which cuprous oxide is in equilibrium with gas. Vogel and Pocher,<sup>(8)</sup> for apparently arbitrary reasons, have placed it on the liquid side of the quadruple point. The experiments described in this paper, however, have seemed to indicate that solid cuprous oxide can decompose down to a temperature at least as low as  $500^\circ\text{C}$ . Accordingly, the maximum sublimation point  $S$  has been placed, in the present diagram, below  $500^\circ\text{C}$ . on the triple curve 5,  $\text{Cu} \cdot \text{Cu}_2\text{O}$ . Gas

According to this interpretation, solid cuprous oxide vaporizes unchanged in composition along the curve 7, but at higher temperatures and pressures is in equilibrium with metallic copper and vapor whose composition is continually changing owing to dilution of the cuprous oxide vapor with oxygen, the gaseous product of the dissociation. Thus, if we desire to show, on the present diagram, the pressures and temperatures at which vapor has the composition  $\text{Cu}_2\text{O}$ , we must introduce a dotted line,  $SC$ , (as done by Vogel and Pocher<sup>(8)</sup> in the case of the other oxide,  $\text{CuO}$ )

which represents the appropriate intersection with the divariant vapor surface, in this case carried to a hypothetical critical curve  $C$  and overlaid by a similar curve  $MC$ , which represents an intersection with the liquidus surface at the concentration  $\text{Cu}_2\text{O}$ , from the minimum melting point to the critical curve

These entirely hypothetical dotted curves are introduced principally to facilitate the construction of typical temperature-concentration diagrams, shown in Fig 6

Between pure copper and cuprous oxide lie two quadruple points,  $Q_1$ , representing the invariant equilibrium,  $\text{Cu} \cdot \text{Cu}_2\text{O} \cdot \text{Liquid} \cdot \text{A} \cdot \text{Gas}$ , and  $Q_2$ , representing that of  $\text{Cu}_2\text{O} \cdot \text{Liquid} \cdot \text{A} \cdot \text{Liquid} \cdot \text{B} \cdot \text{Gas}$ . Both of these points can be located approximately by extrapolation of the data of Roberts and Smyth<sup>(7)</sup> with which the triple curve 9,  $\text{Cu}_2\text{O} \cdot \text{Liquid} \cdot \text{A} \cdot \text{Gas}$ , was established, viz, 0.041 mm Hg at  $1184.6^\circ \text{C}$ , 0.035 mm Hg at  $1150.4^\circ$  and 0.029 mm Hg at  $1119.2^\circ$ . Extrapolating to  $1065^\circ \text{C}$ , the pressure of the quadruple point  $Q_1$  is found to be approximately 0.018 mm Hg. Continuing the curve to higher temperatures it is found to intersect the melting curve 11,  $\text{Cu}_2\text{O} \cdot \text{Liquid} \cdot \text{A} \cdot \text{Liquid} \cdot \text{B}$ , which according to Vogel and Pocheir<sup>(8)</sup> lies at  $1200^\circ \text{C}$ , at a pressure of 0.8 mm Hg, thus locating  $Q_2$ .

Radiating from the quadruple point  $Q_1$  are the four triple curves, (4)  $\text{Cu} \cdot \text{Liquid} \cdot \text{A} \cdot \text{Gas}$ , (5)  $\text{Cu} \cdot \text{Cu}_2\text{O} \cdot \text{Gas}$ , (9)  $\text{Cu}_2\text{O} \cdot \text{Liquid} \cdot \text{A} \cdot \text{Gas}$  and (8)  $\text{Cu} \cdot \text{Cu}_2\text{O} \cdot \text{Liquid} \cdot \text{A}$ . The first of these, 4, is located at its end points by  $Q_1$  and  $T_1$ . No points on curve 5 other than  $Q_1$  have been determined, but according to a recent calculation by Stockdale<sup>(15)</sup> the dissociation pressure of cuprous oxide, which we interpret to mean in this connection the oxygen partial pressure over a mixture of copper and cuprous oxide, is 0.000076 mm Hg at  $927^\circ \text{C}$ . Since the gas pressure along curve 5 will be the sum of the partial pressures of oxygen, cuprous oxide and copper, this curve must lie above the point in question as shown in Fig 5. The melting curve, 8, is assumed to be substantially vertical, passing through  $1065^\circ \text{C}$ . at atmospheric pressure, and the data establishing the position of curve 9 have already been quoted<sup>(16)</sup>.

The triple curves terminating at the quadruple point  $Q_2$  are: (9),  $\text{Cu}_2\text{O} \cdot \text{Liquid} \cdot \text{A} \cdot \text{Gas}$ , (10)  $\text{Liquid} \cdot \text{A} \cdot \text{Liquid} \cdot \text{B} \cdot \text{Gas}$ , (11)  $\text{Cu}_2\text{O} \cdot \text{Liquid} \cdot \text{A} \cdot \text{Liquid} \cdot \text{B}$  and (12)  $\text{Cu}_2\text{O} \cdot \text{Liquid} \cdot \text{B} \cdot \text{Gas}$ . Of these, the first is common with the  $Q_1$  point and has been described. The following four points on curve 10 have been measured by Slade and Farrow:<sup>(6)</sup> 4 mm. Hg at  $1206^\circ \text{C}$ , 10 mm. Hg at  $1240^\circ$ , 12 mm. Hg at  $1260^\circ$  and 25 mm. Hg at  $1324^\circ$ . Their pressure values are probably high, as was pointed out by Roberts and Smyth. The melting curve 11 has again been assumed to be vertical and according to Vogel and Pocheir<sup>(8)</sup> passes through  $1200^\circ \text{C}$  at atmospheric pressure. Curve 12 is located at its end points by  $Q_2$  and  $M$ .

The three univariant curves radiating from the maximum sublimation point  $S$  represent the reactions  $\text{Gas} + \text{Cu} = \text{Cu}_2\text{O}$ , curve 5,  $\text{Gas} = \text{Cu} + \text{Cu}_2\text{O}$ , curve 6 and  $\text{Gas} = \text{Cu}_2\text{O}$ , curve 7, when they are traversed from right to left in Fig 5

All of the curves attached to the minimum melting point  $M$  have been described with the exception of curve 14,  $\text{Cu}_2\text{O}$  Liquid  $B$  Gas, which takes us outside of the range of concentration between copper and cuprous oxide and extends to a quadruple point with cupric oxide, located at approximately  $1080^\circ \text{C}$  and 400 mm Hg, according to Roberts and Smyth <sup>(7)</sup>

In conclusion, a number of theoretical temperature-concentration diagrams (a) at atmospheric pressure,  $p_1$  of Fig 5, (b) at a low pressure,

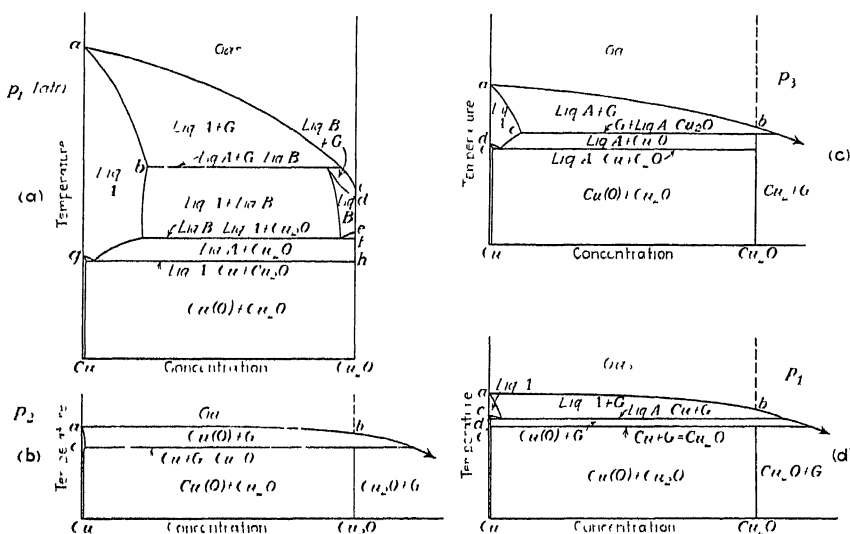


FIG 6—TYPICAL TEMPERATURE-CONCENTRATION SECTIONAL DIAGRAMS THROUGH  $p$ - $t$ - $x$  SPACE DIAGRAM, CONSTRUCTED ON BASIS OF  $p$ - $t$  DIAGRAM SHOWN IN FIG 5

$p_2$ , characteristic of the vacuum technique used in the present experiments, (c) and (d) at two intermediate pressures,  $p_3$  and  $p_4$ , are grouped in Fig 6.

The general plan of developing these sectional diagrams at constant pressures is, first to construct the horizontals of constant temperature as defined by the reactions which occur when each triple curve of Fig 5 is traversed in passing at constant pressure, for example,  $p_1$  from high to low temperatures. Then, to build the divariant and trivariant regions around these horizontals according to the requirements of each case, which establish themselves more or less automatically. The significant points of intersection are lettered in the pressure-temperature diagram, Fig. 5, and the reactions taking place at falling temperature are written along the corresponding horizontals of Fig 6

Thus in constructing Fig 6a, the section at atmospheric pressure, reaction, *b*, occurs when curve 10 of Fig 5 is reached. The divariant field above the reaction horizontal must end at the point *a* on the vaporization curve of liquid copper. One of the divariant fields below the horizontal, representing equilibrium between Liquid *B* and Gas, reaches the points *c* and *d* at the  $\text{Cu}_2\text{O}$  boundary of the diagram, since as explained previously these are the points at which the liquid and vapor reach the composition of the oxide  $\text{Cu}_2\text{O}$ . The next constant temperature horizontal occurs at *f*, where curve 11 of the diagram, Fig 5, is encountered, giving rise to the reaction shown. One of the divariant fields above this horizontal is bounded by a curve ending at the melting point of cuprous oxide, *e*. A final reaction occurs at *h*, and the new field above the horizontal is bounded by a curve which ends at the melting point of copper *g*.

The construction of Figs 6b, 6c and 6d, will be understood by similar cross references to the corresponding letters and curves of Fig 5.

### SUMMARY

The solid solubility of oxygen in copper has been measured in the range  $600^\circ$  to  $1050^\circ$  C and was found to increase from 0.007 per cent oxygen at  $600^\circ$  C to about 0.015 per cent oxygen at  $1050^\circ$  C.

Indirect microscopic evidence of the precipitation of cuprous oxide in solid copper supersaturated with respect to oxygen has been presented.

The solubility values reported are shown to be in fair agreement with those reported by Hanson, Mariyat and Ford and Allen and Street, but do not agree with the values found by Vogel and Pocheur. A possible explanation of the disagreement of the latter is offered.

It has been demonstrated that oxygen can be extracted from solid copper by heating in the absence of oxygen.

Experimental evidence of the decomposition of solid cuprous oxide at low pressures is also presented. The significance of this observation in the construction of a pressure-temperature diagram of the system copper-cuprous oxide has been illustrated.

### BIBLIOGRAPHY

- 1 M S Lucas. Sur l'oxydation de l'argent et du cuivre. *Ann. Chimie et Phys.* (1819) II, 12, 402, *Proc. Manchester Lit. and Phil. Soc.* 1819.
- 2 M Chevallot. Sur l'oxydation de l'argent pendant sa fusion. *Ann. Chim. et Phys.* (1820) II, 13, 299.
- 3 T Graham. On the Absorption and Dialytic Separation of Gases by Collod Septa, II Action of Metallic Septa at Red Heat. *Phil. Mag.* (London) (1866) 32, 503.
- 4 W Hampe. Beitrage der Metallurgie des Kupfers. *Chem. Centralblatt* (1875) 378, *Polytec. Jnl.* (1875) 489.
- 5 E Heyn. Kupfer und Sauerstoff. *Ztsch. f. anorg. Chem.* (1904) 39, 1; *Mitt. Konig. tech. Versuchsanst.* Berlin (1900) 18, 315; *Metallography* (1903) 4, 39.

- 6 R. E. Slade and F. D. Farrow. An Investigation of the Dissociation Pressures and Melting Points of the System Copper-Cuprous Oxide *Proc. Roy. Soc London* (1912) **87A**, 524
- 7 H. S. Roberts and F. H. Smyth. The System Copper-Cupric Oxide. Oxygen *Jnl Amer Chem Soc* (1921) **137**, 1061.
- 8 R. Vogel and W. Poche. Über das System Kupfer-Sauerstoff *Ztsch. f Metallk* (1929) **21**, 333, 368
- 9 D. Hanson, C. Marryat and G. W. Ford. Investigation of the Effects of Impurities on Copper. I, The Effect of Oxygen on Copper. *Jnl Inst Met* (1923) **30**, 197.
- 10 N. P. Allen and A. C. Street. An Investigation of the Effects of Hydrogen and Oxygen on the Unsoundness of Copper-Nickel Alloys *Jnl. Inst. Met* (1933) **51**, 233. Contains quotation from unpublished research by T. Hewitt
- 11 M. Randall, R. F. Nielsen and G. H. West. Free Energy of Some Copper Compounds. *Ind & Eng Chem* (1931) **23**, 388.
- 12 W. H. Bassett and H. A. Bedworth. Estimation of Oxygen and Sulfur in Refined Copper *Trans A.I.M.E.* (1926) **73**, 784
13. H. C. Greenwood. Notiz über die Dampfdruckkurve und die Verdampfungswärme einiger schwerflüchtiger Metalle *Ztsch f Phys Chem* (1911) **76**, 487; *Ztsch f Electrochem.* (1912) **18**, 319, *Trans Faraday Soc* (1911) **7**, 145; *Proc Roy Soc London* (1909) **82A**, 396; (1910) **83A**, 483
- 14 A. Smits *Ztsch f Phys Chem* (1906) **54**, 513
15. D. Stockdale. Discussion of paper by N. P. Allen *Jnl Inst Met* (1930) **43**, 159
- 16 Reference of footnote 7



# An X-ray Study of the Gold-iron Alloys

By ERIC R. JETTE,\* WILLARD L. BRUNER,† AND FRANK FOOTE,‡ NEW YORK, N. Y.

(New York Meeting, February, 1934)

THE alloys of gold and iron were investigated in 1907 by Isaac and Tammann,<sup>1</sup> who determined the thermal diagram for the entire system by thermal analysis and microscopic examination. They also reviewed the previous literature. Since that time the present authors have been able to find only two additional references. Guertler and Schulze<sup>2</sup> examined the electrical resistance of iron alloys containing up to 40 per cent by weight of gold between 0° and 200° C.; the alloys were in the form of wires. The main result of this work was to confirm the solid solubility limit found by Isaac and Tammann; namely, about 20 per cent Au. More recently, Shih<sup>3</sup> has examined the magnetic properties of gold alloys containing up to 10 weight per cent iron and particularly the range below 5 per cent. The alloys in the lower range were found to be paramagnetic; the 10 per cent alloy was ferromagnetic.

The present investigation was undertaken to determine the solid solubility limits at various temperatures, particularly below the  $\alpha$ - $\gamma$  transformation point of iron, since these solubilities are of some importance in connection with the working of the alloys in the manufacture of certain "grey" and "blue" golds.

## MATERIALS AND METHODS

The gold was obtained from the U. S. Metals Refining Co. and contained 99.99+ per cent Au. The electrolytic iron had been annealed in hydrogen and contained impurities as follows: P, 0.035; Si, 0.001; S, C, Mn, Cu, each 0.01 per cent.

Weighed quantities of the two metals were placed in small crucibles lined with pure sintered MgO; a saturated solution of magnesium nitrate

---

Manuscript received at the office of the Institute Nov. 29, 1933.

\* Associate Professor of Metallurgy, School of Mines, Columbia University.

† Research Chemist, Kastenhuber and Lehrfeld, Brooklyn, N. Y.; Special Student School of Mines, Columbia University.

‡ Research Assistant in Metallurgy, School of Mines, Columbia University.

<sup>1</sup> E. Isaac and G. Tammann *Ztsch. anorg. Chem.*, (1907) **53**, 294. Their diagram is reproduced in International Critical Tables, **2**, 450.

<sup>2</sup> W. Guertler and Schulze *Ztsch. phys. Chem.* (1923) **104**, 90.

<sup>3</sup> J. W. Shih *Phys. Rev.* (1931) **38**, 2051.

was used as a binder. Before use the lined crucibles were fired at approximately  $1100^{\circ}\text{C}$ . The crucible containing a charge was placed in a tube that could be flushed with hydrogen and finally evacuated. The alloy was melted and cooled in vacuo; a high-frequency coil was used for heating.

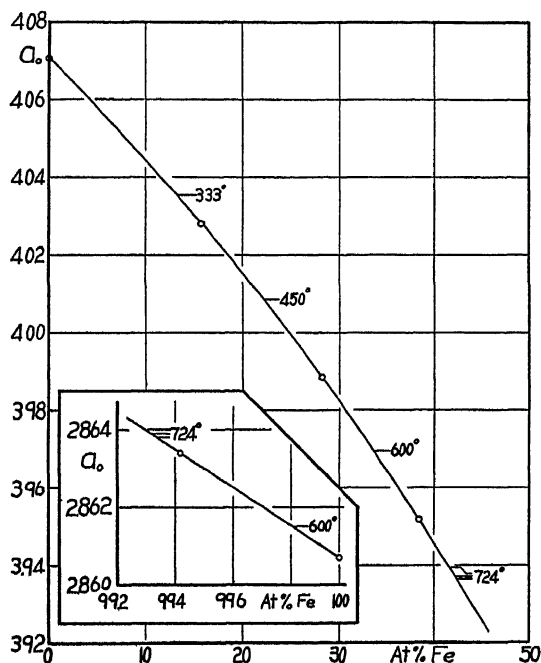


FIG. 1.—EXPERIMENTAL RESULTS ON DETERMINATIONS OF LATTICE CONSTANTS.

In order to secure completely homogeneous alloys, the ingots were annealed in vacuo for a period of a week at temperatures between  $900^{\circ}$  and  $1000^{\circ}\text{C}$ . Most of the alloys being distinctly magnetic, fine particles were prepared by grinding with an alundum wheel. The powders were sealed into small evacuated tubes, annealed for at least 24 hr. and quenched in water. These final annealing temperatures are recorded in Tables 1 and 2. The temperatures were measured by means of either a recently calibrated noble-metal thermocouple or mercury thermometer.

Check analyses were made on all the alloys within the solid solution range and were found to agree exactly with the charges weighed into the crucible. The gold was precipitated by sulfurous acid and weighed as metal. The iron was determined by titration with potassium dichromate.

The X-ray determinations were made by means of Bohlén focussing cameras as modified by Phragmén. These cameras were calibrated empirically against pure NaCl, taking the lattice constant as  $5.6280\text{\AA}$ . and

using radiation from both iron and copper targets. For the work on the iron-gold alloys radiation from an iron target was used. The error in determining the lattice constants of these alloys is certainly not greater than  $\pm 0.001\text{\AA}$  and the experimental points in Fig. 1 agree with the smooth curve drawn through them within considerably smaller limits than this

## RESULTS AND DISCUSSION

The experimental results on the determination of lattice constants are summarized in Tables 1 and 2 and Fig. 1. It may be observed that when the results for the gold-rich solid solution in Table 1 are plotted on a large scale, there is a distinct curvature. This perhaps is not unexpected in view of the difference in the atomic radii ( $r_{\text{Au}} = 1.44\text{\AA}$ ;  $r_{\text{Fe}} = 1.24\text{\AA}$ .) and the wide range over which the solid solution extends. Density measurements proved that this range of solid solutions is of the simple substitution type. On this curve, which is reproduced in Fig. 1, are marked the lattice constants obtained from alloys in the two-phase area annealed at several temperatures. The compositions corresponding to these points are plotted as a function of temperature in Fig. 2. This curve represents the solubility limit of iron in gold at various temperatures.

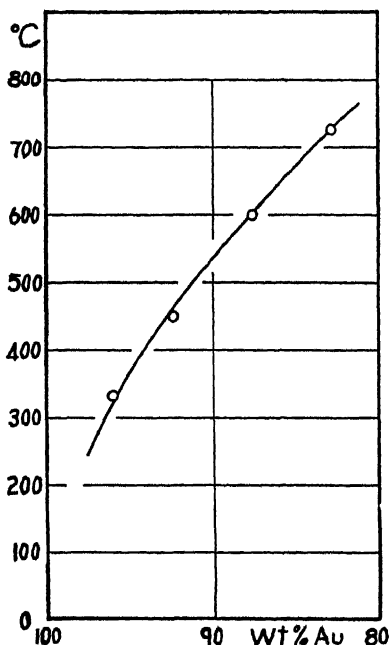


FIG. 2—SOLUBILITY LIMIT OF IRON IN GOLD AT VARIOUS TEMPERATURES

Table 2 also gives lattice constants of the iron-rich phase obtained from the same two-phase alloys.

Inspection shows that gold increases the iron lattice very slightly and this fact is interpreted to mean that the solubility of gold in iron is low. Due to this fact only one determination of the lattice constant within the solid solution range was made. This value agrees closely with the theoretical lattice constant calculated by means of the atomic diameters. For such a narrow range, it is permissible to assume a linear relation between lattice constant and atomic composition. Using this relationship (Fig. 1) the solubility limits of gold in iron were determined. Because of the fact that the gold atom is nearly four times as heavy as the iron atom, these small atomic solubilities became appreciable when expressed in weight per cent. Owing to this

fact and to the small changes observed in the lattice constants of the iron-rich phase, the solubility limits given in Table 2 for this phase may be in error from 0.5 to 1.0 per cent Au by weight. We have not yet succeeded in obtaining sharp lines from this phase at temperatures around 475° C. The solubility curve on the iron side of the system has not been included.

TABLE 1.—*Lattice Constants*  
GOLD-RICH PHASE

Fe, Wt Per Cent	Fe, At Per Cent	Anneal Temp, Deg C	$a_0$ for Au Phase, Å
0	0	724	4 0706
5	15 67	724	4 0280
10	28 18	724	3 9884
15	38 39	724	3 9518

IRON-RICH PHASE

98	99 42	813	2 8634
100	100 0	700	2 8607

TABLE 2.—*Lattice Constants in Two-phase Area*

Gross Composition, Wt Per Cent Au	Anneal Temp, Deg C	$a_0$		Solubility Limits, Wt Per Cent Au	
		Au-rich Phase	Fe-rich Phase	Au-rich	Fe-rich
90	333	4 0353		96 1	
65	450	4 0084		93.1	
20	465		(2 8613)		(0 50)
65	600	3 9694	2 8615	87 5	0 60
20	657		2.8624		1 05
20	724		2 8638		2 00
50	724	3 9394	2 8639	83 1	2 05
65	724	3 9365	2 8640	82 7	2 10
80	724	3 9371		82 8	

In this system, as in several others involving iron as one of the components, it has been impossible to retain by quenching equilibria in which one of the phases has the gamma iron structure. Photograms of alloys quenched from this region are invariably poor. For this reason, measurements could not be extended into the range of existence of gamma iron. This upper region, however, is of small practical importance because if the gamma phase cannot be retained by the very rapid quenching of fine powders, as has been our repeated experience, there is no hope of retaining it in quenched ingots or in cast alloys. Therefore, it is only the properties of the alloys in equilibrium in the alpha range that are encountered in

actual practice Alloys quenched from  $894^{\circ}$  C. showed the diffuse lines typical of iron alloys quenched above the transformation point, from which we may conclude that the transformation temperature of iron saturated with gold lies below this point but above  $724^{\circ}$  C., the next temperature used.

In a general way the constitution of the alloys of the iron-gold system is similar to that proposed by Isaac and Tammann,<sup>1</sup> i. e., there are two terminal solid solution ranges with a two-phase area in between and no indication of a compound of the two elements Quantitatively, however, the equilibrium diagram below the transformation temperature of iron differs considerably from that of the earlier workers The solubility limits reported in the present paper are much lower Isaac and Tammann gave, for example, the solubilities (in weight per cent) at  $400^{\circ}$  as 18 per cent Au and 15 per cent Fe at the iron and gold limits respectively, while the present work gives only 0.5 per cent Au and 5.9 per cent Fe.

It is interesting to note the curious magnetic behavior of the high-gold alloys As mentioned earlier, Shih has determined the magnetic properties for a portion of the range. Pure gold is diamagnetic and the alloys retain the diamagnetic properties up to about 0.1 weight per cent iron when they become paramagnetic The susceptibility increases steadily over the range of 5 per cent iron, which Shih investigated carefully. He observed, however, that the 10 per cent alloy was ferromagnetic. This alloy was well within the solid solution range in the Isaac and Tammann thermal diagram but, on the basis of the solubilities reported in the present paper, the ferromagnetism might well have been due to the presence of the iron-rich phase Shih did not give sufficient details regarding the heat treatment of his alloys to settle this point. In this connection we have investigated the magnetic properties of the alloy containing 15 per cent by weight of iron. A small lump of this alloy was annealed in vacuo for several hours at  $950^{\circ}$  C. and quenched in such a manner that the tube containing the alloy was crushed when it struck the water in the quenching vessel. The ingot could easily be picked up by a magnet. The surface was then polished and carefully etched with dilute aqua regia Microscopic examination up to magnifications of 1200 revealed no trace of a second phase even at the grain boundaries. This is in agreement with X-ray results on the same alloy. Powders, quenched from  $724^{\circ}$  C., of this alloy and of the 90 per cent Au alloy could also be picked up by a magnet. The ferromagnetism is, therefore, a property of the gold-rich solid solution. We have in this series of alloys a continuous change from diamagnetic gold to a ferromagnetic alloy. While 15 per cent by weight of iron seems to be a low concentration, it must be emphasized that this corresponds to 38.4 atomic per cent.

The type of solubility curve on the gold side suggests that these alloys may be precipitation-hardening alloys. Some tests on this were made

on the 85 per cent alloy ingot discussed in the preceding paragraph. A series of six annealings were carried out at 286° C., followed by five more at 465° C. After each anneal the hardness was measured with a Rockwell machine using a 100-kg. load on a  $\frac{1}{8}$ -in. ball. The results, converted to the standard B scale, are summarized in Table 3. Because of the small size of the test specimen, these hardness determinations are not accurate, but they serve to show marked increase in hardness after annealing treatment. The precipitation of the second phase was confirmed by microscopic examination. This precipitation does not take place with measurable velocity at room temperature. The sample of the 15 weight per cent alloy reported in Table 1 was X-rayed again after six months at room temperature; the lattice constant agreed with the previous value within experimental error.

TABLE 3.—*Rockwell B Hardness Number of 85 Per Cent Au Alloy Quenched from 950° C. and Annealed*

Anneal No	0	1	2	3	4	5	6	7	8	9	10	11
Total annealing time, min .		15	30	60	90	130	190	195	200	210	220	240
Annealing temp, deg C		286	286	286	286	286	286	465	465	465	465	465
Rockwell hardness number	43	46	55	64	55	55	59	67	74	97	102	100

### SUMMARY

The gold-iron system has been studied by X-ray methods, particularly at temperatures below the  $\alpha$ - $\gamma$  transformation of iron. It has been established that in this range of temperatures only the two limiting solid solution phases occur. The limits of these solid solutions have been determined at several temperatures. The ferromagnetic character of the solid solutions containing from 10 to 15 per cent by weight of iron has been noted. A series of experiments is reported, which shows that precipitation-hardening of the alloys high in gold is possible.

### DISCUSSION

(*Wheeler P. Davey presiding*)

T. A. WRIGHT,\* New York, N. Y.—I might interject a little commercial comment into a very scientific subject by stating that I am glad the ordinary jewelry manufacturer is not here to hear Dr. Jette tell how to harden an alloy. The manufacturer's main object in life seems to be to get the metallurgist, on the rare occasions when he calls upon him, to give an alloy that will "work like butter"; if it is like butter, he wants it. But we who are in the habit of being called in at times to overcome brittleness in jewelry alloys watch the iron content very, very closely, particularly in the white gold alloys. The iron content is also of interest in the yellow gold alloys. The reason is that we know that if we find iron above certain limits an employee has been

\* Technical Director, Lucius Pitkin Inc.

careless and we are liable to find almost anything else. In other words, contamination has occurred.

I should like to ask one other question. Did you get anything of particular interest from the viewpoint of color in these alloys? Because the jewelry manufacturer today is so far down economically that he is very anxious to find some new developments along the lines of violet and lavender colors.

E. R. JETTE —The colors of these alloys run from the conventional yellow gold to a pale gold and finally to the gray of iron. The two-phase alloys, I think, are not going to be too easy to handle from the standpoint of buffing and getting highly polished surfaces, because the iron phase precipitating out seems to be fairly hard.

Incidentally, silver has a very marked influence on these alloys; the presence of only a small percentage of silver will change the whole appearance of this diagram.

T. A. WRIGHT —Some of the gold the jewelers are buying today from small smelters that have sprung up because of the new gold price contains plenty of silver.

.

■

## X-ray Studies on the Nickel-chromium System

By ERIC R. JETTE,\* V. H. NORDSTROM,† BERNARD QUENEAU‡ AND FRANK FOOTE,‡

NEW YORK, N. Y.

(New York Meeting, February, 1934)

THE nickel-chromium alloys form the base for many industrial heating alloys, so that this system is of considerable practical importance. The literature on these alloys, however, contains much conflicting evidence, not only regarding the solubility limits of the terminal solid solutions at different temperatures but even regarding the number of phases existing in the system. Part of the difficulty undoubtedly arises from the fact that chromium of sufficiently high purity has been available only during the last few years. A second and possibly even more important difficulty arises from the ease with which chromium reacts with silicon and carbon compounds and the atmosphere to form silicides, carbides, nitrides and oxides.

Pilling and Kihlgren<sup>1</sup> in 1929 reviewed the existing scanty information. They did not consider the diagram by which they summarized the various bits of information to be entirely satisfactory.

Matsunaga<sup>2</sup> investigated the system by thermal analysis, microscopic examination and other means. Electrolytic nickel of 99.9 per cent purity and thermit chromium containing 0.30 per cent Al, 0.40 per cent Fe, 0.25 per cent Si and 0.04 per cent C were used. A Tammann furnace with hydrogen flowing through it was used for melting. Sekito and Matsunaga<sup>3</sup> reported an X-ray investigation, presumably on these same alloys, which, as far as can be judged from the abstract, essentially confirmed the thermal and microscopic results.

Nishigori and Hamasumi<sup>4</sup> found compositions for the terminal solid solutions in equilibrium at the eutectic temperature which agreed fairly

---

Manuscript received at the office of the Institute Nov. 29, 1933

\* Associate Professor of Metallurgy, School of Mines, Columbia University.

† Metallurgical Engineering Student, School of Mines, Columbia University.

‡ Research Assistant in Metallurgy, School of Mines, Columbia University.

<sup>1</sup> N. B. Pilling and T. E. Kihlgren. *Trans. Amer. Soc. Steel Treat.* (1929) **15**, 1060.

<sup>2</sup> Y. Matsunaga. *Kinyoku-no-Kenkyu* (Jnl. Study of Metals) (1929) **6**, 207. In Japanese. A translation of part of this article was made available to one of the authors through the courtesy of the International Nickel Co.

<sup>3</sup> S. Sekito and Y. Matsunaga. *Kinyoku-no-Kenkyu* (1929) **6**, 229. Abstract in *Jnl. Inst. Metals* (1930) **42**, 514.

<sup>4</sup> S. Nishigori and M. Hamasumi. *Sci. Rept. Tohoku Univ.* (1929) **18**, 491.



well with those of Matsunaga but their values for the solid solubility limits changed much more rapidly with temperature. Electrolytic nickel containing minor impurities to the extent of 0.15 per cent was used. The

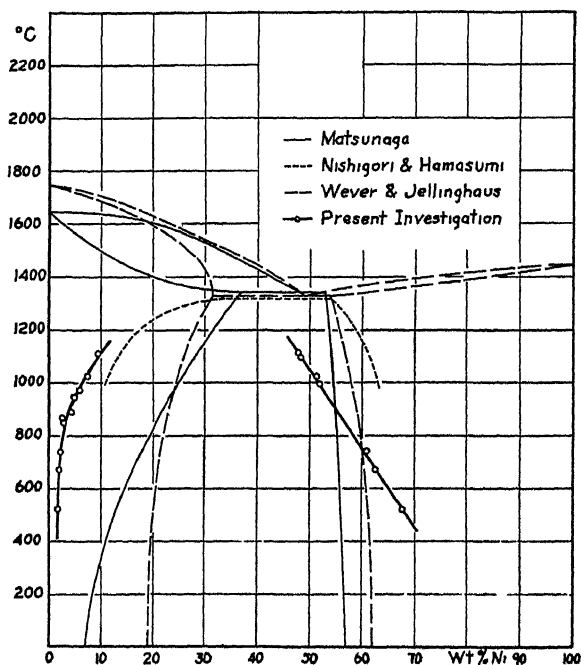


FIG 1.

chromium contained 0.45 per cent Fe, 3.5 per cent Al, 0.9 per cent Si, 0.05 per cent S and 94.21 per cent Cr. However, very little aluminum was found in the alloys; presumably most of it was converted to oxide and absorbed by the walls of the magnesia crucible. The main features of these Japanese investigations, which are of interest in the present article, are included in Fig. 1.

A series of X-ray investigations has been made by Blake and Lord and their collaborators.<sup>5</sup> Unfortunately, the references given are only abstracts of papers presented at various meetings of the American Physical Society and a full description does not seem to have been published; the information is meager therefore, and all the important details are missing. The results available are confusing, but apparently they have found: (1) A face-centered structure between 0 and 63 per cent

<sup>5</sup> W. C. Phebus and F. C. Blake: *Phys. Rev.* (1926) **27**, 798.

F. C. Blake, J. O. Lord and A. E. Focke: *Ibid.* (1927) **29**, 206.

F. C. Blake, J. O. Lord, W. C. Phebus and A. E. Focke: *Ibid.* (1928) **31**, 305.

F. C. Blake and J. O. Lord: *Ibid.* (1930) **35**, 660

chromium (temperature not specified), (2) a body-centered structure at the chromium end of the system, (3) a rhombohedral phase giving photograms with many lines, in alloys high in chromium, (4) a compound

$\text{Cr}_2\text{N}_1$  possessing a tetragonal lattice with  $a = 10.64\text{\AA}$ . and  $\frac{c}{a} = 1.040$ ,

the unit cell containing 96 atoms and the density the same as for body-centered chromium, 6.93, (5) a chromium nitride  $\text{CrN}$  possessing a

hexagonal lattice of  $a = 2.751\text{\AA}$  and  $\frac{c}{a} = 1.605$  with two molecules in

the unit cell. Taken as a whole, these results differ in so many ways from those of the present investigation that further consideration will be given to them in the discussion of our results.

Wever and Jellinghaus<sup>6</sup> determined the liquidus-solidus curves of the system, using electrolytic nickel and chromium containing 0.98 per cent Fe, 0.86 per cent Al, 0.56 per cent Si and 0.01 per cent C. They did not directly determine the phase limits in the solid state. Their diagram is also reproduced in Fig. 1.

The three most recent investigations by thermal and microscopic methods agree in placing the eutectic point close to 50 weight per cent Ni and  $1330^\circ\text{C}$ . They also agree in placing the limiting solidus composition at the eutectic temperature between 32 and 37 weight per cent nickel on the chromium-rich side and at about 54 per cent nickel on the nickel-rich side. The liquidus-solidus curves obtained by the Japanese investigators extrapolate to approximately  $1620^\circ\text{C}$  for pure chromium but Wever and Jellinghaus found approximately  $1750^\circ\text{C}$ . for this point. More recent determinations on chromium of initially high purity, with considerable precautions to prevent contamination, give values well over  $1800^\circ\text{C}$ . Adcock<sup>7</sup> obtained  $1830^\circ\text{C}$ ; Smithells,<sup>8</sup>  $1920^\circ\text{C}$ . The most troublesome impurity seems to be nitrogen, which may lower the melting point to below  $1600^\circ\text{C}$ . Small amounts of iron lower the melting point slightly.<sup>9</sup> The effect of silicon is unknown, but may be expected to be pronounced. In the three investigations of the thermal diagram of the nickel-chromium system discussed above, the chromium used was distinctly impure and no special precautions to keep nitrogen away from the hot or molten metals were mentioned. The precautions adopted to prevent the absorption of carbon may have partly prevented contact with nitrogen. The present writers believe, therefore, that these liquidus-solidus curves should not be taken too seriously as accurate representations of the equilibrium conditions in pure nickel-chromium alloys.

<sup>6</sup> F. Wever and W. Jellinghaus: *Jnl. Kaiser-Wilhelm Inst für Eisenforschung* (1931) **13**, 93.

<sup>7</sup> F. Adcock: *Jnl. Iron and Steel Inst* (1931) **124**, 99.

<sup>8</sup> C. J. Smithells: *Nature* (1929) **124**, 617.

<sup>9</sup> Reference of footnote 7, 124.

Moreover, there is no agreement in the published diagrams regarding the solid solution ranges

### MATERIALS AND PREPARATION OF ALLOYS

The electrolytic nickel used in the authors' investigations contained 0.013 per cent Fe, 0.11 per cent Co, and traces of Si and S. It had previously been heated in purified hydrogen at 1000° C for 72 hr. Spectroscopic test revealed no appreciable amounts of other metallic impurities. The electrolytic chromium supplied by the Electro-Metallurgical Co., through the courtesy of Dr. A. B. Kinzel, contained 0.04 per cent Fe and 0.017 per cent S with a trace of Si. There was also available a small sample of very pure chromium, which had been prepared by reduction with calcium; this sample was obtained through the courtesy of Dr. H. C. Rentschler of the Westinghouse Lamp Works, Bloomfield, N. J. It was used only for determining the lattice constants of the pure metal.

The melts were made in alundum crucibles lined with pure alumina (Norton's Alundum RR). The lining mixture consisted of two-thirds 120-mesh and one-third 200-mesh alumina using a solution of chemically pure  $\text{Al}(\text{NO}_3)_3$  as binder. These crucibles after drying were fired at approximately 1700° C, using a graphite core in a high-frequency furnace as the means of heating. They were afterwards heated in a muffle furnace at about 1100° C under a stream of pure oxygen, to remove any carbon.

The crucible containing a 50-gram charge was placed in a silica tube, which was thoroughly evacuated and flushed with hydrogen several times. The charge was melted in a hydrogen atmosphere using a high-frequency furnace. When the alloy was completely liquid the system was flushed several times with hydrogen as before, and finally evacuated to the limit of a rotary oil pump. The charge was allowed to solidify and cool in vacuo. The resulting ingots were annealed for 24 hr. at 850° C. in vacuo.

In order to secure the material in a form suitable for X-ray analysis, the malleable alloys were filed with very fine steel files and the brittle alloys crushed in a steel mortar and finally ground in an agate mortar to pass a 200-mesh sieve. Steel particles introduced from the file or mortar were removed by a magnet and great care was taken not to introduce any other impurities. Samples thus prepared were finally heat-treated in small evacuated silica tubes. The tubes were always thoroughly heated with a flame during evacuation. The temperatures recorded in Tables 1 and 2 are the final annealing temperatures of the filings or powders. The temperatures were measured by a Pt-Pt 10 per cent Rh thermocouple which had recently been compared with a standard couple. All samples were quenched in ice water from recorded

temperatures The small size of tubes and samples insured rapid cooling. In a few cases, especially in the chromium end of the system where even more rapid quenching was required, arrangements were made to crush the silica tube under water, and thus allow immediate contact between metal and water. The furnace equipped for this technique could be used to temperatures only slightly above  $1100^{\circ}\text{C}$ .

Chemical analyses were made in duplicate on the samples actually used for the X-ray work. In each case the nickel was determined by precipitation with dimethylglyoxime following closely the details of the method given by Lundell, Hoffman and Bright<sup>10</sup> Samples annealed at temperatures between  $1100^{\circ}\text{C}$  and  $1350^{\circ}\text{C}$  were tested for silicon, the tests were negative in every case.

None of the alloys was at any time exposed to air while in a heated condition. This point is important, because nitrogen is probably the most troublesome impurity in chromium alloys. The photograms were carefully examined for the presence of extra lines due to nitride phases. The only case in which such lines were observed will be discussed later.

#### X-RAY METHODS

The powder method with Phragmén's modification of the Bohlin camera was used throughout. These cameras are calibrated empirically, using both iron and copper radiation with sodium chloride as the standard, the lattice constant of sodium chloride was taken as  $5.6280\text{\AA}$ . For the present investigation radiation from a chromium target was the most suitable; the wave lengths of the K radiation used in the computations are  $\alpha_1 = 2.2850$ ,  $\alpha_2 = 2.2889$  and  $\beta = 2.0806\text{\AA}$ . In calculating the constants of the nickel-rich phase, reflections of  $\alpha_1$  and  $\alpha_2$  radiation from the 220 plane and of  $\beta$  radiation from the 311 plane were used, for the chromium-rich phase, the reflections of the  $\alpha_1$  and  $\alpha_2$  radiation from the 211 plane. These reflections were the only ones located in the outermost camera range where the most accurate measurements may be made. The error in measuring the lattice constants of these phases is certainly not greater than  $\pm 0.001\text{\AA}$ . Lattice constants could not be obtained from alloys quenched above  $1150^{\circ}\text{C}$ . because of the rapid changes of solubility in both phases above this temperature and the impossibility of retaining the high-temperature situation by quenching. There is also the possibility of an allotropic modification of chromium, which will be discussed later. Reflections obtained from the alloys quenched at these high temperatures were invariably so badly blurred that accurate measurements were impossible.

---

<sup>10</sup> Lundell, Hoffman and Bright: *Chemical Analysis of Iron and Steel*, 281. New York, 1931. John Wiley & Sons.

## RESULTS

The results are summarized in Tables 1 and 2. Fig. 2 shows the plots of lattice constant versus atomic composition for the two homogeneous phases; along each of the two curves, the lattice constants of the respective phases when in equilibrium with the other phase at several temperatures are indicated. The compositions corresponding to these constants are plotted as a function of temperature in Fig. 1; this is the equilibrium diagram for the system for the temperature range covered by the present

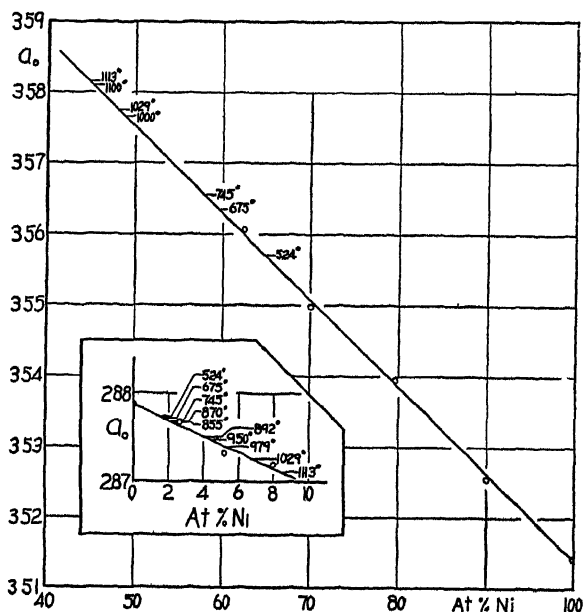


FIG 2

investigation. The average deviation of the points from the curves in Fig. 2 is  $\pm 0.0005\text{\AA}$ .

In addition to the nickel-rich and chromium-rich phases, the alloys high in chromium generally contained a third phase, which was indicated by an additional set of lines on the photograms. Microscopic examination revealed small inclusions. By proper treatment with acids these inclusions were isolated and X-ray photograms were made. The extra lines on the alloy photograms coincided exactly with the strongest lines on the photograms obtained from the inclusions. The structure of these inclusions proved to be rhombohedral. Comparison with material of known composition demonstrated conclusively that these inclusions were chromic oxide ( $\text{Cr}_2\text{O}_3$ ). The failure of these inclusions to dissolve in the acid treatment is due undoubtedly to the slow rate of solution frequently observed with oxides that have been heated to very high temperatures.

A sample of pure chromium that had been heated for an hour at 1340° C and quenched, yielded, besides a few of the strongest  $\text{Cr}_2\text{O}_3$  reflections, lines that calculation showed to be due to a hexagonal close-packed structure. Comparison with the work of Blix<sup>11</sup> showed that the  $\sin^2\theta$  values observed were identical with all the strongest lines (except those of the 112 planes) found by him to belong to the compound  $\text{Cr}_2\text{N}$ <sup>12</sup> The

TABLE 1—*Alloys in Nickel Solid Solution Range*

Alloy No	Ni, Atomic Per Cent	Temperature of Anneal, Deg C	$a_0$ , Ångstroms
1	99 88	1000	3 5143
4	90 08	1029	3 5255
5	79 57	1029	3 5394
6	70 12	1029	3 5498
7	62 46	1029	3 5607

## ALLOYS IN TWO-PHASE AREA

Alloy No	Ni, Atomic Per Cent	Temperature of Anneal, Deg C.	$a_0$ for Alpha Phase	Solubility of Cr in Ni, Per Cent Cr	
				At Per Cent	Wt Per Cent
10	29 05	524	3 5569	35 1	32 4
11	17 93	524	3 5571	35 2	32 5
10	29 05	675	3 5635	40 4	37 5
11	17 93	675	3 5635	40 4	37 5
10	29.05	745	3 5654	42 0	39 1
11	17 93	745	3 5655	42 1	39 2
11	17.93	1000	3 5766	51 1	48 1
10	29 05	1000	3 5767	51 2	48 2
8	49 08	1029	3 5774	51 8	48 8
10	29 05	1100	3 5810	54 7	51 7
10	29.05	1113	3 5815	55 2	52 2
11	17 93	1113	3 5815	55 2	52 2

lattice constant of the chromium sample, which showed the presence of  $\text{Cr}_2\text{N}$  phase was found to be 2 8792 Å., which agrees with the value for pure chromium within the limits of experimental error. This checks the observation of Blix that the solubility of nitrogen in chromium is very low.

<sup>11</sup> R. Blix: *Ztsch. phys. Chem* (1929) 3B, 229

<sup>12</sup> It is not clear how it happened that this sample was exposed to the atmosphere. It had evidently not been properly "degassed" or dried before sealing into the silicon tube, because pressure developed and a bulb was blown on the end of the tube. It is highly probable that this bulb developed small holes or cracks which admitted nitrogen. The failure to find the reflections from the 112 planes was due undoubtedly to the position of these lines at the outermost range of angles and the fact that the lines that did occur were somewhat diffuse

The lattice constant of nickel given in Table 1, which was obtained with radiation from a chromium target, is slightly less than when iron radiation is used, the latter value for  $a_0$  being 3.5158Å. Owen and Iball<sup>13</sup> using copper radiation obtained  $a_0 = 3.5179\text{Å}$ . Chromium radiation was used consistently throughout the present investigation so that any error due to this factor does not affect the solubility limits. Lattice

TABLE 2 — *Alloys in Chromium Solid Solution Range*

Alloy No	Ni, Atomic Per Cent	Temperature of Anneal, Deg C	$a_0$ , Ångstroms
Westinghouse	0	1000	2.8787
Electrolytic	0	1029	2.8787
14	2.66	1000	2.8768
16	5.20	1063	2.8733
15	7.98	1122	2.8720

## ALLOYS IN TWO-PHASE AREA

Alloy No	Ni, Atomic Per Cent	Temperature of Anneal, Deg C	$a_0$ for Beta Phase	Solubility of Ni in Cr, Per Cent Ni	
				At Per Cent	Wt Per Cent
10	29.05	524	2.8774	1.4	1.6
11	17.93	524	2.8774	1.4	1.6
10	29.05	675	2.8772	1.6	1.8
11	17.93	675	2.8772	1.6	1.8
10	29.05	745	2.8769	2.0	2.2
11	17.93	745	2.8769	2.0	2.2
15	7.98	855	2.8767	2.4	2.7
16	5.20	870	2.8768	2.2	2.5
12 <sup>a</sup>	10.98	892	2.8751	3.9	4.4
12 <sup>a</sup>	10.98	950	2.8748	4.3	4.8
12 <sup>a</sup>	10.98	979	2.8740	5.2	5.8
12	10.98	1029	2.8727	6.6	7.4
10	29.05	1029	2.8727	6.6	7.4
11	17.93	1029	2.8729	6.4	7.1
11	17.93	1113	2.8713	8.2	9.2
10	29.05	1113	2.8711	8.4	9.4

<sup>a</sup> Prior anneal and quench from 1029° C in powder form.

constants measured in this laboratory generally differ only in the fourth decimal place from those measured by Professor Owen. Nickel, however, is an exception and this probably is to be traced back to some difference in the materials rather than in the X-ray methods.

The lattice constant of pure chromium given in Table 2 is nearly identical with that found by Preston;<sup>14</sup> that is,  $a_0 = 2.8786\text{Å}$ .

<sup>13</sup> E. A. Owen and J. Iball: *Phil. Mag.* [7] (1932) **13**, 1020.

<sup>14</sup> G. D. Preston: *Jnl. Iron and Steel Inst.* (1931) **124**, 139.

It has been shown by Bradley and Ollard<sup>15</sup> and Sasaki and Sekito<sup>16</sup> that electrolytic chromium prepared under certain conditions of electrolysis has a hexagonal close-packed structure. In order to determine whether this structure could be obtained at high temperatures and retained by quenching, samples of electrolytic chromium, which had been degassed by heating in vacuo for 12 hr at 1000° C., were quenched from 1300° and 1450° C., the samples being sealed in silica tubes. The results were negative, no lines other than those of the body-centered modification and one or two lines from  $\text{Cr}_2\text{O}_3$  were found on the photograms. Similarly negative results in this respect were obtained on quenching high-chromium alloys.

### DISCUSSION OF RESULTS

The solubility limits obtained in the present investigation may be directly compared to those given in earlier articles by a study of Fig. 1. In this diagram the liquidus-solidus curves on the nickel side of the eutectic, obtained in the three investigations quoted, are so nearly the same that only the results by Wever and Jellinghaus are given. On the chromium side these authors' results differ markedly from those of both the Japanese investigations. On account of the essential agreement between these last two sets of results on the liquidus-solidus lines, only Matsunaga's curves are given. The new results differ from the older in two respects:

1. The nickel-rich solid solution range widens out rapidly with increase of temperature with a low-temperature limit of considerably lower nickel content than has previously been assumed. The accuracy and consistency of the experimental results were tested by plotting on a large scale; the maximum difference between a point and the corresponding point on the curve was 0.4 per cent Ni.

2. The solubility of nickel in chromium is much lower than previously supposed, but the conclusion of earlier workers that the solubility increases rapidly at high temperatures is confirmed.

It will be obvious that the solid-phase limits found in the present investigation are not consistent with the liquidus-solidus curves of the system as known at present. If the liquidus-solidus curves are to be accepted, in spite of the known and probable impurities that have been discussed in an earlier section, the newly determined solid-phase equilibria can be reconciled with these curves only by assuming retrograde solubility above 1150° C. on the nickel side. Retrograde solubility, of course, is likely to occur if there is a change in the phase with which the phase under consideration is in equilibrium. This phenomenon can, and does, also occur without the intervention of a phase change. It has

<sup>15</sup> A. J. Bradley and E. F. Ollard: *Nature* (1926) 117, 122.

<sup>16</sup> K. Sasaki and N. Sekito: *Jnl. Soc. Chem. Ind. (Japan)* (1930) 33, 482.



already been noted that a hexagonal close-packed modification of chromium has been prepared by electrolytic methods. A cubic modification having the same structure as  $\alpha$  Mn has also been found.<sup>17</sup> In view of the fact that the high-temperature modifications of manganese may likewise be prepared electrolytically, the possibility that the other modifications of chromium occur at high temperatures is distinctly favorable. The fact that we have been unable to retain such phases by quenching pure chromium cannot be considered as evidence against this possibility, since a similar case occurs with  $\gamma$  and  $\delta$  iron. Experience in this laboratory has shown, for example, that if an iron alloy while being quenched passes through the temperature where the  $\gamma$ - $\alpha$  transformation takes place, the lines on the X-ray photograms will be diffuse. This is due mainly, if not entirely, to the change in solubility accompanying the change of phase. All the films of nickel-chromium alloys quenched above 1150° C contained only such diffuse lines. In this case, however, since there is doubt concerning the existence of a high-temperature modification of chromium, and since it is also possible to explain diffuse lines on the basis of failure to secure adequate quenching from a region of rapidly changing solubility, no final decision can be reached at present. In view of this uncertainty and the doubts already expressed concerning the accuracy of the liquidus-solidus curves, the writers do not feel justified in drawing up a new thermal diagram.

The X-ray work of Blake and Lord and their collaborators has been published only in the form of very brief abstracts, so that in what follows we may misinterpret their work because of the lack of any adequate description of their materials, methods and results. However, it would seem that the rhombohedral phase which they found in high-chromium alloys is probably  $\text{Cr}_2\text{O}_3$ . The compound  $\text{CrN}$  with a hexagonal close-packed structure is in all probability disposed of by the work of Blix<sup>18</sup> already quoted. Blix found a compound of this formula but it has the same structure as  $\text{NaCl}$ . The first new structure occurring in the chromium-nitrogen system is hexagonal close-packed with dimensions not far different from those given by Blake and Lord, but it exists over a range of compositions in the vicinity of the formula  $\text{Cr}_2\text{N}$ . Finally, no evidence has been found indicating the existence of the large tetragonal structure reported by Blake and Lord, which they considered to belong to a chromium nickelide of the formula  $\text{Cr}_2\text{Ni}$ .

#### SUMMARY

The equilibrium diagram of nickel-chromium alloys of a high degree of purity has been studied by X-ray methods of investigating crystal structure. It has been shown that at temperatures below 1150° C. this

---

<sup>17</sup> Reference of footnote 16.

<sup>18</sup> Reference of footnote 11.

system consists of two terminal solid solutions with an intervening two-phase area. On the chromium side of the system the solubility of nickel in chromium is low but increases rapidly at temperatures above 900° C. The solubility of chromium in nickel increases at a rapid but fairly uniform rate as the temperature increases. The solubility found at 1113° C is nearly 53 wt per cent chromium, which is beyond the eutectic point as determined by thermal analysis. Reasons for this discrepancy are discussed. No structures were found other than the body-centered chromium lattice, the face-centered nickel lattice and, occasionally, the rhombohedral structure of  $\text{Cr}_2\text{O}_3$ . The latter substance has been isolated as inclusions from high-chromium alloys.

## DISCUSSION

*(Wheeler P. Davey presiding)*

D. F. McFARLAND,\* State College, Pa.—I have not worked on this system for a great many years. In fact, the work was done back in 1914–15 in connection with work that Oscar Harder was doing for his Doctor's thesis and J. T. Ford for his Master's thesis at the University of Illinois. The thing that impresses me particularly is the great advance that has been made in possibilities of exact work since that time. A period of 18 years has brought about all of these improvements. At that time, the best conditions that we could bring to bear on a study of this equilibrium involved the use of gas-fired crucible furnaces with very distinct limitations. The use of crucibles of graphite, lined with alumina, zirconia or magnesia has developed since then. There was no possibility, under our working conditions, of control of atmosphere. The X-ray was just beginning to be used at that time, so, of course, we could not use that. The high-frequency induction furnace had not yet been made available. And the best metals we could get were of very doubtful purity as compared to those available now. This work represents extremely fine technique and I wish to congratulate Dr. Jette on it, simply on the basis of our experience with the poorer technique that was possible 18 years ago.

J. T. NORTON,† Cambridge, Mass.—I would merely like to ask Dr. Jette if he has made any observations of the changes in these alloys during aging. Obviously, the diagram indicates possibilities of age-hardening, and I wonder if he has made such observations with a view to determining the type of hardening that takes place, whether it is precipitation-hardening or something else.

E. R. JETTE—No, we have not. The chief reason is that we have not had time.

J. S. MARSH,‡ New York, N. Y.—I should like to suggest to Dr. Jette another possibility for that diagram. I doubt very much the probability of retrograde solubility. It seems possible that the diagrams of the German and Japanese investigators are irregular sections through the chromium-nickel-nitrogen diagram. Since nitrogen has a large effect on the melting point of chromium, it seems altogether conceivable that the eutectic point of the chromium-nickel system should move over to the left-hand side of your Fig. 1; that is, containing much more chromium than is shown by these diagrams, which would take care of the solubility curves that you have found.

E. R. JETTE.—I always hesitate to interpret another investigator's thermal analysis, because I do not know the technique myself, and I do not know how many

---

\* Head, Department of Metallurgy, Pennsylvania State College.

† Associate Professor of Physics and Metals, Massachusetts Institute of Technology.

‡ Assistant Editor, Alloys of Iron Research.

things can happen. None of the people who have worked on the systems have, in my opinion, given adequate protection against nitrogen.

The effect of nitrogen was worked out rather carefully at one time by, I think, Adcock.<sup>19</sup> They have found that the melting point of chromium may be lowered below 1600° simply by picking up nitrogen. The chromium-nitrogen system<sup>20</sup> has been worked out. I have forgotten the details but there are at least two compounds, both of which are very stable, that is,  $\text{Cr}_2\text{N}$  and  $\text{CrN}$ . I am not sure about the rest of the diagram now. But it is unquestionable that nitrogen has a tremendous effect.

The reason that I am not willing to include an interpretation of that sort in the paper is that the amount of nitrogen that is going to be absorbed depends entirely upon the experimental set-up.

All those working on this system have appreciated that carbon would seriously affect their results, but the means adopted for preventing the access of carbon or its compounds to the alloy were frequently far from satisfactory. The Japanese investigators, for example, melted their alloys in a carbon-tube resistance furnace and passed a stream of hydrogen through the furnace to prevent or at least reduce the contamination by carbon. Although direct contact with carbon as such was thus avoided, contamination was not prevented, since chromium will react with  $\text{CO}$ ,  $\text{CO}_2$  or hydrocarbons. How completely air was eliminated from the system under these conditions cannot be determined and thus the amount of nitrogen absorbed is unknown.

G EDMUNDS,\* Palmerton, Pa.—Dr. Jette has made somewhat of a wholesale condemnation of thermal methods, and I do not quite agree that the thermal microscopic method is subject to that condemnation. I feel that had Dr. Jette substituted the microscopic for the X-ray method, with technique as accurate and careful as he has used, his results would not have differed greatly from those that he has obtained. In other words, we are today taking the X-ray as a new tool, applying refined methods of stabilizing our samples and then examining by X-ray, and we say the older microscopic method is not as good as the X-ray method, whereas the fundamental preparation of the alloy had more to do with it than the difference in the method.

If there is a difference in solubility in a sample because it was prepared by some inferior technique, that will be reflected just as much with the X-ray as with the thermal microscopic procedure. To be sure, there are some cases where it is almost impossible to detect the presence of a secondary constituent appearing in an alloy; for example, this may be due to the fact that the difference between the etching characteristics or the appearance of the secondary constituent and the matrix is indefinite.

Whenever such a system, as one which changes solubility very rapidly with temperature and in which an adequate quench cannot be obtained, is being examined, there is a very decided advantage in using the X-ray method, provided it can be carried on at the temperature at which the solubility is being determined; but, in line with what I just said, there is no real advantage in the X-ray method if quenched specimens are used.

E R JETTE—I thought I guarded against the notion that I condemned the thermal analysis in the microscopic examination in a wholesale manner, because I had no intention of doing that. But it is certainly true that the ways in which the thermal analysis and the microscopic examination techniques have been handled in the past, have left very much to be desired. The false results that were obtained we are now picking up with the X-ray and the people working along the classical lines are also finding them as they go through their systems more carefully.

<sup>19</sup> Reference of footnote 7.

<sup>20</sup> Reference of footnote 11.

\* Investigator, Research Division, New Jersey Zinc Co.

There has been for some time, of course, a considerable difficulty in convincing metallurgists who have been working along the classical methods that the X-ray methods had anything to tell them at all, and they have, in fact, thought that they could be more certain of their results using the classical method. It is all a question of interpretation. Each investigator is accustomed to handling his own technique.

It is interesting in this connection to note that a year or so ago, Westgren attempted to answer this kind of an objection and had an article in *Metallwirtschaft*<sup>21</sup> on the copper-zinc system. He showed that the X-ray technique gave practically identical results with the best work that had ever been done on that system, and that was, I think, the Hanson and Bauer diagram, that in every detail the two methods checked. That, of course, is what we are ultimately coming to. I have no notion that the X-ray technique is going to do everything, it will not. Precisely the kind of problems that you have indicated, the quenching problems, are one of its disadvantages, because frequently it happens that you can see traces of something that did exist at high temperatures when you look at your microscopic section, which means nothing to us, we do not get that kind of a trace at all. All we know is that we do not have the structure we should have had at the high temperature, and it is not always possible to be certain that there was a high-temperature phase.

As far as the quenching techniques themselves are concerned, there is a slight advantage from the standpoint of the X-ray work in that instead of quenching ingots, blocks of metal, we are quenching powders. Not everybody does that, but it is Westgren's standard practice and it is ours at Columbia. On the high-chromium end, for example, we had to get a very drastic quench in order to get anything like sharp lines. This we accomplish by using a vertical furnace about 15 to 18 in. long. In order to reduce convection currents of air and to keep the temperature gradients within the furnace as constant as possible, long quartz or nichrome tubes extending well beyond the furnace ends are cemented into the main furnace tube; another tube contains a noble metal thermocouple. The finely powdered sample is sealed in a quartz capsule and suspended in one of the inner tubes at the level of the thermocouple tip. The lower end of the inner tubes is kept under water. When a quench is to be made, a heavy brass block is placed in the water just beneath the tube. The capsule suspension is broken and the capsule itself crushed under water by dropping a heavy iron plunger through the tube. The quenching is practically instantaneous but we have found even this to be inadequate in some cases.

In order to make clear my point of view as to the comparative merits of the X-ray and more classical techniques, I shall amplify somewhat the foregoing remarks. Today, if sufficient care is exercised, the latter techniques will yield excellent results which, furthermore, will not be at variance with those obtained from the X-rays. But Mr. Edmunds brought out a fundamental point. The technique used in making the examination is not of as great importance as is the substance that is being examined. No technique for investigating alloys, even when in the best of hands, can yield satisfactory results from improperly prepared specimens; at best the results are then inconclusive, at their worst, false. For many problems either the classical or the X-ray methods may be used with equal success; the choice of method then depends upon expediency and the investigator's own preference. There are other problems which can best be solved by one of the classical methods and still others that are best attacked by the X-ray technique. Common sense compels us to recognize that, as far as the determination of alloy equilibrium diagrams is concerned, the two different sets of techniques are essentially complementary, while, from the standpoint of discovering the more intimate relations between the atoms involved, the classical methods tell us nothing at all and the X-ray technique is, as yet, the only one capable of yielding the desired information.

---

<sup>21</sup> A. Johansson and A. Westgren - *Metallwirtschaft* (1933) 12, 385.



# INDEX

(NOTE: In this index the names of authors of papers and discussions and of men referred to are printed in SMALL CAPITALS, and the title of papers in *italics*.)

## A

- Aging aluminum alloys, 164  
 aluminum-copper alloys, 106  
 aluminum-nickel alloys, 300  
 copper-aluminum alloys, 106  
 nickel bronzes, 218  
 zinc-aluminum alloys, 110
- AKULOV, N S magnetization theory, 48
- Alloys (*See also* names of metals)  
 solid solutions, intermetallic, 75
- Aluminum binary alloys, equilibrium relations, 304  
 crystals *See* Crystals  
 quenching stresses, 158
- Aluminum-copper alloys, effect of quenching, 94
- Aluminum-magnesium alloys constitution, 85
- Aluminum-magnesium silicide alloys equilibrium diagram, 307
- Aluminum-nickel alloys equilibrium relations, 293
- American Institute of Mining and Metallurgical Engineers Divisions' Institute of Metals, officers and committees, 8  
 officers and directors, 7
- ANDERSON, E A, FULLER, M L, WILCOX, R L AND RODDA, J L *High-zinc Region of the Copper-zinc Phase Equilibrium Diagram*, 204
- ANDERSON, E A, SPRINGER, R. D, WILCOX, R L AND WARING, R K *Equilibrium in the Lead-zinc System with Special Reference to Liquid Solubility*, 254
- AUSTIN, C R *Discussion on Comparative Studies on Creep of Metals Using A Modified Rohn Test*, 74
- AUSTIN, C R. AND GREY, J. R. *Comparative Studies on Creep of Metals Using a Modified Rohn Test*, 53

## B

- Barium for deoxidizing nickel bronze, 220
- BARRETT, C S. *Discussions on Crystal Orientations Developed in Alloyed Zinc*, 153  
*on Effect of Quenching Strains on Aluminum-copper Alloys*, 112  
*on Internal Stresses in Quenched Aluminum and Some Alloys*, 180
- Bearing metal, cadmium-nickel, 333
- BECK, K. magnetization studies, 18

- BINGHAM, K E on aluminum-nickel system, 293
- BITTER, F on magnetization, 49
- BOZORTH, R M magnetization theory, 49
- Brass crystals, cold-rolled, orientation, 119
- BRICK, R M AND PHILLIPS, A *Effect of Quenching Strains on Lattice Parameter and Hardness Values of High-purity Aluminum-copper Alloys*, 94, *Discussion*, 116
- Bronzes nickel deoxidizing with barium, 220  
 effect of various metals, 233  
 fatigue strength, 234  
 hard-rolled, properties, 238  
 strength and aging, 218
- BRUNER, W L, JETTE, E R AND FOOTE, F. *An X-ray Study of Gold-iron Alloys*, 354

## C

- Cadmium-nickel alloy, 333
- CARTER, H G *Discussion on Equilibrium Relations in Aluminum-nickel Alloys of High Purity*, 303
- CHRISTIE, J L *Discussions on Influence of Silver on the Softening of Cold-worked Copper*, 203  
*on Testing the Drawing Properties of Rolled Zinc Alloys*, 253
- Chromium effect on nickel bronze, 233
- Chromium-aluminum alloys equilibrium diagram, 308
- Chromium-iron alloys atomic radius, 88
- Chromium-nickel alloys constitution, 83  
 18-8 creep, 66  
 X-ray study, 361
- Chromium-nickel-iron alloys creep, 66
- Cobalt, creep, 57  
 investigations of magnetic properties, 44
- Cobalt-aluminum alloys equilibrium diagram, 307
- Cobalt-iron alloys, magnetic studies, 44
- Conductivity copper influence of silver, 197  
 copper-zinc alloys, 273
- Coordination number as affecting solid solutions, 81
- CORDIANO, H V *Discussion on Lithium-magnesium Equilibrium Diagram*, 332
- CORDIANO, H. V AND HENNEY, O H *Lithium-magnesium Equilibrium Diagram*, 319

- Copper cold-worked influence of silver, 196  
 effect of oxygen, 181  
 embrittlement, 205  
 softening by tinning, 198  
 solid solubility of oxygen in, 337
- Copper-aluminum alloys equilibrium diagram, 306  
 precipitation reactions, 98
- Copper-aluminum-magnesium alloys magnetic properties, 41
- Copper-cuprous oxide eutectic, 181  
 system, 339, 347
- Copper-lithium alloys thermal analysis, 320
- Copper-manganese alloys constitution, 84  
 lattice constants, 84
- Copper-oxygen system, 337
- Copper-tin-nickel alloys strength and aging, 218
- Copper-zinc alloys epsilon structure, 289  
 equilibrium diagram, 264  
 peritectic point, 264, 283
- CRAIG, G L AND KENNY, H C *Influence of Silver on the Softening of Cold-worked Copper*, 196
- Creep of metals modified Rohn test, 53
- Crystals aluminum orientation of cold-rolled, 120  
 brass, alpha cold-rolled, orientation, 119  
 metallic ferromagnetism, 11  
 single orientation in cold-rolled, 119  
 zinc alloyed, orientation, 146  
 deformation, 135
- D
- DAVEY, W P *Discussions on Lithium-magnesium Equilibrium Diagram*, 332  
*on X-ray Study of Orientation Changes in Alpha Brass*, 134
- Dilatation method of measuring, 72
- Drawing rolled zinc alloys, 245
- DRIER, R W *Discussion on Crystal Orientations Developed in Alloyed Zinc*, 154, 155
- Ductility dynamic test applied to zinc, 245  
 nickel bronzes, 222
- DUSSLER, E magnetization studies, 33
- E
- EASE, J T AND WISE, E M *Strength and Aging Characteristics of the Nickel Bronzes*, 218, *Discussion*, 244
- EASTWOOD, L W *Structure and Origin of the Copper-cuprous Oxide Eutectic*, 181, *Discussion*, 195  
*Discussion on Structure and Origin of the Copper-cuprous Oxide Eutectic*, 189, 192
- EDMUNDS, G *Discussions on Testing the Drawing Properties of Rolled Zinc Alloys*, 252, 253  
*on X-ray Studies on the Nickel-chromium System*, 372
- EDMUNDS, G AND FULLER, M L *Crystal Orientations Developed by Progressive Cold Rolling of an Alloyed Zinc*, 146, *Discussion*, 156
- EDMUNDS, G AND KELTON, E H *Testing the Drawing Properties of Rolled Zinc Alloys*, 245
- Equilibrium diagrams aluminum alloys, 305 et seq  
 aluminum-nickel alloys, 293  
 lithium-magnesium, 319  
 nickel-chromium system, 361, 370
- Eutectic aluminum, various, 312  
 cadmium-nickel, 336  
 copper and cuprous oxide, 181  
 nickel-chromium, 363  
 "Eutectic colony," investigation, 191
- F
- Fatigue strength of nickel bronze, 234
- Ferromagnetism in metallic crystals, 11
- Ferrosilicon, constitution, 85
- FIELD, A J *Discussion on Correlation of Equilibrium Relations in Binary Aluminum Alloys of High Purity*, 318
- FINK, W L *Discussions on Correlation of Equilibrium Relations in Binary Aluminum Alloys of High Purity*, 318  
*on Equilibrium Relations in Aluminum-nickel Alloys of High Purity*, 303
- FINK, W L AND FRECH, H R *Correlation of Equilibrium Relations in Binary Aluminum Alloys of High Purity*, 304
- FINK, W L AND WILLEY, L A *Equilibrium Relations in Aluminum-nickel Alloys of High Purity*, 293
- FOOTE, F, JETTE, E R AND BRUNER, W L *An X-ray Study of Gold-iron Alloys*, 354
- FOOTE, F, JETTE, E R, NORDSTROM, V H AND QUENEAU, B. *X-ray Studies on the Nickel-chromium System*, 361
- FRECH, H R AND FINK, W L *Correlation of Equilibrium Relations in Binary Aluminum Alloys of High Purity*, 304
- FULLER, M L *Discussion on Crystal Orientations Developed in Alloyed Zinc*, 154, 155
- FULLER, M L, ANDERSON, E A, WILCOX, R L AND RODDA, J L *High-zinc Region of the Copper-zinc Phase Equilibrium Diagram*, 264
- FULLER, M L AND EDMUNDS, G *Crystal Orientations Developed by Progressive Cold Rolling of an Alloyed Zinc*, 146, *Discussion*, 156
- G
- GANN, J. A *Discussion on Lithium-magnesium Equilibrium Diagram*, 332
- GENSAMER, M *Discussion on X-ray Study of Orientation Changes in Alpha Brass*, 134
- GERLACH, W magnetization studies, 32
- GIER, J R AND AUSTIN, C H: *Comparative Studies on Creep of Metals Using a Modified Rohn Test*, 53
- Gold-iron alloys constitution, 83  
 lattice constants, 83  
 X-ray examination, 354

Gold-silver alloy, lattice, 97  
 GORTER, C J on magnetization, 49  
 Grain boundary influence on deformation, 135  
 GREGG, J L *Influence of Silver on the Softening of Cold-worked Copper*, 204  
 GWYER, A C G on aluminum-nickel system, 293

H

HANSEN, M on copper-zinc system, 286  
 HARGREAVES, F *Discussion on Structure and Origin of the Copper-cuprous Oxide Eutectic*, 194  
 Hardness aluminum-copper alloys, effect of quenching, 94  
     copper-aluminum alloys, 108  
     gold-iron alloys, 359  
     nickel bronzes, 222  
 Haas and Jellinek investigation of lead-zinc system, 262  
 HEAPS, C. W magnetization studies, 24  
 Heat treatment copper-zinc alloys, 267  
     nickel bronze, 235  
 HEISENBERG, W magnetization theory, 48  
 HENRY, O H *Discussion on Lithium-magnesium Equilibrium Diagram*, 332  
 HENRY, O H AND CORDIANO, H V *Lithium-magnesium Equilibrium Diagram*, 319  
 HEYN, E formula for internal stresses, 160  
 HILL, A G magnetization studies, 35  
 HONDA, K magnetization studies, 27, 47  
 HOPKINS, H L, KEMPF, L W AND IVANSO, E V. *Internal Stresses in Quenched Aluminum and Some Aluminum Alloys*, 158  
 Hydrogen reduction of cuprous oxide in copper, 205

I

Intermetallic compound of aluminum and nickel, 296  
 Intermetallic solid solutions, 75  
 Iron creep, 58  
     effect on nickel bronze, 233  
     magnetization, 18  
 Iron-aluminum alloys equilibrium diagram, 305  
 Iron-cobalt alloys magnetic studies, 44  
 Iron-gold alloys X-ray examination, 354  
 Iron-silicon alloys constitution, 85  
 IVANSO, E. V, KEMPF, L W AND HOPKINS, H. L *Internal Stresses in Quenched Aluminum and Some Aluminum Alloys*, 196

J

JETTE, E. R *Intermetallic Solid Solutions*, 75, *Discussion*, 92  
     *Discussions on X-ray Studies on Nickel-Chromium System*, 371, 372  
     *on An X-ray Study of Gold-iron Alloys*, 360  
 JETTE, E. R., BRUNER, W L. AND FOOTE, F. *An X-ray Study of Gold-iron Alloys*, 354

JETTE, E R, NORDSTROM, V H, QUENEAU, B AND FOOTE, F *X-ray Studies on the Nickel-chromium System*, 361

K

KAYA, S magnetization studies, 35, 38  
 KELTON, E H AND EDMUNDS, G *Testing the Drawing Properties of Rolled Zinc Alloys*, 245  
 KEMPF, L W *Discussion on Effect of Quenching Strains on Aluminum-copper Alloys*, 113  
 KEMPF, L W, HOPKINS, H L AND IVANSO, E V *Internal Stresses in Quenched Aluminum and Some Aluminum Alloys*, 158  
 KENNY, H C AND CRAIG, G L *Influence of Silver on the Softening of Cold-worked Copper*, 196

L

Lattice constants copper-aluminum alloys, 96  
     gold-iron alloys, 355  
     Au-Ag, Cu-Pd, and Fe-Cr alloys, 80  
     nickel-chromium, 366  
 Lattice parameter of aluminum-copper alloys, effect of quenching on, 94  
 Lead effect on nickel bronze, 233  
 Lead-zinc system equilibrium, 254  
 LeChatelier thermodynamic equation, 304  
 LICHTENBERGER, F on magnetization of iron-nickel alloys, 42  
 Lithium alloys preparation, 323  
 Lithium-copper alloys thermal analysis, 320  
 Lithium-magnesium alloys equilibrium diagram, 319  
 Lithium-zinc alloys thermal analysis, 320

M

MACNAUGHTAN, D J *Discussion on Strength and Aging Characteristics of Nickel Bronzes*, 243  
 Magnesium-aluminum alloys equilibrium diagram, 307  
 Magnesium-aluminum silicide alloys equilibrium diagram, 307  
 Magnesium-lithium alloys equilibrium diagram, 319  
 Magnetism in gold-iron alloys, 358  
 Magnetization formulas, 13  
 Manganese effect on nickel bronze, 234  
 Manganese-aluminum alloys equilibrium diagram, 308  
 MARSH, J S *Discussion on X-ray Studies on the Nickel-chromium System*, 371  
 Masuyama, Y on magnetism of nickel, 38  
 MATHEWSON, C. H *Discussion on Influence of a Grain Boundary on Deformation of a Single Crystal of Zinc*, 143, 145  
 MATHEWSON, C H AND RHINES, F. N. *Solubility of Oxygen in Solid Copper*, 337  
 MCFARLAND, D F *Discussion on X-ray Studies on the Nickel-chromium System*, 371



McKEEHAN, L. W. *Ferromagnetism in Metallic Crystals*, 11

*Discussions on Correlation of Equilibrium Relations in Binary Aluminum Alloys of High Purity*, 318

*on Influence of a Grain Boundary of Deformation of a Single Crystal of Zinc*, 145

portrait, 10

MEHL, R. F. *Discussions on Correlation of Equilibrium Relations in Binary Aluminum Alloys of High Purity*, 318

*on Influence of a Grain Boundary of Deformation of a Single Crystal of Zinc*, 144

*on Intermetallic Solid Solutions*, 90

*on Structure and Origin of the Copper-cuprous Oxide Eutectic*, 188

MILLER, R. F. *Influence of a Grain Boundary on Deformation of a Single Crystal of Zinc*, 135, *Discussion*, 145

## N

Nickel creep, 56

magnetic properties, 36

Nickel-aluminum alloys equilibrium data, 309 equilibrium relations, 293

Nickel bronzes *See* Bronzes

Nickel-cadmium alloy, 333

Nickel-chromium alloy X-ray study, 361

Nickel-iron alloys magnetic properties, 43

NISHIYAMA, Z. *on magnetism in cobalt*, 46

Nitrogen solubility in chromium, 367

NORDSTROM, V. H., JETTE, E. R., QUENEAU, B. AND FOOTE, F. *X-ray Studies on the Nickel-chromium System*, 361

NORTON, J. T. *Discussions on Influence of a Grain Boundary on Deformation of a Single Crystal of Zinc*, 145

*on X-ray Studies on the Nickel-chromium System*, 371

## O

Oxygen solubility in solid copper, 337

## P

PEIRCE, W. M. *Discussion on Comparative Studies on Creep of Metals Using a Modified Rohn Test*, 73

PERLITZ, H. *on solid solutions*, 82

PHILLIPS, A. AND BRICK, R. M. *Effect of Quenching Strains on Lattice Parameter and Hardness Values of High-purity Aluminum-copper Alloys*, 94, *Discussion*, 116

PHILLIPS, A. J. *Structure and Origin of the Copper-cuprous Oxide Eutectic*, 189

PHILLIPS, A. J. AND SWARTZ, C. E. *Notes on the Cadmium-nickel System*, 333

PORTEVIN, A. M. *Discussion on Structure and Origin of the Copper-cuprous Oxide Eutectic*, 189

"eutectic colony," 181, 189

POTTER, H. H. magnetization studies, 41

## Q

Quenching strains effect on aluminum-copper alloys, 94

Quenching stresses in aluminum, 158

QUENEAU, B., JETTE, E. R., NORDSTROM, V. H. AND FOOTE, F. *X-ray Studies on the Nickel-chromium system*, 361

## R

RHINES, F. N. AND MATHEWSON, C. H. *Solubility of Oxygen in Solid Copper*, 337

RODDA, J. L., ANDERSON, E. A., FULLER, M. L. AND WILCOX, R. L. *High-zinc Region of the Copper-zinc Phase Equilibrium Diagram*, 264

Rods, metallic internal stresses, 160

Rohn test, modified, for creep of metals, 53

ROLLE, S. *Discussion on Copper Embrittlement*, 213

RUDER, W. F. magnetization studies, 30

## S

SACHS, G. method of investigating internal stresses, 108

SAKAO, T. *on cold-rolled aluminum*, 120

SAMANS, C. H. *X-ray Study of Orientation Changes in Cold-rolled Single Crystals of Alpha Brass*, 119, *Discussion*, 134  
*Discussion on Crystal Orientations Developed in Alloyed Zinc*, 155

SCHUMACHER, E. E. *Discussion on Equilibrium in the Lead-zinc System with Special Reference to Liquid Solubility*, 263

SHIH, J. W. *on magnetization of iron-cobalt alloys*, 44

Silchrome steel creep, 66

Silicon, effect on nickel bronze, 233

Silicon-aluminum alloys equilibrium diagram, 306

Silver creep, 57

*influence on cold-worked copper*, 196

SIZOO, G. J. magnetization studies, 34, 41

SMITH, C. S. *Discussions on Copper Embrittlement*, 214, 217

*on Structure and Origin of the Copper cuprous Oxide Eutectic*, 189

Solid solubilities aluminum, binary, 305, 312

copper in zinc, 280

magnesium-lithium, 327

nickel in aluminum, 298

oxygen in copper, 337

Solid solutions, intermetallic, 75

Solubility copper in zinc, 264

iron in gold, 356

liquid, in lead-zinc system, 254

nickel in chromium, 369

nickel in liquid aluminum, 296

oxygen in solid copper, 337

Spring and Romanoff: investigation of lead-zinc system, 261

SPRINGER, R. D., WILCOX, R. L., WARING, R. K. AND ANDERSON, E. A.: *Equilibrium in the Lead-zinc System with Special Reference to Liquid Solubility*, 254

Steel: chrome: creep, 66  
 chrome-nickel: creep, 66  
 chrome-silicon: creep, 66  
 silchrome: creep, 66  
 stainless: creep, 66

STONE, R. H.: *Discussion on Strength and Aging Characteristics of Nickel Bronzes*, 243  
 SUCKSMITH, W. et al.: on magnetism of nickel, 37  
 SWARTZ, C. E. AND PHILLIPS, A. J.: *Notes on the Cadmium-nickel System*, 333

## T

Tanaka, S.: on cold-rolled aluminum, 119  
 Tensile properties: rolled zinc alloys, 251  
 nickel bronzes, 237  
 Thermal analyses: copper-zinc system, 274  
 lead-zinc system, 262  
 nickel-chromium, 372  
 Tin-copper-nickel alloys: system, 218  
 Tinning: softening of copper by, 198  
 Titanium-aluminum alloys: equilibrium data, 310  
 TOUR, S.: *Discussion on Testing the Drawing Properties of Rolled Zinc Alloys*, 252, 253

## V

Van Laar: thermodynamic equation, 305  
 Vegard: theory of solutions, 76

## W

WARING, R. K.: *Discussion on Equilibrium in the Lead-zinc System with Special Reference to Liquid Solubility*, 263  
 WARING, R. K., ANDERSON, E. A., SPRINGER, R. D. AND WILCOX, R. L.: *Equilibrium in the Lead-zinc System with Special Reference to Liquid Solubility*, 254  
 WEBSTER, W. L.: magnetization studies, 24, 30  
 WILCOX, R. L., ANDERSON, E. A., FULLER, R. L. AND RODDA, J. L.: *High-zinc Region of the Copper-zinc Phase Equilibrium Diagram*, 264

WILCOX, R. L., ANDERSON, E. A., WARING, R. K. AND SPRINGER, R. D.: *Equilibrium in the Lead-zinc System with Special Reference to Liquid Solubility*, 254

WILKINS, R. A.: *Discussion on Influence of Silver on the Softening of Cold-worked Copper*, 203

WILLEY, L. A. AND FINE, W. L.: *Equilibrium Relations in Aluminum-nickel Alloys of High Purity*, 293

WISE, E. M. AND EASH, J. T.: *Strength and Aging Characteristics of the Nickel Bronzes*, 218

WRIGHT, T. A.: *Discussion on An X-ray Study of Gold-iron Alloys*, 359, 360

WYMAN, L. L.: *Copper Embrittlement, III*, 205; *Discussion*, 214, 217

*Discussion on Structure and Origin of Copper-cuprous Oxide Eutectic*, 188

## X

X-ray applications: alloys in general, 79  
 aluminum-copper alloys, 94  
 brass crystals, 119  
 copper-zinc alloys, 264, 271  
 gold-iron alloys, 354  
 nickel-chromium system, 361  
 zinc alloys, 146

## Z

Zinc: creep, 73  
 crystals. *See* Crystals.  
 effect on nickel bronze, 233  
 Zinc alloys: drawing, 245  
 orientation in cold-rolled, 146  
 Zinc-aluminum alloys: aging, 110  
 Zinc-copper alloys: equilibrium diagram, 264  
 Zinc-lead alloys: equilibrium, 254  
 Zinc-lithium alloys: thermal analysis, 320

















